

# World Journal of *Gastroenterology*

*World J Gastroenterol* 2021 April 28; 27(16): 1664-1846



## REVIEW

- 1664 Artificial intelligence in gastroenterology and hepatology: Status and challenges  
*Cao JS, Lu ZY, Chen MY, Zhang B, Juengpanich S, Hu JH, Li SJ, Topatana W, Zhou XY, Feng X, Shen JL, Liu Y, Cai XJ*
- 1691 From hepatitis A to E: A critical review of viral hepatitis  
*Castaneda D, Gonzalez AJ, Alomari M, Tandon K, Zervos XB*

## MINIREVIEWS

- 1716 Paediatric gastrointestinal disorders in SARS-CoV-2 infection: Epidemiological and clinical implications  
*Al-Beltagi M, Saeed NK, Bediwy AS, El-Sawaf Y*
- 1728 Hepatitis C virus micro-elimination: Where do we stand?  
*Mangia A, Cotugno R, Cocomazzi G, Squillante MM, Piazzolla V*
- 1738 Coronavirus disease 2019 severity in obesity: Metabolic dysfunction-associated fatty liver disease in the spotlight  
*Vasques-Monteiro IML, Souza-Mello V*
- 1751 Preoperative physiological esophageal assessment for anti-reflux surgery: A guide for surgeons on high-resolution manometry and pH testing  
*Yodice M, Mignucci A, Shah V, Ashley C, Tadros M*

## ORIGINAL ARTICLE

## Basic Study

- 1770 Protective effect and mechanisms of action of Mongolian medicine Sulongga-4 on pyloric ligation-induced gastroduodenal ulcer in rats  
*Tong S, Wang H, A LS, Bai TN, Gong JH, Jin WJ, Dai LL, Ba GN, Cho SB, Fu MH*
- 1785 Depletion of MRPL35 inhibits gastric carcinoma cell proliferation by regulating downstream signaling proteins  
*Yuan L, Li JX, Yang Y, Chen Y, Ma TT, Liang S, Bu Y, Yu L, Nan Y*
- 1805 Mitochondrial pathway of the lysine demethylase 5C inhibitor CPI-455 in the Eca-109 esophageal squamous cell carcinoma cell line  
*Xue XJ, Li FR, Yu J*

## Observational Study

- 1816 Health-related quality of life after curative resection for gastric adenocarcinoma  
*Grosek J, Zavrtanik H, Tomažič A*



**SYSTEMATIC REVIEWS**

- 1828** Surrogate markers of mucosal healing in inflammatory bowel disease: A systematic review  
*State M, Negreanu L, Voiosu T, Voiosu A, Balanescu P, Mateescu RB*

**CASE REPORT**

- 1841** Managing esophagocutaneous fistula after secondary gastric pull-up: A case report  
*Lock JF, Reimer S, Pietryga S, Jakubietz R, Flemming S, Meining A, Germer CT, Seyfried F*

**ABOUT COVER**

Editorial Board Member of *World Journal of Gastroenterology*, Eiji Miyoshi, MD, PhD, Professor, Chairman, Department of Molecular Biochemistry & Clinical Investigation, Osaka University Graduate School of Medicine, 1-7 Yamada-oka, Suita, Osaka 565-0871, Japan. emiyoshi@sahs.med.osaka-u.ac.jp

**AIMS AND SCOPE**

The primary aim of *World Journal of Gastroenterology* (WJG, *World J Gastroenterol*) is to provide scholars and readers from various fields of gastroenterology and hepatology with a platform to publish high-quality basic and clinical research articles and communicate their research findings online. WJG mainly publishes articles reporting research results and findings obtained in the field of gastroenterology and hepatology and covering a wide range of topics including gastroenterology, hepatology, gastrointestinal endoscopy, gastrointestinal surgery, gastrointestinal oncology, and pediatric gastroenterology.

**INDEXING/ABSTRACTING**

The WJG is now indexed in Current Contents®/Clinical Medicine, Science Citation Index Expanded (also known as SciSearch®), Journal Citation Reports®, Index Medicus, MEDLINE, PubMed, PubMed Central, and Scopus. The 2020 edition of Journal Citation Report® cites the 2019 impact factor (IF) for WJG as 3.665; IF without journal self cites: 3.534; 5-year IF: 4.048; Ranking: 35 among 88 journals in gastroenterology and hepatology; and Quartile category: Q2. The WJG's CiteScore for 2019 is 7.1 and Scopus CiteScore rank 2019: Gastroenterology is 17/137.

**RESPONSIBLE EDITORS FOR THIS ISSUE**

Production Editor: Ji-Hong Lin; Production Department Director: Yun-Xiaoqian Wu; Editorial Office Director: Ze-Mao Gong.

**NAME OF JOURNAL**

*World Journal of Gastroenterology*

**ISSN**

ISSN 1007-9327 (print) ISSN 2219-2840 (online)

**LAUNCH DATE**

October 1, 1995

**FREQUENCY**

Weekly

**EDITORS-IN-CHIEF**

Andrzej S Tarnawski, Subrata Ghosh

**EDITORIAL BOARD MEMBERS**

<http://www.wjgnet.com/1007-9327/editorialboard.htm>

**PUBLICATION DATE**

April 28, 2021

**COPYRIGHT**

© 2021 Baishideng Publishing Group Inc

**INSTRUCTIONS TO AUTHORS**

<https://www.wjgnet.com/bpg/gerinfo/204>

**GUIDELINES FOR ETHICS DOCUMENTS**

<https://www.wjgnet.com/bpg/gerinfo/287>

**GUIDELINES FOR NON-NATIVE SPEAKERS OF ENGLISH**

<https://www.wjgnet.com/bpg/gerinfo/240>

**PUBLICATION ETHICS**

<https://www.wjgnet.com/bpg/gerinfo/288>

**PUBLICATION MISCONDUCT**

<https://www.wjgnet.com/bpg/gerinfo/208>

**ARTICLE PROCESSING CHARGE**

<https://www.wjgnet.com/bpg/gerinfo/242>

**STEPS FOR SUBMITTING MANUSCRIPTS**

<https://www.wjgnet.com/bpg/gerinfo/239>

**ONLINE SUBMISSION**

<https://www.f6publishing.com>



## Artificial intelligence in gastroenterology and hepatology: Status and challenges

Jia-Sheng Cao, Zi-Yi Lu, Ming-Yu Chen, Bin Zhang, Sarun Juengpanich, Jia-Hao Hu, Shi-Jie Li, Win Topatana, Xue-Yin Zhou, Xu Feng, Ji-Liang Shen, Yu Liu, Xiu-Jun Cai

**ORCID number:** Jia-Sheng Cao 0000-0002-4047-8899; Zi-Yi Lu 0000-0002-8209-3188; Ming-Yu Chen 0000-0001-5113-754X; Bin Zhang 0000-0002-6888-811X; Sarun Juengpanich 0000-0002-1449-5564; Jia-Hao Hu 0000-0001-5835-1012; Shi-Jie Li 0000-0002-7583-4523; Win Topatana 0000-0001-8580-1920; Xue-Yin Zhou 0000-0002-0209-5248; Xu Feng 0000-0002-4445-8174; Ji-Liang Shen 0000-0001-9702-4735; Yu Liu 0000-0001-9439-0107; Xiu-Jun Cai 0000-0002-6457-0577.

**Author contributions:** Cao JS, Lu ZY, Chen MY, and Cai XJ designed the study and collected the data; Zhang B, Juengpanich S, Hu JH, Li SJ, Topatana W, and Zhou XY analyzed and interpreted the data; Cao JS, Lu ZY, and Chen MY wrote the manuscript; Cai XJ revised the manuscript; all authors approved the final version of the manuscript.

**Supported by** Zhejiang Medical and Health Science and Technology Project, No. 2019321842; National Natural Science Foundation of China, No. 81827804; and Zhejiang Clinical Research Center of Minimally Invasive Diagnosis and Treatment of Abdominal Diseases, No. 2018E50003.

**Conflict-of-interest statement:** The authors deny any conflict of

**Jia-Sheng Cao, Ming-Yu Chen, Bin Zhang, Jia-Hao Hu, Shi-Jie Li, Xu Feng, Ji-Liang Shen, Xiu-Jun Cai**, Department of General Surgery, Sir Run-Run Shaw Hospital, Zhejiang University, Hangzhou 310016, Zhejiang Province, China

**Zi-Yi Lu, Sarun Juengpanich, Win Topatana**, Zhejiang University School of Medicine, Zhejiang University, Hangzhou 310058, Zhejiang Province, China

**Xue-Yin Zhou**, School of Medicine, Wenzhou Medical University, Wenzhou 325035, Zhejiang Province, China

**Yu Liu**, College of Life Sciences, Zhejiang University, Hangzhou 310058, Zhejiang Province, China

**Corresponding author:** Xiu-Jun Cai, FACS, FRCS, MD, PhD, Chief Doctor, Professor, Surgeon, Department of General Surgery, Sir Run-Run Shaw Hospital, Zhejiang University, No. 3 Qingchun East Road, Hangzhou 310016, Zhejiang Province, China.  
[srrsh\\_cxj@zju.edu.cn](mailto:srrsh_cxj@zju.edu.cn)

### Abstract

Originally proposed by John McCarthy in 1955, artificial intelligence (AI) has achieved a breakthrough and revolutionized the processing methods of clinical medicine with the increasing workloads of medical records and digital images. Doctors are paying attention to AI technologies for various diseases in the fields of gastroenterology and hepatology. This review will illustrate AI technology procedures for medical image analysis, including data processing, model establishment, and model validation. Furthermore, we will summarize AI applications in endoscopy, radiology, and pathology, such as detecting and evaluating lesions, facilitating treatment, and predicting treatment response and prognosis with excellent model performance. The current challenges for AI in clinical application include potential inherent bias in retrospective studies that requires larger samples for validation, ethics and legal concerns, and the incomprehensibility of the output results. Therefore, doctors and researchers should cooperate to address the current challenges and carry out further investigations to develop more accurate AI tools for improved clinical applications.

**Key Words:** Artificial intelligence; Gastroenterology; Hepatology; Status; Challenges

interest.

**Open-Access:** This article is an open-access article that was selected by an in-house editor and fully peer-reviewed by external reviewers. It is distributed in accordance with the Creative Commons Attribution NonCommercial (CC BY-NC 4.0) license, which permits others to distribute, remix, adapt, build upon this work non-commercially, and license their derivative works on different terms, provided the original work is properly cited and the use is non-commercial. See: <http://creativecommons.org/licenses/by-nc/4.0/>

**Manuscript source:** Invited manuscript

**Specialty type:** Gastroenterology and hepatology

**Country/Territory of origin:** China

**Peer-review report's scientific quality classification**

Grade A (Excellent): A  
Grade B (Very good): 0  
Grade C (Good): 0  
Grade D (Fair): 0  
Grade E (Poor): 0

**Received:** January 15, 2021

**Peer-review started:** January 15, 2021

**First decision:** February 9, 2021

**Revised:** February 11, 2021

**Accepted:** March 17, 2021

**Article in press:** March 17, 2021

**Published online:** April 28, 2021

**P-Reviewer:** Santos-García G

**S-Editor:** Zhang L

**L-Editor:** Webster JR

**P-Editor:** Wang LL



©The Author(s) 2021. Published by Baishideng Publishing Group Inc. All rights reserved.

**Core Tip:** Artificial intelligence (AI) technologies are widely used for medical image analysis in the gastroenterology and hepatology fields. Several AI models have been developed for accurate diagnosis, treatment, and prognosis based on images of endoscopy, radiology, pathology, achieving high performance comparable to experts. However, we should be aware of the certain constraints that limit the acceptance and utilization of AI tools in clinical practice. To use AI wisely, doctors and researchers should work together to address the current challenges and develop more accurate AI tools to improve patient care.

**Citation:** Cao JS, Lu ZY, Chen MY, Zhang B, Juengpanich S, Hu JH, Li SJ, Topatana W, Zhou XY, Feng X, Shen JL, Liu Y, Cai XJ. Artificial intelligence in gastroenterology and hepatology: Status and challenges. *World J Gastroenterol* 2021; 27(16): 1664-1690

**URL:** <https://www.wjgnet.com/1007-9327/full/v27/i16/1664.htm>

**DOI:** <https://dx.doi.org/10.3748/wjg.v27.i16.1664>

## INTRODUCTION

Originally proposed by John McCarthy in 1955, artificial intelligence (AI) which involves machine learning (ML) and problem solving, has achieved a breakthrough and revolutionized the processing methods of clinical medicine with the increasing workloads of medical records and digital images. In clinical practice, AI consists of several overlapping technologies such as ML, artificial neural networks (ANNs), deep learning (DL), convolutional neural networks (CNNs), and recurrent neural networks<sup>[1,2]</sup> (Figure 1). Since the 1980s, ML has been performed to construct a mathematical model and predict outcomes based on input data, and it is roughly divided into supervised (labeled data), unsupervised (unlabeled data), and semi-supervised (both labeled and unlabeled data) learning techniques<sup>[3]</sup>. Recently, as a subset of ML, ANNs have received increased interest because they can identify and learn input data by themselves instead of being labeled by experts<sup>[4]</sup>. In the last decade, DL, a new model of ML, holds great promise in clinical medicine. DL is particularly suitable for enormous complex or highly dimensional medical image analysis and predictive modeling tasks using the multilayers of ANNs, including CNNs and recurrent neural networks<sup>[5,6]</sup>. Notably, given that convolutional and pooling layers can extract distinct features and fully connected layers can make a final classification, CNNs have demonstrated excellent performance in image recognition such as endoscopy, radiology, and pathology<sup>[7,8]</sup>.

In the fields of gastroenterology and hepatology, doctors are paying attention to AI technologies for the diagnosis, treatment, and prognosis of various diseases due to the heterogeneous expertise levels of doctors (majoring in endoscopy, radiology, and pathology), time-consuming procedures, and increasing workloads. Specifically, doctors usually assess medical images visually to detect and diagnose diseases based on personal expertise and experience. As the maturity of digitalization increases, a quantitative assessment of imaging information has become the reality instead of relatively inaccurate qualitative reasoning<sup>[9,10]</sup>. Although a lot of time is necessary to review and check image analysis traditionally, little information can be obtained. For example, using AI technologies to process pathology images can assess the histopathological classification and predict gene mutations in liver cancer<sup>[11]</sup>, while only the mass nature can be identified by conventional pathology assessment. As a country with a high population, China has produced rapidly increasing medical records, which result in the high workloads<sup>[12]</sup>. Despite the progression of AI, gastroenterologists and hepatologists should always be aware of its limitations such as the retrospective manner of included studies and the utilization of not particularly suitable databases. In addition, it demands that doctors prepare for the effects and changes of AI on clinical practice in the real world.

In this review, we aim to (1) introduce how AI technologies process input data, learn from input data, validate the established model; (2) summarize the AI applications in endoscopy, radiology, pathology for accurate diagnosis, treatment, and prognosis; and (3) discuss the current limitations and future considerations of AI

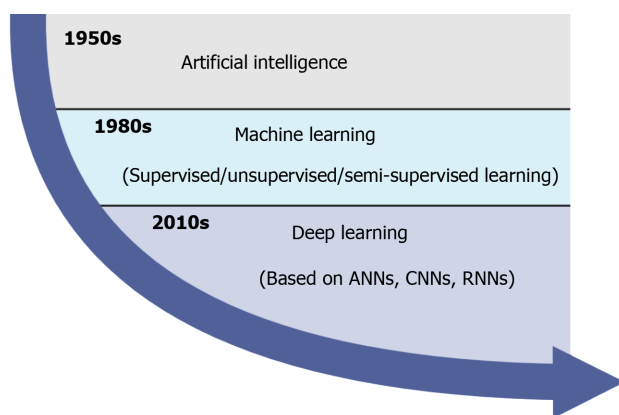


**Figure 1 Timeline and related technologies of artificial intelligence.** AI: Artificial intelligence; ANN: Artificial neural network; CNN: Convolutional neural network; RNN: Recurrent neural network.

applications in the fields of gastroenterology and hepatology (Figure 2).

## METHODS IN DEEP LEARNING

As the most suitable approach for medical image analysis, the DL approach does not require shaped regions of interest on images to complete feature selection and extraction based on a neural network structure<sup>[13,14]</sup>. After data collection and processing, the correct neural network is chosen to establish a model, followed by model validation to assess its true generalizability.

### Data processing

Raw data are collected and analyzed, and corrupt data are identified and cleaned in the processing phase. Data selection methods are provided in Scikit-Learn<sup>[15]</sup>, a Python machine learning library, which consist of univariate selection, feature importance, correlation matrix, and recursive feature elimination or addition. Other programming languages such as R Studio (<http://www.r-project.org>) or MATLAB software (University of New Mexico, New Mexico, United States) also offer a successful environment for AI, and they provide similar approaches to address specific tasks. Useful data and relevant variables from multiple data sources, which are applied to predict outcomes, are selected and divided into an initial training set and a testing set that allow training and internal validation of the model. Data in the training set should be different and nonredundant from that in the testing set. Notably, for small datasets, a higher proportion of data should be included in the testing set to measure the performance of the trained model accurately through cross-validation or in a bootstrapping procedure.

### Modeling

After transforming the data into an appropriate format, different tools are developed for implementing ML. Although several programming tools such as Python, R Studio, and MATLAB vary among themselves, they provide similar options and algorithms to adjust the parameters based on specific tasks. The major classification algorithms for testing are Naive Bayes, Decision Trees, Support Vector Machine, K-Nearest Neighbor, and Ensemble Classifiers. Oversampling or undersampling of the unbalanced training data can be utilized to improve the representation of classes and prevent model bias during the modeling stage. Currently, as the calculation workload of the batch learning process is heavy, minibatch learning is more popularized with repeating epochs, which usually decreases errors for the training and testing phases. However, an early stopping technique would be adopted to address the overfitting problem if repeating epochs cannot ensure error reduction. Based on the evaluations of model performance, developers conduct feature engineering again to manipulate the features and approve the predictive values of the model. After the optimization phase, selection for the model is primarily based on trial-and-error and the best performance for specific problem-solving. Finally, model optimization is performed with adjusted parameters by testing different configurations.

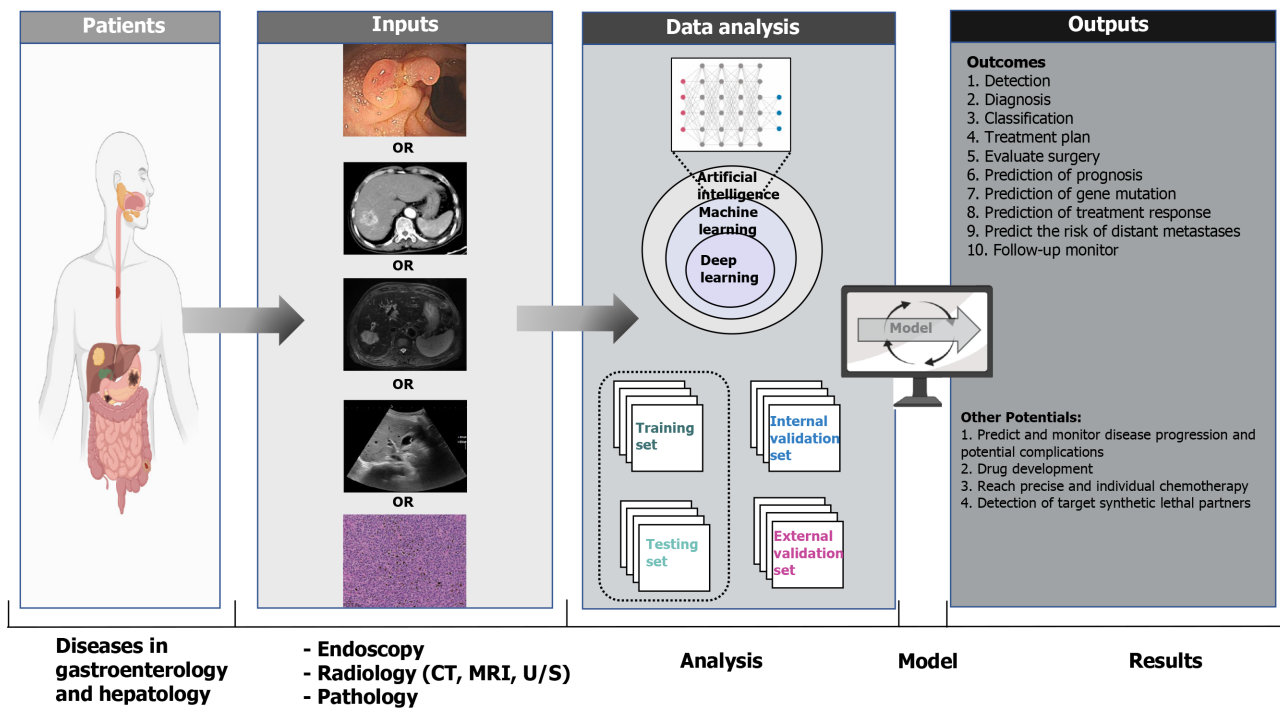


**Figure 2** Artificial intelligence-assisted endoscopy, radiology, and pathology applications for medical image analysis in the fields of gastroenterology and hepatology, including detecting and evaluating lesions, facilitating treatment, and predicting treatment response and prognosis, and other potentials, using several deep learning models. CT: Computed tomography; MRI: Magnetic resonance imaging.

### Model validation

To evaluate the AI approaches, one of the most significant requirements is external validation, which is called the blind test. Any model developed within one dataset will merely reflect its idiosyncrasies, and will have poor performance in analyzing new settings. In addition, models can also be validated by internal data testing (e.g., *k*-fold cross-validation). In *k*-fold cross-validation, the dataset is separated into *k* subsets, including one subset for testing and the remaining (*k*-1) subsets for training a model. With all data used in both training and testing sets, the cross-validation process is repeated *k* times. The model performance is finally calculated as the average value of all *k* iterations. The *k* varies depending on the size of the dataset. For example, leave-one-out validation may be used in a small training set (< 200 data points), which means that *k* is equivalent to the dataset size. The appropriate and robust predictive model should have consistent performance between training and testing sets, preventing overfitting discrepancies.

## ARTIFICIAL INTELLIGENCE IN ENDOSCOPY

With the advent and continuous improvement of fiberoptics, endoscopy has been playing a significant role in the diagnosis and treatment of gastrointestinal diseases. However, gastrointestinal diseases remain an enormous economic burden and lead to high mortality worldwide. AI is applicable in the gastroenterology fields within endoscopy<sup>[16-18]</sup>, such as identification of esophageal and gastric neoplasia in esophago-gastroduodenoscopy (EGD), detection of gastrointestinal bleeding in wireless capsule endoscopy (WCE), and polyp detection and characterization in colonoscopy, *etc*<sup>[19-63]</sup> (Table 1).

### EGD

Inadequate examination of the upper gastrointestinal tract is one of the reasons for misdiagnosing several EGD diseases. Based on AI-assisted EGD, the upper gastrointestinal tract can be divided into the pharynx, esophagus, stomach (upper, middle, lower), and duodenum with high values of the area under the curve (AUC)<sup>[19]</sup>. Furthermore, several AI technologies have classified the images of the stomach within EGD to significantly monitor the blind spots, and their accuracy has reached the ability



**Table 1 Summary of key studies on artificial intelligence-assisted endoscopy in gastroenterology fields**

Ref.	Country	Disease studied	Design of study	Application	Number of cases	Type of machine learning algorithm	Outcomes (%)	
							Accuracy	Sensitivity/Specificity
Esophagogastroduodenoscopy								
Takiyama <i>et al</i> <sup>[19]</sup> , 2018	Japan	Anatomical location of upper gastrointestinal tract	Retrospective	Recognition of the anatomical location of upper gastrointestinal tract	Training: 27335 images: 663 larynx, 3252 esophagus, 5479 upper stomach, 7184 middle stomach, 7539 lower stomach, and 3218 duodenum; Testing: 17081 images: 363 larynx, 2142 esophagus, 3532 upper stomach, 6379 middle stomach, 3137 lower stomach, and 1528 duodenum	CNNs	Larynx: 100; Esophagus: 100; Stomach: 99; Duodenum: 99	Larynx: 93.9/100; Esophagus: 95.8/99.7; Stomach: 98.9/93; Duodenum: 87/99.2
Wu <i>et al</i> <sup>[20]</sup> , 2019	China	Diseases of upper gastrointestinal tract	Prospective	Monitor blind spots of upper gastrointestinal tract	Training: 1.28 million images from 1000 object classes; Testing: 3000 images for DCNN1, and 2160 images for DCNN2	CNNs	90.4	87.57/95.02
van der Sommen <i>et al</i> <sup>[21]</sup> , 2016	Netherlands	EN-BE	Retrospective	Detection of EN in BE	21 patients with EN-BE (60 images), 23 patients without EN-BE (40 images)	SVM	NA	86/87
Swager <i>et al</i> <sup>[22]</sup> , 2017	Netherlands	EN-BE	Retrospective	Detection of EN in BE	60 images: 40 with EN-BE and 30 without EN-BE	SVM	95	90/93
Hashimoto <i>et al</i> <sup>[23]</sup> , 2020	United States	EN-BE	Retrospective	Detection of EN in BE	Training: 916 images with EN-BE; Testing: 458 images: 225 dysplasia and 233 non-dysplasia	CNNs	95.4	96.4/94.2
Ebigbo <i>et al</i> <sup>[24]</sup> , 2020	Germany	EAC-BE	Retrospective	Detection of EAC in BE	Training: 129 images; Testing: 62 images: 36 EAC and 26 normal BE	CNNs	89.9	83.7/100
Horie <i>et al</i> <sup>[25]</sup> , 2019	Japan	EAC and ESCC	Retrospective	Detection of EAC and ESCC	Training: 384 patients with 32 EAC and 397 ESCC (8428 images); Testing: 47 patients with 8 EAC and 41 ESCC (1118 images)	CNNs	98	98/79
Kumagai <i>et al</i> <sup>[26]</sup> , 2019	Japan	ESCC	Retrospective	Detection of ESCC	Training: 240 patients (4715 images: 1141 ESCC and 3574 benign lesions); Testing: 55 patients (1520 images: 467 ESCC and 1053 benign)	CNNs	90.9	92.6/89.3
Zhao <i>et al</i> <sup>[27]</sup> , 2019	China	ESCC	Retrospective	Detection of ESCC	165 patients with ESCC and 54 patients without ESCC (1383 images)	CNNs	89.2	87.0/84.1
Cai <i>et al</i> <sup>[28]</sup> , 2019	China	ESCC	Retrospective	Detection of ESCC	Training: 746 patients (2438 images: 1332 abnormal and 1096 normal); Testing: 52 patients (187 images)	CNNs	91.4	97.8/85.4
Nakagawa <i>et al</i> <sup>[29]</sup> , 2019	Japan	ESCC	Retrospective	Determination of invasion depth	Training: 804 patients with ESCC (14338 images: 8660 non-ME and 5678 ME); Testing: 155 patients with ESCC (914 images: 405 non-ME and 509 ME)	CNNs	SM1/SM2, 3: 91.0; Invasion depth: 89.6	SM1/SM2, 3: 90.1/95.8; Invasion depth: 89.8/88.3
Tokai <i>et al</i> <sup>[30]</sup> , 2020	Japan	ESCC	Retrospective	Determination of invasion depth	Training: 1751 images with ESCC; Testing: 42 patients with ESCC (293 images)	CNNs	80.9	84.1/80.9

Ali <i>et al</i> <sup>[31]</sup> , 2018	Pakistan	EGC	Retrospective	Detection of EGC	56 patients with EGC, 120 patients without EGC	SVM	87	91.0/82.0
Sakai <i>et al</i> <sup>[32]</sup> , 2018	Japan	EGC	Retrospective	Detection of EGC	Training: 58 patients (348943 images: 172555 EGC and 176388 normal); Testing: 58 patients (9650 images: 4653 EGC and 4997 normal)	CNNs	87.6	80.0/94.8
Kanesaka <i>et al</i> <sup>[33]</sup> , 2018	Japan	EGC	Retrospective	Detection of EGC	Training: 126 images: 66 EGC and 60 normal; Testing: 81 images: 61 EGC and 20 normal	SVM	96.3	96.7/95.0
Wu <i>et al</i> <sup>[34]</sup> , 2019	China	EGC	Retrospective	Detection of EGC	Training: 9691 images: 3710 EGC and 5981 normal; Testing: 100 patients: 50 EGC and 50 normal	CNNs	92.5	94.0/91.0
Horiuchi <i>et al</i> <sup>[35]</sup> , 2020	Japan	EGC	Retrospective	Detection of EGC	Training: 2570 images: 1492 EGC and 1078 gastritis; Testing: 285 images: 151 EGC and 107 gastritis	CNNs	85.3	95.4/71.0
Zhu <i>et al</i> <sup>[36]</sup> , 2019	China	Invasive GC	Retrospective	Determination of invasion depth	Training: 245 patients with GC and 545 patients without GC (5056 images); Testing: 203 images: 68 GC and 135 normal	CNNs	89.2	76.5/95.6
Luo <i>et al</i> <sup>[37]</sup> , 2019	China	EAC, ESCC, and GC	Prospective	Detection of upper gastrointestinal cancers	Training: 15040 individuals (125898 images: 31633 cancer and 94265 control); Testing: 1886 individuals (15637 images: 3931 cancer and 11706 control)	CNNs	91.5-97.7	94.2/85.8
Nagao <i>et al</i> <sup>[38]</sup> , 2020	Japan	GC	Retrospective	Determination of invasion depth	1084 patients with GC (16557 images); Training: Testing = 4:1	CNNs	94.5	84.4/99.4
Wireless capsule endoscopy								
Ayaru <i>et al</i> <sup>[39]</sup> , 2015	United Kingdom	Small bowel bleeding	Retrospective	Prediction of outcomes	Training: 170 patients with small bowel bleeding; Testing: 130 patients with small bowel bleeding	ANNs	Recurrent bleeding 88; Therapeutic intervention: 88; Severe bleeding: 78	Recurrent bleeding: 67/91; Therapeutic intervention: 80/89; Severe bleeding: 73/80
Xiao <i>et al</i> <sup>[40]</sup> , 2016	China	Small bowel bleeding	Retrospective	Detection of bleeding in GI tract	Training: 8200 images: 2050 bleeding and 6150 non-bleeding; Testing: 1800 images: 800 bleeding and 1000 non-bleeding	CNNs	99.6	99.2/99.9
Usman <i>et al</i> <sup>[41]</sup> , 2016	South Korea	Small bowel bleeding	Retrospective	Detection of bleeding in GI tract	Training: 75000 pixels: 25000 bleeding and 50000 non-bleeding; Testing: 8000 pixels: 3000 bleeding and 5000 non-bleeding	SVM	91.8	93.7/90.7
Sengupta <i>et al</i> <sup>[42]</sup> , 2017	United States	Small bowel bleeding	Retrospective	Prediction of 30-d mortality	Training: 4044 patients with small bowel bleeding; Testing: 2060 patients with small bowel bleeding	ANNs	81	87.8/90/9
Leenhardt <i>et al</i> <sup>[43]</sup> , 2019	France	Small bowel bleeding	Retrospective	Detection of GIA	Training: 600 images: 300 hemorrhagic GIA and 300 non-hemorrhagic GIA; Testing: 600 images: 300 hemorrhagic GIA and 300 non-hemorrhagic GIA	CNNs	98	100.0/96.0
Aoki <i>et al</i> <sup>[44]</sup> , 2020	Japan	Small bowel bleeding	Retrospective	Detection of small bowel bleeding	Training: 41 patients (27847 images: 6503 bleeding and 21344 normal); Testing: 25 patients (10208 images: 208 bleeding and 10000 non-bleeding)	CNNs	99.89	96.63/99.96
Yang <i>et al</i> <sup>[45]</sup> , 2020	China	Small bowel polyps	Retrospective	Detection of small bowel	1000 images: 500 polyps and 500 non-polyps	SVM	96.00	95.80/96.20



2020				polyps				
Vieira <i>et al</i> <sup>[46]</sup> , 2020	Portugal	Small bowel tumors	Retrospective	Detection of small bowel tumors	39 patients (3936 images: 936 tumors and 3000 normal)	SVM	97.6	96.1/98.3
Colonoscopy								
Fernández-Esparrach <i>et al</i> <sup>[47]</sup> , 2016	Spain	Colorectal polyps	Retrospective	Detection of polyps	24 videos containing 31 different polyps	Energy maps	79	70.4/72.4
Komeda <i>et al</i> <sup>[48]</sup> , 2017	Japan	Colorectal polyps	Retrospective	Detection of polyps	Training: 1800 images: 1200 adenoma and 600 non-adenoma; Testing: 10 cases	CNNs	70.0	83.3/50.0
Misawa <i>et al</i> <sup>[49]</sup> , 2017	Japan	Colorectal polyps	Retrospective	Detection of polyps	Training: 1661 images: 1213 neoplasm and 448 non-neoplasm; Testing: 173 images: 124 neoplasm and 49 non-neoplasm	SVM	87.8	94.3/71.4
Misawa <i>et al</i> <sup>[50]</sup> , 2018	Japan	Colorectal polyps	Retrospective	Detection of polyps	196631 frames: 63135 polyps and 133496 non-polyps	CNNs	76.5	90.0/63.3
Chen <i>et al</i> <sup>[51]</sup> , 2018	China	Colorectal polyps	Retrospective	Detection of diminutive colorectal polyps	Training: 2157 images: 681 hyperplastic and 1476 adenomas; Testing: 284 images: 96 hyperplastic and 188 adenomas	DNNs	90.1	96.3/78.1
Urban <i>et al</i> <sup>[52]</sup> , 2018	United States	Colorectal polyps	Retrospective	Detection of polyps	Training: 8561 images: 4008 polyps and 4553 non-polyps; Testing: 1330 images: 672 polyps and 658 non-polyps	CNNs	96.4	96.9/95.0
Renner <i>et al</i> <sup>[53]</sup> , 2018	Germany	Colorectal polyps	Retrospective	Differentiation of neoplastic from non-neoplastic polyps	Training: 788 images: 602 adenomas and 186 non-adenomatous polyps; Testing: 186 images: 52 adenomas and 48 hyperplastic lesions	DNNs	78.0	92.3/62.5
Wang <i>et al</i> <sup>[54]</sup> , 2018	United States	Colorectal polyps	Retrospective	Detection of polyps	Training: 5545 images: 3634 polyps and 1911 non-polyps; Testing: 27113 images: 5541 polyps and 21572 non-polyps	CNNs	98	94.4/95.9
Mori <i>et al</i> <sup>[55]</sup> , 2018	Japan	Colorectal polyps	Prospective	A diagnose-and-leave strategy for diminutive, non-neoplastic rectosigmoid polyps	Training: 61925 images; Testing: 466 cases (287 neoplastic polyps, 175 nonneoplastic polyps, and 4 missing specimens)	SVM	96.5	93.8/91.0
Byrne <i>et al</i> <sup>[56]</sup> , 2019	Canada	Colorectal polyps	Retrospective	Detection and classification of polyps	Training: 60089 frames of 223 videos (29% NICE type 1, 53% NICE type 2 and 18% of normal mucosa with no polyp); Testing: 125 videos: 51 hyperplastic polyps and 74 adenoma	CNNs	94.0	98.0/83.0
Blanes-Vidal <i>et al</i> <sup>[57]</sup> , 2019	Denmark	Colorectal polyps	Retrospective	Detection of polyps	131 patients with polyps and 124 patients without polyps	CNNs	96.4	97.1/93.3
Lee <i>et al</i> <sup>[58]</sup> , 2020	South Korea	Colorectal polyps	Retrospective	Detection of polyps	Training: 306 patients (8593 images: 8495 polyp and 98 normal); Testing: 15 patients (15 polyps videos)	CNNs	93.4	89.9/93.7
Gohari <i>et al</i> <sup>[59]</sup> , 2011	Iran	CRC	Retrospective	Determination of prognostic factors of CRC	1219 patients with CRC	ANNs	Colon cancer: 89; Rectum cancer: 82.7	NA/NA

Biglarian <i>et al</i> <sup>[60]</sup> , 2012	Iran	CRC	Retrospective	Prediction of distant metastasis in CRC	1219 patients with CRC	ANNs	82	NA/NA
Takeda <i>et al</i> <sup>[61]</sup> , 2017	Japan	CRC	Retrospective	Diagnosis of invasive CRC	Training: 5543 images: 2506 non-neoplasms, 2667 adenomas, and 370 invasive cancers; Testing: 200 images: 100 adenomas and 100 invasive cancers	SVM	94.1	89.4/98.9
Ito <i>et al</i> <sup>[62]</sup> , 2019	Japan	CRC	Retrospective	Diagnosis of cT1b CRC	Training: 9942 images: 5124 cTis + cT1a, 4818 cT1b, and 2604 cTis + cT1a; Testing: 5022 images: 2604 cTis + cT1a, and 2418 cT1b	CNNs	81.2	67.5/89.0
Zhou <i>et al</i> <sup>[63]</sup> , 2020	China	CRC	Retrospective	Diagnosis of CRC	Training: 3176 patients with CRC and 9003 patients without CRC (464105 images: 28071 CRC and 436034 non-CRC); Testing: 307 patients with CRC and 1956 patients without CRC (84615 images: 11675 CRC and 72940 non-CRC)	CNNs	96.3	91.4/98.0

AI: Artificial intelligence; CNN: Convolutional neural network; EN: Early-stage neoplasia; BE: Barrett's esophagus; SVM: Support vector machine; NA: Not available; EAC: Esophageal adenocarcinoma; ESCC: Esophageal squamous cell carcinoma; EGC: Early-stage gastric cancer; GC: Gastric cancer; ANN: Artificial neural network; GI: Gastrointestinal; GIA: Gastrointestinal angioectasia; DNN: Deep neural network; CRC: Colorectal cancer.

of experienced endoscopists<sup>[20,34]</sup>.

Endoscopic surveillance for Barrett's esophagus (BE) is the potential risk factor for esophageal adenocarcinoma (EAC), of which the prognosis is related to disease staging<sup>[64,65]</sup>. However, accurate detection of esophageal neoplasia and early EAC remains difficult for experienced endoscopists<sup>[66]</sup>. An AI system developed by Ebigbo *et al*<sup>[24]</sup> enabled early detection of EAC with high sensitivity and specificity, they subsequently designed a real-time system for neoplasia classification in magnification. Both accurate detection of early EAC is important in BE images and the novel system of high invasion accuracy also deserves clinical attention<sup>[23]</sup>. In esophageal squamous cell carcinoma (ESCC), these tumors are often diagnosed at advanced stages, while early ESCC seems to be detected based on endoscopists' experience because they are almost impossible to visualize with white light endoscopy. Fortunately, with AI technologies, small esophageal lesions (< 10 mm) are recognized, and there is an AI system showing diagnostic accuracy of 91.4%, which is higher than that of high-level (with experience of > 15 years, 88.8%), mid-level (with experience of 5-15 years, 81.6%), and junior-level (with experience of < 5 years, 77.2%) endoscopists<sup>[28]</sup>. In addition, the prognosis of ESCC can be proved by differentiating tumor invasion depth<sup>[29,30]</sup>.

The prognosis of gastric cancer (GC) mainly depends on the early detection and invasion depth of the disease. It is extremely difficult for endoscopists to recognize early gastric cancer (EGC), which is often accompanied by gastric mucosal inflammation, and the false-negative rate of EGC in EGD has reached nearly 25.0%<sup>[67,68]</sup>. AI-assisted EGD has the potential to address tough tissues. However, the first reported CNNs-based AI system for detection of EGC had a low positive predictive value of 30.6%, leading to misdiagnosis of gastritis and misinterpretation of the gastric angle as GC<sup>[69]</sup>. In 2019, Wu *et al*<sup>[34]</sup> examined the detection of GC by AI and

validated 200 endoscopic images, with increased accuracy, sensitivity, and specificity values (92.5%, 94%, and 91%, respectively). Furthermore, the AI system, named GRAIDS, has achieved diagnostic sensitivity close to that of expert endoscopists (94.2% *vs* 94.5%), and it demonstrated a robust performance showing high diagnostic accuracy in a multicenter study<sup>[37]</sup>. Besides detection, one of the most important criteria for curative resection is the invasion depth. The invasion depth prediction of GC by AI was first developed by Kubota *et al*<sup>[70]</sup>, and the model showed the accuracy of T-stages (T1 = 77%, T2 = 49%, T3 = 51%, T4 = 55%, respectively). Considering that endoscopic mucosal resection is appropriate for intramucosal cancers (M) and submucosal cancers (invasion < 500  $\mu$ m) (SM1), a more detailed classification is urgently needed. Therefore, an AI system was developed to differentiate the depths of M or SM1 and SM2 (submucosal invasion  $\geq$  500  $\mu$ m) for GC with significantly higher sensitivity, specificity, and accuracy than those of skilled endoscopists<sup>[38]</sup>.

### WCE

AI-assisted WCE enables endoscopists to highlight suspicious regions on examination of the digestive tract noninvasively, including detection of small bowel bleeding, ulcers, and polyps, celiac disease, *etc.* Based on specific AI classifiers and validation techniques (mainly *k*-fold cross-validation), these models utilized still frames, pixels, or real-time videos to identify patients with small bowel bleeding with accuracy above 90% for most studies<sup>[40,41,43,44]</sup>. A CNNs-based algorithm, established in a retrospective analysis of 10000 WCE images (8200 and 1800 in the training and testing set, respectively) and validated by 10-fold cross-validation, was proposed for automatic detection of small bowel bleeding. The model was performed with a high *F*-1 score of 99.6% and precision of 99.9% for both active and inactive bleeding frames<sup>[40]</sup>. Besides detection, several emerging AI tools have been developed to stratify patients for the possibility of recurrent bleeding, treatment requirement, and mortality estimate to prevent repeated endoscopies in a significant proportion of patients with potential recurrent upper or lower gastrointestinal bleeding<sup>[39,42]</sup>.

### Colonoscopy

Colorectal polyp detection and appropriate polypectomy during colonoscopy is the standard way to prevent colorectal cancer (CRC). Since missed colorectal polyps can potentially progress into CRC, AI-assisted colonoscopy has been developed for polyp detection and characterization, and predicting the prognosis of CRC. In terms of polyp detection, an automated AI system using an energy map was developed in 2016, and it showed barely satisfactory performance<sup>[47]</sup>. Urban *et al*<sup>[52]</sup> used 8641 labeled images and 20 colonoscopy videos as the training and testing set to establish a CNNs model to identify colonic polyps, and the model had an accuracy of 96.4%<sup>[52]</sup>. Notably, the models should be validated to improve accuracy. After validating the model developed by Wang *et al*<sup>[54]</sup> with 27113 newly collected images from 1138 patients, the model showed acceptable performance (sensitivity = 94.38%, specificity = 95.2%, and AUC = 0.984). In addition, polyp characterization with magnifying endoscopic images is useful for identifying pit or vascular patterns to improve performance. AI tools with narrow-band imaging<sup>[51]</sup> or endoscopic videos<sup>[56]</sup> can be used to differentiate diminutive hyperplastic polyps and adenomas with high accuracy. Specifically, diminutive polyps ( $\leq$  5 mm) may also be identified during colonoscopy<sup>[55]</sup>. In addition, AI may assist doctors in predicting the prognosis of CRC. An ANNs model, which was developed from a dataset of 1219 CRC patients, may predict patient survival and influential factors more accurately than a Cox regression model<sup>[59]</sup>, and it also enables doctors to predict the risk of distant metastases<sup>[60]</sup>.

## ARTIFICIAL INTELLIGENCE IN RADIOLOGY

There is a disproportionate growing rate between radiological imaging data and the number of trained radiologists, and it has forced radiologists to compensate by increasing productivity<sup>[71]</sup>. The emergence of AI technologies has eased the current dilemma and dramatically advanced radiology image analysis, including ultrasound, computed tomography (CT), and magnetic resonance imaging (MRI) in the fields of gastroenterology and hepatology. In addition, the rise of radiomics, which is a new technology in radiology and cancer, can extract abundant quantifiable objective data to evaluate surgical resection and predict treatment response<sup>[72-112]</sup> (Table 2).

Table 2 Summary of key studies on artificial intelligence-assisted radiology in hepatology fields

Ref.	Country	Disease studied	Design of study	Application	Number of cases	Type of machine learning algorithm	Outcomes (%)	
							Accuracy	Sensitivity/Specificity
Ultrasound-based medical image recognition								
Gatos <i>et al</i> <sup>[72]</sup> , 2016	United States	Hepatic fibrosis	Retrospective	Classification of CLD	85 images: 54 healthy and 31 CLD	SVM	87	83.3/89.1
Gatos <i>et al</i> <sup>[73]</sup> , 2017	United States	Hepatic fibrosis	Retrospective	Classification of CLD	124 images: 54 healthy and 70 CLD	SVM	87.3	93.5/81.2
Chen <i>et al</i> <sup>[74]</sup> , 2017	China	Hepatic fibrosis	Retrospective	Classification of the stages of hepatic fibrosis in HBV patients	513 HBV patients with different hepatic fibrosis (119 S0, 164 S1, 88 S2, 72 S3, and 70 S4)	SVM, Naive Bayes, RF, KNN	82.87	92.97/82.50
Li <i>et al</i> <sup>[75]</sup> , 2019	China	Hepatic fibrosis	Prospective	Classification of the stages of hepatic fibrosis in HBV patients	144 HBV patients	Adaptive boosting, decision tree, RF, SVM	85	93.8/76.9
Gatos <i>et al</i> <sup>[76]</sup> , 2019	United States	Hepatic fibrosis	Retrospective	Classification of CLD	88 healthy individuals (88 F0 fibrosis stage images) and 112 CLD patients (112 images: 46 F1, 16 F2, 22 F3, and 28 F4)	CNNs	82.5	NA/NA
Wang <i>et al</i> <sup>[77]</sup> , 2019	China	Hepatic fibrosis	Prospective	Classification of the stages of hepatic fibrosis in HBV patients	Training: 266 HBV patients (1330 images); Testing: 132 HBV patients (660 images)	CNNs	F4: 100; ≥ F3: 99; ≥ F2: 99	F4: 100.0/100.0; ≥ F3: 97.4/95.7; ≥ F2: 100.0/97.7
Kuppili <i>et al</i> <sup>[78]</sup> , 2017	United States	MAFLD	Retrospective	Detection and characterization of FLD	63 patients: 27 healthy and 36 MAFLD	ELM, SVM	ELM: 96.75; SVM: 89.01	NA/NA
Byra <i>et al</i> <sup>[79]</sup> , 2018	Poland	MAFLD	Retrospective	Diagnosis of the amount of fat in the liver	55 severely obese patients	CNNs, SVM	96.3	100/88.2
Biswas <i>et al</i> <sup>[80]</sup> , 2018	United States	MAFLD	Retrospective	Detection and risk stratification of FLD	63 patients: 27 healthy and 36 MAFLD	CNNs, SVM, ELM	CNNs: 100; SVM: 82; ELM: 92	NA/NA
Cao <i>et al</i> <sup>[81]</sup> , 2020	China	MAFLD	Retrospective	Detection and classification of MAFLD	240 patients: 106 healthy, 57 mild MAFLD, 67 moderate MAFLD, and 10 severe MAFLD	CNNs	95.8	NA/NA
Guo <i>et al</i> <sup>[82]</sup> , 2018	China	Liver tumors	Retrospective	Diagnosis of liver tumors	93 patients with liver tumors: 47 malignant lesions (22 HCC, 5 CC, and 10 RCLM), and 46 benign lesions	DNNs	90.41	93.56/86.89
Schmauch <i>et al</i> <sup>[83]</sup> , 2019	France	FLL	Retrospective	Detection and characterization of FLL	Training: 367 patients (367 images); Testing: 177 patients	CNNs	Detection: 93.5; Characterization: 91.6	NA/NA
Yang <i>et al</i> <sup>[84]</sup> , 2020	China	FLL	Retrospective	Detection of FLL	Training: 1815 patients with FLL (18000 images); Testing: 328 patients with FLL (3718 images)	CNNs	84.7	86.5/85.5

CT/MRI-based medical image recognition								
Choi <i>et al</i> <sup>[85]</sup> , 2018	South Korea	Hepatic fibrosis	Retrospective	Staging liver fibrosis by using CT images	Training: 7461 patients: 3357 F0, 113 F1, 284 F2, 460 F3, 3247 F4; Testing: 891 patients: 118 F0, 109 F1, 161 F2, 173 F3, 330 F4	CNNs	92.1–95.0	84.6–95.5/89.9–96.6
He <i>et al</i> <sup>[86]</sup> , 2019	United States	Hepatic fibrosis	Retrospective	Staging liver fibrosis by using MRI images	Training: 225 CLD patients; Testing: 84 patients	SVM	81.8	72.2/87.0
Ahmed <i>et al</i> <sup>[87]</sup> , 2020	Egypt	Hepatic fibrosis	Retrospective	Detection and staging of liver fibrosis by using MRI images	37 patients: 15 healthy and 22 CLD	SVM	83.7	81.8/86.6
Hectors <i>et al</i> <sup>[88]</sup> , 2020	United States	Liver fibrosis	Retrospective	Staging liver fibrosis by using MRI images	Training: 178 patients with liver fibrosis; Testing: 54 patients with liver fibrosis	CNNs	F1-F4: 85; F2-F4: 89; F3-F4: 91; F4: 83	F1-F4: 84/90; F2-F4: 87/93; F3-F4: 97/83; F4: 68/94
Vivanti <i>et al</i> <sup>[89]</sup> , 2017	Israel	Liver tumors	Retrospective	Detection and segmentation of new tumors in follow-up by using CT images	246 liver tumors (97 new tumors)	CNNs	86	70/NA
Yasaka <i>et al</i> <sup>[90]</sup> , 2018	Japan	Liver masses	Retrospective	Detection and differentiation of liver masses by using CT images	Training: 460 patients with liver masses (1068 images: 240 Category A, 121 Category B, 320 Category C, 207 Category D, 180 Category E); Testing: 100 images with liver masses: 21 Category A, 9 Category B, 35 Category C, 20 Category D, 15 Category E	CNNs	84	Category A: 71/NA; Category B: 33/NA; Category C: 94/NA; Category D: 90/NA; Category E: 100/NA
Ibragimov <i>et al</i> <sup>[91]</sup> , 2018	United States	Liver diseases requiring SBRT	Retrospective	Prediction of hepatotoxicity after liver SBRT by using CT images	125 patients undergone liver SBRT: 58 liver metastases, 36 HCC, 27 cholangiocarcinoma, and 4 other histopathologies	CNNs	85	NA/NA
Abajian <i>et al</i> <sup>[92]</sup> , 2018	United States	HCC	Retrospective	Prediction of HCC response to TACE by using MRI images	36 HCC patients treated with TACE	RF	78	62.5/82.1
Zhang <i>et al</i> <sup>[93]</sup> , 2018	United States	HCC	Retrospective	Classification of HCC by using MRI images	20 patients with HCC	CNNs	80	NA/NA
Morshid <i>et al</i> <sup>[94]</sup> , 2019	United States	HCC	Retrospective	Prediction of HCC response to TACE by using CT images	105 HCC patients received first-line treatment with TACE	CNNs	74.2	NA/NA
Nayak <i>et al</i> <sup>[95]</sup> , 2019	India	Cirrhosis; HCC	Retrospective	Detection of cirrhosis and HCC by using CT images	40 patients: 14 healthy, 12 cirrhosis, 14 cirrhosis with HCC	SVM	86.9	100/95
Hamm <i>et al</i> <sup>[96]</sup> , 2019	United States	Common hepatic lesions	Retrospective	Classification of common hepatic lesions by using MRI images	Training: 434 patients with common hepatic lesions; Testing: 60 patients with common hepatic lesions	CNNs	92	92/98
Wang <i>et al</i> <sup>[97]</sup> , 2019	United States	Common hepatic lesions	Retrospective	Demonstration of a proof-of-concept interpretable DL system by using MRI images	60 common hepatic lesions patients	CNNs	NA	82.9/NA

Jansen <i>et al</i> <sup>[98]</sup> , 2019	Netherlands	FLL	Retrospective	Classification of FLL by using MRI images	95 patients with FLL (125 benign lesions: 40 adenomas, 29 cysts, and 56 hemangiomas; and 88 malignant lesions: 30 HCC and 58 metastases)	RF	77	Adenoma: 80/78; Cyst: 93/93; Hemangioma: 84/82; HCC: 73/56; Metastasis: 62/77
Mokrane <i>et al</i> <sup>[99]</sup> , 2020	France	HCC	Retrospective	Diagnosis of HCC in patients with cirrhosis by using CT images	Training: 106 patients: 85 HCC and 21 non-HCC; Testing: 36 patients: 23 HCC and 13 non-HCC	SVM, KNN, RF	70	70/54
Shi <i>et al</i> <sup>[100]</sup> , 2020	China	HCC	Retrospective	Detection of HCC from FLL by using CT images	Training: 359 lesions: 155 HCC and 204 non-HCC; Testing: 90 lesions: 39 HCC and 51 non-HCC	CNNs	85.6	74.4/94.1
Alirr <i>et al</i> <sup>[101]</sup> , 2020	Kuwait	Liver tumors	Retrospective	Segmentation of liver tumors	Training: 100 images with liver tumors; Testing: 31 images with liver tumors	CNNs	95.2	NA/NA
Zheng <i>et al</i> <sup>[102]</sup> , 2020	China	Pancreatic cancer	Retrospective	Pancreas segmentation by using MRI images	20 patients with PDAC	CNNs	99.86	NA/NA
Radiomics								
Liang <i>et al</i> <sup>[103]</sup> , 2014	China	HCC	Retrospective	Prediction of recurrence for HCC patients who received RFA	83 patients with HCC receiving RFA as first treatment (18 recurrence and 65 non-recurrence)	SVM	82	67/86
Zhou <i>et al</i> <sup>[104]</sup> , 2017	China	HCC	Retrospective	Characterization of HCC	46 patients with HCC: 21 low-grade (Edmondson grades I and II) and 25 high-grade (Edmondson grades III and IV)	Free-form curve-fitting	86.95	76.00/100.00
Abajian <i>et al</i> <sup>[105]</sup> , 2018	United States	HCC	Retrospective	Prediction of response to intra-arterial treatment	36 patients undergone trans-arterial treatment	RF	78	62.5/82.1
Ibragimov <i>et al</i> <sup>[91]</sup> , 2018	United States	Liver tumors	Retrospective	Prediction of hepatobiliary toxicity of SBRT	125 patients undergone liver SBRT: 58 metapathologies, 36 HCC, 27 cholangiocarcinoma, and 4 other primary liver tumor histopathologies	CNNs	85	NA/NA
Morshid <i>et al</i> <sup>[94]</sup> , 2019	United States	HCC	Retrospective	Prediction of HCC response to TACE	105 patients with HCC: 11 BCLC stage A, 24 BCLC stage B, 67 BCLC stage C, and 3 BCLC stage D	CNNs	74.2	NA/NA
Ma <i>et al</i> <sup>[106]</sup> , 2019	China	HCC	Retrospective	Prediction of MVI in HCC	Training: 110 patients with HCC: 37 with MVI and 73 without MVI; Testing: 47 patients with HCC: 18 with MVI and 29 without MVI	SVM	76.6	65.6/94.4
Dong <i>et al</i> <sup>[107]</sup> , 2020	China	HCC	Retrospective	Prediction and differentiation of MVI in HCC	Prediction: 322 patients with HCC: 144 with MVI and 178 without MVI; Differentiation: 144 patients with HCC and MVI	RF, mRMR	Prediction: 63.4; Differentiation: 73.0	Prediction: 89.2/48.4; Differentiation: 33.3/80.0
He <i>et al</i> <sup>[108]</sup> , 2020	China	HCC	Prospective	Prediction of MVI in HCC	Training: 101 patients with HCC; Testing: 18 patients with HCC	LASSO	84.4	NA/NA
Schoenberg <i>et al</i> <sup>[109]</sup> , 2020	Germany	HCC	Prospective	Prediction of disease-free survival after HCC resection	Training: 127 patients with HCC; Testing: 53 patients with HCC	RF	78.8	NA/NA
Zhao <i>et al</i> <sup>[110]</sup> , 2020	China	HCC	Retrospective	Prediction of ER of HCC	Training: 78 patients with HCC: 40 with ER and	LASSO	80.8	80.0/81.6

2020				after partial hepatectomy	38 without ER; Testing: 35 patients with HCC: 18 with ER and 17 without ER			
Liu <i>et al</i> <sup>[111]</sup> , 2020	China	HCC	Retrospective	Prediction of progression-free survival of HCC patients after RFA and SR	RFA: Training: 149 HCC patients undergone RFA Testing: 65 HCC patients undergone RFA; SR: Training: 144 HCC patients undergone SR Testing: 61 HCC patients undergone SR	Cox-CNNs	RFA: 82.0; SR: 86.3	NA/NA
Chen <i>et al</i> <sup>[112]</sup> , 2021	China	HCC	Retrospective	Prediction of HCC response to first TACE by using CT images	Training: 355 patients with HCC; Testing: 118 patients with HCC	LASSO	81	85.2/77.2

AI: Artificial intelligence; CLD: Chronic liver disease; SVM: Support vector machine; HBV: Hepatitis-B virus; RF: Random forests; KNN: K-nearest neighbor; CNN: Convolutional neural network; NA: Not available; MAFLD: Metabolic associated fatty liver disease; FLD: Fatty liver disease; ELM: Extreme learning machine; HCC: Hepatocellular carcinoma; CC: Cholangiocarcinoma; RCLM: Colorectal cancer liver metastases; DNN: deep neural network; FLL: Focal liver lesions; CLD: Chronic liver disease; SBRT: Stereotactic body radiation therapy; TACE: Transarterial chemotherapy; PDAC: Pancreatic ductal adenocarcinoma; RFA: Radiofrequency ablation; BCLC: Barcelona clinic liver cancer staging; MVI: Microvascular invasion; mRMR: Minimum redundancy maximum relevance; LASSO: Least absolute shrinkage and selection operator; ER: Early recurrence; SR: Surgical resection.

### Abdominal ultrasound

AI technologies have been applied to abdominal ultrasound-based medical images for the assessment of liver diseases, such as hepatic fibrosis and mass lesions. A support vector machine-derived approach was developed by Gatos *et al*<sup>[72]</sup> to detect and classify chronic liver disease (CLD) based on abdominal ultrasound. After quantifying 85 ultrasound images (54 healthy and 31 with CLD), the proposed model showed superior results (accuracy = 87.0%, sensitivity = 83.3%, and specificity = 89.1%), which greatly improved the diagnostic and classification accuracy of CLD. Furthermore, CNNs are employed to identify and isolate regions of different stiffness temporal stability under ultrasound to explore the impact on CLD diagnosis. The updated detection algorithm has augmented the accuracy to 95.5% after excluding unreliable areas and reducing interobserver variability<sup>[76]</sup>. Detecting and classifying hepatic mass lesions as benign or malignant is equally important. Schmauch *et al*<sup>[83]</sup> performed supervised training (367 ultrasonic images together with the radiological reports) to build a DL model, and the resulting algorithm had high receiver operating characteristic curves of 0.93 and 0.916 in lesion detection and characterization, respectively. Although the model could increase the diagnostic accuracy and detect potential malignant mass lesions, it should be further validated. In addition, combining AI technologies with contrast-enhanced ultrasound may improve the performance to identify and characterize liver cancer. For example, after AI-assisted contrast-enhanced ultrasound was applied to detect liver lesions in the arterial, portal, and late phases, the accuracy, sensitivity and specificity of the examination were markedly increased<sup>[82]</sup>. Due to the misty demonstration of gastroenterology within ultrasound, an AI-assisted ultrasound tool was limited.

### CT/MRI

Liver diseases often present indeterminate behaviors on abdominal CT, and a biopsy is



recommended according to the European Association for the Study of the Liver guidelines<sup>[113]</sup>. Based on a large dataset of CT images (7461 patients diagnosed with liver fibrosis), a CNNs model was developed and it outperformed the radiologists' interpretation<sup>[85]</sup>. Furthermore, depending on ANNs-based contrast-enhanced CT images from 460 patients, Yasaka *et al*<sup>[90]</sup> conducted a retrospective study to classify liver masses into five categories with high accuracy, including (1) primary hepatocellular carcinoma (HCC); (2) malignant tumors apart from HCC; (3) early HCC, indeterminate masses, or dysplastic nodules; (4) hemangiomas; and (5) cysts. For patients diagnosed with liver tumors or pancreatic cancer, it is crucial to complete the liver or pancreas segmentation to assess the lesions and make the ideal treatment plan. Instead of conventional manual segmentation, a CNNs model was proposed to segment liver tumors based on CT images, with an accuracy of more than 80.0%, favoring suitable decision-making<sup>[101]</sup>. Additionally, a CNNs model was also developed for pancreas localization and segmentation using CT images<sup>[102]</sup>. Furthermore, monitoring tumor recurrence plays an important role in follow-up CT. Vivanti *et al*<sup>[89]</sup> collected and integrated the initial appearance of tumors, CT behaviors, and quantification of the tumor loads throughout the disease course, and then they designed an automated detection model of tumor recurrence with an accuracy of 86%.

Besides depending on CT images, a DL approach for pancreas segmentation can also be designed from MRI images. Several AI-assisted studies have shown promising results in classifying MRI liver lesions with/without risk factors and patients' clinical data, improving the accuracy and yields of reference models<sup>[93,96,98,102]</sup>.

### Radiomics

Currently, radiomics has received great interest from doctors because this AI-assisted technology can extract indiscoverable quantifiable objective data of the radiological images and reveal the association with potential biological processes<sup>[114,115]</sup>. Preoperative stratification of patients at different risk of recurrence and prediction of survival after resection is fundamental to improve prognosis. As an independent risk factor of recurrence, microvascular invasion (MVI) cannot be provided in conventional radiological techniques<sup>[116]</sup>. Several studies have managed to use radiomic algorithms based on ultrasound, CT, or MRI to elaborate radiomic signatures for preoperative prediction of MVI<sup>[106-108]</sup>. Besides the prediction of recurrence, radiomics may also be utilized to predict survival after surgical resection. However, compared to the excellent AI models based on pathologic images, radiomics-based predictive models merely attain a low value of 0.78<sup>[109]</sup>.

Beyond recurrence and survival prediction purposes, radiomics can also be utilized for prediction of patients' response to transarterial chemoembolization (TACE) and radiofrequency ablation (RFA), and post-radiotherapy hepatotoxicity. A CNNs model developed from 105 HCC patients' CT images had higher accuracy in predicting response to TACE than the Barcelona Clinic Liver Cancer stages<sup>[94]</sup>. In addition, Chen *et al*<sup>[112]</sup> designed an excellent clinical-radiomic model to predict objective response to first TACE based on 595 HCC patients' CT images, which could assist the selection of HCC patients for TACE. Another study used radiomics of MRI images with clinical data to perform prediction of TACE response<sup>[105]</sup>. For HCC in the early stages, RFA is a recommended option. Based on radiomics, Liang *et al*<sup>[103]</sup> designed a model to predict the RFA response and HCC recurrence after RFA, obtaining high AUC, sensitivity, and specificity. Additionally, post-radiotherapy hepatotoxicity should be monitored to adjust the position and dose of radiotherapy. A CNNs model not only identified that irradiation of the proximal portal vein was associated with poor prognosis, it also predicted post-radiotherapy hepatotoxicity with an AUC of 0.85<sup>[91]</sup>. Ibragimov *et al*<sup>[91]</sup> applied a CNNs model to determine the consistent patterns in toxicity-related dose plans, and the AUC of the model for dose planned analysis was increased from 0.79 to 0.85 after the combination with some pre-treatment clinical features, showing that the combined framework can indicate the accurate position and dose of radiotherapy.

## ARTIFICIAL INTELLIGENCE IN PATHOLOGY

Pathological analysis is considered the gold standard for the diagnosis of diseases in the fields of gastroenterology and hepatology. Currently, there is a shortage of pathologists around the world, which has become an obstruction for maintaining the accuracy of pathological analysis<sup>[117]</sup>. With the development of the whole-slide imaging (WSI) scanner and AI technologies, a combination of both technologies can ease the medical burden, improve the diagnosis accuracy, and even predict gene mutations and



prognosis<sup>[118-147]</sup> (Table 3).

### **Basic AI-assisted pathology: diagnosis**

The basic role of pathology is disease diagnosis. In the fields of gastroenterology, there is an increasing need for automatic pathological analysis and diagnosis of GC. Based on the virtual version of pathological slices, several studies were performed to identify and classify GC automatically with high AUCs<sup>[120-122,126]</sup>. For example, a CNNs model was developed to distinguish gastric mass lesions including gastric adenocarcinoma, adenoma and non-neoplastic lesions, and it has achieved the highest AUC of 0.97 for the identification of gastric adenocarcinoma<sup>[126]</sup>. With regard to colorectal lesions, Wei *et al*<sup>[128]</sup> trained an AI-assisted model to classify colorectal polyps on WSIs, and notably, the performance of the model was similar to that of local pathologists whether in a single institution or other institutions. Besides diagnosis, a model based on more than 400 WSIs was developed to differentiate five common subtypes of colorectal polyps with accuracy of 93%<sup>[127]</sup>. In CRC, Shapcott *et al*<sup>[129]</sup> performed a retrospective study to develop a CNNs model for diagnosis based on 853 hand-marked images with an accuracy of 84%.

In the fields of hepatology, AI-assisted pathology is applied in patients with hepatitis B virus (HBV), metabolic associated fatty liver disease, HCC, *etc.* An automated, stain-free AI system can quantify the amount of fibrillar collagen to evaluate the degree of HBV-related fibrosis with the AUC > 0.82<sup>[132]</sup>. For patients with metabolic associated fatty liver disease, AI-assisted pathology tools were used to identify and quantify pathological changes including steatosis, macrosteatosis, lobular inflammation, ballooning, and fibrosis<sup>[133]</sup>, and the algorithm output scores for quantitative comparison with experienced pathologists achieved good agreement. However, limited AI-assisted pathology tools have been built for HCC diagnosis. Notably, the MFC-CNN-ELM program was designed for nuclei grading of biopsy specimens from HCC patients, which revealed high performance in classifying tumor cells of different differentiation stages<sup>[134]</sup>.

### **Advanced AI-assisted pathology: prediction of gene mutations and prognosis**

Apart from AI-assisted pathology tools in diagnosis, it is no surprise that many tools have been developed for the prediction of gene mutations and prognosis in the fields of gastroenterology and hepatology. In CRC, AI tools have shown great effectiveness in predicting prognosis across all tumor stages based on WSIs<sup>[139,140]</sup>, and several prospective multicenter studies have further validated the high prognosis performance<sup>[142]</sup>. Notably, a subset of genetic defects occurring in gastroenterology is related to some morphological features detected on WSIs. Among screened genetic defects, microsatellite instability and mismatch-repair deficiency are associated with the survival of gastrointestinal and colorectal cancer patients receiving immunotherapy. Therefore, an AI tool was designed to predict microsatellite instability and mismatch-repair deficiency directly from pathology, and it finally showed reasonably good performance in assisting immunotherapy<sup>[138,141]</sup>. Notably, Kather *et al*<sup>[140]</sup> further validated the above model's performance in predicting overall survival from CRC pathology slides with a hazard ratio of 2.29 in CRC-specific overall survival (OS) and an hazard ratio of 1.63 in OS, respectively. However, besides the above-mentioned studies that have focused on tumor detection of CRC, few studies were designed to predict gene mutations and prognosis due to the more complicated and heterogeneous histomorphology in gastric diseases than that in the colon<sup>[136,137]</sup>.

In the fields of hepatology, AI tools are mainly used to predict gene mutations and prognosis in HCC. For example, a model has higher accuracy in predicting survival postoperatively than using a composite score of clinical and pathological factors in HCC. In addition, the model may generalize well after validating the performance in an external dataset with different staining and scanning methods<sup>[146]</sup>. Chen *et al*<sup>[11]</sup> investigated a CNN (Inception V3) for automatic classification (benign/malignant classification with 96.0% accuracy, and differentiation degree with 89.6% accuracy) and gene mutation prediction from WSIs after resection of HCC. It was found that *CTNNB1*, *FMN2*, *TP53*, and *ZFX4* could be predicted from WSIs with external AUCs from 0.71 to 0.89. Currently, after integrating clinical data, biological data, genetic data, and pathological data, the novel model may also be a promising approach. The first multi-omics model combined ribonucleic acid (RNA) sequencing, miRNA sequencing and methylation data from The Cancer Genome Atlas, and then employed AI technologies to predict and differentiate survival of HCC patients<sup>[145]</sup>. Other attempts have been made to develop models that can predict gene mutations directly based on WSIs of HCC. Using AI-assisted pathology, some approaches can predict gene expression and RNA sequencing, which may have the potential for clinical

Table 3 Summary of key studies on artificial intelligence-assisted pathology in the gastroenterology and hepatology fields

Ref.	Country	Disease studied	Design of study	Application	Number of cases	Type of machine learning algorithm	Outcomes (%)	
							Accuracy	Sensitivity/Specificity
Basic AI-based pathology: diagnosis								
Tomita <i>et al</i> <sup>[118]</sup> , 2019	United States	BE and EAC	Retrospective	Detection and classification of cancerous and precancerous esophagus tissue	Training: 379 images with 4 classes: normal, BE-no-dysplasia, BE-with-dysplasia, and adenocarcinoma; Testing: 123 images with 4 classes: normal, BE-no-dysplasia, BE-with-dysplasia, and adenocarcinoma	CNNs	Mean: 83; BE-no-dysplasia: 85; BE-with-dysplasia: 89; Adenocarcinoma: 88	Normal: 69/71 BE-no-dysplasia: 77/88; BE-with-dysplasia: 21/97; Adenocarcinoma: 71/91
Sharma <i>et al</i> <sup>[119]</sup> , 2017	Germany	GC	Retrospective	Classification and necrosis detection of GC	454 patients (6810 WSIs: 4994 for cancer classification and 1816 for necrosis detection) (HER2 immunohistochemical stain and HE stained)	CNNs	Cancer classification: 69.90; Necrosis detection: 81.44	NA/NA
Li <i>et al</i> <sup>[120]</sup> , 2018	China	GC	Retrospective	Detection of GC	700 images: 560 GC and 140 normal (HE stained)	CNNs	100	NA/NA
Leon <i>et al</i> <sup>[121]</sup> , 2019	Colombia	GC	Retrospective	Detection of GC	40 images: 20 benign and 20 malignant	CNNs	89.72	NA/NA
Sun <i>et al</i> <sup>[122]</sup> , 2019	China	GC	Retrospective	Diagnosis of GC	500 WSIs of gastric areas with typical cancerous regions	DNNs	91.6	NA/NA
Ma <i>et al</i> <sup>[123]</sup> , 2020	China	GC	Retrospective	Classification of lesions in the gastric mucosa	Training: 534 WSIs (1616713 images: 544925 normal, 544624 chronic gastritis, and 527164 cancer) (HE stained) Testing: 153 WSIs (399240 images: 135446 normal, 125783 chronic gastritis, and 138011 cancer) (HE stained)	CNNs, RF	Benign and cancer: 98.4; Normal, chronic gastritis, and GC: 94.5	Benign and cancer: 98.0/98.9; Normal, chronic gastritis, and GC: NA/NA
Yoshida <i>et al</i> <sup>[124]</sup> , 2018	Japan	Gastric lesions	Retrospective	Classification of gastric biopsy specimens	3062 gastric biopsy specimens (HE stained)	CNNs	55.6	89.5/50.7
Qu <i>et al</i> <sup>[125]</sup> , 2018	Japan	Gastric lesions	Retrospective	Classification of gastric pathology images	Training: 1080 patches: 540 benign and 540 malignant; Testing: 5400 patches: 2700 benign and 2700 malignant	CNNs	96.5	NA/NA
Iizuka <i>et al</i> <sup>[126]</sup> , 2020	Japan	Gastric and colonic epithelial tumors	Retrospective	Classification of gastric and colonic epithelial tumors	4128 cases of human gastric epithelial lesions and 4036 of colonic epithelial lesions (HE stained)	CNNs, RNNs	Gastric adenocarcinoma: 97; Gastric adenoma: 99; Colonic adenocarcinoma: 96; Colonic adenoma: 99	NA/NA
Korbar <i>et al</i> <sup>[127]</sup> , 2017	United States	Colorectal polyps	Retrospective	Classification of different types of colorectal polyps on WSIs	Training: 458 WSIs; Testing: 239 WSIs	A modified version of a residual network	93	88.3/NA
Wei <i>et al</i> <sup>[128]</sup> , 2020	United States	Colorectal polyps	Retrospective	Classification of colorectal polyps on WSIs	Training: 326 slides with colorectal polyps: 37 tubular, 30 tubulovillous or villous, 111 hyperplastic, 140 sessile serrated, and 8 normal;	CNNs	Tubular: 84.5; Tubulovillous or villous: 89.5; Hyperplastic: 85.3;	Tubular: 73.7/91.6; Tubulovillous or villous: 97.6/87.8; Hyperplastic: 60.3/97.5; Sessile

					Testing: 238 slides with colorectal polyps: 95 tubular, 78 tubulovillous or villous, 41 hyperplastic, and 24 sessile serrated		Sessile serrated: 88.7	serrated: 79.2/89.7
Shapcott <i>et al</i> <sup>[129]</sup> , 2018	United Kingdom	CRC	Retrospective	Diagnosis of CRC	853 hand-marked images	CNNs	84	NA/NA
Geessink <i>et al</i> <sup>[130]</sup> , 2019	Netherlands	CRC	Retrospective	Quantification of intratumoral stroma in CRC	129 patients with CRC	CNNs	94.6	91.1/99.4
Song <i>et al</i> <sup>[131]</sup> , 2020	China	CRC	Retrospective	Diagnosis of CRC	Training: 177 slides: 156 adenoma and 21 non-neoplasm; Testing: 362 slides: 167 adenoma and 195 non-neoplasm	CNNs	90.4	89.3/79.0
Wang <i>et al</i> <sup>[132]</sup> , 2015	China	Hepatic fibrosis	Retrospective	Assessment of HBV-related liver fibrosis and detection of liver cirrhosis	Training: 105 HBV patients; Testing: 70 HBV patients	SVM	82	NA/NA
Forlano <i>et al</i> <sup>[133]</sup> , 2020	United Kingdom	MAFLD	Retrospective	Detection and quantification of histological features of MAFLD	Training: 100 MAFLD patients; Testing: 146 MAFLD patients	K-means	Steatosis: 97; Inflammation: 96; Ballooning: 94; Fibrosis: 92	NA/NA
Li <i>et al</i> <sup>[134]</sup> , 2017	China	HCC	Retrospective	Nuclei grading of HCC	4017 HCC nuclei patches	CNNs	96.7	G1: 94.3/97.5; G2: 96.0/97.0; G3: 97.1/96.6; G4: 99.5/95.8
Kiani <i>et al</i> <sup>[135]</sup> , 2020	United States	Liver cancer (HCC and CC)	Retrospective	Histopathologic classification of liver cancer	Training: 70 WSIs: 35 HCC and 35 CC Testing: 80 WSIs: 40 HCC and 40 CC	SVM	84.2	72/95
Advanced AI-based pathology: prediction of gene mutations and prognosis								
Steinbuss <i>et al</i> <sup>[136]</sup> , 2020	Germany	Gastritis	Retrospective	Identification of gastritis subtypes	Training: 92 patients (825 images: 398 low inflammation, 305 severe inflammation, and 122 A gastritis) (HE stained) Testing: 22 patients (209 images: 122 low inflammation, 38 severe inflammation, and 49 A gastritis) (HE stained)	CNNs	84	A gastritis: 88/89; B gastritis: 100/93; C gastritis: 83/100
Liu <i>et al</i> <sup>[137]</sup> , 2020	China	Gastrointestinal neuroendocrine tumor	Retrospective	Prediction of Ki-67 positive cells	12 patients (18762 images: 5900 positive cells, 6086 positive cells, and 6776 background from ROIs) (HE and IHC stained)	CNNs	97.8	97.8/NA
Kather <i>et al</i> <sup>[138]</sup> , 2019	Germany	GC and CRC	Retrospective	Prediction of MSI in GC and CRC	Training: 360 patients (93408 tiles); Testing: 378 patients (896530 tiles)	CNNs	84	NA/NA
Bychkov <i>et al</i> <sup>[139]</sup> , 2018	Finland	CRC	Retrospective	Prediction of CRC outcome	420 CRC tumor tissue microarray samples	CNNs, RNNs	69	NA/NA
Kather <i>et al</i> <sup>[140]</sup> , 2019	Germany	CRC	Retrospective	Prediction of survival from CRC histology slides	Training: 86 CRC tissue slides (> 100000 HE image patches); Testing: 25 CRC patients (7180 images)	CNNs	98.7	NA/NA

Echle <i>et al</i> <sup>[141]</sup> , 2020	Germany	CRC	Retrospective	Detection of dMMR or MSI in CRC	Training: 5500 patients; Testing: 906 patients	A modified shufflenet DL system	92	98/52
Skrede <i>et al</i> <sup>[142]</sup> , 2020	3R23 Song 2020	CRC	Retrospective	Prediction of CRC outcome after resection	Training: 828 patients (> 12000000 image tiles); Testing: 920 patients	CNNs	76	52/78
Sirinukunwattana <i>et al</i> <sup>[143]</sup> , 2020	United Kingdom	CRC	Retrospective	Identification of consensus molecular subtypes of CRC	Training: 278 patients with CRC; Testing: 574 patients with CRC: 144 biopsies and 430 TCGA	Neural networks with domain-adversarial learning	Biopsies: 85; TCGA: 84	NA/NA
Jang <i>et al</i> <sup>[144]</sup> , 2020	South Korea	CRC	Retrospective	Prediction of gene mutations in CRC	Training: 629 WSIs with CRC (HE stained) Testing: 142 WSIs with CRC (HE stained)	CNNs	64.8-88.0	NA/NA
Chaudhary <i>et al</i> <sup>[145]</sup> , 2018	United States	HCC	Retrospective	Identification of survival subgroups of HCC	Training: 360 HCC patients' data using RNA-seq, miRNA-seq and methylation data from TCGA; Testing: 684 HCC patients' data (LIRI-JP cohort: 230; NCI cohort: 221; Chinese cohort: 166, E-TABM-36 cohort: 40, and Hawaiian cohort: 27)	DL	LIRI-JP cohort: 75; NCI cohort: 67; Chinese cohort: 69; E-TABM-36 cohort: 77; Hawaiian cohort: 82	NA/NA
Saillard <i>et al</i> <sup>[146]</sup> , 2020	France	HCC	Retrospective	Prediction of the survival of HCC patients treated by surgical resection	Training: 206 HCC (390 WSIs); Testing: 328 HCC (342 WSIs)	CNNs (SCHMOWDER and CHOWDER)	SCHMOWDER: 78; CHOWDER: 75	NA/NA
Chen <i>et al</i> <sup>[11]</sup> , 2020	China	HCC	Retrospective	Classification and gene mutation prediction of HCC	Training: 472 WSIs: 383 HCC and 89 normal liver tissue; Testing: 101 WSIs: 67 HCC and 34 normal liver tissue	CNNs	Classification: 96.0; Tumor differentiation: 89.6; Gene mutation: 71-89	NA/NA
Fu <i>et al</i> <sup>[147]</sup> , 2020	United Kingdom	EAC, GC, CRC, and liver cancers	Retrospective	Prediction of mutations, tumor composition and prognosis	17335 HE-stained images of 28 cancer types	CNNs	Variable across tumors/gene alterations	NA/NA

AI: Artificial intelligence; BE: Barrett's esophagus; EAC: Esophageal adenocarcinoma; CNN: Convolutional neural network; GC: Gastric cancer; WSI: Whole-slide image; NA: Not available; DNN: Deep neural network; RF: Random forests; RNN: Recurrent neural network; CRC: Colorectal cancer; HBV: Hepatitis-B virus; SVM: Support vector machine; MAFLD: Metabolic associated fatty liver disease; HCC: Hepatocellular carcinoma; CC: Cholangiocarcinoma; ROI: Region of interest; IHC: Immunohistochemistry; MSI: Microsatellite instability; dMMR: Mismatch-repair deficiency; TCGA: The Cancer Genome Atlas; DL: Deep learning.

translation<sup>[147]</sup>. Interestingly, some gene expression such as PD-1 and PD-L1 expression, inflammatory gene signatures, and biomarkers of inflammation did trend with improved survival and response in HCC patients<sup>[148]</sup>.

## LIMITATIONS AND FUTURE CONSIDERATIONS

This review retrospectively summarized some key and representative articles with the possibility of missing some publications in AI-related journals. Although various studies have shown promising results in the fields of AI-assisted gastroenterology and

hepatology, there are still several limitations to be discussed and resolved. One of the major criticisms is the lack of high-quality training, testing, and validation datasets for the development and validation of AI models. Due to the retrospective manner of most studies, selection bias must be considered at the training stage, meanwhile, overfitting and spectrum bias may result in overestimation of the model accuracy and generalization. According to the rigorous “six-steps” translation pipelines<sup>[149]</sup>, doctors and AI researchers should join the calls that advocate for developing interconnected networks of collecting raw acquisition data which was shifted from processed medical images over the world and training AI on a large scale to obtain robust and generalizable models. Furthermore, the black-box nature of AI technologies has become a barrier to clinical practice, because developers and users do not know the details about how computers output the conclusion. Explainable AI for reliable healthcare is worth investigating to reach clinical interpretability and transparency. In addition, from the perspective of ethics and legal liabilities, AI models may potentially cause errors and challenge the patient-doctor relationship despite the fact that they improve the clinical workflow with enhanced precision. Especially in the fields of gastroenterology and hepatology, cancer discrimination may mean a completely different treatment. If misdiagnosis occurs during AI application, who should take responsibility- the doctor, the programmer, the company providing the system, or the patient? Issues such as ethics and legal liabilities should be demonstrated in the early phase to maintain the balance between minimal error rates and maximal patient benefits<sup>[150,151]</sup>.

There have been an increasing number of studies applying AI to gastroenterology and hepatology over the past decade. In the future, the trend will continue and larger studies will be carried out to compare the performance of medical professionals with AI *vs* professionals without AI to highlight the importance of AI assistance. AI technologies will be utilized to develop more accurate models to predict and monitor disease progression and potential complications, and these models may ameliorate the insufficiency of medical resources in the remote underserved or developing regions. Besides, AI-assisted personalized imaging protocols and immediate three-dimensional reconstruction may further improve the diagnostic efficiency and accuracy. Researchers will be able to realize the mechanism of disease progression and treatment response through the combination of multi-modality images or multi-omics data. In addition, there is an emerging trend applying AI to drug development, such as prediction of compound toxicity, physical properties, and biological activities, which may assist chemotherapy for digestive system malignancy. Furthermore, AI could be used to process the data generated from the tissue-on-a-chip platform which could better summarize the tumor microenvironment, thus reach precise and individual chemotherapy in gastroenterology and hepatology. As synthetic lethality becomes a promising genetically targeted cancer therapy<sup>[152,153]</sup>, AI could also be used for the detection of target synthetic lethal partners of overexpressed or mutated genes in tumor cells to kill cancers. Finally, AI tools could not replace endoscopists, radiologists, and pathologists in the near and even distant future. Computers would make predictions and doctors would make the final decision, in other words, they would always work together to benefit patients.

---

## CONCLUSION

AI is rapidly developing and becoming a promising tool in medical image analysis of endoscopy, radiology, and pathology to improve disease diagnosis and treatment in the fields of gastroenterology and hepatology. Nevertheless, we should be aware of the constraints that limit the acceptance and utilization of AI tools in clinical practice. To use AI wisely, doctors and researchers should cooperate to address the current challenges and develop more accurate AI tools to improve patient care.

---

## ACKNOWLEDGEMENTS

We thank Yun Cai for polishing our manuscript. We are grateful to our colleagues for their assistance in checking the data of the studies.

## REFERENCES

- 1 **Laskaris R.** Artificial Intelligence: A Modern Approach, 3<sup>rd</sup> edition. Library Journal, 2015; **140**: 45-45
- 2 **Colom R,** Karama S, Jung RE, Haier RJ. Human intelligence and brain networks. *Dialogues Clin Neurosci* 2010; **12**: 489-501 [PMID: [21319494](#) DOI: [10.31887/DCNS.2010.12.4/rcolom](#)]
- 3 **Darcy AM,** Louie AK, Roberts LW. Machine Learning and the Profession of Medicine. *JAMA* 2016; **315**: 551-552 [PMID: [26864406](#) DOI: [10.1001/jama.2015.18421](#)]
- 4 **Esteva A,** Robicquet A, Ramsundar B, Kuleshov V, DePristo M, Chou K, Cui C, Corrado G, Thrun S, Dean J. A guide to deep learning in healthcare. *Nat Med* 2019; **25**: 24-29 [PMID: [30617335](#) DOI: [10.1038/s41591-018-0316-z](#)]
- 5 **Yang YJ,** Bang CS. Application of artificial intelligence in gastroenterology. *World J Gastroenterol* 2019; **25**: 1666-1683 [PMID: [31011253](#) DOI: [10.3748/wjg.v25.i14.1666](#)]
- 6 **Le Berre C,** Sandborn WJ, Aridhi S, Devignes MD, Fournier L, Smail-Tabbone M, Danese S, Peyrin-Biroulet L. Application of Artificial Intelligence to Gastroenterology and Hepatology. *Gastroenterology* 2020; **158**: 76-94. e2 [PMID: [31593701](#) DOI: [10.1053/j.gastro.2019.08.058](#)]
- 7 **Bengio Y,** Courville A, Vincent P. Representation learning: a review and new perspectives. *IEEE Trans Pattern Anal Mach Intell* 2013; **35**: 1798-1828 [PMID: [23787338](#) DOI: [10.1109/TPAMI.2013.50](#)]
- 8 **Kumar A,** Kim J, Lyndon D, Fulham M, Feng D. An Ensemble of Fine-Tuned Convolutional Neural Networks for Medical Image Classification. *IEEE J Biomed Health Inform* 2017; **21**: 31-40 [PMID: [28114041](#) DOI: [10.1109/JBHI.2016.2635663](#)]
- 9 **Ambinder EP.** A history of the shift toward full computerization of medicine. *J Oncol Pract* 2005; **1**: 54-56 [PMID: [20871680](#) DOI: [10.1200/jop.2005.1.2.54](#)]
- 10 **Chen H,** Sung JY. Potentials of AI in medical image analysis in Gastroenterology and Hepatology. *J Gastroenterol Hepatol* 2021; **36**: 31-38 [PMID: [33140875](#) DOI: [10.1111/jgh.15327](#)]
- 11 **Chen M,** Zhang B, Topatana W, Cao J, Zhu H, Juengpanich S, Mao Q, Yu H, Cai X. Classification and mutation prediction based on histopathology H&E images in liver cancer using deep learning. *NPJ Precis Oncol* 2020; **4**: 14 [PMID: [32550270](#) DOI: [10.1038/s41698-020-0120-3](#)]
- 12 **Fu Y,** Schwebel DC, Hu G. Physicians' Workloads in China: 1998-2016. *Int J Environ Res Public Health* 2018; **15** [PMID: [30081497](#) DOI: [10.3390/ijerph15081649](#)]
- 13 **Miotto R,** Wang F, Wang S, Jiang X, Dudley JT. Deep learning for healthcare: review, opportunities and challenges. *Brief Bioinform* 2018; **19**: 1236-1246 [PMID: [28481991](#) DOI: [10.1093/bib/bbx044](#)]
- 14 **Shen D,** Wu G, Suk HI. Deep Learning in Medical Image Analysis. *Annu Rev Biomed Eng* 2017; **19**: 221-248 [PMID: [28301734](#) DOI: [10.1146/annurev-bioeng-071516-044442](#)]
- 15 **Pedregosa F,** Varoquaux G, Gramfort A, Michel V, Thirion B, Grisel O, Blondel M, Prettenhofer P, Weiss R, Dubourg V, Vanderplas J, Passos A, Cournapeau D, Brucher M, Perrot M, Duchesnay E. Scikit-learn: Machine Learning in Python. *J Mach Learn Res* 2011; **12**: 2825-2830
- 16 **Yu H,** Singh R, Shin SH, Ho KY. Artificial intelligence in upper GI endoscopy - current status, challenges and future promise. *J Gastroenterol Hepatol* 2021; **36**: 20-24 [PMID: [33448515](#) DOI: [10.1111/jgh.15354](#)]
- 17 **Mori Y,** Neumann H, Misawa M, Kudo SE, Bretthauer M. Artificial intelligence in colonoscopy - Now on the market. What's next? *J Gastroenterol Hepatol* 2021; **36**: 7-11 [PMID: [33179322](#) DOI: [10.1111/jgh.15339](#)]
- 18 **Wu J,** Chen J, Cai J. Application of Artificial Intelligence in Gastrointestinal Endoscopy. *J Clin Gastroenterol* 2021; **55**: 110-120 [PMID: [32925304](#) DOI: [10.1097/MCG.0000000000001423](#)]
- 19 **Takiyama H,** Ozawa T, Ishihara S, Fujishiro M, Shichijo S, Nomura S, Miura M, Tada T. Automatic anatomical classification of esophagogastrroduodenoscopy images using deep convolutional neural networks. *Sci Rep* 2018; **8**: 7497 [PMID: [29760397](#) DOI: [10.1038/s41598-018-25842-6](#)]
- 20 **Wu L,** Zhang J, Zhou W, An P, Shen L, Liu J, Jiang X, Huang X, Mu G, Wan X, Lv X, Gao J, Cui N, Hu S, Chen Y, Hu X, Li J, Chen D, Gong D, He X, Ding Q, Zhu X, Li S, Wei X, Li X, Wang X, Zhou J, Zhang M, Yu HG. Randomised controlled trial of WISENSE, a real-time quality improving system for monitoring blind spots during esophagogastrroduodenoscopy. *Gut* 2019; **68**: 2161-2169 [PMID: [30858305](#) DOI: [10.1136/gutjnl-2018-317366](#)]
- 21 **van der Sommen F,** Zinger S, Curvers WL, Bisschops R, Pech O, Weusten BL, Bergman JJ, de With PH, Schoon EJ. Computer-aided detection of early neoplastic lesions in Barrett's esophagus. *Endoscopy* 2016; **48**: 617-624 [PMID: [27100718](#) DOI: [10.1055/s-0042-105284](#)]
- 22 **Swager AF,** van der Sommen F, Klomp SR, Zinger S, Meijer SL, Schoon EJ, Bergman JJGHM, de With PH, Curvers WL. Computer-aided detection of early Barrett's neoplasia using volumetric laser endomicroscopy. *Gastrointest Endosc* 2017; **86**: 839-846 [PMID: [28322771](#) DOI: [10.1016/j.gie.2017.03.011](#)]
- 23 **Hashimoto R,** Requa J, Dao T, Ninh A, Tran E, Mai D, Lugo M, El-Hage Chehade N, Chang KJ, Karnes WE, Samarasena JB. Artificial intelligence using convolutional neural networks for real-time detection of early esophageal neoplasia in Barrett's esophagus (with video). *Gastrointest Endosc* 2020; **91**: 1264-1271. e1 [PMID: [31930967](#) DOI: [10.1016/j.gie.2019.12.049](#)]
- 24 **Ebigbo A,** Mendel R, Probst A, Manzeneder J, Prinz F, de Souza LA Jr, Papa J, Palm C, Messmann H. Real-time use of artificial intelligence in the evaluation of cancer in Barrett's oesophagus. *Gut* 2020; **69**: 615-616 [PMID: [31541004](#) DOI: [10.1136/gutjnl-2019-319460](#)]



- 25 **Horie Y**, Yoshio T, Aoyama K, Yoshimizu S, Horiuchi Y, Ishiyama A, Hirasawa T, Tsuchida T, Ozawa T, Ishihara S, Kumagai Y, Fujishiro M, Maetani I, Fujisaki J, Tada T. Diagnostic outcomes of esophageal cancer by artificial intelligence using convolutional neural networks. *Gastrointest Endosc* 2019; **89**: 25-32 [PMID: [30120958](#) DOI: [10.1016/j.gie.2018.07.037](#)]
- 26 **Kumagai Y**, Takubo K, Kawada K, Aoyama K, Endo Y, Ozawa T, Hirasawa T, Yoshio T, Ishihara S, Fujishiro M, Tamaru JI, Mochiki E, Ishida H, Tada T. Diagnosis using deep-learning artificial intelligence based on the endocytoscopic observation of the esophagus. *Esophagus* 2019; **16**: 180-187 [PMID: [30547352](#) DOI: [10.1007/s10388-018-0651-7](#)]
- 27 **Zhao YY**, Xue DX, Wang YL, Zhang R, Sun B, Cai YP, Feng H, Cai Y, Xu JM. Computer-assisted diagnosis of early esophageal squamous cell carcinoma using narrow-band imaging magnifying endoscopy. *Endoscopy* 2019; **51**: 333-341 [PMID: [30469155](#) DOI: [10.1055/a-0756-8754](#)]
- 28 **Cai SL**, Li B, Tan WM, Niu XJ, Yu HH, Yao LQ, Zhou PH, Yan B, Zhong YS. Using a deep learning system in endoscopy for screening of early esophageal squamous cell carcinoma (with video). *Gastrointest Endosc* 2019; **90**: 745-753. e2 [PMID: [31302091](#) DOI: [10.1016/j.gie.2019.06.044](#)]
- 29 **Nakagawa K**, Ishihara R, Aoyama K, Ohmori M, Nakahira H, Matsuura N, Shichijo S, Nishida T, Yamada T, Yamaguchi S, Ogiyama H, Egawa S, Kishida O, Tada T. Classification for invasion depth of esophageal squamous cell carcinoma using a deep neural network compared with experienced endoscopists. *Gastrointest Endosc* 2019; **90**: 407-414 [PMID: [31077698](#) DOI: [10.1016/j.gie.2019.04.245](#)]
- 30 **Tokai Y**, Yoshio T, Aoyama K, Horie Y, Yoshimizu S, Horiuchi Y, Ishiyama A, Tsuchida T, Hirasawa T, Sakakibara Y, Yamada T, Yamaguchi S, Fujisaki J, Tada T. Application of artificial intelligence using convolutional neural networks in determining the invasion depth of esophageal squamous cell carcinoma. *Esophagus* 2020; **17**: 250-256 [PMID: [31980977](#) DOI: [10.1007/s10388-020-00716-x](#)]
- 31 **Ali H**, Yasmin M, Sharif M, Rehmani MH. Computer assisted gastric abnormalities detection using hybrid texture descriptors for chromoendoscopy images. *Comput Methods Programs Biomed* 2018; **157**: 39-47 [PMID: [29477434](#) DOI: [10.1016/j.cmpb.2018.01.013](#)]
- 32 **Sakai Y**, Takemoto S, Hori K, Nishimura M, Ikematsu H, Yano T, Yokota H. Automatic detection of early gastric cancer in endoscopic images using a transferring convolutional neural network. *Annu Int Conf IEEE Eng Med Biol Soc* 2018; **2018**: 4138-4141 [PMID: [30441266](#) DOI: [10.1109/EMBC.2018.8513274](#)]
- 33 **Kanesaka T**, Lee TC, Uedo N, Lin KP, Chen HZ, Lee JY, Wang HP, Chang HT. Computer-aided diagnosis for identifying and delineating early gastric cancers in magnifying narrow-band imaging. *Gastrointest Endosc* 2018; **87**: 1339-1344 [PMID: [29225083](#) DOI: [10.1016/j.gie.2017.11.029](#)]
- 34 **Wu L**, Zhou W, Wan X, Zhang J, Shen L, Hu S, Ding Q, Mu G, Yin A, Huang X, Liu J, Jiang X, Wang Z, Deng Y, Liu M, Lin R, Ling T, Li P, Wu Q, Jin P, Chen J, Yu H. A deep neural network improves endoscopic detection of early gastric cancer without blind spots. *Endoscopy* 2019; **51**: 522-531 [PMID: [30861533](#) DOI: [10.1055/a-0855-3532](#)]
- 35 **Horiuchi Y**, Aoyama K, Tokai Y, Hirasawa T, Yoshimizu S, Ishiyama A, Yoshio T, Tsuchida T, Fujisaki J, Tada T. Convolutional Neural Network for Differentiating Gastric Cancer from Gastritis Using Magnified Endoscopy with Narrow Band Imaging. *Dig Dis Sci* 2020; **65**: 1355-1363 [PMID: [31584138](#) DOI: [10.1007/s10620-019-05862-6](#)]
- 36 **Zhu Y**, Wang QC, Xu MD, Zhang Z, Cheng J, Zhong YS, Zhang YQ, Chen WF, Yao LQ, Zhou PH, Li QL. Application of convolutional neural network in the diagnosis of the invasion depth of gastric cancer based on conventional endoscopy. *Gastrointest Endosc* 2019; **89**: 806-815. e1 [PMID: [30452913](#) DOI: [10.1016/j.gie.2018.11.011](#)]
- 37 **Luo H**, Xu G, Li C, He L, Luo L, Wang Z, Jing B, Deng Y, Jin Y, Li Y, Li B, Tan W, He C, Seeruttun SR, Wu Q, Huang J, Huang DW, Chen B, Lin SB, Chen QM, Yuan CM, Chen HX, Pu HY, Zhou F, He Y, Xu RH. Real-time artificial intelligence for detection of upper gastrointestinal cancer by endoscopy: a multicentre, case-control, diagnostic study. *Lancet Oncol* 2019; **20**: 1645-1654 [PMID: [31591062](#) DOI: [10.1016/S1470-2045\(19\)30637-0](#)]
- 38 **Nagao S**, Tsuji Y, Sakaguchi Y, Takahashi Y, Minatsuki C, Niimi K, Yamashita H, Yamamichi N, Seto Y, Tada T, Koike K. Highly accurate artificial intelligence systems to predict the invasion depth of gastric cancer: efficacy of conventional white-light imaging, nonmagnifying narrow-band imaging, and indigo-carmin dye contrast imaging. *Gastrointest Endosc* 2020; **92**: 866-873. e1 [PMID: [32592776](#) DOI: [10.1016/j.gie.2020.06.047](#)]
- 39 **Ayaru L**, Ypsilantis PP, Nanapragasam A, Choi RC, Thillanathan A, Min-Ho L, Montana G. Prediction of Outcome in Acute Lower Gastrointestinal Bleeding Using Gradient Boosting. *PLoS One* 2015; **10**: e0132485 [PMID: [26172121](#) DOI: [10.1371/journal.pone.0132485](#)]
- 40 **Xiao Jia**, Meng MQ. A deep convolutional neural network for bleeding detection in Wireless Capsule Endoscopy images. *Annu Int Conf IEEE Eng Med Biol Soc* 2016; **2016**: 639-642 [PMID: [28268409](#) DOI: [10.1109/EMBC.2016.7590783](#)]
- 41 **Usman MA**, Satria GB, Usman MR, Shin SY. Detection of small colon bleeding in wireless capsule endoscopy videos. *Comput Med Imaging Graph* 2016; **54**: 16-26 [PMID: [27793502](#) DOI: [10.1016/j.compmedimag.2016.09.005](#)]
- 42 **Sengupta N**, Tapper EB. Derivation and Internal Validation of a Clinical Prediction Tool for 30-Day Mortality in Lower Gastrointestinal Bleeding. *Am J Med* 2017; **130**: 601.e1-601. e8 [PMID: [28065767](#) DOI: [10.1016/j.amjmed.2016.12.009](#)]

- 43 **Leenhardt R**, Vasseur P, Li C, Saurin JC, Rahmi G, Cholet F, Becq A, Marteau P, Histace A, Dray X; CAD-CAP Database Working Group. A neural network algorithm for detection of GI angiectasia during small-bowel capsule endoscopy. *Gastrointest Endosc* 2019; **89**: 189-194 [PMID: [30017868](#) DOI: [10.1016/j.gie.2018.06.036](#)]
- 44 **Aoki T**, Yamada A, Kato Y, Saito H, Tsuboi A, Nakada A, Niikura R, Fujishiro M, Oka S, Ishihara S, Matsuda T, Nakahori M, Tanaka S, Koike K, Tada T. Automatic detection of blood content in capsule endoscopy images based on a deep convolutional neural network. *J Gastroenterol Hepatol* 2020; **35**: 1196-1200 [PMID: [31758717](#) DOI: [10.1111/jgh.14941](#)]
- 45 **Yang J**, Chang L, Li S, He X, Zhu T. WCE polyp detection based on novel feature descriptor with normalized variance locality-constrained linear coding. *Int J Comput Assist Radiol Surg* 2020; **15**: 1291-1302 [PMID: [32447521](#) DOI: [10.1007/s11548-020-02190-3](#)]
- 46 **Vieira PM**, Freitas NR, Valente J, Vaz IF, Rolanda C, Lima CS. Automatic detection of small bowel tumors in wireless capsule endoscopy images using ensemble learning. *Med Phys* 2020; **47**: 52-63 [PMID: [31299096](#) DOI: [10.1002/mp.13709](#)]
- 47 **Fernández-Esparrach G**, Bernal J, López-Cerón M, Córdova H, Sánchez-Montes C, Rodríguez de Miguel C, Sánchez FJ. Exploring the clinical potential of an automatic colonic polyp detection method based on the creation of energy maps. *Endoscopy* 2016; **48**: 837-842 [PMID: [27285900](#) DOI: [10.1055/s-0042-108434](#)]
- 48 **Komeda Y**, Handa H, Watanabe T, Nomura T, Kitahashi M, Sakurai T, Okamoto A, Minami T, Kono M, Arizumi T, Takenaka M, Hagiwara S, Matsui S, Nishida N, Kashida H, Kudo M. Computer-Aided Diagnosis Based on Convolutional Neural Network System for Colorectal Polyp Classification: Preliminary Experience. *Oncology* 2017; **93** Suppl 1: 30-34 [PMID: [29258081](#) DOI: [10.1159/000481227](#)]
- 49 **Misawa M**, Kudo SE, Mori Y, Takeda K, Maeda Y, Kataoka S, Nakamura H, Kudo T, Wakamura K, Hayashi T, Katagiri A, Baba T, Ishida F, Inoue H, Nimura Y, Oda M, Mori K. Accuracy of computer-aided diagnosis based on narrow-band imaging endocytoscopy for diagnosing colorectal lesions: comparison with experts. *Int J Comput Assist Radiol Surg* 2017; **12**: 757-766 [PMID: [28247214](#) DOI: [10.1007/s11548-017-1542-4](#)]
- 50 **Misawa M**, Kudo SE, Mori Y, Cho T, Kataoka S, Yamauchi A, Ogawa Y, Maeda Y, Takeda K, Ichimasa K, Nakamura H, Yagawa Y, Toyoshima N, Ogata N, Kudo T, Hisayuki T, Hayashi T, Wakamura K, Baba T, Ishida F, Itoh H, Roth H, Oda M, Mori K. Artificial Intelligence-Assisted Polyp Detection for Colonoscopy: Initial Experience. *Gastroenterology* 2018; **154**: 2027-2029. e3 [PMID: [29653147](#) DOI: [10.1053/j.gastro.2018.04.003](#)]
- 51 **Chen PJ**, Lin MC, Lai MJ, Lin JC, Lu HH, Tseng VS. Accurate Classification of Diminutive Colorectal Polyps Using Computer-Aided Analysis. *Gastroenterology* 2018; **154**: 568-575 [PMID: [29042219](#) DOI: [10.1053/j.gastro.2017.10.010](#)]
- 52 **Urban G**, Tripathi P, Alkayali T, Mittal M, Jalali F, Karnes W, Baldi P. Deep Learning Localizes and Identifies Polyps in Real Time With 96% Accuracy in Screening Colonoscopy. *Gastroenterology* 2018; **155**: 1069-1078. e8 [PMID: [29928897](#) DOI: [10.1053/j.gastro.2018.06.037](#)]
- 53 **Renner J**, Philipsen H, Haller B, Navarro-Avila F, Saint-Hill-Feblès Y, Mateus D, Ponchon T, Poszler A, Abdelhafez M, Schmid RM, von Delius S, Klare P. Optical classification of neoplastic colorectal polyps - a computer-assisted approach (the COACH study). *Scand J Gastroenterol* 2018; **53**: 1100-1106 [PMID: [30270677](#) DOI: [10.1080/00365521.2018.1501092](#)]
- 54 **Wang P**, Xiao X, Glissen Brown JR, Berzin TM, Tu M, Xiong F, Hu X, Liu P, Song Y, Zhang D, Yang X, Li L, He J, Yi X, Liu J, Liu X. Development and validation of a deep-learning algorithm for the detection of polyps during colonoscopy. *Nat Biomed Eng* 2018; **2**: 741-748 [PMID: [31015647](#) DOI: [10.1038/s41551-018-0301-3](#)]
- 55 **Mori Y**, Kudo SE, Misawa M, Saito Y, Ikematsu H, Hotta K, Ohtsuka K, Urushibara F, Kataoka S, Ogawa Y, Maeda Y, Takeda K, Nakamura H, Ichimasa K, Kudo T, Hayashi T, Wakamura K, Ishida F, Inoue H, Itoh H, Oda M, Mori K. Real-Time Use of Artificial Intelligence in Identification of Diminutive Polyps During Colonoscopy: A Prospective Study. *Ann Intern Med* 2018; **169**: 357-366 [PMID: [30105375](#) DOI: [10.7326/M18-0249](#)]
- 56 **Byrne MF**, Chapados N, Soudan F, Oertel C, Linares Pérez M, Kelly R, Iqbal N, Chandelier F, Rex DK. Real-time differentiation of adenomatous and hyperplastic diminutive colorectal polyps during analysis of unaltered videos of standard colonoscopy using a deep learning model. *Gut* 2019; **68**: 94-100 [PMID: [29066576](#) DOI: [10.1136/gutjnl-2017-314547](#)]
- 57 **Blanes-Vidal V**, Baatrup G, Nadimi ES. Addressing priority challenges in the detection and assessment of colorectal polyps from capsule endoscopy and colonoscopy in colorectal cancer screening using machine learning. *Acta Oncol* 2019; **58**: S29-S36 [PMID: [30836800](#) DOI: [10.1080/0284186X.2019.1584404](#)]
- 58 **Lee JY**, Jeong J, Song EM, Ha C, Lee HJ, Koo JE, Yang DH, Kim N, Byeon JS. Real-time detection of colon polyps during colonoscopy using deep learning: systematic validation with four independent datasets. *Sci Rep* 2020; **10**: 8379 [PMID: [32433506](#) DOI: [10.1038/s41598-020-65387-1](#)]
- 59 **Gohari MR**, Biglarian A, Bakhshi E, Pourhoseingholi MA. Use of an artificial neural network to determine prognostic factors in colorectal cancer patients. *Asian Pac J Cancer Prev* 2011; **12**: 1469-1472 [PMID: [22126483](#)]
- 60 **Biglarian A**, Bakhshi E, Gohari MR, Khodabakhshi R. Artificial neural network for prediction of distant metastasis in colorectal cancer. *Asian Pac J Cancer Prev* 2012; **13**: 927-930 [PMID: [22126483](#)]



- 22631673 DOI: [10.7314/apjcp.2012.13.3.927](https://doi.org/10.7314/apjcp.2012.13.3.927)]
- 61 **Takeda K**, Kudo SE, Mori Y, Misawa M, Kudo T, Wakamura K, Katagiri A, Baba T, Hidaka E, Ishida F, Inoue H, Oda M, Mori K. Accuracy of diagnosing invasive colorectal cancer using computer-aided endocytoscopy. *Endoscopy* 2017; **49**: 798-802 [PMID: [28472832](https://pubmed.ncbi.nlm.nih.gov/28472832/) DOI: [10.1055/s-0043-105486](https://doi.org/10.1055/s-0043-105486)]
  - 62 **Ito N**, Kawahira H, Nakashima H, Uesato M, Miyauchi H, Matsubara H. Endoscopic Diagnostic Support System for cT1b Colorectal Cancer Using Deep Learning. *Oncology* 2019; **96**: 44-50 [PMID: [30130758](https://pubmed.ncbi.nlm.nih.gov/30130758/) DOI: [10.1159/000491636](https://doi.org/10.1159/000491636)]
  - 63 **Zhou D**, Tian F, Tian X, Sun L, Huang X, Zhao F, Zhou N, Chen Z, Zhang Q, Yang M, Yang Y, Guo X, Li Z, Liu J, Wang J, Wang B, Zhang G, Sun B, Zhang W, Kong D, Chen K, Li X. Diagnostic evaluation of a deep learning model for optical diagnosis of colorectal cancer. *Nat Commun* 2020; **11**: 2961 [PMID: [32528084](https://pubmed.ncbi.nlm.nih.gov/32528084/) DOI: [10.1038/s41467-020-16777-6](https://doi.org/10.1038/s41467-020-16777-6)]
  - 64 **Shaheen NJ**, Falk GW, Iyer PG, Gerson LB; American College of Gastroenterology. ACG Clinical Guideline: Diagnosis and Management of Barrett's Esophagus. *Am J Gastroenterol* 2016; **111**: 30-50; quiz 51 [PMID: [26526079](https://pubmed.ncbi.nlm.nih.gov/26526079/) DOI: [10.1038/ajg.2015.322](https://doi.org/10.1038/ajg.2015.322)]
  - 65 **Fitzgerald RC**, di Pietro M, Ragunath K, Ang Y, Kang JY, Watson P, Trudgill N, Patel P, Kaye PV, Sanders S, O'Donovan M, Bird-Lieberman E, Bhandari P, Jankowski JA, Attwood S, Parsons SL, Loft D, Lagergren J, Moayyedi P, Lyratzopoulos G, de Caestecker J; British Society of Gastroenterology. British Society of Gastroenterology guidelines on the diagnosis and management of Barrett's oesophagus. *Gut* 2014; **63**: 7-42 [PMID: [24165758](https://pubmed.ncbi.nlm.nih.gov/24165758/) DOI: [10.1136/gutjnl-2013-305372](https://doi.org/10.1136/gutjnl-2013-305372)]
  - 66 **Schölvinck DW**, van der Meulen K, Bergman JJGHM, Weusten BLAM. Detection of lesions in dysplastic Barrett's esophagus by community and expert endoscopists. *Endoscopy* 2017; **49**: 113-120 [PMID: [27855466](https://pubmed.ncbi.nlm.nih.gov/27855466/) DOI: [10.1055/s-0042-118312](https://doi.org/10.1055/s-0042-118312)]
  - 67 **Menon S**, Trudgill N. How commonly is upper gastrointestinal cancer missed at endoscopy? *Endosc Int Open* 2014; **2**: E46-E50 [PMID: [26135259](https://pubmed.ncbi.nlm.nih.gov/26135259/) DOI: [10.1055/s-0034-1365524](https://doi.org/10.1055/s-0034-1365524)]
  - 68 **Hosokawa O**, Hattori M, Douden K, Hayashi H, Ohta K, Kaizaki Y. Difference in accuracy between gastroscopy and colonoscopy for detection of cancer. *Hepatogastroenterology* 2007; **54**: 442-444 [PMID: [17523293](https://pubmed.ncbi.nlm.nih.gov/17523293/)]
  - 69 **Hirasawa T**, Aoyama K, Tanimoto T, Ishihara S, Shichijo S, Ozawa T, Ohnishi T, Fujishiro M, Matsuo K, Fujisaki J, Tada T. Application of artificial intelligence using a convolutional neural network for detecting gastric cancer in endoscopic images. *Gastric Cancer* 2018; **21**: 653-660 [PMID: [29335825](https://pubmed.ncbi.nlm.nih.gov/29335825/) DOI: [10.1007/s10120-018-0793-2](https://doi.org/10.1007/s10120-018-0793-2)]
  - 70 **Kubota K**, Kuroda J, Yoshida M, Ohta K, Kitajima M. Medical image analysis: computer-aided diagnosis of gastric cancer invasion on endoscopic images. *Surg Endosc* 2012; **26**: 1485-1489 [PMID: [22083334](https://pubmed.ncbi.nlm.nih.gov/22083334/) DOI: [10.1007/s00464-011-2036-z](https://doi.org/10.1007/s00464-011-2036-z)]
  - 71 **Boland GW**, Guimaraes AS, Mueller PR. The radiologist's conundrum: benefits and costs of increasing CT capacity and utilization. *Eur Radiol* 2009; **19**: 9-11; discussion 12 [PMID: [18766347](https://pubmed.ncbi.nlm.nih.gov/18766347/) DOI: [10.1007/s00330-008-1159-7](https://doi.org/10.1007/s00330-008-1159-7)]
  - 72 **Gatos I**, Tsantis S, Spiliopoulos S, Karnabatidis D, Theotokas I, Zoumpoulis P, Loupas T, Hazle JD, Kagadis GC. A new computer aided diagnosis system for evaluation of chronic liver disease with ultrasound shear wave elastography imaging. *Med Phys* 2016; **43**: 1428-1436 [PMID: [26936727](https://pubmed.ncbi.nlm.nih.gov/26936727/) DOI: [10.1118/1.4942383](https://doi.org/10.1118/1.4942383)]
  - 73 **Gatos I**, Tsantis S, Spiliopoulos S, Karnabatidis D, Theotokas I, Zoumpoulis P, Loupas T, Hazle JD, Kagadis GC. A Machine-Learning Algorithm Toward Color Analysis for Chronic Liver Disease Classification, Employing Ultrasound Shear Wave Elastography. *Ultrasound Med Biol* 2017; **43**: 1797-1810 [PMID: [28634041](https://pubmed.ncbi.nlm.nih.gov/28634041/) DOI: [10.1016/j.ultrasmedbio.2017.05.002](https://doi.org/10.1016/j.ultrasmedbio.2017.05.002)]
  - 74 **Chen Y**, Luo Y, Huang W, Hu D, Zheng RQ, Cong SZ, Meng FK, Yang H, Lin HJ, Sun Y, Wang XY, Wu T, Ren J, Pei SF, Zheng Y, He Y, Hu Y, Yang N, Yan H. Machine-learning-based classification of real-time tissue elastography for hepatic fibrosis in patients with chronic hepatitis B. *Comput Biol Med* 2017; **89**: 18-23 [PMID: [28779596](https://pubmed.ncbi.nlm.nih.gov/28779596/) DOI: [10.1016/j.combiomed.2017.07.012](https://doi.org/10.1016/j.combiomed.2017.07.012)]
  - 75 **Li W**, Huang Y, Zhuang BW, Liu GJ, Hu HT, Li X, Liang JY, Wang Z, Huang XW, Zhang CQ, Ruan SM, Xie XY, Kuang M, Lu MD, Chen LD, Wang W. Multiparametric ultrasomics of significant liver fibrosis: A machine learning-based analysis. *Eur Radiol* 2019; **29**: 1496-1506 [PMID: [30178143](https://pubmed.ncbi.nlm.nih.gov/30178143/) DOI: [10.1007/s00330-018-5680-z](https://doi.org/10.1007/s00330-018-5680-z)]
  - 76 **Gatos I**, Tsantis S, Spiliopoulos S, Karnabatidis D, Theotokas I, Zoumpoulis P, Loupas T, Hazle JD, Kagadis GC. Temporal stability assessment in shear wave elasticity images validated by deep learning neural network for chronic liver disease fibrosis stage assessment. *Med Phys* 2019; **46**: 2298-2309 [PMID: [30929260](https://pubmed.ncbi.nlm.nih.gov/30929260/) DOI: [10.1002/mp.13521](https://doi.org/10.1002/mp.13521)]
  - 77 **Wang K**, Lu X, Zhou H, Gao Y, Zheng J, Tong M, Wu C, Liu C, Huang L, Jiang T, Meng F, Lu Y, Ai H, Xie XY, Yin LP, Liang P, Tian J, Zheng R. Deep learning Radiomics of shear wave elastography significantly improved diagnostic performance for assessing liver fibrosis in chronic hepatitis B: a prospective multicentre study. *Gut* 2019; **68**: 729-741 [PMID: [29730602](https://pubmed.ncbi.nlm.nih.gov/29730602/) DOI: [10.1136/gutjnl-2018-316204](https://doi.org/10.1136/gutjnl-2018-316204)]
  - 78 **Kuppili V**, Biswas M, Sreekumar A, Suri HS, Saba L, Edla DR, Marinho RT, Sanches JM, Suri JS. Extreme Learning Machine Framework for Risk Stratification of Fatty Liver Disease Using Ultrasound Tissue Characterization. *J Med Syst* 2017; **41**: 152 [PMID: [28836045](https://pubmed.ncbi.nlm.nih.gov/28836045/) DOI: [10.1007/s10916-017-0797-1](https://doi.org/10.1007/s10916-017-0797-1)]
  - 79 **Byra M**, Styczynski G, Szmigielski C, Kalinowski P, Michałowski Ł, Paluszkiwicz R, Ziarkiewicz-Wróblewska B, Zieniewicz K, Sobieraj P, Nowicki A. Transfer learning with deep

- convolutional neural network for liver steatosis assessment in ultrasound images. *Int J Comput Assist Radiol Surg* 2018; **13**: 1895-1903 [PMID: 30094778 DOI: 10.1007/s11548-018-1843-2]
- 80 **Biswas M**, Kuppli V, Edla DR, Suri HS, Saba L, Marinho RT, Sanches JM, Suri JS. Symtosis: A liver ultrasound tissue characterization and risk stratification in optimized deep learning paradigm. *Comput Methods Programs Biomed* 2018; **155**: 165-177 [PMID: 29512496 DOI: 10.1016/j.cmpb.2017.12.016]
  - 81 **Cao W**, An X, Cong L, Lyu C, Zhou Q, Guo R. Application of Deep Learning in Quantitative Analysis of 2-Dimensional Ultrasound Imaging of Nonalcoholic Fatty Liver Disease. *J Ultrasound Med* 2020; **39**: 51-59 [PMID: 31222786 DOI: 10.1002/jum.15070]
  - 82 **Guo LH**, Wang D, Qian YY, Zheng X, Zhao CK, Li XL, Bo XW, Yue WW, Zhang Q, Shi J, Xu HX. A two-stage multi-view learning framework based computer-aided diagnosis of liver tumors with contrast enhanced ultrasound images. *Clin Hemorheol Microcirc* 2018; **69**: 343-354 [PMID: 29630528 DOI: 10.3233/CH-170275]
  - 83 **Schmauch B**, Herent P, Jehanno P, Dehaene O, Saillard C, Aubé C, Luciani A, Lassau N, Jégou S. Diagnosis of focal liver lesions from ultrasound using deep learning. *Diagn Interv Imaging* 2019; **100**: 227-233 [PMID: 30926443 DOI: 10.1016/j.diii.2019.02.009]
  - 84 **Yang Q**, Wei J, Hao X, Kong D, Yu X, Jiang T, Xi J, Cai W, Luo Y, Jing X, Yang Y, Cheng Z, Wu J, Zhang H, Liao J, Zhou P, Song Y, Zhang Y, Han Z, Cheng W, Tang L, Liu F, Dou J, Zheng R, Yu J, Tian J, Liang P. Improving B-mode ultrasound diagnostic performance for focal liver lesions using deep learning: A multicentre study. *EBioMedicine* 2020; **56**: 102777 [PMID: 32485640 DOI: 10.1016/j.ebiom.2020.102777]
  - 85 **Choi KJ**, Jang JK, Lee SS, Sung YS, Shim WH, Kim HS, Yun J, Choi JY, Lee Y, Kang BK, Kim JH, Kim SY, Yu ES. Development and Validation of a Deep Learning System for Staging Liver Fibrosis by Using Contrast Agent-enhanced CT Images in the Liver. *Radiology* 2018; **289**: 688-697 [PMID: 30179104 DOI: 10.1148/radiol.2018180763]
  - 86 **He L**, Li H, Dudley JA, Maloney TC, Brady SL, Somasundaram E, Trout AT, Dillman JR. Machine Learning Prediction of Liver Stiffness Using Clinical and T2-Weighted MRI Radiomic Data. *AJR Am J Roentgenol* 2019; **213**: 592-601 [PMID: 31120779 DOI: 10.2214/AJR.19.21082]
  - 87 **Ahmed Y**, Hussein RS, Basha TA, Khalifa AM, Ibrahim AS, Abdelmoaty AS, Abdella HM, Fahmy AS. Detecting liver fibrosis using a machine learning-based approach to the quantification of the heart-induced deformation in tagged MR images. *NMR Biomed* 2020; **33**: e4215 [PMID: 31730265 DOI: 10.1002/nbm.4215]
  - 88 **Hectors SJ**, Kennedy P, Huang KH, Stocker D, Carbonell G, Greenspan H, Friedman S, Taouli B. Fully automated prediction of liver fibrosis using deep learning analysis of gadoteric acid-enhanced MRI. *Eur Radiol* 2020 [PMID: 33201285 DOI: 10.1007/s00330-020-07475-4]
  - 89 **Vivanti R**, Szeskin A, Lev-Cohain N, Sosna J, Jaskowicz L. Automatic detection of new tumors and tumor burden evaluation in longitudinal liver CT scan studies. *Int J Comput Assist Radiol Surg* 2017; **12**: 1945-1957 [PMID: 28856515 DOI: 10.1007/s11548-017-1660-z]
  - 90 **Yasaka K**, Akai H, Abe O, Kiryu S. Deep Learning with Convolutional Neural Network for Differentiation of Liver Masses at Dynamic Contrast-enhanced CT: A Preliminary Study. *Radiology* 2018; **286**: 887-896 [PMID: 29059036 DOI: 10.1148/radiol.2017170706]
  - 91 **Ibragimov B**, Toesca D, Chang D, Yuan Y, Koong A, Xing L. Development of deep neural network for individualized hepatobiliary toxicity prediction after liver SBRT. *Med Phys* 2018; **45**: 4763-4774 [PMID: 30098025 DOI: 10.1002/mp.13122]
  - 92 **Abajian A**, Murali N, Savic LJ, Laage-Gaupp FM, Nezami N, Duncan JS, Schlachter T, Lin M, Geschwind JF, Chapiro J. Predicting Treatment Response to Intra-arterial Therapies for Hepatocellular Carcinoma with the Use of Supervised Machine Learning-An Artificial Intelligence Concept. *J Vasc Interv Radiol* 2018; **29**: 850-857. e1 [PMID: 29548875 DOI: 10.1016/j.jvir.2018.01.769]
  - 93 **Zhang F**, Yang J, Nezami N, Laage-Gaupp F, Chapiro J, De Lin M, Duncan J. Liver Tissue Classification Using an Auto-context-based Deep Neural Network with a Multi-phase Training Framework. *Patch Based Tech Med Imaging (2018)* 2018; **11075**: 59-66 [PMID: 32432233 DOI: 10.1007/978-3-030-00500-9\_7]
  - 94 **Morshid A**, Elsayes KM, Khalaf AM, Elmohr MM, Yu J, Kaseb AO, Hassan M, Mahvash A, Wang Z, Hazle JD, Fuentes D. A machine learning model to predict hepatocellular carcinoma response to transcatheter arterial chemoembolization. *Radiol Artif Intell* 2019; **1** [PMID: 31858078 DOI: 10.1148/ryai.2019180021]
  - 95 **Nayak A**, Baidya Kayal E, Arya M, Culli J, Krishan S, Agarwal S, Mehndiratta A. Computer-aided diagnosis of cirrhosis and hepatocellular carcinoma using multi-phase abdomen CT. *Int J Comput Assist Radiol Surg* 2019; **14**: 1341-1352 [PMID: 31062266 DOI: 10.1007/s11548-019-01991-5]
  - 96 **Hamm CA**, Wang CJ, Savic LJ, Ferrante M, Schobert I, Schlachter T, Lin M, Duncan JS, Weinreb JC, Chapiro J, Letzen B. Deep learning for liver tumor diagnosis part I: development of a convolutional neural network classifier for multi-phasic MRI. *Eur Radiol* 2019; **29**: 3338-3347 [PMID: 31016442 DOI: 10.1007/s00330-019-06205-9]
  - 97 **Wang CJ**, Hamm CA, Savic LJ, Ferrante M, Schobert I, Schlachter T, Lin M, Weinreb JC, Duncan JS, Chapiro J, Letzen B. Deep learning for liver tumor diagnosis part II: convolutional neural network interpretation using radiologic imaging features. *Eur Radiol* 2019; **29**: 3348-3357 [PMID: 31093705 DOI: 10.1007/s00330-019-06214-8]
  - 98 **Jansen MJA**, Kuijf HJ, Veldhuis WB, Wessels FJ, Viergever MA, Pluim JPW. Automatic

- classification of focal liver lesions based on MRI and risk factors. *PLoS One* 2019; **14**: e0217053 [PMID: 31095624 DOI: 10.1371/journal.pone.0217053]
- 99 **Mokrane FZ**, Lu L, Vavasour A, Otal P, Peron JM, Luk L, Yang H, Ammari S, Saenger Y, Rousseau H, Zhao B, Schwartz LH, Dercle L. Radiomics machine-learning signature for diagnosis of hepatocellular carcinoma in cirrhotic patients with indeterminate liver nodules. *Eur Radiol* 2020; **30**: 558-570 [PMID: 31444598 DOI: 10.1007/s00330-019-06347-w]
  - 100 **Shi W**, Kuang S, Cao S, Hu B, Xie S, Chen S, Chen Y, Gao D, Zhu Y, Zhang H, Liu H, Ye M, Sirlin CB, Wang J. Deep learning assisted differentiation of hepatocellular carcinoma from focal liver lesions: choice of four-phase and three-phase CT imaging protocol. *Abdom Radiol (NY)* 2020; **45**: 2688-2697 [PMID: 32232524 DOI: 10.1007/s00261-020-02485-8]
  - 101 **Alirr OI**. Deep learning and level set approach for liver and tumor segmentation from CT scans. *J Appl Clin Med Phys* 2020; **21**: 200-209 [PMID: 33113290 DOI: 10.1002/acm2.13003]
  - 102 **Zheng H**, Chen Y, Yue X, Ma C, Liu X, Yang P, Lu J. Deep pancreas segmentation with uncertain regions of shadowed sets. *Magn Reson Imaging* 2020; **68**: 45-52 [PMID: 31987903 DOI: 10.1016/j.mri.2020.01.008]
  - 103 **Liang JD**, Ping XO, Tseng YJ, Huang GT, Lai F, Yang PM. Recurrence predictive models for patients with hepatocellular carcinoma after radiofrequency ablation using support vector machines with feature selection methods. *Comput Methods Programs Biomed* 2014; **117**: 425-434 [PMID: 25278224 DOI: 10.1016/j.cmpb.2014.09.001]
  - 104 **Zhou W**, Zhang L, Wang K, Chen S, Wang G, Liu Z, Liang C. Malignancy characterization of hepatocellular carcinomas based on texture analysis of contrast-enhanced MR images. *J Magn Reson Imaging* 2017; **45**: 1476-1484 [PMID: 27626270 DOI: 10.1002/jmri.25454]
  - 105 **Abajian A**, Murali N, Savic LJ, Laage-Gaupp FM, Nezami N, Duncan JS, Schlachter T, Lin M, Geschwind JF, Chapiro J. Predicting Treatment Response to Image-Guided Therapies Using Machine Learning: An Example for Trans-Arterial Treatment of Hepatocellular Carcinoma. *J Vis Exp* 2018 [PMID: 30371657 DOI: 10.3791/58382]
  - 106 **Ma X**, Wei J, Gu D, Zhu Y, Feng B, Liang M, Wang S, Zhao X, Tian J. Preoperative radiomics nomogram for microvascular invasion prediction in hepatocellular carcinoma using contrast-enhanced CT. *Eur Radiol* 2019; **29**: 3595-3605 [PMID: 30770969 DOI: 10.1007/s00330-018-5985-y]
  - 107 **Dong Y**, Zhou L, Xia W, Zhao XY, Zhang Q, Jian JM, Gao X, Wang WP. Preoperative Prediction of Microvascular Invasion in Hepatocellular Carcinoma: Initial Application of a Radiomic Algorithm Based on Grayscale Ultrasound Images. *Front Oncol* 2020; **10**: 353 [PMID: 32266138 DOI: 10.3389/fonc.2020.00353]
  - 108 **He M**, Zhang P, Ma X, He B, Fang C, Jia F. Radiomic Feature-Based Predictive Model for Microvascular Invasion in Patients With Hepatocellular Carcinoma. *Front Oncol* 2020; **10**: 574228 [PMID: 33251138 DOI: 10.3389/fonc.2020.574228]
  - 109 **Schoenberg MB**, Bucher JN, Koch D, Börner N, Hesse S, De Toni EN, Seidensticker M, Angele MK, Klein C, Bazhin AV, Werner J, Guba MO. A novel machine learning algorithm to predict disease free survival after resection of hepatocellular carcinoma. *Ann Transl Med* 2020; **8**: 434 [PMID: 32395478 DOI: 10.21037/atm.2020.04.16]
  - 110 **Zhao Y**, Wu J, Zhang Q, Hua Z, Qi W, Wang N, Lin T, Sheng L, Cui D, Liu J, Song Q, Li X, Wu T, Guo Y, Cui J, Liu A. Radiomics Analysis Based on Multiparametric MRI for Predicting Early Recurrence in Hepatocellular Carcinoma After Partial Hepatectomy. *J Magn Reson Imaging* 2020 [PMID: 33217114 DOI: 10.1002/jmri.27424]
  - 111 **Liu F**, Liu D, Wang K, Xie X, Su L, Kuang M, Huang G, Peng B, Wang Y, Lin M, Tian J. Deep Learning Radiomics Based on Contrast-Enhanced Ultrasound Might Optimize Curative Treatments for Very-Early or Early-Stage Hepatocellular Carcinoma Patients. *Liver Cancer* 2020; **9**: 397-413 [PMID: 32999867 DOI: 10.1159/000505694]
  - 112 **Chen M**, Cao J, Hu J, Topatana W, Li S, Juengpanich S, Lin J, Tong C, Shen J, Zhang B, Wu J, Pocha C, Kudo M, Amedei A, Trevisani F, Sung PS, Zaydfudim VM, Kanda T, Cai X. Clinical-Radiomic Analysis for Pretreatment Prediction of Objective Response to First Transarterial Chemoembolization in Hepatocellular Carcinoma. *Liver Cancer* 2021; **10**: 38-51 [PMID: 33708638 DOI: 10.1159/000512028]
  - 113 **European Association for the Study of the Liver**. EASL Clinical Practice Guidelines: Management of hepatocellular carcinoma. *J Hepatol* 2018; **69**: 182-236 [PMID: 29628281 DOI: 10.1016/j.jhep.2018.03.019]
  - 114 **Gillies RJ**, Kinahan PE, Hricak H. Radiomics: Images Are More than Pictures, They Are Data. *Radiology* 2016; **278**: 563-577 [PMID: 26579733 DOI: 10.1148/radiol.2015151169]
  - 115 **Lambin P**, Leijenaar RTH, Deist TM, Peerlings J, de Jong EEC, van Timmeren J, Sanduleanu S, Larue RTHM, Even AJG, Jochems A, van Wijk Y, Woodruff H, van Soest J, Lustberg T, Roelofs E, van Elmpt W, Dekker A, Mottaghy FM, Wildberger JE, Walsh S. Radiomics: the bridge between medical imaging and personalized medicine. *Nat Rev Clin Oncol* 2017; **14**: 749-762 [PMID: 28975929 DOI: 10.1038/nrclinonc.2017.141]
  - 116 **Erstad DJ**, Tanabe KK. Prognostic and Therapeutic Implications of Microvascular Invasion in Hepatocellular Carcinoma. *Ann Surg Oncol* 2019; **26**: 1474-1493 [PMID: 30788629 DOI: 10.1245/s10434-019-07227-9]
  - 117 **Metter DM**, Colgan TJ, Leung ST, Timmons CF, Park JY. Trends in the US and Canadian Pathologist Workforces From 2007 to 2017. *JAMA Netw Open* 2019; **2**: e194337 [PMID: 31150073]

- DOI: [10.1001/jamanetworkopen.2019.4337](https://doi.org/10.1001/jamanetworkopen.2019.4337)]
- 118 **Tomita N**, Abdollahi B, Wei J, Ren B, Suriawinata A, Hassanpour S. Attention-Based Deep Neural Networks for Detection of Cancerous and Precancerous Esophagus Tissue on Histopathological Slides. *JAMA Netw Open* 2019; **2**: e1914645 [PMID: [31693124](https://pubmed.ncbi.nlm.nih.gov/31693124/) DOI: [10.1001/jamanetworkopen.2019.14645](https://doi.org/10.1001/jamanetworkopen.2019.14645)]
  - 119 **Sharma H**, Zerbe N, Klempert I, Hellwich O, Hufnagl P. Deep convolutional neural networks for automatic classification of gastric carcinoma using whole slide images in digital histopathology. *Comput Med Imaging Graph* 2017; **61**: 2-13 [PMID: [28676295](https://pubmed.ncbi.nlm.nih.gov/28676295/) DOI: [10.1016/j.compmedimag.2017.06.001](https://doi.org/10.1016/j.compmedimag.2017.06.001)]
  - 120 **Li Y**, Li X, Xie X, Shen L. Deep learning based gastric cancer identification. Proceedings of the 2018 IEEE 15th International Symposium on Biomedical Imaging; 2018: 182-185 [DOI: [10.1109/ISBI.2018.8363550](https://doi.org/10.1109/ISBI.2018.8363550)]
  - 121 **Leon F**, Gelvez M, Jaimes Z, Gelvez T, Arguello H. Supervised Classification of Histopathological Images Using Convolutional Neuronal Networks for Gastric Cancer Detection. Proceedings of the 2019 XXII Symposium on Image, Signal Processing and Artificial Vision; 2019: 1-5 [DOI: [10.1109/STSIVA.2019.8730284](https://doi.org/10.1109/STSIVA.2019.8730284)]
  - 122 **Sun M**, Zhang G, Dang H, Qi X, Zhou X, Chang Q. Accurate Gastric Cancer Segmentation in Digital Pathology Images Using Deformable Convolution and Multi-Scale Embedding Networks. *IEEE Access* 2019; **7**: 75530-75541 [DOI: [10.1109/ACCESS.2019.2918800](https://doi.org/10.1109/ACCESS.2019.2918800)]
  - 123 **Ma B**, Guo Y, Hu W, Yuan F, Zhu Z, Yu Y, Zou H. Artificial Intelligence-Based Multiclass Classification of Benign or Malignant Mucosal Lesions of the Stomach. *Front Pharmacol* 2020; **11**: 572372 [PMID: [33132910](https://pubmed.ncbi.nlm.nih.gov/33132910/) DOI: [10.3389/fphar.2020.572372](https://doi.org/10.3389/fphar.2020.572372)]
  - 124 **Yoshida H**, Shimazu T, Kiyuna T, Marugame A, Yamashita Y, Cosatto E, Taniguchi H, Sekine S, Ochiai A. Automated histological classification of whole-slide images of gastric biopsy specimens. *Gastric Cancer* 2018; **21**: 249-257 [PMID: [28577229](https://pubmed.ncbi.nlm.nih.gov/28577229/) DOI: [10.1007/s10120-017-0731-8](https://doi.org/10.1007/s10120-017-0731-8)]
  - 125 **Qu J**, Hiruta N, Terai K, Nosato H, Murakawa M, Sakanashi H. Gastric Pathology Image Classification Using Stepwise Fine-Tuning for Deep Neural Networks. *J Healthc Eng* 2018; **2018**: 8961781 [PMID: [30034677](https://pubmed.ncbi.nlm.nih.gov/30034677/) DOI: [10.1155/2018/8961781](https://doi.org/10.1155/2018/8961781)]
  - 126 **Iizuka O**, Kanavati F, Kato K, Rambeau M, Arihiro K, Tsuneki M. Deep Learning Models for Histopathological Classification of Gastric and Colonic Epithelial Tumours. *Sci Rep* 2020; **10**: 1504 [PMID: [32001752](https://pubmed.ncbi.nlm.nih.gov/32001752/) DOI: [10.1038/s41598-020-58467-9](https://doi.org/10.1038/s41598-020-58467-9)]
  - 127 **Korbar B**, Olofson AM, Miraflor AP, Nicka CM, Suriawinata MA, Torresani L, Suriawinata AA, Hassanpour S. Deep Learning for Classification of Colorectal Polyps on Whole-slide Images. *J Pathol Inform* 2017; **8**: 30 [PMID: [28828201](https://pubmed.ncbi.nlm.nih.gov/28828201/) DOI: [10.4103/jpi.jpi\\_34\\_17](https://doi.org/10.4103/jpi.jpi_34_17)]
  - 128 **Wei JW**, Suriawinata AA, Vaickus LJ, Ren B, Liu X, Lisovsky M, Tomita N, Abdollahi B, Kim AS, Snover DC, Baron JA, Barry EL, Hassanpour S. Evaluation of a Deep Neural Network for Automated Classification of Colorectal Polyps on Histopathologic Slides. *JAMA Netw Open* 2020; **3**: e203398 [PMID: [32324237](https://pubmed.ncbi.nlm.nih.gov/32324237/) DOI: [10.1001/jamanetworkopen.2020.3398](https://doi.org/10.1001/jamanetworkopen.2020.3398)]
  - 129 **Shapcott M**, Hewitt KJ, Rajpoot N. Deep Learning With Sampling in Colon Cancer Histology. *Front Bioeng Biotechnol* 2019; **7**: 52 [PMID: [30972333](https://pubmed.ncbi.nlm.nih.gov/30972333/) DOI: [10.3389/fbioe.2019.00052](https://doi.org/10.3389/fbioe.2019.00052)]
  - 130 **Geessink OGF**, Baidoshvili A, Klaase JM, Ehteshami Bejnordi B, Litjens GJS, van Pelt GW, Mesker WE, Nagtegaal ID, Ciompi F, van der Laak JAWM. Computer aided quantification of intratumoral stroma yields an independent prognosticator in rectal cancer. *Cell Oncol (Dordr)* 2019; **42**: 331-341 [PMID: [30825182](https://pubmed.ncbi.nlm.nih.gov/30825182/) DOI: [10.1007/s13402-019-00429-z](https://doi.org/10.1007/s13402-019-00429-z)]
  - 131 **Song Z**, Yu C, Zou S, Wang W, Huang Y, Ding X, Liu J, Shao L, Yuan J, Gou X, Jin W, Wang Z, Chen X, Chen H, Liu C, Xu G, Sun Z, Ku C, Zhang Y, Dong X, Wang S, Xu W, Lv N, Shi H. Automatic deep learning-based colorectal adenoma detection system and its similarities with pathologists. *BMJ Open* 2020; **10**: e036423 [PMID: [32912980](https://pubmed.ncbi.nlm.nih.gov/32912980/) DOI: [10.1136/bmjopen-2019-036423](https://doi.org/10.1136/bmjopen-2019-036423)]
  - 132 **Wang TH**, Chen TC, Teng X, Liang KH, Yeh CT. Automated biphasic morphological assessment of hepatitis B-related liver fibrosis using second harmonic generation microscopy. *Sci Rep* 2015; **5**: 12962 [PMID: [26260921](https://pubmed.ncbi.nlm.nih.gov/26260921/) DOI: [10.1038/srep12962](https://doi.org/10.1038/srep12962)]
  - 133 **Forlano R**, Mullish BH, Giannakeas N, Maurice JB, Angkathunyakul N, Lloyd J, Tzallas AT, Tsipouras M, Yee M, Thursz MR, Goldin RD, Manousou P. High-Throughput, Machine Learning-Based Quantification of Steatosis, Inflammation, Ballooning, and Fibrosis in Biopsies From Patients With Nonalcoholic Fatty Liver Disease. *Clin Gastroenterol Hepatol* 2020; **18**: 2081-2090. e9 [PMID: [31887451](https://pubmed.ncbi.nlm.nih.gov/31887451/) DOI: [10.1016/j.cgh.2019.12.025](https://doi.org/10.1016/j.cgh.2019.12.025)]
  - 134 **Li S**, Jiang H, Pang W. Joint multiple fully connected convolutional neural network with extreme learning machine for hepatocellular carcinoma nuclei grading. *Comput Biol Med* 2017; **84**: 156-167 [PMID: [28365546](https://pubmed.ncbi.nlm.nih.gov/28365546/) DOI: [10.1016/j.combiomed.2017.03.017](https://doi.org/10.1016/j.combiomed.2017.03.017)]
  - 135 **Kiani A**, Uyumazturk B, Rajpurkar P, Wang A, Gao R, Jones E, Yu Y, Langlotz CP, Ball RL, Montine TJ, Martin BA, Berry GJ, Ozawa MG, Hazard FK, Brown RA, Chen SB, Wood M, Allard LS, Ylagan L, Ng AY, Shen J. Impact of a deep learning assistant on the histopathologic classification of liver cancer. *NPJ Digit Med* 2020; **3**: 23 [PMID: [32140566](https://pubmed.ncbi.nlm.nih.gov/32140566/) DOI: [10.1038/s41746-020-0232-8](https://doi.org/10.1038/s41746-020-0232-8)]
  - 136 **Steinbuss G**, Kriegsmann K, Kriegsmann M. Identification of Gastritis Subtypes by Convolutional Neuronal Networks on Histological Images of Antrum and Corpus Biopsies. *Int J Mol Sci* 2020; **21** [PMID: [32932860](https://pubmed.ncbi.nlm.nih.gov/32932860/) DOI: [10.3390/ijms21186652](https://doi.org/10.3390/ijms21186652)]
  - 137 **Liu Y**, Li X, Zheng A, Zhu X, Liu S, Hu M, Luo Q, Liao H, Liu M, He Y, Chen Y. Predict Ki-67



- Positive Cells in H&E-Stained Images Using Deep Learning Independently From IHC-Stained Images. *Front Mol Biosci* 2020; **7**: 183 [PMID: [32903653](#) DOI: [10.3389/fmolb.2020.00183](#)]
- 138 **Kather JN**, Pearson AT, Halama N, Jäger D, Krause J, Loosen SH, Marx A, Boor P, Tacke F, Neumann UP, Grabsch HI, Yoshikawa T, Brenner H, Chang-Claude J, Hoffmeister M, Trautwein C, Luedde T. Deep learning can predict microsatellite instability directly from histology in gastrointestinal cancer. *Nat Med* 2019; **25**: 1054-1056 [PMID: [31160815](#) DOI: [10.1038/s41591-019-0462-y](#)]
  - 139 **Bychkov D**, Linder N, Turkki R, Nordling S, Kovanen PE, Verrill C, Walliander M, Lundin M, Haglund C, Lundin J. Deep learning based tissue analysis predicts outcome in colorectal cancer. *Sci Rep* 2018; **8**: 3395 [PMID: [29467373](#) DOI: [10.1038/s41598-018-21758-3](#)]
  - 140 **Kather JN**, Krisam J, Charoentong P, Luedde T, Herpel E, Weis CA, Gaiser T, Marx A, Valous NA, Ferber D, Jansen L, Reyes-Aldasoro CC, Zörnig I, Jäger D, Brenner H, Chang-Claude J, Hoffmeister M, Halama N. Predicting survival from colorectal cancer histology slides using deep learning: A retrospective multicenter study. *PLoS Med* 2019; **16**: e1002730 [PMID: [30677016](#) DOI: [10.1371/journal.pmed.1002730](#)]
  - 141 **Echle A**, Grabsch HI, Quirke P, van den Brandt PA, West NP, Hutchins GGA, Heij LR, Tan X, Richman SD, Krause J, Alwers E, Jenniskens J, Offermans K, Gray R, Brenner H, Chang-Claude J, Trautwein C, Pearson AT, Boor P, Luedde T, Gaisa NT, Hoffmeister M, Kather JN. Clinical-Grade Detection of Microsatellite Instability in Colorectal Tumors by Deep Learning. *Gastroenterology* 2020; **159**: 1406-1416. e11 [PMID: [32562722](#) DOI: [10.1053/j.gastro.2020.06.021](#)]
  - 142 **Skrede OJ**, De Raedt S, Kleppe A, Hveem TS, Liestøl K, Maddison J, Askautrud HA, Pradhan M, Nesheim JA, Albrechtsen F, Farstad IN, Domingo E, Church DN, Nesbakken A, Shepherd NA, Tomlinson I, Kerr R, Novelli M, Kerr DJ, Danielsen HE. Deep learning for prediction of colorectal cancer outcome: a discovery and validation study. *Lancet* 2020; **395**: 350-360 [PMID: [32007170](#) DOI: [10.1016/S0140-6736\(19\)32998-8](#)]
  - 143 **Sirinukunwattana K**, Domingo E, Richman SD, Redmond KL, Blake A, Verrill C, Leedham SJ, Chatzipli A, Hardy C, Whalley CM, Wu CH, Beggs AD, McDermott U, Dunne PD, Meade A, Walker SM, Murray GI, Samuel L, Seymour M, Tomlinson I, Quirke P, Maughan T, Rittscher J, Koelzer VH; S:CORT consortium. Image-based consensus molecular subtype (imCMS) classification of colorectal cancer using deep learning. *Gut* 2021; **70**: 544-554 [PMID: [32690604](#) DOI: [10.1136/gutjnl-2019-319866](#)]
  - 144 **Jang HJ**, Lee A, Kang J, Song IH, Lee SH. Prediction of clinically actionable genetic alterations from colorectal cancer histopathology images using deep learning. *World J Gastroenterol* 2020; **26**: 6207-6223 [PMID: [33177794](#) DOI: [10.3748/wjg.v26.i40.6207](#)]
  - 145 **Chaudhary K**, Poirion OB, Lu L, Garmire LX. Deep Learning-Based Multi-Omics Integration Robustly Predicts Survival in Liver Cancer. *Clin Cancer Res* 2018; **24**: 1248-1259 [PMID: [28982688](#) DOI: [10.1158/1078-0432.CCR-17-0853](#)]
  - 146 **Saillard C**, Schmauch B, Laifa O, Moarii M, Toldo S, Zaslavskiy M, Pronier E, Laurent A, Amaddeo G, Regnault H, Sommacale D, Ziol M, Pawlotsky JM, Mulé S, Luciani A, Wainrib G, Clozel T, Courtiol P, Calderaro J. Predicting Survival After Hepatocellular Carcinoma Resection Using Deep Learning on Histological Slides. *Hepatology* 2020; **72**: 2000-2013 [PMID: [32108950](#) DOI: [10.1002/hep.31207](#)]
  - 147 **Fu Y**, Jung AW, Torne RV, Gonzalez S, Vöhringer H, Shmatko A, Yates LR, Jimenez-Linan M, Moore L, Gerstung M. Pan-cancer computational histopathology reveals mutations, tumor composition and prognosis. *Nature Cancer* 2020; **1**: 800-810 [DOI: [10.1038/s43018-020-0085-8](#)]
  - 148 **Sangro B**, Melero I, Wadhawan S, Finn RS, Abou-Alfa GK, Cheng AL, Yau T, Furuse J, Park JW, Boyd Z, Tang HT, Shen Y, Tschaika M, Neely J, El-Khoueiry A. Association of inflammatory biomarkers with clinical outcomes in nivolumab-treated patients with advanced hepatocellular carcinoma. *J Hepatol* 2020; **73**: 1460-1469 [PMID: [32710922](#) DOI: [10.1016/j.jhep.2020.07.026](#)]
  - 149 **Stead WW**. Clinical Implications and Challenges of Artificial Intelligence and Deep Learning. *JAMA* 2018; **320**: 1107-1108 [PMID: [30178025](#) DOI: [10.1001/jama.2018.11029](#)]
  - 150 **Sung JJ**, Poon NC. Artificial intelligence in gastroenterology: where are we heading? *Front Med* 2020; **14**: 511-517 [PMID: [32458189](#) DOI: [10.1007/s11684-020-0742-4](#)]
  - 151 **Poon NC**, Sung JJ. Self-driving cars and AI-assisted endoscopy: Who should take the responsibility when things go wrong? *J Gastroenterol Hepatol* 2019; **34**: 625-626 [PMID: [30920688](#) DOI: [10.1111/jgh.14641](#)]
  - 152 **Li S**, Topatana W, Juengpanich S, Cao J, Hu J, Zhang B, Ma D, Cai X, Chen M. Development of synthetic lethality in cancer: molecular and cellular classification. *Signal Transduct Target Ther* 2020; **5**: 241 [PMID: [33077733](#) DOI: [10.1038/s41392-020-00358-6](#)]
  - 153 **Topatana W**, Juengpanich S, Li S, Cao J, Hu J, Lee J, Suliyanto K, Ma D, Zhang B, Chen M, Cai X. Advances in synthetic lethality for cancer therapy: cellular mechanism and clinical translation. *J Hematol Oncol* 2020; **13**: 118 [PMID: [32883316](#) DOI: [10.1186/s13045-020-00956-5](#)]



## From hepatitis A to E: A critical review of viral hepatitis

Daniel Castaneda, Adalberto Jose Gonzalez, Mohammad Alomari, Kanwarpreet Tandon, Xaralambos Bobby Zervos

**ORCID number:** Daniel Castaneda 0000-0002-0825-772X; Adalberto Jose Gonzalez 0000-0001-8108-5402; Mohammad Alomari 0000-0003-1201-0866; Kanwarpreet Tandon 0000-0003-0941-1589; Xaralambos Bobby Zervos 0000-0001-6783-0525.

**Author contributions:** Castaneda D, Gonzalez AJ, Alomari M and Tandon K performed the literature search, drafted the article and made the manuscript corrections; Zervos XB performed critical review and supervision of the article; all authors have read and approved the final manuscript.

**Conflict-of-interest statement:** None of the authors have any compelling conflict of interest.

**Open-Access:** This article is an open-access article that was selected by an in-house editor and fully peer-reviewed by external reviewers. It is distributed in accordance with the Creative Commons Attribution NonCommercial (CC BY-NC 4.0) license, which permits others to distribute, remix, adapt, build upon this work non-commercially, and license their derivative works on different terms, provided the original work is properly cited and the use is non-commercial. See: <http://creativecommons.org/licenses/by-nc/4.0/>

**Manuscript source:** Invited

**Daniel Castaneda, Adalberto Jose Gonzalez, Mohammad Alomari, Kanwarpreet Tandon,** Digestive Disease Institute, Cleveland Clinic Florida, Weston, FL 33331, United States

**Xaralambos Bobby Zervos,** Transplant Department, Cleveland Clinic Florida, Weston, FL 33331, United States

**Corresponding author:** Daniel Castaneda, MD, Academic Fellow, Digestive Disease Institute, Cleveland Clinic Florida, 2950 Cleveland Clinic Boulevard, Weston, FL 33331, United States. [daniel.castaneda.m@gmail.com](mailto:daniel.castaneda.m@gmail.com)

### Abstract

Viral infections affecting the liver have had an important impact on humanity, as they have led to significant morbidity and mortality in patients with acute and chronic infections. Once an unknown etiology, the discovery of the viral agents triggered interest of the scientific community to establish the pathogenesis and diagnostic modalities to identify the affected population. With the rapid scientific and technological advances in the last centuries, controlling and even curing the infections became a possibility, with a large focus on preventive medicine through vaccination. Hence, a comprehensive understanding of hepatitis A, B, C, D and E is required by primary care physicians and gastroenterologists to provide care to these patients. The review article describes the epidemiology, pathogenesis, clinical presentation, diagnostic tools and current medication regimens, with a focus on upcoming treatment options and the role of liver transplantation.

**Key Words:** Hepatitis A; Hepatitis B; Hepatitis C; Hepatitis D; Hepatitis E; Treatment

©The Author(s) 2021. Published by Baishideng Publishing Group Inc. All rights reserved.

**Core Tip:** Viral hepatitis (A, B, C, D and E) diagnosis and treatment have evolved through the last decades, with recent investigations aiming to cure and prevent them pharmacologically or through liver transplantation. This state-of-art review focuses on the epidemiology, pathogenesis, clinical presentation, with a special focus on upcoming diagnostic tools and treatments.

**Citation:** Castaneda D, Gonzalez AJ, Alomari M, Tandon K, Zervos XB. From hepatitis A to E: A critical review of viral hepatitis. *World J Gastroenterol* 2021; 27(16): 1691-1715



manuscript

**Specialty type:** Gastroenterology and hepatology**Country/Territory of origin:** United States**Peer-review report's scientific quality classification**

Grade A (Excellent): A, A, A

Grade B (Very good): 0

Grade C (Good): 0

Grade D (Fair): 0

Grade E (Poor): 0

**Received:** January 25, 2021**Peer-review started:** January 25, 2021**First decision:** February 27, 2021**Revised:** March 2, 2021**Accepted:** April 9, 2021**Article in press:** April 9, 2021**Published online:** April 28, 2021**P-Reviewer:** Cheng H, Shayesteh AA**S-Editor:** Gao CC**L-Editor:** A**P-Editor:** Liu JH**URL:** <https://www.wjgnet.com/1007-9327/full/v27/i16/1691.htm>**DOI:** <https://dx.doi.org/10.3748/wjg.v27.i16.1691>

## INTRODUCTION

Viral hepatitis has been a formidable challenge eliciting epidemic dating back to ancient times, with documented outbreaks 5000 years ago in China and similar jaundice descriptions by Hippocrates in the fifth century BC in the island of Thassos<sup>[1,2]</sup>. Technological advancements over the modern era allowed for the viruses to be identified and subsequent scientific inquiry revolutionized the morbidity and mortality caused by these viral pathogens. We aim to provide an overview of viral hepatitis with discussion of current and prospective therapies. Though most remain dominant in certain parts of the world, globalization demands a fundamental understanding of each virus as we all have the daily potential of encountering any of them at our doorstep.

## HEPATITIS A

### Epidemiology

First discovered in 1973 by Feinstone, a spherical 27 nanometer particle was seen on immune electron microscopy in the fecal sample of hepatitis A patients<sup>[3]</sup>. A member of the picornavirus family, the hepatitis A virus (HAV) is an RNA virus responsible for 1.4 million cases per year globally<sup>[4]</sup>, with an estimated 7134 deaths in 2016; almost half of these cases were reported in Asia<sup>[5]</sup>. In the United States, the annual incidence rate was reported to be 2 cases per 100000 people, in 2006. Recent outbreaks of the disease have shown a 294% increase in infections between 2016-2018 compared to 2013-2015<sup>[6,7]</sup>.

### Recent outbreaks

In 1988, about 300000 people in Shanghai reported symptoms of HAV after consumption of raw clams, described as one of the largest outbreaks in the modern era<sup>[8,9]</sup>. Several outbreaks related to specific food products affecting over 300 patients from multiple states in the United States have been reported in the recent years (2013-2019). The outbreaks have been related to consumption of fresh blackberries, frozen strawberries, raw scallops, and pomegranate seeds. A recent study in 2017 conducted over 4 states (California, Kentucky, Michigan, and Utah) has shown evidence for shift towards large community outbreaks with person-to-person transmission. The majority of these infections have been reported among persons with injection or non-injection drug use and/or persons experiencing homelessness<sup>[10]</sup>.

Current data from state health departments shows, over 37000 new outbreak related cases with greater than 22600 hospital admissions and approximately 350 HAV deaths reported between July 2016 and December 2020<sup>[11]</sup>.

On the contrary, 19947 cases of HAV from 24 European Union countries have been reported between January and December 2017, which is four times higher when compared to similar time periods between 2012 and 2015<sup>[12]</sup>. The number of outbreak related cases from 22 European Union countries was 4475 in 2016 and most outbreaks were related to men who have sex with men.

### Pathogenesis

The transmission of HAV occurs *via* fecal-oral route, which includes consumption of contaminated food or water and person to person contact. Polymerase chain reaction testing for blood donors is performed as transmission through blood transfusion is noted on rare occasions<sup>[13]</sup>. The dissemination of the HAV into the liver occurs *via* the portal vein after the virus traverses the mucosa of the small intestinal wall. The virus particles subsequently replicate and are secreted into the biliary canaliculi, reaching back to the small intestine through the bile ducts and being re-excreted in the feces. Until the body responds with appropriate immune reaction in antibodies, the HAV enterohepatic cycle continues. Human leukocyte antigen-restricted, HAV-specific CD8+ T lymphocytes and natural killer cells have been implicated in the damage and destruction of infected hepatocytes<sup>[14-16]</sup>.

### Clinical presentation

The usual HAV incubation period is about 2-4 wk<sup>[17]</sup>. Fever, malaise, jaundice have been described as the most common presenting symptoms for HAV infection<sup>[18]</sup>. Other common symptoms include weakness, fatigue, nausea, vomiting, abdominal pain, arthralgias, myalgias, diarrhea and anorexia<sup>[12]</sup>. Patients rarely enter a prolonged cholestatic phase through recovery, while relapsing infections have been described as well<sup>[19]</sup>.

About 10%-15% of patients present with a relapsing course within a 6-mo period of the initial infection<sup>[20]</sup>. The symptoms during the relapse are usually less severe than the initial infection. Notably, on extremely rare occasions a type 1 autoimmune hepatitis has been observed in genetically predisposed patients<sup>[21]</sup>. The spectrum of infections can range from asymptomatic patients without jaundice, symptomatic patients with jaundice, cholestasis with prolonged jaundice, to relapsing infections or acute liver failure<sup>[19]</sup>.

Serum aminotransferases above 1000 U/dL are usually noted, with total bilirubin typically  $\leq 10$  mg/dL, and alkaline phosphatase below 400 U/L. Usually the serum alanine aminotransferase (ALT) is higher than the aspartate aminotransferase (AST)<sup>[22,23]</sup>. In general, older patients are more likely to have severe hepatocellular derangements, hospital admissions and higher mortality<sup>[24]</sup>. These findings can be attributed to an impaired regeneration capacity of the liver and a relatively weaker immune system in the older population<sup>[25]</sup>. In addition to old age, higher mortality has been reported in males<sup>[26]</sup>. Old age, underlying liver pathology and chronic viral hepatitis are reported risk factors for acute liver failure. In patients who develop acute liver failure, higher mortality has been associated with creatinine  $> 2$  mg/dL (strongest predictor) total bilirubin  $> 9.6$  mg/dL and albumin  $< 2.5$  g/L<sup>[18]</sup>.

### Diagnosis

Specific antibodies against HAV (anti-HAV) in the serum can be detected. The diagnosis is confirmed by the presence of immunoglobulin (Ig) M anti-HAV. The antibodies can be detected at the time of onset of symptoms. Serum IgM levels peak during the acute infection and remain positive for up to 4 mo on an average from the onset of symptoms<sup>[27]</sup>. Immunity is usually tested with HAV total antibody to determine HAV natural exposure or secondary to vaccination<sup>[28]</sup>. The presence of IgM antibodies without any clinical symptoms is indicative of HAV infection in the past with persistent antibodies, asymptomatic infection or false positive test<sup>[29]</sup>.

Liver biopsy or imaging studies are not required to make a diagnosis. If performed, a liver biopsy may show marked portal inflammation with typically a lesser degree of necrosis, Kupffer cell proliferation, acidophil bodies, or ballooning when compared to non-HAV viral hepatitis<sup>[30]</sup>.

### Management

No specific treatment is available for HAV and the management is mainly symptomatic. The primary focus remains on improving sanitary conditions to minimize the transmission in the community. Historically, immunoglobulins have been used in the prevention of HAV infections. With the availability of an effective vaccine, the use of immunoglobulins has been largely abandoned except in infants below the age of 12 mo. Post exposure prophylaxis with hepatitis A vaccine has been approved since 2007 for immunocompetent patients without chronic liver disease, who are between the ages of 12 mo and 40 years of age<sup>[11]</sup>.

An inactivated HAV vaccine has been licensed in Europe since 1991, while a live attenuated hepatitis A vaccine has been in use in China since 1992<sup>[31]</sup>. The inactivated virus vaccine was first approved for use in United States in 1995. The vaccine is given in 2 to 3 dose series at least 6 mo apart, depending on the vaccine formulation used. In 1996, the Advisory Committee on Immunization Practices (ACIP) recommended vaccination for people at high risk for HAV infection or adverse consequences of the infection<sup>[32]</sup>. In 2006, ACIP recommended routine vaccination of all children 12-23 mo of age; and in 2019, the committee recommended routine HAV vaccination of people experiencing homelessness<sup>[33,34]</sup>. Other recommendations for groups that would benefit from vaccination are described in Table 1<sup>[35]</sup>.

The vaccine has had significant effect on the decrease in HAV infections, although coverage rates remain lower when compared to other childhood vaccines. These rates were noted to be around 87% for first dose and 57% for the second dose. Long term immune response up to 40 years in noted in over 90% patients who receive both doses of the 2-vaccine series<sup>[36]</sup>.

**Table 1 Centers for Disease Control and Prevention recommendations for hepatitis A vaccination**

	Recommendations
Children	Children age 12-23 mo Age 2-18 yr who have not received the vaccine (catch up vaccination)
High risk population	International travelers Men who have sex with men Illicit drug users People at occupational risk of exposure People anticipating close personal contact with international adoptee People experiencing Homeless
Population at high risk of severe hepatitis A	People with chronic liver disease HIV+ people
Others	Pregnant women at high risk or at risk of severe hepatitis A Any person requesting the vaccine

HIV: Human immunodeficiency virus.

### Role of liver transplant

Acute liver failure occurs in less than 1% of acute HAV infections<sup>[6]</sup>. From these patients, only 31% require emergent liver transplant for treatment of fulminant disease, while the remaining patients recover spontaneously with symptomatic management<sup>[37]</sup>. In a study comparing liver transplant outcomes in patients with HAV *vs* hepatitis B infection, the patients with HAV were found to have lower 1- and 5-year survival rates. Presence of acute pancreatitis and HAV recurrence in this population was identified as risk factors for shorter graft and patient survival. Following transplant, patients should be carefully monitored for HAV recurrence as it is common and is associated with poor outcomes<sup>[38]</sup>.

## HEPATITIS B

### Epidemiology

Chronic hepatitis B virus (HBV) infection had an estimated prevalence of 257 million people in 2015 worldwide, with the highest proportion of cases in Western Pacific and African regions (68% of the cases) and with the lowest prevalence in North America<sup>[39]</sup>. An estimated 29% of cirrhosis-related deaths worldwide were due to HBV in 2017<sup>[40]</sup>, while also contributing to the majority of liver cancer-deaths the same year. There are ten identified HBV genotypes (A-J) collectively, with 35 identified sub-genotypes; the distribution of the genotypes varies broadly worldwide (Figure 1)<sup>[41]</sup>. The variation in the genotype distribution and risk factors relies on common factors in high-risk populations, such as vertical transmission which is associated to higher risk of chronic disease and hepatocellular carcinoma (HCC)<sup>[42]</sup>. Risk factors for HBV transmission include a history of blood transfusion, intravenous drug or paraphernalia use<sup>[43]</sup>, contaminated piercing instruments<sup>[44]</sup>, sexual intercourse with an infected person and organ transplantation from HBV positive donors<sup>[45]</sup>.

### Pathogenesis

The HBV is a double-stranded DNA virus belonging to the *Hepadnaviridae* family, first identified in 1963 and named the Australian Antigen due to the protein reacting to antibodies from a hemophiliac patient. The virus has a special tropism for hepatocytes, to which it adheres and integrates upon initial infection<sup>[46]</sup>. After viral uncoating, the DNA integrates to the host nucleus as a covalently closed circular DNA (cccDNA) that can persist indefinitely in the hepatocytes; this explains the possibility of HBV reactivation in chronic inactive disease<sup>[47]</sup>. Ultimately, through a process driven by reverse transcriptase, new viral molecules are assembled from the cccDNA and are released by exocytosis. This process leads to immune-mediated liver injury as antigens

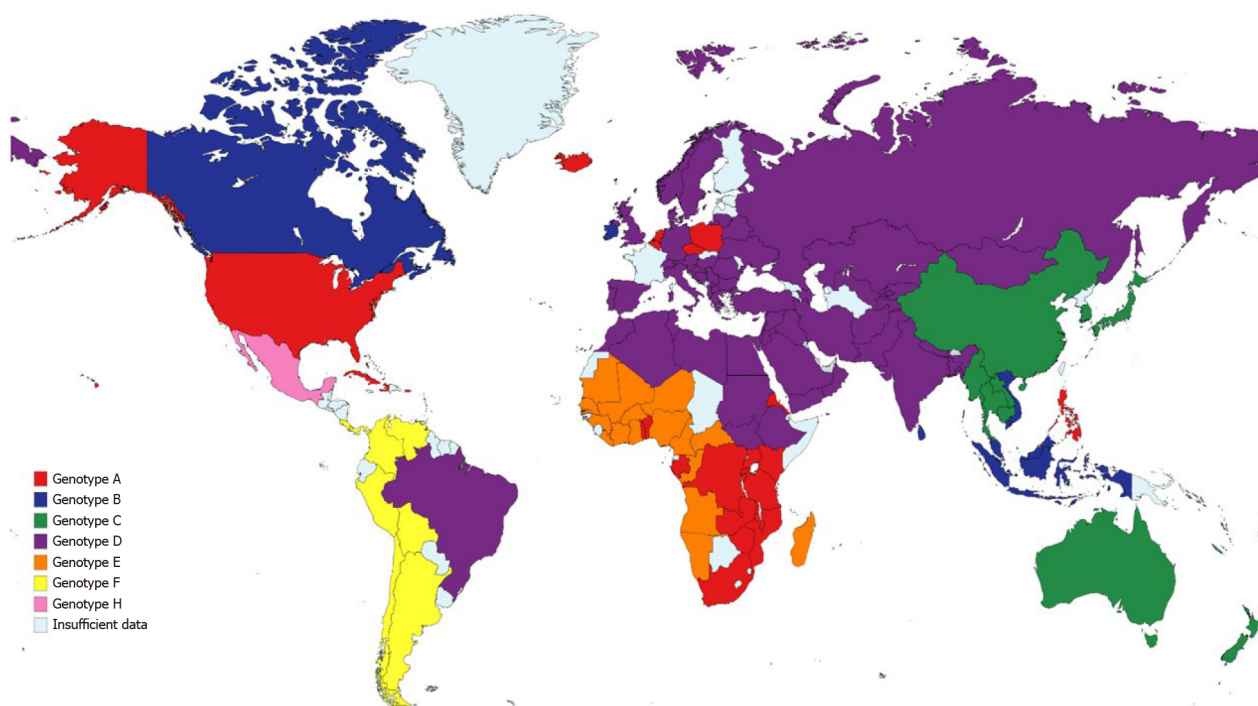


**Figure 1** Global geographic distribution of most common hepatitis B virus genotypes per country.

are recognized by the immunologic system, with a lesser effect from direct viral cytotoxicity. Importantly, the DNA expresses important proteins for its survival including two capsid core proteins—core antigen and e antigen (hepatitis B e antigen, HBeAg), and the surface antigen (hepatitis B surface antigen, HBsAg), all of which are relevant for diagnosis and surveillance. Variations in genotypes have been described, with differences clinically relevant for pegylated (PEG)-interferon response and HCC risk<sup>[48]</sup>.

### **Clinical presentation**

Acute HBV infection can range from a subclinical disease to an icteric hepatitis, the former being the most common presentation<sup>[49]</sup>. Patients may present fatigue, nausea, vomiting and right upper quadrant pain before or during jaundice onset. Notably, less than 1% of cases may present fulminant hepatitis. During the acute phase, there is a rapid HBV viral load increase in the 10000-100000 ng/mL range, along with ALT and AST elevation in the 1000-2000 IU/L range, and total bilirubin elevation<sup>[50]</sup>. At this point, HBsAg and IgM core antibody (HBcAb) become positive, supporting an acute HBV diagnosis. Although a subset of acute HBV can have resolution of the infection with liver enzyme normalization, if the ALT remains elevated after 6 mo from initial presentation, a chronic HBV phase is established.

Chronic HBV may develop in patients exposed at a younger age<sup>[51]</sup>, with genetic predisposition or in those that did not develop symptoms when acute HBV infection occurred<sup>[52]</sup>. These patients are usually asymptomatic for years, unless there is HBV exacerbation<sup>[53]</sup> or development of complications<sup>[54]</sup>. The occurrence of HBV exacerbations is best explained by four phases reflecting the disease activity<sup>[55]</sup>. The first phase (known as immune tolerant) shows markedly elevated HBV titers and positive HBeAg, without ALT elevation or liver inflammation for which patients are asymptomatic. The second phase (immune clearance) is characterized by activation of the immune system, leading to elevation of ALT at least five-fold the upper limit, HBV DNA decrease and histological evidence of inflammation, possibly leading to fatigue, jaundice, and right upper quadrant pain. The third phase (immune control) shows negative HBeAg, as there is seroconversion to positive HBeAb (hepatitis B e antibody) and undetectable to low HBV DNA titers. The fourth phase (immune active) is characterized by ALT and HBV DNA elevation due to triggers such as hepatitis D virus (HDV) superinfection or immunosuppression, leading to similar symptoms seen in the immune clearance phase with potential risk for acute liver failure. Importantly, the disease can fluctuate between the third and fourth phases.



### Diagnosis

Patients that present with acute HBV present with serologies as previously discussed. However, some patients will be in the “window period”, where the immune system has cleared the HBsAg, but no HBV surface antibody (HBsAb) is present; in this scenario, the only positive marker is an elevated IgM HBcAb. Ultimately, once the patient clears the infection, both positive IgG HBcAb and HBsAb will be present. On the other hand, if the patient develops chronic HBV infection, no HBsAb will be detected and HBsAg will persist, even if IgG HBcAb is present. Also, the HBeAg status, HBV DNA and aminotransferases level help determining the phase of the disease and tailor treatment considerations. Finally, the population that has been vaccinated and has never been exposed to HBV will only show positive HBsAb<sup>[56]</sup>.

### Complications

Due to parenchymal inflammation and fibrosis with long-term disease, patients with chronic HBV are predisposed to develop liver cirrhosis. Also, patients with HBV have an increased risk to develop HCC, regardless of the presence of cirrhosis; this risk is well established, but the mechanisms of carcinogenicity are hypothesized to be multifactorial including length<sup>[57]</sup> and severity<sup>[58]</sup> of HBV DNA elevation, ethnicity of the patients and more recently has been associated to the actual genome strain of the virus, especially patients with genotype C<sup>[59]</sup>.

### Current treatment options

Based on consensus from multiple societies, treatment with viral suppression therapy is recommended if patients have extrahepatic manifestations, pregnancy, family history of HCC, hepatitis C virus (HCV)/HDV co-infection, immunosuppression prophylaxis, compensated/decompensated liver cirrhosis<sup>[60]</sup>, or if in the immune active phase and meeting specific criteria established by liver society guidelines (Table 2)<sup>[61-63]</sup>.

Current HBV treatments include nucleoside/nucleotide analogs and PEG-interferon. Overall, the HBsAg seroconversion is higher with PEG-interferon regimen compared to other medications, but its efficacy is limited due to poor patient tolerance<sup>[64]</sup>. Available nucleoside/nucleotide analogs include lamivudine, adefovir, telvidudine, entecavir, tenofovir fumarate and tenofovir alafenamide<sup>[61,63]</sup>. From these medications, the first line regimen for treatment consists of entecavir, tenofovir fumarate or tenofovir alafenamide monotherapy due to high genetic resistance barrier, while the other medications can be considered as options based on medication availability and poor access to first line agents.

### Role for liver transplant

Patients with HBV that develop acute liver failure, decompensated liver cirrhosis or HCC can potentially undergo liver transplantation as ultimate therapy. In the setting of posttransplant immunosuppression, the rate of HBV recurrence is high with survival rates < 50% after 2 years if no preventive measures are taken<sup>[65]</sup>. Hence, based on donor and recipient serologies different strategies have been developed including the use of combination of HBV immunoglobulin during the anhepatic and postoperative phase when indicated, with indefinite use of high-genetic barrier nucleoside/nucleotide analogs demonstrating the lowest rates of HBV recurrence and post-transplant decompensation<sup>[66]</sup>.

### Ongoing research and future directions

Current treatment options have changed the prognosis for HBV patients, but have been limited by its low cure rates. Hence, other targets in the viral life cycle have been evaluated to improve HBsAg seroconversion and potential cure. For example, inhibition of the HBV entry into the uninfected hepatocytes by blockage of the sodium taurocholate co-transporting peptide (NTCP) receptor in the HBV capsid has been studied with three drugs in different trial stages. Bulevirtide is a NTCP antagonist found to inhibit infection in mice injected with HBV<sup>[67]</sup>; in a phase 1 study it showed to be safe without occurrence of serious side effects in 36 healthy subjects at a max dose of 20 mg<sup>[68]</sup>. Subsequently, a multicenter phase 2b randomized trial in 60 HBV/HDV patients receiving PEG-interferon, bulevirtide 2 mg or both with bulevirtide at 2 mg and 5 mg dosing for 48 wk showed a higher proportion of HBsAg decline or loss in patients with combination therapy<sup>[69]</sup>. Other potential NTCP inhibitor are the cyclosporin derivatives such as SCY450 and SCY995<sup>[70]</sup>, which have been found to inhibit hepatocyte HBV entry *in vitro* without affecting bile acid uptake, opening a new therapeutic window. Other experimental medications from the cyclophilin inhibitor family like alisporivir<sup>[71]</sup> and CRV431<sup>[72]</sup>, have shown reduction of HBV DNA and

**Table 2 Treatment criteria in patients with chronic hepatitis B virus and immune active phase per society guidelines**

Criteria	American Association for the Study of Liver Disease <sup>[61]</sup>	European Association for the Study of the Liver <sup>[63]</sup>	Asian Pacific Association for the study of Liver Diseases <sup>[62]</sup>
ALT	≥ 2 times ULN – males 35 U/L, females 25 U/L	> 1 time ULN – 40 U/L	> 2 times ULN – 40 U/L
HBV DNA viral load	> 2000 IU/mL if HBeAg negative or > 20000 IU/mL if HBeAg positive	> 2000 IU/mL, regardless of HBeAg status	> 2000 IU/mL if HBeAg negative or > 20000 IU/mL if HBeAg positive
Degree of liver fibrosis/inflammation	Liver biopsy with moderate-severe inflammation or advanced liver fibrosis (F3-F4). Liver elastography or serum markers showing advanced liver fibrosis (F3-F4)	Liver biopsy, liver elastography or non-invasive testing consistent with moderate-severe fibrosis (F3-F4)	Liver biopsy with moderate-severe inflammation or advanced liver fibrosis (F3-F4). Fibroscan or serum markers showing advanced liver fibrosis (F3-F4)

ALT: Alanine aminotransferase; HBV: Hepatitis B virus; HBeAg: Hepatitis B e antigen; ULN: Upper limit of normal.

HBsAg in lab models possibly through a similar mechanism with promising results.

Another potential target is at the level of capsid assembly, where core assembly modulators have been found to disrupt the assembly by producing abnormal capsid proteins (Type I) or virions without DNA (Type II)<sup>[73]</sup>. *In vitro* evaluation of infected hepatocytes showed a decrease in HBV DNA with different investigational molecules such as JNJ-6379, RO7049389, EDP 514, GLS4 and BAY 41-4109. From these, JNJ-6379, RO7019389 and GLS4 have advanced to phase 2 and 3 clinical studies<sup>[64]</sup>.

High interest has focused on the use of interfering RNA molecules. These are small molecules administered intravenously, with the capacity of covalently binding to RNA before assembly and leading to RNA degradation, which could decrease the HBV DNA, HBeAg, HBsAg and HBcAg titers while increasing the seroconversion rates. A few molecules have advanced to phase 2 studies with no delivery method concern, with most of the studies presented at major hepatology conferences. The use of GSK3389404 in a phase IIa study showed a dose-dependent reduction in HBsAg, with an adequate safety profile in 66 patients<sup>[74]</sup>. Similarly, JNJ-3989 Led to sustained HBsAg reduction in 56% of 39 patients in a phase II study<sup>[75]</sup>. Also, a phase 2a randomized study evaluating GSK3228836 showed several log HBsAg reduction among 17 HBV patients<sup>[76]</sup>. Further phase 3 studies are needed to evaluate the seroconversion and functional cure rates in larger populations.

Other relevant target has been the inhibition of HBsAg release from infected hepatocytes to decrease the immunogenic tolerance induced by this molecule. A phase 2 trial study evaluating the combination of PEG-interferon and REP 2139 in 12 patients with HDV coinfection showed a titer reduction to < 50 IU/mL in 6 subjects and HBV DNA suppression in 10 subjects<sup>[77]</sup>. A second study on REP 2139 and a derivative (REP 2165) in combination with tenofovir and PEG-interferon showed functional cure rates up to 40% in HBeAg negative HBV patients<sup>[78]</sup>.

Lastly, newer nucleoside/nucleotide analogs affecting the HBV life cycle have been developed. Besifovir is a molecule with similar chemical structure to tenofovir fumarate. These two medications were compared in a phase 3 randomized trial including 197 HBV patients receiving the medications for 48 wk. There was no difference in HBV DNA suppression rate with the use of besifovir (80.9%) compared to tenofovir (84.9%), showing equivalence in treatment rates between both arms<sup>[79]</sup>.

On another hand, modulation of the immune system to increase HBV clearance has been a hot topic since the introduction of interferon-based treatments. Recently, the use of immune checkpoint inhibitor *via* programmed death receptor 1 (PD-1) blockage has been explored as a mechanism to overcome the T-cell anergy seen in chronic HBV. Nivolumab is a PD-1 inhibitor that was studied in a phase I trial along with and without a therapeutic vaccine in 24 patients with HBeAg negative chronic HBV, showing a significant HBV DNA log reduction but no significant HBsAg seroconversion rates (only seen in one patient)<sup>[80]</sup>. Other studied mechanisms include the innate immunity stimulation through stimulation of toll-like receptors (TLR). However, in phase 1 studies neither TLR-7 nor TLR-8 agonists have shown to decrease significantly the HBsAg titers in the short term<sup>[81]</sup>; further phase 2 studies with longer treatment duration may help elucidate its role in HBV treatment.

Finally, HBV vaccination has become revolutionary in public health infection prevention by reducing vertical transmission and decreasing HCC incidence in younger populations<sup>[82]</sup>. While the currently widespread regimen with recombinant HBsAg (Engerix-B/Recombivax HB) includes three doses for immunization, a recent regimen utilizing an adjuvant in conjunction with recombinant HBsAg (Heplisav) has



shown to be as efficacious after two doses, with consideration to administer in non-compliant patients or patients with HBsAb titers < 10 IU/mL. Special interest has been directed to therapeutic vaccines to achieve functional HBV cure. Even though different therapeutic vaccines have been studied, the HeberNavac HBsAg-HBcAg is the only vaccine that has shown significant HBeAg seroconversion rates compared to PEG-interferon in a randomized phase III trial<sup>[83]</sup>. Although promising, immunotherapy remains a territory to be explored and similar to HCV the goal of viral eradication remains at the core of research efforts.

## HEPATITIS C

### Epidemiology

Greater than 71 million persons worldwide are infected with HCV<sup>[84]</sup>. Prevalence has increased from 1990 to 2010<sup>[85]</sup>. The Eastern Mediterranean region has an HCV prevalence greater than 2%, considered to be the highest in the world. The continents of Africa and Europe have a prevalence of 1%-2%. North and South America and the Western Pacific region have a prevalence of less than 1% (Figure 2)<sup>[84]</sup>.

There are seven main genotypes and 67 subtypes. HCV genotype 1 represents about half of all HCV infections, making it the most prevalent genotype in the world. The second most common is HCV genotype 3, involving approximately one-third of HCV infections; it is found more commonly in south Asia, Australia, and several European countries. Genotypes 2 is found in Asia and West Africa, while genotype 4 is found in central and eastern sub-Saharan Africa, North Africa, and the Middle East. Genotypes 2 and 4 represent about 9%-13% of all HCV cases. Genotypes 5, 6, and 7 are restricted to South Africa, South-east Asia, and Democratic Republic of Congo, respectively<sup>[86-88]</sup> (Figure 3).

### Pathogenesis

Hepatitis C is a small, enveloped, positive single-stranded RNA virus that was first discovered in 1989 as a member of the *Flaviridae* family and is the only member of genus *Hepacivirus*. It enters the body percutaneously through needlestick injuries (including healthcare or intravenous drug use) containing contaminated blood. It may also enter non-percutaneously through organ transplantation, blood transfusions, sexual intercourse, perinatal transmission, hemodialysis, religious scarification, body piercings, tattoos, and immunoglobulin injection<sup>[89]</sup>. There are 4 host-derived factors that facilitate the entry of HCV into the bloodstream: Scavenger receptor class B type I, Occludin, Claudin-I and CD81<sup>[90]</sup>. Additionally, CD81 binds with the viral particle, either through viral envelope protein (E)2 or other molecules and facilitates its entry into the hepatocyte<sup>[91]</sup>.

Although it is considered a non-cytopathic virus, once HCV enters the hepatocyte, it replicates and causes cell necrosis *via* immune-mediated cytolysis (innate immunity and adaptive immunity) and metabolism-mediated inflammation (hepatic steatosis, oxidative stress, and insulin resistance)<sup>[90]</sup>.

Non-structural protein 5A (NS5A) and E2 regions of HCV also play an important role in the pathogenesis. NS5A inactivates RNA dependent protein kinase (PKR) in hepatocytes, inhibiting the apoptotic pathway and inducing anti-inflammatory interleukin secretion, allowing for viral replication. E2 protein inhibits PKR, allowing the evasion of HCV. The role that different HCV genotypes play in the progression of liver disease is still controversial, but genotype 1b seems to have a more aggressive course, as it has been more associated to cirrhosis progression and liver disease decompensation requiring transplantation<sup>[92]</sup>.

HCV core proteins leads to insulin resistance by direct receptor effect or through increased secretion of tumor necrosis factor- $\alpha$ ; this leads to further hepatic steatosis, inflammation, and fibrosis. HCV associated oxidative stress is mainly caused by HCV-core protein which induces oxidation of glutathione and increase in reactive oxygen species<sup>[93]</sup>. NS5A promotes production of reactive oxygen species in the membrane of the endoplasmic reticulum<sup>[94]</sup>. NS3 is also thought to directly induce oxidative stress<sup>[95]</sup>. Finally, HCV causes steatosis through impaired secretion of lipids from liver cells, increased production of free fatty acids, and impaired fatty acid breakdown<sup>[96]</sup>.

### Clinical presentation

Chronic HCV infection can occur in 50%-85% of patients, while 15%-45% of patients may present spontaneous clearance of the virus<sup>[96]</sup>. Most patients with HCV infection

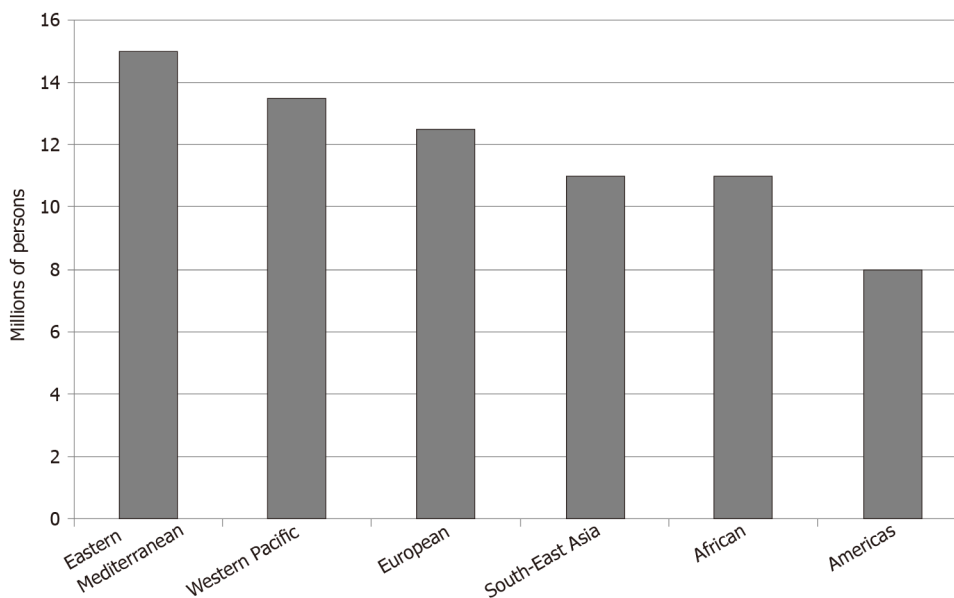


Figure 2 World Health Organization estimated chronic hepatitis C infection prevalence worldwide per region in 2015.

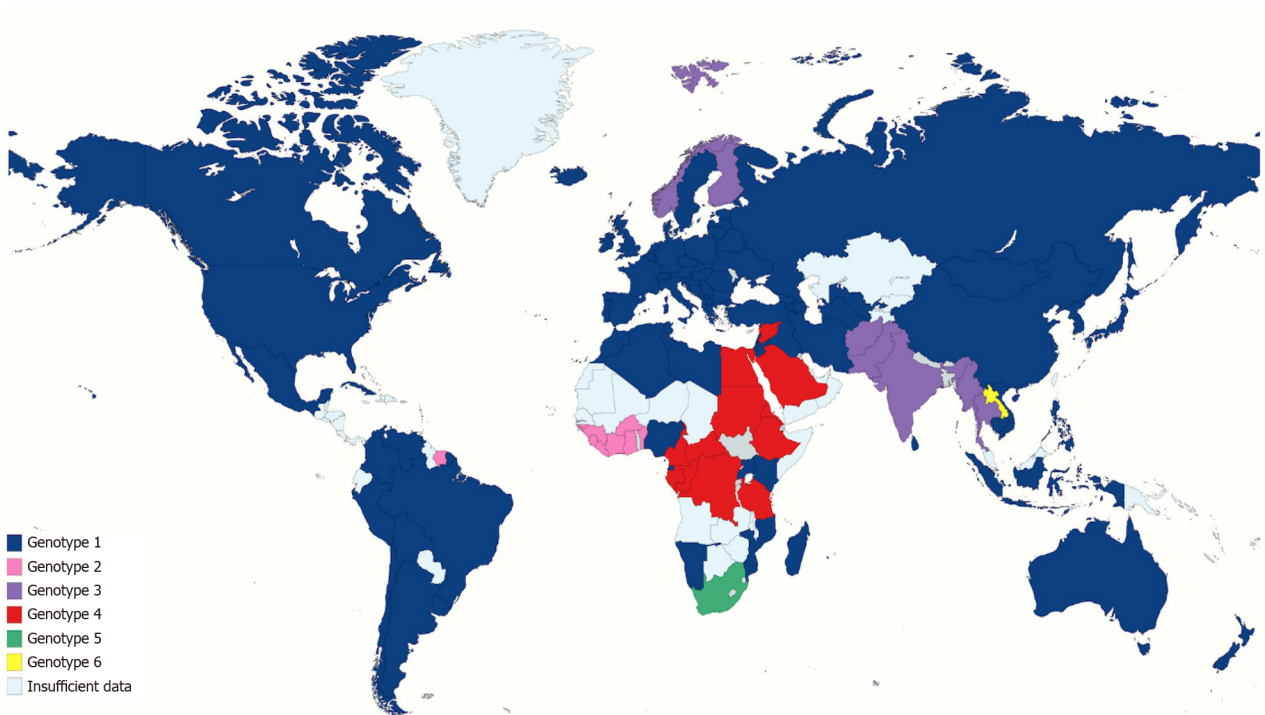


Figure 3 Global geographic distribution of most common hepatitis C virus genotype per country.

are asymptomatic or have nonspecific symptoms. These may include fatigue, sleep disturbances, nausea, diarrhea, abdominal pain, anorexia, myalgia, arthralgia, weakness, depression, anxiety, and weight loss<sup>[97]</sup>. Patients who develop cirrhosis may develop jaundice, ascites, and other stigmata of cirrhosis.

Serum aminotransferase levels remain relatively stable over time in chronic HCV patients. One in three patients have a normal ALT; only one fourth have a serum ALT more than twice the upper limit of normal; the rest of patients have slight enzyme elevations, usually less than twice the upper limit of normal. Rarely, ALT elevations more than 10-fold the upper limit of normal may occur<sup>[98]</sup>. There is little correlation between aminotransferase levels and liver histologic findings<sup>[99]</sup>.

On the other hand, it is estimated that acute HCV accounts for 15%-20% of cases of acute hepatitis<sup>[100]</sup>. More than two thirds of acute HCV infections are usually asymptomatic<sup>[101]</sup>. Symptomatic patients present similarly to other acute hepatitis, with

jaundice, nausea, dark urine, and right upper quadrant pain. These symptoms develop 2-26 wk after exposure and lasts 2-12 wk<sup>[102]</sup>. Aminotransferase levels tend to be greater than 10 times to 20 times the upper limit of normal but fluctuate widely and may even normalize<sup>[103]</sup>. Acute liver failure due to acute HCV infection is extremely rare, but patients with chronic HBV<sup>[104]</sup> or other underlying chronic liver conditions may be predisposed to this outcome.

Extrahepatic manifestations are found in up to 38% of patients with chronic HCV<sup>[105]</sup>. These may include hematologic abnormalities, such as essential mixed cryoglobulinemia and lymphoma; glomerular renal disease, most notably membranoproliferative glomerulonephritis and cryoglobulinemia; dermatologic disorders such as porphyria cutanea tarda and lichen planus; rheumatologic complaints such as arthralgias/myalgias; neurological involvement with sensory or motor neuropathy; and autoimmune conditions such as thyroiditis. Resolution of these manifestations can be expected with treatment.

### Complications

Spontaneous clearance of HCV occurs in about one fourth to one half of patients<sup>[106]</sup>. This usually occurs within 12 wk of exposure. A C/C type allele polymorphism in the chromosomal locus close to interleukin-28B has been associated with higher spontaneous clearance (50%) compared to the 15% rate of spontaneous viral clearance seen with the T/T allele<sup>[107]</sup>. Other favorable factors associated with higher rates of clearance include HLA-DRB1 and DQB1 alleles, white race, female sex, childhood infection, symptomatic acute infection, and high titers of neutralizing antibodies<sup>[106]</sup>.

Rate of progression of chronic HCV infection to cirrhosis varies widely among the literature, but pooled data estimates that 16% of patients develop cirrhosis within 20 years<sup>[108]</sup>. It estimated that an HCV infected liver develops cirrhosis after approximately 20-30 years<sup>[109,110]</sup> with approximately 700000 deaths annually worldwide<sup>[111]</sup>. Risk factors for progression of hepatic fibrosis in patients with chronic HCV infection include age > 40 years<sup>[110]</sup>, alcohol consumption, HBV coinfection, human immunodeficiency virus coinfection, immunosuppressed stage, marijuana use, obesity, diabetes mellitus<sup>[112]</sup>, schistosomiasis, severe hepatic necroinflammation, smoking, male sex<sup>[113]</sup>, and white race<sup>[114]</sup>. The viral load has not correlated with risk of progression to cirrhosis. Studies have described a 3.9% risk of decompensation per year with ascites presence representing the most common form of decompensation<sup>[115]</sup>. Once patients develop cirrhosis, there is a 1.4%-4.9% yearly incidence rate of HCC<sup>[115-117]</sup>. It is estimated that HCV accounts for 25% of HCC cases worldwide<sup>[118]</sup>.

### Diagnosis

Third generation enzyme immunoassays (EIAs) detect antibodies against different HCV antigens, including HCV core, NS3, NS4, and NS5 as early as 8 wk, with sensitivity and specificity of 99% after 2-6 mo after exposure<sup>[119]</sup>. False negatives may arise in patients on hemodialysis and immunocompromised patients. These are considered indirect assays.

Quantitative, HCV RNA tests are a type of direct immunoassays that may detect HCV viremia in patients with at least 10-15 IU/mL<sup>[120]</sup>. HCV core antigen immunoassay is an alternative to HCV RNA testing but cannot be used to monitor response to antiviral therapy as it has limitations in sensitivity<sup>[121]</sup>.

In patients with low pre-test probability for HCV infection, a negative EIA for anti-HCV antibody effectively excludes HCV infection. However, in patients suspected acute HCV infection, HCV RNA viral load by polymerase chain reaction (PCR) must also be obtained as antibodies may not become positive until 2-6 mo on average. A positive HCV antibody and positive HCV RNA confirms HCV infection but cannot distinguish between acute and chronic infection. Acute infection can be confirmed if a patient previously tested negative in the 6 mo prior to infection and has not tested positive for both RNA and antibody, or if the RNA and antibody become negative within 6 mo. Chronic HCV infection is defined as positive HCV RNA of at least 6 mo duration.

For patients with suspected exposure to HCV, HCV RNA, anti-HCV antibody, and serum aminotransferases are obtained within 48 h to obtain baseline values. If HCV RNA is positive, infection is confirmed, and acuity will depend on whether HCV antibody is positive (chronic) or negative (acute). However, if HCV RNA is negative, it should be rechecked in 4 wk and if positive it is considered an acute HCV infection. If HCV RNA is negative 4 wk after exposure, it should be re-checked at 12-16 wk. If negative again, HCV should be checked once more at 6 mo.

### Currently available treatments

Antiviral therapy should be contemplated for almost all patients with HCV. Clinicians should consider withholding treatment in patients with decompensated cirrhosis listed for liver transplant with a high Model for End-Stage Liver Disease (MELD) score, pregnant patients, and patients with less than 12 mo of life expectancy.

The intent of HCV treatment is to eradicate the virus to mitigate cirrhosis and associated complications, such as portal hypertension, HCC, need for liver transplantation, and death. The goal is to obtain sustained viral remission (SVR), which is the absence of virus in the blood 12 wk after treatment completion. SVR has been associated with improvement in elastography fibrosis scores<sup>[122]</sup>, while decreasing hepatic decompensation<sup>[123]</sup>, HCC<sup>[124]</sup>, and liver-related deaths<sup>[125]</sup>.

The major groups of therapy include interferon-alpha, ribavirin, and direct acting antivirals (DAAs). Interferon was the first treatment available for HCV in the 1980s. More recently, interferon has been bound to PEG, which increases its half-life and has increased SVR rates<sup>[126]</sup>. Ribavirin, an oral guanosine analog, may be used in a synergistic combination interferon to increase response and reduce relapse. Ribavirin is usually well tolerated but may produce hemolytic anemia, especially in patients with renal disease given its excretion in the kidney. It should be avoided in patients with a creatinine clearance less than 50 mL/min. In addition, ribavirin is teratogenic<sup>[127]</sup>.

DAAs inhibit replication of HCV by targeting the NS3/NS4 protease, NS5A protein, and the NS5B polymerase. NS3/NS4 protease inhibitors end in the suffix “-previr” and include boceprevir, telaprevir, simeprevir, paritaprevir, grazoprevir, glecaprevir, and voxilaprevir. NS5A inhibitors end in suffix “-asvirs” and include daclatasvir, ledipasvir, ombitasvir, and elbasvir, velpatasvir, and pibrentasvir. NS5B polymerase inhibitors end in “-buvirs” and are either nucleoside, nucleotide (sofosbuvir), or non-nucleoside (dasabuvir).

The classes of DAAs are typically used in combination: sofosbuvir/ledipasvir, elbasvir/grazoprevir, sofosbuvir/velpatasvir, sofosbuvir/velpatasvir/voxilaprevir, and glecaprevir/pibrentasvir. The choice of regimen and duration depend on the patient's genotype, renal function, and concurrent medications. The genotypic coverage provided by each regimen is outside of the scope of this review, but importantly sofosbuvir/velpatasvir and glecaprevir/pibrentasvir are considered pangenotypic regimens. Protease inhibitors are primarily hepatically excreted and thus are contraindicated in Child-Pugh B and C cirrhosis. Nucleoside NS5B inhibitor sofosbuvir is primarily renally excreted and should be avoided in patients an estimated glomerular filtration rate less than 30 mL/min per 1.73 m<sup>2</sup>.

### Role of liver transplant

Liver transplantation frequently provides destination treatment for HCV decompensated cirrhosis or HCC in candidates who are not deemed appropriate for surgical resection. HCV infection remains one of the leading etiologies for liver transplantation worldwide<sup>[128]</sup>. Since 2012, the percentage of liver transplants allocated for chronic HCV infection has steadily decreased in United States<sup>[129]</sup> due to the use of DAAs. The use of liver transplant for acute liver failure secondary to HCV infection has not been a common phenomenon.

Virtually all recipients who are serologically positive for HCV at the time of transplant develop recurrent HCV infection during reperfusion of the transplanted liver graft<sup>[130]</sup>. The main consequence is the development of post-transplant liver injury in the form of fibrosis in up to 40%<sup>[130]</sup>, recurrent cirrhosis in up to 30% after 5 years<sup>[131]</sup>, and fibrosing cholestatic HCV in up to 10%<sup>[132]</sup>. This has been associated with lower overall survival in HCV infected recipients in comparison to HCV negative recipients<sup>[133]</sup>. To counteract this, therapy with DAAs have been used and have increased post-transplant one-year survival rates in HCV viremic recipients from 90%-92%<sup>[129]</sup>. DAAs may be used to cure HCV prior to transplant, eliminating the chance of HCV recurrence<sup>[134]</sup>, or can be used post-transplant. Reasons why HCV treatment with DAAs may be delayed until after transplant include: improvement of MELD score leading to de-listing or increased wait time on transplant list, lower likelihood of SVR, and limited access to available regimens for advanced cirrhosis<sup>[135]</sup>.

Utilization of HCV infected organs has been one of the major advancements aimed at increasing the donor organ pool and decreasing waitlist time. Initially, this was primarily performed in recipients already infected with chronic HCV. Between 2010 to 2015, the proportion of HCV positive livers transplanted into HCV seropositive recipients increased 2.4-fold<sup>[136]</sup>. More recently, the transplantation of HCV infected organs including livers into HCV seronegative recipients has been utilized with



similarly good outcomes<sup>[137,138]</sup>. Donors positive for HCV RNA have a high risk of transmitting infection to HCV negative recipients but this may also occur with HCV antibody positive HCV RNA negative donors in up to 16% of cases<sup>[139]</sup>.

HCV negative recipients who receive HCV positive organs may receive DAA therapy prophylactically or reactively after they are found to be positive for HCV. In liver transplantation, DAA therapy is typically given for at least 12 wk to recipients once they are found to have positive HCV RNA, usually within 3 mo. Thus far, studies have shown SVR of up to 100%<sup>[140,141]</sup>. Questions are easing surrounding the concern whether the risk of rejection is increased in recipients of HCV organs, either from HCV or DAA therapy<sup>[140]</sup>. Initial 2-year outcomes of HCV positive organ transplantation in HCV negative recipients have shown promising similar patient and graft survival<sup>[138]</sup>. Short duration of DAA has been considered but not extensively studied in HCV positive liver transplantation.

In non-hepatic transplantation, prophylactic DAA therapy is favored before viremia to reduce the chances of complications and the duration of DAA therapy<sup>[142]</sup>. Some authors have even limited duration of DAA therapy to as few as 8 d, but this is not currently recommended outside a clinical trial setting<sup>[143]</sup>. A pangenotypic regimen is typically utilized if prophylactic DAA therapy is used. Thus far, outcomes of transplantation of HCV positive nonhepatic organs in HCV negative patients have been promising, but data is limited. There is still some concern regarding risks such as DAA treatment failure with evolution of resistance associated substitutions and fibrosing cholestatic hepatitis<sup>[144]</sup>.

### **Ongoing research and future directions**

Much of the future research and guidelines will aim to answer questions regarding the safety, ethical, and practical concerns regarding the transplantation of HCV viremic organs into HCV negative recipients. Several factors related to the HCV donor organ remain nebulous. It is unclear whether duration of HCV infection, viral load, genotype, and failed prior treatment of the donor will affect SVR rates post-transplant in this patient population as studies have not controlled for these factors<sup>[145]</sup>. In addition, several optimal donor factors, specifically age and fibrosis grade, are not clear. Previous studies showed that HCV infected livers of donors 50 years or older have been found to have increased fibrosis progression and worse graft survival<sup>[146]</sup>, but this data is prior to the advent of DAAs and should be re-examined. Similarly, data prior to the widespread use of DAAs showed that HCV positive donor kidneys had worse outcomes; because of this, the kidney donor profile index includes HCV status as a relevant factor but more recent data from the DAA era shows similar outcomes in these HCV positive donor kidneys<sup>[147]</sup>. Further studies are needed to establish its effects in the outcomes and limit the number of discarded HCV infected organs.

Recipient selection to match donor characteristics when utilizing HCV organs need further investigation to establish best practice guidelines for HCV organ utilization. For now, HCV infected donor allografts are used mainly in patients whose waitlist duration is expected to exceed their duration of transplant-free survival, but no studies have explicitly examined this. Another scarcely studied but relevant risk is how healthy the recipient's liver condition factors to receive an HCV infected non-liver organ, and what the long-term outcomes of this are. Timing of DAA therapy, optimal regimen, duration, cost effectiveness of different strategies, interactions between DAAs and calcineurin inhibitors, and other drug interactions with DAAs will also need to be investigated. Finally, data on long-term outcomes, specifically efficacy and safety, following transplantation of HCV viremic organs into HCV negative recipients is lacking, as current data is limited to 1-2 years.

The ongoing pursuit for a HCV vaccine remains prudent, especially since DAAs do not prevent against reinfection. To date, there have been a few clinical trials studying different methods for active immunity, including viral vectors<sup>[148]</sup>, DNA-plasmid, recombinant proteins, and prime-boost vaccination strategies<sup>[149]</sup>. However, thus far, many of these trials are still in the early phases or have not conferred consistent long-term immunity.

In 2020, the United States Center for Disease Control and Prevention increased the previous screening expanse by recommending one-time universal screening for all adults at least 18 years of age. Similarly, the United States Preventive Services Task Force recommended one-time universal screening for patients 18-79 years old. The World Health Organization (WHO), the American Association for the Study of Liver Diseases/Infectious Diseases Society of America joint guideline group, the European Association for the Study of the Liver, the National Health Service in the United Kingdom, the Canadian Task Force on Preventive Health Care, the Canadian

Association for the Study of the Liver, and other groups have yet to recommend universal screening.

Given the vast prevalence of HCV infections worldwide, there has been an increased effort in the last five years to encourage primary care physicians to treat HCV. This has been aided by the ease of using DAAs and the advent of pangenotypic drugs. However, studies have shown that up to 59% of primary care physicians still refer all of their HCV patients to specialists, citing needing additional training to feel comfortable treating the infection<sup>[150]</sup>. Thus, further studies investigating the best methods in educating and involving primary care physicians to treat HCV are needed.

## HEPATITIS D

### **Epidemiology**

In a recent large meta-analysis by Chen *et al*<sup>[58]</sup> with 182 articles included from 61 countries, it was estimated that 62-72 million individuals around the globe are infected with HDV. Approximately 10.58% of HBsAg carriers were coinfecting with HDV, which is two-fold higher than what has been estimated previously<sup>[150,151]</sup>. Areas of highest HDV infection carriage include western and middle Africa, the Amazon Basin, eastern and Mediterranean Europe, the Middle East, and parts of Asia. Notably, a recent epidemiological study examining a cohort of HBV-positive intravenous drug users revealed an alarming increase in HDV seroprevalence from 29% in 1988-1989 to 50% in 2005-2006<sup>[152]</sup>. Nonetheless, the lack of HDV RNA validation in many of these studies hinders a true estimation of HDV prevalence.

### **Pathogenesis**

HDV is a single-stranded RNA virus, considered a defective virus that requires the existence of HBV for full expression and replication. It was first described in 1977 by Rizzetto *et al*<sup>[153]</sup> in Italy, when they detected a new antigen-antibody system associated with but immunologically distinct from HBV by direct immunofluorescence. Although there are 8 different described HDV genotypes, HDV-1 is responsible for most cases in North America, Europe, and the Middle East<sup>[154]</sup>.

Like HBV, HDV is transmitted *via* the parenteral route through exposure to infected blood or body fluids with an exceedingly small inoculum needed to transmit infection<sup>[155]</sup>.

### **Clinical presentation**

The clinical spectrum of HDV infection ranges from inactive asymptomatic carrier to acute liver failure<sup>[156]</sup>. Concomitant infection of HBV and HDV typically leads to mild self-limited disease or less likely severe acute hepatitis with spontaneous resolution of both infections<sup>[157]</sup>. In contrast, HDV superinfection in chronic HBV carriers usually results in a protracted clinical course<sup>[158]</sup>. Nevertheless, patients exhibit heterogeneous clinical presentations with more severe disease reported in genotypes 1 and 3<sup>[159]</sup>, intravenous drug users, and older patients in European cohorts. This could be due to the variable direct cytotoxic effect and immunogenic response to HDV on the host hepatocytes<sup>[160-162]</sup>.

Screening for HDV should be considered in all HBsAg-positive patients especially those presenting with worsening liver disease. Initially, testing for total anti-HDV antibody (IgM and IgG) should be attempted by EIAs or radioimmunoassays. A positive test warrants confirmation by serum reverse transcriptase-PCR assays for HDV RNA. Quantification of serum HDV RNA is important in evaluating the need for and efficacy of antiviral therapy.

### **Currently available treatments**

Current evidence supports treating chronic HDV infection in those with detectable viral RNA and evidence of biochemical or histological active liver disease, particularly if significant fibrosis exists<sup>[61]</sup>. On the contrary, asymptomatic patients with normal liver enzymes do not require therapy.

With nearly 34 years lapsed since the introduction of interferon for the treatment of chronic HDV infection, it remains the only available treatment option of proven benefit<sup>[163]</sup>. Nonetheless, sustained virologic response is low even with the newer PEG-interferon and rarely exceeds 25%<sup>[164]</sup>. A meta-analysis of five trials comparing standard 48-wk PEG-interferon with no treatment confirmed not only a modest benefit to PEG-interferon but such benefit was not sustained<sup>[165]</sup>.



### Ongoing research and future directions

The past decade has witnessed the evolution of multiple novel antiviral agents that target various critical steps of HDV life cycle. Three new drugs have emerged for the treatment of chronic HDV infection. Among them is the specific inhibitor of HDV prenylation lonafarnib which showed promising results as a monotherapy or when combined with ritonavir or PEG-interferon. Reduction in viral RNA load and improvement in liver enzymes were observed at variable endpoints<sup>[166]</sup>. Although observed therapeutic benefits correlated with lonafarnib dose used, that was challenged by its universal limiting adverse effects like nausea, diarrhea, abdominal bloating, and weight loss.

Other new therapies included HDV entry inhibitors such as bulevirtide. As mentioned above, this medication was evaluated in patients with HBV coinfection for 24 wk as a monotherapy or in combination with PEG-interferon or tenofovir. The majority of bulevirtide treated patients experienced a > 1 log<sub>10</sub> reduction in HDV RNA after 24 wk of therapy with combination therapy being more effective than monotherapy. Finally, as mentioned in the hepatitis B section, REP 2139 was introduced as an inhibitor of virion secretion with potential for viral load suppression in patients with HBV-HDV coinfection. However, marked ALT elevations were noted in these studies<sup>[77,78]</sup>. Combination of inhibitors over an enduring treatment regimen are likely required. These novel agents are being considered in combination with PEG-interferon, which carries known side effects that may be prohibitive in its use with HDV cirrhosis.

Animal studies suggest that vaccine strategies for preventing HDV superinfection may be feasible<sup>[167,168]</sup>. Those studies used groundhogs as animal models and focused on inducing active immunity by injecting the animal with a full-sized HDV antigen or synthetic peptides. These investigations, although promising, were limited by their small size and heterogenous results. As of today, vaccination against HBV remains the most cost-effective means to prevent HDV infection.

### Role of liver transplant

Liver transplantation is indicated in patients with fulminant liver failure. Communication and arrangement for transfer to a transplant facility are paramount in the ability to rescue these individuals. Post liver transplantation recurrence of HDV infection despite appropriate medical therapy was estimated to be 13.4%<sup>[169]</sup> with comparable outcomes between patients with and without recurrence.

---

## HEPATITIS E

---

### Epidemiology

The WHO reported an estimated 20 million new hepatitis E virus (HEV) infections every year globally, leading to 3.3 million symptomatic cases of acute hepatitis and in another report to over 44000 deaths in 2015<sup>[39]</sup>. Although the use of current antibody assays in seroprevalence studies remains debatable, the overall seroprevalence of the HEV in the United States between 1988 and 1994 was projected to be 21%<sup>[170]</sup>. Other more recent analyses reported a lower but rising overall seroprevalence in the United States born individuals from 4.5% in 2013-2014 to 8.1% in 2015-2016, with increasing age, female sex, and Asian ethnicity being significant predictors of HEV seropositivity<sup>[171]</sup>.

### Pathogenesis

The HEV is a small, single-stranded RNA virus that is considered one of the most common, yet underdiagnosed etiologies of acute viral hepatitis with the earliest epidemic going back to 1955 in New Delhi<sup>[172]</sup>. While it stands as the only member of the genus *Hepevirus* in the family *Hepeviridae*, a plethora of genotypes were identified to date with four of particular clinical significance; genotypes 1 and 2 being confined to humans, while genotypes 3 and 4 can infect humans and animals largely *via* the fecal-oral route<sup>[173,174]</sup>.

### Clinical presentation

Most HEV infected patients are either asymptomatic or may develop mild, self-limited, HAV-like illness. Typically preceded by an incubation period ranging between 2 wk to 10 wk<sup>[175]</sup>. This is essentially true of HEV genotypes 1 and 2. However, the zoonotic genotypes HEV 3 and 4 have been increasingly reported as causes of

chronic hepatitis almost exclusively in those who are immunocompromised<sup>[176,177]</sup>. Less than 5% of acutely infected HEV patients will progress to acute liver failure and those patients are more likely to be pregnant, malnourished, or have a preexisting liver condition<sup>[178,179]</sup>.

Although a uniform diagnostic approach for HEV infection is limited by the lack of standardized antibody assays, patients with consistent clinical presentation should be tested for anti-HEV IgM antibody assay with a confirmatory HEV RNA viral load if positive.

### **Currently available treatments**

Similar to HAV infection, the majority of patients with acute HEV infection require no specific treatment and the management is mostly supportive. However, patients who develop acute liver failure may warrant liver transplantation<sup>[180]</sup>. A rising body of literature investigated the role of ribavirin in treating chronic HEV infection in immunosuppressed patients with variable success<sup>[181]</sup>. Whenever possible, treatment should be accompanied by reducing immunosuppressive therapy and followed by testing for clearance to confirm eradication<sup>[182]</sup>. A 3-mo course of ribavirin has been proposed for the above indication, while its use in acute fulminant hepatitis appear promising<sup>[183]</sup>, more robust evidence is yet awaited.

Prevention remains the most effective approach to combat HEV-related disease. This can be achieved by maintaining quality standards for public water supplies and maintaining hygienic practices as per the WHO recommendation<sup>[175]</sup>.

In 2011, a recombinant vaccine to prevent HEV infection was registered in China. Although it is not approved yet in other countries, few studies have emerged to evaluate efficacy and safety of this vaccine. In a large, randomized trial from China including 112604 healthy adults that evaluated different doses of HEV vaccine compared to placebo, a protective effect of 100% was reported at 1 year following 30 d from the last dose received. Another trial revealed a protective efficacy of the vaccine against HEV to be 86.8% after 4.5 years of the first vaccination<sup>[184]</sup>. Other preventive options such as immune globulin remain experimental<sup>[185]</sup>.

### **Ongoing research and future directions**

For chronic HEV patients who fail ribavirin therapy, some alternatives such as PEG-interferon<sup>[186]</sup> and sofosbuvir are being considered pending more evidence<sup>[187]</sup>. Their routine use is being hindered by the lack of safety and efficacy profile in this setting besides the perceived higher risk of acute rejection with PEG-interferon due to its immunostimulatory effect in organ transplant recipients.

### **Role of liver transplant**

Although liver transplant recipients may develop chronic HEV in the setting of prolonged immunosuppression, acute HEV infection may rarely result in acute liver failure necessitating liver transplant. Accumulating epidemiologic evidence described significant heterogeneity in HEV infection prevalence and outcomes. For example, HEV remains the most common cause of acute viral hepatitis and acute liver failure (up to 44%) in some Asian countries such as India and Bangladesh<sup>[187,188]</sup>. This contrasts with Western Europe and the United States where it is a rare cause of acute liver failure<sup>[189]</sup>.

---

## **CONCLUSION**

The recognition of the epidemiological and clinical features of hepatitis A, B, C, D and E is crucial to guide the diagnosis of these conditions. Fortunately, the medical advances in the last centuries have allowed to effectively diagnose them and comprehensively establish its multisystemic impact in this population. With the advent of new therapies, the possibility of achieving control of the disease is a reality, while reaching the cure and eradication of chronic hepatitis B, C and D is around the corner.

---

## **REFERENCES**

- 1 Fonseca JC. [History of viral hepatitis]. *Rev Soc Bras Med Trop* 2010; 43: 322-330 [PMID: 20563505 DOI: 10.1590/s0037-86822010000300022]

- 2 **Martin NA.** The discovery of viral hepatitis: a military perspective. *J R Army Med Corps* 2003; **149**: 121-124 [PMID: [12929519](#) DOI: [10.1136/jramc-149-02-04](#)]
- 3 **Koff RS.** Feinstone SM, Kapikian AZ, Purcell RH. Hepatitis A: detection by immune electron microscopy of a virus like antigen associated with acute illness [Science 1973;182:1026-1028]. *J Hepatol* 2002; **37**: 2-6 [PMID: [12076855](#) DOI: [10.1016/s0168-8278\(02\)00169-1](#)]
- 4 **Melnick JL.** Properties and classification of hepatitis A virus. *Vaccine* 1992; **10** Suppl 1: S24-S26 [PMID: [1335653](#) DOI: [10.1016/0264-410x\(92\)90536-s](#)]
- 5 **World Health Organization.** Hepatitis A. [cited 19 January 2021]. In: World Health Organization [Internet]. Available from: <https://www.who.int/news-room/fact-sheets/detail/hepatitis-a>
- 6 **Wasley A, Fiore A, Bell BP.** Hepatitis A in the era of vaccination. *Epidemiol Rev* 2006; **28**: 101-111 [PMID: [16775039](#) DOI: [10.1093/epirev/mxj012](#)]
- 7 **Foster MA, Hofmeister MG, Kupronis BA, Lin Y, Xia GL, Yin S, Teshale E.** Increase in Hepatitis A Virus Infections - United States, 2013-2018. *MMWR Morb Mortal Wkly Rep* 2019; **68**: 413-415 [PMID: [31071072](#) DOI: [10.15585/mmwr.mm6818a2](#)]
- 8 **Cooksley WG.** What did we learn from the Shanghai hepatitis A epidemic? *J Viral Hepat* 2000; **7** Suppl 1: 1-3 [PMID: [10870174](#) DOI: [10.1046/j.1365-2893.2000.00021.x](#)]
- 9 **Halliday ML, Kang LY, Zhou TK, Hu MD, Pan QC, Fu TY, Huang YS, Hu SL.** An epidemic of hepatitis A attributable to the ingestion of raw clams in Shanghai, China. *J Infect Dis* 1991; **164**: 852-859 [PMID: [1658157](#) DOI: [10.1093/infdis/164.5.852](#)]
- 10 **Foster M, Ramachandran S, Myatt K, Donovan D, Bohm S, Fiedler J, Barbeau B, Collins J, Thoroughman D, McDonald E, Ballard J, Eason J, Jorgensen C.** Hepatitis A Virus Outbreaks Associated with Drug Use and Homelessness - California, Kentucky, Michigan, and Utah, 2017. *MMWR Morb Mortal Wkly Rep* 2018; **67**: 1208-1210 [PMID: [30383739](#) DOI: [10.15585/mmwr.mm6743a3](#)]
- 11 **Centers for Disease Control and Prevention.** Widespread person-to-person outbreaks of hepatitis A across the United States. [cited 28 July 2020]. In: Centers for Disease Control and Prevention [Internet]. Available from: <https://www.cdc.gov/hepatitis/outbreaks/2017March-HepatitisA.htm>
- 12 **European Centre for Disease Prevention and Control.** Epidemiological update: Hepatitis A outbreak in the EU/EEA mostly affecting men who have sex with men. [cited 28 July 2020]. In: European Centre for Disease Prevention and Control [Internet]. <https://www.ecdc.europa.eu/en/news-events/epidemiological-update-hepatitis-outbreak-eueea-mostly-affecting-men-who-have-sex-men-2>
- 13 **Manka P, Verheyen J, Gerken G, Canbay A.** Liver Failure due to Acute Viral Hepatitis (A-E). *Visc Med* 2016; **32**: 80-85 [PMID: [27413724](#) DOI: [10.1159/000444915](#)]
- 14 **Baba M, Hasegawa H, Nakayabu M, Fukai K, Suzuki S.** Cytolytic activity of natural killer cells and lymphokine activated killer cells against hepatitis A virus infected fibroblasts. *J Clin Lab Immunol* 1993; **40**: 47-60 [PMID: [7932628](#)]
- 15 **Fleischer B, Fleischer S, Maier K, Wiedmann KH, Sacher M, Thaler H, Vallbracht A.** Clonal analysis of infiltrating T lymphocytes in liver tissue in viral hepatitis A. *Immunology* 1990; **69**: 14-19 [PMID: [2312151](#)]
- 16 **Vallbracht A, Fleischer B, Busch FW.** Hepatitis A: hepatotropism and influence on myelopoiesis. *Intervirology* 1993; **35**: 133-139 [PMID: [8407240](#) DOI: [10.1159/000150304](#)]
- 17 **Richardson M, Elliman D, Maguire H, Simpson J, Nicoll A.** Evidence base of incubation periods, periods of infectiousness and exclusion policies for the control of communicable diseases in schools and preschools. *Pediatr Infect Dis J* 2001; **20**: 380-391 [PMID: [11332662](#) DOI: [10.1097/00006454-200104000-00004](#)]
- 18 **Mackinney-Novelo I, Barahona-Garrido J, Castillo-Albarran F, Santiago-Hernández JJ, Méndez-Sánchez N, Uribe M, Chávez-Tapia N.** Clinical course and management of acute hepatitis A infection in adults. *Ann Hepatol* 2012; **11**: 652-657 [PMID: [22947525](#)]
- 19 **Gordon SC, Reddy KR, Schiff L, Schiff ER.** Prolonged intrahepatic cholestasis secondary to acute hepatitis A. *Ann Intern Med* 1984; **101**: 635-637 [PMID: [6486595](#) DOI: [10.7326/0003-4819-101-5-635](#)]
- 20 **Matheny SC, Kingery JE.** Hepatitis A. *Am Fam Physician* 2012; **86**: 1027-34; quiz 1010 [PMID: [23198670](#)]
- 21 **Tagle Arrospe M, León Barúa R.** [Viral hepatitis A as a triggering agent of autoimmune hepatitis report of a case and review of literature]. *Rev Gastroenterol Peru* 2003; **23**: 134-137 [PMID: [12853990](#)]
- 22 **Koff RS.** Clinical manifestations and diagnosis of hepatitis A virus infection. *Vaccine* 1992; **10** Suppl 1: S15-S17 [PMID: [1335649](#) DOI: [10.1016/0264-410x\(92\)90533-p](#)]
- 23 **Tong MJ, el-Farra NS, Grew MI.** Clinical manifestations of hepatitis A: recent experience in a community teaching hospital. *J Infect Dis* 1995; **171** Suppl 1: S15-S18 [PMID: [7876641](#) DOI: [10.1093/infdis/171.supplement\\_1.s15](#)]
- 24 **Carrion AF, Martin P.** Viral hepatitis in the elderly. *Am J Gastroenterol* 2012; **107**: 691-697 [PMID: [22290404](#) DOI: [10.1038/ajg.2012.7](#)]
- 25 **Ponnappan S, Ponnappan U.** Aging and immune function: molecular mechanisms to interventions. *Antioxid Redox Signal* 2011; **14**: 1551-1585 [PMID: [20812785](#) DOI: [10.1089/ars.2010.3228](#)]
- 26 **National Center for Health Statistics.** Health Data Interactive. [cited 30 December 2020]. In: Centers for Disease Control and Prevention [Internet]. In: Available from: <https://www.cdc.gov/nchs/hdi.htm>

- 27 **Liaw YF**, Yang CY, Chu CM, Huang MJ. Appearance and persistence of hepatitis A IgM antibody in acute clinical hepatitis A observed in an outbreak. *Infection* 1986; **14**: 156-158 [PMID: [3759243](#) DOI: [10.1007/BF01645253](#)]
- 28 **Lemon SM**, Binn LN, Marchwicki R, Murphy PC, Ping LH, Jansen RW, Asher LV, Stapleton JT, Taylor DG, LeDuc JW. In vivo replication and reversion to wild type of a neutralization-resistant antigenic variant of hepatitis A virus. *J Infect Dis* 1990; **161**: 7-13 [PMID: [1688601](#) DOI: [10.1093/infdis/161.1.7](#)]
- 29 **Centers for Disease Control and Prevention**. Positive test results for acute hepatitis A virus infection among persons with no recent history of acute hepatitis--United States, 2002-2004. *MMWR Morb Mortal Wkly Rep* 2005; **54**: 453-456 [PMID: [15889006](#)]
- 30 **Kryger P**, Christoffersen P. Liver histopathology of the hepatitis A virus infection: a comparison with hepatitis type B and non-a, non-b. *J Clin Pathol* 1983; **36**: 650-654 [PMID: [6406559](#) DOI: [10.1136/jcp.36.6.650](#)]
- 31 **Werzberger A**, Kuter B, Shouval D, Mensch B, Brown L, Wiens B, Lewis J, Miller W, Sitrin R, Provost P. Anatomy of a trial: a historical view of the Monroe inactivated hepatitis A protective efficacy trial. *J Hepatol* 1993; **18** Suppl 2: S46-S50 [PMID: [8182273](#) DOI: [10.1016/s0168-8278\(05\)80378-2](#)]
- 32 Prevention of hepatitis A through active or passive immunization: Recommendations of the Advisory Committee on Immunization Practices (ACIP). *MMWR Recomm Rep* 1996; **45**: 1-30 [PMID: [9005304](#)]
- 33 **Advisory Committee on Immunization Practices (ACIP)**, Fiore AE, Wasley A, Bell BP. Prevention of hepatitis A through active or passive immunization: recommendations of the Advisory Committee on Immunization Practices (ACIP). *MMWR Recomm Rep* 2006; **55**: 1-23 [PMID: [16708058](#)]
- 34 **Doshani M**, Weng M, Moore KL, Romero JR, Nelson NP. Recommendations of the Advisory Committee on Immunization Practices for Use of Hepatitis A Vaccine for Persons Experiencing Homelessness. *MMWR Morb Mortal Wkly Rep* 2019; **68**: 153-156 [PMID: [30763295](#) DOI: [10.15585/mmwr.mm6806a6](#)]
- 35 **Centers for Disease Control and Prevention**. Hepatitis A Questions and Answers for Health Professionals. [cited 28 July 2020]. In: Centers for Disease Control and Prevention [Internet]. Available from: <https://www.cdc.gov/hepatitis/hav/havfaq.htm#vaccine>
- 36 **Hill HA**, Elam-Evans LD, Yankey D, Singleton JA, Kolasa M. National, State, and Selected Local Area Vaccination Coverage Among Children Aged 19-35 Months - United States, 2014. *MMWR Morb Mortal Wkly Rep* 2015; **64**: 889-896 [PMID: [26313470](#) DOI: [10.15585/mmwr.mm6433a1](#)]
- 37 **Taylor RM**, Davern T, Munoz S, Han SH, McGuire B, Larson AM, Hynan L, Lee WM, Fontana RJ; US Acute Liver Failure Study Group. Fulminant hepatitis A virus infection in the United States: Incidence, prognosis, and outcomes. *Hepatology* 2006; **44**: 1589-1597 [PMID: [17133489](#) DOI: [10.1002/hep.21439](#)]
- 38 **Jung DH**, Hwang S, Lim YS, Kim KH, Ahn CS, Moon DB, Ha TY, Song GW, Park GC, Lee SG. Outcome comparison of liver transplantation for hepatitis A-related vs hepatitis B-related acute liver failure in adult recipients. *Clin Transplant* 2018; **32** [PMID: [29044729](#) DOI: [10.1111/ctr.13140](#)]
- 39 **World Health Organization**. Global hepatitis report, 2017. [cited 19 January 2021]. In: World Health Organization [Internet]. Available from: <https://www.who.int/publications/i/item/global-hepatitis-report-2017>
- 40 **Paik JM**, Golabi P, Younossi Y, Mishra A, Younossi ZM. Changes in the Global Burden of Chronic Liver Diseases From 2012 to 2017: The Growing Impact of NAFLD. *Hepatology* 2020; **72**: 1605-1616 [PMID: [32043613](#) DOI: [10.1002/hep.31173](#)]
- 41 **Velkov S**, Ott JJ, Protzer U, Michler T. The Global Hepatitis B Virus Genotype Distribution Approximated from Available Genotyping Data. *Genes (Basel)* 2018; **9** [PMID: [30326600](#) DOI: [10.3390/genes9100495](#)]
- 42 **Meireles LC**, Marinho RT, Van Damme P. Three decades of hepatitis B control with vaccination. *World J Hepatol* 2015; **7**: 2127-2132 [PMID: [26328023](#) DOI: [10.4254/wjh.v7.i18.2127](#)]
- 43 **Busch MP**, Bloch EM, Kleinman S. Prevention of transfusion-transmitted infections. *Blood* 2019; **133**: 1854-1864 [PMID: [30808637](#) DOI: [10.1182/blood-2018-11-833996](#)]
- 44 **Jafari S**, Buxton JA, Afshar K, Copes R, Baharlou S. Tattooing and risk of hepatitis B: a systematic review and meta-analysis. *Can J Public Health* 2012; **103**: 207-212 [PMID: [22905640](#) DOI: [10.1007/BF03403814](#)]
- 45 **Bixler D**, Annambholta P, Abara WE, Collier MG, Jones J, Mixson-Hayden T, Basavaraju SV, Ramachandran S, Kamili S, Moorman A. Hepatitis B and C virus infections transmitted through organ transplantation investigated by CDC, United States, 2014-2017. *Am J Transplant* 2019; **19**: 2570-2582 [PMID: [30861300](#) DOI: [10.1111/ajt.15352](#)]
- 46 **Scaglioni PP**, Melegari M, Wands JR. Recent advances in the molecular biology of hepatitis B virus. *Baillieres Clin Gastroenterol* 1996; **10**: 207-225 [PMID: [8864030](#) DOI: [10.1016/s0950-3528\(96\)90003-2](#)]
- 47 **Rybicka M**, Bielawski KP. Recent Advances in Understanding, Diagnosing, and Treating Hepatitis B Virus Infection. *Microorganisms* 2020; **8** [PMID: [32942584](#) DOI: [10.3390/microorganisms8091416](#)]
- 48 **Revill PA**, Tu T, Netter HJ, Yuen LKW, Locarnini SA, Littlejohn M. The evolution and clinical impact of hepatitis B virus genome diversity. *Nat Rev Gastroenterol Hepatol* 2020; **17**: 618-634



- [PMID: [32467580](#) DOI: [10.1038/s41575-020-0296-6](#)]
- 49 **Liaw YF**, Tsai SL, Sheen IS, Chao M, Yeh CT, Hsieh SY, Chu CM. Clinical and virological course of chronic hepatitis B virus infection with hepatitis C and D virus markers. *Am J Gastroenterol* 1998; **93**: 354-359 [PMID: [9517639](#) DOI: [10.1111/j.1572-0241.1998.00354.x](#)]
  - 50 **Jindal A**, Kumar M, Sarin SK. Management of acute hepatitis B and reactivation of hepatitis B. *Liver Int* 2013; **33** Suppl 1: 164-175 [PMID: [23286861](#) DOI: [10.1111/liv.12081](#)]
  - 51 **Chu CM**, Liaw YF. Chronic hepatitis B virus infection acquired in childhood: special emphasis on prognostic and therapeutic implication of delayed HBeAg seroconversion. *J Viral Hepat* 2007; **14**: 147-152 [PMID: [17305879](#) DOI: [10.1111/j.1365-2893.2006.00810.x](#)]
  - 52 **Yan ZH**, Fan Y, Wang XH, Mao Q, Deng GH, Wang YM. Relationship between HLA-DR gene polymorphisms and outcomes of hepatitis B viral infections: a meta-analysis. *World J Gastroenterol* 2012; **18**: 3119-3128 [PMID: [22791948](#) DOI: [10.3748/wjg.v18.i24.3119](#)]
  - 53 **Chang ML**, Liaw YF. Hepatitis B flares in chronic hepatitis B: pathogenesis, natural course, and management. *J Hepatol* 2014; **61**: 1407-1417 [PMID: [25178562](#) DOI: [10.1016/j.jhep.2014.08.033](#)]
  - 54 **Lapointe-Shaw L**, Chung H, Holder L, Kwong JC, Sander B, Austin PC, Janssen HLA, Feld JJ. Diagnosis of Chronic Hepatitis B Peri-Complication: Risk factors and Trends over Time. *Hepatology* 2020 [PMID: [32931613](#) DOI: [10.1002/hep.31557](#)]
  - 55 **Croagh CM**, Lubel JS. Natural history of chronic hepatitis B: phases in a complex relationship. *World J Gastroenterol* 2014; **20**: 10395-10404 [PMID: [25132755](#) DOI: [10.3748/wjg.v20.i30.10395](#)]
  - 56 **Prasidhrathsint K**, Stapleton JT. Laboratory Diagnosis and Monitoring of Viral Hepatitis. *Gastroenterol Clin North Am* 2019; **48**: 259-279 [PMID: [31046974](#) DOI: [10.1016/j.gtc.2019.02.007](#)]
  - 57 **Seo SI**, Kim HS, Yang BK, Kang JG, Shin WG, Lee JH, Kim HY, Jang MK. Predictive factors for risk of hepatocellular carcinoma in immune inactive chronic hepatitis B. *Clin Res Hepatol Gastroenterol* 2020; **44**: 711-717 [PMID: [31959567](#) DOI: [10.1016/j.clinre.2019.10.009](#)]
  - 58 **Chen CJ**, Yang HI, Su J, Jen CL, You SL, Lu SN, Huang GT, Iloeje UH; REVEAL-HBV Study Group. Risk of hepatocellular carcinoma across a biological gradient of serum hepatitis B virus DNA level. *JAMA* 2006; **295**: 65-73 [PMID: [16391218](#) DOI: [10.1001/jama.295.1.65](#)]
  - 59 **Chan HL**, Hui AY, Wong ML, Tse AM, Hung LC, Wong VW, Sung JJ. Genotype C hepatitis B virus infection is associated with an increased risk of hepatocellular carcinoma. *Gut* 2004; **53**: 1494-1498 [PMID: [15361502](#) DOI: [10.1136/gut.2003.033324](#)]
  - 60 **Jeng WJ**, Lok AS. Should Treatment Indications for Chronic Hepatitis B Be Expanded? *Clin Gastroenterol Hepatol* 2020 [PMID: [32434068](#) DOI: [10.1016/j.cgh.2020.04.091](#)]
  - 61 **Terrault NA**, Lok ASF, McMahon BJ, Chang KM, Hwang JP, Jonas MM, Brown RS Jr, Bzowej NH, Wong JB. Update on prevention, diagnosis, and treatment of chronic hepatitis B: AASLD 2018 hepatitis B guidance. *Hepatology* 2018; **67**: 1560-1599 [PMID: [29405329](#) DOI: [10.1002/hep.29800](#)]
  - 62 **Sarin SK**, Kumar M, Lau GK, Abbas Z, Chan HL, Chen CJ, Chen DS, Chen HL, Chen PJ, Chien RN, Dokmeci AK, Gane E, Hou JL, Jafri W, Jia J, Kim JH, Lai CL, Lee HC, Lim SG, Liu CJ, Locarnini S, Al Mahtab M, Mohamed R, Omata M, Park J, Piratvisuth T, Sharma BC, Sollano J, Wang FS, Wei L, Yuen MF, Zheng SS, Kao JH. Asian-Pacific clinical practice guidelines on the management of hepatitis B: a 2015 update. *Hepatol Int* 2016; **10**: 1-98 [PMID: [26563120](#) DOI: [10.1007/s12072-015-9675-4](#)]
  - 63 **European Association for the Study of the Liver**. EASL 2017 Clinical Practice Guidelines on the management of hepatitis B virus infection. *J Hepatol* 2017; **67**: 370-398 [PMID: [28427875](#) DOI: [10.1016/j.jhep.2017.03.021](#)]
  - 64 **Tao Y**, Wu D, Zhou L, Chen E, Liu C, Tang X, Jiang W, Han N, Li H, Tang H. Present and Future Therapies for Chronic Hepatitis B. *Adv Exp Med Biol* 2020; **1179**: 137-186 [PMID: [31741336](#) DOI: [10.1007/978-981-13-9151-4\\_6](#)]
  - 65 **Jothimani D**, Venugopal R, Vij M, Rela M. Post liver transplant recurrent and de novo viral infections. *Best Pract Res Clin Gastroenterol* 2020; **46-47**: 101689 [PMID: [33158469](#) DOI: [10.1016/j.bpg.2020.101689](#)]
  - 66 **Park JS**, Gayam V, Pan CQ. Review article: preventing hepatitis B graft infection in hepatitis B patients after liver transplantation: immunoglobulin vs anti-virals. *Aliment Pharmacol Ther* 2020; **52**: 944-954 [PMID: [32743822](#) DOI: [10.1111/apt.15999](#)]
  - 67 **Volz T**, Allweiss L, Ben MBarek M, Warlich M, Lohse AW, Pollok JM, Alexandrov A, Urban S, Petersen J, Lütgehetmann M, Dandri M. The entry inhibitor Myrcludex-B efficiently blocks intrahepatic virus spreading in humanized mice previously infected with hepatitis B virus. *J Hepatol* 2013; **58**: 861-867 [PMID: [23246506](#) DOI: [10.1016/j.jhep.2012.12.008](#)]
  - 68 **Blank A**, Markert C, Hohmann N, Carls A, Mikus G, Lehr T, Alexandrov A, Haag M, Schwab M, Urban S, Haefeli WE. First-in-human application of the novel hepatitis B and hepatitis D virus entry inhibitor myrcludex B. *J Hepatol* 2016; **65**: 483-489 [PMID: [27132172](#) DOI: [10.1016/j.jhep.2016.04.013](#)]
  - 69 **Weldemeyer H**, Shoneweis L, Bogomolov P, Voronka N, Stepanova T, Bremer B, Allweiss L, Dandri M, Burhenne J, Haefeli WE, Ciesek S, Dittmer U, Alexandrov A, Urban S. GS-13-Final results of a multicenter open label phase 2 clinical trial (MYR203) to assess safety and efficacy of Myrcludex B with Peg interferon a-2a in Patients with Chronic Hepatitis HBV/HDV Co-Infection. *J Hepatol* 2019; **70**: e81 [DOI: [10.1016/S0618-8278\(19\)30141-0](#)]
  - 70 **Shimura S**, Watashi K, Fukano K, Peel M, Sluder A, Kawai F, Iwamoto M, Tsukuda S, Takeuchi JS, Miyake T, Sugiyama M, Ogasawara Y, Park SY, Tanaka Y, Kusuha H, Mizokami M, Sureau C, Wakita T. Cyclosporin derivatives inhibit hepatitis B virus entry without interfering with NTCP

- transporter activity. *J Hepatol* 2017; **66**: 685-692 [PMID: [27890789](#) DOI: [10.1016/j.jhep.2016.11.009](#)]
- 71 **Phillips S**, Chokshi S, Chatterji U, Riva A, Bobardt M, Williams R, Gallay P, Naoumov NV. Alisporivir inhibition of hepatocyte cyclophilins reduces HBV replication and hepatitis B surface antigen production. *Gastroenterology* 2015; **148**: 403-14. e7 [PMID: [25305505](#) DOI: [10.1053/j.gastro.2014.10.004](#)]
  - 72 **Gallay P**, Ure D, Bobardt M, Chatterji U, Ou J, Trepanier D, Foster R. The cyclophilin inhibitor CRV431 inhibits liver HBV DNA and HBsAg in transgenic mice. *PLoS One* 2019; **14**: e0217433 [PMID: [31181107](#) DOI: [10.1371/journal.pone.0217433](#)]
  - 73 **Alexopoulou A**, Vasilieva L, Karayiannis P. New Approaches to the Treatment of Chronic Hepatitis B. *J Clin Med* 2020; **9** [PMID: [33019573](#) DOI: [10.3390/jcm9103187](#)]
  - 74 **Yuen MF**, Heo J, Kumada H, Suzuki F, Suzuki Y, Xie Q, Jia J, Karino Y, Hou J, Chayama K, Imamura M, Lao-Tan JY, Lim SG, Tanaka Y, Xie W, Yoon JH, Duan Z, Kurosaki M, Park SJ, Labio E, Kumar R, Kweon YO, Yim HJ, Cremer J, Elston R, Chen S, Davies M, Baptiste-Brown S, Han K, Campbell FM, Paff M, Theodore D. Results after 12 wk treatment of multiple doses of GSK3389404 in chronic hepatitis B subjects on stable nucleos(t)ide therapy in a phase 2a double-blind, placebo-controlled study. *Hepatology* 2019; **70**: 433A
  - 75 **Gane E**, Locarnini S, Lim TH, Strasser S, Sievert W, Cheng W, Thompson A, Given B, Schluep T, Hamilton J, Biermer M, Kalmeijer R, Beumont-Mauviel M, Lenz O, Cloherty G, Wong DKH, Schwabe C, Jackson K, Ferrari C, Lai CL, Gish RG, Yuen MF. Short-term treatment with RNA interference therapy, JNJ-3989, results in sustained hepatitis B surface antigen suppression in patients with chronic hepatitis B receiving nucleos(t)ide analogue treatment. *J Hepatol* 2020; **73**: S20 [DOI: [10.1016/S0168-8278\(20\)30597-3](#)]
  - 76 **Yuen MF**, Heo J, Jang JW, Yoon JH, Kweon YO, Park SJ. Hepatitis B virus (HBV) surface antigen (HBsAg) inhibition with is 505358 in chronic hepatitis B (CHB) patients on stable nucleos (t)ide analogue (NA) regimen and in NA -naive CHB patients: phase 2a, randomized, double-blind, placebo-controlled study. *J Hepatol* 2020; **73**: S49-S50
  - 77 **Bazinnet M**, Pântea V, Cebotarescu V, Cojuhari L, Jimbei P, Albrecht J, Schmid P, Le Gal F, Gordien E, Krawczyk A, Mijočević H, Karimzadeh H, Roggendorf M, Vaillant A. Safety and efficacy of REP 2139 and pegylated interferon alfa-2a for treatment-naïve patients with chronic hepatitis B virus and hepatitis D virus co-infection (REP 301 and REP 301-LTF): a non-randomised, open-label, phase 2 trial. *Lancet Gastroenterol Hepatol* 2017; **2**: 877-889 [PMID: [28964701](#) DOI: [10.1016/S2468-1253\(17\)30288-1](#)]
  - 78 **Bazinnet M**, Pantea V, Placinta G, Moscalu I, Cebotarescu V, Cojuhari L, Jimbei P, Iarovoi L, Smesnoi V, Musteata T, Jucov A, Krawczyk A, Vaillant A. FRI-210 Establishment of high rates of functional cure of HBeAg negative chronic HBV infection with REP 2139-Mg based combination therapy: Ongoing follow-up results from the REP 401 study. *J Hepatol* 2019; **70**: E486
  - 79 **Ahn SH**, Kim W, Jung YK, Yang JM, Jang JY, Kweon YO, Cho YK, Kim YJ, Hong GY, Kim DJ, Um SH, Sohn JH, Lee JW, Park SJ, Lee BS, Kim JH, Kim HS, Yoon SK, Kim MY, Yim HJ, Lee KS, Lim YS, Lee WS, Park NH, Jin SY, Kim KH, Choi W, Han KH. Efficacy and Safety of Besifovir Dipivoxil Maleate Compared With Tenofovir Disoproxil Fumarate in Treatment of Chronic Hepatitis B Virus Infection. *Clin Gastroenterol Hepatol* 2019; **17**: 1850-1859. e4 [PMID: [30448598](#) DOI: [10.1016/j.cgh.2018.11.001](#)]
  - 80 **Gane E**, Verdon DJ, Brooks AE, Gaggar A, Nguyen AH, Subramanian GM, Schwabe C, Dunbar PR. Anti-PD-1 blockade with nivolumab with and without therapeutic vaccination for virally suppressed chronic hepatitis B: A pilot study. *J Hepatol* 2019; **71**: 900-907 [PMID: [31306680](#) DOI: [10.1016/j.jhep.2019.06.028](#)]
  - 81 **Boni C**, Vecchi A, Rossi M, Laccabue D, Giuberti T, Alfieri A, Lampertico P, Grossi G, Facchetti F, Brunetto MR, Coco B, Cavallone D, Mangia A, Santoro R, Piazzolla V, Lau A, Gaggar A, Subramanian GM, Ferrari C. TLR7 Agonist Increases Responses of Hepatitis B Virus-Specific T Cells and Natural Killer Cells in Patients With Chronic Hepatitis B Treated With Nucleos(T)Ide Analogues. *Gastroenterology* 2018; **154**: 1764-1777. e7 [PMID: [29378197](#) DOI: [10.1053/j.gastro.2018.01.030](#)]
  - 82 **Lin CL**, Kao JH. Hepatitis B: Immunization and Impact on Natural History and Cancer Incidence. *Gastroenterol Clin North Am* 2020; **49**: 201-214 [PMID: [32389359](#) DOI: [10.1016/j.gtc.2020.01.010](#)]
  - 83 **Fernández G**, L Sanchez A, Jerez E, E Anillo L, Freyre F, A Aguiar J, Leon Y, Cinza Z, A Diaz P, Figueroa N, Muzio V, G Nieto G, Lobaina Y, Aguilar A, Penton E, C Aguilar J. Five-year Follow-up of Chronic Hepatitis B Patients Immunized by Nasal Route with the Therapeutic Vaccine HeberNasvac. *Euroasian J Hepatogastroenterol* 2018; **8**: 133-139 [PMID: [30828555](#) DOI: [10.5005/jp-journals-10018-1279](#)]
  - 84 **World Health Organization**. Web Annex B. WHO estimates of the prevalence and incidence of hepatitis C virus infection by WHO region, 2015. [cited 19 January 2021]. In: World Health Organization [Internet]. Available from: <https://apps.who.int/iris/bitstream/handle/10665/277005/WHO-CDS-HIV-18.46-eng.pdf>
  - 85 **Polaris Observatory HCV Collaborators**. Global prevalence and genotype distribution of hepatitis C virus infection in 2015: a modelling study. *Lancet Gastroenterol Hepatol* 2017; **2**: 161-176 [PMID: [28404132](#) DOI: [10.1016/S2468-1253\(16\)30181-9](#)]
  - 86 **Smith DB**, Bukh J, Kuiken C, Muerhoff AS, Rice CM, Stapleton JT, Simmonds P. Expanded classification of hepatitis C virus into 7 genotypes and 67 subtypes: updated criteria and genotype



- assignment web resource. *Hepatology* 2014; **59**: 318-327 [PMID: [24115039](#) DOI: [10.1002/hep.26744](#)]
- 87 **Gower E**, Estes C, Blach S, Razavi-Shearer K, Razavi H. Global epidemiology and genotype distribution of the hepatitis C virus infection. *J Hepatol* 2014; **61**: S45-S57 [PMID: [25086286](#) DOI: [10.1016/j.jhep.2014.07.027](#)]
  - 88 **Mohd Hanafiah K**, Groeger J, Flaxman AD, Wiersma ST. Global epidemiology of hepatitis C virus infection: new estimates of age-specific antibody to HCV seroprevalence. *Hepatology* 2013; **57**: 1333-1342 [PMID: [23172780](#) DOI: [10.1002/hep.26141](#)]
  - 89 **Murphy EL**, Bryzman SM, Glynn SA, Ameti DI, Thomson RA, Williams AE, Nass CC, Ownby HE, Schreiber GB, Kong F, Neal KR, Nemo GJ. Risk factors for hepatitis C virus infection in United States blood donors. *Hepatology* 2000; **31**: 756-762 [PMID: [10706569](#) DOI: [10.1002/hep.510310329](#)]
  - 90 **Irshad M**, Mankotia DS, Irshad K. An insight into the diagnosis and pathogenesis of hepatitis C virus infection. *World J Gastroenterol* 2013; **19**: 7896-7909 [PMID: [24307784](#) DOI: [10.3748/wjg.v19.i44.7896](#)]
  - 91 **Zeisel MB**, Felmlee DJ, Baumert TF. Hepatitis C virus entry. *Curr Top Microbiol Immunol* 2013; **369**: 87-112 [PMID: [23463198](#) DOI: [10.1007/978-3-642-27340-7\\_4](#)]
  - 92 **Zein NN**. Clinical significance of hepatitis C virus genotypes. *Clin Microbiol Rev* 2000; **13**: 223-235 [PMID: [10755999](#) DOI: [10.1128/cmr.13.2.223-235.2000](#)]
  - 93 **Clément S**, Pascarella S, Negro F. Hepatitis C virus infection: molecular pathways to steatosis, insulin resistance and oxidative stress. *Viruses* 2009; **1**: 126-143 [PMID: [21994542](#) DOI: [10.3390/v1020126](#)]
  - 94 **Bengsch B**, Seigel B, Ruhl M, Timm J, Kuntz M, Blum HE, Pircher H, Thimme R. Coexpression of PD-1, 2B4, CD160 and KLRG1 on exhausted HCV-specific CD8+ T cells is linked to antigen recognition and T cell differentiation. *PLoS Pathog* 2010; **6**: e1000947 [PMID: [20548953](#) DOI: [10.1371/journal.ppat.1000947](#)]
  - 95 **Dionisio N**, Garcia-Mediavilla MV, Sanchez-Campos S, Majano PL, Benedicto I, Rosado JA, Salido GM, Gonzalez-Gallego J. Hepatitis C virus NS5A and core proteins induce oxidative stress-mediated calcium signalling alterations in hepatocytes. *J Hepatol* 2009; **50**: 872-882 [PMID: [19303156](#) DOI: [10.1016/j.jhep.2008.12.026](#)]
  - 96 **Westbrook RH**, Dusheiko G. Natural history of hepatitis C. *J Hepatol* 2014; **61**: S58-S68 [PMID: [25443346](#) DOI: [10.1016/j.jhep.2014.07.012](#)]
  - 97 **Evon DM**, Stewart PW, Amador J, Serper M, Lok AS, Sterling RK, Sarkar S, Golin CE, Reeve BB, Nelson DR, Reau N, Lim JK, Reddy KR, Di Bisceglie AM, Fried MW. . A comprehensive assessment of patient reported symptom burden, medical comorbidities, and functional well being in patients initiating direct acting antiviral therapy for chronic hepatitis C: Results from a large US multi-center observational study. *PLoS One* 2018; **13**: e0196908 [PMID: [30067745](#) DOI: [10.1371/journal.pone.0196908](#)]
  - 98 **Conry-Cantilena C**, VanRaden M, Gobble J, Melpolder J, Shakil AO, Viladomiu L, Cheung L, DiBisceglie A, Hoofnagle J, Shih JW. Routes of infection, viremia, and liver disease in blood donors found to have hepatitis C virus infection. *N Engl J Med* 1996; **334**: 1691-1696 [PMID: [8637513](#) DOI: [10.1056/NEJM199606273342602](#)]
  - 99 **Haber MM**, West AB, Haber AD, Reuben A. Relationship of aminotransferases to liver histological status in chronic hepatitis C. *Am J Gastroenterol* 1995; **90**: 1250-1257 [PMID: [7639225](#)]
  - 100 **Mosley JW**, Operskalski EA, Tobler LH, Andrews WW, Phelps B, Dockter J, Giachetti C, Busch MP. Viral and host factors in early hepatitis C virus infection. *Hepatology* 2005; **42**: 86-92 [PMID: [15954090](#) DOI: [10.1002/hep.20742](#)]
  - 101 **Seeff LB**. Natural history of hepatitis C. *Hepatology* 1997; **26**: 21S-28S [PMID: [9305659](#) DOI: [10.1002/hep.510260704](#)]
  - 102 **Marcellin P**. Hepatitis C: the clinical spectrum of the disease. *J Hepatol* 1999; **31** Suppl 1: 9-16 [PMID: [10622554](#) DOI: [10.1016/s0168-8278\(99\)80368-7](#)]
  - 103 **Loomba R**, Rivera MM, McBurney R, Park Y, Haynes-Williams V, Rehmann B, Alter HJ, Herrine SK, Liang TJ, Hoofnagle JH, Heller T. The natural history of acute hepatitis C: clinical presentation, laboratory findings and treatment outcomes. *Aliment Pharmacol Ther* 2011; **33**: 559-565 [PMID: [21198704](#) DOI: [10.1111/j.1365-2036.2010.04549.x](#)]
  - 104 **Chu CM**, Yeh CT, Liaw YF. Fulminant hepatic failure in acute hepatitis C: increased risk in chronic carriers of hepatitis B virus. *Gut* 1999; **45**: 613-617 [PMID: [10486374](#) DOI: [10.1136/gut.45.4.613](#)]
  - 105 **Cacoub P**, Renou C, Rosenthal E, Cohen P, Louri I, Loustaud-Ratti V, Yamamoto AM, Camproux AC, Hausfater P, Musset L, Veyssier P, Raguin G, Piette JC. Extrahepatic manifestations associated with hepatitis C virus infection. A prospective multicenter study of 321 patients. The GERMIVIC. Groupe d'Etude et de Recherche en Medecine Interne et Maladies Infectieuses sur le Virus de l'Hépatite C. *Medicine (Baltimore)* 2000; **79**: 47-56 [PMID: [10670409](#) DOI: [10.1097/00005792-200001000-00005](#)]
  - 106 **Grebely J**, Raffa JD, Lai C, Krajden M, Conway B, Tyndall MW. Factors associated with spontaneous clearance of hepatitis C virus among illicit drug users. *Can J Gastroenterol* 2007; **21**: 447-451 [PMID: [17637948](#) DOI: [10.1155/2007/796325](#)]
  - 107 **Thomas DL**, Thio CL, Martin MP, Qi Y, Ge D, O'Huigin C, Kidd J, Kidd K, Khakoo SI, Alexander G, Goedert JJ, Kirk GD, Donfield SM, Rosen HR, Tobler LH, Busch MP, McHutchison JG, Goldstein DB, Carrington M. Genetic variation in IL28B and spontaneous clearance of hepatitis C

- virus. *Nature* 2009; **461**: 798-801 [PMID: [19759533](#) DOI: [10.1038/nature08463](#)]
- 108 **Thein HH**, Yi Q, Dore GJ, Krahn MD. Estimation of stage-specific fibrosis progression rates in chronic hepatitis C virus infection: a meta-analysis and meta-regression. *Hepatology* 2008; **48**: 418-431 [PMID: [18563841](#) DOI: [10.1002/hep.22375](#)]
  - 109 **Tong MJ**, el-Farra NS, Reikes AR, Co RL. Clinical outcomes after transfusion-associated hepatitis C. *N Engl J Med* 1995; **332**: 1463-1466 [PMID: [7739682](#) DOI: [10.1056/NEJM199506013322202](#)]
  - 110 **Poynard T**, Bedossa P, Opolon P. Natural history of liver fibrosis progression in patients with chronic hepatitis C. The OBSVIRC, METAVIR, CLINIVIR, and DOSVIRC groups. *Lancet* 1997; **349**: 825-832 [PMID: [9121257](#) DOI: [10.1016/s0140-6736\(96\)07642-8](#)]
  - 111 **Global Burden of Disease Study 2013 Collaborators**. Global, regional, and national incidence, prevalence, and years lived with disability for 301 acute and chronic diseases and injuries in 188 countries, 1990-2013: a systematic analysis for the Global Burden of Disease Study 2013. *Lancet* 2015; **386**: 743-800 [PMID: [26063472](#) DOI: [10.1016/S0140-6736\(15\)60692-4](#)]
  - 112 **Huang YW**, Yang SS, Fu SC, Wang TC, Hsu CK, Chen DS, Hu JT, Kao JH. Increased risk of cirrhosis and its decompensation in chronic hepatitis C patients with new-onset diabetes: a nationwide cohort study. *Hepatology* 2014; **60**: 807-814 [PMID: [24919583](#) DOI: [10.1002/hep.27212](#)]
  - 113 **Marabita F**, Aghemo A, De Nicola S, Rumi MG, Cheroni C, Scavelli R, Crimi M, Soffredini R, Abrignani S, De Francesco R, Colombo M. Genetic variation in the interleukin-28B gene is not associated with fibrosis progression in patients with chronic hepatitis C and known date of infection. *Hepatology* 2011; **54**: 1127-1134 [PMID: [21721028](#) DOI: [10.1002/hep.24503](#)]
  - 114 **Wiley TE**, Brown J, Chan J. Hepatitis C infection in African Americans: its natural history and histological progression. *Am J Gastroenterol* 2002; **97**: 700-706 [PMID: [11922566](#) DOI: [10.1111/j.1572-0241.2002.05555.x](#)]
  - 115 **Fattovich G**, Giustina G, Degos F, Tremolada F, Diodati G, Almasio P, Nevens F, Solinas A, Mura D, Brouwer JT, Thomas H, Njapoum C, Casarin C, Bonetti P, Fuschi P, Basho J, Tocco A, Bhalla A, Galassini R, Noventa F, Schalm SW, Realdi G. Morbidity and mortality in compensated cirrhosis type C: a retrospective follow-up study of 384 patients. *Gastroenterology* 1997; **112**: 463-472 [PMID: [9024300](#) DOI: [10.1053/gast.1997.v112.pm9024300](#)]
  - 116 **Hu KQ**, Tong MJ. The long-term outcomes of patients with compensated hepatitis C virus-related cirrhosis and history of parenteral exposure in the United States. *Hepatology* 1999; **29**: 1311-1316 [PMID: [10094980](#) DOI: [10.1002/hep.510290424](#)]
  - 117 **Lok AS**, Seeff LB, Morgan TR, di Bisceglie AM, Sterling RK, Curto TM, Everson GT, Lindsay KL, Lee WM, Bonkovsky HL, Dienstag JL, Ghany MG, Morishima C, Goodman ZD; HALT-C Trial Group. Incidence of hepatocellular carcinoma and associated risk factors in hepatitis C-related advanced liver disease. *Gastroenterology* 2009; **136**: 138-148 [PMID: [18848939](#) DOI: [10.1053/j.gastro.2008.09.014](#)]
  - 118 **Tanaka Y**, Kurbanov F, Mano S, Orito E, Vargas V, Esteban JI, Yuen MF, Lai CL, Kramvis A, Kew MC, Smuts HE, Netesov SV, Alter HJ, Mizokami M. Molecular tracing of the global hepatitis C virus epidemic predicts regional patterns of hepatocellular carcinoma mortality. *Gastroenterology* 2006; **130**: 703-714 [PMID: [16530512](#) DOI: [10.1053/j.gastro.2006.01.032](#)]
  - 119 **Alborino F**, Burighel A, Tiller FW, van Helden J, Gabriel C, Raineri A, Catapano R, Stekel H. Multicenter evaluation of a fully automated third-generation anti-HCV antibody screening test with excellent sensitivity and specificity. *Med Microbiol Immunol* 2011; **200**: 77-83 [PMID: [20865278](#) DOI: [10.1007/s00430-010-0171-0](#)]
  - 120 **Cobb B**, Pockros PJ, Vilchez RA, Vierling JM. HCV RNA viral load assessments in the era of direct-acting antivirals. *Am J Gastroenterol* 2013; **108**: 471-475 [PMID: [23552304](#) DOI: [10.1038/ajg.2012.248](#)]
  - 121 **Mederacke I**, Wedemeyer H, Ciesek S, Steinmann E, Raupach R, Wursthorn K, Manns MP, Tillmann HL. Performance and clinical utility of a novel fully automated quantitative HCV-core antigen assay. *J Clin Virol* 2009; **46**: 210-215 [PMID: [19766055](#) DOI: [10.1016/j.jcv.2009.08.014](#)]
  - 122 **Singh S**, Facciorusso A, Loomba R, Falck-Ytter YT. Magnitude and Kinetics of Decrease in Liver Stiffness After Antiviral Therapy in Patients With Chronic Hepatitis C: A Systematic Review and Meta-analysis. *Clin Gastroenterol Hepatol* 2018; **16**: 27-38. e4 [PMID: [28479504](#) DOI: [10.1016/j.cgh.2017.04.038](#)]
  - 123 **Hutchinson S**, Valerio H, Dillon J, Fox R, Innes H, Weir A, Barclay S, McDonald S, Kennedy N, Fraser A, Stanley A, Bramley P, Hayes P, Goldberg D. Reduction in the incidence of hepatitis C related decompensated cirrhosis associated with national scale up of direct-acting antiviral therapies targeting patients with advanced liver fibrosis. *J Hepatol* 2018; **68**: S67 [DOI: [10.1016/S0168-8278\(18\)30355-6](#)]
  - 124 **Backus LI**, Belperio PS, Shahoumian TA, Mole LA. Impact of sustained virologic response with direct-acting antiviral treatment on mortality and hepatocellular carcinoma. *Hepatology* 2017; **66**: 46A
  - 125 **Kim KR**, Osinusi A, Mannalithara A, Aguilar R, Brainard D. Survival benefit of direct acting antiviral therapy in patients with decompensated cirrhosis. *J Hepatol* 2018; **68**: S84
  - 126 **Dusheiko G**, Wedemeyer H. New protease inhibitors and direct-acting antivirals for hepatitis C: interferon's long goodbye. *Gut* 2012; **61**: 1647-1652 [PMID: [22936671](#) DOI: [10.1136/gutjnl-2012-302910](#)]
  - 127 **Thomas E**, Ghany MG, Liang TJ. The application and mechanism of action of ribavirin in therapy

- of hepatitis C. *Antivir Chem Chemother* 2012; **23**: 1-12 [PMID: [22592135](#) DOI: [10.3851/IMP2125](#)]
- 128 **Younossi ZM**, Stepanova M, Ong J, Trimble G, AlQahtani S, Younossi I, Ahmed A, Racila A, Henry L. Nonalcoholic Steatohepatitis Is the Most Rapidly Increasing Indication for Liver Transplantation in the United States. *Clin Gastroenterol Hepatol* 2021; **19**: 580-589. e5 [PMID: [32531342](#) DOI: [10.1016/j.cgh.2020.05.064](#)]
  - 129 **Cholankeril G**, Ahmed A. Alcoholic Liver Disease Replaces Hepatitis C Virus Infection as the Leading Indication for Liver Transplantation in the United States. *Clin Gastroenterol Hepatol* 2018; **16**: 1356-1358 [PMID: [29199144](#) DOI: [10.1016/j.cgh.2017.11.045](#)]
  - 130 **Dickson RC**, Caldwell SH, Ishitani MB, Lau JY, Driscoll CJ, Stevenson WC, McCullough CS, Pruett TL. Clinical and histologic patterns of early graft failure due to recurrent hepatitis C in four patients after liver transplantation. *Transplantation* 1996; **61**: 701-705 [PMID: [8607170](#) DOI: [10.1097/00007890-199603150-00005](#)]
  - 131 **Berenguer M**. Natural history of recurrent hepatitis C. *Liver Transpl* 2002; **8**: S14-S18 [PMID: [12362293](#) DOI: [10.1053/jlts.2002.35781](#)]
  - 132 **Verna EC**, Abdelmessih R, Salomao MA, Lefkowitz J, Moreira RK, Brown RS Jr. Cholestatic hepatitis C following liver transplantation: an outcome-based histological definition, clinical predictors, and prognosis. *Liver Transpl* 2013; **19**: 78-88 [PMID: [23081888](#) DOI: [10.1002/lt.23559](#)]
  - 133 **Forman LM**, Lewis JD, Berlin JA, Feldman HI, Lucey MR. The association between hepatitis C infection and survival after orthotopic liver transplantation. *Gastroenterology* 2002; **122**: 889-896 [PMID: [11910340](#) DOI: [10.1053/gast.2002.32418](#)]
  - 134 **Curry MP**, Forns X, Chung RT, Terrault NA, Brown R Jr, Fenkel JM, Gordon F, O'Leary J, Kuo A, Schiano T, Everson G, Schiff E, Befeler A, Gane E, Saab S, McHutchison JG, Subramanian GM, Symonds WT, Denning J, McNair L, Arterburn S, Svarovskaia E, Moonka D, Afdhal N. Sofosbuvir and ribavirin prevent recurrence of HCV infection after liver transplantation: an open-label study. *Gastroenterology* 2015; **148**: 100-107. e1 [PMID: [25261839](#) DOI: [10.1053/j.gastro.2014.09.023](#)]
  - 135 **Verna EC**. The dynamic landscape of liver transplant in the era of effective hepatitis C virus therapy. *Hepatology* 2017; **65**: 763-766 [PMID: [28093781](#) DOI: [10.1002/hep.29054](#)]
  - 136 **Bowring MG**, Kucirka LM, Massie AB, Luo X, Cameron A, Sulkowski M, Rakestraw K, Gurakar A, Kuo I, Segev DL, Durand CM. Changes in Utilization and Discard of Hepatitis C-Infected Donor Livers in the Recent Era. *Am J Transplant* 2017; **17**: 519-527 [PMID: [27456927](#) DOI: [10.1111/ajt.13976](#)]
  - 137 **Kapila N**, Menon KVN, Al-Khalloufi K, Vanatta JM, Murgas C, Reino D, Ebaid S, Shaw JJ, Agrawal N, Rhazouani S, Navas V, Sheffield C, Rahman AU, Castillo M, Lindenmeyer CC, Miller C, Quintini C, Zervos XB. Hepatitis C Virus NAT-Positive Solid Organ Allografts Transplanted Into Hepatitis C Virus-Negative Recipients: A Real-World Experience. *Hepatology* 2020; **72**: 32-41 [PMID: [31659775](#) DOI: [10.1002/hep.31011](#)]
  - 138 **Cotter TG**, Paul S, Sandıkcı B, Couri T, Bodzin AS, Little EC, Sundaram V, Charlton M. Increasing Utilization and Excellent Initial Outcomes Following Liver Transplant of Hepatitis C Virus (HCV)-Viremic Donors Into HCV-Negative Recipients: Outcomes Following Liver Transplant of HCV-Viremic Donors. *Hepatology* 2019; **69**: 2381-2395 [PMID: [30706517](#) DOI: [10.1002/hep.30540](#)]
  - 139 **Bari K**, Luckett K, Kaiser T, Diwan T, Cuffy M, Schoech MR, Safdar K, Blackard JT, Apewokin S, Paterno F, Sherman KE, Zucker SD, Anwar N, Shah SA. Hepatitis C transmission from seropositive, nonviremic donors to non-hepatitis C liver transplant recipients. *Hepatology* 2018; **67**: 1673-1682 [PMID: [29205441](#) DOI: [10.1002/hep.29704](#)]
  - 140 **Kwong AJ**, Wall A, Melcher M, Wang U, Ahmed A, Subramanian A, Kwo PY. Liver transplantation for hepatitis C virus (HCV) non-viremic recipients with HCV viremic donors. *Am J Transplant* 2019; **19**: 1380-1387 [PMID: [30378723](#) DOI: [10.1111/ajt.15162](#)]
  - 141 **Bethea E**, Arvind A, Gustafson J, Andersson K, Pratt D, Bhan I, Thiim M, Corey K, Bloom P, Markmann J, Yeh H, Elias N, Kimura S, Dageforde LA, Cuenca A, Kawai T, Safa K, Williams W, Gilligan H, Sise M, Fishman J, Kotton C, Kim A, Rogers CC, Shao S, Cote M, Irwin L, Myoung P, Chung RT. Immediate administration of antiviral therapy after transplantation of hepatitis C-infected livers into uninfected recipients: Implications for therapeutic planning. *Am J Transplant* 2020; **20**: 1619-1628 [PMID: [31887236](#) DOI: [10.1111/ajt.15768](#)]
  - 142 **Woolley AE**, Singh SK, Goldberg HJ, Mallidi HR, Givertz MM, Mehra MR, Coppolino A, Kusztos AE, Johnson ME, Chen K, Haddad EA, Fanikos J, Harrington DP, Camp PC, Baden LR; DONATE HCV Trial Team. Heart and Lung Transplants from HCV-Infected Donors to Uninfected Recipients. *N Engl J Med* 2019; **380**: 1606-1617 [PMID: [30946553](#) DOI: [10.1056/NEJMoa1812406](#)]
  - 143 **Feld JJ**, Cypel M, Kumar D, Dahari H, Pinto Ribeiro RV, Marks N, Kamkar N, Bahinskaya I, Onofrio FQ, Zahoor MA, Cerrochi O, Tinckam K, Kim SJ, Schiff J, Reichman TW, McDonald M, Alba C, Waddell TK, Sapisochin G, Selzner M, Keshavjee S, Janssen HLA, Hansen BE, Singer LG, Humar A. Short-course, direct-acting antivirals and ezetimibe to prevent HCV infection in recipients of organs from HCV-infected donors: a phase 3, single-centre, open-label study. *Lancet Gastroenterol Hepatol* 2020; **5**: 649-657 [PMID: [32389183](#) DOI: [10.1016/S2468-1253\(20\)30081-9](#)]
  - 144 **Kapila N**, Al-Khalloufi K, Bejarano PA, Vanatta JM, Zervos XB. Fibrosing cholestatic hepatitis after kidney transplantation from HCV-viremic donors to HCV-negative recipients: A unique complication in the DAA era. *Am J Transplant* 2020; **20**: 600-605 [PMID: [31448549](#) DOI: [10.1111/ajt.15583](#)]
  - 145 **Weinfurter K**, Reddy KR. Hepatitis C viraemic organs in solid organ transplantation. *J Hepatol*

- 2021; **74**: 716-733 [PMID: [33212088](#) DOI: [10.1016/j.jhep.2020.11.014](#)]
- 146 **Khapra AP**, Agarwal K, Fiel MI, Kontorinis N, Hossain S, Emre S, Schiano TD. Impact of donor age on survival and fibrosis progression in patients with hepatitis C undergoing liver transplantation using HCV+ allografts. *Liver Transpl* 2006; **12**: 1496-1503 [PMID: [16964597](#) DOI: [10.1002/Lt.20849](#)]
  - 147 **Potluri VS**, Goldberg DS, Mohan S, Bloom RD, Sawinski D, Abt PL, Blumberg EA, Parikh CR, Sharpe J, Reddy KR, Molnar MZ, Sise M, Reese PP. National Trends in Utilization and 1-Year Outcomes with Transplantation of HCV-Viremic Kidneys. *J Am Soc Nephrol* 2019; **30**: 1939-1951 [PMID: [31515244](#) DOI: [10.1681/ASN.2019050462](#)]
  - 148 **Swadling L**, Capone S, Antrobus RD, Brown A, Richardson R, Newell EW, Halliday J, Kelly C, Bowen D, Fergusson J, Kurioka A, Ammendola V, Del Sorbo M, Grazioli F, Esposito ML, Siani L, Traboni C, Hill A, Colloca S, Davis M, Nicosia A, Cortese R, Folgori A, Klennerman P, Barnes E. A human vaccine strategy based on chimpanzee adenoviral and MVA vectors that primes, boosts, and sustains functional HCV-specific T cell memory. *Sci Transl Med* 2014; **6**: 261ra153 [PMID: [25378645](#) DOI: [10.1126/scitranslmed.3009185](#)]
  - 149 **Masavuli MG**, Wijesundara DK, Underwood A, Christiansen D, Earnest-Silveira L, Bull R, Torresi J, Gowans EJ, Grubor-Bauk B. A Hepatitis C Virus DNA Vaccine Encoding a Secreted, Oligomerized Form of Envelope Proteins Is Highly Immunogenic and Elicits Neutralizing Antibodies in Vaccinated Mice. *Front Immunol* 2019; **10**: 1145 [PMID: [31178869](#) DOI: [10.3389/fimmu.2019.01145](#)]
  - 150 **Doshi RK**, Ruben M, Drezner K, Lachmann A, Kuo I, Chanes-Mora P, Varga L, Saafir-Callaway B, Visconti A, Kharfen M. Knowledge, Attitudes, and Behaviors Related to Hepatitis C Screening and Treatment among Health Care Providers in Washington, DC. *J Community Health* 2020; **45**: 785-794 [PMID: [32125591](#) DOI: [10.1007/s10900-020-00794-z](#)]
  - 151 **Farci P**. Delta hepatitis: an update. *J Hepatol* 2003; **39** Suppl 1: S212-S219 [PMID: [14708706](#) DOI: [10.1016/s0168-8278\(03\)00331-3](#)]
  - 152 **Kucirka LM**, Farzadegan H, Feld JJ, Mehta SH, Winters M, Glenn JS, Kirk GD, Segev DL, Nelson KE, Marks M, Heller T, Golub ET. Prevalence, correlates, and viral dynamics of hepatitis delta among injection drug users. *J Infect Dis* 2010; **202**: 845-852 [PMID: [20701536](#) DOI: [10.1086/655808](#)]
  - 153 **Rizzetto M**, Canese MG, Aricò S, Crivelli O, Trepo C, Bonino F, Verme G. Immunofluorescence detection of new antigen-antibody system (delta/anti-delta) associated to hepatitis B virus in liver and in serum of HBsAg carriers. *Gut* 1977; **18**: 997-1003 [PMID: [75123](#) DOI: [10.1136/gut.18.12.997](#)]
  - 154 **Rizzetto M**, Smedile A. Pegylated interferon therapy of chronic hepatitis D: in need of revision. *Hepatology* 2015; **61**: 1109-1111 [PMID: [25348580](#) DOI: [10.1002/hep.27585](#)]
  - 155 **Ponzetto A**, Hoyer BH, Popper H, Engle R, Purcell RH, Gerin JL. Titration of the infectivity of hepatitis D virus in chimpanzees. *J Infect Dis* 1987; **155**: 72-78 [PMID: [3794405](#) DOI: [10.1093/infdis/155.1.72](#)]
  - 156 **Govindarajan S**, De Cock KM, Redeker AG. Natural course of delta superinfection in chronic hepatitis B virus-infected patients: histopathologic study with multiple liver biopsies. *Hepatology* 1986; **6**: 640-644 [PMID: [3525368](#) DOI: [10.1002/hep.1840060415](#)]
  - 157 **Smedile A**, Farci P, Verme G, Caredda F, Cargnel A, Caporaso N, Dentico P, Trepo C, Opolon P, Gimson A, Vergani D, Williams R, Rizzetto M. Influence of delta infection on severity of hepatitis B. *Lancet* 1982; **2**: 945-947 [PMID: [6127458](#) DOI: [10.1016/s0140-6736\(82\)90156-8](#)]
  - 158 **Smedile A**, Dentico P, Zanetti A, Sagnelli E, Nordenfelt E, Actis GC, Rizzetto M. Infection with the delta agent in chronic HBsAg carriers. *Gastroenterology* 1981; **81**: 992-997 [PMID: [7286594](#)]
  - 159 **Su CW**, Huang YH, Huo TI, Shih HH, Sheen IJ, Chen SW, Lee PC, Lee SD, Wu JC. Genotypes and viremia of hepatitis B and D viruses are associated with outcomes of chronic hepatitis D patients. *Gastroenterology* 2006; **130**: 1625-1635 [PMID: [16697726](#) DOI: [10.1053/j.gastro.2006.01.035](#)]
  - 160 **Bockmann JH**, Grube M, Hamed V, von Felden J, Landahl J, Wehmeyer M, Giersch K, Hall MT, Murray JM, Dandri M, Lütth S, Lohse AW, Lütgehetmann M, Schulze Zur Wiesch J. High rates of cirrhosis and severe clinical events in patients with HBV/HDV co-infection: longitudinal analysis of a German cohort. *BMC Gastroenterol* 2020; **20**: 24 [PMID: [32000689](#) DOI: [10.1186/s12876-020-1168-9](#)]
  - 161 **Cole SM**, Gowans EJ, Macnaughton TB, Hall PD, Burrell CJ. Direct evidence for cytotoxicity associated with expression of hepatitis delta virus antigen. *Hepatology* 1991; **13**: 845-851 [PMID: [1709411](#)]
  - 162 **Guilhot S**, Huang SN, Xia YP, La Monica N, Lai MM, Chisari FV. Expression of the hepatitis delta virus large and small antigens in transgenic mice. *J Virol* 1994; **68**: 1052-1058 [PMID: [8289334](#) DOI: [10.1128/JVI.68.2.1052-1058.1994](#)]
  - 163 **Rizzetto M**, Rosina F, Saracco G, Bellando PC, Actis GC, Bonino F, Smedile A, Trinchero P, Sansalvadore F, Pintus C. Treatment of chronic delta hepatitis with alpha-2 recombinant interferon. *J Hepatol* 1986; **3** Suppl 2: S229-S233 [PMID: [3298410](#) DOI: [10.1016/s0168-8278\(86\)80125-8](#)]
  - 164 **Wedemeyer H**, Yurdaydin C, Dalekos GN, Erhardt A, Çakaloğlu Y, Değertekin H, Gürel S, Zeuzem S, Zachou K, Bozkaya H, Koch A, Bock T, Dienes HP, Manns MP; HIDIT Study Group. Peginterferon plus adefovir vs either drug alone for hepatitis delta. *N Engl J Med* 2011; **364**: 322-331 [PMID: [21268724](#) DOI: [10.1056/NEJMoa0912696](#)]
  - 165 **Abbas Z**, Khan MA, Salih M, Jafri W. Interferon alpha for chronic hepatitis D. *Cochrane Database*



- Syst Rev* 2011; CD006002 [PMID: 22161394 DOI: 10.1002/14651858.CD006002.pub2]
- 166 **Yurdaydin C**, Keskin O, Kalkan Ç, Karakaya F, Çalışkan A, Karataylı E, Karataylı S, Bozdayı AM, Koh C, Heller T, Idilman R, Glenn JS. Optimizing lonaferib treatment for the management of chronic delta hepatitis: The LOWR HDV-1 study. *Hepatology* 2018; **67**: 1224-1236 [PMID: 29152762 DOI: 10.1002/hep.29658]
  - 167 **Karayiannis P**, Saldanha J, Jackson AM, Luther S, Goldin R, Monjardino J, Thomas HC. Partial control of hepatitis delta virus superinfection by immunisation of woodchucks (*Marmota monax*) with hepatitis delta antigen expressed by a recombinant vaccinia or baculovirus. *J Med Virol* 1993; **41**: 210-214 [PMID: 8263503 DOI: 10.1002/jmv.1890410308]
  - 168 **Ponzetto A**, Eckart M, D'Urso N, Negro F, Silvestro M, Bonino F, Wang KS, Chien D, Choo QL, Houghton M. Towards a vaccine for the prevention of hepatitis delta virus superinfection in HBV carriers. *Prog Clin Biol Res* 1993; **382**: 207-210 [PMID: 8502681]
  - 169 **Serin A**, Tokat Y. Recurrence of Hepatitis D Virus in Liver Transplant Recipients With Hepatitis B and D Virus-Related Chronic Liver Disease. *Transplant Proc* 2019; **51**: 2457-2460 [PMID: 31405744 DOI: 10.1016/j.transproceed.2019.01.163]
  - 170 **Kuniholm MH**, Purcell RH, McQuillan GM, Engle RE, Wasley A, Nelson KE. Epidemiology of hepatitis E virus in the United States: results from the Third National Health and Nutrition Examination Survey, 1988-1994. *J Infect Dis* 2009; **200**: 48-56 [PMID: 19473098 DOI: 10.1086/599319]
  - 171 **Cangin C**, Focht B, Harris R, Strunk JA. Hepatitis E seroprevalence in the United States: Results for immunoglobulins IGG and IGM. *J Med Virol* 2019; **91**: 124-131 [PMID: 30168589 DOI: 10.1002/jmv.25299]
  - 172 **Gupta DN**, Smetana HF. The histopathology of viral hepatitis as seen in the Delhi epidemic (1955-56). *Indian J Med Res* 1957; **45**: 101-113 [PMID: 13438544]
  - 173 **Xia J**, Zeng H, Liu L, Zhang Y, Liu P, Geng J, Wang L, Zhuang H. Swine and rabbits are the main reservoirs of hepatitis E virus in China: detection of HEV RNA in feces of farmed and wild animals. *Arch Virol* 2015; **160**: 2791-2798 [PMID: 26303139 DOI: 10.1007/s00705-015-2574-0]
  - 174 **Andonov A**, Robbins M, Borlang J, Cao J, Hatchette T, Stueck A, Deschambault Y, Murnaghan K, Varga J, Johnston L. Rat Hepatitis E Virus Linked to Severe Acute Hepatitis in an Immunocompetent Patient. *J Infect Dis* 2019; **220**: 951-955 [PMID: 30649379 DOI: 10.1093/infdis/jiz025]
  - 175 **World Health Organization**. Hepatitis E. [cited 19 January 2021]. In: World Health Organization [Internet]. Available from: <https://www.who.int/news-room/fact-sheets/detail/hepatitis-e#:~:text=Symptoms,%20after%20onset%20of%20the%20disease>
  - 176 **Perumpail RB**, Ahmed A, Higgins JP, So SK, Cochran JL, Drobeniuc J, Mixson-Hayden TR, Teo CG. Fatal Accelerated Cirrhosis after Imported HEV Genotype 4 Infection. *Emerg Infect Dis* 2015; **21**: 1679-1681 [PMID: 26291424 DOI: 10.3201/eid2109.150300]
  - 177 **Behrendt P**, Steinmann E, Manns MP, Wedemeyer H. The impact of hepatitis E in the liver transplant setting. *J Hepatol* 2014; **61**: 1418-1429 [PMID: 25195557 DOI: 10.1016/j.jhep.2014.08.047]
  - 178 **Aggarwal R**. Hepatitis E: clinical presentation in disease-endemic areas and diagnosis. *Semin Liver Dis* 2013; **33**: 30-40 [PMID: 23564387 DOI: 10.1055/s-0033-1338112]
  - 179 **Zhu FC**, Zhang J, Zhang XF, Zhou C, Wang ZZ, Huang SJ, Wang H, Yang CL, Jiang HM, Cai JP, Wang YJ, Ai X, Hu YM, Tang Q, Yao X, Yan Q, Xian YL, Wu T, Li YM, Miao J, Ng MH, Shih JW, Xia NS. Efficacy and safety of a recombinant hepatitis E vaccine in healthy adults: a large-scale, randomised, double-blind placebo-controlled, phase 3 trial. *Lancet* 2010; **376**: 895-902 [PMID: 20728932 DOI: 10.1016/S0140-6736(10)61030-6]
  - 180 **Wedemeyer H**, Pischke S, Manns MP. Pathogenesis and treatment of hepatitis e virus infection. *Gastroenterology* 2012; **142**: 1388-1397. e1 [PMID: 22537448 DOI: 10.1053/j.gastro.2012.02.014]
  - 181 **Dalton HR**, Kamar N. Treatment of hepatitis E virus. *Curr Opin Infect Dis* 2016; **29**: 639-644 [PMID: 27607911 DOI: 10.1097/QCO.0000000000000316]
  - 182 **Kamar N**, Garrouste C, Haagsma EB, Garrigue V, Pischke S, Chauvet C, Dumortier J, Cannesson A, Cassuto-Viguier E, Thervet E, Conti F, Lebray P, Dalton HR, Santella R, Kanaan N, Essig M, Mousson C, Radenne S, Roque-Afonso AM, Izopet J, Rostaing L. Factors associated with chronic hepatitis in patients with hepatitis E virus infection who have received solid organ transplants. *Gastroenterology* 2011; **140**: 1481-1489 [PMID: 21354150 DOI: 10.1053/j.gastro.2011.02.050]
  - 183 **Bhatia V**, Singhal A, Panda SK, Acharya SK. A 20-year single-center experience with acute liver failure during pregnancy: is the prognosis really worse? *Hepatology* 2008; **48**: 1577-1585 [PMID: 18925633 DOI: 10.1002/hep.22493]
  - 184 **Zhang J**, Zhang XF, Huang SJ, Wu T, Hu YM, Wang ZZ, Wang H, Jiang HM, Wang YJ, Yan Q, Guo M, Liu XH, Li JX, Yang CL, Tang Q, Jiang RJ, Pan HR, Li YM, Shih JW, Ng MH, Zhu FC, Xia NS. Long-term efficacy of a hepatitis E vaccine. *N Engl J Med* 2015; **372**: 914-922 [PMID: 25738667 DOI: 10.1056/NEJMoal406011]
  - 185 **Tsarev SA**, Tsareva TS, Emerson SU, Govindarajan S, Shapiro M, Gerin JL, Purcell RH. Successful passive and active immunization of cynomolgus monkeys against hepatitis E. *Proc Natl Acad Sci USA* 1994; **91**: 10198-10202 [PMID: 7937861 DOI: 10.1073/pnas.91.21.10198]
  - 186 **Kamar N**, Rostaing L, Abravanel F, Garrouste C, Esposito L, Cardeau-Desangles I, Mansuy JM, Selves J, Peron JM, Otal P, Muscari F, Izopet J. Pegylated interferon-alpha for treating chronic hepatitis E virus infection after liver transplantation. *Clin Infect Dis* 2010; **50**: e30-e33 [PMID:

20113176 DOI: [10.1086/650488](https://doi.org/10.1086/650488)]

- 187 **Dao Thi VL**, Debing Y, Wu X, Rice CM, Neyts J, Moradpour D, Gouttenoire J. Sofosbuvir Inhibits Hepatitis E Virus Replication In Vitro and Results in an Additive Effect When Combined With Ribavirin. *Gastroenterology* 2016; **150**: 82-85. e4 [PMID: [26408347](https://pubmed.ncbi.nlm.nih.gov/26408347/) DOI: [10.1053/j.gastro.2015.09.011](https://doi.org/10.1053/j.gastro.2015.09.011)]
- 188 **Khuroo MS**, Kamili S. Aetiology and prognostic factors in acute liver failure in India. *J Viral Hepat* 2003; **10**: 224-231 [PMID: [12753342](https://pubmed.ncbi.nlm.nih.gov/12753342/) DOI: [10.1046/j.1365-2893.2003.00415.x](https://doi.org/10.1046/j.1365-2893.2003.00415.x)]
- 189 **Fontana RJ**, Engle RE, Scaglione S, Araya V, Shaikh O, Tillman H, Attar N, Purcell RH, Lee WM; US Acute Liver Failure Study Group. The role of hepatitis E virus infection in adult Americans with acute liver failure. *Hepatology* 2016; **64**: 1870-1880 [PMID: [27215797](https://pubmed.ncbi.nlm.nih.gov/27215797/) DOI: [10.1002/hep.28649](https://doi.org/10.1002/hep.28649)]





## Paediatric gastrointestinal disorders in SARS-CoV-2 infection: Epidemiological and clinical implications

Mohammed Al-Beltagi, Nermin Kamal Saeed, Adel Salah Bediwy, Yasser El-Sawaf

**ORCID number:** Mohammed Al-Beltagi 0000-0002-7761-9536; Nermin Kamal Saeed 0000-0001-7875-8207; Adel Salah Bediwy 0000-0002-0281-0010; Yasser El-Sawaf 0000-0001-8083-3042.

**Author contributions:** Al-Beltagi M, Saeed NK, Bediwy AS, and El-Sawaf Y collected the data and wrote and revised the manuscript.

**Conflict-of-interest statement:** The authors declare no conflicts of interest for this article.

**Open-Access:** This article is an open-access article that was selected by an in-house editor and fully peer-reviewed by external reviewers. It is distributed in accordance with the Creative Commons Attribution NonCommercial (CC BY-NC 4.0) license, which permits others to distribute, remix, adapt, build upon this work non-commercially, and license their derivative works on different terms, provided the original work is properly cited and the use is non-commercial. See: <http://creativecommons.org/licenses/by-nc/4.0/>

**Manuscript source:** Invited manuscript

**Specialty type:** Gastroenterology and hepatology

**Mohammed Al-Beltagi**, Department of Pediatric, Faculty of Medicine, Tanta University, Tanta 31527, Algharbia, Egypt

**Mohammed Al-Beltagi**, Department of Pediatrics, University Medical Center, Arabian Gulf University, Manama 26671, Bahrain

**Nermin Kamal Saeed**, Microbiology Section, Pathology Department, Salmaniya Medical Complex, Manama 12, Bahrain

**Nermin Kamal Saeed**, Department of Microbiology, Royal College of Surgeons in Ireland - Bahrain, Bahrain, Busaiteen 15503, Muharraq, Bahrain

**Adel Salah Bediwy**, Department of Chest Diseases, Tanta University, Tanta 31527, Algharbia, Egypt

**Adel Salah Bediwy**, Department of Pulmonology, University Medical Center, Arabian Gulf University, Manama 26671, Bahrain

**Yasser El-Sawaf**, Department of Tropical Medicine, Tanta University, Tanta 31527, Algharbia, Egypt

**Yasser El-Sawaf**, Department of Gastroenterology, University Medical Center, Arabian Gulf University, Manama 26671, Bahrain

**Corresponding author:** Mohammed Al-Beltagi, MD, PhD, Professor, Department of Pediatric, Faculty of Medicine, Tanta University, Medical Complex, El Bahr St. Tanta Qism 2, Tanta 31527, Algharbia, Egypt. [mbelrem@hotmail.com](mailto:mbelrem@hotmail.com)

### Abstract

The coronavirus disease 2019 (COVID-19) pandemic is a threat worldwide for individuals of all ages, including children. Gastrointestinal manifestations could be the initial presenting manifestation in many patients, especially in children. These symptoms are more common in patients with severe disease than in patients with non-severe disease. Approximately 48.1% of patients had a stool sample that was positive for severe acute respiratory syndrome coronavirus 2 (SARS-CoV-2) viral RNA. Children typically form 1%-8% of all laboratory-confirmed cases of SARS-CoV-2. Gastrointestinal manifestations of COVID-19 in children are not rare, with a prevalence between 0 and 88%, and a wide variety of presentations, including diarrhoea, vomiting, and abdominal pain, can develop before, with or after the development of respiratory symptoms. Atypical

**Country/Territory of origin:** Egypt**Peer-review report's scientific quality classification**

Grade A (Excellent): A

Grade B (Very good): 0

Grade C (Good): 0

Grade D (Fair): 0

Grade E (Poor): 0

**Received:** December 16, 2020**Peer-review started:** December 16, 2020**First decision:** March 7, 2021**Revised:** March 12, 2021**Accepted:** April 5, 2021**Article in press:** April 5, 2021**Published online:** April 28, 2021**P-Reviewer:** Lambrecht NW**S-Editor:** Fan JR**L-Editor:** A**P-Editor:** Liu JH

manifestations such as appendicitis or liver injury could also appear, especially in the presence of multisystem inflammatory disease. In this review, we discussed the epidemiology of COVID-19 gastrointestinal diseases in children as well as their implications on the diagnosis, misdiagnosis, prognosis, and faecal-oral transmission route of COVID-19 and the impact of gastrointestinal diseases on the gut microbiome, child nutrition, and disease management.

**Key Words:** COVID-19; SARS-CoV-2; Gastrointestinal diseases; Children; Dysbiosis; Faecal-oral transmission

©The Author(s) 2021. Published by Baishideng Publishing Group Inc. All rights reserved.

**Core Tip:** Coronavirus disease 2019 (COVID-19) presents with different manifestations, including gastrointestinal inflammation, especially in children. Gastrointestinal effects of COVID-19 have a significant impact on the diagnosis, misdiagnosis, prognosis, faecal-oral transmission route, gut microbiota, and child nutrition. The presence of gastrointestinal symptoms in children with COVID-19 should not be ignored.

**Citation:** Al-Beltagi M, Saeed NK, Bediwy AS, El-Sawaf Y. Paediatric gastrointestinal disorders in SARS-CoV-2 infection: Epidemiological and clinical implications. *World J Gastroenterol* 2021; 27(16): 1716-1727

**URL:** <https://www.wjgnet.com/1007-9327/full/v27/i16/1716.htm>

**DOI:** <https://dx.doi.org/10.3748/wjg.v27.i16.1716>

## INTRODUCTION

The rise of coronavirus disease 2019 (COVID-19) at the end of 2019 became a real and significant challenge to humanity, especially as the outbreak escalated to a global pandemic in March 2020. The challenge was related not only to the rapid transmission of COVID-19 but also to the dilemma and conflict in the clinical presentations, rate of mutation, laboratory diagnosis, and management of the disease. COVID-19 is caused by severe acute respiratory syndrome coronavirus 2 (SARS-CoV-2), a virus that is related to a large group of enveloped, positive-stranded RNA viruses called coronaviruses because of the crown-like spikes on their surface. There are four subgroups (genera) of coronaviruses, named alpha, beta, gamma, and delta; the alpha and beta subgroups can cause disease in humans, causing respiratory infections, gastrointestinal infections, and hepatic and central nervous system diseases<sup>[1]</sup>. The most recent outbreaks of coronavirus belong to beta coronaviruses and include the SARS-CoV outbreak, the Middle East respiratory syndrome coronavirus outbreak, and the recent SARS-CoV-2 pandemic. In humans, coronaviruses primarily affect the upper respiratory tract, causing different manifestations of respiratory infections. However, gastrointestinal manifestations could be the initial presenting manifestation in many patients, especially in children. These manifestations could also be the sole manifestations in a small percentage of patients. This article will review the different gastrointestinal disorders in association with SARS-CoV-2 infection (COVID-19) and discuss their epidemiological and clinical implications<sup>[2]</sup>.

## EPIDEMIOLOGY OF COVID-19 AND GASTROINTESTINAL DISORDERS IN CHILDREN

Although it predominantly affects adults of higher age groups, SARS-CoV-2 can infect children at any age, even during the neonatal period; intrauterine or perinatal transmission of the virus is uncertain, and vertical transmission is not yet proven<sup>[3]</sup>. Children typically form 1%-8% of all laboratory-confirmed cases of COVID-19: 7% in neonates, 29% in infants less than 1 year old, 10% in the 2<sup>nd</sup> year of life, 11% between 2 and 5 years old, 16% between 5 and 10 years old, and 34% between 10 and 18 years of

age<sup>[4]</sup>. However, the percentage of the disease in children may differ from one country to another and from one ethnic group to another according to the underlying health, social, and economic status of individuals<sup>[5]</sup>. As the number of children infected is currently increasing, studies have shown that most infected children have mild disease. However, approximately 4.4% of infected children have severe disease, with a mortality rate of 0.2%, with no deaths reported below the age of 9 years. Infants less than 1 year old and children who have other underlying comorbidities are more prone to severe COVID-19. There was no sex difference in the infected children, unlike that observed in adults with a male to female ratio of 1.1:1. The source of infection was usually an infected family member as a part of a family cluster outbreak<sup>[6]</sup>.

The low prevalence of COVID-19 in children is multifactorial. Children have few outdoor activities, especially with school shutdowns, lower travelling rates than adults, and less exposure to smoking and air pollution; hence, children are less likely to be exposed to infection. Their immune status plays an important role in modifying their risk of infection with SARS-CoV-2. Children have a more active innate immune response and a healthier respiratory system than adults, especially children less than 10 years of age. They also respond with a normal or high lymphocytic count in response to infection with SARS-CoV-2, in contrast to adults, who respond with a decreased lymphocytic count. Coinfection with other viruses may limit the replication of SARS-CoV-2 *via* direct virus-to-virus interactions and competitive inhibition and may be a possible mechanism like what is observed with the common cold and influenza. However, the main factor for the low incidence of COVID-19 in children is related to the age-dependent immaturity of angiotensin-converting enzyme 2 (ACE2) receptors in children and their different distribution and function compared to adults. These receptors serve as a binding site for SARS-CoV-2 and a portal of entry to the inside of the cell by the binding of the viral spike proteins to ACE2 receptors. The degree of cell susceptibility to viral infection is correlated with the number of ACE2 receptors on those cells. However, ACE2 has dual effects on cell infection by the virus. In addition to ACE2 receptors acting as a binding site for the virus, they have a very important pulmonary protective role, as they protect against severe lung injury caused by the virus. Therefore, this dual role of ACE2 pushes us to perform more research to confirm its implication in COVID-19 pathogenesis<sup>[7-10]</sup>. The low number of children infected with SARS-CoV-2 does not necessarily mean a high resistance to the infection. Another possible theoretical reason is related to Bacillus Calmette-Guérin (BCG) vaccination in children. BCG may provide some protection against COVID-19 as it modulates cell-mediated immunity, including innate cells such as macrophages, monocytes, and epithelia, and many children are vaccinated with BCG<sup>[11]</sup>. However, the protective effects of BCG against COVID-19 are still unknown. As more than 95% of children infected with SARS-CoV-2 are asymptomatic and less likely to be tested, epidemiological surveillance may be inadequate, and children may still contribute to viral transmission.

Although fever and respiratory manifestations are the most common features of COVID-19, approximately 17.6% of patients present with gastrointestinal symptoms that usually appear 1-2 d before respiratory symptoms. Verified cases of COVID-19 with the sole gastrointestinal manifestation have been described in both adults and children. Gastrointestinal manifestations were more common in patients with severe disease (17.1%) than in patients with non-severe disease (11.8%). Approximately 48.1% of the patients had stool that was positive for viral RNA, even in stool samples collected after the respiratory samples turned negative for the virus. The exact rate of gastrointestinal symptoms is a matter of debate, with various incidences among the different studies. Anorexia and poor appetite were the most common gastrointestinal symptoms (a range between 34.7% and 67% and a mean of 47%), followed by diarrhoea (range between 2.1% and 32.5% and a mean of 11.6%), abdominal pain and discomfort (range between 1% and 11.9% and a mean of 5.2%), and nausea and vomiting (range between 1% and 11.7%, and a mean of 5.1%), while the incidence of liver damage ranged from 15% to 53%<sup>[12-18]</sup>. Liver damage is doubled in the presence of gastrointestinal manifestations compared to in the absence of gastrointestinal manifestations. Gastrointestinal manifestations usually deteriorate with disease progression, and severe gastrointestinal bleeding has been reported in some cases<sup>[19]</sup>.

Gastrointestinal manifestations of COVID-19 in children are not rare, with a prevalence between 0 and 88%, and a wide variety of presentations, including diarrhoea, vomiting, and abdominal pain, that can develop before, with or after the development of respiratory symptoms. Atypical manifestations such as acute appendicitis or liver injury could also appear, especially in the presence of multisystem inflammatory disease<sup>[20]</sup>. An American study including 44 children showed that gastrointestinal manifestations were present in 84.1% of children

admitted to the hospital and were most often associated with fever and rash<sup>[21]</sup>. In a meta-analysis including 280 children from 9 studies, the pooled prevalence of gastrointestinal manifestations was 22.8%. Diarrhoea was the most common presentation (12.4%), followed by vomiting (10.3%) and abdominal pain (5.4%)<sup>[22]</sup>. In a prospective study including 992 healthy children of healthcare workers in the United Kingdom, approximately 7% tested positive for SARS-CoV-2 antibodies, half of them were asymptomatic, and 19% had gastrointestinal symptoms, including diarrhoea, vomiting, and abdominal cramps<sup>[23]</sup>. Another study in Wuhan, China showed that gastrointestinal manifestations were observed in 15.2% of children infected with SARS-CoV-2 (diarrhoea 8.8% and vomiting 6.4%). In contrast to adults, gastrointestinal manifestations in children were associated with less severe disease and less need for oxygen therapy<sup>[24]</sup>.

### **Pathogenesis of gastrointestinal infection in COVID-19**

The exact mechanism of gastrointestinal symptoms caused by SARS-CoV-2 infection is still unclear. The detection of SARS-CoV-2 RNA in the stool suggests faecal-oral transmission. The presence of gastrointestinal manifestations before respiratory symptoms in a group of patients, along with the presence of viral shedding from the gastrointestinal tract in cases with a more aggressive clinical course, may indicate the role of the gastrointestinal tract in modifying the course of COVID-19 and help in predicting prognosis<sup>[25]</sup>. Several studies suggest that the virus actively infects the cells of the gastrointestinal tract, replicating itself in the epithelium of the small and large intestine and producing an excessive immunological reaction in the host<sup>[26]</sup>. ACE2 is highly expressed in lung alveolar type II cells and the upper oesophagus, in absorptive enterocytes from the ileum and colon, and in hepatocytes and cholangiocytes. The ACE2 receptor is an important receptor on the cell membrane of host cells. The interaction between the S protein of SARS-CoV-2 and ACE2 promotes the invasion of host cells by SARS-CoV-2. Abundant expression of ACE2 throughout the endothelial surface of the gastrointestinal tract, especially in enterocytes, may act as a secondary entry site for SARS-CoV-2 infection. The magnitude of ACE2 expression in the gut may ameliorate or worsen gut dysbiosis and gastrointestinal leakage<sup>[27]</sup>. Dysbiosis and the consequent leaky gut further impair the gut-lung axis and are related to the onset of pulmonary hypertension as well as the hyperactivation of the ACE/Ang II/AT1R (angiotensin II type 1 receptor) axis from ACE2 Loss. At the same time, infection with SARS-CoV-2 causes infiltration with many plasma cells and lymphocytes and potentially induces interstitial oedema and the degeneration of the gut-blood barrier, leading to the spread of viruses, bacteria, endotoxins, and microbial metabolites into the systemic circulation, affecting the host's response to SARS-CoV-2 infection and inducing multisystem dysfunction and septic shock<sup>[28]</sup>. Persistent viral faecal shedding alters the gut into a base for sustained viral replication and consequently may explain the associated poor prognosis. On the other side of the gut-lung axis, SARS-CoV-2-infection-induced respiratory lesions impair the respiratory tract microbiota, which adversely compromises the digestive tract through immune dysregulation<sup>[29]</sup>.

Failure to detect viral RNA in the stool in some patients infected with SARS-CoV-2 that have gastrointestinal manifestations suggests the presence of other mechanisms of indirect gastrointestinal injury in COVID-19 patients. Disturbed cellular immunity has a significant impact on gastrointestinal health in patients with COVID-19. Lung-derived C-C chemokine receptor type 9-CD4<sup>+</sup> T cells were significantly increased in patients infected with SARS-CoV-2 compared to healthy individuals. These cells are important for mucosal immunity and have a significant role in the development of chronic enteritis by intestinal immune damage and the disruption of the intestinal flora<sup>[30]</sup>. The resulting dysbiosis will further promote the polarization of Th17 cells in the small intestine, and the production of excessive interleukin (IL)-17A leads to the recruitment of neutrophils, causing more intestinal immune damage, and inducing diarrhoea and other gastrointestinal symptoms<sup>[31]</sup>. The induced intestinal inflammation impairs the intestinal mucosal barrier, allowing easy access of the bacteria and its toxin to circulate in the blood and affect other organs, including the liver (gut-liver axis). Intestinal inflammation-induced host and microbial metabolites can reach the liver through the portal vein, impairing liver function<sup>[32]</sup>. Consequently, the inflamed liver releases bile acids and other bioactive materials into the biliary and systemic circulation, reaching the intestines and causing more intestinal lesions (bidirectional effect). The liver could also be affected by the adverse effects of various drugs used to treat COVID-19 (Figure 1).



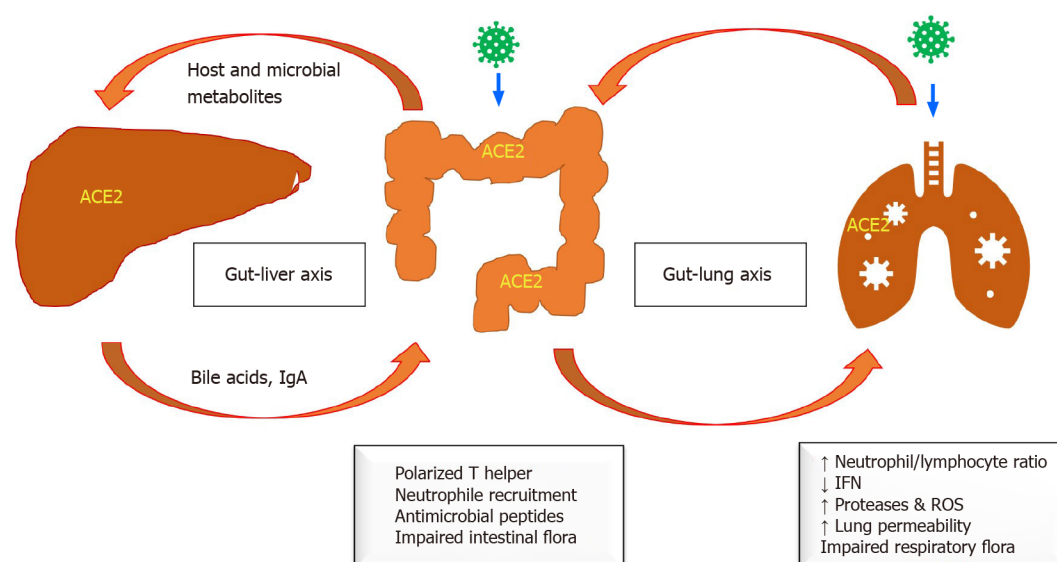


**Figure 1 Pathogenesis of gastrointestinal infection in coronavirus disease 2019.** ACE2: Angiotensin-converting enzyme 2; IFN: Interferon; IgA: Immunoglobulin A; ROS: Reactive oxygen species.

### Diagnosis

Gastrointestinal manifestations are present in more than half (57%) of the patients infected with commonly circulating coronaviruses, especially in children. These manifestations are considered a warning in the presence of other medical comorbidities<sup>[33]</sup>. Children infected with SARS-CoV-2 usually have milder clinical manifestations of the disease than adults, and occasionally, they act as asymptomatic carriers. Gastrointestinal symptoms are common in children with COVID-19; approximately 25% of them exhibit at least one gastrointestinal symptom. These symptoms may occur in the absence of respiratory symptoms. The most common gastrointestinal symptoms in children are diarrhoea, followed by vomiting and abdominal pain. The manifestations usually come in combination. Gastrointestinal bleeding was reported in adults, but no data were reported in children. Abdominal pain is sometimes severe enough to be mistaken with acute abdomen such as acute appendicitis or systemic sepsis<sup>[20]</sup>.

Infants less than one year of age may present with food intolerance or feeding difficulties. These atypical presentations, especially as initial symptoms, may be misleading and lead to delayed diagnosis of COVID-19. Diagnosis is usually based on the detection of viral nucleic acids in respiratory tract specimens, while faecal nucleic acid detection is often neglected. Therefore, children with gastrointestinal symptoms as the predominant manifestation of COVID-19 are often misdiagnosed<sup>[34]</sup>. Gastrointestinal manifestations are a prominent presenting feature of multisystem inflammatory syndrome in children (MIS-C). When presenting with MIS-C, COVID-19 could be confused with gastrointestinal infections or even inflammatory bowel disease. Therefore, any child with a history of recent SARS-CoV-2 exposure or infection and prominent gastrointestinal symptoms should be considered to have MIS-C, especially in the presence of other clinical comorbidities and extremely high inflammatory markers<sup>[21]</sup>.

### Diagnostic tools

The initial diagnostic tools to monitor infected children are the same as those used for adults, *i.e.*, tracing the history of contact with any infected individuals. Real-time reverse transcription-polymerase chain reaction (RT-PCR) testing of nose and throat swabs for the detection of SARS-CoV-2 nucleic acid is the gold-standard confirmatory test for COVID-19. The virus can be detected from the stool until 12 d after disease onset. Stool can still give positive results despite negative respiratory tests. Patients who present with gastrointestinal symptoms may have a longer duration between symptom onset and viral clearance and may have increased faecal virus positivity compared with those who present with respiratory symptoms<sup>[35]</sup>. Children have a higher nucleic acid positivity rate of faeces and prolonged faecal viral shedding compared to adults<sup>[34]</sup>. SARS-CoV-2 RNA can be found in stool specimens and anal/rectal swabs, often with more positivity than oral samples, in the late phase of



the disease. Next-generation sequencing is utilized to identify SARS-CoV-2 strains and mutations for epidemiological and research purposes. Rapid antigen detection tests depend on the detection of the viral antigen in the nose and throat swab in cases with high viral load and in pre-symptomatic and early symptomatic cases up to five days from symptom onset. These tests offer multiple benefits in comparison to RT-PCR tests, including shorter turnaround times, easier techniques, and reduced costs, especially in situations with limited RT-PCR testing capacity. However, there is a high chance of cross-reactivity with other coronavirus families. Additionally, rapid antigen detection tests have lower sensitivity and specificity than RT-PCR. Therefore, positive results should be confirmed with RT-PCR. On the other hand, antibody detection tests are usually negative during the first 7–10 d of infection, with a high risk of missing cases of SARS-CoV-2 infection<sup>[36,37]</sup>.

There are relatively lower rates of lymphopenia and higher inflammatory markers in children than in adults, and thrombocytopenia may occur. Monitoring the lymphocyte count and C-reactive protein level as signs of severe infection while using procalcitonin levels to detect potential bacterial coinfection is encouraged. Patients with severe infection may have high plasma levels of IL-2, IL-7, IL-10, granulocyte colony-stimulating factor, interferon-gamma-inducible protein 10, monocyte chemoattractant protein 1, macrophage inflammatory protein 1-alpha and tumour necrosis factor alpha. Levels of bilirubin and hepatic enzymes are excellent markers for the severity of infections. Elevated lactate dehydrogenase levels, abnormal coagulation, elevated D-dimers, and progressively decreased lymphocytic count may also be observed in severe cases<sup>[6,38,39]</sup>.

Positive faecal occult blood testing indicates upper gastrointestinal bleeding. Endoscopy may show mucosal damage to the oesophageal, gastric, duodenal, and colonic mucosa. Biopsy could show numerous infiltrating plasma cells and lymphocytes, as well as interstitial oedema in the lamina propria of the stomach, duodenum, and rectum. Viral-induced gastrointestinal inflammation causes elevated serum IL-6 levels and elevated levels of faecal calprotectin with significantly higher concentrations in patients with COVID-19 suffering from diarrhoea<sup>[26]</sup>. The ACE2 protein, used by the virus as a receptor for entry, could be stained mainly in the cytoplasm of gastrointestinal epithelial cells. Immunofluorescence testing may show abundant expression of ACE2 in the glandular cells of the gastric, duodenal, and rectal epithelia<sup>[40]</sup>. Lung imaging examination has been considered a complimentary confirmation method. Chest X-ray findings in children appear to be nonspecific. However, children with mild disease should not routinely have computed tomography chest imaging in view of high radiation exposure<sup>[13]</sup>.

## IMPLICATIONS OF GASTROINTESTINAL INFECTION IN COVID-19

### *Faecal-oral transmission*

Oral gastrointestinal infection with SARS-CoV-2 alters the gastrointestinal tract into a reservoir for viral replication, leading to virus spread to other organs, as well as viral shedding in the stool. Faecal viral shedding could continue for 1 wk after clearance from the respiratory tract. This was observed to be more prevalent in children than in adults, with possible long-term faecal-oral transmission, increasing the potential risk for stools to become a source of the contamination of airdrops and several environmental surfaces and may play an important role in viral spread. Therefore, negative nasopharyngeal or oral samples for the virus may not be sufficient to confirm “non-infectivity”, as the virus might still be intermittently shed in body fluids and excreta, including stool. Adding one negative stool sample may increase the negativity yield, especially in patients with gastrointestinal symptoms. However, intermittent shedding should also be considered. The risk of faecal-oral transmission of SARS-CoV-2 is suspected to increase, especially with studies reporting that viral particles in environmental settings may remain viable in aerosols for up to 3 h and for 72 h on solid surfaces. When combined with poor hygiene, including poor handwashing techniques, children have a high risk of transmitting the disease to their contacts. Children should be taught the importance of proper hygiene in an easily understandable language. They should also avoid contact with elderly people if they test positive for COVID-19<sup>[41–43]</sup>.

### *Impact on the gut microbiome*

The gut microbiome is the collection of microorganisms (bacteria, yeast, fungi, archaea, protozoa, and viruses) found in the gastrointestinal tract, mostly in the large bowel,

and it performs many beneficial functions, including immune modulation, with pro-/anti-inflammatory effects. The relation between infection with SARS-CoV-2 and the microbiota is bidirectional. Infection with SARS-CoV-2 is well known to cause the dysbiosis of both the respiratory and gastrointestinal microbiota, which negatively impacts gastrointestinal health and contributes to the development of gastrointestinal disease. The dysbiosis of the gut microbiota creates a suitable environment for SARS-CoV-2 replication and subsequent effects. The inflammatory proteins, cytokines and other mediators that are released because of gut dysbiosis will be augmented with coronavirus infection, which may induce a “cytokine storm” causing more damage than the virus alone, which can ultimately result in multiorgan injury<sup>[44]</sup>. Zuo *et al*<sup>[45]</sup> examined the effect of infection with SARS-CoV-2 on the gut microbiome. They found that the virus induces dysbiosis, an effect that begins even before the start of antiviral therapy. They observed the enrichment of opportunistic pathogens and the depletion of beneficial commensals, an effect that could persist even after the clearance of SARS-CoV-2 from the body, suggesting a more long-lasting detrimental effect on the gut microbiome. They observed a decline in beneficial microbes such as *Lactobacillus*, *Bifidobacterium* and *Faecalibacterium prausnitzii*, which are inversely correlated with the severity of the disease. They also observed the enrichment of *Clostridium hathewayi*, *Clostridium ramosum*, and *Coprobacillus*, which are positively correlated with disease severity<sup>[45]</sup>. Zuo *et al*<sup>[46]</sup> also found heterogeneous configurations of the faecal mycobiome, with the enrichment of fungal pathogens from the genera *Candida* and *Aspergillus*, during the hospitalization of patients with COVID-19 compared with controls. This effect persisted even after nasopharyngeal clearance of SARS-CoV-2<sup>[46]</sup>. Other factors could also play a role in inducing dysbiosis in patients with COVID-19, including the presence of other comorbidities that negatively affect the gut microbiota, such as diabetes mellitus, hypertension, and old age; the use of antibiotics, antivirals, antifungals, and steroids; and other intensive care units milia that could negatively affect and alter the gut microbiome<sup>[47]</sup>.

### **Impact on patient nutrition**

COVID-19 affects the nutrition of patients in many aspects. The poor appetite found in a significant number of patients with COVID-19 makes it difficult to achieve the desired nutrition goals with an oral diet alone, causing undernutrition and sarcopenia. Diarrhoea and vomiting, which are common presentations in children with COVID-19, play an important role in undernutrition development. Anosmia may impair taste perception and interfere with nutritional supplementation or food intake. At the same time, the disruption of normal intestinal mucosal integrity by SARS-CoV-2 could compromise the digestion and absorption of nutrients and may even prevent trophic enteral nutrition<sup>[48]</sup>. Mechanical ventilation that may be needed in the management of children with severe respiratory disease causes excessive swallowing of air and further gastric distention, which predisposes them to gastroesophageal reflux. Pneumonia and respiratory distress may also cause delayed gastric emptying and intestinal hypomotility, leading to constipation, which is an important factor able to interfere with proper nutritional therapy<sup>[49]</sup>.

### **Impact on patient management**

Gut dysbiosis is an important cause of/and results from gastrointestinal inflammation in patients with COVID-19. Gut microbiota diversity and the presence of beneficial microorganisms in the gut may play an important role in determining the course of the disease. The restoration of gut microbiota diversity could help ameliorate the severity of the disease. Since the gut microbiota is malleable and can be modulated by dietary modification, the addition of specialized pre-/probiotics such as fructooligosaccharides, galactooligosaccharides and various *Lactobacillus* strains to the diet could help to improve gut dysbiosis, especially for patients presenting with diarrhoea, thereby improving the overall immune response in these patients<sup>[50]</sup>. Fermented food with probiotics can produce bioactive peptides able to inhibit ACE enzymes by blocking the active sites. Furthermore, fragments of dead probiotic cells can also serve as ACE inhibitors. Consequently, probiotics could have the potential to block the ACE receptor, which acts as an entryway for SARS-CoV-2 to attack gastro-intestinal cells<sup>[51]</sup>. At the same time, prebiotics, probiotics, or symbiotics could be supplied as a prophylactic measure to high-risk groups, such as front-line caregivers and healthy contacts with a suspected case of COVID-19<sup>[50]</sup>. However, microbiota modulation as a method of treatment of patients with COVID-19 is based on indirect evidence and needs further study.

Dietary management plays an important role in patients with COVID-19. Oral intake is the preferred method of nutrition if the patient condition allows. Oral intake is of paramount importance, as a lack of nutrient contact with intestinal mucosa could lead to the atrophy of lymphoid tissue and functional decline of the immune system, as well as the intensification of bacterial translocation. The patients are advised to take a high-calorie and high-protein diet (1-2.5 g/kg/d) to maintain adequate metabolic functions and proper body weight. If the nutrition targets are not met by the oral diet, oral nutrition supplements are recommended and should be started within 1-2 d of hospitalization. Supplementation with digestive enzymes can be given for patients with poor general conditions and impaired digestion. Breast milk is a true immune nutrient, and breastfeeding should be encouraged<sup>[52]</sup>. If oral intake fails or is not tolerated, enteral nutrition is still the preferred method of nutrition therapy, as it stimulates the gut. Gastric feeding is preferred to optimize digestive activity, and the post-pyloric route (preferably jejunal) is recommended in the presence of a high risk of reflux aspiration, intolerance, or the failure of nasogastric tube feeding. Prokinetic agents may be used to enhance motility prior to this intervention. As enteral feeding (especially when using post-pyloric tubes) carries a high risk of aerosol generation, healthcare professionals should use proper personal protective equipment during insertion of the tubes. Enteral nutrition ensures adequate anthropometric progression and decreases the length of hospital stay, costs, mortality rate, and septic complications compared with parenteral nutrition. Overfeeding should be avoided in patients with COVID-19 and severe respiratory disease, as this can increase the risk of hypercapnia. The prone position during enteral feeding is permitted and may lead to a better prognosis. Parenteral nutrition is indicated when nutrition targets cannot be met by enteral nutrition or gastrointestinal intolerance is present despite different measures to address intolerance<sup>[53-55]</sup>.

Occasionally, children with severe gastrointestinal symptoms may need endoscopy. This procedure could stimulate excessive saliva and other digestive secretions that increase the risk of choking, vomiting, or diarrhoea with a greater risk of transmission of infection during digestive endoscopy, biopsy, and treatment *via* an airborne route, including the aspiration of oral and faecal material *via* endoscopes. Therefore, these procedures should be performed in a specialized endoscopic operation room, if possible, with negative pressure with standard level-three protection and strict disinfection procedures<sup>[56,57]</sup>.

### **Impact on misdiagnosis and prognosis**

Children with COVID-19 have been reported to present as asymptomatic or with only mild symptoms of the respiratory or gastrointestinal system. Infants are more likely to present with atypical clinical symptoms than older children. A study reported five infants diagnosed with COVID-19 who presented with isolated fever and reduced oral intake without associated respiratory symptoms<sup>[58,59]</sup>. The characteristics of gastrointestinal symptoms in COVID-19 are more insidious than the characteristics of respiratory symptoms, making them easy to overlook. However, some patients might have only gastrointestinal symptoms during the whole course of the disease, and some continue to shed the virus in faeces, despite respiratory samples testing negative<sup>[60]</sup>. An awareness of these insidious or atypical presentations will allow appropriate investigation and help to decrease the risk of misdiagnosis and consequently decrease the risk of the spread of the disease in the community.

Compared to patients without digestive symptoms, those presenting with digestive symptoms have a longer time from onset to admission and a worse prognosis<sup>[61]</sup>. A study by Chen *et al*<sup>[62]</sup> showed that the presence of gastrointestinal symptoms was associated with a high risk of adult respiratory distress syndrome, non-invasive mechanical ventilation, and tracheal intubation, but not mortality, in patients with COVID-19<sup>[62]</sup>. Another study by Zhou *et al*<sup>[63]</sup> showed that patients with gastrointestinal symptoms have a similar rate of complications, treatment, and clinical prognosis as patients without gastrointestinal symptom in medical and nonmedical staff<sup>[63]</sup>. However, these studies were performed in the adult population and cannot be extrapolated in children.

## **CONCLUSION**

COVID-19 has a wide variety of clinical presentations, and gastrointestinal effects are not rare. Gastrointestinal manifestations could be the initial presenting manifestation in many patients, especially in children, and are more common in patients with severe

disease. Gastrointestinal inflammation associated with COVID-19 greatly affects diagnosis and may increase the rate of misdiagnosis, with a significant impact on prognosis, faecal-oral transmission, the gut microbiome, and patient nutrition and management.

## REFERENCES

- Hong KH**, Lee SW, Kim TS, Huh HJ, Lee J, Kim SY, Park JS, Kim GJ, Sung H, Roh KH, Kim JS, Kim HS, Lee ST, Seong MW, Ryoo N, Lee H, Kwon KC, Yoo CK. Guidelines for Laboratory Diagnosis of Coronavirus Disease 2019 (COVID-19) in Korea. *Ann Lab Med* 2020; **40**: 351-360 [PMID: [32237288](#) DOI: [10.3343/alm.2020.40.5.351](#)]
- Rabaan AA**, Al-Ahmed SH, Haque S, Sah R, Tiwari R, Malik YS, Dhama K, Yatoo MI, Bonilla-Aldana DK, Rodriguez-Morales AJ. SARS-CoV-2, SARS-CoV, and MERS-CoV: A comparative overview. *Infez Med* 2020; 174-184 [PMID: [32275259](#)]
- Molloy EJ**, Lavizzari A, Klingenberg C, Profit J, Zupancic JAF, Davis AS, Mosca F, Bearer CF, Roehr CC; International Neonatal COVID-19 Consortium. Neonates in the COVID-19 pandemic. *Pediatr Res* 2020 [PMID: [32746446](#) DOI: [10.1038/s41390-020-1096-y](#)]
- Götzinger F**, Santiago-García B, Noguera-Julian A, Lanaspá M, Lancella L, Calò Carducci FI, Gabrovská N, Velizarova S, Prunk P, Osterman V, Krivec U, Lo Vecchio A, Shingadia D, Soriano-Arandes A, Melendo S, Lanari M, Pierantoni L, Wagner N, L'Huillier AG, Heininger U, Ritz N, Bandi S, Krajcar N, Roglić S, Santos M, Christiaens C, Creuven M, Buonsenso D, Welch SB, Bogyi M, Brinkmann F, Tebruegge M; ptbnet COVID-19 Study Group. COVID-19 in children and adolescents in Europe: a multinational, multicentre cohort study. *Lancet Child Adolesc Health* 2020; **4**: 653-661 [PMID: [32593339](#) DOI: [10.1016/S2352-4642\(20\)30177-2](#)]
- Tai DBG**, Shah A, Doubeni CA, Sia IG, Wieland ML. The Disproportionate Impact of COVID-19 on Racial and Ethnic Minorities in the United States. *Clin Infect Dis* 2021; **72**: 703-706 [PMID: [32562416](#) DOI: [10.1093/cid/ciaa815](#)]
- Zare-Zardini H**, Soltaninejad H, Ferdosian F, Hamidieh AA, Memarpour-Yazdi M. Coronavirus Disease 2019 (COVID-19) in Children: Prevalence, Diagnosis, Clinical Symptoms, and Treatment. *Int J Gen Med* 2020; **13**: 477-482 [PMID: [32848446](#) DOI: [10.2147/IJGM.S262098](#)]
- Lee PI**, Hu YL, Chen PY, Huang YC, Hsueh PR. Are children less susceptible to COVID-19? *J Microbiol Immunol Infect* 2020; **53**: 371-372 [PMID: [32147409](#) DOI: [10.1016/j.jmii.2020.02.011](#)]
- Cristiani L**, Mancino E, Matera L, Nenna R, Pierangeli A, Scagnolari C, Midulla F. Will children reveal their secret? *Eur Respir J* 2020; **55** [PMID: [32241833](#) DOI: [10.1183/13993003.00749-2020](#)]
- Nickbakhsh S**, Mair C, Matthews L, Reeve R, Johnson PCD, Thorburn F, von Wissmann B, Reynolds A, McMenamin J, Gunson RN, Murcia PR. Virus-virus interactions impact the population dynamics of influenza and the common cold. *Proc Natl Acad Sci USA* 2019 [PMID: [31843887](#) DOI: [10.1073/pnas.1911083116](#)]
- Skarstein Kolberg E**. ACE2, COVID19 and serum ACE as a possible biomarker to predict severity of disease. *J Clin Virol* 2020; **126**: 104350 [PMID: [32283335](#) DOI: [10.1016/j.jcv.2020.104350](#)]
- Covián C**, Fernández-Fierro A, Retamal-Díaz A, Díaz FE, Vasquez AE, Lay MK, Riedel CA, González PA, Bueno SM, Kalergis AM. BCG-Induced Cross-Protection and Development of Trained Immunity: Implication for Vaccine Design. *Front Immunol* 2019; **10**: 2806 [PMID: [31849980](#) DOI: [10.3389/fimmu.2019.02806](#)]
- Aguila EJT**, Cua IHY, Dumagpi JEL, Francisco CPD, Raymundo NTV, Sy-Janairo MLL, Cabral-Prodigalidad PAI, Lontok MAD. COVID-19 and its effects on the digestive system and endoscopy practice. *JGH Open* 2020; **4**: 324-331 [PMID: [32514432](#) DOI: [10.1002/jgh3.12358](#)]
- Huang C**, Wang Y, Li X, Ren L, Zhao J, Hu Y, Zhang L, Fan G, Xu J, Gu X, Cheng Z, Yu T, Xia J, Wei Y, Wu W, Xie X, Yin W, Li H, Liu M, Xiao Y, Gao H, Guo L, Xie J, Wang G, Jiang R, Gao Z, Jin Q, Wang J, Cao B. Clinical features of patients infected with 2019 novel coronavirus in Wuhan, China. *Lancet* 2020; **395**: 497-506 [PMID: [31986264](#) DOI: [10.1016/S0140-6736\(20\)30183-5](#)]
- Guan WJ**, Ni ZY, Hu Y, Liang WH, Ou CQ, He JX, Liu L, Shan H, Lei CL, Hui DSC, Du B, Li LJ, Zeng G, Yuen KY, Chen RC, Tang CL, Wang T, Chen PY, Xiang J, Li SY, Wang JL, Liang ZJ, Peng YX, Wei L, Liu Y, Hu YH, Peng P, Wang JM, Liu JY, Chen Z, Li G, Zheng ZJ, Qiu SQ, Luo J, Ye CJ, Zhu SY, Zhong NS; China Medical Treatment Expert Group for Covid-19. Clinical Characteristics of Coronavirus Disease 2019 in China. *N Engl J Med* 2020; **382**: 1708-1720 [PMID: [32109013](#) DOI: [10.1056/NEJMoa2002032](#)]
- Xu XW**, Wu XX, Jiang XG, Xu KJ, Ying LJ, Ma CL, Li SB, Wang HY, Zhang S, Gao HN, Sheng JF, Cai HL, Qiu YQ, Li LJ. Clinical findings in a group of patients infected with the 2019 novel coronavirus (SARS-Cov-2) outside of Wuhan, China: retrospective case series. *BMJ* 2020; **368**: m606 [PMID: [32075786](#) DOI: [10.1136/bmj.m606](#)]
- Young BE**, Ong SWX, Kalimuddin S, Low JG, Tan SY, Loh J, Ng OT, Marimuthu K, Ang LW, Mak TM, Lau SK, Anderson DE, Chan KS, Tan TY, Ng TY, Cui L, Said Z, Kurupatham L, Chen MI, Chan M, Vasoo S, Wang LF, Tan BH, Lin RTP, Lee VJM, Leo YS, Lye DC; Singapore 2019 Novel Coronavirus Outbreak Research Team. Epidemiologic Features and Clinical Course of Patients Infected With SARS-CoV-2 in Singapore. *JAMA* 2020; **323**: 1488-1494 [PMID: [32125362](#) DOI: [10.1001/jama.2020.3204](#)]



- 17 **Cheung KS**, Hung IFN, Chan PPY, Lung KC, Tso E, Liu R, Ng YY, Chu MY, Chung TWH, Tam AR, Yip CCY, Leung KH, Fung AY, Zhang HM, Zhang AJX, To KKW, Chan KH, Yuen KY, Leung WK. Gastrointestinal Manifestations of SARS-CoV-2 Infection and Virus Load in Fecal Samples From a Hong Kong Cohort: Systematic Review and Meta-analysis. *Gastroenterology* 2020; **159**: 81-95 [PMID: [32251668](#) DOI: [10.1053/j.gastro.2020.03.065](#)]
- 18 **Jin X**, Lian JS, Hu JH, Gao J, Zheng L, Zhang YM, Hao SR, Jia HY, Cai H, Zhang XL, Yu GD, Xu KJ, Wang XY, Gu JQ, Zhang SY, Ye CY, Jin CL, Lu YF, Yu X, Yu XP, Huang JR, Xu KL, Ni Q, Yu CB, Zhu B, Li YT, Liu J, Zhao H, Zhang X, Yu L, Guo YZ, Su JW, Tao JJ, Lang GJ, Wu XX, Wu WR, Qv TT, Xiang DR, Yi P, Shi D, Chen Y, Ren Y, Qiu YQ, Li LJ, Sheng J, Yang Y. Epidemiological, clinical and virological characteristics of 74 cases of coronavirus-infected disease 2019 (COVID-19) with gastrointestinal symptoms. *Gut* 2020; **69**: 1002-1009 [PMID: [32213556](#) DOI: [10.1136/gutjnl-2020-320926](#)]
- 19 **Carvalho A**, Alqusairi R, Adams A, Paul M, Kothari N, Peters S, DeBenedet AT. SARS-CoV-2 Gastrointestinal Infection Causing Hemorrhagic Colitis: Implications for Detection and Transmission of COVID-19 Disease. *Am J Gastroenterol* 2020; **115**: 942-946 [PMID: [32496741](#) DOI: [10.14309/ajg.0000000000000667](#)]
- 20 **Tullie L**, Ford K, Bisharat M, Watson T, Thakkar H, Mullassery D, Giuliani S, Blackburn S, Cross K, De Coppi P, Curry J. Gastrointestinal features in children with COVID-19: an observation of varied presentation in eight children. *Lancet Child Adolesc Health* 2020; **4**: e19-e20 [PMID: [32442420](#) DOI: [10.1016/S2352-4642\(20\)30165-6](#)]
- 21 **Miller J**, Cantor A, Zachariah P, Ahn D, Martinez M, Margolis KG. Gastrointestinal Symptoms as a Major Presentation Component of a Novel Multisystem Inflammatory Syndrome in Children That Is Related to Coronavirus Disease 2019: A Single Center Experience of 44 Cases. *Gastroenterology* 2020; **159**: 1571-1574. e2 [PMID: [32505742](#) DOI: [10.1053/j.gastro.2020.05.079](#)]
- 22 **Akobeng AK**, Grafton-Clarke C, Abdelgadir I, Twum-Barimah E, Gordon M. Gastrointestinal manifestations of COVID-19 in children: a systematic review and meta-analysis. *Front Gastroenterol* 2020; **8** [DOI: [10.1136/flgastro-2020-101529](#)]
- 23 **Mayor S**. Covid-19: UK studies find gastrointestinal symptoms are common in children. *BMJ* 2020; **370**: m3484 [PMID: [32895221](#) DOI: [10.1136/bmj.m3484](#)]
- 24 **Lu X**, Zhang L, Du H, Zhang J, Li YY, Qu J, Zhang W, Wang Y, Bao S, Li Y, Wu C, Liu H, Liu D, Shao J, Peng X, Yang Y, Liu Z, Xiang Y, Zhang F, Silva RM, Pinkerton KE, Shen K, Xiao H, Xu S, Wong GWK; Chinese Pediatric Novel Coronavirus Study Team. SARS-CoV-2 Infection in Children. *N Engl J Med* 2020; **382**: 1663-1665 [PMID: [32187458](#) DOI: [10.1056/NEJMc2005073](#)]
- 25 **Cheng PK**, Wong DA, Tong LK, Ip SM, Lo AC, Lau CS, Yeung EY, Lim WW. Viral shedding patterns of coronavirus in patients with probable severe acute respiratory syndrome. *Lancet* 2004; **363**: 1699-1700 [PMID: [15158632](#) DOI: [10.1016/S0140-6736\(04\)16255-7](#)]
- 26 **Ojetti V**, Saviano A, Covino M, Acampora N, Troiani E, Franceschi F; GEMELLI AGAINST COVID-19 group. COVID-19 and intestinal inflammation: Role of fecal calprotectin. *Dig Liver Dis* 2020; **52**: 1231-1233 [PMID: [33060042](#) DOI: [10.1016/j.dld.2020.09.015](#)]
- 27 **Hashimoto T**, Perlot T, Rehman A, Trichereau J, Ishiguro H, Paolino M, Sigl V, Hanada T, Hanada R, Lipinski S, Wild B, Camargo SM, Singer D, Richter A, Kuba K, Fukamizu A, Schreiber S, Clevers H, Verrey F, Rosenstiel P, Penninger JM. ACE2 Links amino acid malnutrition to microbial ecology and intestinal inflammation. *Nature* 2012; **487**: 477-481 [PMID: [22837003](#) DOI: [10.1038/nature11228](#)]
- 28 **Kim S**, Rigatto K, Gazzana MB, Knorst MM, Richards EM, Pepine CJ, Raizada MK. Altered Gut Microbiome Profile in Patients With Pulmonary Arterial Hypertension. *Hypertension* 2020; **75**: 1063-1071 [PMID: [32088998](#) DOI: [10.1161/HYPERTENSIONAHA.119.14294](#)]
- 29 **Villapol S**. Gastrointestinal symptoms associated with COVID-19: impact on the gut microbiome. *Transl Res* 2020; **226**: 57-69 [PMID: [32827705](#) DOI: [10.1016/j.trsl.2020.08.004](#)]
- 30 **Stenstad H**, Ericsson A, Johansson-Lindbom B, Svensson M, Marsal J, Mack M, Picarella D, Soler D, Marquez G, Briskin M, Agace WW. Gut-associated lymphoid tissue-primed CD4+ T cells display CCR9-dependent and -independent homing to the small intestine. *Blood* 2006; **107**: 3447-3454 [PMID: [16391017](#) DOI: [10.1182/blood-2005-07-2860](#)]
- 31 **Zhang D**, Li S, Wang N, Tan HY, Zhang Z, Feng Y. The Cross-Talk Between Gut Microbiota and Lungs in Common Lung Diseases. *Front Microbiol* 2020; **11**: 301 [PMID: [32158441](#) DOI: [10.3389/fmicb.2020.00301](#)]
- 32 **Tripathi A**, Debelius J, Brenner DA, Karin M, Loomba R, Schnabl B, Knight R. The gut-liver axis and the intersection with the microbiome. *Nat Rev Gastroenterol Hepatol* 2018; **15**: 397-411 [PMID: [29748586](#) DOI: [10.1038/s41575-018-0011-z](#)]
- 33 **Giacomet V**, Barcellini L, Stracuzzi M, Longoni E, Folgari L, Leone A, Zuccotti GV; COVID-19 Pediatric network. Gastrointestinal Symptoms in Severe COVID-19 Children. *Pediatr Infect Dis J* 2020; **39**: e317-e320 [PMID: [32932333](#) DOI: [10.1097/INF.0000000000002843](#)]
- 34 **Wang JG**, Cui HR, Tang HB, Deng XL. Gastrointestinal symptoms and fecal nucleic acid testing of children with 2019 coronavirus disease: a systematic review and meta-analysis. *Sci Rep* 2020; **10**: 17846 [PMID: [33082472](#) DOI: [10.1038/s41598-020-74913-0](#)]
- 35 **Han C**, Duan C, Zhang S, Spiegel B, Shi H, Wang W, Zhang L, Lin R, Liu J, Ding Z, Hou X. Digestive Symptoms in COVID-19 Patients With Mild Disease Severity: Clinical Presentation, Stool Viral RNA Testing, and Outcomes. *Am J Gastroenterol* 2020; **115**: 916-923 [PMID: [32301761](#) DOI: [10.14309/ajg.0000000000000664](#)]



- 36 **European Centre for Disease Prevention and Control.** Options for the use of rapid antigen tests for COVID-19 in the EU/EEA and the UK. 19 November 2020. Stockholm: ECDC; 2020. [cited 2 December 2020]. Available from: [https://europa.eu/european-union/coronavirus-response\\_en](https://europa.eu/european-union/coronavirus-response_en)
- 37 **Schohy A, Anantharajah A, Bodéus M, Kabamba-Mukadi B, Verroken A, Rodriguez-Villalobos H.** Low performance of rapid antigen detection test as frontline testing for COVID-19 diagnosis. *J Clin Virol* 2020; **129**: 104455 [PMID: [32485618](#) DOI: [10.1016/j.jcv.2020.104455](#)]
- 38 **Huang I, Pranata R, Lim MA, Oehadian A, Alisjahbana B.** C-reactive protein, procalcitonin, D-dimer, and ferritin in severe coronavirus disease-2019: a meta-analysis. *Ther Adv Respir Dis* 2020; **14**: 1753466620937175 [PMID: [32615866](#) DOI: [10.1177/1753466620937175](#)]
- 39 **Balasubramanian S, Rao NM, Goenka A, Roderick M, Ramanan AV.** Coronavirus Disease 2019 (COVID-19) in Children - What We Know So Far and What We Do Not. *Indian Pediatr* 2020; **57**: 435-442 [PMID: [32273490](#) DOI: [10.1007/s13312-020-1819-5](#)]
- 40 **Cipriano M, Ruberti E, Giacalone A.** Gastrointestinal Infection Could Be New Focus for Coronavirus Diagnosis. *Cureus* 2020; **12**: e7422 [PMID: [32351807](#) DOI: [10.7759/cureus.7422](#)]
- 41 **Altamimi E.** Effect of COVID-19 Pandemic and Lockdown on Children With Gastrointestinal Disorders. *Gastroenterology Res* 2020; **13**: 125-128 [PMID: [32655731](#) DOI: [10.14740/gr1290](#)]
- 42 **van Doremalen N, Bushmaker T, Morris DH, Holbrook MG, Gamble A, Williamson BN, Tamin A, Harcourt JL, Thornburg NJ, Gerber SI, Lloyd-Smith JO, de Wit E, Munster VJ.** Aerosol and Surface Stability of SARS-CoV-2 as Compared with SARS-CoV-1. *N Engl J Med* 2020; **382**: 1564-1567 [PMID: [32182409](#) DOI: [10.1056/NEJMc2004973](#)]
- 43 **Donà D, Minotti C, Costenaro P, Da Dalt L, Giaquinto C.** Fecal-Oral Transmission of SARS-CoV-2 In Children: is it Time to Change Our Approach? *Pediatr Infect Dis J* 2020; **39**: e133-e134 [PMID: [32304466](#) DOI: [10.1097/INF.0000000000002704](#)]
- 44 **Janda L, Mihalčin M, Šfastná M.** Is a healthy microbiome responsible for lower mortality in COVID-19? *Biologia (Bratisl)* 2020; 1-11 [PMID: [33078028](#) DOI: [10.2478/s11756-020-00614-8](#)]
- 45 **Zuo T, Zhang F, Lui GCY, Yeoh YK, Li AYL, Zhan H, Wan Y, Chung ACK, Cheung CP, Chen N, Lai CKC, Chen Z, Tso EYK, Fung KSC, Chan V, Ling L, Joynt G, Hui DSC, Chan FKL, Chan PKS, Ng SC.** Alterations in Gut Microbiota of Patients With COVID-19 During Time of Hospitalization. *Gastroenterology* 2020; **159**: 944-955. e8 [PMID: [32442562](#) DOI: [10.1053/j.gastro.2020.05.048](#)]
- 46 **Zuo T, Zhan H, Zhang F, Liu Q, Tso EYK, Lui GCY, Chen N, Li A, Lu W, Chan FKL, Chan PKS, Ng SC.** Alterations in Fecal Fungal Microbiome of Patients With COVID-19 During Time of Hospitalization until Discharge. *Gastroenterology* 2020; **159**: 1302-1310. e5 [PMID: [32598884](#) DOI: [10.1053/j.gastro.2020.06.048](#)]
- 47 **Din AU, Mazhar M, Waseem M, Ahmad W, Bibi A, Hassan A, Ali N, Gang W, Qian G, Ullah R, Shah T, Ullah M, Khan I, Nisar MF, Wu J.** SARS-CoV-2 microbiome dysbiosis linked disorders and possible probiotics role. *Biomed Pharmacother* 2021; **133**: 110947 [PMID: [33197765](#) DOI: [10.1016/j.biopha.2020.110947](#)]
- 48 **Aguila EJT, Cua IHY, Fontanilla JAC, Yabut VLM, Causing MFP.** Gastrointestinal Manifestations of COVID-19: Impact on Nutrition Practices. *Nutr Clin Pract* 2020; **35**: 800-805 [PMID: [32668037](#) DOI: [10.1002/ncp.10554](#)]
- 49 **Oba J, Carvalho WB, Silva CA, Delgado AF.** Gastrointestinal manifestations and nutritional therapy during COVID-19 pandemic: a practical guide for pediatricians. *Einstein (Sao Paulo)* 2020; **18**: eRW5774 [PMID: [32667418](#) DOI: [10.31744/einstein\\_journal/2020rw5774](#)]
- 50 **Dhar D, Mohanty A.** Gut microbiota and Covid-19- possible link and implications. *Virus Res* 2020; **285**: 198018 [PMID: [32430279](#) DOI: [10.1016/j.virusres.2020.198018](#)]
- 51 **Olaimat AN, Aolymat I, Al-Holy M, Ayyash M, Abu Ghoush M, Al-Nabulsi AA, Osaili T, Apostolopoulos V, Liu SQ, Shah NP.** The potential application of probiotics and prebiotics for the prevention and treatment of COVID-19. *NPJ Sci Food* 2020; **4**: 17 [PMID: [33083549](#) DOI: [10.1038/s41538-020-00078-9](#)]
- 52 **ASPEN.** Nutrition and hydration: Key weapons in the fight against COVID-19. [cited 10 December 2020]. Available from: <http://www.nutritioncare.org/>
- 53 **Barazzoni R, Bischoff SC, Breda J, Wickramasinghe K, Krznaric Z, Nitzan D, Pirlich M, Singer P;** endorsed by the ESPEN Council. ESPEN expert statements and practical guidance for nutritional management of individuals with SARS-CoV-2 infection. *Clin Nutr* 2020; **39**: 1631-1638 [PMID: [32305181](#) DOI: [10.1016/j.clnu.2020.03.022](#)]
- 54 **Singer P, Blaser AR, Berger MM, Alhazzani W, Calder PC, Casaer MP, Hiesmayr M, Mayer K, Montejo JC, Pichard C, Preiser JC, van Zanten ARH, Oczkowski S, Szczeklik W, Bischoff SC.** ESPEN guideline on clinical nutrition in the intensive care unit. *Clin Nutr* 2019; **38**: 48-79 [PMID: [30348463](#) DOI: [10.1016/j.clnu.2018.08.037](#)]
- 55 **Dunn CG, Kenney E, Fleischhacker SE, Bleich SN.** Feeding Low-Income Children during the Covid-19 Pandemic. *N Engl J Med* 2020; **382**: e40 [PMID: [32227759](#) DOI: [10.1056/NEJMp2005638](#)]
- 56 **Repici A, Maselli R, Colombo M, Gabbiadini R, Spadaccini M, Anderloni A, Carrara S, Fugazza A, Di Leo M, Galtieri PA, Pellegatta G, Ferrara EC, Azzolini E, Lagioia M.** Coronavirus (COVID-19) outbreak: what the department of endoscopy should know. *Gastrointest Endosc* 2020; **92**: 192-197 [PMID: [32179106](#) DOI: [10.1016/j.gie.2020.03.019](#)]
- 57 **Elshaarawy O, Lashen SA, Makhoulf NA, Abdeltawab D, Zaghloul MS, Ahmed RM, Fathy H, Afifi S, Abdel-Gawad M, Abdelsameea E, Abd-Elsalam S, Mohamed SY, Tag-Adeen M, Tharwat M, Alzamzamy A, Bekhit AN, Eid AM, Awad A, Aamr M, Dayem WAAE, Wifi MN, Alborae M.** Barriers for resuming endoscopy service in the context of COVID-19 pandemic: A multicenter survey

- from Egypt. *World J Gastroenterol* 2020; **26**: 6880-6890 [PMID: [33268968](#) DOI: [10.3748/wjg.v26.i43.6880](#)]
- 58 **Dong Y**, Mo X, Hu Y, Qi X, Jiang F, Jiang Z, Tong S. Epidemiology of COVID-19 Among Children in China. *Pediatrics* 2020; **145** [PMID: [32179660](#) DOI: [10.1542/peds.2020-0702](#)]
  - 59 **Nathan N**, Prevost B, Corvol H. Atypical presentation of COVID-19 in young infants. *Lancet* 2020; **395**: 1481 [PMID: [32353326](#) DOI: [10.1016/S0140-6736\(20\)30980-6](#)]
  - 60 **Yang L**, Tu L. Implications of gastrointestinal manifestations of COVID-19. *Lancet Gastroenterol Hepatol* 2020; **5**: 629-630 [PMID: [32405602](#) DOI: [10.1016/S2468-1253\(20\)30132-1](#)]
  - 61 **Pan L**, Mu M, Yang P, Sun Y, Wang R, Yan J, Li P, Hu B, Wang J, Hu C, Jin Y, Niu X, Ping R, Du Y, Li T, Xu G, Hu Q, Tu L. Clinical Characteristics of COVID-19 Patients With Digestive Symptoms in Hubei, China: A Descriptive, Cross-Sectional, Multicenter Study. *Am J Gastroenterol* 2020; **115**: 766-773 [PMID: [32287140](#) DOI: [10.14309/ajg.0000000000000620](#)]
  - 62 **Chen R**, Yu YL, Li W, Liu Y, Lu JX, Chen F, Zhou Q, Xia ZY, Gao L, Meng QT, Ma D. Gastrointestinal Symptoms Associated With Unfavorable Prognosis of COVID-19 Patients: A Retrospective Study. *Front Med (Lausanne)* 2020; **7**: 608259 [PMID: [33262996](#) DOI: [10.3389/fmed.2020.608259](#)]
  - 63 **Zhou Z**, Zhao N, Shu Y, Han S, Chen B, Shu X. Effect of Gastrointestinal Symptoms in Patients With COVID-19. *Gastroenterology* 2020; **158**: 2294-2297 [PMID: [32199880](#) DOI: [10.1053/j.gastro.2020.03.020](#)]



## Hepatitis C virus micro-elimination: Where do we stand?

Alessandra Mangia, Rosa Cotugno, Giovanna Cocomazzi, Maria Maddalena Squillante, Valeria Piazzolla

**ORCID number:** Alessandra Mangia 0000-0002-2600-3555; Rosa Cotugno 0000-0001-5431-592X; Giovanna Cocomazzi 0000-0003-2831-934X; Maria Maddalena Squillante 0000-0002-1101-0041; Valeria Piazzolla 0000-0002-8653-0138.

**Author contributions:** Mangia A designed the review, supervised the drafting of the manuscript, and finalized the version for publication; Cotugno R and Squillante MM searched the literature and collected the references; Piazzolla V and Cocomazzi G wrote the first draft of the manuscript.

### Conflict-of-interest statement:

Mangia A has served in an advisory role and received research grants from Gilead Sciences, MSD, Intercept, and Spring Bank; all other authors declare having no conflicts of interest.

**Open-Access:** This article is an open-access article that was selected by an in-house editor and fully peer-reviewed by external reviewers. It is distributed in accordance with the Creative Commons Attribution NonCommercial (CC BY-NC 4.0) license, which permits others to distribute, remix, adapt, build upon this work non-commercially, and license their derivative works on different terms, provided the original work is properly cited and

**Alessandra Mangia, Rosa Cotugno, Giovanna Cocomazzi, Maria Maddalena Squillante, Valeria Piazzolla**, Liver Unit, Department of Medical Sciences, IRCCS Casa Sollievo della Sofferenza, San Giovanni Rotondo 71013, Fg, Italy

**Corresponding author:** Alessandra Mangia, MD, Chief Doctor, Liver Unit, Department of Medical Sciences, IRCCS Casa Sollievo della Sofferenza, Viale Cappuccini 1, San Giovanni Rotondo 71013, Fg, Italy. [a.mangia@tin.it](mailto:a.mangia@tin.it)

### Abstract

Hepatitis C virus (HCV) elimination by 2030, using direct-acting antiviral treatments, has been promoted by the World Health Organization. This achievement is not attainable, however, particularly after the 2020 pandemic of the coronavirus disease 2019. Consequently, the more realistic objective of eliminating HCV from population segments for which targeted strategies of prevention and treatment are easily attained has been promoted in Europe, as a valid alternative. The underlying idea is that micro-elimination will ultimately lead to macro-elimination. The micro-elimination strategy may target different specific populations and at-risk groups. Different settings, including prisons and hospitals, have also been identified as micro-elimination scenarios. In addition, dedicated micro-elimination strategies have been designed that are tailored at the geographical level according to HCV epidemiology and individual country's income. The main elements of a valid and successful micro-elimination project are reliable epidemiological data and active involvement of all the stakeholders. Community involvement represents another essential component for a successful program.

**Key Words:** Hepatitis C virus antibodies; Hepatitis C virus elimination; Hepatitis C virus epidemiology; Hepatitis C virus RNA; Hepatitis C virus diagnosis; Hepatitis C virus infection

©The Author(s) 2021. Published by Baishideng Publishing Group Inc. All rights reserved.

**Core Tip:** Achievement of hepatitis C virus (HCV) elimination using direct-acting antiviral drugs treatment by 2030 promoted by World Health Organization is hardly attainable especially amidst the coronavirus disease 2019 pandemic. The smaller goal of eliminating HCV from population segments for which tailored strategies of prevention and treatment can be easily implemented appears more realistic. Different

the use is non-commercial. See: <http://creativecommons.org/licenses/by-nc/4.0/>

**Manuscript source:** Invited manuscript

**Specialty type:** Gastroenterology and hepatology

**Country/Territory of origin:** Italy

**Peer-review report's scientific quality classification**

Grade A (Excellent): A  
Grade B (Very good): B, B, B  
Grade C (Good): 0  
Grade D (Fair): D  
Grade E (Poor): 0

**Received:** January 14, 2021

**Peer-review started:** January 14, 2021

**First decision:** February 10, 2021

**Revised:** February 28, 2021

**Accepted:** April 5, 2021

**Article in press:** April 5, 2021

**Published online:** April 28, 2021

**P-Reviewer:** Carneiro B, Fhkm MFL, Poustchi H, Su WW

**S-Editor:** Fan JR

**L-Editor:** A

**P-Editor:** Ma YJ



specific populations and at-risk groups, as well as different settings including prisons and hospitals have been selected for micro-elimination campaigns. Dedicated micro-elimination strategies have also been designed at geographical level according to the countries income and HCV epidemiology. The success of micro-elimination depends on reliable epidemiological data and active involvement of all the different stakeholders.

**Citation:** Mangia A, Cotugno R, Cocomazzi G, Squillante MM, Piazzolla V. Hepatitis C virus micro-elimination: Where do we stand? *World J Gastroenterol* 2021; 27(16): 1728-1737

**URL:** <https://www.wjgnet.com/1007-9327/full/v27/i16/1728.htm>

**DOI:** <https://dx.doi.org/10.3748/wjg.v27.i16.1728>

## INTRODUCTION

Chronic hepatitis C is a major public health problem, affecting approximately 71 million people worldwide<sup>[1]</sup>. In 2016, the World Health Organization (WHO) published a document highlighting their global strategy aiming to achieve viral hepatitis elimination by 2030<sup>[2,3]</sup>. The objectives of this strategy for hepatitis C virus (HCV) infection-as a public health problem-are 90% reduction of new infections, 65% reduction in mortality, 90% increase in HCV diagnosis, and 80% increase in treatment rates.

The availability of low cost and highly efficient pangenotypic regimens for HCV treatment has led to the treatment of 5 million infected persons across the world. However, all the steps along the HCV care cascade need to be enhanced, starting with the proportion of infected people screened, followed by the number of patients testing positive for HCV antibodies and diagnosed with HCV RNA, and finishing with the consequent proportion of patients linked to care and treatment<sup>[4]</sup>. While safety improvements and harm reductions can be achieved and will ensure a reduction in incidence, HCV diagnoses remain largely suboptimal, with less than 20% of the estimated 71 million chronic HCV-infected individuals identified globally. Razavi *et al*<sup>[5]</sup> reported that, among high-income countries, only 11 are on track to eliminate HCV by 2030 and 5 more countries are on track for elimination by 2040; all the remaining are expected to eliminate HCV by 2050 or later. This is mostly due to an insufficient number of patients diagnosed, linked to care and treated, across the majority of countries.

A low level of community awareness as well as stigma and fears related to special populations, such as people who use intravenous drugs (PWID), prevent an expanded screening. Referral of patients already diagnosed represents another major challenge. Even more critical are geographical and transportation barriers. Long wait times before the start of treatment and reimbursement policies in some countries account for additional obstacles. Although pre-treatment evaluations, including viral load confirmation and liver disease staging, can be simplified using the pangenotypic and panfibrotic regimens currently available<sup>[4]</sup>, treatment restrictions related to the stage of fibrosis remain a limiting factor in several countries.

More recently it has become evident that a key aspect in improving the results of treatment strategies is patient engagement. In addition, the coronavirus disease 2019 (COVID-19) pandemic is having a deep impact on management of chronic liver diseases in general. Screening campaigns appear more difficult to implement, and testing and access to treatment have been reduced<sup>[6]</sup>. Moreover, modeling the global impact of COVID-19 on global HCV elimination efforts has shown that a 1-year delay scenario could result in an excess of incidence of HCV cases and liver-related events among such cases, as well as an excess of cases with the infection's consequent hepatocellular carcinoma development<sup>[7]</sup>.

Thus, it is clear that a one-size-fits-all strategy would be unsuccessful to achieve global elimination and that different populations with chronic HCV infection require dedicated programs<sup>[8,9]</sup>. Achievement of elimination in a well-defined group or context currently appears more feasible and checkable than a macro-elimination plan<sup>[10]</sup>. The inclusion of key interventions and the adoption of test-and-treat strategies and simplified treatment regimens were then considered more tangible and achievable milestones. In particular, since 2017, the European Association for Study of the Liver

adopted a micro-elimination strategy as a stepwise, savvy approach in the fight against HCV. The goal of macro-elimination was accordingly adjusted in order to pursue micro-elimination in defined subgroups of patients, such as patients with human immunodeficiency virus (HIV)/HCV coinfection or hemophilia, and prisoners or PWID<sup>[10]</sup>.

Micro-elimination requires involvement of all the different stakeholders, including administrative local representatives, health providers, and patients representatives. This strategy is based on different criteria that allow stakeholders to adapt to different situations. The key aspect is to individualize access to the services on the basis of the patients' needs in order to overcome barriers and to achieve higher rates of diagnosis and treatment in a given population of interest during an established period of time. It is important that the progress attained is publicly announced and analyzed using adequate performance indicators<sup>[11]</sup>. One of the advantages of this strategy is that once results are achieved in a given context, the success translates into leverage for new initiatives. Of course, stakeholders' engagement is key to successful micro-elimination, together with funding, advocacy efforts and ability to scale, and most importantly involvement of the community. The approaches to micro-elimination may differ and they might be based on different locations, different settings, or different populations<sup>[11]</sup>.

## AVAILABLE HCV TREATMENT REGIMENS

Current developments in the treatment of chronic hepatitis C are dramatic. Indeed, several direct-acting antiviral drugs (DAA) have been approved from 2013 to 2017 for treatment of HCV-infected patients, with high rates of sustained virological response (Table 1). The arrival of these highly effective treatment regimens has improved prospects for the eradication of HCV worldwide. DAA are well tolerated. The first approved DAA was sofosbuvir a once-daily pangenotypic oral nucleotide analog polymerase inhibitor as a component of combination antiviral regimens. It was approved on December 2013<sup>[4]</sup>. The protease inhibitor simeprevir was used as a two pills combination with sofosbuvir for all the different HCV genotypes but 2 and 3 on 2014<sup>[4]</sup>. Sofosbuvir was later in the same year used as a single pill fixed dose combination with the NS5A inhibitor, ledipasvir for genotype 1 and 4 treatment<sup>[4]</sup>. Simultaneously, on 2014 the three compounds combination of ombitasvir, paritaprevir /ritonavir boosted and dasabuvir not including polymerase inhibitor was approved for genotype 1 treatment<sup>[4]</sup>. Daclatasvir another NS5A inhibitor was approved for genotype 2 and 3 on 2015<sup>[4]</sup>. The combination of NS5 and NS3 protease inhibitor elbasvir and grazoprevir with or without ribavirin for GT1 and 4 infection was approved on 2016<sup>[4]</sup>. However, the true revolution was the approval on January 2016 of sofosbuvir/velpatasvir (SOF/VEL). Velpatasvir is a second generation NS5A inhibitor administered with sofosbuvir as single pill fixed combination<sup>[4]</sup>. This was the first pangenotypic regimen to be used without ribavirin for 12 wk regardless of severity of liver disease even in patients with compensated cirrhosis<sup>[4]</sup>. The other pangenotypic regimen based on glecaprevir and pibrentasvir without the inclusion of a polymerase inhibitor to be administered as three pills daily initially for a variable duration of treatment of 8 or 12 wk and later for only 8 wk in patients with or without cirrhosis infected with genotypes 1, 2, 4 and for no cirrhotic genotype 3 and for 12 wk in patients with cirrhosis of genotype 3 was approved on 2017. The use of easy to manage and safe pangenotypic regimens provide not only effective treatment options but also the most powerful opportunity to achieve HCV elimination.

## MICRO-ELIMINATION IN DIFFERENT GEOGRAPHICAL LOCATIONS

Egypt has a very high burden of HCV infections and severe HCV-related liver diseases. In 2015, the reported prevalence of HCV chronic infection in the general population was 7%<sup>[12]</sup>. The national plan involved testing of 35 million Egyptians for HCV antibodies, over a 6-mo period. As a result, over 2.4 million Egyptians had been treated by 2019. This is an example of strong political commitment and industry support, allowing barriers to be removed. However, implementation of systems to track patients who were treated and cured, and to monitor the achievement of HCV elimination have not been properly developed. Pilot projects conducted at community level were recently completed<sup>[12]</sup>. From 2018, a test-and-treat strategy was started, targeting each individual aged 18-80 years in 73 villages under the auspices of 7



**Table 1 Treatment compounds available for hepatitis C virus infection**

	No cirrhosis		Cirrhosis (Child-Pugh class A)	
	Naïve	Experienced	Naïve	Experienced
HCV-1a, 1b, 2, 4, 5	SOF/VEL 12 wk	SOF/VEL 12 wk	SOF/VEL 12 wk	SOF/VEL 12 wk
	GLE/PIB 8 wk	GLE/PIB 8 wk	GLE/PIB 8 wk	GLE/PIB 12 wk
	GZR/ELB (GT 1b or 4 only) 12 wk	GZR/ELB (GT 1b or 4 only) 12 wk	GZR/ELB (GT 1b or 4 only) 12 wk	GZR/ELB (GT 1b or 4 only) 12 wk
	SOF/VEL/VOX 8 wk	SOF/VEL/VOX 8 wk	SOF/VEL/VOX 12 wk	SOF/VEL/VOX 12 wk
HCV-3	SOF/VEL 12 wk	SOF/VEL 12 wk	SOF/VEL 12 wk	SOF/VEL 12 wk
	GLE/PIB 8 wk	GLE/PIB 12 wk	GLE/PIB 8-12 wk	GLE/PIB 16 wk
	SOF/VEL/VOX 8 wk	SOF/VEL/VOX 8 wk	SOF/VEL/VOX 8 wk	SOF/VEL/VOX 8 wk

SOF: Sofosbuvir; VEL: Velpatasvir; GLE: Glecaprevir; PIB: Pibentavir; EBR: Elbasvir; GZR: Grazoprevir; VOX: Voxilaprevir; HCV: Hepatitis C virus.

governates. Free testing was offered, and patients were linked to care and offered free treatment during an educational and prevention campaign. Of the 200000 early tested individuals, 34000 tested positive for HCV antibodies and 14500 were treated. Of those, 99.9% completed the assigned treatment and 97% achieved viral clearance<sup>[13]</sup>.

Another example of a well-conducted HCV micro-elimination campaign comes from Iceland, where the HCV prevalence before the direct-acting antivirals revolution was low. Of 1000 persons infected with HCV in the country, nearly all have been diagnosed within a test-and-treat campaign started in 2016. Treatment was supported by pharmaceutical companies. So far, the island is on track to eliminate HCV by 2021<sup>[14]</sup>.

Georgia was the first European country that started an active national hepatitis elimination program tailored to local needs, based on the 5.4% HCV prevalence in the country. A nationwide case-finding integrated program was designed according to previous experiences in HIV prevention and a control program was initiated for HCV<sup>[15]</sup>. The HCV testing was integrated in the country's healthcare services for substance users, patients with mental health disorders, and HIV-coinfected subjects. The initial program expanded its scope in 2016, aiming for complete HCV elimination. Of the 150000 estimated HCV-infected subjects, 58% were diagnosed and 80% initiated the HCV treatment; the cure rate was 98.8% for those who completed it. Identification of HCV infection among the remaining population appears to be challenging. According to a recent model based on the Georgia data, in 2019, mortality was reduced by 14% and both prevalence and incidence were reduced by 37%<sup>[16]</sup>.

Among the other European countries, Scotland raised awareness on the impact of HCV through strong campaigns. This led to political support in scaling up the issue, with consequent reduction in HCV incidence and prevalence as well as in mortality. The improvements in harm reduction settings were mainly driven by the use of rapid and accurate diagnosis through dried blood spot testing. Given that there remain undiagnosed subgroups, the next challenge will be involving primary care physicians to increase the diagnosis rate and treatment access<sup>[17]</sup>. In Spain, with 46.9 million inhabitants and an HCV prevalence of 0.22%, a nationwide plan was initiated in 2016. According to the national data, while HCV testing has been performed in 90% of the general population, testing and linkage to care in at-risk groups remain suboptimal<sup>[18]</sup>.

In other countries, including some from Europe and the United States, the lack of comprehensive data on local situations in terms of prevalence and incidence, or the lack of good quality data in given high-risk groups-other than the lack of affordable tests or harm reductions programs-seem to be affecting achievement of the WHO's goal.

In particular, HCV elimination in low- and middle-income countries has been considered prohibitive until recently. Low-cost screening and drop of drug cost attained only recently are the cornerstone of a published experience involving Cambodia, India, Indonesia, Myanmar, Nigeria, Rwanda and Vietnam by intensive screening and decentralized programs this program has led to cure over 120 people with cure rate higher than 90%. This initiative-supported by Clinton Health Access-proves that the combination of political will, modest financial investment and adequate training pave the way for viral elimination even in the presence of limited

infrastructures<sup>[19]</sup>.

Exploring worldwide progresses in the path to achieve a testing cure protocol for HCV, special attention needed to be reserved to Pakistan. Pakistan has the second highest global burden of HCV infection worldwide with very low level of infection awareness<sup>[20]</sup>. The Government launched a National Hepatitis Framework for 2017-2021 planning to cure 95% of infected people with DAA (generic sofosbuvir in combination with ribavirin). This initiative resulted in a doubled number of treatments. Despite this success, the country should develop an extensive monitoring and evaluation system and should further implement the national plan<sup>[21]</sup>.

Moving to other countries, low testing rate and poor linkage to care are barriers to treatment in China. Due to its large population a considerable number of infected patients have not yet been discovered. In order to curb the spread of HCV infection and relate morbidity hospitals conduct blood-borne virus screening for inpatients<sup>[22]</sup>. In addition, several projects are exploring the impact of social media in increasing HCV infection awareness. Among them an interesting randomized controlled study based on crowdsourcing is ongoing in Shenzhen in the setting of primary care. This study aims at enrolling more than 1000 subjects older than 30 years. Subjects randomized into the active arm will receive promotional material by social media campaigns and their HCV testing uptake will be compared to those of the control group just attending the primary care departments and not involved in crowdsourcing activities<sup>[23]</sup>. A model of targeted HCV screening in past PWID has been adopted in Hong Kong since 2012. Although based on a limited number of subjects, this project represents the first example of targeted screening in Asia<sup>[24]</sup>.

## MICRO-ELIMINATION IN DIFFERENT SETTINGS

Prisons' and hospitals' emergency departments are considered appropriate settings for universal screening programs. HCV is common in prisons and guidelines recommend that HCV treatment should be offered to all HCV-infected prisoners. However, a significant proportion of incarcerated patients remain untreated and, once released, contribute to the spread of HCV through the local community. The incidence of HCV infection among prisoners is consequent to drug use and has been estimated globally as 16 *per* 100 person-years (1-34 years)<sup>[25]</sup>. Prisoners are difficult to engage, due to established high-risk behaviors and psychological disorders<sup>[26]</sup>. On the other hand, the specific context of prisons allows, after a rapid testing, a quick treatment plan implementation and completion, with the only limiting factor being a short permanence in the same prison<sup>[27]</sup>. A study conducted in Australia showed that of 562 HCV RNA-positive patients, 416 started treatment with different direct-acting antiviral agents. A sustained virological response (SVR) at 12 wk of 72% was attained, with patients lost to treatment after release accounting for this particular SVR rate. For patients able to complete treatment, per protocol analysis revealed higher SVR at 12 wk (SVR12) rates, up to 96% and comparable to those for the general population<sup>[28]</sup>. This study was based on a nurse-centered strategy.

Other models based on multidisciplinary networks and telemedicine have been explored in the United Kingdom<sup>[29]</sup>. Initiatives based on telemedicine were promoted and associated with a high number of treatments and treatment responders in Spain, in a large experiment conducted in "El Dueso" prison between May 2016 and July 2017. Overall, 847 inmates agreed to participate. Among them, 110 were HCV antibodies-positive and 86 HCV RNA-positive. Only 69 patients were treated and 66 of those completed the treatment, yielding a 96.9% SVR rate by intention-to-treat analysis<sup>[30]</sup>. In the United Kingdom, 128 of 266 individuals who started treatment based on telemedicine had available follow-up data. Of them, 87% achieved SVR; however, the proportion of patients who experienced reinfection was high<sup>[31]</sup>.

The feasibility of a test-and-treat strategy in incarcerated subjects has been highlighted recently in a study by Wong *et al*<sup>[32]</sup>. This study was based on a pangenotypic regimen, with minimal monitoring required. Of the 526 incarcerated adults treated with SOF/VEL in different countries across the world, SVR12 was attained by 437, representing 98.9% of those who completed treatment. A non-virological failure was reported in 82 individuals.

Another example of micro-elimination in a dedicated setting is provided by various interventions implemented in hospital emergency or surgical departments. Examples of these strategies are provided by studies conducted in Spain, in Italy and, more recently, in the United States. In a Spanish study conducted at the emergency department of Hospital Val d'Hebron on 5000 subjects, it was shown that the rate of

HCV antibodies positivity was 4%, higher than that in the general population; in contrast, the rate of active infections was low, with only 16% being HCV RNA-positive. Interestingly, the study showed that in 40% of cases, patients were unaware of their infectious condition<sup>[33]</sup>.

An Italian survey evaluated 11000 patients from the Venetian area. Each patient was tested upon admission to the surgery department<sup>[34]</sup>. Overall, 2% showed HCV antibodies positivity. Again, the rate was slightly higher than in the general population. Unfortunately, in this study, the results from HCV RNA data were not available for all and estimating active infections was not possible.

In the United States, an automated emergency department cohort screening for viral hepatitis was started in 2018 in New Jersey. The strategy was based on testing Baby Boomers until 2019 and was implemented by extending screening to at-risk in-patients from 2019 to 2020, with further expansion of the screening according to the Centers for Disease Control (CDC) screening guidelines from 2020 onwards. With the aid of a patient navigator, subjects testing HCV RNA-positive were linked to treatment. Universal screening results showed a 3.4% rate for HCV antibodies positivity and 0.9% of HCV RNA positivity among missed Baby Boomers subjects; the rates among non-Baby Boomers were 0.8% and 0.2%, respectively. Rates were higher for subjects aged 55-75 years. The combined cohort and universal screening led to identification of 195 infected individuals among the 37000 subjects who were screened to be linked to care<sup>[35]</sup>.

## MICRO-ELIMINATION IN DIFFERENT POPULATIONS

As reported by Degenhardt *et al.*<sup>[36]</sup>, the estimated prevalence of PWID by country is variable, with the highest rates reported in United States, Russia, Australia, Brazil, and the European Union. In the United States, PWID account for 60% of new HCV infections (60%) (CDC 2018), while in the European Union, 53.2% of PWID are reportedly HCV antibodies-positive. In the United Kingdom, 80% of individuals infected with HCV are PWID. Therefore, PWID are a key population for targeted micro-elimination strategies. In this population, pangenotypic regimens are associated with high rates of SVR, regardless of the recent use of substances<sup>[37]</sup>.

A large number of studies have investigated different strategies to eliminate HCV in this target population. Integrated approaches based on harm reduction in community settings to enable scale-up and use of simplified models based on low-cost diagnostics have been shown successful in improving screening, linkage to care, treatment access, and response. Studies have suggested that scale-up treatment in this population is mandatory<sup>[38]</sup>. A study conducted in Scotland in Tayside, a region with a population of 400000 and with an HCV prevalence of 0.55%-0.56%, explored enhanced testing and treatment service focusing on the HCV/HIV coinfection subpopulation. Of the total 2700 subjects, 2300 were diagnosed. In comparison to the pegylated-interferon treatment era, higher rates of patients were linked to treatment and cured. Multidisciplinary involvement included pharmacies, drug treatment centers and prisons, and was based on dedicated educational programs. Of the positive patients, 76% were treated<sup>[39]</sup>.

Multidisciplinary involvement has been pursued by other groups, including ours. In late 2019, our center launched a program promoting ad hoc transportation from "SERDS" (*i.e.*, Centers Taking Care of People with Substance Disorders) to prescribing centers, fast-track baseline evaluation at our center, and a close on-treatment monitoring at 15 different SERDS by the SERDS physician. Of 1500 patients screened, 239 (16%) were HCV RNA-positive, and all were linked to care and started treatment. Of them, 30% were active drug users and 70% were past drug users. High SVR12 rates were reported overall, being 98%. No reinfection was experienced during a short follow-up<sup>[40]</sup>.

Other initiatives, within substance users disorders programs, have targeted their efforts to decentralization. Among them, one-within a continuum program adopted in Philadelphia, United States to compare navigator *vs* embedded treatment models-recently showed that navigators are not sufficient to link HCV PWID to HCV cure<sup>[41]</sup>. By contrast, embedding HCV treatment within a substance use disorders (SUD) treatment program increases the number of patients linked to care.

The feasibility of HCV eradication in intravenous drug use in Italy has been evaluated within the San Patrignano Therapeutic community. Results showed that one-third of the resident patients were unaware of their HCV infection status. The rate of HCV antibodies-positive patients was 65%, and 238 of the 293 patients who tested

HCV RNA-positive started treatment. As in our study, no case of reinfection was experienced after a short follow-up<sup>[42]</sup>. The SVR rate was 96.6%. In both these studies, patients were treated with a pangenotypic regimen of SOF/VEL for 12 wk.

Decentralization of the confirmatory testing in harm-reduction sites has been recently implemented. Test-and-treat in point-of care at harm-reduction and addiction centers was proposed as a strategy to treat patients monitored at these centers or at addiction centers in Catalonia, Italy<sup>[43]</sup>. In both cases, an increase in the number of treatments was registered (+ 57% and + 19%, respectively), although SVR remained suboptimal and associated with a reinfection rate of 6% in harm-reduction centers<sup>[43]</sup>. In Georgia, a decentralizing screening strategy was shown to be associated with an increase in every step of the HCV care cascade<sup>[44]</sup>. In the United States, decentralization was implemented with an internist addiction medicine specialist evaluating opiate-dependent patients in a hepatology clinic. This co-localization model was associated with an improvement in the number of patients taking treatment, with an adherence rate of 87.4% and SVR of 98.9%<sup>[45]</sup>.

Among the higher risk groups, MSM cannot be forgotten. Data from population based on systems evaluating the progress through the cascade of care in this group are limited. In France, incidence continue to rise. Among 21,519 HIV positive, HCV negative patients followed between 2012 and 2016 in 16 centers, 218 first HCV infections occurred. Simultaneously, among 3392 patients with cured HCV infection, 74 reinfections were registered<sup>[46]</sup>. This data show why this is a target population for micro-elimination even despite the high uptake of DAA. As shown in a study from Switzerland, DAA use was able to halve HCV incidence in HIV positive MSM<sup>[47]</sup>.

Very recently a study was designed to compare progress in care and treatment in MSM and non-MSM with HCV infection living in British Columbia<sup>[48]</sup>. Slightly more MSM *vs* non-MSM received HCV RNA confirmatory testing (83% *vs* 82%) and initiated treatment. In 2019 as compared to 2012, treatment uptake among MSM increased significantly (63% *vs* 37%). SVR rates of 91% and 90% were registered among MSM and non-MSM, respectively. These results suggest that DAAs were associated with substantial improvement in progression across the different HCV care cascade steps.

---

## COVID-19 CHALLENGES CAN HELP HCV SCALE-UP

---

COVID-19 emergency is demonstrating a greater impact in HCV testing and diagnosis. In United States, at Boston Medical Center, testing decreased by 50, while new diagnoses decreased by more than 60%<sup>[49]</sup>. Consequently, nontraditional methods of preventive healthcare delivery as telemedicine and technology need to be used in order to emphasize the importance of prevention.

In African Countries integration of diagnostics platforms and implementation of digital technologies were rapidly promoted during the pandemic. Testing and treatment services are facilitating the continuation of essential prevention and are ensuring that people are not further marginalized. Although prevention interventions that require mass gathering are suspended, internet and postal systems may ensuring treatment distribution and help is assisting patients with self-testing<sup>[50]</sup>.

---

## CONCLUSION

---

The simplification of treatment access, and treatments tailored to the different settings are key aspects towards achieving HCV elimination. All the described interventions have demonstrated an ability to increase in one or more of the HCV cascade steps. The success of micro-elimination initiatives relies on correct targeting of a patient population or appropriate geographical context identification and patient setting.

The COVID-19 pandemic is affecting the results of some of these initiatives, requiring an extension of the timelines and further adjustments to reduce interpersonal contacts. However, it may also result in opportunities to spread awareness of the risks related to infectious disease and of the chances of combined screening programs for HCV and COVID-19.

As the WHO goal for HCV elimination seems hard to reach in the proposed timeframe, micro-elimination is a key alternative strategy. Provided that community involvement represents a free pass for a successful program, micro-elimination will ultimately lead to macro-elimination.



## REFERENCES

- 1 **Polaris Observatory HCV Collaborators.** Global prevalence and genotype distribution of hepatitis C virus infection in 2015: a modelling study. *Lancet Gastroenterol Hepatol* 2017; **2**: 161-176 [PMID: 28404132 DOI: 10.1016/S2468-1253(16)30181-9]
- 2 **Ward JW, Hinman AR.** What Is Needed to Eliminate Hepatitis B Virus and Hepatitis C Virus as Global Health Threats. *Gastroenterology* 2019; **156**: 297-310 [PMID: 30391470 DOI: 10.1053/j.gastro.2018.10.048]
- 3 **AASLD.** Call to Action for Liver Associations to Advance Progress Towards Viral Hepatitis Elimination: A Focus on Simplified Approaches to HCV Testing and Cure. AASLD 2019. [cited 26 October 2020]. Available from: <https://www.aasld.org/>
- 4 **European Association for the Study of the Liver;** Clinical Practice Guidelines Panel: Chair; EASL Governing Board representative; Panel members. EASL recommendations on treatment of hepatitis C: Final update of the series<sup>☆</sup>. *J Hepatol* 2020; **73**: 1170-1218 [PMID: 32956768 DOI: 10.1016/j.jhep.2020.08.018]
- 5 **Razavi H, Sanchez Gonzalez Y, Yuen C, Cornberg M.** Global timing of hepatitis C virus elimination in high-income countries. *Liver Int* 2020; **40**: 522-529 [PMID: 31815353 DOI: 10.1111/liv.14324]
- 6 **Wingrove C, Ferrier L, James C, Wang S.** The impact of COVID-19 on hepatitis elimination. *Lancet Gastroenterol Hepatol* 2020; **5**: 792-794 [PMID: 32730783 DOI: 10.1016/S2468-1253(20)30238-7]
- 7 **Blach S, Kondili LA, Aghemo A, Cai Z, Dugan E, Estes C, Gamkrelidze I, Ma S, Pawlotsky JM, Razavi-Shearer D, Razavi H, Waked I, Zeuzem S, Craxi A.** Impact of COVID-19 on global HCV elimination efforts. *J Hepatol* 2021; **74**: 31-36 [PMID: 32777322 DOI: 10.1016/j.jhep.2020.07.042]
- 8 **Lens S, Miralpeix A, Galvez M, Marto E, Gonzalez N, Rodriguez-Trajes S, Mariño Z, Saludes V, Reyes-Ureña J, Major X, Colom J, Fornis X.** Impact of the lockdown in an externalized HCV linkage-to-care model focusing on PWID patients with ongoing high risk practices. The Liver Meeting Digital Experience AASLD. 13-16 November 2020. [cited 26 December 2020]. Available from: [http://www.lingyuint.com/2020/2020\\_aasld.html](http://www.lingyuint.com/2020/2020_aasld.html)
- 9 **Bruggmann P, Litwin AH.** Models of care for the management of hepatitis C virus among people who inject drugs: one size does not fit all. *Clin Infect Dis* 2013; **57** Suppl 2: S56-S61 [PMID: 23884067 DOI: 10.1093/cid/cit271]
- 10 **Lazarus JV, Wiktor S, Colombo M, Thursz M;** EASL International Liver Foundation. Micro-elimination - A path to global elimination of hepatitis C. *J Hepatol* 2017; **67**: 665-666 [PMID: 28760329 DOI: 10.1016/j.jhep.2017.06.033]
- 11 **Lazarus JV, Safreed-Harmon K, Thursz MR, Dillon JF, El-Sayed MH, Elsharkawy AM, Hatzakis A, Jadoul M, Prestileo T, Razavi H, Rockstroh JK, Wiktor SZ, Colombo M.** The Micro-Elimination Approach to Eliminating Hepatitis C: Strategic and Operational Considerations. *Semin Liver Dis* 2018; **38**: 181-192 [PMID: 29986353 DOI: 10.1055/s-0038-1666841]
- 12 **Kandeel A, Genedy M, El-Refai S, Funk AL, Fontanet A, Talaat M.** The prevalence of hepatitis C virus infection in Egypt 2015: implications for future policy on prevention and treatment. *Liver Int* 2017; **37**: 45-53 [PMID: 27275625 DOI: 10.1111/liv.13186]
- 13 **Shiha G, Soliman R, Mikhail NNH, Easterbrook P.** An educate, test and treat model towards elimination of hepatitis C infection in Egypt: Feasibility and effectiveness in 73 villages. *J Hepatol* 2020; **72**: 658-669 [PMID: 31734097 DOI: 10.1016/j.jhep.2019.11.004]
- 14 **Olafsson S, Fridriksdottir RH, Tyrfinngsson T, Runarsdottir V, Hansdottir I, Bergmann OM, Björnsson ES, Johannsson B, Sigurdardottir B, Löve A, Baldvinsdottir GE, Löve T J, Sigmundsdottir G, Jósefsdóttir KS, Hernandez UB, Heimisdottir M, Gottfredsson M.** Iceland may already have reached the WHO 2030 targets for diagnosis and treatment of hepatitis C virus infection. Results from the Treatment as Prevention for Hepatitis C (TrapHepC) program. *J Hepatol* 2019; **70**: THU 412
- 15 **Gvinjilia L, Nasrullah M, Sergeenko D, Tsertsvadze T, Kamkamidze G, Butsashvili M, Gamkrelidze A, Imnadze P, Kvaratskhelia V, Chkhartishvili N, Sharvadze L, Drobeniuc J, Hagan L, Ward JW, Morgan J, Averhoff F.** National Progress Toward Hepatitis C Elimination - Georgia, 2015-2016. *MMWR Morb Mortal Wkly Rep* 2016; **65**: 1132-1135 [PMID: 27764081 DOI: 10.15585/mmwr.mm6541a2]
- 16 **Walker JG, Kuchuloria T, Sergeenko D, Fraser H, Lim AG, Shadaker S, Hagan L, Gamkrelidze A, Kvaratskhelia V, Gvinjilia L, Aladashvili M, Asatiani A, Baliashvili D, Butsashvili M, Chikovani I, Khonelidze I, Kirtadze I, Kuniholm MH, Otiaishvili D, Sharvadze L, Stvilia K, Tsertsvadze T, Zakalashvili M, Hickman M, Martin NK, Morgan J, Nasrullah M, Averhoff F, Vickerman P.** Interim effect evaluation of the hepatitis C elimination programme in Georgia: a modelling study. *Lancet Glob Health* 2020; **8**: e244-e253 [PMID: 31864917 DOI: 10.1016/S2214-109X(19)30483-8]
- 17 **Schröder SE, Pedrana A, Scott N, Wilson D, Kuschel C, Aufegger L, Atun R, Baptista-Leite R, Butsashvili M, El-Sayed M, Getahun A, Hamid S, Hammad R, 't Hoen E, Hutchinson SJ, Lazarus JV, Lesi O, Li W, Binti Mohamed R, Olafsson S, Peck R, Sohn AH, Sonderup M, Spearman CW, Swan T, Thursz M, Walker T, Hellard M, Howell J.** Innovative strategies for the elimination of viral hepatitis at a national level: A country case series. *Liver Int* 2019; **39**: 1818-1836 [PMID: 31433902 DOI: 10.1111/liv.14222]
- 18 **PEAHC.** Plan Estratégico para el abordaje de la hepatitis C en el sistema nacional de salud 2020. [cited 26 October 2020]. Available from: [http://www.msssi.gob.es/ciudadanos/enfLesiones/enfTrasmisibles/docs/plan\\_estrategico\\_hepatitis\\_C.pdf](http://www.msssi.gob.es/ciudadanos/enfLesiones/enfTrasmisibles/docs/plan_estrategico_hepatitis_C.pdf)



- 19 **Boeke CE**, Adesigbin C, Agwuocha C, Anartati A, Aung HT, Aung KS, Grover GS, Ngo D, Okamoto E, Ngwije A, Nsanzimana S, Sindhwani S, Singh G, Sun LP, Kinh NV, Waworuntu W, McClure C. Initial success from a public health approach to hepatitis C testing, treatment and cure in seven countries: the road to elimination. *BMJ Glob Health* 2020; **5** [PMID: [33328200](#) DOI: [10.1136/bmjgh-2020-003767](#)]
- 20 **Moin A**, Fatima H, Qadir TF. Tackling hepatitis C-Pakistan's road to success. *Lancet* 2018; **391**: 834-835 [PMID: [29508739](#) DOI: [10.1016/S0140-6736\(18\)30462-8](#)]
- 21 **Mahmood H**, Qureshi H, Glass N, Averhoff F. Optimizing medicines and treatment regimens for hepatitis C patients in Pakistan. World Hepatitis Summit; November 1-3, 2017; Sao Paulo, Brazil, 2017: 4a. [cited 10 October 2020]. Available from: [https://www.researchgate.net/publication/327361674\\_Optimizing\\_medicines\\_and\\_treatment\\_regimens\\_for\\_hepatitis\\_C\\_patients\\_in\\_Pakistan](https://www.researchgate.net/publication/327361674_Optimizing_medicines_and_treatment_regimens_for_hepatitis_C_patients_in_Pakistan)
- 22 **Liu L**, Xu H, Hu Y, Shang J, Jiang J, Yu L, Zhao C, Zhang D, Zhang X, Li J, Li W, Wu Y, Hu D, Wang X, Zhao Q, Zhang Q, Luo W, Chen J, Zhou W, Niu J. Hepatitis C screening in hospitals: find the missing patients. *Virol J* 2019; **16**: 47 [PMID: [30992019](#) DOI: [10.1186/s12985-019-1157-1](#)]
- 23 **Wong WCW**, Yang NS, Li J, Li H, Wan EYF, Fitzpatrick T, Xiong Y, Seto WK, Chan P, Liu R, Tang W, Tucker JD. Crowdsourcing to promote hepatitis C testing and linkage-to-care in China: a randomized controlled trial protocol. *BMC Public Health* 2020; **20**: 1048 [PMID: [32615951](#) DOI: [10.1186/s12889-020-09152-z](#)]
- 24 **Wong VW**, Wong GL, Chim AM, Cheng TF, Cheung SW, Lai CM, Szeto KJ, Tsang S, Wu SH, Yan KK, Hui AY, Yiu DC, Wu BB, Cheung D, Chung CS, Lai CW, Chan HL. Targeted hepatitis C screening among ex-injection drug users in the community. *J Gastroenterol Hepatol* 2014; **29**: 116-120 [PMID: [24033786](#) DOI: [10.1111/jgh.12355](#)]
- 25 **Larney S**, Kopinski H, Beckwith CG, Zaller ND, Jarlais DD, Hagan H, Rich JD, van den Bergh BJ, Degenhardt L. Incidence and prevalence of hepatitis C in prisons and other closed settings: results of a systematic review and meta-analysis. *Hepatology* 2013; **58**: 1215-1224 [PMID: [23504650](#) DOI: [10.1002/hep.26387](#)]
- 26 **Fazel S**, Baillargeon J. The health of prisoners. *Lancet* 2011; **377**: 956-965 [PMID: [21093904](#) DOI: [10.1016/S0140-6736\(10\)61053-7](#)]
- 27 **Stöver H**, Meroueh F, Marco A, Keppler K, Saiz de la Hoya P, Littlewood R, Wright N, Nava F, Alam F, Walcher S, Somaini L. Offering HCV treatment to prisoners is an important opportunity: key principles based on policy and practice assessment in Europe. *BMC Public Health* 2019; **19**: 30 [PMID: [30621658](#) DOI: [10.1186/s12889-018-6357-x](#)]
- 28 **Papaluca T**, McDonald L, Craigie A, Gibson A, Desmond P, Wong D, Winter R, Scott N, Howell J, Doyle J, Pedrana A, Lloyd A, Stooze M, Hellard M, Iser D, Thompson A. Outcomes of treatment for hepatitis C in prisoners using a nurse-led, statewide model of care. *J Hepatol* 2019; **70**: 839-846 [PMID: [30654067](#) DOI: [10.1016/j.jhep.2019.01.012](#)]
- 29 **Ustianowski A**, White M, Bell S, Bennet J, Pavey K, O'Connell L, Smiles J, Hammond S, Horne M, Roberts D, Vilar FJ. Rapid test & treat program successfully facilitating hepatitis C micro-elimination in a women's prison. *EASL* 2020; SAT280
- 30 **Cuadrado A**, Llerena S, Cobo C, Pallás JR, Mateo M, Cabezas J, Fortea JJ, Alvarez S, Pellón R, Crespo J, Echevarría S, Ayasa R, Setién E, Lopez-Hoyos M, Crespo-Facorro B, Agüero J, Chueca N, García F, Calleja JL. Microenvironment Eradication of Hepatitis C: A Novel Treatment Paradigm. *Am J Gastroenterol* 2018; **113**: 1639-1648 [PMID: [29946175](#) DOI: [10.1038/s41395-018-0157-x](#)]
- 31 **Bhandari R**, Morey S, Hamoodi A, Thompson C, Jones D, Hewett M, Hunter E, Taha Y, McPherson S. High rate of hepatitis C reinfection following antiviral treatment in the North East England Prisons. *J Viral Hepat* 2020; **27**: 449-452 [PMID: [31749225](#) DOI: [10.1111/jvh.13240](#)]
- 32 **Wong A**, Jimenez-Mutiloa E, Di Marco V, Perez F, Macedo G, Brixko C, Ranieri R, Campanale F, Bascia A, Fernandez-Rodriguez CM, De Ledinghen V, Maida I, Mangia A, Barrett L, Teti E, Figueiredo LM, AmadoLEM, Retortillo MG, Borgia SM, Mertens M, Hernandez C, Ntalla I, Vanstraelen K, Rosati S. Value of SOF/VEL as pangenotypic pan fibrotic HCV treatment in implementing a test and treat strategy in prisons: real-world care management from 6 countries. *Hepatology* 2020; **72**: 944
- 33 **Llaneras J**, Barreira-Díaz A, Uriona S, Rando A, Barciela MR, Velasquez F, Rodríguez-Frías F, Rodríguez-Frías F, Arranz M, Esteban-Mur R, Ferret MAB. A hospital free of hepatitis C: hepatitis C virus screening program in an emergency department of a tertiary hospital of a high-income country. *Hepatology* 2020; **72**: 858
- 34 **Caroli A**, Franceschet I, Fasci-Spurio F, Girardi L, Cappuccio R, Checchin D, Lamboglia F, Forti A, Scarpato C. Is hospital admission an ideal condition for HCV condition for HCV screening? *EASL* 2020; SAT278
- 35 **Wang SH**, Brogden R. Automated viral Hepatitis (HCV and HBV) screening: lesson on expansion and sustainability amidst the COVID-19 pandemic. *Hepatology* 2020; **72**: 947
- 36 **Degenhardt L**, Peacock A, Colledge S, Leung J, Grebely J, Vickerman P, Stone J, Cunningham EB, Trickey A, Dumchev K, Lynskey M, Griffiths P, Mattick RP, Hickman M, Larney S. Global prevalence of injecting drug use and sociodemographic characteristics and prevalence of HIV, HBV, and HCV in people who inject drugs: a multistage systematic review. *Lancet Glob Health* 2017; **5**: e1192-e1207 [PMID: [29074409](#) DOI: [10.1016/S2214-109X\(17\)30375-3](#)]
- 37 **Hajarizadeh B**, Cunningham EB, Reid H, Law M, Dore GJ, Grebely J. Direct-acting antiviral treatment for hepatitis C among people who use or inject drugs: a systematic review and meta-analysis. *Lancet Gastroenterol Hepatol* 2018; **3**: 754-767 [PMID: [30245064](#) DOI: [10.1016/S2468-2667\(18\)30100-0](#)]

- 10.1016/S2468-1253(18)30304-2]
- 38 **Fraser H**, Zibbell J, Hoerger T, Hariri S, Vellozzi C, Martin NK, Kral AH, Hickman M, Ward JW, Vickerman P. Scaling-up HCV prevention and treatment interventions in rural United States-model projections for tackling an increasing epidemic. *Addiction* 2018; **113**: 173-182 [PMID: 28734093 DOI: 10.1111/add.13948]
  - 39 **Byrne C**, Robinson E, Rae N, Dillon JF. Toward microelimination of hepatitis C and HIV coinfection in NHS Tayside, Scotland: Real-world outcomes. *Health Sci Rep* 2020; **3**: e191 [PMID: 33033752 DOI: 10.1002/hsr2.191]
  - 40 **Mangia A**, Campanozzi F, Cotugno R, Canosa A, De Giorgi A, Piazzolla AV, Iannuzziello C, Augello N, Cocomazzi G, campanozzi F. Intensified screening, diagnosis and linkage to care program for SUD patients is associated with improvement in HCV care cascade. *Hepatology* 2020; **72**: 970
  - 41 **Addish E**, Zellman H, Kuncio D, Kostman J, Viner K, Trooskin S. Microelimination among PWUD: outcomes of a patient navigation model vs an embedded treatment mode. *Hepatology* 2020; **72**: 657
  - 42 **Boschini A**, Piselli P, Smacchia C, Poletti R, Begnini M, Ottogalli P, Cimaglia C, Parracino MP, Girardi E. HCV treatment and reinfection risk in injecting drug users in residential treatment setting for drug addiction. San Patrignano HCV-free. *Hepatology* 2020; **72**: 917
  - 43 **Forns X**, Colom J, Garcia-Retortillo M, Quer JC, Lens S, Dominguez-Hernandez R, Casado M. Point of care hepatitis C testing and treating strategy in people who inject drugs in Harm reduction and addiction centers for hepatitis C elimination. The Liver Meeting Digital Experience AASLD. 13-16 November 2020. [cited 26 December 2020]. Available from: <https://www.aasld.org/event/liver-meeting>
  - 44 Erratum for Research Article: "Single-cell RNA-seq and computational analysis using temporal mixture modeling resolves  $T_H1/T_{FH}$  fate bifurcation in malaria" by T. Lönnberg, V. Svensson, K. R. James, D. Fernandez-Ruiz, I. Sebina, R. Montandon, M. S. F. Soon, L. G. Fogg, A. S. Nair, U. N. Liligeto, M. J. T. Stubbington, L.-H. Ly, F. Otzen Bagger, M. Zwiessele, N. D. Lawrence, F. Souza-Fonseca-Guimaraes, P. T. Bunn, C. R. Engwerda, W. R. Heath, O. Billker, O. Stegle, A. Haque, S. A. Teichmann. *Sci Immunol* 2018; **3** [PMID: 29523583 DOI: 10.1126/sciimmunol.aat1469]
  - 45 **Nallapeta NS**, Jindal R, Edwards J, Martinez A. HCV micro-elimination: implementation of the internist-addiction medicine-hepatology colocalization (IAHC) model. *INHSU* 2019; 118
  - 46 **Cotte L**, Huleux T, Raffi F, Rey D, Delobel P, Gagneux-Brunon A, Jacomet C, Palich R, Laroche H, Cabié A, Hoen B, Chidiac C, Pradat P. HCV incidence is still increasing in French HIV-infected MSM. 25th Conference on Retroviruses and Opportunistic Infections (CROI). 4-7 March 2018. Boston. Abstract 591
  - 47 **Braun DL**, Hampel BH, Nguyen H. A treatment as prevention trial to eliminate HCV in HIV+MSM: the Swiss HCV free Trial. 25th Conference on Retroviruses and Opportunistic Infections (CROI). 4-7 March 2018. Boston. Abstract 81LB
  - 48 **Janjua N**, Yu A, Wilton J, Adu P, Pearce M, Samji H, McKee G. Population-level hepatitis C cascade of care among men who have sex with men in British Columbia, Canada. *J Hepatol* 2020; **73**: S32 [DOI: 10.1016/S0168-8278(20)30617-6]
  - 49 **Sperring H**, Ruiz-Mercado G, Schechter-Perkins EM. Impact of the 2020 COVID-19 Pandemic on Ambulatory Hepatitis C Testing. *J Prim Care Community Health* 2020; **11**: 2150132720969554 [PMID: 33225792 DOI: 10.1177/2150132720969554]
  - 50 **IFRC**. Community-based health care, including outreach and campaigns, in the context of the COVID-19 pandemic. [cited 26 October 2020]. Available from: <https://www.unicef.org/media/68811/file/Guidance-Community-based>



## Coronavirus disease 2019 severity in obesity: Metabolic dysfunction-associated fatty liver disease in the spotlight

Isabela Macedo Lopes Vasques-Monteiro, Vanessa Souza-Mello

**ORCID number:** Isabela Macedo Lopes Vasques-Monteiro [0000-0003-1729-3201](https://orcid.org/0000-0003-1729-3201); Vanessa Souza-Mello [0000-0002-2510-9569](https://orcid.org/0000-0002-2510-9569).

**Author contributions:** Souza-Mello V conceived the idea for the manuscript; Vasques-Monteiro IML and Souza-Mello V performed the literature search and data analysis and drafted the manuscript; Vasquez-Monteiro IML designed the figures; Souza-Mello V critically revised the work; all authors read and approved the final version of the manuscript.

**Supported by** Conselho Nacional de Desenvolvimento Científico e Tecnológico (Brazil), No. 305867/2017-2; and Fundação Carlos Chagas Filho de Amparo à Pesquisa do Estado do Rio de Janeiro, No. E-26/202.657/2018.

**Conflict-of-interest statement:** The authors have nothing to disclose.

**Open-Access:** This article is an open-access article that was selected by an in-house editor and fully peer-reviewed by external reviewers. It is distributed in accordance with the Creative Commons Attribution NonCommercial (CC BY-NC 4.0) license, which permits others to distribute, remix, adapt, build upon this work non-commercially, and license their derivative works

**Isabela Macedo Lopes Vasques-Monteiro, Vanessa Souza-Mello**, Anatomy, Rio de Janeiro State University, Rio de Janeiro 20551030, Brazil

**Isabela Macedo Lopes Vasques-Monteiro**, Food Science and Technology, Federal University of the State of Rio de Janeiro, Rio de Janeiro 22290250, Brazil

**Vanessa Souza-Mello**, Laboratory of Morphometry, Metabolism, and Cardiovascular Diseases, Biomedical Center, Institute of Biology, Anatomy Department, Rio de Janeiro State University, Rio de Janeiro 20551030, Brazil

**Corresponding author:** Vanessa Souza-Mello, PhD, Associate Professor, Laboratory of Morphometry, Metabolism, and Cardiovascular Diseases, Biomedical Center, Institute of Biology, Anatomy Department, Rio de Janeiro State University, Blvd. 28 de setembro 87, Rio de Janeiro 20551030, Brazil. [souzamello.uerj@gmail.com](mailto:souzamello.uerj@gmail.com)

### Abstract

The coronavirus disease 2019 (COVID-19) outbreak has drawn the scientific community's attention to pre-existing metabolic conditions that could aggravate the infection, causing extended viral shedding, prolonged hospitalization, and high death rates. Metabolic dysfunction-associated fatty liver disease (MAFLD) emerges as a surrogate for COVID-19 severity due to the constellation of metabolic alterations it entails. This review outlines the impact MAFLD exerts on COVID-19 severity in obese subjects, besides the possible mechanistic links to the poor outcomes. The data collected showed that MAFLD patients had poorer COVID-19 outcomes than non-MAFLD obese subjects. MAFLD is generally accompanied by impaired glycemic control and systemic arterial hypertension, both of which can decompensate during the COVID-19 clinical course. Also, MAFLD subjects had higher plasma inflammatory marker concentrations than non-MAFLD subjects, which might be related to an intensified cytokine storm syndrome frequently associated with the need for mechanical ventilation and death. In conclusion, MAFLD represents a higher risk than obesity for COVID-19 severity, resulting in poor outcomes and even progression to non-alcoholic steatohepatitis. Hepatologists should include MAFLD subjects in the high-risk group, intensify preventive measurements, and prioritize their vaccination.

**Key Words:** Metabolic dysfunction-associated fatty liver disease; Obesity; COVID-19; Severity; Cytokine storm syndrome

on different terms, provided the original work is properly cited and the use is non-commercial. See: <http://creativecommons.org/licenses/by-nc/4.0/>

**Manuscript source:** Invited manuscript

**Specialty type:** Gastroenterology and hepatology

**Country/Territory of origin:** Brazil

**Peer-review report's scientific quality classification**

Grade A (Excellent): 0  
Grade B (Very good): B  
Grade C (Good): 0  
Grade D (Fair): 0  
Grade E (Poor): 0

**Received:** January 10, 2021

**Peer-review started:** January 10, 2021

**First decision:** February 11, 2021

**Revised:** February 15, 2021

**Accepted:** March 22, 2021

**Article in press:** March 22, 2021

**Published online:** April 28, 2021

**P-Reviewer:** Ma J

**S-Editor:** Zhang L

**L-Editor:** Filipodia

**P-Editor:** Liu JH



©The Author(s) 2021. Published by Baishideng Publishing Group Inc. All rights reserved.

**Core Tip:** It is notorious that obesity represents a risk for coronavirus disease 2019 (COVID-19) severity. However, COVID-19 often causes liver alterations or provokes the progression of pre-existing liver diseases. This review outlines the role of metabolic dysfunction-associated fatty liver disease in COVID-19 severity. The evidence available thus far supports the notion that metabolic dysfunction-associated fatty liver disease represents a more intense risk than obesity for hospitalization, extended viral shedding, and death. A pro-inflammatory state with inflammasome activation, implying increased susceptibility to cytokine storm syndrome, underlies these findings and emerges as, in addition to massive vaccination of subjects with liver diseases, potential targets for therapeutic strategies.

**Citation:** Vasques-Monteiro IML, Souza-Mello V. Coronavirus disease 2019 severity in obesity: Metabolic dysfunction-associated fatty liver disease in the spotlight. *World J Gastroenterol* 2021; 27(16): 1738-1750

**URL:** <https://www.wjgnet.com/1007-9327/full/v27/i16/1738.htm>

**DOI:** <https://dx.doi.org/10.3748/wjg.v27.i16.1738>

## INTRODUCTION

The infection caused by the coronavirus severe acute respiratory syndrome coronavirus 2 (SARS-CoV-2) [coronavirus disease 2019 (COVID-19), *Beta-coronavirus* genus, *Coronaviridae* family] was declared as a pandemic in March 2020 by the World Health Organization and caused an unprecedented burden to health systems worldwide because of its harmful evolution to severe acute respiratory syndrome<sup>[1,2]</sup>. Although most cases are asymptomatic, this fact facilitated the rapid viral spread worldwide, resulting in overloaded hospitals due to the extended hospitalizations and the frequent need for mechanical ventilation that severe COVID-19 requires<sup>[3,4]</sup>. From December 2019 to February 14, 2021, COVID-19 caused almost 2.4 million deaths, and more than 108 million confirmed cases in 222 countries or territories<sup>[1]</sup>.

The SARS-CoV-2 relies on binding to the angiotensin-converting enzyme 2 (ACE2) receptor to enter target cells and start viral shedding<sup>[5]</sup>. Much as the infection frequently happens through the nasopharyngeal epithelium and has the lungs as the chief target with respiratory commitment, COVID-19 represents a systemic disease with adverse cardiac, circulatory, and cerebral outcomes after hematogenic propagation and virus neurotropism for the vagus nerve that links lungs to the central nervous system<sup>[6-8]</sup>. Of note, the presence of ACE2 receptors in the brush border of intestinal enterocytes and cholangiocytes makes possible the occurrence of gastrointestinal symptoms and aggravation of pre-existing metabolic diseases<sup>[9,10]</sup>. **Figure 1** summarizes the most common infection and propagation pathways of SARS-CoV-2 with adverse effects in the human body.

In this regard, overweight emerged as a high-risk factor to hospitalization due to COVID-19, surpassed only by age  $\geq 65$  in the New York population<sup>[11]</sup>, emphasizing the high risk of severe COVID-19. Body mass gain yields metabolic alterations that start in the adipose tissue, with hypertrophy and hyperplasia as attempts to buffer excessive energy intake by fat storage<sup>[12]</sup>. In the long run, adipogenesis capacity exhausts, and the existing enlarged adipocytes trigger lipolysis to manage a continuous lipid accumulation through lipogenesis<sup>[13,14]</sup>. At this stage, excessive non-esterified fatty acids (NEFAs) are diverted to other organs like the liver and drive steatosis<sup>[15]</sup>.

Hepatic steatosis is known as the hepatic manifestation of metabolic syndrome. Hence, metabolic disturbances such as insulin resistance, systemic arterial hypertension, and meta-inflammation, typical from obesity, coexist with this hepatic impairment<sup>[15,16]</sup>. Therefore, it was recently renamed metabolic dysfunction-associated fatty liver disease (MAFLD) as it represents better the constellation of metabolic impairments involved in its etiology than the former acronym non-alcoholic fatty liver disease<sup>[17]</sup>.

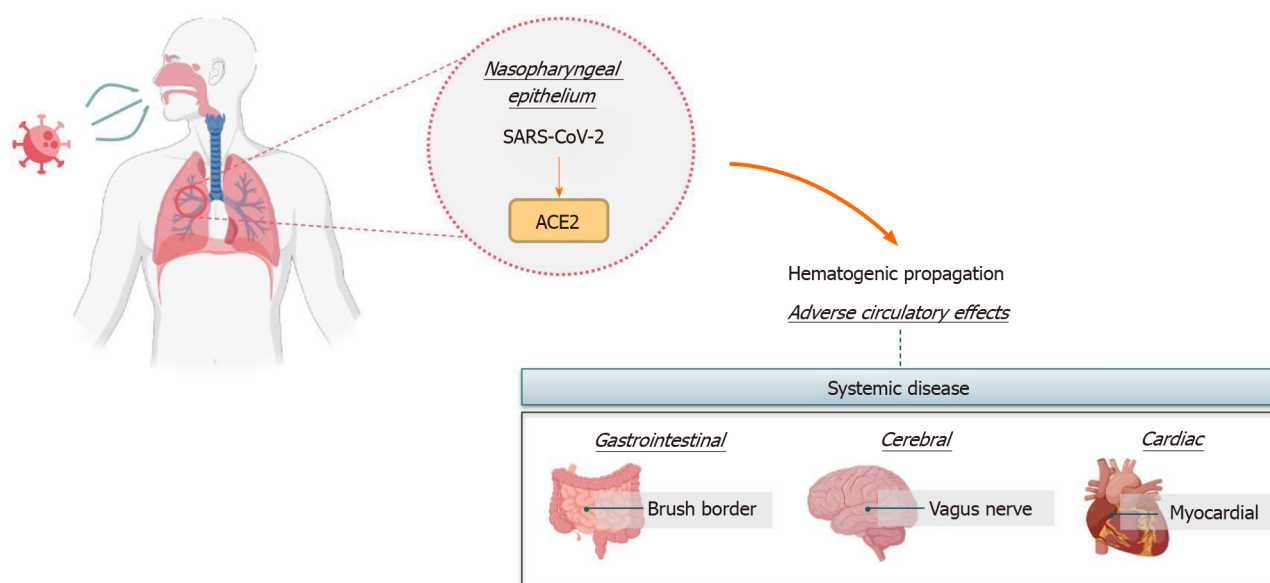


**Figure 1** Most common infection and propagation pathways of severe acute respiratory syndrome coronavirus 2 in the human body. SARS-CoV-2: Severe acute respiratory syndrome coronavirus 2; ACE2: Angiotensin-converting enzyme 2.

MAFLD in obesity comprises lipotoxic effects on the liver by proinflammatory adipokines that influence hepatic energy metabolism in an endocrine fashion<sup>[18]</sup>. The inflamed adipose tissue has been linked to enhanced viral systemic spread, entry, and viral shedding in COVID-19 obese subjects<sup>[19]</sup>. This hypothesis complies with an intensified cytokine storm in obese patients with COVID-19, explaining the poor outcomes<sup>[20]</sup>.

Among the metabolic impairments caused by excessive body fat, pre-existing MAFLD can result in COVID-19 patients being more prone to hospitalization and worsening metabolic conditions<sup>[21]</sup>. This review outlined the impact MAFLD exerts on COVID-19 severity in obese subjects in addition to the possible mechanistic links to poor outcomes. The information gathered relating to COVID-19 was that available on PubMed from the beginning of the pandemic until the end of 2020.

## OBESITY AND FATTY LIVER: EPIDEMIOLOGY AND PATHOGENESIS

MAFLD is the most common chronic hepatic disease worldwide. Its global prevalence is around 25%, with the highest prevalence in the Middle East (31.79%) and South America (30.45%)<sup>[22]</sup>. MAFLD is not a disease exclusive of obesity, but obese subjects fall victim to fatty liver more frequently, as their insulin-resistant and pro-inflammatory adipokine profile converge to the accumulation of ectopic fat<sup>[18,23]</sup>. Recent evidence shows the presence of obesity among 51.34% of MAFLD patients and 81.83% of patients with non-alcoholic steatohepatitis (NASH)<sup>[22]</sup>. Although MAFLD silently initiates without symptoms, its harmful progression towards NASH (with hepatic fibrosis), cirrhosis, or hepatocellular carcinoma challenges the scientific community to understand its metabolic basis.

The pathogenesis of fatty liver is multifactorial and linked to diet, metabolic factors, intestinal microorganisms, and genetics. Exposure of hepatocytes to high levels of lipids and carbohydrates, usually included in the diet of obese individuals, leads to glucolipotoxicity and predisposes to MAFLD. Excessive circulating NEFAs come from accelerated lipolysis and reduced fatty acid uptake in subcutaneous adipose tissue, triggering ectopic fat accumulation (in the liver, skeletal muscle) and, therefore, insulin resistance in multiple organs<sup>[24]</sup>. The release of NEFAs from dysfunctional and insulin-resistant adipocytes causes lipotoxicity, induced by the ectopic accumulation of toxic metabolites stemmed from triglycerides. Hence, inflammatory pathways are activated, and cellular dysfunction occurs with liver incapacity to eliminate excessive NEFAs, ending up in lipoapoptosis, an essential feature of NASH<sup>[18]</sup>.

Hepatic steatosis comprises approximately 60% of hepatic triglycerides from adipose tissue, 25% from *de novo* lipogenesis and 15% from dietary lipids<sup>[25]</sup>. Moreover, visceral adipose tissue is more closely related to the fatty liver than subcutaneous



adipose tissue, possibly because the former is more resistant to insulin than the latter<sup>[26]</sup>. Increasing evidence shows that during adipose tissue expansion in obesity, there are changes in the expression and secretion of adipokines, favoring pro-inflammatory mediators for the development of MAFLD, progression to NASH, and possible development of liver cirrhosis<sup>[27]</sup>. Leptin and adiponectin are the adipokines widely described in the literature as influences on fatty liver development.

In animal models of MAFLD, leptin seems to have a double action: It can protect from hepatic steatosis, at least in the early stages of the disease, but it also can act as an inflammatory and fibrogenic factor when the disease persists or progresses, that is when the mechanisms of counterweight do not limit it<sup>[28-30]</sup>. In this sense, leptin can directly increase the production of pro-inflammatory cytokines, such as tumor necrosis factor (TNF)- $\alpha$ , interleukin (IL)-6, IL-12, and IL-18, the chemokines IL-8 and monocyte chemoattractant protein 1, and the lipid mediators prostaglandin E2, leukotrienes, and LTB4, being responsible for the noxious MAFLD progression<sup>[26]</sup>. Persisting hyperleptinemia promotes liver inflammation and fibrosis as the disease progresses to NASH.

On the contrary, adiponectin decreases as the fat mass increases. At physiological conditions, adiponectin exerts an anti-steatotic effect on hepatocytes by increasing beta-oxidation, while decreasing gluconeogenesis, fatty acid input to the liver, and *de novo* lipogenesis. Furthermore, high molecular weight adiponectin isoform has anti-inflammatory properties like TNF- $\alpha$  blockade and downregulation, resulting in insulin resistance alleviation<sup>[29]</sup>. In the case of positive energy balance and overweight onset, this critical balance is disrupted towards the side of TNF- $\alpha$ , contributing to chronic low-grade inflammation, insulin resistance, and MAFLD<sup>[26]</sup>. In humans, patients with fatty liver exhibit low adiponectin concentrations, whereas control subjects show high adiponectin concentrations. However, the adiponectin concentrations are even lower in patients with NASH than in MAFLD. It can be argued that, initially, adipokine actions can limit hepatic steatosis, but as adipose tissue expands, adipokine changes become harmful and contribute to MAFLD progression<sup>[18]</sup>.

An innovative concept proposes that the gut-liver axis plays a crucial role in the pathogenesis and progression of MAFLD<sup>[31]</sup>. Although there are some controversies, animal and human studies show that gut microbiota from obese subjects comprises an increase in the relative abundance of firmicutes followed by a decrease of bacteroidetes<sup>[32]</sup>. Moreover, a higher prevalence of gram-negative bacteria, such as proteobacteria, and reduced phylum-level diversity are usual features in non-alcoholic fatty liver disease patients<sup>[33]</sup>. Changes in the gut microbiota in obesity disrupt the intestinal endothelial barrier, eliciting systemic bacterial translocation and hepatic inflammation by microbiota-related endotoxins and short-chain fatty acids that reach the liver through the portal vein<sup>[26]</sup>.

Concerning a possible genetic predisposition to MAFLD, the adipose tissue of obese patients with fatty liver has upregulation of pro-inflammatory genes and macrophages-producing cytokines compared to obese subjects that do not develop MAFLD<sup>[34]</sup>. This observation raises the hypothesis of a genetic polymorphism that explains why some obese individuals develop MAFLD, while others do not<sup>[35]</sup>. Briefly, an allele in the *PNPLA3* gene is a surrogate for the MAFLD onset and hepatic inflammation<sup>[36]</sup>. Other genes like *FDFT1*, *TM6SF2*, *GCKR*, and *MBAT7* have already been linked to the progression of MAFLD<sup>[37]</sup>. However, the complete identity of "MAFLD related to genetics" still needs to be further investigated.

## CORONAVIRUS DISEASE 2019 PROGNOSIS IN METABOLIC DYSFUNCTION-ASSOCIATED FATTY LIVER DISEASE PATIENTS

### *Hepatic outcomes of COVID-19*

The clinical course of COVID-19 encompasses elevated aspartate aminotransferase and alanine aminotransferase combined with a mild rise in bilirubin levels<sup>[38]</sup>. A study in China found that 37.3% of patients had an abnormal liver function at hospital admission<sup>[39]</sup>. In Mexico, 96.8% of patients ( $n = 150$ ) had a liver impairment but without an association between abnormal liver function tests and mortality<sup>[40]</sup>. A Chinese study has suggested aspartate aminotransferase as a promising marker to predict hospital stay, with higher values suggestive of prolonged periods. However, this information might not apply to different populations and should be better addressed<sup>[41]</sup>.

Concerning histological liver changes, a post-mortem study in Belgium revealed histological alterations in all 14 deceased COVID-19 patients, with central lobular necrosis and portal inflammation as the most frequent hepatic histological damages<sup>[42]</sup>.

In agreement with this, COVID-19 patients with acute respiratory distress syndrome showed mild microvesicular steatosis and lobular and portal activity in China<sup>[43]</sup>. The most common post-mortem histological findings in 40 North Americans that died from COVID-19 were fatty liver (75%), mild acute hepatitis (50%), and portal inflammation (50%). However, the fat distribution pattern was not typical of MAFLD and might stem from the administration of steroids during hospitalization<sup>[44]</sup>.

In line with these previous findings, a Chinese study showed 96% of hepatocellular liver injury among COVID-19 hospitalized subjects, with 50% of them presenting liver injury at hospital admission and 75.2% showing liver injury during hospital stay<sup>[45]</sup>. This observation emphasizes that not only could the pre-existing hepatic disease produce a severe form of COVID-19, but the virus itself can trigger liver damage. Indeed, it is hard to distinguish whether liver injury during hospital stay stemmed from the COVID-19 infection or some drugs used as attempts to stop viral replication<sup>[45,46]</sup>. Hepatotoxic effects of paracetamol, lopinavir/ritonavir, remdesivir, chloroquine, tocilizumab, and uminefovir can cause microvesicular steatosis and mild hepatic inflammation<sup>[47]</sup>. These findings are depicted in **Figure 2**.

## **METABOLIC DYSFUNCTION-ASSOCIATED FATTY LIVER DISEASE IN CORONAVIRUS DISEASE 2019 PATIENTS: INCREASED SEVERITY WHEN COMPARED TO OBESITY?**

MAFLD is considered a pre-existing condition that turns individuals more vulnerable to COVID-19 infection and virus-related complications. Furthermore, these patients may have an increased risk of MAFLD to NASH progression, a long-term consequence of viral infection<sup>[48]</sup>. As MAFLD is frequently associated with overweight/obesity, it is sometimes hard to separate the single effect each one exerts on COVID-19 severity. Herein, we outlined the most recent evidence after almost 1 year from the beginning of the pandemic.

The presence of MAFLD could predict severe COVID-19 (more than 2-fold prevalence) and critical illness in patients younger than 60 years old in China<sup>[49]</sup>, in addition to longer viral shedding time (17.5 d *vs* 12.1 d on average)<sup>[45]</sup>. Furthermore, Chinese MAFLD patients without type 2 diabetes showed a 4-fold high risk for severe COVID-19, and a 12% increase in the risk for severe COVID-19 for each 1-unit augmentation in body mass index<sup>[50]</sup>. Obesity conferred a 6 times greater risk of severe infection in Chinese patients with MAFLD [odds ratio (OR) did not adapt 5.77,  $P = 0.029$ ]. The association of obesity with COVID-19 severity remained after adjusting for many factors (age, sex, smoking habits, diabetes, hypertension, and dyslipidemia, OR compatible 6.32,  $P = 0.033$ )<sup>[51]</sup>.

Conversely, a study considering a large sample in the United States pointed out MAFLD/NASH as a greater risk for hospitalization than obesity itself<sup>[52]</sup>. In line with this, increased rates of COVID-19 clinical severity among MAFLD patients have been observed even after controlling for obesity, suggesting that the effect of MAFLD on disease severity may be more expressive than increased body mass index<sup>[53]</sup>. MAFLD/NASH might have a significant role in maximizing chronic inflammation and hypercoagulability, emerging as a pivotal surrogate for severe COVID-19 cases<sup>[52]</sup>.

A study in Brazil showed that hepatic steatosis was found in computed tomography (CT) among 31.9% of COVID-19 positive patients, while only 7.1% of COVID-19 negative subjects showed hepatic steatosis. The OR was 4.698 after adjusting for age and sex, but they did not evaluate the severity or poor clinical outcomes<sup>[54]</sup>. In this context, a meta-analysis carried out with six Chinese studies with 1293 participants revealed that patients with COVID-19 showed a high percentage of MAFLD and increased risk of COVID-19 severity, indicating a need for intensive monitoring of MAFLD patients with COVID-19<sup>[55]</sup>.

In agreement with this, MAFLD entails a constellation of metabolic abnormalities that can be aggravated during viral infection. Through univariate analysis, it was shown that metabolic syndrome leads to a higher cumulative incidence of COVID-19, with liver damage being the most associated with this outcome<sup>[56]</sup>. Moreover, COVID-19 can cause hypoglycemia or hyperglycemia, compromising glycemic control due to sedentarism, anxiety, or viral tropism to pancreatic tissue<sup>[57]</sup>. Continuous monitoring of blood glucose is encouraged as hypoglycemia should be avoided, and glycemia should not exceed 180 mg/dL or 10 mmol/L in COVID-19 patients. MAFLD patients commonly show hypertension, and surveillance of medication and blood pressure levels can avoid shock in severe COVID-19 cases<sup>[58]</sup>.

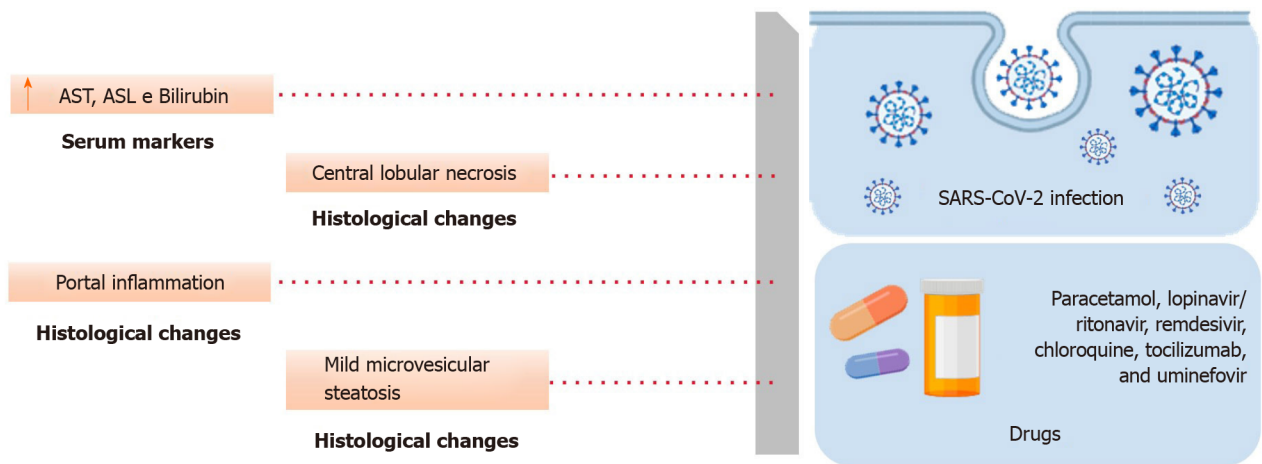


**Figure 2** Clinical features and hepatological changes due to severe acute respiratory syndrome coronavirus 2 infection (upper panel) and hepatotoxic effects of some drugs used as an attempt to treat coronavirus disease 2019 (lower panel). SARS-CoV-2: Severe acute respiratory syndrome coronavirus 2; AST: Aspartate aminotransferase.

Despite showing similar COVID-19 symptoms to non-MAFLD, fever in 66.8% and cough in 55.7% of patients<sup>[39]</sup>, MAFLD patients showed higher chances of intensive care unit admission (intensive care unit, OR: 1.60), intubation (2.51), need for vasopressors (1.22), and alanine aminotransferase > 5 times upper limit of normal (2.12)<sup>[59]</sup>. In univariate analyses, when compared with patients without chronic liver disease, subjects with MAFLD had significantly higher rates of intensive care unit admission (50.9% *vs* 35.2%,  $P = 0.0095$ ) and need for mechanical ventilation (49.1% *vs* 30.4%,  $P = 0.006$ )<sup>[53]</sup>.

A possible explanation for increased COVID-19 severity due to MAFLD includes higher C reactive protein (CRP) (107 *vs* 91.2 mg/L,  $P = 0.05$ ) concentrations in COVID-19 patients with MAFLD than controls without MAFLD in London<sup>[60]</sup>. This favored pro-inflammatory state can result in high death rates, as MAFLD patients who died during hospitalization had higher concentrations of inflammatory markers like ferritin<sup>[61]</sup>, prothrombin time, and lactate dehydrogenase than patients with MAFLD who survived hospitalization<sup>[60]</sup>. Notably, the combination of high CRP levels with low lymphocyte count predicted prolonged hospital stay (median 23 *vs* 18 d;  $P = 0.037$ ) and a higher proportion of severe COVID-19 (33.3% *vs* 14.7%,  $P = 0.007$ ) compared to non-obese patients<sup>[50]</sup>. Figure 3 outlines the mild symptoms and the factors that lead to severe forms of COVID-19.

Concerning imaging exams and COVID-19 prognosis in MAFLD patients, a CT study in the Mexican population proposed the liver to spleen ratio (CTL/S) as a surrogate for the diagnosis of MAFLD in COVID-19 patients, given that spleen does not store fat. Both organs are visualized in the CT performed to evaluate the degree of pulmonary commitment because it shows the upper abdomen, and the CTL/S  $\leq 0.9$  indicated the presence of fatty liver. Hepatic steatosis was associated with severe COVID-19 pneumonia, and CTL/S could be a substantial aid to estimate the prognosis of COVID-19 in MAFLD patients<sup>[62]</sup>.

A recent systematic review evaluating clinical studies from China, Israel, and the United States showed that the presence of hepatic steatosis is a predictor for symptomatic and severe COVID-19, even after the adjustment for obesity presence (OR: 2.358,  $P < 0.001$ )<sup>[63]</sup>. Moreover, COVID-19 infection in pre-existing chronic liver disease patients from 13 different Asian countries caused decompensation in 20% of the cirrhotic patients with high mortality. Among MAFLD patients, the presence of comorbidities like obesity and type 2 diabetes entailed a risk of liver injuries due to COVID-19 infection<sup>[64]</sup>. In agreement, a recent Indian study using non-COVID-19 cirrhotic patients as controls showed that COVID-19 infection resulted in a 100% mortality rate in patients with acute-on-chronic liver failure in comparison with 53.3% in acute-on-chronic liver failure controls. The poor outcome that COVID-19 imposes on cirrhotic patients includes the need for mechanical ventilation and urges physicians and hepatologists to consider patients with chronic liver diseases as a high-risk group for COVID-19 and guarantee rigorous preventive measures<sup>[65]</sup>.

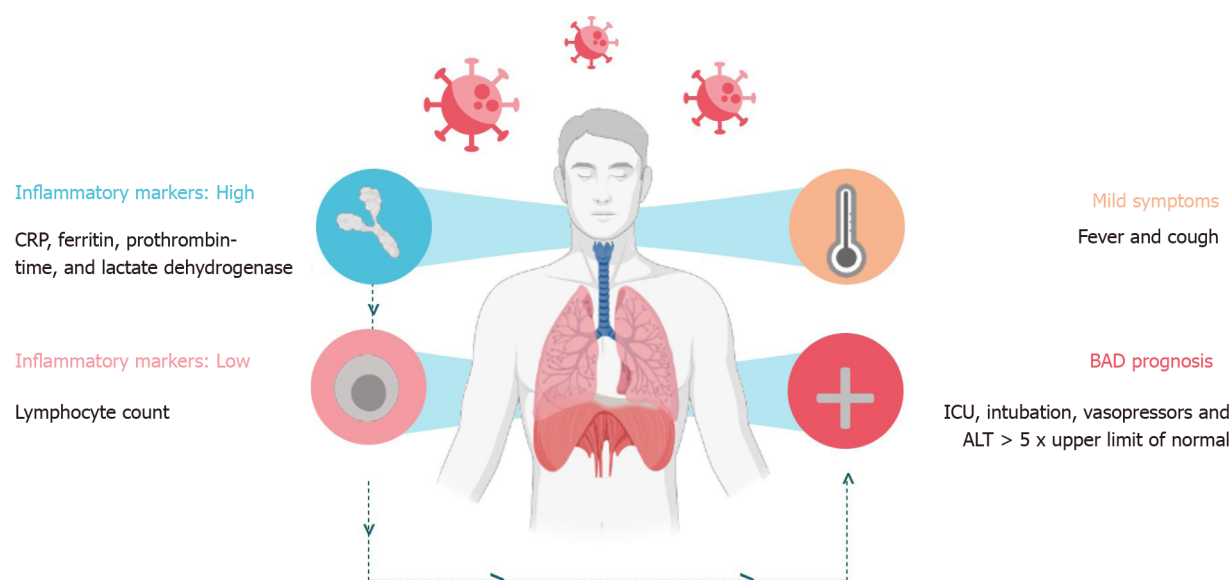


**Figure 3** Mild symptoms, inflammatory markers, and serious developments of coronavirus disease 2019. ALT: Alanine aminotransferase; CRP: C reactive protein; ICU: Intensive care unit.

### INVOLVED PATHWAYS IN INCREASED SEVERITY OF CORONAVIRUS DISEASE 2019 IN OBESE SUBJECTS WITH METABOLIC DYSFUNCTION-ASSOCIATED FATTY LIVER DISEASE

The post-mortem evaluation of the livers from people that died of COVID-19 often reveals that the virus causes inflammatory and immune-mediated liver damage rather than cytopathic harm<sup>[43]</sup>. The observation of different immune cell exudates near the portal area reinforces this hypothesis and links hepatic damage to the cytokine storm syndrome (CSS), which emerges as a promising explanation for the increased severity of COVID-19 in obese patients with MAFLD<sup>[66,67]</sup>.

To put it simply, CSS comprises the activation of inflammasomes and the following release of pro-inflammatory cytokines like IL-1 $\beta$  and IL-6<sup>[68,69]</sup>. The inflammasomes are complexes of proteins that reside in macrophages, activated by toll-like receptors binding to a pathogen-associated molecular pattern or damage-associated molecular patterns<sup>[70,71]</sup>. The liver has the largest macrophage reservoir in the body (the Kupfer cells); and, therefore, the activation of the NLR family pyrin domain containing 3 (NLRP3) inflammasome can damage this organ and acts as a promising marker of COVID-19 severity in obese patients<sup>[43,72]</sup>.

The adipose tissue expansion in obesity triggers fatty liver and inflammasome activity by lipotoxicity<sup>[73]</sup>. The dramatic changes that adipose tissue macrophages undergo during weight gain (polarization to M1 state) reflect in the Kupfer cells that produce inflammatory chemokines and cytokines, generating hepatic insulin resistance and inflammation<sup>[74,75]</sup>. In this context, IL-6 emerges as a pivotal marker of COVID-19 worsening as it can trigger the CSS<sup>[76]</sup>, besides being generally high in obese and MAFLD subjects<sup>[77]</sup>.

It can be supposed that the obese patient with MAFLD before catching COVID-19 could show a maximized CSS, which might be linked to the increased need for longer hospitalizations and intensive care. Consistent with this suggestion, inflammasome activation elicits massive augmentation of pro-inflammatory cytokine concentrations and induces pyroptosis<sup>[78]</sup>. Cell death mediated by pyroptosis in macrophages relies on NLRP3 activation and provokes severe acute respiratory syndrome in COVID-19 patients, picturing a frame of aggravated disease by the CSS in MAFLD patients<sup>[79]</sup>. Furthermore, severe obese subjects can show serious infections in the lower respiratory tract due to mechanical dysfunction, which also makes them more prone to secondary infections<sup>[80]</sup>.

Additional mechanisms related to the intensification of COVID-19 in MAFLD obese patients include the hepatocellular hypoxia in chronic liver diseases that leads to ACE2 overexpression<sup>[81]</sup>. Hence, these changes can cope with MAFLD progression towards NASH by the overexpression of ACE2 in endothelial cells and the consequent



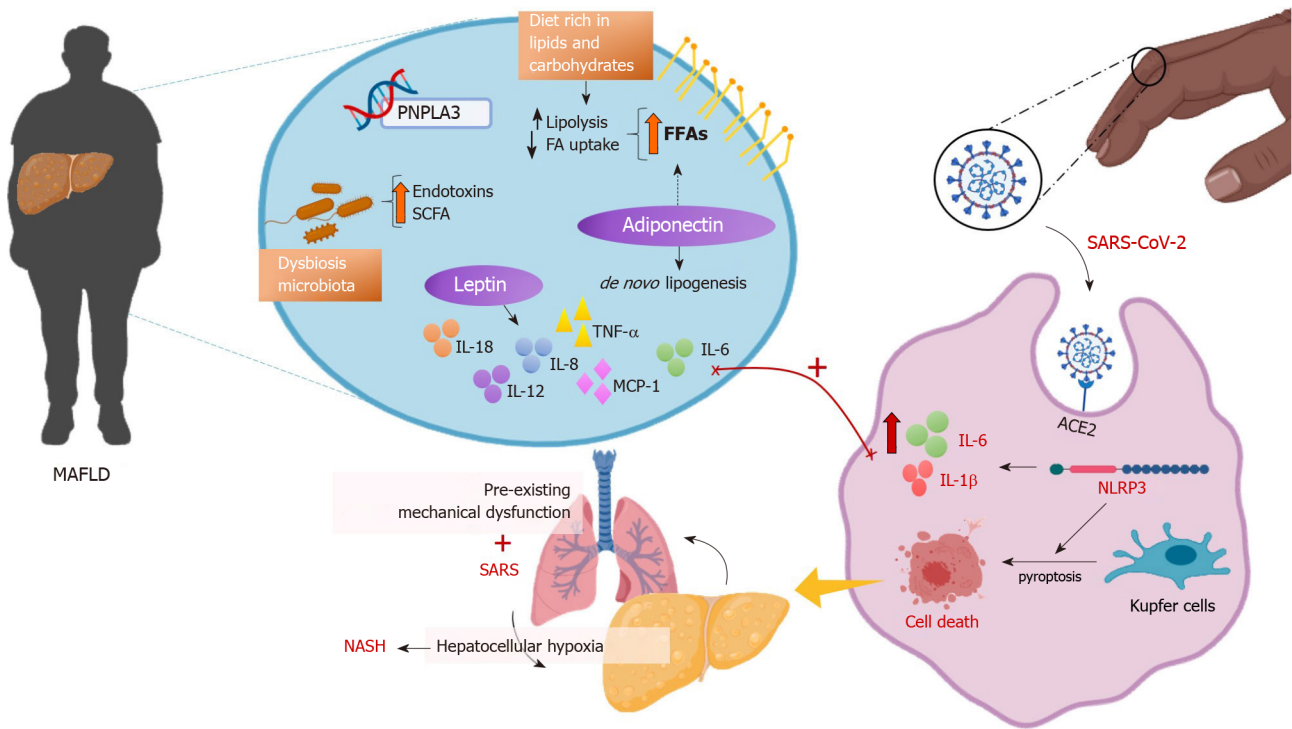


**Figure 4 Graphical abstract.** Metabolic dysfunction-associated fatty liver disease (MAFLD) patients usually show a constellation of metabolic impairments that include altered adipokine profile, glucolipotoxicity with ectopic lipid accumulation, and gut dysbiosis, besides a genetic background that favors these hepatic alterations and pre-existing mechanical lung dysfunction when obese. These clinical conditions before coronavirus disease 2019 (COVID-19) infection can aggravate the cytokine storm syndrome, with activation of macrophages that reside in the liver (Kupffer cells), resulting in inflammasome activation and cell death by pyroptosis. MAFLD patients are at high risk of complications and severe COVID-19 clinical course, with frequent mechanical ventilation, prolonged hospitalizations, and extended viral shedding. Upon survival, COVID-19 may act as a surrogate for MAFLD-non-alcoholic steatohepatitis progression, and hepatocellular hypoxia seems to underlie this process. ACE2: Angiotensin-converting enzyme 2; FFA: Free Fatty Acid; IL: Interleukin; MAFLD: Metabolic dysfunction-associated fatty liver disease; MCP1: Monocyte chemoattractant protein 1; NASH: Non-alcoholic steatohepatitis; NEFAs: Non-esterified fatty acids; NLRP: NLR family pyrin domain-containing; SARS-CoV-2: Severe acute respiratory syndrome coronavirus 2; SCFA: Short-chain fatty acid; TNF- $\alpha$ : Tumor necrosis factor.

increased reactive oxygen species production, inflammatory pathways activated in the Kupfer cells, and peroxisome proliferator-activated receptor- $\alpha$  down-regulation with pro-lipogenic gene expression and steatosis maximization<sup>[82,83]</sup>. In this regard, the presence of hepatic steatosis before viral infection can amplify the symptoms of COVID-19 as the lipotoxicity sustains the activation of Kupfer cells and allows the progression to liver fibrosis. The main pathways involved with the severity of COVID-19 in MAFLD patients are depicted in **Figure 4**.

## CONCLUSION

In conclusion, pre-existing MAFLD increases the risk of severe COVID-19 that requires hospitalization. MAFLD itself can represent an increased predisposition to CSS, and high CRP concentrations, NLRP3 activation, and IL-6 concentrations emerge as likely surrogates for the need for mechanical ventilation, with high death rates or evolution to NASH among survivors.

It is urgent to consider that MAFLD surpassed obesity as a risk factor to COVID-19 severity in populations with diverse genetic backgrounds. Therefore, MAFLD subjects should be ranked high-risk to catch COVID-19, submitted to rigorous preventive measurements, and classified as a prioritized group for vaccination.

## ACKNOWLEDGEMENTS

The authors would like to thank all physicians, health professionals, and researchers for working uninterruptedly during pandemics. Your dedication helped to gather the information that saved millions of lives and resulted in vaccines in an unprecedented



minimal time.

## REFERENCES

- 1 **World Health Organization.** WHO Coronavirus Disease (COVID-19) Dashboard 2021 [cited 19 January 2021]. Available from: <https://covid19.who.int/>
- 2 **Wu D,** Wu T, Liu Q, Yang Z. The SARS-CoV-2 outbreak: What we know. *Int J Infect Dis* 2020; **94**: 44-48 [PMID: [32171952](#) DOI: [10.1016/j.ijid.2020.03.004](#)]
- 3 **Albano D,** Bertagna F, Bertoli M, Bosio G, Lucchini S, Motta F, Panarotto MB, Peli A, Camoni L, Bengel FM, Giubbini R. Incidental Findings Suggestive of COVID-19 in Asymptomatic Patients Undergoing Nuclear Medicine Procedures in a High-Prevalence Region. *J Nucl Med* 2020; **61**: 632-636 [PMID: [32238429](#) DOI: [10.2967/jnumed.120.246256](#)]
- 4 **Goyal P,** Choi JJ, Pinheiro LC, Schenck EJ, Chen R, Jabri A, Satlin MJ, Campion TR Jr, Nahid M, Ringel JB, Hoffman KL, Alshak MN, Li HA, Wehmeyer GT, Rajan M, Reshetnyak E, Hupert N, Horn EM, Martinez FJ, Gulick RM, Safford MM. Clinical Characteristics of Covid-19 in New York City. *N Engl J Med* 2020; **382**: 2372-2374 [PMID: [32302078](#) DOI: [10.1056/NEJMc2010419](#)]
- 5 **Zubair AS,** McAlpine LS, Gardin T, Farhadian S, Kuruvilla DE, Spudich S. Neuropathogenesis and Neurologic Manifestations of the Coronaviruses in the Age of Coronavirus Disease 2019: A Review. *JAMA Neurol* 2020; **77**: 1018-1027 [PMID: [32469387](#) DOI: [10.1001/jamaneurol.2020.2065](#)]
- 6 **Chigr F,** Merzouki M, Najimi M. Autonomic Brain Centers and Pathophysiology of COVID-19. *ACS Chem Neurosci* 2020; **11**: 1520-1522 [PMID: [32427468](#) DOI: [10.1021/acscchemneuro.0c00265](#)]
- 7 **Ellul MA,** Benjamin L, Singh B, Lant S, Michael BD, Easton A, Kneen R, Defres S, Sejvar J, Solomon T. Neurological associations of COVID-19. *Lancet Neurol* 2020; **19**: 767-783 [PMID: [32622375](#) DOI: [10.1016/S1474-4422\(20\)30221-0](#)]
- 8 **Mitrani RD,** Dabas N, Goldberger JJ. COVID-19 cardiac injury: Implications for long-term surveillance and outcomes in survivors. *Heart Rhythm* 2020; **17**: 1984-1990 [PMID: [32599178](#) DOI: [10.1016/j.hrthm.2020.06.026](#)]
- 9 **Hamming I,** Timens W, Bulthuis ML, Lely AT, Navis G, van Goor H. Tissue distribution of ACE2 protein, the functional receptor for SARS coronavirus. A first step in understanding SARS pathogenesis. *J Pathol* 2004; **203**: 631-637 [PMID: [15141377](#) DOI: [10.1002/path.1570](#)]
- 10 **Qi F,** Qian S, Zhang S, Zhang Z. Single cell RNA sequencing of 13 human tissues identify cell types and receptors of human coronaviruses. *Biochem Biophys Res Commun* 2020; **526**: 135-140 [PMID: [32199615](#) DOI: [10.1016/j.bbrc.2020.03.044](#)]
- 11 **Petrilli CM,** Jones SA, Yang J, Rajagopalan H, O'Donnell L, Chernyak Y, Tobin KA, Cerfolio RJ, Francois F, Horwitz LI. Factors associated with hospital admission and critical illness among 5279 people with coronavirus disease 2019 in New York City: prospective cohort study. *BMJ* 2020; **369**: m1966 [PMID: [32444366](#) DOI: [10.1136/bmj.m1966](#)]
- 12 **Gustafson B,** Smith U. Regulation of white adipogenesis and its relation to ectopic fat accumulation and cardiovascular risk. *Atherosclerosis* 2015; **241**: 27-35 [PMID: [25957567](#) DOI: [10.1016/j.atherosclerosis.2015.04.812](#)]
- 13 **Gustafson B,** Hammarstedt A, Hedjazifar S, Smith U. Restricted adipogenesis in hypertrophic obesity: the role of WISP2, WNT, and BMP4. *Diabetes* 2013; **62**: 2997-3004 [PMID: [23970518](#) DOI: [10.2337/db13-0473](#)]
- 14 **Saponaro C,** Gaggini M, Carli F, Gastaldelli A. The Subtle Balance between Lipolysis and Lipogenesis: A Critical Point in Metabolic Homeostasis. *Nutrients* 2015; **7**: 9453-9474 [PMID: [26580649](#) DOI: [10.3390/nu7115475](#)]
- 15 **Cusi K.** Role of insulin resistance and lipotoxicity in non-alcoholic steatohepatitis. *Clin Liver Dis* 2009; **13**: 545-563 [PMID: [19818304](#) DOI: [10.1016/j.cld.2009.07.009](#)]
- 16 **Cildir G,** Akincilar SC, Tergaonkar V. Chronic adipose tissue inflammation: all immune cells on the stage. *Trends Mol Med* 2013; **19**: 487-500 [PMID: [23746697](#) DOI: [10.1016/j.molmed.2013.05.001](#)]
- 17 **Eslam M,** Sanyal AJ, George J; International Consensus Panel. MAFLD: A Consensus-Driven Proposed Nomenclature for Metabolic Associated Fatty Liver Disease. *Gastroenterology* 2020; **158**: 1999-2014. e1 [PMID: [32044314](#) DOI: [10.1053/j.gastro.2019.11.312](#)]
- 18 **Polyzos SA,** Kountouras J, Mantzoros CS. Obesity and nonalcoholic fatty liver disease: From pathophysiology to therapeutics. *Metabolism* 2019; **92**: 82-97 [PMID: [30502373](#) DOI: [10.1016/j.metabol.2018.11.014](#)]
- 19 **Ryan PM,** Caplice NM. Is Adipose Tissue a Reservoir for Viral Spread, Immune Activation, and Cytokine Amplification in Coronavirus Disease 2019? *Obesity (Silver Spring)* 2020; **28**: 1191-1194 [PMID: [32314868](#) DOI: [10.1002/oby.22843](#)]
- 20 **Dugail I,** Amri EZ, Vitale N. High prevalence for obesity in severe COVID-19: Possible links and perspectives towards patient stratification. *Biochimie* 2020; **179**: 257-265 [PMID: [32649962](#) DOI: [10.1016/j.biochi.2020.07.001](#)]
- 21 **Portincasa P,** Krawczyk M, Smyk W, Lammert F, Di Ciaula A. COVID-19 and non-alcoholic fatty liver disease: Two intersecting pandemics. *Eur J Clin Invest* 2020; **50**: e13338 [PMID: [32589264](#) DOI: [10.1111/eci.13338](#)]
- 22 **Younossi ZM,** Koenig AB, Abdelatif D, Fazel Y, Henry L, Wymer M. Global epidemiology of nonalcoholic fatty liver disease-Meta-analytic assessment of prevalence, incidence, and outcomes.

- Hepatology* 2016; **64**: 73-84 [PMID: 26707365 DOI: 10.1002/hep.28431]
- 23 **Xian YX**, Weng JP, Xu F. MAFLD vs. NAFLD: shared features and potential changes in epidemiology, pathophysiology, diagnosis, and pharmacotherapy. *Chin Med J (Engl)* 2020; **134**: 8-19 [PMID: 33323806 DOI: 10.1097/CM9.0000000000001263]
  - 24 **Magkos F**, Mantzoros CS. Body fat redistribution and metabolic abnormalities in HIV-infected patients on highly active antiretroviral therapy: novel insights into pathophysiology and emerging opportunities for treatment. *Metabolism* 2011; **60**: 749-753 [PMID: 20965525 DOI: 10.1016/j.metabol.2010.09.011]
  - 25 **Donnelly KL**, Smith CI, Schwarzenberg SJ, Jessurun J, Boldt MD, Parks EJ. Sources of fatty acids stored in liver and secreted via lipoproteins in patients with nonalcoholic fatty liver disease. *J Clin Invest* 2005; **115**: 1343-1351 [PMID: 15864352 DOI: 10.1172/JCI23621]
  - 26 **Polyzos SA**, Kountouras J, Mantzoros CS. Adipose tissue, obesity and non-alcoholic fatty liver disease. *Minerva Endocrinol* 2017; **42**: 92-108 [PMID: 27711029 DOI: 10.23736/S0391-1977.16.02563-3]
  - 27 **Polyzos SA**, Kountouras J, Mantzoros CS. Adipokines in nonalcoholic fatty liver disease. *Metabolism* 2016; **65**: 1062-1079 [PMID: 26725002 DOI: 10.1016/j.metabol.2015.11.006]
  - 28 **Polyzos SA**, Kountouras J, Mantzoros CS. Leptin in nonalcoholic fatty liver disease: a narrative review. *Metabolism* 2015; **64**: 60-78 [PMID: 25456097 DOI: 10.1016/j.metabol.2014.10.012]
  - 29 **Polyzos SA**, Kountouras J, Zavos C, Tsiaousi E. The role of adiponectin in the pathogenesis and treatment of non-alcoholic fatty liver disease. *Diabetes Obes Metab* 2010; **12**: 365-383 [PMID: 20415685 DOI: 10.1111/j.1463-1326.2009.01176.x]
  - 30 **Imajo K**, Fujita K, Yoneda M, Nozaki Y, Ogawa Y, Shinohara Y, Kato S, Mawatari H, Shibata W, Kitani H, Ikejima K, Kirikoshi H, Nakajima N, Saito S, Maeyama S, Watanabe S, Wada K, Nakajima A. Hyperresponsivity to low-dose endotoxin during progression to nonalcoholic steatohepatitis is regulated by leptin-mediated signaling. *Cell Metab* 2012; **16**: 44-54 [PMID: 22768838 DOI: 10.1016/j.cmet.2012.05.012]
  - 31 **Silva-Veiga FM**, Miranda CS, Martins FF, Daleprane JB, Mandarin-de-Lacerda CA, Souza-Mello V. Gut-liver axis modulation in fructose-fed mice: a role for PPAR-alpha and linagliptin. *J Endocrinol* 2020; **247**: 11-24 [PMID: 32698143 DOI: 10.1530/JOE-20-0139]
  - 32 **Turnbaugh PJ**, Ley RE, Mahowald MA, Magrini V, Mardis ER, Gordon JL. An obesity-associated gut microbiome with increased capacity for energy harvest. *Nature* 2006; **444**: 1027-1031 [PMID: 17183312 DOI: 10.1038/nature05414]
  - 33 **Porras D**, Nistal E, Martínez-Flórez S, González-Gallego J, García-Mediavilla MV, Sánchez-Campos S. Intestinal Microbiota Modulation in Obesity-Related Non-alcoholic Fatty Liver Disease. *Front Physiol* 2018; **9**: 1813 [PMID: 30618824 DOI: 10.3389/fphys.2018.01813]
  - 34 **du Plessis J**, van Pelt J, Korf H, Mathieu C, van der Schueren B, Lannoo M, Oyen T, Topal B, Fetter G, Nayler S, van der Merwe T, Windmolders P, Van Gaal L, Verrijken A, Hubens G, Gericke M, Cassiman D, Francque S, Nevens F, van der Merwe S. Association of Adipose Tissue Inflammation With Histologic Severity of Nonalcoholic Fatty Liver Disease. *Gastroenterology* 2015; **149**: 635-48. e14 [PMID: 26028579 DOI: 10.1053/j.gastro.2015.05.044]
  - 35 **Lonardo A**, Mantovani A, Lugari S, Targher G. Epidemiology and pathophysiology of the association between NAFLD and metabolically healthy or metabolically unhealthy obesity. *Ann Hepatol* 2020; **19**: 359-366 [PMID: 32349939 DOI: 10.1016/j.aohp.2020.03.001]
  - 36 **Romeo S**, Kozlitina J, Xing C, Pertsemlidis A, Cox D, Pennacchio LA, Boerwinkle E, Cohen JC, Hobbs HH. Genetic variation in PNPLA3 confers susceptibility to nonalcoholic fatty liver disease. *Nat Genet* 2008; **40**: 1461-1465 [PMID: 18820647 DOI: 10.1038/ng.257]
  - 37 **Lau LHS**, Wong SH. Microbiota, Obesity and NAFLD. *Adv Exp Med Biol* 2018; **1061**: 111-125 [PMID: 29956210 DOI: 10.1007/978-981-10-8684-7\_9]
  - 38 **Sharma P**, Kumar A. Metabolic dysfunction associated fatty liver disease increases risk of severe Covid-19. *Diabetes Metab Syndr* 2020; **14**: 825-827 [PMID: 32540736 DOI: 10.1016/j.dsx.2020.06.013]
  - 39 **Huang R**, Zhu L, Wang J, Xue L, Liu L, Yan X, Huang S, Li Y, Zhang B, Xu T, Li C, Ji F, Ming F, Zhao Y, Cheng J, Wang Y, Zhao H, Hong S, Chen K, Zhao XA, Zou L, Sang D, Shao H, Guan X, Chen X, Chen Y, Wei J, Zhu C, Wu C. Clinical features of COVID-19 patients with non-alcoholic fatty liver disease. *Hepatol Commun* 2020 [PMID: 32838108 DOI: 10.1002/hep4.1592]
  - 40 **Lopez-Mendez I**, Aquino-Matus J, Gall SM, Prieto-Nava JD, Juarez-Hernandez E, Uribe M, Castro-Narro G. Association of liver steatosis and fibrosis with clinical outcomes in patients with SARS-CoV-2 infection (COVID-19). *Ann Hepatol* 2021; **20**: 100271 [PMID: 33099028 DOI: 10.1016/j.aohp.2020.09.015]
  - 41 **Gu X**, Li X, An X, Yang S, Wu S, Yang X, Wang H. Elevated serum aspartate aminotransferase level identifies patients with coronavirus disease 2019 and predicts the length of hospital stay. *J Clin Lab Anal* 2020; **34**: e23391 [PMID: 32488888 DOI: 10.1002/jcla.23391]
  - 42 **Schmit G**, Lelotte J, Vanhaebost J, Horsmans Y, Van Bockstal M, Baldin P. The Liver in COVID-19-Related Death: Protagonist or Innocent Bystander? *Pathobiology* 2021; **88**: 88-94 [PMID: 33108789 DOI: 10.1159/000512008]
  - 43 **Xu Z**, Shi L, Wang Y, Zhang J, Huang L, Zhang C, Liu S, Zhao P, Liu H, Zhu L, Tai Y, Bai C, Gao T, Song J, Xia P, Dong J, Zhao J, Wang FS. Pathological findings of COVID-19 associated with acute respiratory distress syndrome. *Lancet Respir Med* 2020; **8**: 420-422 [PMID: 32085846 DOI: 10.1016/S2213-2600(20)30076-X]

- 44 **Lagana SM**, Kudose S, Iuga AC, Lee MJ, Fazlollahi L, Remotti HE, Del Portillo A, De Michele S, de Gonzalez AK, Saqi A, Khairallah P, Chong AM, Park H, Uhlemann AC, Lefkowitz JH, Verna EC. Hepatic pathology in patients dying of COVID-19: a series of 40 cases including clinical, histologic, and virologic data. *Mod Pathol* 2020; **33**: 2147-2155 [PMID: [32792598](#) DOI: [10.1038/s41379-020-00649-x](#)]
- 45 **Ji D**, Qin E, Xu J, Zhang D, Cheng G, Wang Y, Lau G. Non-alcoholic fatty liver diseases in patients with COVID-19: A retrospective study. *J Hepatol* 2020; **73**: 451-453 [PMID: [32278005](#) DOI: [10.1016/j.jhep.2020.03.044](#)]
- 46 **Sun J**, Aghemo A, Forner A, Valenti L. COVID-19 and liver disease. *Liver Int* 2020; **40**: 1278-1281 [PMID: [32251539](#) DOI: [10.1111/liv.14470](#)]
- 47 **Zhang P**, Zhu L, Cai J, Lei F, Qin JJ, Xie J, Liu YM, Zhao YC, Huang X, Lin L, Xia M, Chen MM, Cheng X, Zhang X, Guo D, Peng Y, Ji YX, Chen J, She ZG, Wang Y, Xu Q, Tan R, Wang H, Lin J, Luo P, Fu S, Cai H, Ye P, Xiao B, Mao W, Liu L, Yan Y, Liu M, Chen M, Zhang XJ, Wang X, Touyz RM, Xia J, Zhang BH, Yuan Y, Loomba R, Liu PP, Li H. Association of Inpatient Use of Angiotensin-Converting Enzyme Inhibitors and Angiotensin II Receptor Blockers With Mortality Among Patients With Hypertension Hospitalized With COVID-19. *Circ Res* 2020; **126**: 1671-1681 [PMID: [32302265](#) DOI: [10.1161/CIRCRESAHA.120.317134](#)]
- 48 **Portincasa P**, Krawczyk M, Machill A, Lammert F, Di Ciaula A. Hepatic consequences of COVID-19 infection. Lapping or biting? *Eur J Intern Med* 2020; **77**: 18-24 [PMID: [32507608](#) DOI: [10.1016/j.ejim.2020.05.035](#)]
- 49 **Zhou YJ**, Zheng KI, Wang XB, Yan HD, Sun QF, Pan KH, Wang TY, Ma HL, Chen YP, George J, Zheng MH. Younger patients with MAFLD are at increased risk of severe COVID-19 illness: A multicenter preliminary analysis. *J Hepatol* 2020; **73**: 719-721 [PMID: [32348790](#) DOI: [10.1016/j.jhep.2020.04.027](#)]
- 50 **Gao F**, Zheng KI, Wang XB, Sun QF, Pan KH, Wang TY, Chen YP, Targher G, Byrne CD, George J, Zheng MH. Obesity Is a Risk Factor for Greater COVID-19 Severity. *Diabetes Care* 2020; **43**: e72-e74 [PMID: [32409499](#) DOI: [10.2337/dc20-0682](#)]
- 51 **Zheng KI**, Gao F, Wang XB, Sun QF, Pan KH, Wang TY, Ma HL, Chen YP, Liu WY, George J, Zheng MH. Letter to the Editor: Obesity as a risk factor for greater severity of COVID-19 in patients with metabolic associated fatty liver disease. *Metabolism* 2020; **108**: 154244 [PMID: [32320741](#) DOI: [10.1016/j.metabol.2020.154244](#)]
- 52 **Bramante C**, Tignanelli CJ, Dutta N, Jones E, Tamariz L, Clark JM, Usher M, Metlon-Meaux G, Ikramuddin S. Non-alcoholic fatty liver disease (NAFLD) and risk of hospitalization for Covid-19. *medRxiv* 2020 [PMID: [32909011](#) DOI: [10.1101/2020.09.01.20185850](#)]
- 53 **Hashemi N**, Viveiros K, Redd WD, Zhou JC, McCarty TR, Bazarbashi AN, Hathorn KE, Wong D, Njie C, Shen L, Chan WW. Impact of chronic liver disease on outcomes of hospitalized patients with COVID-19: A multicentre United States experience. *Liver Int* 2020; **40**: 2515-2521 [PMID: [32585065](#) DOI: [10.1111/liv.14583](#)]
- 54 **Medeiros AK**, Barbisan CC, Cruz IR, de Araújo EM, Libânio BB, Albuquerque KS, Torres US. Higher frequency of hepatic steatosis at CT among COVID-19-positive patients. *Abdom Radiol (NY)* 2020; **45**: 2748-2754 [PMID: [32683613](#) DOI: [10.1007/s00261-020-02648-7](#)]
- 55 **Pan L**, Huang P, Xie X, Xu J, Guo D, Jiang Y. Metabolic associated fatty liver disease increases the severity of COVID-19: A meta-analysis. *Dig Liver Dis* 2021; **53**: 153-157 [PMID: [33011088](#) DOI: [10.1016/j.dld.2020.09.007](#)]
- 56 **Ghoneim S**, Butt MU, Hamid O, Shah A, Asaad I. The incidence of COVID-19 in patients with metabolic syndrome and non-alcoholic steatohepatitis: A population-based study. *Metabol Open* 2020; **8**: 100057 [PMID: [32924000](#) DOI: [10.1016/j.metop.2020.100057](#)]
- 57 **Zhou J**, Tan J. Diabetes patients with COVID-19 need better blood glucose management in Wuhan, China. *Metabolism* 2020; **107**: 154216 [PMID: [32220612](#) DOI: [10.1016/j.metabol.2020.154216](#)]
- 58 **Wong GL**, Wong VW, Thompson A, Jia J, Hou J, Lesmana CRA, Susilo A, Tanaka Y, Chan WK, Gane E, Ong-Go AK, Lim SG, Ahn SH, Yu ML, Piratvisuth T, Chan HL; Asia-Pacific Working Group for Liver Derangement during the COVID-19 Pandemic. Management of patients with liver derangement during the COVID-19 pandemic: an Asia-Pacific position statement. *Lancet Gastroenterol Hepatol* 2020; **5**: 776-787 [PMID: [32585136](#) DOI: [10.1016/S2468-1253\(20\)30190-4](#)]
- 59 **Chen VL**, Hawa F, Berinstein JA, Reddy CA, Kassab I, Platt KD, Hsu CY, Steiner CA, Louissaint J, Gunaratnam NT, Sharma P. Hepatic Steatosis Is Associated with Increased Disease Severity and Liver Injury in Coronavirus Disease-19. *Dig Dis Sci* 2020 [PMID: [32980956](#) DOI: [10.1007/s10620-020-06618-3](#)]
- 60 **Forlano R**, Mullish BH, Mukherjee SK, Nathwani R, Harlow C, Crook P, Judge R, Soubieries A, Middleton P, Daunt A, Perez-Guzman P, Selvapatt N, Lemoine M, Dhar A, Thursz MR, Nayagam S, Manousou P. In-hospital mortality is associated with inflammatory response in NAFLD patients admitted for COVID-19. *PLoS One* 2020; **15**: e0240400 [PMID: [33031439](#) DOI: [10.1371/journal.pone.0240400](#)]
- 61 **Ji D**, Zhang D, Yang T, Mu J, Zhao P, Xu J, Li C, Cheng G, Wang Y, Chen Z, Qin E, Lau G. Effect of COVID-19 on patients with compensated chronic liver diseases. *Hepatol Int* 2020; **14**: 701-710 [PMID: [32734407](#) DOI: [10.1007/s12072-020-10058-6](#)]
- 62 **Palomar-Lever A**, Barraza G, Galicia-Alba J, Echeverri-Bolaños M, Escarria-Panesso R, Padua-Barrios J, Halabe-Cherem J, Hernandez-Molina G, Chargo-Loustaunau TN, Kimura-Hayama E. Hepatic steatosis as an independent risk factor for severe disease in patients with COVID-19: A

- computed tomography study. *JGH Open* 2020 [PMID: 32838045 DOI: 10.1002/jgh3.12395]
- 63 **Sachdeva S**, Khandait H, Kopel J, Aloysius MM, Desai R, Goyal H. NAFLD and COVID-19: a Pooled Analysis. *SN Compr Clin Med* 2020; 1-4 [PMID: 33173850 DOI: 10.1007/s42399-020-00631-3]
  - 64 **Sarin SK**, Choudhury A, Lau GK, Zheng MH, Ji D, Abd-Elsalam S, Hwang J, Qi X, Cua IH, Suh JJ, Park JG, Putharoen O, Kaewdech A, Piratvisuth T, Treeprasertsuk S, Park S, Wejnaruemarn S, Payawal DA, Baatarkhuu O, Ahn SH, Yeo CD, Alonzo UR, Chinbayer T, Loho IM, Yokosuka O, Jafri W, Tan S, Soo LI, Tanwandee T, Gani R, Anand L, Esmail ES, Khalaf M, Alam S, Lin CY, Chuang WL, Soin AS, Garg HK, Kalista K, Batsukh B, Purnomo HD, Dara VP, Rathi P, Al Mahtab M, Shukla A, Sharma MK, Omata M; APASL COVID Task Force, APASL COVID Liver Injury Spectrum Study (APCOLIS Study-NCT 04345640). Pre-existing liver disease is associated with poor outcome in patients with SARS CoV2 infection; The APCOLIS Study (APASL COVID-19 Liver Injury Spectrum Study). *Hepatol Int* 2020; 14: 690-700 [PMID: 32623632 DOI: 10.1007/s12072-020-10072-8]
  - 65 **Shalimar**, Elhence A, Vaishnav M, Kumar R, Pathak P, Soni KD, Aggarwal R, Soneja M, Jorwal P, Kumar A, Khanna P, Singh AK, Biswas A, Nischal N, Dar L, Choudhary A, Rangarajan K, Mohan A, Acharya P, Nayak B, Gunjan D, Saraya A, Mahapatra S, Makharia G, Trikha A, Garg P. Poor outcomes in patients with cirrhosis and Corona Virus Disease-19. *Indian J Gastroenterol* 2020; 39: 285-291 [PMID: 32803716 DOI: 10.1007/s12664-020-01074-3]
  - 66 **Li J**, Fan JG. Characteristics and Mechanism of Liver Injury in 2019 Coronavirus Disease. *J Clin Transl Hepatol* 2020; 8: 13-17 [PMID: 32274341 DOI: 10.14218/JCTH.2020.00019]
  - 67 **Conti P**, Ronconi G, Caraffa A, Gallenga CE, Ross R, Frydas I, Kritas SK. Induction of pro-inflammatory cytokines (IL-1 and IL-6) and lung inflammation by Coronavirus-19 (COVI-19 or SARS-CoV-2): anti-inflammatory strategies. *J Biol Regul Homeost Agents* 2020; 34: 327-331 [PMID: 32171193 DOI: 10.23812/CONTI-E]
  - 68 **Tisoncik JR**, Korth MJ, Simmons CP, Farrar J, Martin TR, Katze MG. Into the eye of the cytokine storm. *Microbiol Mol Biol Rev* 2012; 76: 16-32 [PMID: 22390970 DOI: 10.1128/MMBR.05015-11]
  - 69 **Schmidt-Arras D**, Rose-John S. IL-6 pathway in the liver: From physiopathology to therapy. *J Hepatol* 2016; 64: 1403-1415 [PMID: 26867490 DOI: 10.1016/j.jhep.2016.02.004]
  - 70 **López-Reyes A**, Martínez-Armenta C, Espinosa-Velázquez R, Vázquez-Cárdenas P, Cruz-Ramos M, Palacios-Gonzalez B, Gomez-Quiroz LE, Martínez-Nava GA. NLRP3 Inflammasome: The Stormy Link Between Obesity and COVID-19. *Front Immunol* 2020; 11: 570251 [PMID: 33193349 DOI: 10.3389/fimmu.2020.570251]
  - 71 **Swanson KV**, Deng M, Ting JP. The NLRP3 inflammasome: molecular activation and regulation to therapeutics. *Nat Rev Immunol* 2019; 19: 477-489 [PMID: 31036962 DOI: 10.1038/s41577-019-0165-0]
  - 72 **Lefere S**, Tacke F. Macrophages in obesity and non-alcoholic fatty liver disease: Crosstalk with metabolism. *JHEP Rep* 2019; 1: 30-43 [PMID: 32149275 DOI: 10.1016/j.jhepr.2019.02.004]
  - 73 **Rheinheimer J**, de Souza BM, Cardoso NS, Bauer AC, Crispim D. Current role of the NLRP3 inflammasome on obesity and insulin resistance: A systematic review. *Metabolism* 2017; 74: 1-9 [PMID: 28764843 DOI: 10.1016/j.metabol.2017.06.002]
  - 74 **Vandanmagsar B**, Youm YH, Ravussin A, Galgani JE, Stadler K, Mynatt RL, Ravussin E, Stephens JM, Dixit VD. The NLRP3 inflammasome instigates obesity-induced inflammation and insulin resistance. *Nat Med* 2011; 17: 179-188 [PMID: 21217695 DOI: 10.1038/nm.2279]
  - 75 **Luo W**, Xu Q, Wang Q, Wu H, Hua J. Effect of modulation of PPAR- $\gamma$  activity on Kupffer cells M1/M2 polarization in the development of non-alcoholic fatty liver disease. *Sci Rep* 2017; 7: 44612 [PMID: 28300213 DOI: 10.1038/srep44612]
  - 76 **Feng G**, Zheng KI, Yan QQ, Rios RS, Targher G, Byrne CD, Poucke SV, Liu WY, Zheng MH. COVID-19 and Liver Dysfunction: Current Insights and Emergent Therapeutic Strategies. *J Clin Transl Hepatol* 2020; 8: 18-24 [PMID: 32274342 DOI: 10.14218/JCTH.2020.00018]
  - 77 **Simon TG**, Trejo MEP, McClelland R, Bradley R, Blaha MJ, Zeb I, Corey KE, Budoff MJ, Chung RT. Circulating Interleukin-6 is a biomarker for coronary atherosclerosis in nonalcoholic fatty liver disease: Results from the Multi-Ethnic Study of Atherosclerosis. *Int J Cardiol* 2018; 259: 198-204 [PMID: 29579601 DOI: 10.1016/j.ijcard.2018.01.046]
  - 78 **Shi CS**, Nabar NR, Huang NN, Kehrl JH. SARS-Coronavirus Open Reading Frame-8b triggers intracellular stress pathways and activates NLRP3 inflammasomes. *Cell Death Discov* 2019; 5: 101 [PMID: 31231549 DOI: 10.1038/s41420-019-0181-7]
  - 79 **Chen IY**, Moriyama M, Chang MF, Ichinohe T. Severe Acute Respiratory Syndrome Coronavirus Viroporin 3a Activates the NLRP3 Inflammasome. *Front Microbiol* 2019; 10: 50 [PMID: 30761102 DOI: 10.3389/fmicb.2019.00050]
  - 80 **Peters U**, Suratt BT, Bates JHT, Dixon AE. Beyond BMI: Obesity and Lung Disease. *Chest* 2018; 153: 702-709 [PMID: 28728934 DOI: 10.1016/j.chest.2017.07.010]
  - 81 **Paizis G**, Tikellis C, Cooper ME, Schembri JM, Lew RA, Smith AI, Shaw T, Warner FJ, Zuilli A, Burrell LM, Angus PW. Chronic liver injury in rats and humans upregulates the novel enzyme angiotensin converting enzyme 2. *Gut* 2005; 54: 1790-1796 [PMID: 16166274 DOI: 10.1136/gut.2004.062398]
  - 82 **Chen J**, Chen J, Fu H, Li Y, Wang L, Luo S, Lu H. Hypoxia exacerbates nonalcoholic fatty liver disease via the HIF-2 $\alpha$ /PPAR $\alpha$  pathway. *Am J Physiol Endocrinol Metab* 2019; 317: E710-E722 [PMID: 31430204 DOI: 10.1152/ajpendo.00052.2019]

- 83 **Hernández A**, Reyes D, Geng Y, Arab JP, Cabrera D, Sepulveda R, Solis N, Buist-Homan M, Arrese M, Moshage H. Extracellular vesicles derived from fat-laden hepatocytes undergoing chemical hypoxia promote a pro-fibrotic phenotype in hepatic stellate cells. *Biochim Biophys Acta Mol Basis Dis* 2020; **1866**: 165857 [PMID: [32512191](#) DOI: [10.1016/j.bbadis.2020.165857](#)]





## Preoperative physiological esophageal assessment for anti-reflux surgery: A guide for surgeons on high-resolution manometry and pH testing

Michael Yodice, Alexandra Mignucci, Virali Shah, Christopher Ashley, Micheal Tadros

**ORCID number:** Michael Yodice 0000-0002-2738-2606; Alexandra Mignucci 0000-0002-8303-7997; Virali Shah 0000-0001-9229-5288; Christopher Ashley 0000-0002-7824-5556; Micheal Tadros 0000-0003-3118-3893.

**Author contributions:** Yodice M contributed as lead author with manuscript preparation. Mignucci A and Shah V contributed equally with manuscript preparation and critical review; Ashley C contributed critical review for the manuscript; Tadros M is the guarantor of the manuscript and also provided critical review.

**Conflict-of-interest statement:** The authors disclose no conflicts of interest or external funding for this publication.

**Open-Access:** This article is an open-access article that was selected by an in-house editor and fully peer-reviewed by external reviewers. It is distributed in accordance with the Creative Commons Attribution NonCommercial (CC BY-NC 4.0) license, which permits others to distribute, remix, adapt, build upon this work non-commercially, and license their derivative works on different terms, provided the original work is properly cited and

**Michael Yodice, Alexandra Mignucci, Virali Shah,** Department of Gastroenterology, Albany Medical College, Albany, NY 12208, United States

**Christopher Ashley,** Section of Gastroenterology, Stratton VA Medical Center, Albany, NY 12208, United States

**Micheal Tadros,** Department of Gastroenterology, Albany Medical Center, Schenectady, NY 12309, United States

**Corresponding author:** Micheal Tadros, FACG, MD, Associate Professor, Doctor, Department of Gastroenterology, Albany Medical Center, 1769 Union Street 2<sup>nd</sup> Floor, Schenectady, NY 12309, United States. [tadrosml@amc.edu](mailto:tadrosml@amc.edu)

### Abstract

Gastroesophageal reflux disease (GERD) is one of the most commonly encountered digestive diseases in the world, with the prevalence continuing to increase. Many patients are successfully treated with lifestyle modifications and proton pump inhibitor therapy, but a subset of patients require more aggressive intervention for control of their symptoms. Surgical treatment with fundoplication is a viable option for patients with GERD, as it attempts to improve the integrity of the lower esophageal sphincter (LES). While surgery can be as effective as medical treatment, it can also be associated with side effects such as dysphagia, bloating, and abdominal pain. Therefore, a thorough pre-operative assessment is crucial to select appropriate surgical candidates. Newer technologies are becoming increasingly available to help clinicians identify patients with true LES dysfunction, such as pH-impedance studies and high-resolution manometry (HRM). Pre-operative evaluation should be aimed at confirming the diagnosis of GERD, ruling out any major motility disorders, and selecting appropriate surgical candidates. HRM and pH testing are key tests to consider for patients with GERD like symptoms, and the addition of provocative measures such as straight leg raises and multiple rapid swallows to HRM protocol can assess the presence of underlying hiatal hernias and to test a patient's peristaltic reserve prior to surgery.

**Key Words:** Gastroesophageal reflux disease; Fundoplication; High resolution manometry; pH-impedance; Anti-reflux surgery; Pre-operative assessment

the use is non-commercial. See: <http://creativecommons.org/licenses/by-nc/4.0/>

**Manuscript source:** Invited manuscript

**Specialty type:** Gastroenterology and hepatology

**Country/Territory of origin:** United States

**Peer-review report's scientific quality classification**

Grade A (Excellent): A, A  
Grade B (Very good): B, B  
Grade C (Good): C  
Grade D (Fair): 0  
Grade E (Poor): 0

**Received:** January 23, 2021

**Peer-review started:** January 23, 2021

**First decision:** February 10, 2021

**Revised:** February 18, 2021

**Accepted:** March 25, 2021

**Article in press:** March 25, 2021

**Published online:** April 28, 2021

**P-Reviewer:** Liu Y, Sawada A, Uygun I, Wang D

**S-Editor:** Zhang H

**L-Editor:** A

**P-Editor:** Ma YJ



©The Author(s) 2021. Published by Baishideng Publishing Group Inc. All rights reserved.

**Core Tip:** The goal of this review is to discuss recent technological advancements that have utility for patients with gastroesophageal reflux disease (GERD) as a pre-operative assessment for anti-reflux surgery. Surgical treatment of GERD is centered around improving the integrity of the lower esophageal sphincter, therefore it is crucial to rule out other esophageal pathologies that may present with GERD-like symptoms. Advances in pH-impedance studies allow for assessment of patients with weak acid reflux of non-erosive reflux disease. High resolution manometry with the addition of provocative measures can uncover underlying esophageal motility disorders with GERD-like symptoms.

**Citation:** Yodice M, Mignucci A, Shah V, Ashley C, Tadros M. Preoperative physiological esophageal assessment for anti-reflux surgery: A guide for surgeons on high-resolution manometry and pH testing. *World J Gastroenterol* 2021; 27(16): 1751-1769

**URL:** <https://www.wjgnet.com/1007-9327/full/v27/i16/1751.htm>

**DOI:** <https://dx.doi.org/10.3748/wjg.v27.i16.1751>

## INTRODUCTION

Gastroesophageal reflux disease (GERD), defined as an abnormal reflux of gastric contents with associated symptoms, is one of the most common digestive diseases in the world, and currently affects up to 30% of individuals in North America<sup>[1,2]</sup>. While the disease is commonly encountered in the outpatient setting, the true number of individuals with GERD could be even higher, as some patients may self-treat with over-the-counter medications<sup>[3]</sup>. Studies have also found the number of patients with GERD continues to rise, which may be due to the growing obesity epidemic<sup>[1]</sup>. Additionally, GERD is one of the costliest digestive diseases in the United States, with up to half of the cost attributed to the long term use of proton pump inhibitor (PPI) therapy<sup>[4]</sup>.

The American College of Gastroenterology (ACG) guidelines state that a presumptive diagnosis of GERD can be made in patients with classical symptoms such as heartburn or regurgitation, with further diagnostic evaluation such as an upper endoscopy recommended for patients with alarm symptoms<sup>[5]</sup>. The ACG recommends management of these patients begin with lifestyle modifications, including weight loss and dietary changes, along with an 8-week course of PPI therapy<sup>[5]</sup>. While this approach is effective for most patients, a subset of patients may require further management including surgical options such as fundoplication. Surgical treatment of GERD is as effective as medical management in appropriate candidates and is currently recommended for reasons including complications from PPIs, medication non-compliance, and large hiatal hernias<sup>[3,5]</sup>. Additionally, the Society of American Gastrointestinal and Endoscopic Surgeons (SAGES) recommends surgical therapy for patients with GERD who: have failed medical management, request surgery due to quality of life issues related to long term medication use, have complications such as Barrett's esophagus, or have extra-esophageal symptoms related to their GERD<sup>[6]</sup>.

While surgical treatment of GERD may be as effective as medical therapy, complications are also possible. The most commonly reported side effects of surgery include dysphagia, belching, and increased abdominal bloating, though it is also possible to develop more severe complications requiring repeat surgery<sup>[7]</sup>. A total 360° Nissen Fundoplication is the most common surgical treatment for GERD, but variations also exist involving differing degrees of wrapping. Studies have found partial fundoplication to be similarly effective for reducing reflux symptoms, and may also have less post-operative dysphagia and bloating<sup>[8]</sup>. This is supported by a level 1 recommendation from the SAGES that partial fundoplication is associated with less dysphagia and similar patient satisfaction<sup>[6]</sup>. Additionally, newer techniques such as the Linx procedure [which uses a circlet of magnets to augment the lower esophageal sphincter (LES)] have shown similar short-term outcomes for the treatment of GERD when compared to fundoplication. More research is needed on the long-term outcomes<sup>[9]</sup>.

While surgical treatment of GERD can successfully relieve symptoms in up to 90% of patients<sup>[10]</sup>, a thorough pre-operative assessment is necessary to identify appropriate surgical candidates. The underlying mechanism of anti-reflux surgery is to improve the integrity of the LES. Therefore, in order to achieve the best post-operative outcomes, it is crucial to confirm a patient's symptoms are due to GERD and not another underlying pathology. Otherwise, a patient would likely continue experiencing symptoms post-operatively along with potentially developing complications such as dysphagia.

Newer technologies are becoming increasingly available for the assessment of patients with reflux symptoms and can help confirm the diagnosis of GERD. Improvements in pH studies with the inclusion of impedance measurements may help identify patients with non-erosive reflux disease (NERD). Additionally, advancements in high resolution manometry (HRM) help further classify esophageal pathologies and identify patients as having disorders with GERD like symptoms (Table 1). In this review, we aim to provide a guide for the pre-operative assessment and evaluation of patients with reflux. We will focus on newer technologies that can be used to identify appropriate candidates for anti-reflux surgery by confirming the diagnosis of GERD and ruling out other esophageal diseases.

The ACG guidelines state that a presumptive diagnosis of GERD can be made in patients with classical symptoms such as heartburn or regurgitation, with further diagnostic evaluation such as an upper endoscopy recommended for patients with alarm symptoms<sup>[5]</sup>. The ACG recommends management of these patients begin with lifestyle modifications, including weight loss and dietary changes, along with an 8-wk course of PPI therapy<sup>[5]</sup>. While this approach is effective for most patients, a subset of patients may require further management including surgical options such as fundoplication. Surgical treatment of GERD is as effective as medical management in appropriate candidates and is currently recommended for reasons including complications from PPIs, medication non-compliance, and large hiatal hernias<sup>[3,5]</sup>. Additionally, the SAGES recommends surgical therapy for patients with GERD who: have failed medical management, request surgery due to quality of life issues related to long term medication use, have complications such as Barrett's esophagus, or have extra-esophageal symptoms related to their GERD<sup>[6]</sup>.

While surgical treatment of GERD may be as effective as medical therapy, complications are also possible. The most commonly reported side effects of surgery include dysphagia, belching, and increased abdominal bloating, though it is also possible to develop more severe complications requiring repeat surgery<sup>[7]</sup>. A total 360° Nissen fundoplication is the most common surgical treatment for GERD, but variations also exist involving differing degrees of wrapping. Studies have found partial fundoplication to be similarly effective for reducing reflux symptoms, and may also have less post-operative dysphagia and bloating<sup>[8]</sup>. This is supported by a level 1 recommendation from the SAGES that partial fundoplication is associated with less dysphagia and similar patient satisfaction<sup>[6]</sup>. Additionally, newer techniques such as the Linx procedure (which uses a circlet of magnets to augment the LES) have shown similar short-term outcomes for the treatment of GERD when compared to fundoplication. More research is needed on the long-term outcomes<sup>[9]</sup>.

While surgical treatment of GERD can successfully relieve symptoms in up to 90% of patients<sup>[10]</sup>, a thorough pre-operative assessment is necessary to identify appropriate surgical candidates. The underlying mechanism of anti-reflux surgery is to improve the integrity of the LES. Therefore, in order to achieve the best post-operative outcomes, it is crucial to confirm a patient's symptoms are due to GERD and not another underlying pathology. Otherwise, a patient would likely continue experiencing symptoms post-operatively along with potentially developing complications such as dysphagia.

Newer technologies are becoming increasingly available for the assessment of patients with reflux symptoms and can help confirm the diagnosis of GERD. Improvements in pH studies with the inclusion of impedance measurements may help identify patients with NERD. Additionally, advancements in HRM help further classify esophageal pathologies and identify patients as having disorders with GERD like symptoms (Table 1). In this review, we aim to provide a guide for the pre-operative assessment and evaluation of patients with reflux. We will focus on newer technologies that can be used to identify appropriate candidates for anti-reflux surgery by confirming the diagnosis of GERD and ruling out other esophageal diseases.

**Table 1 Esophageal disorders with gastroesophageal reflux disease-like symptoms**

Diagnosis	Definition	Clinical symptoms	Pathophysiology	Diagnostic evaluation
<b>Structural disorders</b>				
GERD	Symptoms and complications secondary to the reflux of gastric contents above the lower esophageal sphincter <sup>[5]</sup>	Regurgitation, reflux, dysphagia, retrosternal non-cardiac chest pain, globus sensation, extra esophageal symptoms	Abnormal transient LES relaxation, LES dysfunction secondary to anatomic abnormality such as hiatal hernia	Upper endoscopy, high resolution manometry, ambulatory pH testing, ambulatory impedance testing
Weak acid reflux	Symptoms secondary to reflux of gastric contents above the LES with pH ranging from 4-7 <sup>[32]</sup>	Reflux, regurgitation, non-cardiac chest pain	Persistent reflux with pH from 4-7 due to transient LES relaxation	pH studies - on maximum PPI therapy
Eosinophilic esophagitis	Presence of symptoms of esophageal dysfunction such as reflux or dysphagia, eosinophilic inflammation on esophageal biopsy with $\geq 15$ eosinophils per high power field, and exclusion of other disorders with similar presentations <sup>[61]</sup>	Dysphagia, reflux, non-cardiac chest pain	Eosinophil mediated inflammatory response in the esophagus secondary to allergenic antigens	Upper endoscopy with biopsy
<b>Motility disorders</b>				
Achalasia	Elevated IRP > 15 mmHg and absence of normal peristalsis <sup>[44]</sup>	Dysphagia, regurgitation, non-cardiac chest pain	Failure of LES relaxation and absence of normal peristalsis	High resolution manometry, upper endoscopy, barium studies
Absent peristalsis	Systemic symptoms with aperistalsis with failed peristalsis on 100% of swallows <sup>[49]</sup>	Reflux, dysphagia, non-cardiac chest pain	Lower esophageal collagen deposition leading to LES dysfunction	High resolution manometry, autoimmune antibody workup
Distal esophageal spasm	Normal IRP and $\geq 20\%$ premature contractions with DCI > 450 mmHg <sup>[44]</sup>	Dysphagia, regurgitation, reflux, non-cardiac chest pain	Impaired inhibition and coordination of esophageal muscle contraction	High resolution manometry, Barium swallow "corkscrew esophagus"
Hypercontractile esophagus	Minimum of 2 swallows with DCI > 8000 mmHg <sup>[44]</sup>	Retrosternal non-cardiac chest pain, dysphagia, regurgitation	Increased contraction of esophageal smooth muscle	Upper endoscopy, barium studies, high resolution manometry
Esophagogastric junction outflow obstruction	Elevated median IRP > 15 mmHg with evidence of peristalsis on swallows <sup>[44]</sup>	Dysphagia, reflux, regurgitation	Impairment of esophagogastric junction relaxation with normal or weakened esophageal peristalsis	High resolution manometry, needs to be confirmed with further studies such as barium swallow or endoflip, must rule out artifact that can be seen with a hiatal hernia
Opioid induced esophageal dysfunction	Presence of symptoms of esophageal dysfunction with manometric evidence of esophageal dysmotility in the presence of chronic opioid use <sup>[55]</sup>	Regurgitation, dysphagia, reflux	Opioid induced blocking of esophageal inhibitory signals leading to increased spastic contraction and decreased LES relaxation	Clinical history, high resolution manometry
Gastroparesis	Presence of symptoms such as nausea, vomiting, and early satiety with mechanical obstruction ruled out and evidence of delayed gastric emptying on testing <sup>[82]</sup>	Nausea, reflux, regurgitation, early satiety, abdominal pain and bloating	Multiple etiologies caused slowed peristalsis and delayed gastric emptying	Gastric emptying study
<b>Functional disorders</b>				
Functional heartburn	Presence of burning retrosternal discomfort, no symptoms relief on optimal therapy, absence of GERD or EOE as cause of symptoms, and absence of major motility disorder <sup>[83]</sup>	Reflux, regurgitation, globus sensation	Potentially secondary to increased esophageal sensitivity	Upper endoscopy, high resolution manometry, pH-impedance studies
Reflux hypersensitivity	Presence of retrosternal chest pain, normal endoscopy and absence of EOE, absence of major motility disorder, and symptom association with reflux events with normal acid exposure on pH-impedance tests <sup>[83]</sup>	Reflux	Hypersensitization of esophageal nerve endings leading to pain secondary to physiologic esophageal stimuli	Upper endoscopy, high resolution manometry, pH-impedance studies
Rumination	Must include both persistent regurgitation of recently ingested food with subsequent spitting or re-mastication, and regurgitation that is not preceded by retching <sup>[83]</sup>	Regurgitation (frequently after meals), reflux	Behavioral contraction of abdominal muscles leading to increased intragastric pressure and reflux	Clinical history, high resolution manometry, pH-impedance studies
Supragastric	Presence of frequent repetitive	Frequent belching, reflux,	Behavioral swallowing of air	Clinical history, high

belching	belching, no established clinical correlate for gastric belching, and evidence of supragastric origin on impedance testing <sup>[83]</sup>	regurgitation, globus sensation	without LES relaxation	resolution manometry, pH-impedance studies
----------	--	---------------------------------	------------------------	--

LES: Lower esophageal sphincter; GERD: Gastroesophageal reflux disease; IRP: Integrated relaxation pressure; DCI: Distal contractile integral; EOE: Eosinophilic esophagitis.

## HISTORY TAKING

The most important step in evaluating a patient's candidacy for anti-reflux surgery is to confirm the diagnosis of GERD. This starts with careful history taking to assess the signs and symptoms a patient is suffering from. While the presence of typical GERD symptoms is enough for a presumptive diagnosis<sup>[5]</sup>, these symptoms can also be present in a wide range of diseases and do not confirm the diagnosis of GERD. One recent systematic review found that classic symptoms such as heartburn and regurgitation had a varying degree of sensitivity, ranging from 30%-76%, for the presence of underlying GERD<sup>[11]</sup>. Additionally, the researchers found the studied symptoms were associated with a wide range of specificities (62%-96%)<sup>[11]</sup>. It is also important to identify if patients are suffering from extra-esophageal symptoms of GERD, as they are less likely to find symptom relief with surgery. One randomized control study compared patients with asthma on medical *vs* surgical therapy for reflux. While all patients experienced clinical improvement of their symptoms, researchers found no significant difference between the two modalities<sup>[12]</sup>. Overall, while a patient may display classic symptoms of GERD, further assessment must be completed to determine their appropriateness for surgery.

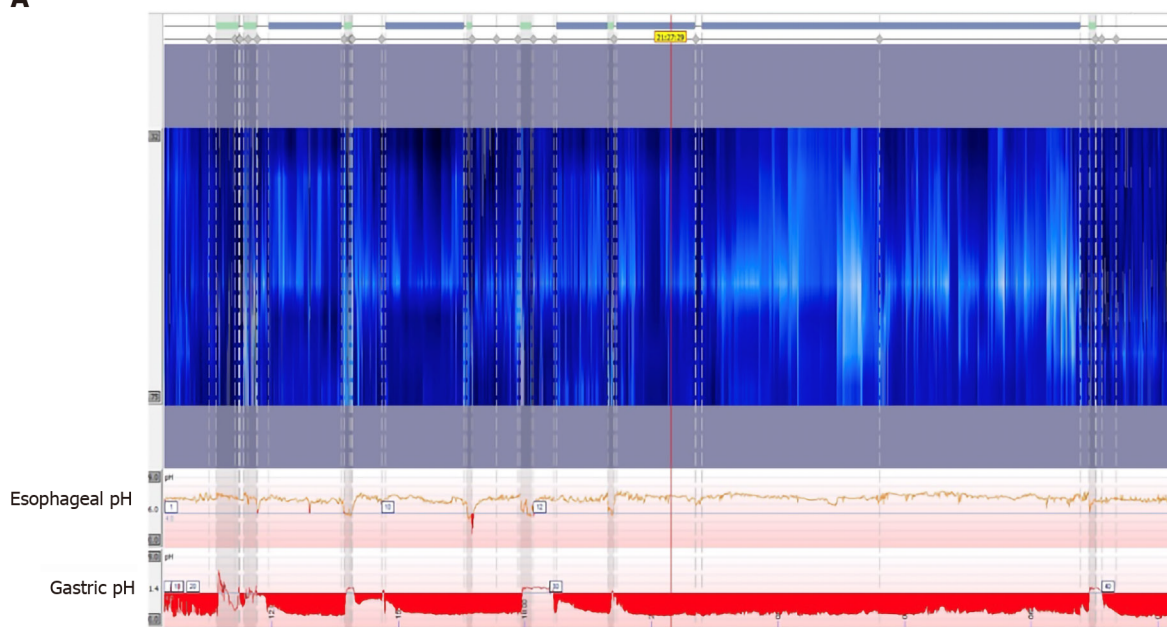
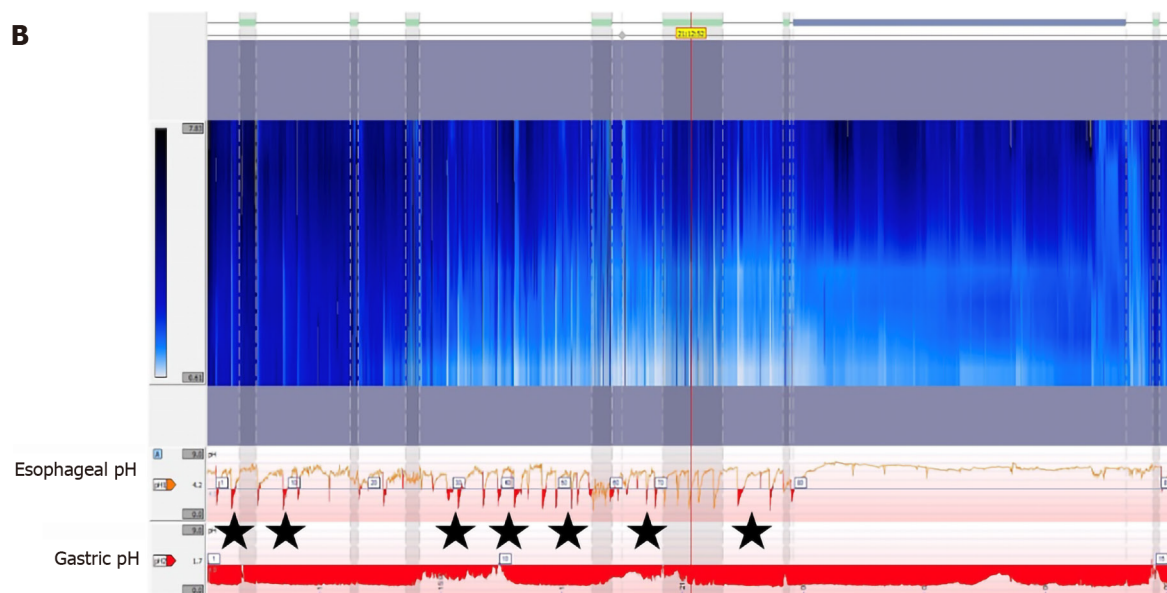
Another important aspect of the patient's history is to assess their response to PPI therapy, which may be a good predictor of outcomes after anti-reflux surgery<sup>[13]</sup>. One recent study involving 370 patients undergoing laparoscopic Nissen fundoplication found patients who responded well to PPI therapy had a significantly greater reduction in reflux symptoms after surgery<sup>[14]</sup>. Previous studies have also indicated that patients with symptoms refractory to PPI therapy may have a higher likelihood of poor surgical outcomes<sup>[15]</sup>. However, while PPI effectiveness may help predict surgical outcomes, it should not be used to confirm or rule out a diagnosis. One meta-analysis found that a successful response to PPI therapy was only 78% sensitive and 54% specific for an underlying diagnosis of GERD<sup>[16]</sup>.

When assessing a patient for anti-reflux surgery, it is also important to understand the role of obesity in surgical outcomes. It is known that GERD is more common in obese patients, as greater central adipose tissue may lead to increased intraabdominal pressure stressing the LES<sup>[17]</sup>. While some studies indicated the morbidly obese are at a higher risk for surgical failure, more recent studies found similar outcomes of fundoplication in obese patients<sup>[18,19]</sup>. An alternative surgical option for obese patients includes Roux-en-Y gastric bypass surgery. The SAGES currently recommends bypass surgery for morbidly obese patients with GERD, as it can help decrease GERD symptoms in addition to the weight loss benefits for the patient<sup>[6]</sup>. However, evidence is still unclear regarding the optimal surgical treatment for patients with class I obesity, and while anti-reflux surgery is a safe option, these patients should be evaluated on a case-by-case basis. Additionally, it is still important to fully assess the reflux symptoms of patients undergoing weight loss surgery. While obese patients are more likely to have GERD, they may also have an underlying esophageal motility disorders, and the use of HRM can help distinguish between these conditions<sup>[20]</sup>.

## ESOPHAGEAL PH TESTING

After thorough history taking to identify patients with GERD like symptoms, a upper endoscopy can help make a diagnosis by directly visualizing esophageal lesions such as esophagitis. However, a subset of patients may still have gastric reflux without evidence of any erosions<sup>[5]</sup>. In these patients with NERD, further testing is required to accurately diagnose reflux and confirm if a patient might be a good candidate for surgical correction. Esophageal pH testing can be a useful modality to identify acidic reflux above the LES<sup>[21,22]</sup>. Standard ambulatory pH monitoring involves placement of a trans-nasal probe 5 cm above the LES<sup>[23]</sup>. The probe then measures acid exposure time (AET) by recording any drops in pH below 4 over a 24-h period (**Figure 1**). The



**A****B**

**Figure 1 Twenty-four hours pH studies.** A: Normal 24 h pH study showing acid in the stomach without acid reflux events in the esophagus; B: Abnormal 24 h pH monitoring test with multiple acid reflux events in the esophagus (star indicating reflux events).

DeMeester score was a system developed in the 1970's to categorize a patient's reflux based on parameters including the number and timing of reflux events as well as supine *vs* upright positioning during these periods<sup>[24]</sup>. More recently, the Lyon consensus recommends using only AET when determining GERD, and defined pathologic reflux as having greater than 6% AET<sup>[22]</sup>. Although there is debate regarding which method is more reliable, both have similar strengths and weaknesses, and there is no current evidence that one method is superior to the other<sup>[25]</sup>. In general, the ACG recommends pH monitoring for all patients with NERD as a pre-operative assessment, and more recent studies have also found utility in measuring AET for patients with LA grade A or B esophagitis prior to surgery<sup>[5,26]</sup>. Additionally, pH testing has utility for confirming reflux in patients with GERD or NERD who are unresponsive to PPI therapy<sup>[21]</sup>.

One drawback of ambulatory pH monitoring is the discomfort patients may experience from the trans-nasal catheter, with some studies showing patients tend to decrease typical daily activities that might promote reflux after the probe is placed<sup>[27]</sup>. Wireless capsule pH monitoring is also available, and while it must be placed endoscopically, it is often better tolerated than the catheter probe and may provide

better measurements of physiologic reflux (Figure 2)<sup>[28]</sup>. In addition to improved patient tolerance, the capsule can record AET for 48-96 h depending on battery life, improving the sensitivity of the test<sup>[29]</sup>. However, both catheter and capsule pH monitoring are limited by the fact that they only measure acidic reflux. Studies have shown up to 30% of patients with pathologic reflux may have normal pH measurements on ambulatory monitoring<sup>[30]</sup>. This indicates up to 1/3 of patients with LES dysfunction who may benefit from surgery are missed with this form of testing (Table 2).

### **pH-impedance testing**

Multichannel intraluminal impedance pH monitoring (MII-pH) is a newer technology that measures changes in electrical conductivity between multiple points on the probe<sup>[23]</sup>. This data is combined with the pH probe to measure reflux of any material above the LES, independent of pH (Figure 3)<sup>[30]</sup>. The Lyon consensus defines physiologic reflux as 40 or less reflux events, with pathologic defined as greater than 80 episodes of reflux<sup>[22]</sup>. This definition allows for patients to continue PPI therapy during testing, as pH does not factor into the diagnosis<sup>[31]</sup>. MII-pH testing also has utility in identifying patients with weak acid reflux (pH 4-7). Up to 30% of patients with GERD may continue to have symptoms refractory to acid suppression therapy<sup>[32]</sup>. While these symptoms could potentially be secondary to any of the diagnoses seen in Table 1, MII-pH testing can identify patients with weak reflux by independently measuring reflux and pH (Figure 3). Treatment of patients with weak acid reflux is controversial, especially because previous studies have shown failure of PPIs is an indicator for poor outcomes after anti-reflux surgery<sup>[15]</sup>. However, if clinicians can confirm refractory GERD is secondary to weak acid reflux and not alternative diagnoses such as functional heartburn, they can identify patients who would still be good surgical candidates<sup>[33]</sup>.

Limitations of MII-pH testing include using a trans-nasal catheter and required manometry testing for all patients prior to placement<sup>[29]</sup>. Additionally, visual analysis of the data is time consuming, but computerized electronic review software can be imprecise. One study found that computer interpretation of results identified only 74% of reflux events confirmed by visual analysis<sup>[34]</sup>. The authors suggested visual review of the data may be necessary to confirm test accuracy<sup>[34]</sup>. There also remains a potential for patients to have increased AET and reflux events secondary to other esophageal pathologies not related to LES dysfunction or GERD. This is important to keep in mind during pre-operative assessment for anti-reflux surgery, as patients without underlying LES dysfunction would not be good candidates for surgical treatment. Patients with rumination syndrome can have false positives on pH testing due to frequent regurgitation, not transient LES relaxation<sup>[35]</sup>. Increased AET can also be secondary to a hypomotility disorders, such as in patients with achalasia or scleroderma. This is not limited to only pH testing, as impedance studies may also have inconclusive or misleading results in patients with achalasia, scleroderma, or rumination syndrome<sup>[29]</sup>. Due to these possibilities, the ACG recommends that all patients undergo manometry as part of their pre-operative assessment to rule out any motility disorders that may cause reflux<sup>[5]</sup>.

Another important aspect of utilizing pH or pH-impedance testing is the measurement of any associated symptoms during testing (Figure 4). Since there is still the potential for false positives when looking at AET or number of reflux episodes during testing, it is also important for a patient to log any symptoms they experience during testing<sup>[36]</sup>. This also has utility with extra-esophageal symptoms and can help in identifying if symptoms are causing reflux or are secondary to reflux, such as coughing<sup>[36]</sup>. The Symptoms Association Probability (SAP) is one example of a methods to assess the association of symptoms with reflux events. This involves using a 2 × 2 table assessing the presence of symptoms and reflux events in 2-min blocks over a 24 h period<sup>[37]</sup>. Analysis then allows the determination of whether the symptoms were more likely secondary to reflux events or caused by chance. While there are other methods to assess symptom association, a SAP can provide a probability of symptom association and is thought to have the best clinical utility<sup>[36]</sup>.

## **MANOMETRY AND MOTILITY TESTING**

Another important aspect of the pre-operative assessment is to rule out major esophageal motility disorders with HRM (Figure 5). Patients with GERD often have findings of decreased LES pressures on HRM, indicating an impaired ability for the

**Table 2 Esophageal pH measurement options**

	Overview	Benefits	Limitations
Twenty-four hours ambulatory catheter	Trans-nasal catheter placed 5 cm above the LES. Measures time of pH < 4	Can be placed in office	Catheter may cause discomfort; Patients may deviate from daily routine; Patients should refrain from taking PPI therapy during testing; False positives secondary eating/drinking acidic food
Wireless capsule	Small probe that is placed endoscopically in esophagus 5-6 cm above LES. Measures time of pH < 4	Little patient discomfort; Battery life of 48-96 h allows for better measurement of physiologic acid exposure	Must be placed endoscopically; Patients should refrain from taking PPI therapy during testing; False positives secondary eating/drinking acidic food
MII-pH catheter	Trans-nasal catheter placed 5 cm above LES. Contains pH probe along with electrodes to measure reflux episodes	Can be done on or off PPI; Measures pH and reflux independently; Patients can continue taking PPIs; Can identify patients with weak acid reflux	Catheter may cause discomfort; Patients must have prior manometry testing; False positive possible in patients with rumination, achalasia, and scleroderma

LES: Lower esophageal sphincter; PPI: Proton pump inhibitor.

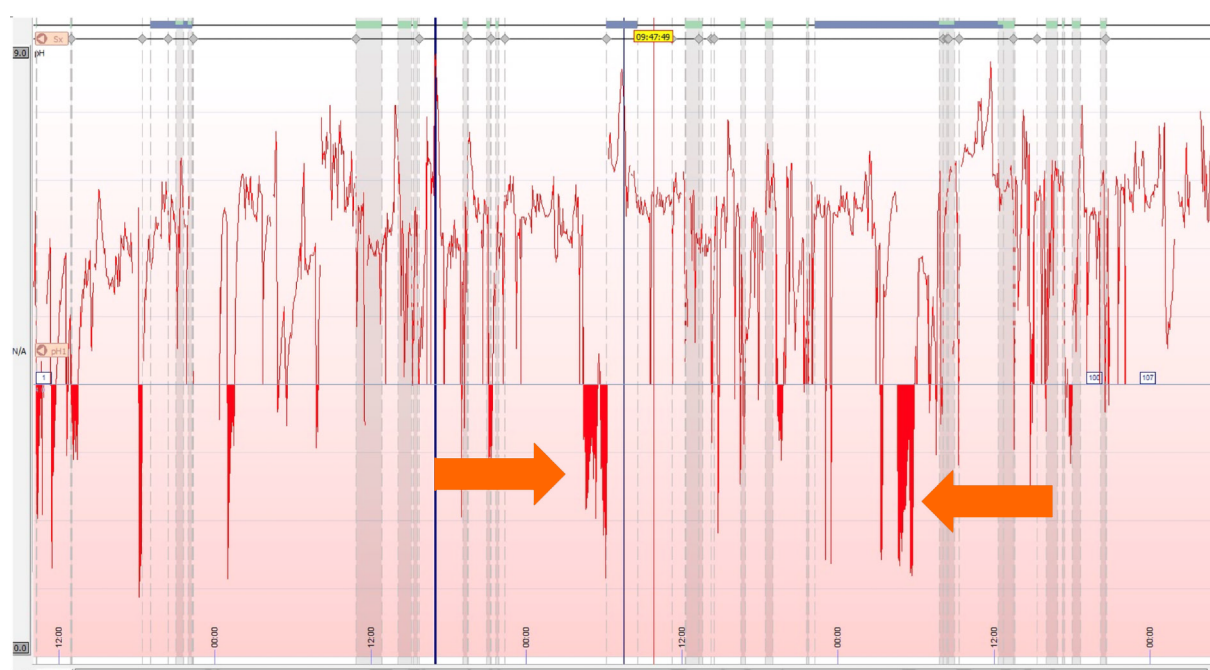


**Figure 2** Abnormal wireless capsule pH study (arrows indicating prolonged reflux events).

LES to act as an anti-reflux barrier and prevent gastric contents from entering the esophagus<sup>[38]</sup>. The smooth muscle in the LES is also augmented by pressure generated from the crural diaphragm, and because HRM utilizes an increased number of sensors, these pressures can be differentiated when evaluating the LES strength<sup>[39]</sup>. The esophagogastric junction contractile integral can also be quantified on HRM and may identify patients with severe reflux, but further research is needed to create a standardized metric for evaluating patients<sup>[22]</sup>. Additionally, LES physiology can be altered in the presence of a hiatal hernia, and HRM can be used to assess and measure the size of a patient's hiatal hernia<sup>[40]</sup>. While esophageal manometry is not a confirmatory test for diagnosing GERD, HRM is useful in identifying any underlying motility issues (Figure 6)<sup>[41,42]</sup>. While there is limited data to support mandatory pre-operative manometry testing, the ACG still recommends manometry to specifically rule out achalasia and absent peristalsis seen in conditions such as scleroderma<sup>[5]</sup>. In the 2019 ICARUS guidelines, 94% of experts also strongly agreed with pre-op HRM testing, but this could only be supported with grade D evidence<sup>[42]</sup>. Additionally, HRM can be used to assess baseline esophageal physiology to predict the risk of post-operative dysphagia.

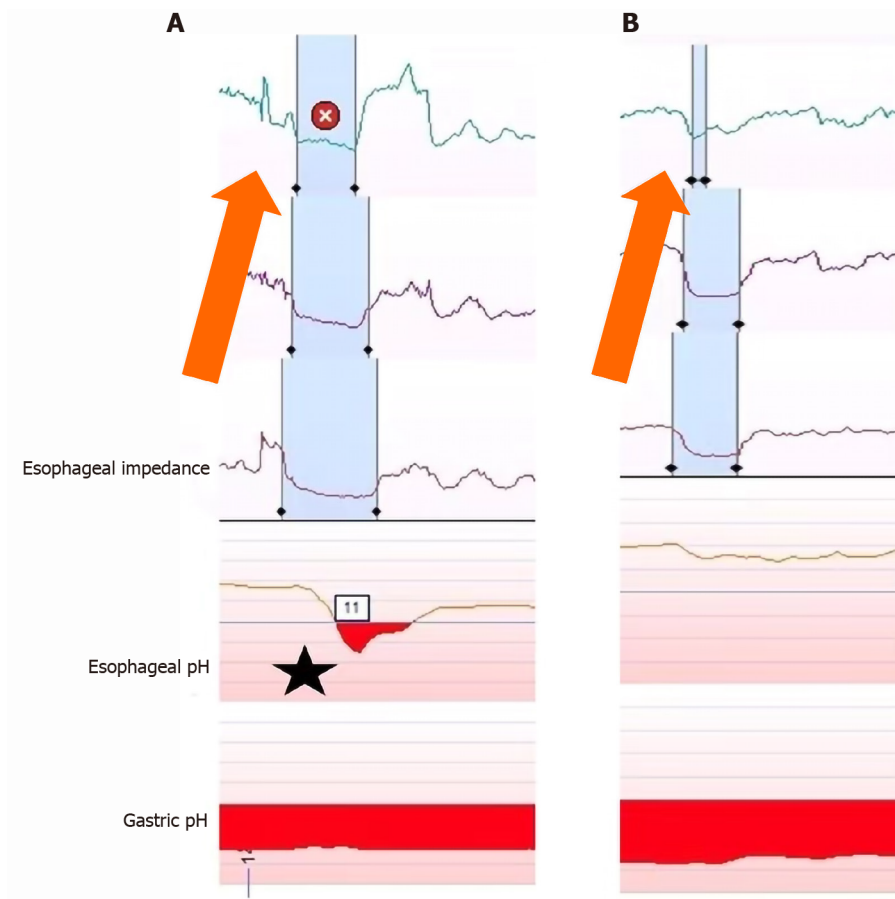


**Figure 3 Examples of pH-impedance measurements.** A: Reflux event recorded during 48 h pH-impedance study; B: Weak acid reflux event in the esophagus without acid exposure in the stomach detected on pH-impedance study (arrows indicating impedance events, star indicating pH drop and acid event).

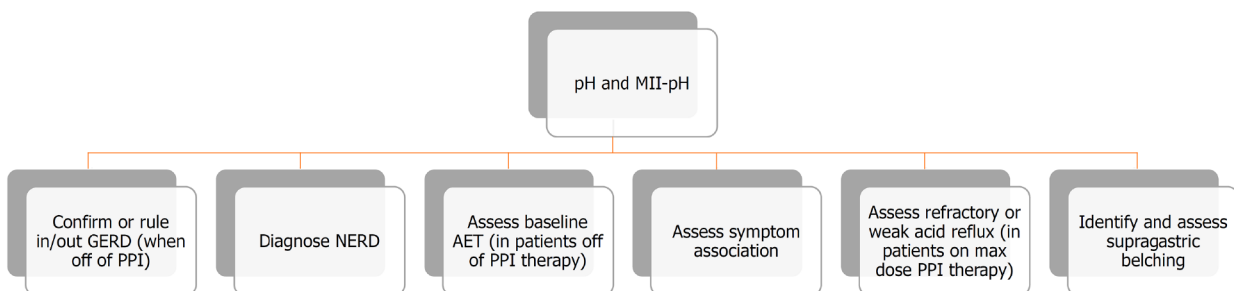


**Figure 4 Utility of pH and multichannel intraluminal impedance pH testing for pre-operative assessment.** GERD: Gastroesophageal reflux disease; NERD: Non-erosive reflux disease; PPI: Proton pump inhibitor; AET: Acid exposure time; MII-pH: Multichannel intraluminal impedance pH monitoring.

### ***Ruling out major motility disorders***

The main indication for HRM should be used to rule out major motility disorders, as these may be the underlying cause of a patient's reflux symptoms, and may also be a contraindication for fundoplication<sup>[6]</sup>.

**Achalasia:** Abnormal esophageal peristalsis can manifest as GERD-like symptoms in patients with achalasia. The integrated relaxation pressure (IRP) is an important measurement during manometry that assesses esophageal pressures and transit across the esophagogastric junction<sup>[43]</sup>. According to the Chicago Classification (CC), type I achalasia is diagnosed in patients found to have an IRP > 15 mmHg and 100% failed peristalsis on HRM, with type II having the same characteristics as well as panesophageal pressurization in ≥ 20% of swallows<sup>[44]</sup>. Type III achalasia is defined as an elevated IRP > 15 mmHg, the absences of any normal peristalsis, and spastic contractions greater > 450 mmHg on ≥ 20% of swallows (Figure 7)<sup>[44]</sup>. As previously



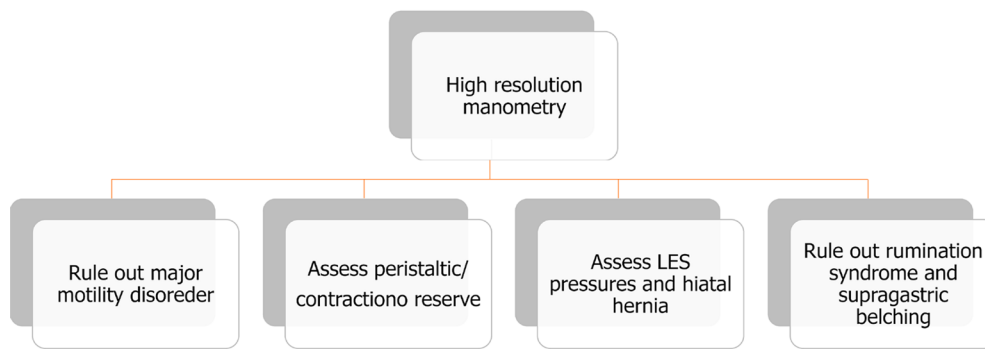


**Figure 5 Utility of high-resolution manometry for pre-operative assessment.** LES: Lower esophageal sphincter.

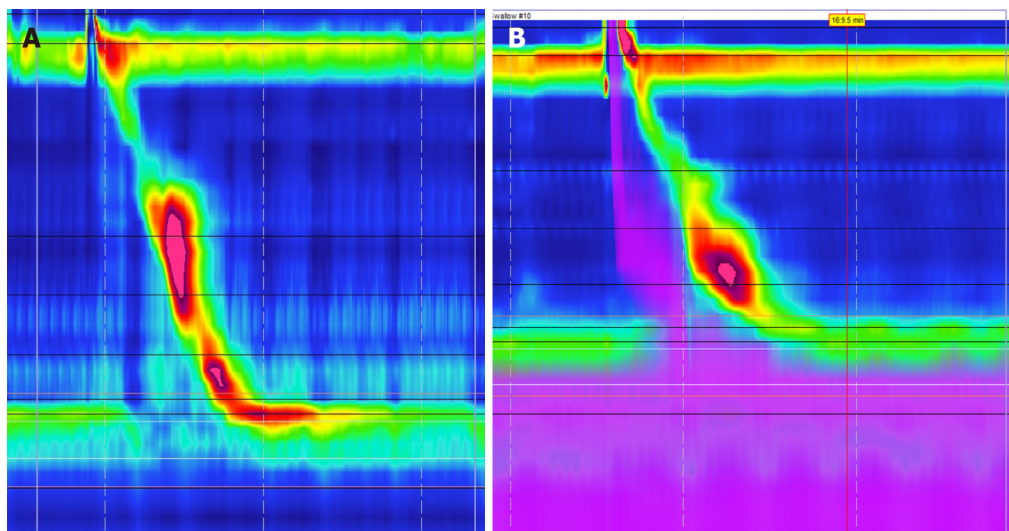


**Figure 6 Normal peristalsis and lower esophageal sphincter relaxation on high-resolution manometry.** A: Example of normal swallow on high-resolution manometry; B: Normal swallow with complete esophageal clearance by impedance.

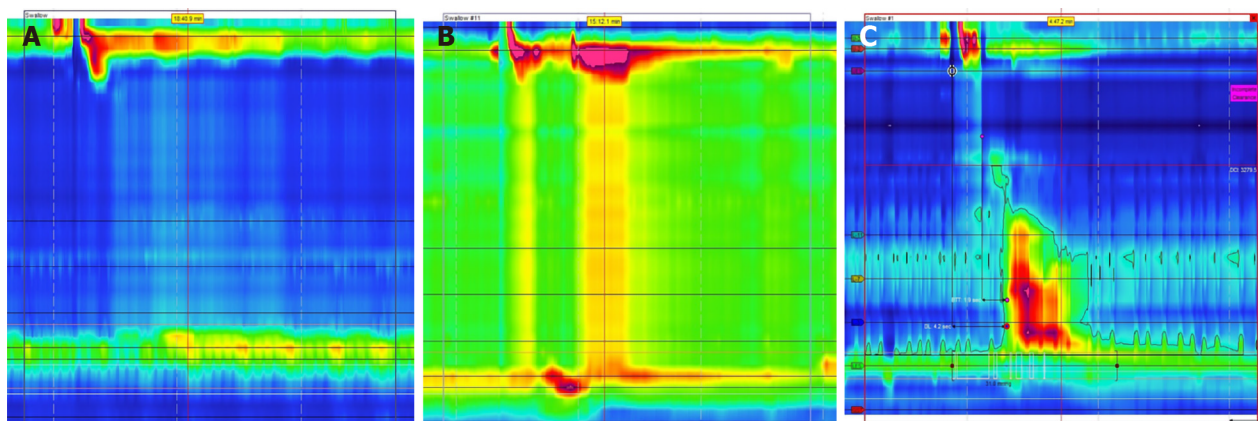


**Figure 7 Examples of achalasia diagnosed on high-resolution manometry.** A: Type I achalasia with failure of lower esophageal sphincter relaxation and absence of peristalsis; B: Type II achalasia with panesophageal pressurization; C: Type III achalasia with abnormal peristalsis (spastic/premature contractions).

discussed, the goal of fundoplication is to improve the integrity of the LES, but patients with achalasia suffer from impaired LES relaxation along with esophageal aperistalsis. While these patients may also have underlying GERD, surgical treatment revolves around addressing the LES with myotomy<sup>[42,45]</sup>. However, after myotomy weakens the LES, GERD can become a common side effect. While these patients would benefit from fundoplication, there is debate regarding the risk of post-operative



dysphagia<sup>[46]</sup>. One prospective randomized study compared outcomes of myotomy alone *vs* myotomy with fundoplication for 43 patients with achalasia. Researchers found that patients receiving myotomy with fundoplication had significantly less GERD and AET, with no significant difference in dysphagia between the two groups<sup>[47]</sup>. The group also followed patients long-term and concluded there was no significant differences in post-op dysphagia in patients who received myotomy with fundoplication<sup>[48]</sup>. Current guidelines from both the ACG and the SAGES recommend patients with achalasia undergo both myotomy and fundoplication for the best outcomes<sup>[45,46]</sup>.

**Absent peristalsis:** Conflicting data also exists regarding fundoplication for patients with absent peristalsis. Evidence of aperistalsis, defined as failed peristalsis with 100% of swallows, on HRM can indicate patients with scleroderma-like esophagus (Figure 8)<sup>[49]</sup>. Older studies have confirmed anti-reflux surgery can lead to improved symptoms, but more recent studies indicated these patients might have a higher risk for post-operative dysphagia<sup>[42,50]</sup>. Additionally, studies have shown that alternative surgeries such as a Roux-en-Y bypass may lead to better outcomes. A 2018 study followed patients with systemic sclerosis undergoing surgical treatment for their GERD and compared fundoplication *vs* Roux-en-Y bypass. While the sample size was small, researchers found patients had better GERD symptom relief after Roux-en-Y compared to fundoplication<sup>[51]</sup>.

**Esophagogastric junction outflow obstruction:** Esophagogastric junction outflow obstruction (EGJOO) is another esophageal motility disorder that can present with GERD like symptoms. In this disorder, patients have normal or weakened esophageal peristalsis on HRM with an elevated IRP<sup>[44]</sup>. While the current CC provides a guideline on making a diagnosis with HRM, it is important to remember that other factors can lead to an increased IRP. In some patients with hiatal hernias, the manometry catheter may be incorrectly positioned due to the underlying anatomical abnormality, which can contribute to increased IRP measurements<sup>[52]</sup>. These patients require confirmatory testing, and some centers have adopted the use of upright HRM measurements with an IRP > 12 mmHg as a cutoff<sup>[53]</sup>. Additionally, other esophageal abnormalities such as Schatzki's ring can lead to altered HRM results<sup>[54]</sup>. Data is currently limited regarding the outcomes of fundoplication in patients with EGJOO, but an accurate diagnosis is still important as it identifies esophageal dysmotility as the cause of a patient's GERD like symptoms.

Opioid induced esophageal dysfunction is increasingly being recognized as a potential cause of esophageal dysmotility. Just as chronic opioid use can lead to bowel hypomotility, it is theorized that opioids may block esophageal inhibitory signals leading to increased contractions and decreased LES sphincter relaxation<sup>[55]</sup>. This can in turn lead to findings of EGJOO, esophageal spasm, and hypercontractile esophagus on HRM (Figure 9)<sup>[56]</sup>. It is important to recognize the effect of chronic opioid use on esophageal motility, as cessation of opioid drugs may lead to resolution of GERD like symptoms.

**Hypercontractile disorders:** In addition to uncovering evidence of esophageal hypomotility, HRM can also identify hypercontractile patterns such as jackhammer esophagus and esophageal spasm (Figure 10). While the pathophysiology behind these diseases is still under investigation, both involve impaired inhibition and coordination of esophageal peristalsis and can present with dysphagia, non-cardiac chest pain, and reflux<sup>[57,58]</sup>. Jackhammer esophagus can be diagnosed on HRM if at least 20% of swallows have a distal contractile integral (DCI) of greater than 8000 mmHg<sup>[44]</sup>. According to the 2019 ICARUS guidelines, 64% of experts agreed that patients with jackhammer esophagus are still good candidates for anti-reflux surgery, but this assertion is only supported by grade D evidence<sup>[42]</sup>. Data is limited regarding outcomes of patients with jackhammer esophagus after anti-reflux surgery, but one retrospective study found no difference in outcomes when compared to patients with physiologic esophageal motility<sup>[59]</sup>. Distal esophageal spasm is diagnosed in patients with a normal IRP but  $\geq 20\%$  of premature contractions with a DCI of > 450 mmHg<sup>[44]</sup>. 64% of experts agreed that these patients were not good surgical candidates, but this again was only supported with grade D evidence<sup>[42]</sup>. Instead, the authors suggested specific therapeutic measures for esophageal spasm such as botulinum injections and myotomy instead of anti-reflux surgery<sup>[42]</sup>.

### Utility of provocative maneuvers during HRM

Provocative studies such as multiple rapid swallow (MRS) or rapid drink challenge

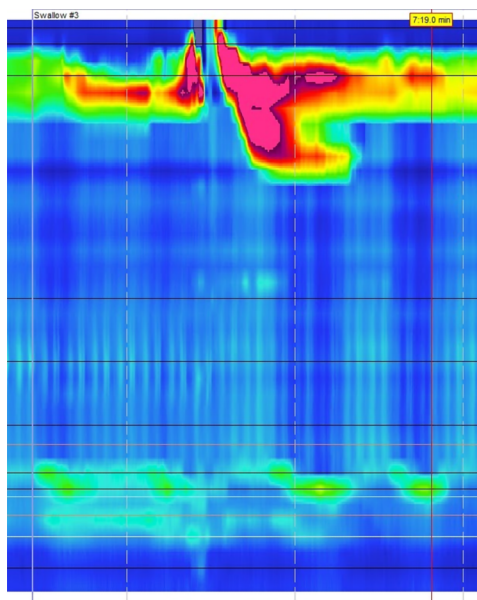


Figure 8 Scleroderma esophagus with absent peristalsis and hypotensive lower esophageal sphincter.

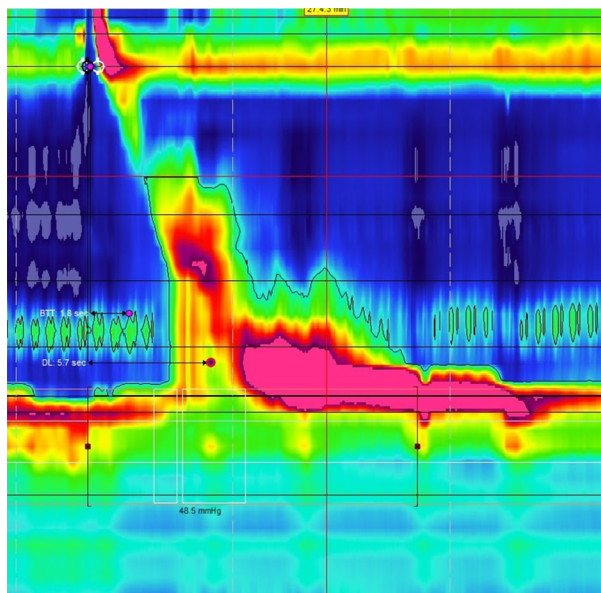
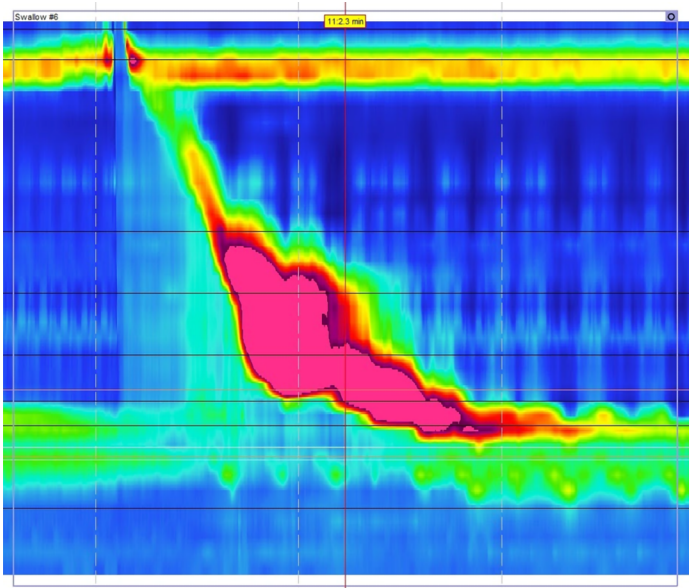


Figure 9 Outflow obstruction with elevated residual pressure and distal pressurization from chronic opioid use.

(RDC) tests can also be added to HRM to further evaluate esophageal physiology. MRS testing involves swallowing small amounts of water over a quick period of time which stresses the coordination of esophageal contraction and LES relaxation<sup>[60]</sup>. Recent studies have found the addition of MRS during HRM can help uncover pathologies that might have been missed on manometry alone such as distal esophageal spasm and achalasia variants<sup>[61]</sup>. MRS also allows for visualization of esophageal pressurization patterns which can help identify hypercontractility and EGJOO<sup>[62,63]</sup>. RDC is also a simple test that can be added to HRM to stress the esophagus and uncover motility disorders. RDC is a similar test to MRS, but involves drinking a larger total amount of water. A recent study in 2017 compared HRM and RDC results between healthy individuals and a cohort of patients with dysphagia and reflux. They found that the addition of RDC improved the sensitivity and specificity of HRM for identifying esophageal motility disorders to 85% and 95% respectively<sup>[64]</sup>.

Another provocative test that can be added to HRM is apple viscous swallows (AVS). AVS involves patients swallowing apple sauce during manometry, and the increased viscosity may help better simulate physiologic swallowing of food. A study from 2011 Looked at patients with dysphagia and compared results of HRM with AVS



**Figure 10** Example of hypercontractile esophagus with distal contractile integral > 8000 mmHg.

and standard water swallows. The researchers found that 4% of patients had abnormal results with water swallows, but this increased to 30% with AVS<sup>[65]</sup>. Overall, the additions of provocative maneuvers such as MRS, RDC, and AVS to HRM are quick and simple and can help identify esophageal motility disorders in patients with GERD like symptoms.

Provocative testing also has important utility as a pre-operative assessment by predicting the risk of post-operative dysphagia. The DCI is another measurement that can be used to assess the strength of esophageal contractions during HRM<sup>[63]</sup>. According to the CC, a DCI ratio can be calculated from standard manometry and MRS testing to assess peristaltic or contraction reserve (Figure 11)<sup>[44]</sup>. This can help indicate the ability of the esophageal body to augment contractions and may be predictive of multiple pathologies in patients with impaired esophageal motility<sup>[22,66]</sup>. Patients with weak contractions on HRM with MRS may have low peristaltic reserve and a DCI ratio cutoff of > 0.85 was found to be 67% sensitive and 64% specific for identifying late post-operative dysphagia in patients with GERD<sup>[67]</sup>. Additionally, a lack of manometric response can identify patients with esophageal involvement of their systemic sclerosis, as peristaltic reserve is typically absent in this population<sup>[68]</sup>.

It is known from previous studies that impaired LES pressures are associated with increased esophageal acid exposure<sup>[69]</sup>. A 2012 retrospective study included over 2000 patients who underwent manometry and pH testing and found that patients with incompetent LES pressures had significantly higher DeMeester scores<sup>[70]</sup>. A hiatal hernia is one example of why the LES can be compromised in patients and lead to lower closing pressures<sup>[71]</sup>. The straight leg raise is another simple provocative maneuver that can be completed during HRM to assess patients with a hiatal hernia (Figure 12). Previous studies have indicated the size of a hiatal hernia is the best predictor for the severity of GERD<sup>[72]</sup>. Straight leg raises during HRM can increase intraabdominal pressure and stress the LES. A recent study measured trans-esophagogastric junction gradient pressures during straight leg raises on HRM and found a significant decrease in peak pressure gradient in patients with a hiatal hernia of 3 cm or greater<sup>[73]</sup>. Straight leg raises are a simple provocative maneuver to add during HRM and can identify patients that could benefit from surgical treatment for both their GERD and hiatal hernia with good outcomes<sup>[74]</sup> (Table 3).

### ***Ruling out supragastric belching and rumination syndrome***

Patients with GERD may also commonly complain of increased belching<sup>[75]</sup>. Supragastric belching is another disorder with many GERD-like symptoms, and is common in patients with GERD, NERD, reflux hypersensitivity, and functional dyspepsia<sup>[76,77]</sup>. Distinguishing between the two disorders is important, as both are due to different underlying pathologies requiring specific treatment approaches. Supragastric belching is seen as a learned behavioral disorder where air is pulled into the esophagus, but there is no transient relaxation of the LES as seen in physiologic

**Table 3 Key measurements on high resolution manometry**

Measurement	Utility
Integrated relaxation pressure	Measures esophageal pressures during transit and passage through esophagogastric junction. Can be used to diagnose achalasia and other hypomotility disorders
Distal contractile integral	Measures strength of esophageal contractions. Can diagnose hypercontractile disorders such as jackhammer esophagus
Distal latency	Measurement of esophageal transit and contraction time. Can indicate impaired or spastic peristalsis
DCI ratio	Ratio of DCI on normal swallows and MRS testing. Used to assess peristaltic reserve. This can be used to predict risk of post-operative dysphagia

DCI: Distal contractile integral; MRS: Multiple rapid swallow.

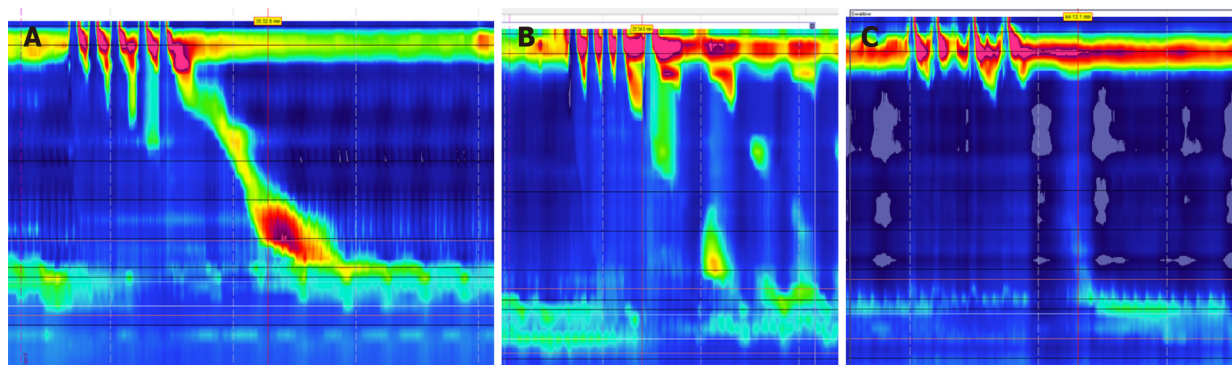


**Figure 11 Findings on high-resolution manometry with multiple rapid swallow.** A: Normal multiple rapid swallow (MRS) with good contraction distal contractile integral; B: Weak esophageal contractions with MRS; C: Failed esophageal contractions with MRS.

belching<sup>[78]</sup>. Even though these patients present with symptoms of reflux, the treatment is directed at behavioral therapy to decrease bringing air into the esophagus. These patients would not be good candidates for anti-reflux surgery. Recent improvements in high resolution impedance manometry (HRIM) allow for clinicians to measure both esophageal pressure and flow during swallows<sup>[79]</sup>. While supragastric belching can induce GERD, HRIM can identify episodes of supragastric belching with no LES relaxation and confirm only esophageal air is released instead of gastric air<sup>[80]</sup>.

Rumination syndrome is another functional disorder involving patients suffering with GERD-like symptoms of frequent reflux and regurgitation. Like supragastric belching, HRM can be useful in identifying the underlying mechanism of the dysfunction. A recent study found that different subtypes of rumination can be identified on HRM, with some having pathophysiologies similar to supragastric belching, and others showing evidence of gastric contents refluxing above the LES<sup>[35]</sup>. While the first line treatment of rumination syndrome involves cognitive behavioral therapy, HRM can help identify patients with gastric rumination as the cause of their reflux symptoms, and these patients may benefit from further treatments such as anti-reflux surgery<sup>[35]</sup>.

## CONCLUSION

Fundoplication is a safe and effective treatment for individuals with GERD, but a thorough pre-operative assessment is critical to achieving good surgical outcomes. Newer technologies continue to become more widely available and can help clinicians in selecting appropriate surgical candidates. By accurately diagnosing GERD, assessing peristaltic reserve, and ruling out major motility disorders and diseases with GERD-like symptoms, clinicians can confidently identify patients with true LES dysfunction who would benefit from surgical intervention.



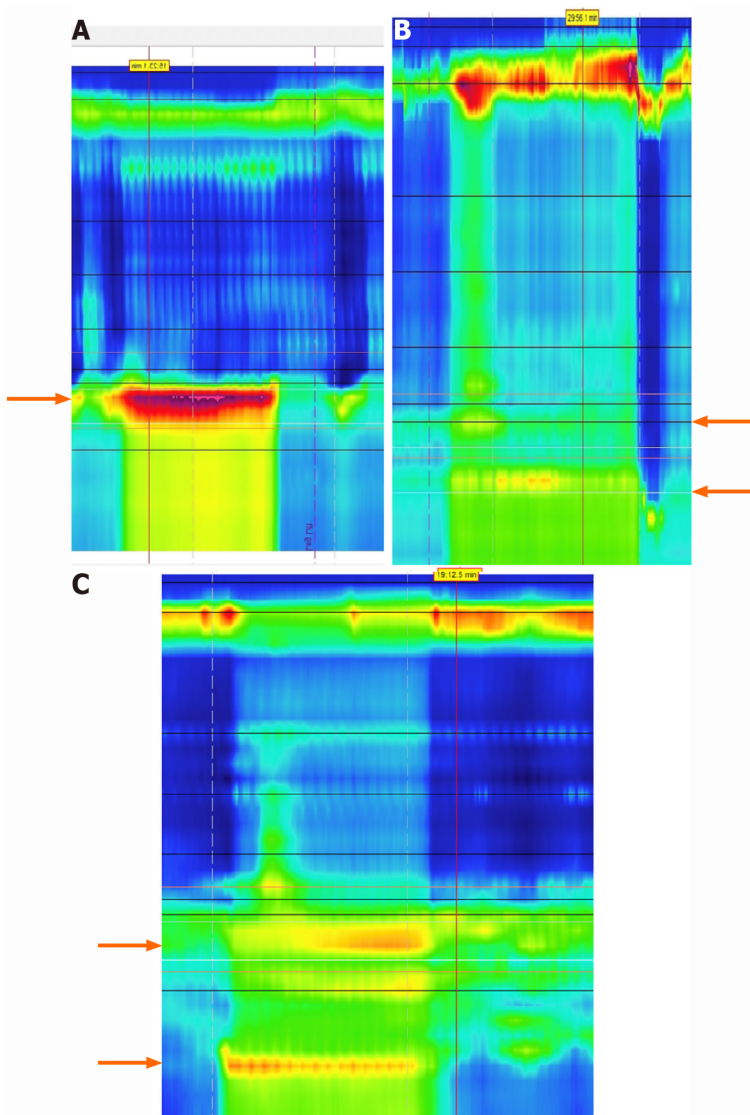


**Figure 12** Examples of straight leg raise testing during high-resolution manometry. A: Normal straight leg raise test with single pressurization zone; B: Two pressurization zones after straight leg raise indicating presence of small hiatal hernia; C: Example of two pressurization zones after straight leg raise in patient with large hiatal hernia (Arrows indicate pressurization zones).

## REFERENCES

- 1 El-Serag HB, Sweet S, Winchester CC, Dent J. Update on the epidemiology of gastro-oesophageal reflux disease: a systematic review. *Gut* 2014; **63**: 871-880 [PMID: 23853213 DOI: 10.1136/gutjnl-2012-304269]
- 2 Dent J, Becher A, Sung J, Zou D, Agr us L, Bazzoli F. Systematic review: patterns of reflux-induced symptoms and esophageal endoscopic findings in large-scale surveys. *Clin Gastroenterol Hepatol* 2012; **10**: 863-873. e3 [PMID: 22401904 DOI: 10.1016/j.cgh.2012.02.028]
- 3 Patti MG. An Evidence-Based Approach to the Treatment of Gastroesophageal Reflux Disease. *JAMA Surg* 2016; **151**: 73-78 [PMID: 26629969 DOI: 10.1001/jamasurg.2015.4233]
- 4 Gawron AJ, French DD, Pandolfino JE, Howden CW. Economic evaluations of gastroesophageal reflux disease medical management. *Pharmacoeconomics* 2014; **32**: 745-758 [PMID: 24807469 DOI: 10.1007/s40273-014-0164-8]
- 5 Katz PO, Gerson LB, Vela MF. Guidelines for the diagnosis and management of gastroesophageal reflux disease. *Am J Gastroenterol* 2013; **108**: 308-28; quiz 329 [PMID: 23419381 DOI: 10.1038/ajg.2012.444]
- 6 Stefanidis D, Hope WW, Kohn GP, Reardon PR, Richardson WS, Fanelli RD; SAGES Guidelines Committee. Guidelines for surgical treatment of gastroesophageal reflux disease. *Surg Endosc* 2010; **24**: 2647-2669 [PMID: 20725747 DOI: 10.1007/s00464-010-1267-8]
- 7 Frazzoni M, Piccoli M, Conigliaro R, Frazzoni L, Melotti G. Laparoscopic fundoplication for gastroesophageal reflux disease. *World J Gastroenterol* 2014; **20**: 14272-14279 [PMID: 25339814 DOI: 10.3748/wjg.v20.i39.14272]
- 8 Broeders JA, Roks DJ, Ahmed Ali U, Watson DI, Baigrie RJ, Cao Z, Hartmann J, Maddern GJ.



- Laparoscopic anterior 180-degree versus nissen fundoplication for gastroesophageal reflux disease: systematic review and meta-analysis of randomized clinical trials. *Ann Surg* 2013; **257**: 850-859 [PMID: 23470572 DOI: 10.1097/SLA.0b013e31828604dd]
- 9 **Skubleny D**, Switzer NJ, Dang J, Gill RS, Shi X, de Gara C, Birch DW, Wong C, Hutter MM, Karmali S. LINX<sup>®</sup> magnetic esophageal sphincter augmentation versus Nissen fundoplication for gastroesophageal reflux disease: a systematic review and meta-analysis. *Surg Endosc* 2017; **31**: 3078-3084 [PMID: 27981382 DOI: 10.1007/s00464-016-5370-3]
  - 10 **Davis CS**, Baldea A, Johns JR, Joehl RJ, Fisichella PM. The evolution and long-term results of laparoscopic antireflux surgery for the treatment of gastroesophageal reflux disease. *JSLs* 2010; **14**: 332-341 [PMID: 21333184 DOI: 10.4293/108680810X12924466007007]
  - 11 **Moayyedi P**, Talley NJ, Fennerty MB, Vakil N. Can the clinical history distinguish between organic and functional dyspepsia? *JAMA* 2006; **295**: 1566-1576 [PMID: 16595759 DOI: 10.1001/jama.295.13.1566]
  - 12 **Larrain A**, Carrasco E, Galleguillos F, Sepulveda R, Pope CE 2nd. Medical and surgical treatment of nonallergic asthma associated with gastroesophageal reflux. *Chest* 1991; **99**: 1330-1335 [PMID: 2036812 DOI: 10.1378/chest.99.6.1330]
  - 13 **Oelschlager BK**, Quiroga E, Parra JD, Cahill M, Polissar N, Pellegrini CA. Long-term outcomes after laparoscopic antireflux surgery. *Am J Gastroenterol* 2008; **103**: 280-7; quiz 288 [PMID: 17970835 DOI: 10.1111/j.1572-0241.2007.01606.x]
  - 14 **Hamdy E**, El Nakeeb A, Hamed H, El Hemaly M, ElHak NG. Outcome of laparoscopic Nissen fundoplication for gastroesophageal reflux disease in non-responders to proton pump inhibitors. *J Gastrointest Surg* 2014; **18**: 1557-1562 [PMID: 24985244 DOI: 10.1007/s11605-014-2584-3]
  - 15 **Campos GM**, Peters JH, DeMeester TR, Oberg S, Crookes PF, Tan S, DeMeester SR, Hagen JA, Bremner CG. Multivariate analysis of factors predicting outcome after laparoscopic Nissen fundoplication. *J Gastrointest Surg* 1999; **3**: 292-300 [PMID: 10481122 DOI: 10.1016/s1091-255x(99)80071-7]
  - 16 **Numans ME**, Lau J, de Wit NJ, Bonis PA. Short-term treatment with proton-pump inhibitors as a test for gastroesophageal reflux disease: a meta-analysis of diagnostic test characteristics. *Ann Intern Med* 2004; **140**: 518-527 [PMID: 15068979 DOI: 10.7326/0003-4819-140-7-200404060-00011]
  - 17 **Herbella FA**, Sweet MP, Tedesco P, Nipomnick I, Patti MG. Gastroesophageal reflux disease and obesity. Pathophysiology and implications for treatment. *J Gastrointest Surg* 2007; **11**: 286-290 [PMID: 17458599 DOI: 10.1007/s11605-007-0097-z]
  - 18 **Luketina RR**, Koch OO, Köhler G, Antoniou SA, Emmanuel K, Pointner R. Obesity does not affect the outcome of laparoscopic antireflux surgery. *Surg Endosc* 2015; **29**: 1327-1333 [PMID: 25294529 DOI: 10.1007/s00464-014-3842-x]
  - 19 **Morgenthal CB**, Lin E, Shane MD, Hunter JG, Smith CD. Who will fail laparoscopic Nissen fundoplication? *Surg Endosc* 2007; **21**: 1978-1984 [PMID: 17623236 DOI: 10.1007/s00464-007-9490-7]
  - 20 **Kuna M**, Tran V, Tadros M. The Role of High-Resolution Manometry in Management of Patients with Sleeve Gastrectomy. *Obes Surg* 2021; **31**: 409-412 [PMID: 32617925 DOI: 10.1007/s11695-020-04797-6]
  - 21 **Savarino E**, Bredenoord AJ, Fox M, Pandolfino JE, Roman S, Gyawali CP; International Working Group for Disorders of Gastrointestinal Motility and Function. Advances in the physiological assessment and diagnosis of GERD. *Nat Rev Gastroenterol Hepatol* 2018; **15**: 323 [PMID: 29622813 DOI: 10.1038/nrgastro.2018.32]
  - 22 **Gyawali CP**, Kahrilas PJ, Savarino E, Zerbib F, Mion F, Smout AJPM, Vaezi M, Sifrim D, Fox MR, Vela MF, Tutuian R, Tack J, Bredenoord AJ, Pandolfino J, Roman S. Modern diagnosis of GERD: the Lyon Consensus. *Gut* 2018; **67**: 1351-1362 [PMID: 29437910 DOI: 10.1136/gutjnl-2017-314722]
  - 23 **Vardar R**, Keskin M. Indications of 24-h esophageal pH monitoring, capsule pH monitoring, combined pH monitoring with multichannel impedance, esophageal manometry, radiology and scintigraphy in gastroesophageal reflux disease? *Turk J Gastroenterol* 2017; **28**: S16-S21 [PMID: 29199161 DOI: 10.5152/tjg.2017.06]
  - 24 **Johnson LF**, DeMeester TR. Development of the 24-hour intraesophageal pH monitoring composite scoring system. *J Clin Gastroenterol* 1986; **8** Suppl 1: 52-58 [PMID: 3734377 DOI: 10.1097/00004836-198606001-00008]
  - 25 **Neto RML**, Herbella FAM, Schlottmann F, Patti MG. Does DeMeester score still define GERD? *Dis Esophagus* 2019; **32** [PMID: 30561585 DOI: 10.1093/dote/doy118]
  - 26 **Schwameis K**, Lin B, Roman J, Olengue K, Siegal S, DeMeester SR. Is pH Testing Necessary Before Antireflux Surgery in Patients with Endoscopic Erosive Esophagitis? *J Gastrointest Surg* 2018; **22**: 8-12 [PMID: 28842858 DOI: 10.1007/s11605-017-3554-3]
  - 27 **Fass R**, Hell R, Sampliner RE, Pulliam G, Graver E, Hartz V, Johnson C, Jaffe P. Effect of ambulatory 24-hour esophageal pH monitoring on reflux-provoking activities. *Dig Dis Sci* 1999; **44**: 2263-2269 [PMID: 10573372 DOI: 10.1023/a:1026608804938]
  - 28 **Richter JE**, Pandolfino JE, Vela MF, Kahrilas PJ, Lacy BE, Ganz R, Dengler W, Oelschlager BK, Peters J, DeVault KR, Fass R, Gyawali CP, Conklin J, DeMeester T; Esophageal Diagnostic Working Group. Utilization of wireless pH monitoring technologies: a summary of the proceedings from the esophageal diagnostic working group. *Dis Esophagus* 2013; **26**: 755-765 [PMID: 22882487 DOI: 10.1111/j.1442-2050.2012.01384.x]
  - 29 **Chae S**, Richter JE. Wireless 24, 48, and 96 Hour or Impedance or Oropharyngeal Prolonged pH

- Monitoring: Which Test, When, and Why for GERD? *Curr Gastroenterol Rep* 2018; **20**: 52 [PMID: 30259210 DOI: 10.1007/s11894-018-0659-0]
- 30 **Frazzoni M**, de Bortoli N, Frazzoni L, Tolone S, Savarino V, Savarino E. Impedance-pH Monitoring for Diagnosis of Reflux Disease: New Perspectives. *Dig Dis Sci* 2017; **62**: 1881-1889 [PMID: 28550489 DOI: 10.1007/s10620-017-4625-8]
  - 31 **Zerbib F**, Roman S, Ropert A, des Varannes SB, Poudoux P, Chaput U, Mion F, V  rin E, Galmiche JP, Sifrim D. Esophageal pH-impedance monitoring and symptom analysis in GERD: a study in patients off and on therapy. *Am J Gastroenterol* 2006; **101**: 1956-1963 [PMID: 16848801 DOI: 10.1111/j.1572-0241.2006.00711.x]
  - 32 **Sifrim D**, Zerbib F. Diagnosis and management of patients with reflux symptoms refractory to proton pump inhibitors. *Gut* 2012; **61**: 1340-1354 [PMID: 22684483 DOI: 10.1136/gutjnl-2011-301897]
  - 33 **Scarpellini E**, Ang D, Pauwels A, De Santis A, Vanuytsel T, Tack J. Management of refractory typical GERD symptoms. *Nat Rev Gastroenterol Hepatol* 2016; **13**: 281-294 [PMID: 27075264 DOI: 10.1038/nrgastro.2016.50]
  - 34 **Koop AH**, Francis DL, DeVault KR. Visual and Automated Computer Analysis Differ Substantially in Detection of Acidic Reflux in Multichannel Intraluminal Impedance-pH Monitoring. *Clin Gastroenterol Hepatol* 2018; **16**: 979-980 [PMID: 29108959 DOI: 10.1016/j.cgh.2017.10.039]
  - 35 **Tucker E**, Knowles K, Wright J, Fox MR. Rumination variations: aetiology and classification of abnormal behavioural responses to digestive symptoms based on high-resolution manometry studies. *Aliment Pharmacol Ther* 2013; **37**: 263-274 [PMID: 23173868 DOI: 10.1111/apt.12148]
  - 36 **Kamal AN**, Clarke JO, Oors JM, Smout AJ, Bredenoord AJ. The Role of Symptom Association Analysis in Gastroesophageal Reflux Testing. *Am J Gastroenterol* 2020; **115**: 1950-1959 [PMID: 32740077 DOI: 10.14309/ajg.0000000000000754]
  - 37 **Weusten BL**, Roelofs JM, Akkermans LM, Van Berge-Henegouwen GP, Smout AJ. The symptom-association probability: an improved method for symptom analysis of 24-hour esophageal pH data. *Gastroenterology* 1994; **107**: 1741-1745 [PMID: 7958686 DOI: 10.1016/0016-5085(94)90815-x]
  - 38 **Pandolfino JE**, Roman S. High-resolution manometry: an atlas of esophageal motility disorders and findings of GERD using esophageal pressure topography. *Thorac Surg Clin* 2011; **21**: 465-475 [PMID: 22040629 DOI: 10.1016/j.thorsurg.2011.08.007]
  - 39 **Pandolfino JE**, Kim H, Ghosh SK, Clarke JO, Zhang Q, Kahrilas PJ. High-resolution manometry of the EGJ: an analysis of crural diaphragm function in GERD. *Am J Gastroenterol* 2007; **102**: 1056-1063 [PMID: 17319930 DOI: 10.1111/j.1572-0241.2007.01138.x]
  - 40 **Tolone S**, Savarino E, Zaninotto G, Gyawali CP, Frazzoni M, de Bortoli N, Frazzoni L, Del Genio G, Bodini G, Furnari M, Savarino V, Docimo L. High-resolution manometry is superior to endoscopy and radiology in assessing and grading sliding hiatal hernia: A comparison with surgical in vivo evaluation. *United European Gastroenterol J* 2018; **6**: 981-989 [PMID: 30228885 DOI: 10.1177/2050640618769160]
  - 41 **Mittal R**, Vaezi MF. Esophageal Motility Disorders and Gastroesophageal Reflux Disease. *N Engl J Med* 2020; **383**: 1961-1972 [PMID: 33176086 DOI: 10.1056/NEJMra2000328]
  - 42 **Pauwels A**, Boeckstaens V, Andrews CN, Attwood SE, Berrisford R, Bisschops R, Boeckstaens GE, Bor S, Bredenoord AJ, Cicala M, Corsetti M, Fornari F, Gyawali CP, Hatlebakk J, Johnson SB, Lerut T, Lundell L, Mattioli S, Miwa H, Naftoux P, Omari T, Pandolfino J, Penagini R, Rice TW, Roelandt P, Rommel N, Savarino V, Sifrim D, Suzuki H, Tutuian R, Vanuytsel T, Vela MF, Watson DI, Zerbib F, Tack J. How to select patients for antireflux surgery? *Gut* 2019; **68**: 1928-1941 [PMID: 31375601 DOI: 10.1136/gutjnl-2019-318260]
  - 43 **Ghosh SK**, Pandolfino JE, Rice J, Clarke JO, Kwiatek M, Kahrilas PJ. Impaired deglutitive EGJ relaxation in clinical esophageal manometry: a quantitative analysis of 400 patients and 75 controls. *Am J Physiol Gastrointest Liver Physiol* 2007; **293**: G878-G885 [PMID: 17690172 DOI: 10.1152/ajpgi.00252.2007]
  - 44 **Kahrilas PJ**, Bredenoord AJ, Fox M, Gyawali CP, Roman S, Smout AJ, Pandolfino JE; International High Resolution Manometry Working Group. The Chicago Classification of esophageal motility disorders, v3.0. *Neurogastroenterol Motil* 2015; **27**: 160-174 [PMID: 25469569 DOI: 10.1111/nmo.12477]
  - 45 **Stefanidis D**, Richardson W, Farrell TM, Kohn GP, Augenstein V, Fanelli RD; Society of American Gastrointestinal and Endoscopic Surgeons. SAGES guidelines for the surgical treatment of esophageal achalasia. *Surg Endosc* 2012; **26**: 296-311 [PMID: 22044977 DOI: 10.1007/s00464-011-2017-2]
  - 46 **Vaezi MF**, Pandolfino JE, Yadlapati RH, Greer KB, Kavitt RT. ACG Clinical Guidelines: Diagnosis and Management of Achalasia. *Am J Gastroenterol* 2020; **115**: 1393-1411 [PMID: 32773454 DOI: 10.14309/ajg.0000000000000731]
  - 47 **Richards WO**, Torquati A, Holzman MD, Khaitan L, Byrne D, Lutfi R, Sharp KW. Heller myotomy versus Heller myotomy with Dor fundoplication for achalasia: a prospective randomized double-blind clinical trial. *Ann Surg* 2004; **240**: 405-12; discussion 412 [PMID: 15319712 DOI: 10.1097/01.sla.0000136940.32255.51]
  - 48 **Kummerow Broman K**, Phillips SE, Faqih A, Kaiser J, Pierce RA, Poulouse BK, Richards WO, Sharp KW, Holzman MD. Heller myotomy versus Heller myotomy with Dor fundoplication for achalasia: long-term symptomatic follow-up of a prospective randomized controlled trial. *Surg Endosc* 2018; **32**: 1668-1674 [PMID: 29046957 DOI: 10.1007/s00464-017-5845-x]
  - 49 **Bakhos CT**, Petrov RV, Parkman HP, Malik Z, Abbas AE. Role and safety of fundoplication in

- esophageal disease and dysmotility syndromes. *J Thorac Dis* 2019; **11**: S1610-S1617 [PMID: 31489228 DOI: 10.21037/jtd.2019.06.62]
- 50 **Poirier NC**, Taillefer R, Topart P, Duranceau A. Antireflux operations in patients with scleroderma. *Ann Thorac Surg* 1994; **58**: 66-72; discussion 72 [PMID: 8037562 DOI: 10.1016/0003-4975(94)91073-1]
  - 51 **Yan J**, Strong AT, Sharma G, Gabbard S, Thota P, Rodriguez J, Kroh M. Surgical management of gastroesophageal reflux disease in patients with systemic sclerosis. *Surg Endosc* 2018; **32**: 3855-3860 [PMID: 29435755 DOI: 10.1007/s00464-018-6115-2]
  - 52 **Roman S**, Kahrilas PJ, Kia L, Luger D, Soper N, Pandolfino JE. Effects of large hiatal hernias on esophageal peristalsis. *Arch Surg* 2012; **147**: 352-357 [PMID: 22508779 DOI: 10.1001/archsurg.2012.17]
  - 53 **Triggs JR**, Carlson DA, Beveridge C, Jain A, Tye MY, Kahrilas PJ, Pandolfino JE. Upright Integrated Relaxation Pressure Facilitates Characterization of Esophagogastric Junction Outflow Obstruction. *Clin Gastroenterol Hepatol* 2019; **17**: 2218-2226. e2 [PMID: 30708108 DOI: 10.1016/j.cgh.2019.01.024]
  - 54 **Müller M**, Gockel I, Hedwig P, Eckardt AJ, Kuhr K, König J, Eckardt VF. Is the Schatzki ring a unique esophageal entity? *World J Gastroenterol* 2011; **17**: 2838-2843 [PMID: 21734791 DOI: 10.3748/wjg.v17.i23.2838]
  - 55 **Snyder DL**, Vela MF. Opioid-induced esophageal dysfunction. *Curr Opin Gastroenterol* 2020; **36**: 344-350 [PMID: 32427604 DOI: 10.1097/MOG.0000000000000648]
  - 56 **Snyder DL**, Crowell MD, Horsley-Silva J, Ravi K, Lacy BE, Vela MF. Opioid-Induced Esophageal Dysfunction: Differential Effects of Type and Dose. *Am J Gastroenterol* 2019; **114**: 1464-1469 [PMID: 31403963 DOI: 10.14309/ajg.0000000000000369]
  - 57 **Jung HY**, Puckett JL, Bhalla V, Rojas-Feria M, Bhargava V, Liu J, Mittal RK. Asynchrony between the circular and the longitudinal muscle contraction in patients with nutcracker esophagus. *Gastroenterology* 2005; **128**: 1179-1186 [PMID: 15887102 DOI: 10.1053/j.gastro.2005.02.002]
  - 58 **Rohof WOA**, Bredenoord AJ. Chicago Classification of Esophageal Motility Disorders: Lessons Learned. *Curr Gastroenterol Rep* 2017; **19**: 37 [PMID: 28730503 DOI: 10.1007/s11894-017-0576-7]
  - 59 **Dell'Acqua-Cassão B**, Mardiros-Herbella FA, Farah JF, Bonadiman A, Silva LC, Patti MG. Outcomes of laparoscopic Nissen fundoplication in patients with manometric patterns of esophageal motility disorders. *Am Surg* 2013; **79**: 361-365 [PMID: 23574844]
  - 60 **Leopold A**, Yu D, Bhuta R, Kataria R, Lu X, Jehangir A, Harrison M, Friedenber F, Malik Z, Schey R, Parkman HP. Multiple Rapid Swallows (MRS) Complements Single-Swallow (SS) Analysis for High-Resolution Esophageal Manometry (HREM). *Dig Dis Sci* 2019; **64**: 2206-2213 [PMID: 30805798 DOI: 10.1007/s10620-019-05545-2]
  - 61 **Tadros M**, Tran V, Shah V, Yodice M. Patterns of esophageal dysmotility elicited by multiple rapid swallows. *Esophagus* 2021; **18**: 353-361 [PMID: 33011871 DOI: 10.1007/s10388-020-00784-z]
  - 62 **Marin I**, Serra J. Patterns of esophageal pressure responses to a rapid drink challenge test in patients with esophageal motility disorders. *Neurogastroenterol Motil* 2016; **28**: 543-553 [PMID: 26686375 DOI: 10.1111/nmo.12749]
  - 63 **Tadros M**, Yodice M. The Challenges of Esophagogastric Junction Outflow Obstruction, Is It Really a Diagnosis? *Dysphagia* 2020 [PMID: 32676750 DOI: 10.1007/s00455-020-10156-5]
  - 64 **Ang D**, Hollenstein M, Misselwitz B, Knowles K, Wright J, Tucker E, Sweis R, Fox M. Rapid Drink Challenge in high-resolution manometry: an adjunctive test for detection of esophageal motility disorders. *Neurogastroenterol Motil* 2017; **29** [PMID: 27420913 DOI: 10.1111/nmo.12902]
  - 65 **Basseri B**, Pimentel M, Shaye OA, Low K, Soffer EE, Conklin JL. Apple sauce improves detection of esophageal motor dysfunction during high-resolution manometry evaluation of dysphagia. *Dig Dis Sci* 2011; **56**: 1723-1728 [PMID: 21181443 DOI: 10.1007/s10620-010-1513-x]
  - 66 **Shaker A**, Stoikes N, Drapekin J, Kushnir V, Brunt LM, Gyawali CP. Multiple rapid swallow responses during esophageal high-resolution manometry reflect esophageal body peristaltic reserve. *Am J Gastroenterol* 2013; **108**: 1706-1712 [PMID: 24019081 DOI: 10.1038/ajg.2013.289]
  - 67 **Stoikes N**, Drapekin J, Kushnir V, Shaker A, Brunt LM, Gyawali CP. The value of multiple rapid swallows during preoperative esophageal manometry before laparoscopic antireflux surgery. *Surg Endosc* 2012; **26**: 3401-3407 [PMID: 22648115 DOI: 10.1007/s00464-012-2350-0]
  - 68 **Carlson DA**, Crowell MD, Kimmel JN, Patel A, Gyawali CP, Hinchcliff M, Griffing WL, Pandolfino JE, Vela MF. Loss of Peristaltic Reserve, Determined by Multiple Rapid Swallows, Is the Most Frequent Esophageal Motility Abnormality in Patients With Systemic Sclerosis. *Clin Gastroenterol Hepatol* 2016; **14**: 1502-1506 [PMID: 27062902 DOI: 10.1016/j.cgh.2016.03.039]
  - 69 **Zaninotto G**, DeMeester TR, Schwizer W, Johansson KE, Cheng SC. The lower esophageal sphincter in health and disease. *Am J Surg* 1988; **155**: 104-111 [PMID: 3341525 DOI: 10.1016/s0002-9610(88)80266-6]
  - 70 **Tsuboi K**, Hoshino M, Sundaram A, Yano F, Mittal SK. Role of the lower esophageal sphincter on esophageal acid exposure - a review of over 2000 patients. *Trop Gastroenterol* 2012; **33**: 107-111 [PMID: 23025056 DOI: 10.7869/tg.2012.26]
  - 71 **Tolone S**, Gualtieri G, Savarino E, Frazzoni M, de Bortoli N, Furnari M, Casalino G, Parisi S, Savarino V, Docimo L. Pre-operative clinical and instrumental factors as antireflux surgery outcome predictors. *World J Gastrointest Surg* 2016; **8**: 719-728 [PMID: 27933133 DOI: 10.4240/wjgs.v8.i11.719]
  - 72 **Jones MP**, Sloan SS, Rabine JC, Ebert CC, Huang CF, Kahrilas PJ. Hiatal hernia size is the dominant

- determinant of esophagitis presence and severity in gastroesophageal reflux disease. *Am J Gastroenterol* 2001; **96**: 1711-1717 [PMID: [11419819](#) DOI: [10.1111/j.1572-0241.2001.03926.x](#)]
- 73 **Rogers B**, Hasak S, Hansalia V, Gyawali CP. Trans-esophagogastric junction pressure gradients during straight leg raise maneuver on high-resolution manometry associate with large hiatus hernias. *Neurogastroenterol Motil* 2020; **32**: e13836 [PMID: [32163648](#) DOI: [10.1111/nmo.13836](#)]
- 74 **Lei Y**, Li JY, Jiang J, Wang J, Zhang QY, Wang TY, Krasna MJ. Outcome of floppy Nissen fundoplication with intraoperative manometry to treat sliding hiatal hernia. *Dis Esophagus* 2008; **21**: 364-369 [PMID: [18477260](#) DOI: [10.1111/j.1442-2050.2007.00777.x](#)]
- 75 **Lin M**, Triadafilopoulos G. Belching: dyspepsia or gastroesophageal reflux disease? *Am J Gastroenterol* 2003; **98**: 2139-2145 [PMID: [14572558](#) DOI: [10.1111/j.1572-0241.2003.07627.x](#)]
- 76 **Conchillo JM**, Selimah M, Bredenoord AJ, Samsom M, Smout AJ. Air swallowing, belching, acid and non-acid reflux in patients with functional dyspepsia. *Aliment Pharmacol Ther* 2007; **25**: 965-971 [PMID: [17403001](#) DOI: [10.1111/j.1365-2036.2007.03279.x](#)]
- 77 **Sawada A**, Guzman M, Nikaki K, Sonmez S, Yazaki E, Aziz Q, Woodland P, Rogers B, Gyawali CP, Sifrim D. Identification of Different Phenotypes of Esophageal Reflux Hypersensitivity and Implications for Treatment. *Clin Gastroenterol Hepatol* 2020 [PMID: [32272249](#) DOI: [10.1016/j.cgh.2020.03.063](#)]
- 78 **Bredenoord AJ**. Excessive belching and aerophagia: two different disorders. *Dis Esophagus* 2010; **23**: 347-352 [PMID: [20095992](#) DOI: [10.1111/j.1442-2050.2009.01038.x](#)]
- 79 **Holloway RH**. Combined impedance-manometry for the evaluation of esophageal disorders. *Curr Opin Gastroenterol* 2014; **30**: 422-427 [PMID: [24859805](#) DOI: [10.1097/MOG.0000000000000079](#)]
- 80 **Kessing BF**, Bredenoord AJ, Smout AJ. The pathophysiology, diagnosis and treatment of excessive belching symptoms. *Am J Gastroenterol* 2014; **109**: 1196-203; (Quiz) 1204 [PMID: [25001253](#) DOI: [10.1038/ajg.2014.165](#)]
- 81 **Dellon ES**, Liacouras CA, Molina-Infante J, Furuta GT, Spergel JM, Zevit N, Spechler SJ, Attwood SE, Straumann A, Aceves SS, Alexander JA, Atkins D, Arva NC, Blanchard C, Bonis PA, Book WM, Capocelli KE, Chehade M, Cheng E, Collins MH, Davis CM, Dias JA, Di Lorenzo C, Dohil R, Dupont C, Falk GW, Ferreira CT, Fox A, Gonsalves NP, Gupta SK, Katzka DA, Kinoshita Y, Menard-Katcher C, Kodroff E, Metz DC, Miehke S, Muir AB, Mukkada VA, Murch S, Nurko S, Ohtsuka Y, Orel R, Papadopoulou A, Peterson KA, Philpott H, Putnam PE, Richter JE, Rosen R, Rothenberg ME, Schoepfer A, Scott MM, Shah N, Sheikh J, Souza RF, Strobel MJ, Talley NJ, Vaezi MF, Vandenplas Y, Vieira MC, Walker MM, Wechsler JB, Wershil BK, Wen T, Yang GY, Hirano I, Bredenoord AJ. Updated International Consensus Diagnostic Criteria for Eosinophilic Esophagitis: Proceedings of the AGREE Conference. *Gastroenterology* 2018; **155**: 1022-1033. e10 [PMID: [30009819](#) DOI: [10.1053/j.gastro.2018.07.009](#)]
- 82 **Camilleri M**, Chedid V, Ford AC, Haruma K, Horowitz M, Jones KL, Low PA, Park SY, Parkman HP, Stanghellini V. Gastroparesis. *Nat Rev Dis Primers* 2018; **4**: 41 [PMID: [30385743](#) DOI: [10.1038/s41572-018-0038-z](#)]
- 83 **Rome IV Criteria**. Rome Foundation. 2016. [cited 20 January 2021]. Available from: <https://theromefoundation.org/rome-iv/rome-iv-criteria/>

## Basic Study

# Protective effect and mechanisms of action of Mongolian medicine Sulongga-4 on pyloric ligation-induced gastroduodenal ulcer in rats

Shan Tong, Huan Wang, Li-Sha A, Ta-Na Bai, Ju-Hua Gong, Wen-Jie Jin, Li-Li Dai, Gen-Na Ba, Sung-Bo Cho, Ming-Hai Fu

**ORCID number:** Shan Tong 0000-0002-6145-0721; Huan Wang 0000-0002-5457-665X; Li-Sha A 0000-0002-0137-1677; Ta-Na Bai 0000-0002-3590-4355; Ju-Hua Gong 0000-0001-6433-4518; Wen-Jie Jin 0000-0002-9288-8697; Li-Li Dai 0000-0003-4821-596X; Gen-Na Ba 0000-0002-0834-3863; Sung-Bo Cho 0000-0002-2593-2758; Ming-Hai Fu 0000-0002-5096-8744.

**Author contributions:** Tong S, Wang H and Fu MH conceived and designed the project; Tong S, Wang H, Jin WJ and Dai LL performed the experiments; Bai TN and Gong JH performed the animal experiment; Cho SB, A LS, Ba GN and Fu MH performed microarray data analysis and interpreted the results; Cho SB and Fu MH wrote the manuscript; All authors have read and approved the final manuscript.

**Supported by** Mongolian Medicine Food and Drug Source Protection and Utilization Innovation Team Construction Project, No. 190301; National Natural Science Foundation of China, No. 81760765; Inner Mongolia University for Nationalities Doctoral Start-up Grant, No. BS412 and No. BS413; Mongolian Medicine Engineering Technology Research Centre Open Fund

**Shan Tong, Huan Wang, Li-Sha A, Ta-Na Bai, Ju-Hua Gong, Wen-Jie Jin, Li-Li Dai, Gen-Na Ba, Sung-Bo Cho, Ming-Hai Fu**, School of Mongolian Medicine, Inner Mongolia University for Nationalities, Tongliao 028000, Inner Mongolia Autonomous Region, China

**Shan Tong**, Mongolian Medicine Surgery Department, Affiliated Hospital of Inner Mongolia University for Nationalities, Tongliao 028000, Inner Mongolia Autonomous Region, China

**Li-Sha A, Wen-Jie Jin, Li-Li Dai, Ming-Hai Fu**, Traditional Mongolian Medicine Research Institute, Inner Mongolia University for Nationalities, Tongliao 028000, Inner Mongolia Autonomous Region, China

**Corresponding author:** Ming-Hai Fu, PhD, Associate Professor, School of Mongolian Medicine, Inner Mongolia University for Nationalities, No. 996 Xilamulun Street, Tongliao 028000, Inner Mongolia Autonomous Region, China. [mfu@imn.edu.cn](mailto:mfu@imn.edu.cn)

## Abstract

### BACKGROUND

Sulongga-4 (SL-4) is a herbal formula used in traditional Mongolian medical clinics for the treatment of peptic ulcers and gastroenteritis, even though its pharmacological mechanism has not been well characterized.

### AIM

To evaluate the protective effect and identify the mechanisms of action of SL-4 on gastroduodenal ulcer induced by pyloric ligation (PL) in rats.

### METHODS

PL was performed to induce gastric and duodenal ulcers in rats, which were then treated with oral SL-4 (1.3, 2.6, or 3.9 g/kg per day) for 15 d. PL-induced gastroduodenal ulceration. Therapeutic effects were characterized by pathological and histological evaluations and inflammatory indicators were analyzed by enzyme-linked immunosorbent assay. Microarray analyses were conducted to identify gene expression profiles of gastroduodenal tissue in PL rats with or without SL-4 treatment. The candidate target genes were selected and verified by quantitative reverse transcription polymerase chain reaction (qRT-PCR).

### RESULTS

SL-4 decreased histopathological features in the PL-induced ulcerated rats. SL-4



Project, No. MDK2017072; and Inner Mongolia Autonomous Region Talent Development Fund Project, No. RC201802.

#### Institutional animal care and use

**committee statement:** This research was reviewed and approved by the Committee on the Ethics of Animal Experiments of Inner Mongolia University for Nationalities.

**Conflict-of-interest statement:** The authors declare that they have no competing interests.

**Data sharing statement:** No additional data are available.

**ARRIVE guidelines statement:** The authors have read the ARRIVE Guidelines, and the manuscript was prepared and revised according to the ARRIVE Guidelines.

**Open-Access:** This article is an open-access article that was selected by an in-house editor and fully peer-reviewed by external reviewers. It is distributed in accordance with the Creative Commons Attribution NonCommercial (CC BY-NC 4.0) license, which permits others to distribute, remix, adapt, build upon this work non-commercially, and license their derivative works on different terms, provided the original work is properly cited and the use is non-commercial. See: <http://creativecommons.org/licenses/by-nc/4.0/>

**Manuscript source:** Unsolicited manuscript

**Specialty type:** Gastroenterology and hepatology

**Country/Territory of origin:** China

#### Peer-review report's scientific quality classification

Grade A (Excellent): 0  
Grade B (Very good): B  
Grade C (Good): C, C  
Grade D (Fair): 0  
Grade E (Poor): 0

**Received:** November 20, 2020

**Peer-review started:** November 20, 2020

significantly ( $P < 0.05$ ) decreased expression of tumor necrosis factor- $\alpha$ , interleukin (IL)-1 $\beta$ , IL-6, endotoxin, platelet-activating factor, and increased prostaglandin E2 and epidermal growth factor in ulcer tissue. Microarray analysis was used to identify a panel of candidate target genes for SL-4 acting on PL-induced ulceration. Genes included some complement and coagulation cascade and retinol metabolism pathways that are closely associated with inflammatory responses and gastric mucosal protective mechanisms. qRT-PCR showed that altered expression of the selected genes, such as *CYP2b2*, *UGT2b1*, *A2m*, and *MASP1* was consistent with the microarray results.

#### CONCLUSION

SL-4 exerts protective effects against PL-induced gastroduodenal ulcers *via* reducing inflammatory cytokines and elevating expression of gastric acid inhibitory factors. Downregulation of *CYP2b2* and *UGT2b1* genes in retinol metabolism and upregulation of *A2m* and *MASP1* genes in the complement and coagulation cascades pathways are possibly involved in SL-4-mediated protection against gastroduodenal ulcer.

**Key Words:** Sulongga-4; Peptic ulcer; Pyloric ligation; Microarray analysis; Inflammatory reaction; Retinol metabolism

©The Author(s) 2021. Published by Baishideng Publishing Group Inc. All rights reserved.

**Core Tip:** Sulongga-4 (SL-4) is a classic herbal formula used in Mongolian medical clinics for the treatment of peptic ulcers and gastroenteritis. This study investigated the protective effects and molecular mechanisms of SL-4 in pyloric ligation (PL)-induced gastroduodenal ulcers in rats *via* microarray analysis. Our results suggest that SL-4 was strongly protective against PL-induced gastroduodenal ulcers *via* reducing inflammatory cytokines and elevating the expression of gastric acid inhibitory factors. Downregulation of *CYP2b2* and *UGT2b1*, and upregulation of *A2m* and *MASP1* may be involved in the gastroduodenal ulcer protection mechanism of SL-4.

**Citation:** Tong S, Wang H, A LS, Bai TN, Gong JH, Jin WJ, Dai LL, Ba GN, Cho SB, Fu MH. Protective effect and mechanisms of action of Mongolian medicine Sulongga-4 on pyloric ligation-induced gastroduodenal ulcer in rats. *World J Gastroenterol* 2021; 27(16): 1770-1784

**URL:** <https://www.wjgnet.com/1007-9327/full/v27/i16/1770.htm>

**DOI:** <https://dx.doi.org/10.3748/wjg.v27.i16.1770>

#### INTRODUCTION

Peptic ulcer disease is the most prevalent chronic disease of the digestive system, with complications resulting in high morbidity and mortality<sup>[1]</sup>. Many factors can lead to the formation of peptic ulcers, and one of the basic mechanisms is impairment of gastric mucosal barrier function by acidic gastric secretion<sup>[2]</sup>. Inflammation or injury of the digestive system cause visceral hypersensitivity that can drive the development of chronic pain and patient discomfort<sup>[3]</sup>, while inflammation is a key driver of gastric ulcer formation<sup>[4]</sup>. For protection against inflammation, cells respond with attenuated production of proinflammatory cytokines such as interleukin (IL)-12, tumor necrosis factor (TNF)- $\alpha$ , IL1 $\beta$ , IL-6, IL-8, and interferon (IFN)<sup>[5,6]</sup>. These cytokines drive the aggregation and trigger activation of T cells in areas of inflammation. Mediators of inflammation protect against peptic ulcer formation. Although peptic ulcer disease can be treated with drugs such as proton pump inhibitors, H2 receptor antagonists and prostaglandin analogs, most of these drugs have adverse reactions and limitations when used for the long term<sup>[7]</sup>. Safer and more effective antiulcer agents are therefore needed.

The use of plant extracts as natural medications is well documented, with multifunctional effects reported such as immunostimulatory, anti-inflammatory, antiviral, anticancer, and radioprotective effects<sup>[8]</sup>. Plant or herbal extracts are also recognized as a source of therapeutics for gastric ulcers<sup>[9]</sup>. Traditional Mongolian

**First decision:** December 17, 2020**Revised:** January 29, 2021**Accepted:** March 24, 2021**Article in press:** March 24, 2021**Published online:** April 28, 2021**P-Reviewer:** Carri JH, Nakajima N, Shelat VG**S-Editor:** Gao CC**L-Editor:** Filipodia**P-Editor:** Ma YJ

medicine (TMM) has been used to treat peptic ulcers and is proven to be effective in clinical treatment. The use of TMM is widespread in North China, Mongolia, and the Buryat Republic. The use of TMM is spreading to more Asian countries because of its profound curative effects on some common diseases in the northern region. The Mongolian medicine Sulongga-4 (SL-4) is composed of four medicinal herbs: *Forsythia suspensa*, *Persicaria bistorta*, *Caulis clematidis armandii*, and *Ophiopogon japonicus*. According to ethnopharmacological records, SL-4 has shown good efficacy against *Hododenbaoru*, a term in TMM referring to peptic ulcer<sup>[10]</sup>. Modern clinical applications and preliminary studies have shown that SL-4 is generally used for abdominal pain, gastroenteritis, peptic ulcer, and diarrhea. For example, SL-4 has been found to have clinical therapeutic effects against infantile diarrhea and to improve intestinal health<sup>[11-13]</sup>. Wang *et al.*<sup>[14,15]</sup> reported that SL-4 was protective against acute liver damage induced by pyloric ligation (PL) and CCl<sub>4</sub>. To further evaluate the efficacy of SL-4, we investigated whether it had a protective effect on PL-induced gastroduodenal ulcer in a rat model. Additionally, combined microarray analysis and data mining were conducted to uncover the underlying molecular mechanisms of the gastroprotective effects of SL-4.

## MATERIALS AND METHODS

### Ethics statement

Male Sprague-Dawley rats (200 ± 20 g, 6 wk of age, SPF grade, batch no. SCXK 2015-0001) were purchased from Liaoning Chang-Sheng Biotechnology Co. The experimental procedures were approved by the Committee on the Ethics of Animal Experiments of Inner Mongolia University for Nationalities (approval no. NM-LL-2016-12-15-01), in accordance with the requirements and general guidelines of the Chinese Experimental Animals Administration Legislation. All surgery was conducted under sodium pentobarbital anesthesia, and every attempt was made to alleviate suffering.

### Animal treatment

Sixty male rats were housed in environmentally controlled conditions (22 ± 2 °C, relative humidity of 50% ± 5%) with a 12-h light/dark cycle and had free access to food and water for 7 d acclimatization. SL-4 was provided by the Drug Manufacturing section of the Affiliated Hospital of Inner Mongolia University for Nationalities (batch No.: 20190312). Rats were randomly divided into five groups (*n* = 12) that were treated by a sham operation, PL, and 1.3, 2.6, or 3.9 g/kg SL-4. Rats in the sham operation and PL groups were given 0.5% carboxymethylcellulose sodium (CMC-Na, Sigma). Rats in the three SL-4 groups were given 1.3, 2.6, or 3.9 g/kg SL-4 in 0.5% CMC-Na suspension by gastric lavage once daily. The rats in all five groups were pretreated for 15 consecutive days.

### Ulcer model induced by PL

One hour after the last drug administration, all rats were fasted for 24 h with free access to water prior to ulceration. Each rat was anesthetized by intraperitoneal injection of pentobarbital for induction of PL-induced gastric ulcer as previously described<sup>[16]</sup>. The abdominal cavity was opened and the pylorus was ligated, avoiding injury of the adjacent blood vessels. The stomach was gently replaced and the belly was sutured. After being deprived of food and water for 18 h, the animals were killed and the stomach and duodenum were dissected for subsequent analysis.

### Pathological and histological examination

Rats were anesthetized intraperitoneally with sodium pentobarbital and killed. Gastric and duodenal sections were harvested for pathological examination. For histological examination, gastroduodenal ulcer tissue was fixed with 4% paraformaldehyde for 48 h; decalcified in 10% aqueous EDTA solution (Sigma-Aldrich, St. Louis, MO, United States) at room temperature and constant agitation, processed, and embedded in paraffin. The tissues were cut into 4 µm serial sections and dewaxed twice in xylene at 37 °C for 15 min; rehydrated through decreasing concentrations of ethanol, and washed in distilled water at room temperature for 5 min. The tissues were stained with hematoxylin and eosin (H&E, Nanjing Jiancheng Bioengineering Institute, Nanjing, China).

### Measurement of tissue cytokine expression

Gastroduodenal tissues were homogenized in Tris buffer on ice and centrifuged at 12 000 g at 4 °C for 10 min. The supernatants were used to determine the activities of endotoxin (ET), IL-6, and platelet-activating factor (PAF) in the duodenal tissue and TNF- $\alpha$ , prostaglandin E2 (PGE2), epidermal growth factor (EGF) and IL-1 $\beta$  in the gastric tissue. Enzyme activity was determined with commercial assay kits (Nanjing Jiancheng Bioengineering Institute).

### Total RNA extraction

Total RNA was extracted for microarray and qRT-PCR assay from gastric and duodenal tissue with TRIzol reagent (Invitrogen, Gaithersburg, MD, United States) and purified with mirVana miRNA Isolation Kits (Ambion, Austin, TX, United States). RNA was quantified with a Qubit fluorometer (Thermo Fisher Scientific, United States), and RNA integrity was assessed with a Bioanalyzer 2100 (Agilent, CA, United States). Only RNA extracts with an RNA integrity of > 6 were used in subsequent analyses.

### Microarray analysis

Microarray hybridization, scanning, and analysis were performed by the Capital Biotechnology Corporation (Beijing, China). Using 100 ng total RNA, double-stranded cDNA containing the T7 RNA polymerase promoter sequence was prepared with CbcScript reverse transcriptase using a cDNA synthesis system (CapitalBio, Beijing, China) with the T7 Oligo(dT). cDNA labeled with a fluorescent dye (Cy5 or Cy3-dCTP) was produced by Eberwine's linear RNA amplification method and subsequent enzymatic reactions. The procedure was improved by using CapitalBio cRNA Amplification and Labeling Kits to produce higher yields of labeled cDNA. The microarray slides were read with an Agilent G2565CA Microarray Scanner to obtain the microarray hybridization images. The array data were analyzed for data summation, normalization, and quality control with GeneSpring V13 (Agilent).

### Differentially expressed genes and Kyoto Encyclopedia of Genes and Genomes (KEGG) pathway analysis

Chip signal intensities  $\geq 400$  were included for comparison. A two-class unpaired algorithm in the CapitalBio expression microarray analyzer software (CBC analyzer) was applied to identify differentially expressed genes in the sham operation and PL groups, and the PL and SL-4 groups in both gastric and duodenal tissues. Differentially expressed genes with fold-change  $\geq 2.0$  or  $\leq 2$  and  $P$  values  $\leq 0.05$  were evaluated. KEGG pathways were analyzed with a CapitalBio Molecule Annotation System integrated with the KEGG database as previously described.

### qRT-PCR validation

To validate the microarray results, qRT-PCR was used to validate the expression of the selected genes in the SL-4 (3.9 g/kg), PL and sham groups. The RNA samples used for qRT-PCR were the same samples from individual rats that made up the pools. One microgram of total RNA and an oligo(dT) primer were used for cDNA synthesis following the manufacturer's protocol for SuperScript III reverse transcriptase (Invitrogen, Carlsbad, CA, United States). Primers for the four genes chosen for verification were designed based on sequences published in GeneBank (Table 1). The validated genes were *CYP2b2*, *UGT2b1*, *MASP1*, and *A2m*. qRT-PCR was performed with an ABI PRISM 7900 sequence detection system (PE Applied Biosystems, Foster City, CA, United States) under the following conditions: 50 °C for 10 min, 40 cycles of 95 °C for 1 min, and 60 °C for 1 min. The program was ended with a melting curve from 72 °C to 95 °C and cooling to 40 °C. The *GAPDH* gene was used as a house-keeping control. Relative gene expression ( $\Delta\Delta Ct$ ) was calculated and graphed as a fold-change.

### Statistical analysis

Pharmacological data were analyzed using SPSS 17.0 and reported as means  $\pm$  SD. Intergroup comparisons were conducted with  $t$ -tests, and  $P < 0.05$  was taken to indicate a significant difference. Regarding the microarray, a CBC analyzer (expression profile analysis procedures based on R Bioconductor and PERL) was used for the analysis. To select the DEGs, the threshold values were  $\geq 2$  and  $\leq 2$  fold-change and a  $t$ -test  $P$  value of 0.05. The data were Log<sub>2</sub> transformed and median centered by genes using the adjust data function of CLUSTER 3.0 software and further analyzed by hierarchical

**Table 1 Primers used for quantitative reverse transcription polymerase chain reaction analysis of gene expression in gastric and duodenal tissue**

Gene	Accession No.	Forward primer	Reverse primer
MASP1	NM_022257.1	CAACTACATCGGCGGCTACTACTG	GCTGGTGATGTGCGCTGTCCTC
A2m	NM_012488.2	TCATCCAAGTCTGGTCTCTCTC	CCAGAACCATACTACTGCGGT
CYP2b2	NM_001198676.1	GGAAGAACGGATTACAGGAGGAAGC	CTGTGATGCACTGGAAGAGGAAGG
UGT2b1	NM_173295.1	ATGTCATTCTCGCAGATGCTGTGG	ATAGGAAGGAGGCAGTGGAAAGTCC

clustering with average linkage.

## RESULTS

### **SL-4 decreased histopathological features in ulcerated rats**

In the PL group, rats showed severe injury and inflammation of the gastroduodenal epithelium and edema of the submucosa. SL-4 improved these alterations dose-dependently, and showed less mucosal damage and milder inflammation than the PL group (Figure 1). H&E staining confirmed the pathological alterations of gastroduodenal tissues. The SL-4-treated groups showed a recovery trend toward normal histology and only superficial lesions. More precisely, the mucosal structure and the epithelium were intact, with normal glandular size, morphology, and distribution in the SL-4 3.9 g/kg group compared with PL untreated rats, which was essentially the same as the control sham group.

### **SL-4 modulated cytokine expression in the damaged gastroduodenal tissue**

The levels of enzymes present in tissue homogenates were determined by enzyme-linked immunosorbent assays. SL-4 pretreatment significantly ameliorated elevation of the inflammatory factors TNF- $\alpha$  and IL-1 $\beta$  in rat gastric tissue and increased the expression of prostaglandin E<sub>2</sub> (PGE<sub>2</sub>) and EGF hormones that inhibit gastric acid secretion compared with the PL group (Figure 2). In comparison, SL-4 treatment attenuated the expression of IL-6, ET and PAF in ulcerated duodenal tissue compared with the PL group in (Figure 3).

### **SL-4 altered gene expression in rats with PL-induced gastroduodenal ulcers**

DEGs were identified in the ulcerated gastroduodenal tissues by an mRNA fold-change between two experimental groups of  $\geq 2$  and a  $P$  value  $\leq 0.05$ . Volcano plot analysis showed that 1415 genes (731 upregulated and 784 downregulated) and 1460 genes (792 upregulated and 668 downregulated) were differentially expressed in gastric tissue from sham and PL, and PL and SL-4 groups (Figure 4A and B), and 2610 (1344 upregulated and 1266 downregulated) and 209 (100 upregulated and 109 downregulated) DEGs were identified in sham *vs* PL and PL *vs* SL-4 in the duodenal tissue (Figure 4C and D).

### **KEGG pathways analysis**

To define the biological pathways associated with PL and SL-4 treatment in rat gastroduodenal ulceration, we analyzed the microarray data using R software, which was based on the KEGG database. The top ten DEG-enriched pathways in the sham *vs* PL and PL *vs* SL-4 groups in gastric and duodenal tissue are summarized in Tables 2 and 3. In gastric tissue, four pathways were engaged in the crosstalk of sham *vs* PL and PL *vs* SL-4, including *Staphylococcus aureus* infection, retinol metabolism, cytokine-cytokine receptor interaction, and the hematopoietic cell lineage pathway. In duodenal tissue, among the top 10 KEGG pathways in the sham *vs* PL and PL *vs* SL-4, two were the same in both groups, which were the complement and coagulation cascade pathways and *S. aureus* infection pathway.

According to the rat phenotype, retinol metabolism in the gastric tissue and complement and coagulation cascade pathways in the duodenal tissue were both closely associated with inflammatory responses and gastric mucosal protection mechanisms. Twelve genes were found to have  $> 2$ -fold expression and  $P$  values  $\leq 0.05$  in the two pathways. Gene expression pattern variations had the same trends in the PL and SL-4 groups. More precisely, when gene expression associated with retinol

**Table 2** Top 10 Kyoto Encyclopedia of Genes and Genomes pathways enriched with differentially expressed mRNAs in gastric tissue from rats the study groups

Treatment	KEGG pathway	P value
Sham vs PL	<i>Staphylococcus aureus</i> infection	$1.83 \times 10^{-5}$
	Cytokine-cytokine receptor interaction	$2.93 \times 10^{-4}$
	Renin-angiotensin system	$7.29 \times 10^{-4}$
	Inflammatory bowel disease	$8.59 \times 10^{-4}$
	Rheumatoid arthritis	$1.52 \times 10^{-3}$
	Retinol metabolism	$1.57 \times 10^{-3}$
	Amoebiasis	$1.59 \times 10^{-3}$
	Mineral absorption	$1.75 \times 10^{-3}$
	Hematopoietic cell lineage	$2.35 \times 10^{-3}$
	Ascorbate and aldarate metabolism	$2.51 \times 10^{-3}$
PL vs SL-4	Complement and coagulation cascades	$2.59 \times 10^{-11}$
	<i>Staphylococcus aureus</i> infection	$5.95 \times 10^{-8}$
	Cytokine-cytokine receptor interaction	$2.06 \times 10^{-7}$
	Steroid hormone biosynthesis	$8.49 \times 10^{-6}$
	Hematopoietic cell lineage	$3.10 \times 10^{-5}$
	Malaria	$6.08 \times 10^{-5}$
	Chemical carcinogenesis	$1.22 \times 10^{-4}$
	Metabolism of xenobiotics by cytochrome P450	$1.28 \times 10^{-4}$
	Pertussis	$1.99 \times 10^{-4}$
	Retinol metabolism	$2.25 \times 10^{-4}$

KEGG: Kyoto Encyclopedia of Genes and Genomes; PL: Pyloric ligation; Sham: Sham operation; SL-4: Sulongga-4 decoction.

metabolism was upregulated in the PL group, SL-4 downregulated the same genes relative to the PL group. In contrast, the pathways for certain genes in the complement and coagulation cascade were downregulated in the PL group and upregulated in the SL-4 group (Table 4).

#### qRT-PCR validation

The SL-4-mediated increase or decrease in *CYP2b2* and *UGT2b1* in the retinol metabolism pathway, and *A2m* and *MASP1* in the complement and coagulation cascades pathway were verified by qRT-PCR. Changes in the expression patterns of the four selected genes were consistent with the microarray results (Figure 5). Expression of *CYP2b2* and *UGT2b1* mRNA were increased in the PL group and decreased by SL-4 treatment. In contrast, expression of *A2m* and *MASP1* were decreased in the PL group and increased in the SL-4 group.

## DISCUSSION

In Mongolian folk medicine, SL-4 is traditionally used to treat peptic ulcers and gastroenteritis. Previous studies have shown that SL-4 has therapeutic effects against infantile diarrhea and improves intestinal health<sup>[13-15]</sup>. However, the anti-ulcerogenic effect of SL-4 and its pharmacological mechanism have not been well investigated. Thus, we aimed to study whether SL-4 had a protective effect on PL-induced gastroduodenal ulcers in a rat model and examined its molecular mechanism by microarray analysis.

PL is a well-established methodology to develop gastric ulceration in rats<sup>[16]</sup>. PL induces accumulation of gastric acid and pepsin, resulting in breakdown of the gastric



**Table 3 Top 10 Kyoto Encyclopedia of Genes and Genomes pathways enriched with differentially expressed mRNAs in duodenal tissue from rats the study groups**

Treatment	KEGG pathway	P value
Sham vs PL	Complement and coagulation cascades	$3.93 \times 10^{-9}$
	<i>Staphylococcus aureus</i> infection	$4.53 \times 10^{-9}$
	Cytokine-cytokine receptor interaction	$6.48 \times 10^{-7}$
	Hematopoietic cell lineage	$9.84 \times 10^{-6}$
	Rheumatoid arthritis	$2.78 \times 10^{-5}$
	Osteoclast differentiation	$4.40 \times 10^{-5}$
	PI3K-Akt signalling pathway	$2.13 \times 10^{-4}$
	Tuberculosis	$2.89 \times 10^{-4}$
	ECM-receptor interaction	$3.02 \times 10^{-4}$
	Amoebiasis	$3.37 \times 10^{-4}$
PL vs SL-4	Maturity onset diabetes of the young	$2.10 \times 10^{-7}$
	Complement and coagulation cascades	$7.39 \times 10^{-6}$
	<i>Staphylococcus aureus</i> infection	$7.99 \times 10^{-5}$
	Regulation of autophagy	$2.26 \times 10^{-3}$
	Type II diabetes mellitus	$8.47 \times 10^{-3}$
	Longevity regulating pathway – multiple species	$1.51 \times 10^{-2}$
	Phototransduction	$2.05 \times 10^{-2}$
	Mucin type O-Glycan biosynthesis	$2.35 \times 10^{-2}$
	Porphyrin and chlorophyll metabolism	$3.51 \times 10^{-2}$
	Longevity regulating pathway	$4.01 \times 10^{-2}$

KEGG: Kyoto Encyclopedia of Genes and Genomes; Sham: PL: Pyloric ligation; Sham operation; SL-4: Sulongga-4 decoction.

mucosal barrier and causes inflammatory injury, which are key drivers of gastric ulcer formation<sup>[17]</sup>. To protect against inflammation, the cells respond with attenuated production of proinflammatory cytokines such as IL-12, TNF- $\alpha$ , IL-1, IL-6, and IFN $\gamma$ <sup>[18]</sup>. Our findings show that SL-4 significantly improved the protective effects against gastroduodenal mucosal hemorrhage and inflammation, as confirmed by histopathology. Additionally, inflammatory factors such as IL-6, TNF- $\alpha$  and IL-1 $\beta$  were significantly reduced by SL-4 in contrast to the PL group, which indicates that the antiulcer effects of SL-4 can be attributed to anti-inflammatory activity. PAF, a potent phospholipid mediator of leukocyte activation, is a potent mediator of endogenous ulcer formation<sup>[19]</sup>. ET is a hormone secreted by the endothelial cells of blood vessels that can also promote ulceration<sup>[18]</sup>. Our data showed that SL-4 suppressed expression of PAF and ET in the gastroduodenal tissues in PL model mice in a dose-dependent manner, suggesting an inhibitory role for SL-4 in the activation of endothelial cells during ulcer maintenance. Additionally, SL-4 increased expression of PGE2 and EGF in gastroduodenal tissue, which indicates that it may effectively inhibit the secretion of gastric acid, enhance the gastric mucosal defensive function, promote the repair of gastric mucosal injury, and reduce recurrence rate of gastric ulcer<sup>[20]</sup>. A previous study reported that PGE2 was responsible for the production and maintenance of the cellular integrity of the gastric mucosa, and that depletion of PGE2 could cause gastric ulcers<sup>[21]</sup>. Histological evaluation showed that SL-4 reduced mean ulcer size and minimized ulcer formation, congestion, inflammation, hemorrhage, and necrosis of the gastric mucosa. Together, these findings demonstrated the antiulcer effect of SL-4 in PL rats.

*Forsythia suspensa* is a major herbal component of SL-4. It has been reported that its active ingredients forsythiaside and forsythin exert potent anti-inflammatory and antibacterial activities, which may have possible use as antiulcer agents<sup>[22]</sup>. A number of medicinal plants have been reported useful for the treatment of gastrointestinal

**Table 4** Sequence of major genes involved in two main Kyoto Encyclopedia of Genes and Genomes pathways in gastric and duodenal tissue

Tissue pathway	Gene symbol	Gene name	Sham vs PL	PL vs SL-4	GeneBank accession No.
Gastric (retinol metabolism)	<i>UGT2b1</i>	UDP glucuronosyl transferase 2 family, polypeptide B1"	+13.71	-30.56	NM_173295
	<i>SDR16c5</i>	Short chain dehydrogenase/reductase family 16C, member 5	+7.16	+3.12	NM_001106634
	<i>RDH7</i>	Retinol dehydrogenase 7	+5.89	-45.38	NM_133543
	<i>CYP2b2</i>	Cytochrome P450, family 2, subfamily b, polypeptide 2	+5.57	-12.51	NM_001198676
	<i>CYP4a1</i>	Cytochrome P450, family 4, subfamily a, polypeptide 1	+3.93	-83.27	NM_175837
	<i>CYP1a1</i>	Cytochrome P450, family 1, subfamily a, polypeptide 1	-3.47	+1.86	NM_012540
Duodenal (complement and coagulation cascades)	<i>A2m</i>	Alpha-2-macroglobulin	-20.37	+33.00	NM_012488
	<i>FGG</i>	Fibrinogen gamma chain	-41.01	+15.50	NM_012559
	<i>FGA</i>	Fibrinogen alpha chain	-23.51	+6.49	NM_001008724
	<i>MASP1</i>	Mannan-binding lectin serine peptidase 1	-11.09	+3.19	AY149996
	<i>VSIG4</i>	V-set and immunoglobulin domain containing 4	-6.37	+3.26	NM_001025004
	<i>CFB</i>	Complement factor B	+3.08	-5.43	NM_212466

Genes involved in the retinol metabolism pathway in gastric tissue and in the complement and coagulation cascade pathways in duodenal tissue with > 2-fold change associated with different experimental treatments were determined by microarray analysis. Fold-induction was calculated as the normalized intensity in the study groups. Positive and negative numbers represent up- and downregulated gene expression. PL: Pyloric ligation; Sham: Sham operation; SL-4: Sulongga-4 decoction.

disorders. Wu *et al*<sup>[23]</sup> reported that a Chinese medicinal herb, *Pogostemon cablin*, and its main active compound  $\beta$ -patchoulene profoundly inhibited ulcer formation by reducing the inflammatory response and improving angiogenesis. Kumar *et al*<sup>[24]</sup> studied the antiulcer activity of an Indian medicine *Cedrus deodara* and found that its volatile oil had a potent gastroprotective effect on ulceration and inflammation in PL- and ethanol-treated rats. Al-Wajeeh *et al*<sup>[25]</sup> reported that a Malaysian medicine *Cibotium barometz* hair protected against ethanol-induced ulceration through regulation of antioxidant enzymes and gastric secretory actions. Consistent with those findings, our data confirmed that the gastroprotective effects of SL-4 components primarily work through modulation of inflammatory and gastric secretory mechanisms.

Microarray techniques are crucial for understanding and interpreting the activity of traditional medicines, particularly in revealing their mechanisms of action and drug targets<sup>[26]</sup>. To investigate the underlying molecular mechanisms of SL-4, we determined the gene expression profiles of gastric and duodenal tissues obtained from rats with PL-induced ulcers with or without SL-4 treatment. Retinol metabolism was one of the most significantly modified pathways in gastric tissue after SL-4 treatment. Retinoic acid (RA) intake and metabolism change dramatically during the acute-phase response (APR) to inflammation<sup>[27]</sup>. The APR is a metabolic system responding to infection, trauma, or tissue injury, and the PL method used in this study may have caused a strong APR in the intestinal tract. Inflammation drives decreased retinol usage by a reduction of retinol-binding protein synthesis<sup>[28]</sup>. RA increases the synthesis of inflammatory cytokines including transforming growth factor (TGF)- $\beta$ , IL-10, IL-4, IL-5, and IL-6, and enhances white blood cell production<sup>[29]</sup>. Microarray analysis found that SL-4 decreased the expression of key transcriptomes associated with retinol metabolism. RA concentration is controlled by glucuronosyltransferases, including UGT2b1, and P450 cytochromes including CYP26A1, CYP26B1, and CYP26C1. These subfamilies catalyze RA oxidation to forms including 5,8-epoxy RA, 4-oxo RA, 4-hydroxy RA, and 18-hydroxy RA<sup>[30,31]</sup>. Thus, decreased enzyme activation blocks RA accumulation in the other areas and maintains a suitable physiological RA concentra-

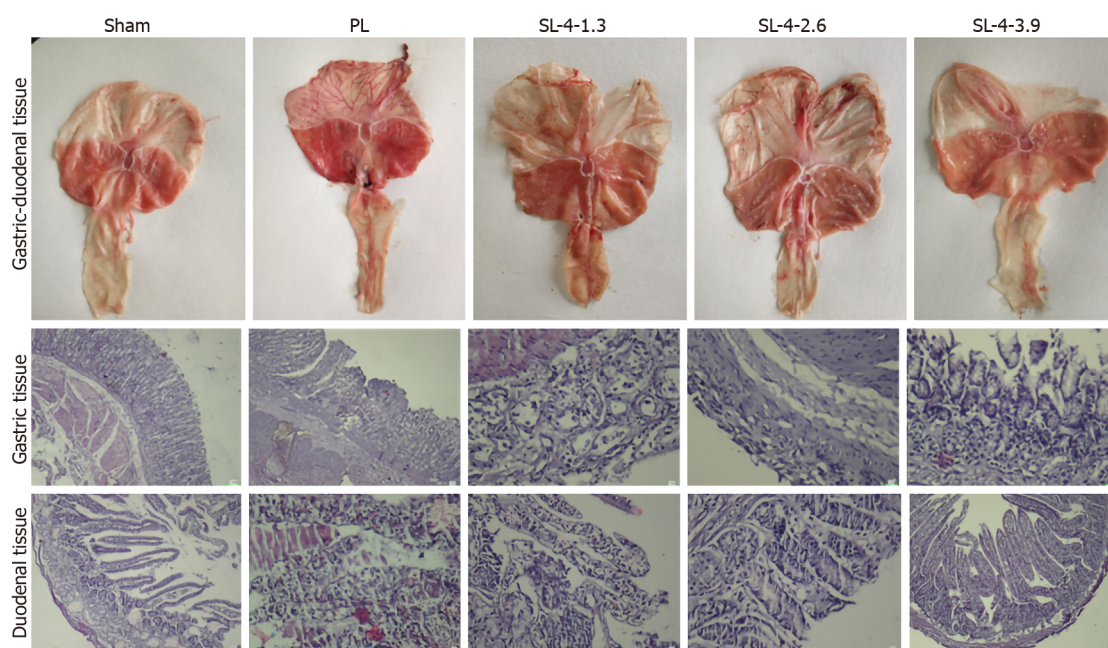


**Figure 1** Histopathological assessment of the effects of Sulongga-4 on pyloric ligation-induced gastric and duodenal ulcers in rats. The gastroduodenal tissues were fixed with 4% paraformaldehyde, embedded in paraffin, and sectioned. The tissue sections were dewaxed, rehydrated, and stained with hematoxylin and eosin before observation by light microscopy (10 × 10). PL: Pyloric ligation; Sham: Sham surgery; SL-4: Sulongga-4 decoction.

tion to achieve the anti-inflammatory function of the gastrointestinal tract. Therefore, SL-4 can enhance the role of RA in maintaining homeostasis at the intestinal barrier and equilibrating immunity and tolerance. Together with vitamin A supplementation, SL-4 treatment may improve the protective effect against gastric ulcers in a clinical setting. The current results also suggest that SL-4 accelerates the anti-inflammatory effects of retinol metabolism. This further indicates the therapeutic effect of SL-4 on inflammatory bowel disease and other clinical inflammatory symptoms.

Additionally, KEGG analysis found significant differences in the complement and coagulation cascade pathways that could have been caused by an inflammatory response. Damage of the intestinal tract activates the coagulation cascade. Fibrin formation provides a physical barrier that can be a potential shield from inflammation<sup>[32]</sup>. Our microarray results indicated that SL-4 elevated the transcriptome expression of A2m, which acts as a carrier protein to bind numerous growth factors and cytokines, such as platelet-derived growth factor, basic fibroblast growth factor, TGF- $\beta$  and IL-1 $\beta$ , thus inhibiting inflammation<sup>[33]</sup>. MASP1 is a serine protease that functions as a component of the lectin pathway of complement systems, which plays a pivotal role in the defense against infection<sup>[34]</sup>. Elevation of MASP1 expression by SL-4 may be responsible for improving the immune activity and defense against gastric infections. The above results suggest that SL-4 may have several active substances that promote anti-inflammatory responses that prevent peptic ulcer formation *via* retinol metabolism and the complement and coagulation systems.

*S. aureus* infection was found in both gastric and duodenal tissues, which indicated that PL activated the immune system against *S. aureus* infection. Although our KEGG analysis did not find a direct protective effect, antimicrobial activity for SL-4 has been reported<sup>[12]</sup>. The intestinal immune system plays a vital role in the prevention of and defense against inflammation caused by harmful pathogens. In our study, PL induced an increase in IL-1 $\beta$  secretion in gastric tissues. Although the IL-1 $\beta$ -mediated immune response to *S. aureus* has not been confirmed, IL-1 $\beta$  is a key cytokine in orchestrating host defenses against the organism<sup>[35]</sup>. Therefore, the effect of SL-4 on bacterial infection of the intestinal tract should be investigated in a future study.

## CONCLUSION

Our data demonstrate that SL-4 protected against PL-induced gastroduodenal ulceration by reducing inflammatory cytokines and increasing the expression of gastric acid inhibitory factors. We propose that regulation of *CYP2b2* and *UGT2b1* gene

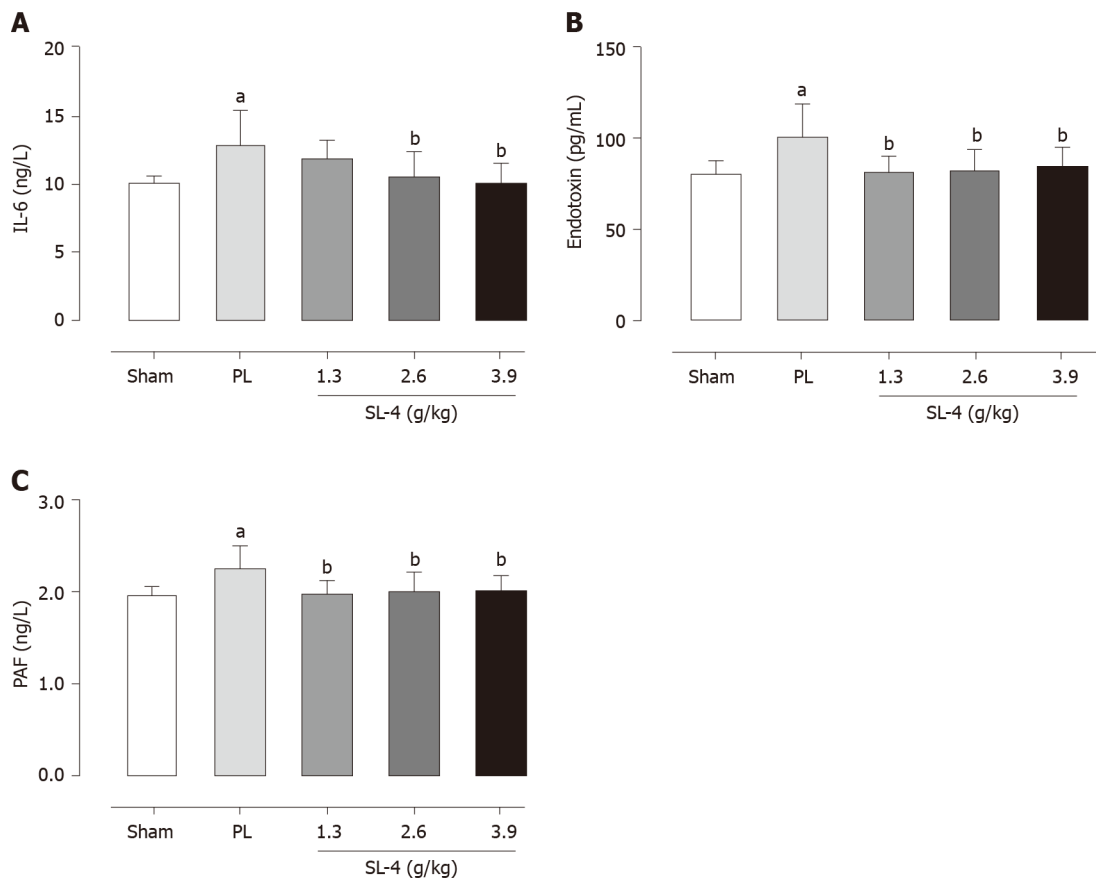


**Figure 2** Expression of interleukin-6, endotoxin, and platelet-activating factor in duodenal tissue obtained from rats in different groups, and determined by enzyme-linked immunosorbent assay. Data are reported as means  $\pm$  standard error ( $n = 10-12$ ). A: Interleukin-6; B: Endotoxin; C: Platelet-activating factor. <sup>a</sup> $P < 0.05$  vs the sham group; <sup>b</sup> $P < 0.05$  vs the pyloric ligation (PL) group. Sham: Sham surgery; SL-4: Sulongga-4 decoction.

expression in the retinol metabolism pathway and *A2m* and *MASP1* genes in the complement and coagulation cascade pathways are may be involved in mechanism by which SL-4 protects against gastroduodenal ulcers. Most notable are the effects of SL-4 on the transcriptome involved in retinol metabolism, which has not been described previously. The Mongolian folk medicine SL-4 is a promising gastroprotective agent with potential use for treating gastric ulcers in clinical practice.

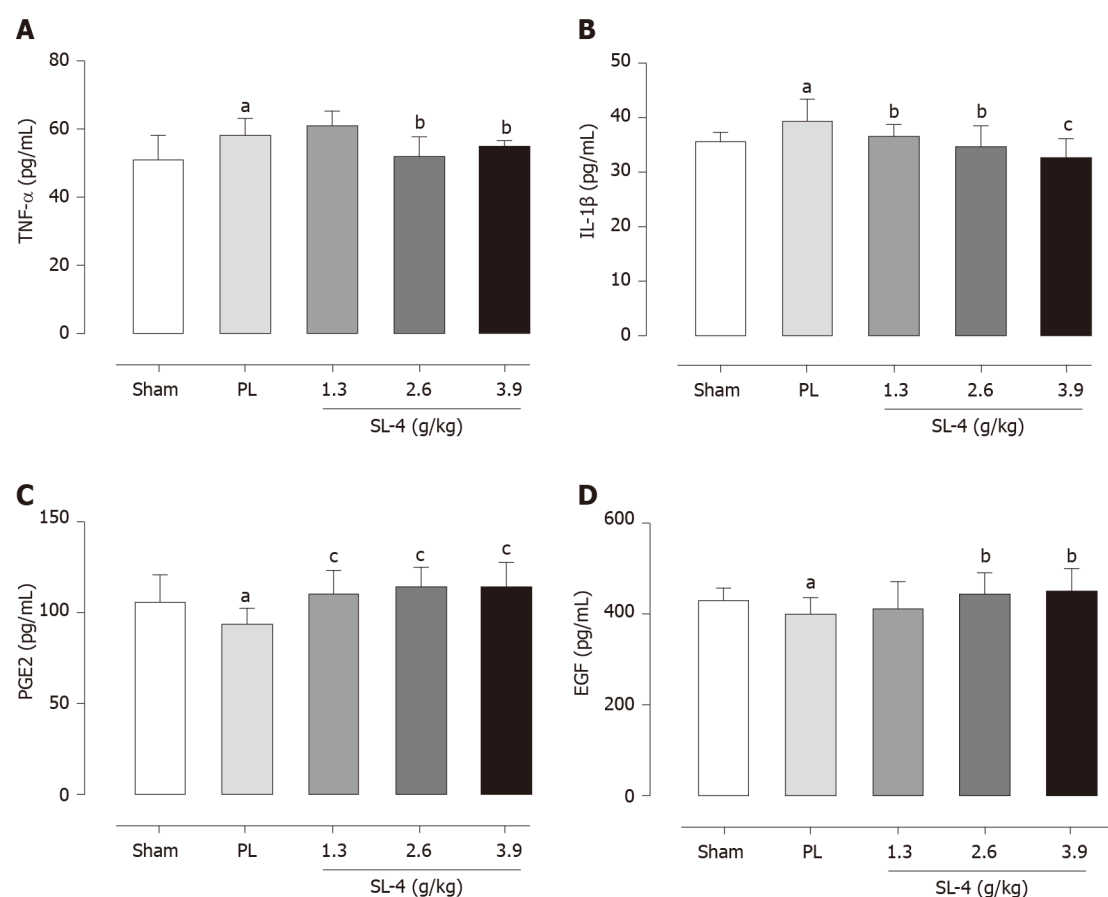


**Figure 3** Expression of tumor necrosis factor- $\alpha$ , interleukin-1 $\beta$ , prostaglandin E2 and epidermal growth factor in the gastric tissue from rats in different groups, and determined by enzyme-linked immunosorbent assay. Data are means  $\pm$  standard error ( $n = 10-12$ ). A: Tumor necrosis factor- $\alpha$ ; B: Interleukin-1 $\beta$ ; C: Prostaglandin E2; D: Epidermal growth factor. <sup>a</sup> $P < 0.05$  vs the sham group; <sup>b</sup> $P < 0.05$  and <sup>c</sup> $P < 0.01$  vs the pyloric ligation (PL) group, respectively. Sham: Sham surgery; SL-4: Sulongga-4 decoction.



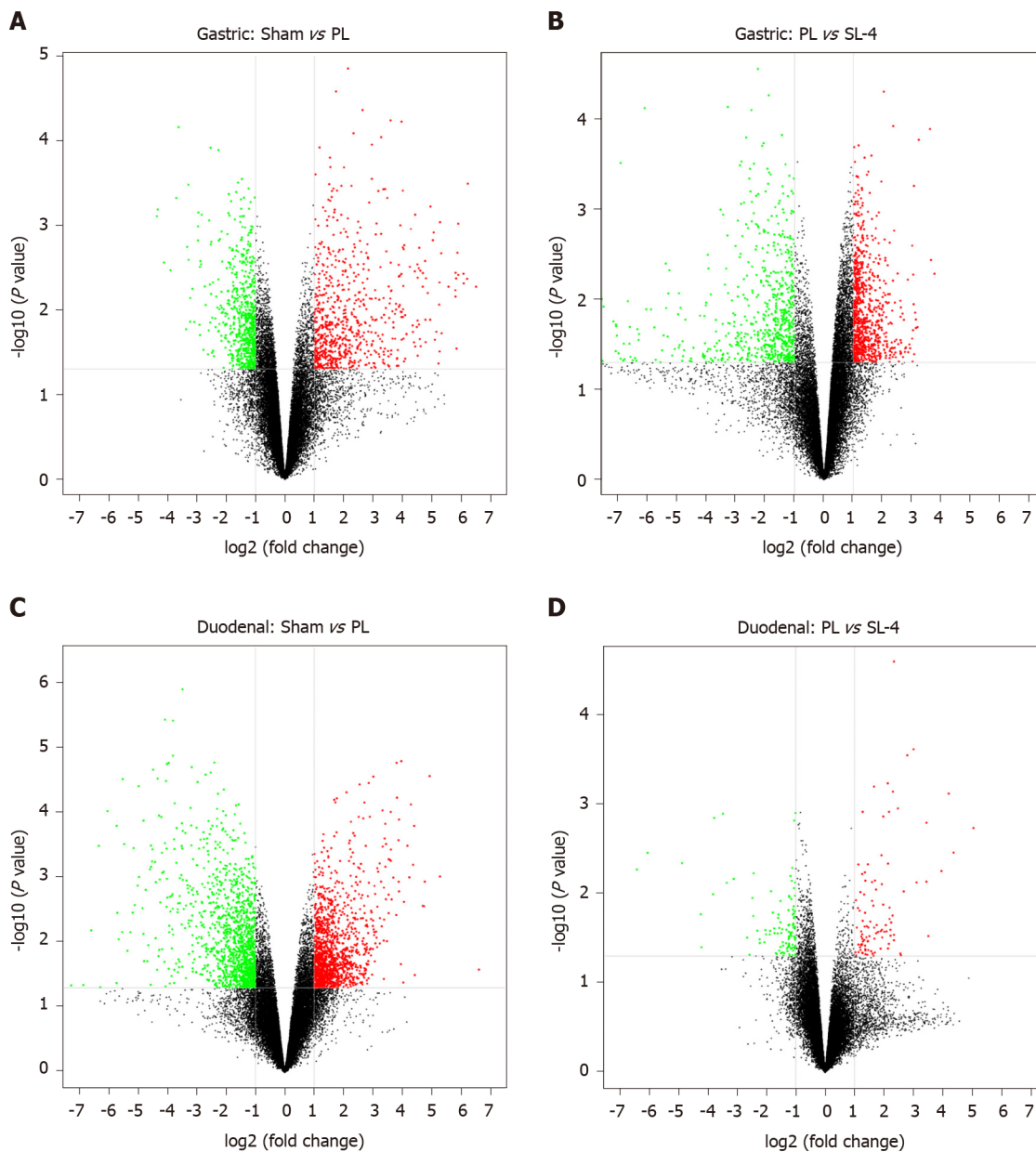


**Figure 4** Volcano plots of microarray data on differentially expressed mRNA in gastric and duodenal tissue. A and B: There were 1415 and 1460 differentially expressed genes in the sham operation vs pyloric ligation (PL) (A) and PL vs SL-4 groups (B), respectively in gastric tissue; C and D: There were 2610 and 209 differentially expressed genes in the sham operation vs PL (C) and PL vs SL-4 groups (D), respectively in duodenal tissue. Vertical lines correspond to 2-fold up- and downregulation. The horizontal line represents a *P* value of 0.05. Significantly up- and downregulated genes are shown in red and green, respectively. Statistical significance was defined as a fold-change of 2.0 and *P* value of 0.05 between groups. Sham: Sham operation, SL-4: Sulonga-4 decoction.

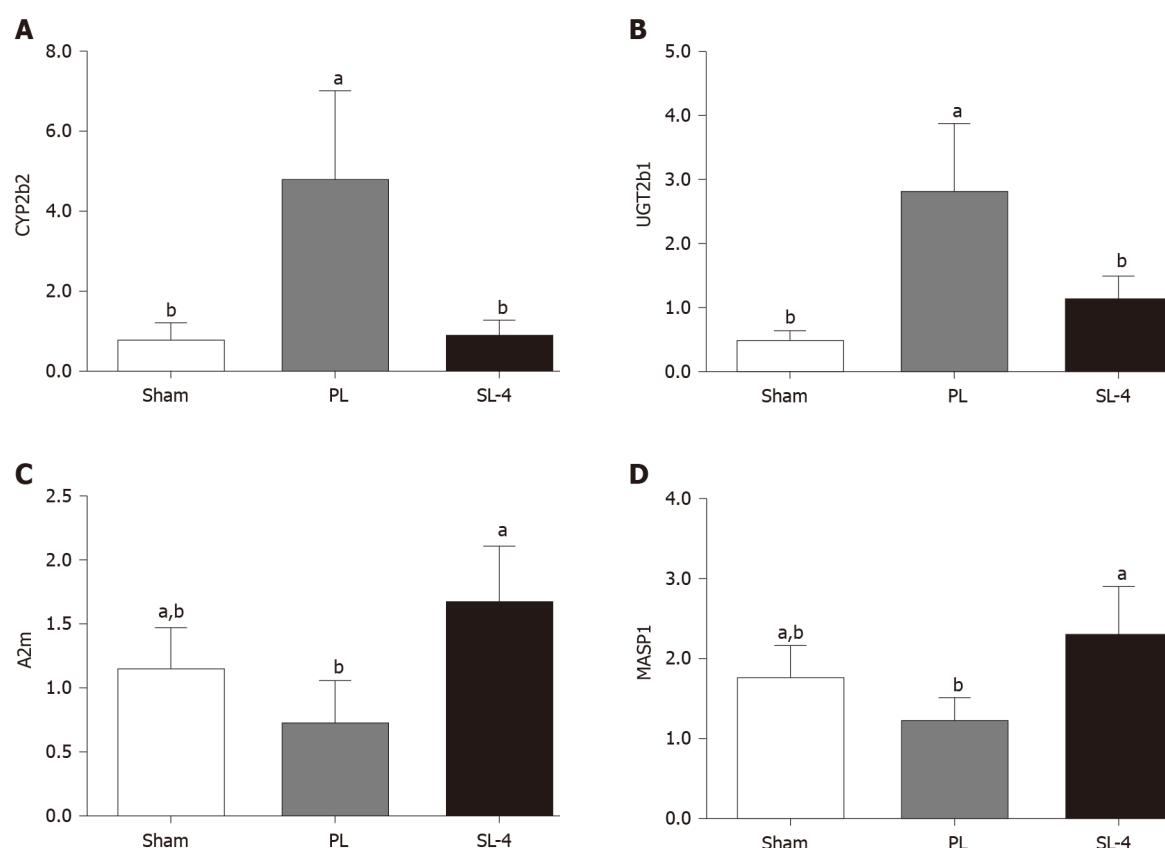


**Figure 5** Relative expression of *CYP2b2* and *UGT2b1* mRNA in gastric tissue and *A2m* and *MASP1* mRNA in duodenal tissue by reverse transcription polymerase chain reaction assay. A: *CYP2b2*; B: *UGT2b1*; C: *A2m*; D: *MASP1*. *GAPDH* was used as the reference gene. Values are means  $\pm$  standard error ( $n = 6$ ). <sup>a</sup> $P < 0.05$  vs sham operation; <sup>b</sup> $P < 0.05$  vs pyloric ligation (PL). Sham: Sham operation; SL-4: Sulongga-4 decoction.

## ARTICLE HIGHLIGHTS

### Research background

Sulongga-4 (SL-4) is a classic herbal formula used in traditional Mongolian medical clinics for the treatment of peptic ulcers and gastroenteritis, even though its pharmacological mechanism has not been well characterized.

### Research motivation

The study objective was to identify the protective effect and mechanism of SL-4 against peptic ulcer disease.

### Research objectives

To evaluate the protective effect and identify the mechanisms of action of SL-4 on gastroduodenal ulcer induced by pyloric ligation (PL) in rats.

### Research methods

PL was performed to induce gastric and duodenal ulcers in rats that were then treated with oral SL-4 (1.3, 2.6, or 3.9 g/kg per day) for 15 d. PL-induced gastroduodenal ulceration. Therapeutic effects were evaluated by pathological and histological evaluation. Inflammatory indicators were analyzed by enzyme-linked immunosorbent assay. Microarray analyses were conducted to determine the gene expression profiles of gastroduodenal tissue in PL rats with or without SL-4 treatment. The candidate target genes were selected and verified by quantitative reverse transcription polymerase chain reaction (qRT-PCR).

### Research results

SL-4 improved the histopathology of the PL-induced ulcers. SL-4 significantly ( $P < 0.05$ ) decreased the expression of tumor necrosis factor- $\alpha$ , interleukin (IL)-1 $\beta$ , IL-6, endotoxin, PAF, and increased prostaglandin E2 and EGF in ulcer tissue. Microarray

analysis was used to identify a list of candidate target genes for SL-4 acting on PL-induced ulceration. The genes included some that modulate complement and coagulation cascade pathways, and retinol metabolism pathways that are closely associated with inflammatory responses and gastric mucosal protective mechanisms. qRT-PCR showed that altered expression of the selected genes, such as *CYP2b2*, *UGT2b1*, *A2m*, and *MASP1*, was consistent with the microarray results.

### Research conclusions

SL-4 exerted protective effects against PL-induced gastroduodenal ulcers *via* reducing inflammatory cytokines and elevating the expression of gastric acid inhibitory factors. Downregulation of the *CYP2b2* and *UGT2b1* genes in retinol metabolism and upregulation of the *A2m* and *MASP1* genes in the complement and coagulation cascade pathways may have been involved in the protection against gastroduodenal ulcers.

### Research perspectives

SL-4, a Mongolian folk medicine, is a promising gastroprotective agent with potential clinical use as a treatment of gastric ulcers.

## REFERENCES

- 1 Lanas A, Chan FKL. Peptic ulcer disease. *Lancet* 2017; **390**: 613-624 [PMID: 28242110 DOI: 10.1016/S0140-6736(16)32404-7]
- 2 Chung KT, Shelat VG. Perforated peptic ulcer - an update. *World J Gastrointest Surg* 2017; **9**: 1-12 [PMID: 28138363 DOI: 10.4240/wjgs.v9.i1.1]
- 3 Spiller R, Aziz Q, Creed F, Emmanuel A, Houghton L, Hungin P, Jones R, Kumar D, Rubin G, Trudgill N, Whorwell P; Clinical Services Committee of The British Society of Gastroenterology. Guidelines on the irritable bowel syndrome: mechanisms and practical management. *Gut* 2007; **56**: 1770-1798 [PMID: 17488783 DOI: 10.1136/gut.2007.119446]
- 4 Aziz RS, Siddiqua A, Shahzad M, Shabbir A, Naseem N. Oxyresveratrol ameliorates ethanol-induced gastric ulcer *via* downregulation of IL-6, TNF- $\alpha$ , NF- $\kappa$ B, and COX-2 Levels, and upregulation of TFF-2 Levels. *Biomed Pharmacother* 2019; **110**: 554-560 [PMID: 30530291 DOI: 10.1016/j.biopha.2018.12.002]
- 5 Biswas SK, Lopez-Collazo E. Endotoxin tolerance: new mechanisms, molecules and clinical significance. *Trends Immunol* 2009; **30**: 475-487 [PMID: 19781994 DOI: 10.1016/j.it.2009.07.009]
- 6 Scully P, McKernan DP, Keohane J, Groeger D, Shanahan F, Dinan TG, Quigley EM. Plasma cytokine profiles in females with irritable bowel syndrome and extra-intestinal co-morbidity. *Am J Gastroenterol* 2010; **105**: 2235-2243 [PMID: 20407431 DOI: 10.1038/ajg.2010.159]
- 7 Beg S, Swain S, Hasan H, Barkat MA, Hussain MS. Systematic review of herbals as potential anti-inflammatory agents: Recent advances, current clinical status and future perspectives. *Pharmacogn Rev* 2011; **5**: 120-137 [PMID: 22279370 DOI: 10.4103/0973-7847.91102]
- 8 Kuna L, Jakab J, Smolic R, Raguz-Lucic N, Vcev A, Smolic M. Peptic Ulcer Disease: A Brief Review of Conventional Therapy and Herbal Treatment Options. *J Clin Med* 2019; **8** [PMID: 30717467 DOI: 10.3390/jcm8020179]
- 9 Bi WP, Man HB, Man MQ. Efficacy and safety of herbal medicines in treating gastric ulcer: a review. *World J Gastroenterol* 2014; **20**: 17020-17028 [PMID: 25493014 DOI: 10.3748/wjg.v20.i45.17020]
- 10 Ba DRH, Li J. Encyclopedia of Mongolian studies: medical science. 1st ed. Huhhot: IM People's Publishing House, 2012: 253-254
- 11 Ge RL. Traditional Mongolian medicine treatment of infantile diarrhea. *Menggu Chuantong Yiyao Zazhi* 1995; **1**: 24-25
- 12 Gang B, Tu Y. A comparative study on the bacterial inhibitory effect of Sulongga-4, Saorilao-4 decoction and Yongwa-4 decoction. *Zhongguo Minzu Yiyao Zazhi* 2005; **11**: 21-22
- 13 Qi WM, Wu L, Bai YH. Effect of Sulongga-4 decoction on the intestinal villus epithelial cell movement and goblet cells in diarrhea young rats. *Zhongguo Minzu Yiyao Zazhi* 2015; **21**: 61-63
- 14 Wang H, Tong S, Xiao M, Wang BGL, Wang TY. A study on the protective effect of traditional Mongolian medicine Lianqiao-4 decoction on pyloric ligation-induced liver damage. *Zhongguo Shiyang Fangjixue Zazhi* 2013; **20**: 238-241
- 15 Wang H, Bai MR, Bao ML, Wang TY, Ba GN. A study on screening for effective sites for the liver-protecting and enzyme-lowering effects of traditional Mongolian medicine Lianqiao-4 decoction in CCl<sub>4</sub>-induced acute liver damage. *Zhongguo Mianyixue Zazhi* 2014; **20**: 45-46
- 16 Zhang SL, Li H, He X, Zhang RQ, Sun YH, Zhang CF, Wang CZ, Yuan CS. Alkaloids from *Mahonia bealei* possess anti-H<sup>+</sup>/K<sup>+</sup>-ATPase and anti-gastrin effects on pyloric ligation-induced gastric ulcer in rats. *Phytomedicine* 2014; **21**: 1356-1363 [PMID: 25172799 DOI: 10.1016/j.phymed.2014.07.007]
- 17 Wang XY, Yin JY, Zhao MM, Liu SY, Nie SP, Xie MY. Gastroprotective activity of polysaccharide from *Herichium erinaceus* against ethanol-induced gastric mucosal lesion and pylorus ligation-induced

- gastric ulcer, and its antioxidant activities. *Carbohydr Polym* 2018; **186**: 100-109 [PMID: 29455967 DOI: 10.1016/j.carbpol.2018.01.004]
- 18 **Liu D**, Cao S, Zhou Y, Xiong Y. Recent advances in endotoxin tolerance. *J Cell Biochem* 2019; **120**: 56-70 [PMID: 30246452 DOI: 10.1002/jcb.27547]
  - 19 **Jeong YI**, Jung ID, Lee CM, Chang JH, Chun SH, Noh KT, Jeong SK, Shin YK, Lee WS, Kang MS, Lee SY, Lee JD, Park YM. The novel role of platelet-activating factor in protecting mice against lipopolysaccharide-induced endotoxic shock. *PLoS One* 2009; **4**: e6503 [PMID: 19652714 DOI: 10.1371/journal.pone.0006503]
  - 20 **Fang YF**, Xu WL, Wang L, Lian QW, Qiu LF, Zhou H, Chen SJ. Effect of Hydrotalcite on Indometacin-Induced Gastric Injury in Rats. *Biomed Res Int* 2019; **2019**: 4605748 [PMID: 31111054 DOI: 10.1155/2019/4605748]
  - 21 **Ercan G**, Ilbar Tartar R, Solmaz A, Gulcicek OB, Karagulle OO, Meric S, Cayoren H, Kusan R, Kemik A, Gokceoglu Kayali D, Cetinel S, Celik A. Potent therapeutic effects of ruscogenin on gastric ulcer established by acetic acid. *Asian J Surg* 2020; **43**: 405-416 [PMID: 31345657 DOI: 10.1016/j.asjsur.2019.07.001]
  - 22 **Qu H**, Zhang Y, Wang Y, Li B, Sun W. Antioxidant and antibacterial activity of two compounds (forsythiaside and forsythin) isolated from *Forsythia suspensa*. *J Pharm Pharmacol* 2008; **60**: 261-266 [PMID: 18237475 DOI: 10.1211/jpp.60.2.0016]
  - 23 **Wu JZ**, Liu YH, Liang JL, Huang QH, Dou YX, Nie J, Zhuo JY, Wu X, Chen JN, Su ZR, Wu QD. Protective role of  $\beta$ -patchoulene from *Pogostemon cablin* against indomethacin-induced gastric ulcer in rats: Involvement of anti-inflammation and angiogenesis. *Phytomedicine* 2018; **39**: 111-118 [PMID: 29433672 DOI: 10.1016/j.phymed.2017.12.024]
  - 24 **Kumar A**, Singh V, Chaudhary AK. Gastric antisecretory and antiulcer activities of *Cedrus deodara* (Roxb.) Loud. in Wistar rats. *J Ethnopharmacol* 2011; **134**: 294-297 [PMID: 21182918 DOI: 10.1016/j.jep.2010.12.019]
  - 25 **Al-Wajeeh NS**, Hajerezaie M, Noor SM, Halabi MF, Al-Henhena N, Azizan AH, Kamran S, Hassandarvish P, Shwter AN, Karimian H, Ali HM, Abdulla MA. The gastro protective effects of Cibatium barometz hair on ethanol-induced gastric ulcer in Sprague-Dawley rats. *BMC Vet Res* 2017; **13**: 27 [PMID: 28103938 DOI: 10.1186/s12917-017-0949-z]
  - 26 **Kiyama R**. DNA Microarray-Based Screening and Characterization of Traditional Chinese Medicine. *Microarrays (Basel)* 2017; **6**: 4 [PMID: 28146102 DOI: 10.3390/microarrays6010004]
  - 27 **Couch Y**, Akbar N, Roodselaar J, Evans MC, Gardiner C, Sargent I, Romero IA, Bristow A, Buchan AM, Haughey N, Anthony DC. Circulating endothelial cell-derived extracellular vesicles mediate the acute phase response and sickness behaviour associated with CNS inflammation. *Sci Rep* 2017; **7**: 9574 [PMID: 28851955 DOI: 10.1038/s41598-017-09710-3]
  - 28 **Gieng SH**, Raila J, Rosales FJ. Accumulation of retinol in the liver after prolonged hyporetinolemia in the vitamin A-sufficient rat. *J Lipid Res* 2005; **46**: 641-649 [PMID: 15627651 DOI: 10.1194/jlr.M400415-JLR200]
  - 29 **Akanda MR**, Kim IS, Ahn D, Tae HJ, Nam HH, Choo BK, Kim K, Park BY. Anti-Inflammatory and Gastroprotective Roles of *Rabdosia inflexa* through Downregulation of Pro-Inflammatory Cytokines and MAPK/NF- $\kappa$ B Signaling Pathways. *Int J Mol Sci* 2018; **19** [PMID: 29462911 DOI: 10.3390/ijms19020584]
  - 30 **Sakai Y**, Meno C, Fujii H, Nishino J, Shiratori H, Saijoh Y, Rossant J, Hamada H. The retinoic acid-inactivating enzyme CYP26 is essential for establishing an uneven distribution of retinoic acid along the antero-posterior axis within the mouse embryo. *Genes Dev* 2001; **15**: 213-225 [PMID: 11157777 DOI: 10.1101/gad.851501]
  - 31 **Takeuchi H**, Yokota A, Ohoka Y, Iwata M. Cyp26b1 regulates retinoic acid-dependent signals in T cells and its expression is inhibited by transforming growth factor- $\beta$ . *PLoS One* 2011; **6**: e16089 [PMID: 21249211 DOI: 10.1371/journal.pone.0016089]
  - 32 **Degen JL**, Bugge TH, Goguen JD. Fibrin and fibrinolysis in infection and host defense. *J Thromb Haemost* 2007; **5** Suppl 1: 24-31 [PMID: 17635705 DOI: 10.1111/j.1538-7836.2007.02519.x]
  - 33 **Mocchegiani E**, Malavolta M. Zinc dyshomeostasis, ageing and neurodegeneration: implications of A2M and inflammatory gene polymorphisms. *J Alzheimers Dis* 2007; **12**: 101-109 [PMID: 17851198 DOI: 10.3233/jad-2007-12110]
  - 34 **Beltrame MH**, Boldt AB, Catarino SJ, Mendes HC, Boschmann SE, Goeldner I, Messias-Reason I. MBL-associated serine proteases (MASPs) and infectious diseases. *Mol Immunol* 2015; **67**: 85-100 [PMID: 25862418 DOI: 10.1016/j.molimm.2015.03.245]
  - 35 **Gutierrez Jauregui R**, Fleige H, Bubke A, Rohde M, Weiss S, Förster R. IL-1 $\beta$  Promotes *Staphylococcus aureus* Biofilms on Implants *in vivo*. *Front Immunol* 2019; **10**: 1082 [PMID: 31156635 DOI: 10.3389/fimmu.2019.01082]



## Basic Study

# Depletion of MRPL35 inhibits gastric carcinoma cell proliferation by regulating downstream signaling proteins

Ling Yuan, Jia-Xin Li, Yi Yang, Yan Chen, Ting-Ting Ma, Shuang Liang, Yang Bu, Lei Yu, Yi Nan

**ORCID number:** Ling Yuan 0000-0003-2838-0976; Jia-Xin Li 0000-0002-6413-2542; Yi Yang 0000-0002-8466-5717; Yan Chen 0000-0002-8673-398X; Ting-Ting Ma 0000-0002-2415-2354; Shuang Liang 0000-0003-3031-6172; Yang Bu 0000-0003-0303-5607; Lei Yu 0000-0002-8837-2022; Yi Nan 0000-0002-5511-9266.

**Author contributions:** Nan Y provided the conceptual and technical guidance, designed the study, and revised the manuscript critically for important intellectual content; Yuan L carried out most of *in vivo* studies, analyzed the data, and wrote the manuscript; Li JX carried out all of *in vitro* experiments and wrote the manuscript; Yang Y and Ma TT performed parts of *in vivo* studies; Chen Y conducted statistical analysis of all of the data; Liang S, Bu Y, and Yu L supervised the clinical relevance and coordinated the clinic pathological features; all authors have read and approved the manuscript.

**Supported by** Ningxia Natural Science Foundation, No. 2020AAC03130.

**Institutional review board statement:** The study was reviewed and approved by the Institutional Review Board of Ningxia Medical University (No.

**Ling Yuan, Jia-Xin Li, Yi Yang, Ting-Ting Ma,** Pharmacy College of Ningxia Medical University, Yinchuan 750004, Ningxia Hui Autonomous Region, China

**Ling Yuan, Yi Nan,** Key Laboratory of Hui Ethnic Medicine Modernization of Ministry of Education, Ningxia Medical University, Yinchuan 750004, Ningxia Hui Autonomous Region, China

**Yan Chen,** Traditional Chinese Medicine College, Ningxia Medical University, Yinchuan 750004, Ningxia Hui Autonomous Region, China

**Shuang Liang,** Department of Oncology and Endocrinology, Yinchuan Hospital of Traditional Chinese Medicine Affiliated to Ningxia Medical University, Yinchuan 750004, Ningxia Hui Autonomous Region, China

**Yang Bu,** Department of Hepatobiliary Surgery, General Hospital of Ningxia Medical University, Yinchuan 750004, Ningxia Hui Autonomous Region, China

**Lei Yu,** Department of Infectious Diseases, The Fourth Hospital of Harbin Medical University, Harbin 150001, Heilongjiang Province, China

**Corresponding author:** Yi Nan, MD, PhD, Professor, Key Laboratory of Hui Ethnic Medicine Modernization of Ministry of Education, Ningxia Medical University, No. 1160 Shengli Street, Yinchuan 750004, Ningxia Hui Autonomous Region, China. [20080011@nxmu.edu.cn](mailto:20080011@nxmu.edu.cn)

## Abstract

### BACKGROUND

Gastric carcinoma (GC) is a digestive system disease with high morbidity and mortality. However, early clinical detection is difficult, and the therapeutic effect for advanced disease is not satisfactory. Thus, finding new tumor markers and therapeutic targets conducive to the treatment of GC is imperative. MRPL35 is a member of the large subunit family of mitochondrial ribosomal protein. MRPL35 shows the characteristic of oncogene in colorectal cancer and esophageal cancer, which promotes the exploration of the correlation between MRPL35 and GC. We proposed that the expression of MRPL35 might be critical in GC.

### AIM

To study the effect of MRPL35 knockdown on GC cell proliferation.

### METHODS



2020-071).

**Institutional animal care and use committee statement:**

All procedures involving animals were reviewed and approved by the Institutional Animal Care and Use Committee of the Ningxia Medical University (IACUC protocol number: 2019-083).

**Conflict-of-interest statement:** All authors declare no financial or commercial conflict of interest.

**Data sharing statement:** All data generated or analyzed during this study are included in this published article.

**ARRIVE guidelines statement:** The authors have read the ARRIVE guidelines, and the manuscript was prepared and revised according to the ARRIVE guidelines.

**Open-Access:** This article is an open-access article that was selected by an in-house editor and fully peer-reviewed by external reviewers. It is distributed in accordance with the Creative Commons Attribution NonCommercial (CC BY-NC 4.0) license, which permits others to distribute, remix, adapt, build upon this work non-commercially, and license their derivative works on different terms, provided the original work is properly cited and the use is non-commercial. See: <http://creativecommons.org/licenses/by-nc/4.0/>

**Manuscript source:** Unsolicited manuscript

**Specialty type:** Gastroenterology and hepatology

**Country/Territory of origin:** China

**Peer-review report's scientific quality classification**

Grade A (Excellent): A  
Grade B (Very good): B  
Grade C (Good): C  
Grade D (Fair): 0  
Grade E (Poor): 0

**Received:** December 22, 2020

**Peer-review started:** December 22,

The expression of MRPL35 in GC was evaluated based on data from the public tumor database UALCAN ([www.ualcan.path.uab.edu](http://www.ualcan.path.uab.edu)). The effect of the expression of MRPL35 on the prognosis was evaluated with KMplot ([www.kmplot.com](http://www.kmplot.com)). The expression of MRPL35 was assessed on the tissue microarray by immunohistochemistry and the level of MRPL35 mRNA in 25 pairs of clinical GC tissues and matched adjacent tissues was detected by quantitative reverse transcription-polymerase chain reaction. Celigo cell count assay, colony formation assay, and flow cytometry were used to assess the role of MRPL35 in GC cell proliferation and apoptosis *in vitro*. Additionally, tumor formation experiment in BALB/c nude mice was utilized to determine the effect of MRPL35 on GC cell proliferation. After knockdown of MRPL35, related proteins were identified by isobaric tags for relative and absolute quantification analysis, and the expression of related proteins was detected by Western blot.

**RESULTS**

The expression of MRPL35 was up-regulated in GC ( $P = 1.77 \times 10^{-4}$ ). The Kaplan-Meier plots of the overall survival indicated that high expression of MRPL35 was associated with a poor survival in GC. Compared with adjacent tissues, the expression of MRPL35 in GC tissues was increased, which was related to age ( $P = 0.03$ ), lymph node metastasis ( $P = 0.007$ ), and pathological tumor-node-metastasis stage ( $P = 0.024$ ). Knockdown of MRPL35 inhibited GC cell proliferation and colony formation and induced apoptosis. Animal experiment results showed that knockdown of MRPL35 inhibited tumor formation in BALB/c nude mice. Western blotting analysis showed that after knockdown of MRPL35, the expression of PICK1 and BCL-XL proteins decreased, and that of AGR2 protein increased.

**CONCLUSION**

Collectively, our findings demonstrate that knockdown of MRPL35 inhibits GC cell proliferation through related proteins including PICK1, BCL-XL, and AGR2.

**Key Words:** Gastric carcinoma; MRPL35; Apoptosis; Proliferation; Tissue microarray; Isobaric tags for relative and absolute quantification

©The Author(s) 2021. Published by Baishideng Publishing Group Inc. All rights reserved.

**Core Tip:** MRPL35 is a member of the large subunit family of mitochondrial ribosomal protein. Our results showed that compared with adjacent tissues, the expression of MRPL35 in gastric carcinoma (GC) tissues was increased significantly, which was related to age, lymph node metastasis, and pathological tumor-node-metastasis stage of GC patients. Knockdown of MRPL35 inhibited GC cell proliferation, clone formation, and tumor formation in BALB/c nude mice, induced apoptosis, reduced the expression of PICK1 and BCL-XL proteins, and increased that of AGR2 protein. These data indicate that MRPL35 might be an oncogene and be used as a new therapeutic target for GC.

**Citation:** Yuan L, Li JX, Yang Y, Chen Y, Ma TT, Liang S, Bu Y, Yu L, Nan Y. Depletion of MRPL35 inhibits gastric carcinoma cell proliferation by regulating downstream signaling proteins. *World J Gastroenterol* 2021; 27(16): 1785-1804

**URL:** <https://www.wjgnet.com/1007-9327/full/v27/i16/1785.htm>

**DOI:** <https://dx.doi.org/10.3748/wjg.v27.i16.1785>

**INTRODUCTION**

Gastric carcinoma (GC) is a common digestive system disease, the fourth most common cancer, and the second leading cause of cancer-related mortality worldwide. About 1033701 new cases of GC and 782685 GC-related deaths occurred worldwide in 2018, accounting for 8.2% of all cancer deaths in this year<sup>[1,2]</sup>. In China, the incidence of GC has always been high, and the mortality rate of the disease has also increased

2020

**First decision:** January 23, 2021**Revised:** February 4, 2021**Accepted:** March 11, 2021**Article in press:** March 11, 2021**Published online:** April 28, 2021**P-Reviewer:** Cheng TH, Exbrayat JM**S-Editor:** Gao CC**L-Editor:** Wang TQ**P-Editor:** Liu JH

gradually, which is threatening human life and health.

At present, the treatment for GC mainly includes surgery, chemotherapy, radiotherapy, and drug treatment<sup>[3]</sup>. Most patients with early and advanced GC can be treated by surgery. However, the metastasis of GC is a major problem faced by surgery. The surgical treatment cannot cope with the distant metastasis of GC. Chemotherapy and radiotherapy reduce the recurrence and metastasis of GC, treat residual lesions, protect surrounding normal tissues and important organs, and improve survival<sup>[4]</sup>. During chemotherapy and radiotherapy, patients have to bear a specific degree of discomfort and pain, resulting in lower patient compliance, which in turn, affects the treatment effect. Therefore, finding effective drug treatment target is a major issue in the treatment of GC.

MRPL35, a 39S large subunit, encoded by a nuclear gene, is a member of the large subunit family of mitochondrial ribosomal protein. It is a specific component of mitochondrial ribosomes and plays a key role in the assembly of cytochrome C oxidase, involved in the translation of mitochondrial proteins<sup>[5,6]</sup>. The *MRPL35* gene is localized on chromosome 2p11.2, and the protein contains 188 amino acids and has a molecular weight of about 25 ku. Survival analysis revealed that high expression of *MRPL35* indicated a prolonged survival in patients with glioblastoma<sup>[7]</sup>. The expression of *MRPL35* in colorectal cancer tissues is higher than that of the matched adjacent tissues<sup>[8]</sup>. Furthermore, down-regulation of *MRPL35* leads to increased production of reactive oxygen species and DNA damage and can inhibit cell proliferation, block the G2/M phase cell cycle, reduce the mitochondrial membrane potential, and induce apoptosis and autophagy *in vitro*. After the transfection of esophageal cancer TE-1 cells with lentivirus, compared with shCtrl (negative control virus) group, the expression of *MRPL35* was reduced in the sh*MRPL35* (lentiviral particles of *MRPL35*) group, and *MRPL35* silencing suppresses the proliferation of esophageal cancer TE-1 cells and promotes apoptosis<sup>[9]</sup>. Other studies found that *MRPL35* was negatively correlated with the survival time of patients after surgery<sup>[10]</sup>. *MRPL35* knockdown in colorectal cancer HCT116 cell and SW480 cell inhibited cell proliferation, promoted apoptosis, and blocked the G2/M phase of the cell cycle.

The MRP family regulates cells by participating in the transcriptional translation function of ribosomal proteins, which is closely related to tumor genesis and development<sup>[11]</sup>. Previous studies have confirmed that *MRPS18-2* is an oncogene<sup>[12]</sup>; *MRPL44* is up-regulated in the tissues of cervical lymph node metastasis of thyroid cancer<sup>[13]</sup>; *MRPS22*, which is found in large cell lung cancer, is highly expressed in squamous cell carcinoma and adenocarcinoma, and is low in other types of cancer<sup>[14]</sup>; *MRPL41* is down-regulated in colorectal cancer, pancreatic cancer, and other cancers<sup>[15]</sup>; *MRPS23*, down-regulated in breast cancer, can activate P21 WAF1/CIP1 and P53, inhibit cell proliferation, and promote apoptosis<sup>[16]</sup>; and *MRPL35* is associated with the occurrence and development of glioblastoma, esophageal cancer, and colorectal cancer. However, the expression and functional role of *MRPL35* in GC remain largely unknown. Therefore, we analyzed the correlation between *MRPL35* and GC by tissue microarray, cell function experiments, nude mouse tumor formation experiments, and proteomic analysis. The expression of *MRPL35* might be critical in GC according to the experimental results, and it could be a potential therapeutic target for GC.

## MATERIALS AND METHODS

### Patients

GC tissues and matched adjacent tissues were obtained from Department of Hepatobiliary Surgery, General Hospital of Ningxia Medical University. Following surgical removal, the tissue samples were immediately stored in liquid nitrogen before total RNA extraction. All tissues were histopathologically identified as GC or adjacent tissues. None of the patients had received preoperative adjuvant therapy, and all patients provided informed consent in accordance with the protocol approved by the Ethics Committee of Ningxia Medical University.

### Immunohistochemistry staining

Immunohistochemistry (IHC) staining was performed on the tissue microarray (TMA)<sup>[17,18]</sup>. The method of staining is immunohistochemical streptavidin-peroxidase (SP) method. The section contained 64 pairs of GC tissues and matched adjacent tissues. The section was deparaffinized in xylene and washed in 700 mL/L ethanol. The antigen was recovered using citrate buffer (pH 6.0) under high pressure for 10

min. Endogenous peroxidase was blocked with 30 mL/L H<sub>2</sub>O<sub>2</sub> (MERCK, Germany) in methanol for 10 min. Then, the section was incubated overnight with primary antibody (mouse polyclonal anti-MRPL35 antibody, HPA026631; Sigma-Aldrich, St. Louis, MO, United States) at 4 °C and secondary antibody successively, and developed with diaminobenzidine (DAB) reagent. The section was washed in TBST three times for 5 min, rinsed with tap water for 5 min, and then counterstained with hematoxylin. A negative control was run by omission of primary antibody (phosphate buffered saline instead of primary antibody) on another slide that was for testing the proper antibody concentration. Subsequently, the TMA was analyzed independently by two pathologists without knowing the patients' clinical information. The areas of the brown-yellow particles are the signs of positively stained tumor cells which represent the MRPL35 protein in the tissues. The staining intensity was scored from 0-3 as negative (0), weak (1), medium (2), or strong (3). The degree of staining was scored by the area of positively stained tumor cells relative to the entire tumor area: 0 (0%), 1 (1%-25%), 2 (26%-50%), 3 (51%-75%), and 4 (76%-100%). The overall protein expression score (the overall score range was 0-12) was calculated by multiplying the intensity and the positive score.

### **Cell culture and transfection**

Human GC cell lines (AGS, NCI-N87, MKN-45, and HGC-27) were purchased from the Cell Bank of the Chinese Academy of Sciences. The cell lines were cultured in a cell incubator at 37 °C and 50 mL/L CO<sub>2</sub> in RPMI-1640 medium (Gibco, New York, United States) containing 100 mL/L fetal bovine serum (FBS, Gibco) and penicillin and streptomycin (Invitrogen, Carlsbad, United States). shMRPL35 and shCtrl were designed and produced by GeneChem (Shanghai, China). Lentiviral transfection and the specific steps were performed according to the manufacturer's instructions.

### **Quantitative reverse transcription-polymerase chain reaction**

Total RNA of the cultured cells was extracted using TRIzol reagent (PuFei, Shanghai, China). PrimeScript RT Master Mix Perfect Real-Time (TaKaRa, Shiga, Japan) was used to synthesize first-strand cDNA from total RNA. Quantitative reverse transcription-polymerase chain reaction (qRT-PCR) was performed using SYBR Master Mixture (TaKaRa) according to the manufacturer's instructions. The primers used are as follows: MRPL35: Forward, 5'-TTGGCATCTTCAACCTACCGC-3' and reverse, 5'-GGAGGAAACAACCTGGTGTCTGA-3'; GAPDH: Forward, 5'-TGACTTCAACAGCGACACCCA-3' and reverse, 5'-CACCTGTGTGCTGTAGCCAAA-3'. Data are presented as the mean ± SD for duplicate runs. The relative quantification of MRPL35 expression was evaluated using the 2<sup>-ΔΔCT</sup> method. All experiments were repeated three times.

### **Celigo cell count assay**

The infected cells were seeded in a six-well plate at a density of 2000 cells/well and cultured at 37 °C and 50 mL/L CO<sub>2</sub>. On the following day, the Celigo assay was performed daily for 5 consecutive days according to the manufacturer's instructions. All experiments were repeated three times.

### **Colony formation assay**

The infected cells were inoculated in a six-well plate at a density of 1000 cells/well. The medium was changed every 3 d during the interval. After 2 wk, the colonies were fixed with 4% paraformaldehyde for 40 min and stained with 0.1% crystal violet (Sigma-Aldrich) for 4 min. The visible colonies were counted manually. Triplicate wells were assessed for each treatment group. All experiments were repeated three times.

### **Flow cytometry analysis of apoptosis**

Apoptotic and necrotic cells were evaluated with Annexin V-fluorescein isothiocyanate (FITC) and propidium iodide (PI) (KeyGEN, Jiangsu, China). All the samples were analyzed in triplicate by flow cytometry (BD Bioscience, Bedford, MA, United States). All experiments were repeated three times.

### **Tumor formation experiment in BABL/c nude mice**

Four-week-old male BABL/c nude mice of specific pathogen-free (SPF) grade were purchased from the Animal Experiment Center of Ningxia Medical University. All animals were housed in polypropylene cages and fed standard laboratory chow and water *ad libitum*, and maintained at a temperature of 22 ± 1 °C, with 50% ± 5% relative

humidity and 12:12 h light-dark cycles. First, MKN-45 cells were infected with shMRPL35 and shCtrl ( $n = 10$  per group). A microsyringe was used to extract 200  $\mu$ L of the infected and uninfected MKN-45 cell suspension at a concentration of  $1.25 \times 10^7$  /mL, and injected into the skin of nude mice. The tumor volume was measured daily using the formula  $V = W^2 \times L \times 0.5$  ( $V$ , volume;  $W$ , width;  $L$ , length). The animal protocols (IACUC-NYLAC-2019-083) were approved by the Institutional Animal Care and Use Committee of Ningxia Medical University.

### **Isobaric tags for relative and absolute quantification analysis**

SDT lysis method was used for GC cell sample preparation, and the bicinchoninic acid (BCA) method (Beyotime, Shanghai, China) was used for protein quantification. After protein samples were subjected to sodium dodecyl sulfate-polyacrylamide gel electrophoresis (SDS-PAGE), Coomassie brilliant blue staining, and filter aided sample preparation enzymolysis, the resulting peptides were quantified using NanoDrop (Thermo Scientific ND2000, Shanghai, China), and the sample peptides were labeled according to the instructions of the isobaric tags for relative and absolute quantification (iTRAQ) labeling kit (AB SCIEX, Framingham, MA, United States). The labeled peptides of each group were mixed and graded using Agilent 1260 infinity II HPLC system, and Easy nLC chromatographic system (Thermo Scientific) analysis and mass spectrometry were performed. The high-resolution mass spectrometer Q Exactive Plus (Thermo Scientific) and Proteome Discoverer 2.1 (Thermo Scientific) software were used for iTRAQ analysis, and the database search was performed on the MASCOT2.5 (Matrix Science, Boston, MA, United States) server. The Protein Database used was Uniprot\_HomoSapiens\_159615\_20170811.fasta ([http:// www.uniprot.org](http://www.uniprot.org)). A homology search was first performed for the identified sequences with a localized sequence comparison tool NCBI BLAST+ against the NCBI database, and top 10 aligned sequences were selected according to the E value from the lowest to the highest for subsequent analysis. Then, Blast2GO Command Line was utilized to perform GO (Gene Ontology) annotation on the identified proteins. The enrichment analysis of GO annotation or KEGG pathway annotation was performed on the identified proteins through Fisher's exact test. The expression of identified proteins was analyzed with Cluster 3.0 software, and hierarchical clustering heat map was generated with Java Trewview software.

### **Western blot analysis**

Total protein was extracted using the Whole Cell Lysis Assay (KeyGEN, Jiangsu, China), and the concentration was determined by BCA Protein Quantitation Assay (KeyGEN, Jiangsu, China). The protein was separated by SDS-PAGE (60-100 mL/L gel) with a sample amount of 50  $\mu$ g and transferred to polyvinylidene difluoride (PVDF) membranes that were probed with specific primary antibodies overnight at 4 °C. Then, the membranes were incubated with secondary antibodies for 1 h. The immune-reactive bands were visualized using ECL Reagent (Affinity Biosciences, Jiangsu, China) and images were analyzed by Bio-Rad Laboratories (Inc., Hercules, United States). All the primary antibodies and secondary antibodies were from Abcam (MA, United States).

### **Statistical analysis**

The statistical methods of this study were reviewed by Sun J from Department of Occupational and Environmental Health and Department of Medical Statistics, Institute of Public Health and Management, Ningxia Medical University. All analyses were performed using GraphPad Prism 7.0. All the data are expressed as the mean  $\pm$  SE. Statistical significance was analyzed using one-way ANOVA.  $P < 0.05$  was considered statistically significant.

## **RESULTS**

### **The expression of MRPL35 is up-regulated in GC tissues**

The expression of MRPL35 between GC tissues and adjacent tissues was compared through the public tumor database UALCAN ([www.ualcan.path.uab.edu](http://www.ualcan.path.uab.edu)). The results showed that the expression of MRPL35 was increased in GC tissues in comparison with matched adjacent tissues ( $P = 1.77 \times 10^{-4}$ ; 10-4; **Figure 1A**). In different pathological grades, the expression of MRPL35 in moderate and well grades was higher than that in matched adjacent tissues ( $P = 8.25 \times 10^{-5}$ ;  $P = 4.19 \times 10^{-5}$ ; 10-5;



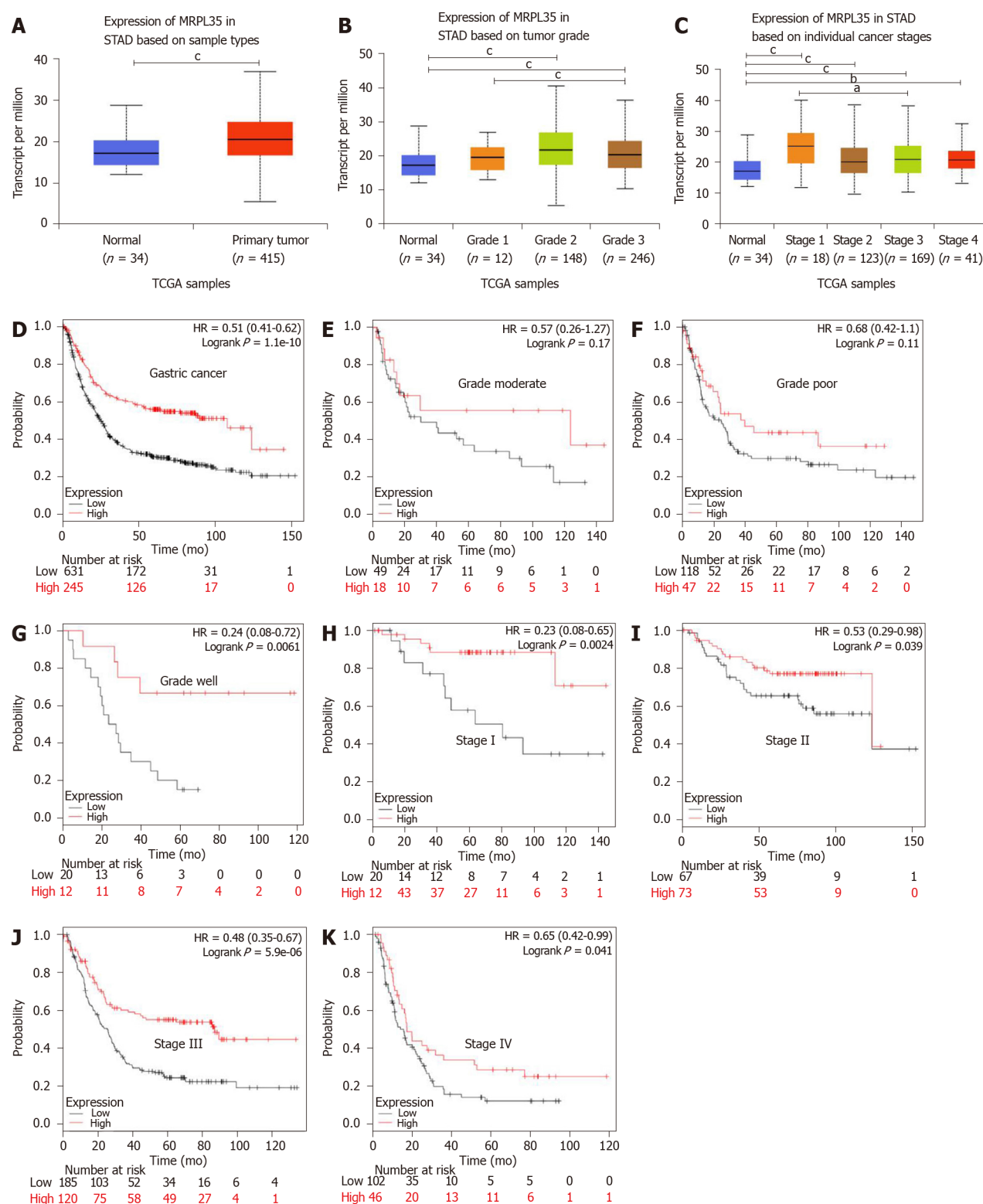


**Figure 1** MRPL35 is highly up-regulated in gastric carcinoma. A-C: The expression of MRPL35 in stomach adenocarcinoma based on sample type (A), tumor grade (B), and individual cancer stage (C). The results were based on data from the public database UALCAN ([www.ualcan.path.uab.edu](http://www.ualcan.path.uab.edu)); D: Kaplan-Meier overall survival chart. The results were based on data from the public database KMplot ([www.kmplot.com](http://www.kmplot.com)); E-G: Overall survival of patients with high and low expression of MRPL35 in different pathological grades of gastric carcinoma (GC) (E, moderate; F, poor; G, well); H-K: Overall survival of patients with high and low expression of MRPL35 in different pathological stages of GC (H, stage I; I, stage II; J, stage III; K, stage IV). The results were based on data from the public database KMplot ([www.kmplot.com](http://www.kmplot.com)). <sup>a</sup>*P* < 0.05, <sup>b</sup>*P* < 0.01, <sup>c</sup>*P* < 0.001. STAD: Stomach adenocarcinoma; HR: Hazard ratio.

Figure 1B). In different pathological stages, the expression of MRPL35 in stages I, II, III, and IV was higher than that in matched adjacent tissues (*P* = 0.0012, *P* < 6.42 × 10<sup>-4</sup>, *P* = 4.36 × 10<sup>-4</sup>, and *P* = 0.0021, respectively; Figure 1C). Next, the effect of MRPL35 expression on the prognosis was evaluated with KMplot ([www.kmplot.com](http://www.kmplot.com)). The



Kaplan-Meier plots of the overall survival indicated that high expression of MRPL35 was associated with a poor survival in GC (Figure 1D). When stratified according to different histological types and disease stages, patients with high MRPL35 expression had a poor overall survival in well grade and in stage I, stage II, stage III, and stage IV (Figure 1G-K), but not in poor and moderate grades (Figure 1E and F).

Furthermore, the expression of MRPL35 in clinical samples was detected by IHC method in 64 pairs of GC tissues and matched adjacent tissues. The immunostaining of MRPL35 protein was mainly located in the cell (Figure 2A-C). The negative control pictures are shown in the supplementary materials (Supplementary Figure 1). According to the staining site, the MRPL35 protein expression score was calculated by multiplying the intensity and the positive score (total score range 0-12). The expression of MRPL35 protein in GC tissues was higher than that in matched adjacent tissues ( $P < 0.05$ ) (Figure 2D and E). These data indicated that up-regulation of MRPL35 might play an important role in the development of GC. In addition, the expression of MRPL35 mRNA in 25 pairs of clinical GC tissues and matched adjacent tissues was detected by qRT-PCR, and the expression of MRPL35 mRNA was up-regulated in GC tissues ( $P = 0.009$ ; Figure 2F and G).

The correlation between the high expression of MRPL35 and clinicopathological factors in patients with GC proved the importance of high expression of MRPL35 in GC patients (Table 1). According to the average expression (staining score), 68 patients were divided into two groups; for the expression of MRPL35,  $< 6$  was defined as low expression and  $\geq 6$  defined as high expression. The result of statistical analysis showed that high expression of MRPL35 was correlated with age ( $P = 0.03$ ), lymph node metastasis ( $P = 0.007$ ), and pathological tumor-node-metastasis stage (p-TNM stage) ( $P = 0.024$ ). On the other hand, the correlation between the expression of MRPL35 and other clinicopathological features was not significant.

### Expression of MRPL35 in GC cells

Next, qRT-PCR analysis was performed to determine the expression of MRPL35 in four human GC cell lines. The result showed that the expression of MRPL35 was elevated in AGS and HGC-27 cell lines, but was lower in MKN-45 and NCI-N87 cell lines (Figure 3A). Thus, lentiviral vectors were used to knock down MRPL35 in both cell lines. At 72 h post-transfection, bright light and fluorescence observation under a microscope showed that the cell transfection rate was  $> 80\%$  (Figure 3B and C). qRT-PCR data revealed that the expression of MRPL35 mRNA (PSC32114 and PSC32115) in AGS and HGC-27 cells was inhibited after shRNA lentivirus transfection ( $P < 0.05$ ), and the knockdown efficiency reached 73.7% and 76.5% in AGS cells, and 67% and 77.5% in HGC-27 cells (Figure 3D and E). Subsequently, the expression of MRPL35 protein after MRPL35 knockdown in AGS cells was assessed by Western blot; in contrast with the shCtrl group, the expression of MRPL35 (PSC32114 and PSC32115) was reduced in AGS cells ( $P < 0.05$ ) (Figure 3F).

### Effect of MRPL35 knockdown on GC cell proliferation, colony formation, and apoptosis

In contrast with the shCtrl group, the shMRPL35 (PSC32114 and PSC32115) group had inhibited proliferation of the two cell lines as monitored by Celigo cell count assay ( $P < 0.01$ ), indicating that knockdown of MRPL35 had an inhibitory effect on cell proliferation (Figure 4A and B). In addition, knockdown of MRPL35 greatly reduced the colony-forming ability of AGS and HGC-27 cells (Figure 4C and D). Finally, the apoptosis was analyzed using flow cytometry. The numbers of apoptosis of AGS cells and HGC-27 cells in the shMRPL35 (PSC32114 and PSC32115) group increased compared with the shCtrl group ( $P < 0.01$ ) (Figure 4E and F). These result indicated that MRPL35 might be essential for the proliferation of GC cells.

### Knockdown of MRPL35 inhibits tumor formation in BABL/c nude mice

The tumor volume of the shMRPL35 group was smaller than that of the shCtrl group (Figure 5A and B). Within 3 wk of tumor formation, the tumor growth curve was drawn. Compared with the shCtrl and the NC groups, the tumor growth rate of the shMRPL35 group was lower (Figure 5C) ( $P < 0.01$ ).

### Proteomic and bioinformatic analysis identified proteins

Among 5993 proteins, 100 differentially expressed proteins (DEPs) were identified (Figure 6A). In comparison with the shCtrl group, 49 DEPs were up-regulated and 51 were down-regulated in the shMRPL35 group. The DEPs were screened based on the multiple of expression difference  $> 1.2$  times and  $P$  value ( $t$ -test)  $< 0.05$ . The

**Table 1** Correlation of expression of MRPL35 with various clinicopathological features in 68 gastric carcinoma patients

Pathological feature	<i>n</i>	Expression of MRPL35		
		High	Low	<i>P</i> value
	68	28	40	
Gender				
Male	48	19	29	0.685
Female	20	9	11	
Age (yr)				
< 65	33	18	15	0.03 <sup>a</sup>
≥ 65	35	10	25	
p-TNM stage				
I/II	33	9	24	0.024 <sup>a</sup>
III/IV	35	19	16	
Size of tumour				
≤ 5 cm	29	9	20	0.1
> 5 cm	39	19	20	
Pathological T grade				
T1/T2	11	3	8	0.313
T3/T4	57	25	32	
Lymph node metastasis (pN)				
N0/N1	30	7	23	0.007 <sup>b</sup>
N2/N3	38	21	17	

<sup>a</sup>*P* < 0.05.<sup>b</sup>*P* < 0.01. p-TNM stage: Pathological tumor-node-metastasis stage.

enrichment analysis was performed through GO functional annotation, describing the differential proteins from a large variety of biological processes, including cellular process, single-organism process, biological regulation, regulation of the biological process, and metabolic process (Figure 6B and C). The significance level of protein enrichment in each pathway was obtained by analyzing DEPs based on the KEGG database pathway annotation analysis (Figure 6D). The result of cluster analysis showed that the expression of all DEPs was different in the groups of shMRPL35 and shCtrl (Figure 6E).

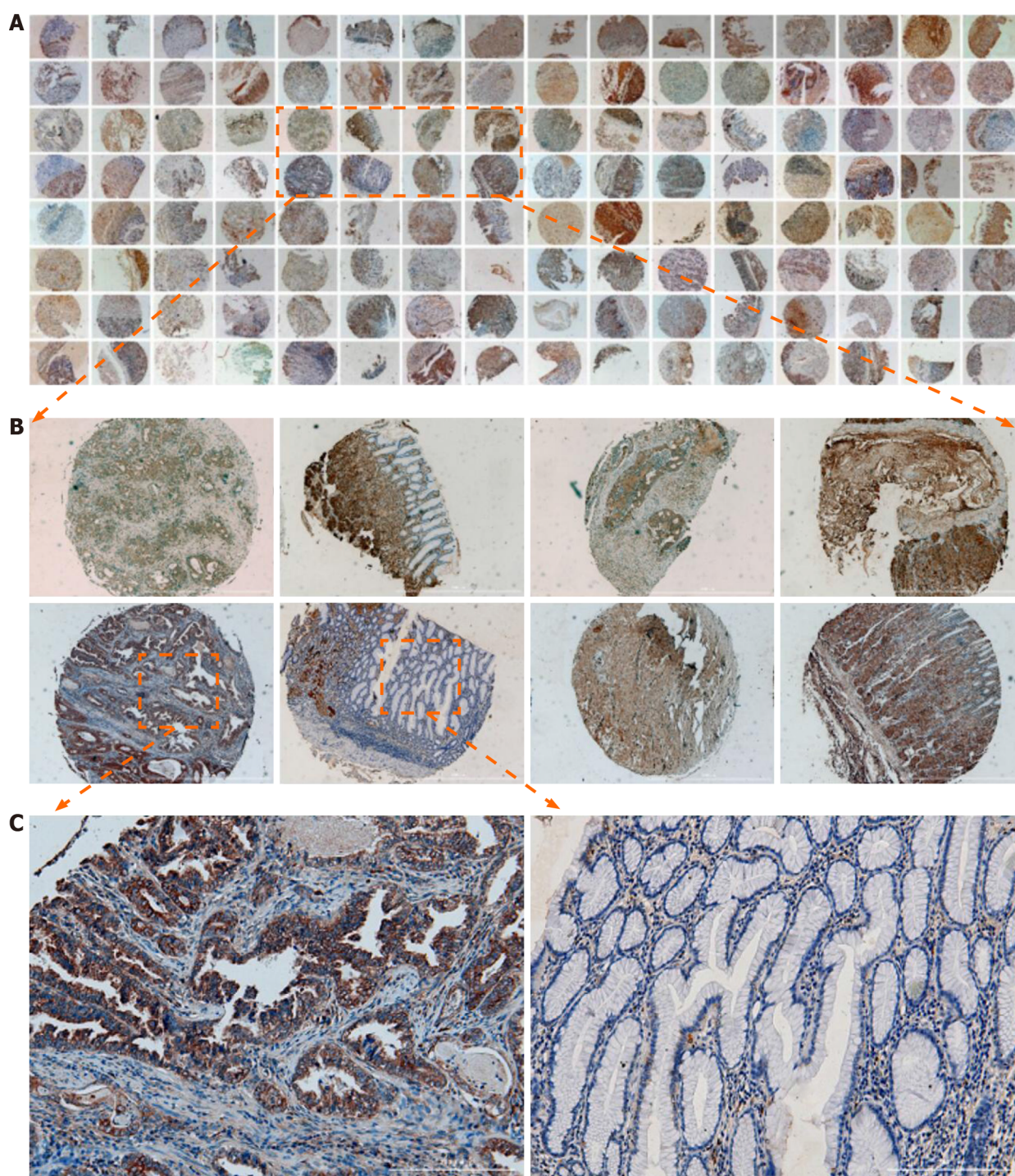
### **Knockdown of MRPL35 alters the expression of PICK1, BCL-XL, and AGR2 proteins in GC cells**

PHLDA1, MAPK8, PICK1, BCL-XL, AGR2, and ZFP36L1 proteins were selected for Western blot verification, and these proteins ranked the top 30 in biological process, molecular function, and cellular component. The expression of PHLDA1, MAPK8, PICK1, BCL-XL, AGR2, and ZFP36L1 proteins in AGS cell was detected by Western blot, and these proteins were contained in DEPs. Compared with the shCtrl group, the expression of PICK1 and BCL-XL proteins was decreased, and that of AGR2 was increased in the shMRPL35 group (*P* < 0.01) (Figure 7A and B). Based on the above result, knockdown of MRPL35 may inhibit the proliferation of GC cells through PICK1, BCL-XL, and AGR2 proteins.

## **DISCUSSION**

A major finding of this study is that knockdown of MRPL35 could inhibit the proliferation of human GC cells and promote apoptosis through nude mouse tumor





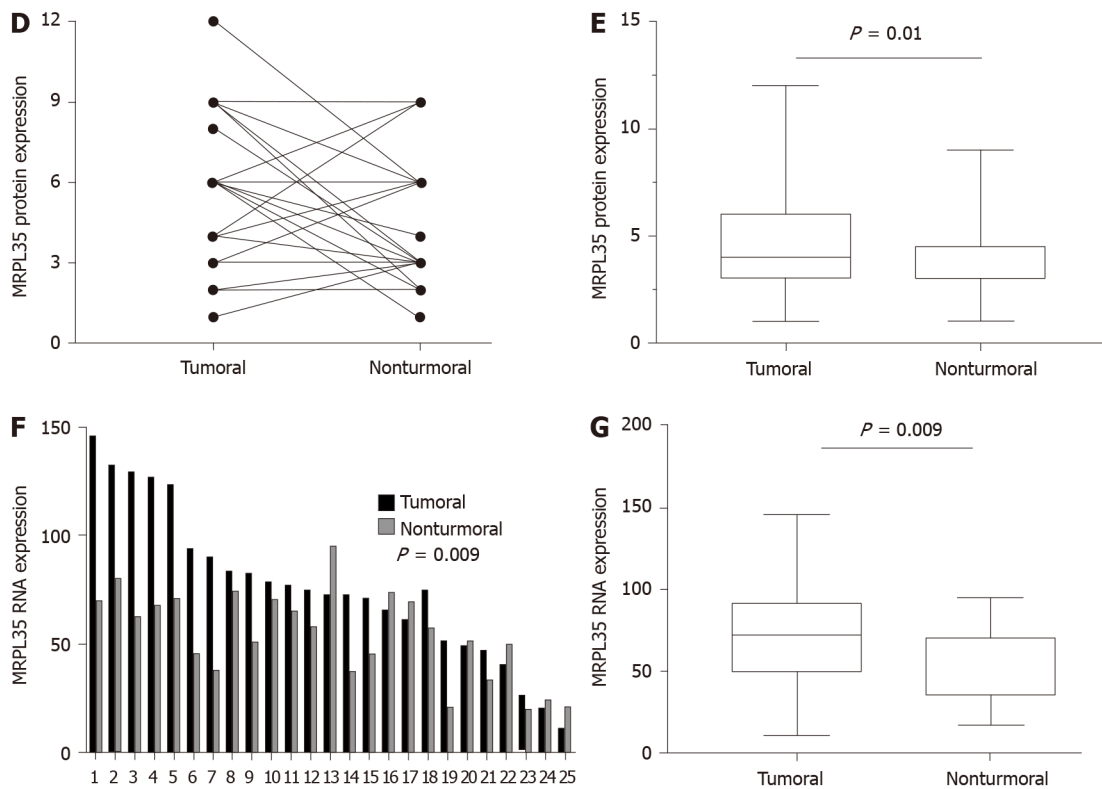
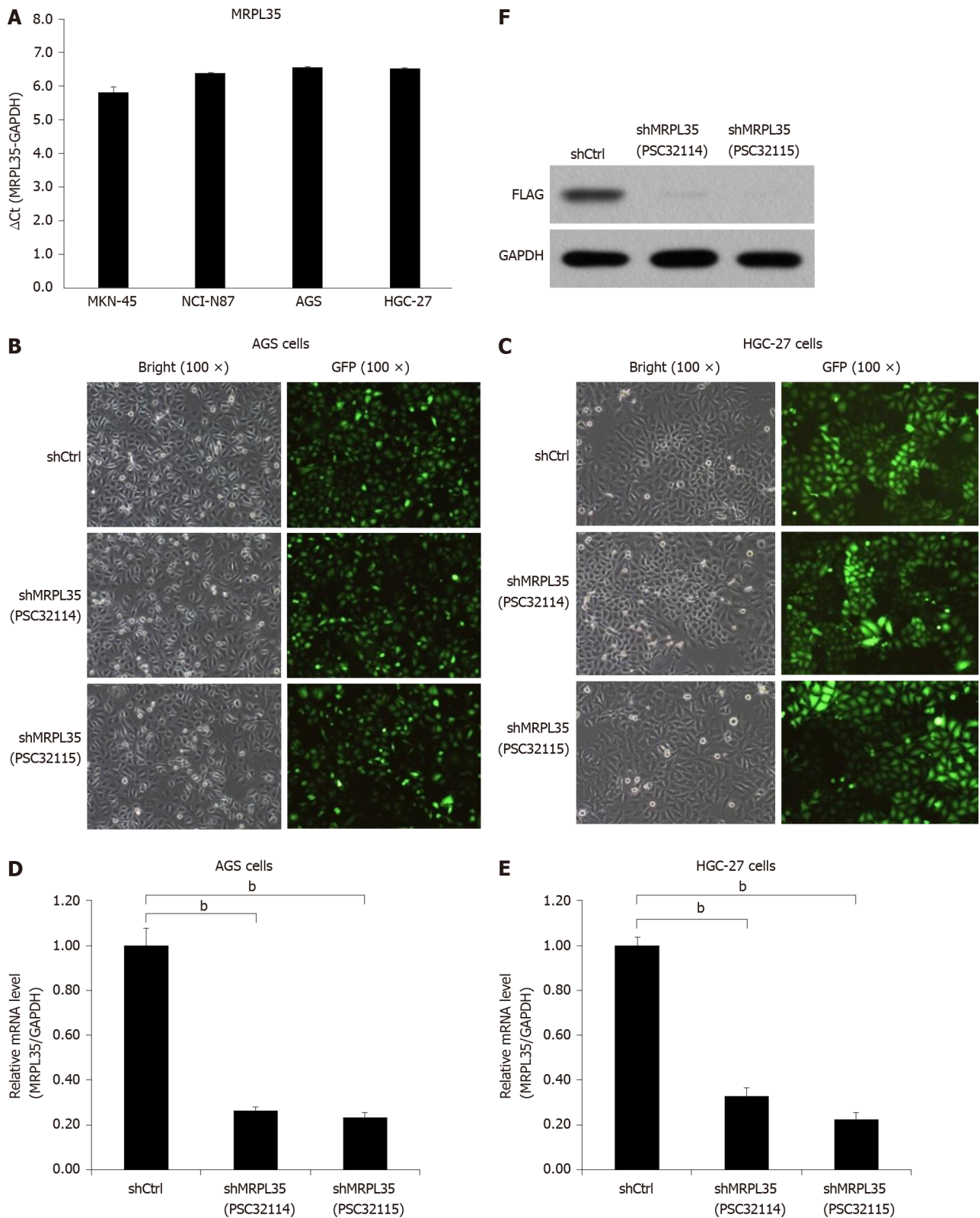


**Figure 2** The expression of MRPL35 is up-regulated in gastric carcinoma tissues. A-C: Immunohistochemistry was performed on 64 pairs of gastric carcinoma (GC) tissues and matched adjacent tissues. Magnification: 4 × (A), 40 × (B), 200 × (C); D and E: The relative expression of MRPL35 in GC tissues and matched adjacent tissues; F and G: The relative expression of MRPL35 mRNA in GC tissues and matched adjacent tissues (n = 25).

formation experiment *in vivo*, together with cell function experiment *in vitro*. In addition, proteomic analysis found that related downstream proteins changed after knockdown of MRPL35. And then, the six proteins were assessed by Western blot, which showed that the expression of PICK1 and BCL-XL proteins decreased, while that of AGR2 protein increased. In addition, the expression of MRPL35 was up-regulated in GC tissues, and high expression of MRPL35 was associated with a low survival rate in GC. Sixty-four pairs of clinical samples of GC tissues and matched adjacent tissues were examined for the expression of MRPL35 by IHC. The expression of MRPL35 in GC tissues was increased compared with matched adjacent tissues, and high expression of MRPL35 was correlated with age, lymph node metastasis, and p-TNM stage. Moreover, the results of other studies on MRPL35 in other cancers were similar to those of the current study, suggested that MRPL35 has the potential to serve as a new therapeutic target for GC. It is necessary to explain the number of tissues on the TMA. Originally, there were 75 pairs of GC tissues and matched adjacent tissues on the section, but a few of them were worn out during the IHC process. Finally, the tissues that could present on the slide and be used for analysis included 68 GC tissues and 64 matched adjacent tissues, that is to say, there were 64 GC tissues and 64 matched adjacent tissues, as well as the extra four GC tissues of which the matched adjacent tissues were worn out. We performed clinicopathological feature analysis on the remaining 68 GC tissues, and then obtained the data in Table 1. However, we carried out the IHC analysis on the remaining 64 pairs of GC tissues and matched adjacent tissues, because it should make a comparative analysis between GC tissues and the matched adjacent tissues. So only 64 pairs of tissues are shown in Figure 2A, for there were no matched adjacent tissues to be compared with the extra four GC tissues. The figures of the extra four GC tissues are shown in the supplementary materials (Supplementary Figure 2).

From the previous studies, we noticed that the expression of MRPL35 was decreased and cell proliferation inhibited, while apoptosis was promoted after knockdown of MRPL35 in esophageal cancer TE-1 cells<sup>[9]</sup>. This phenomenon was similar to the results of the current study. The expression of MRPL35 in cancer tissues was higher than that in matched adjacent tissues in colorectal cancer, and MRPL35 knockdown *in vitro* can inhibit cell proliferation and promote apoptosis<sup>[8]</sup>. The expression of MRPL35 was decreased in the nude mouse xenograft model of colorectal

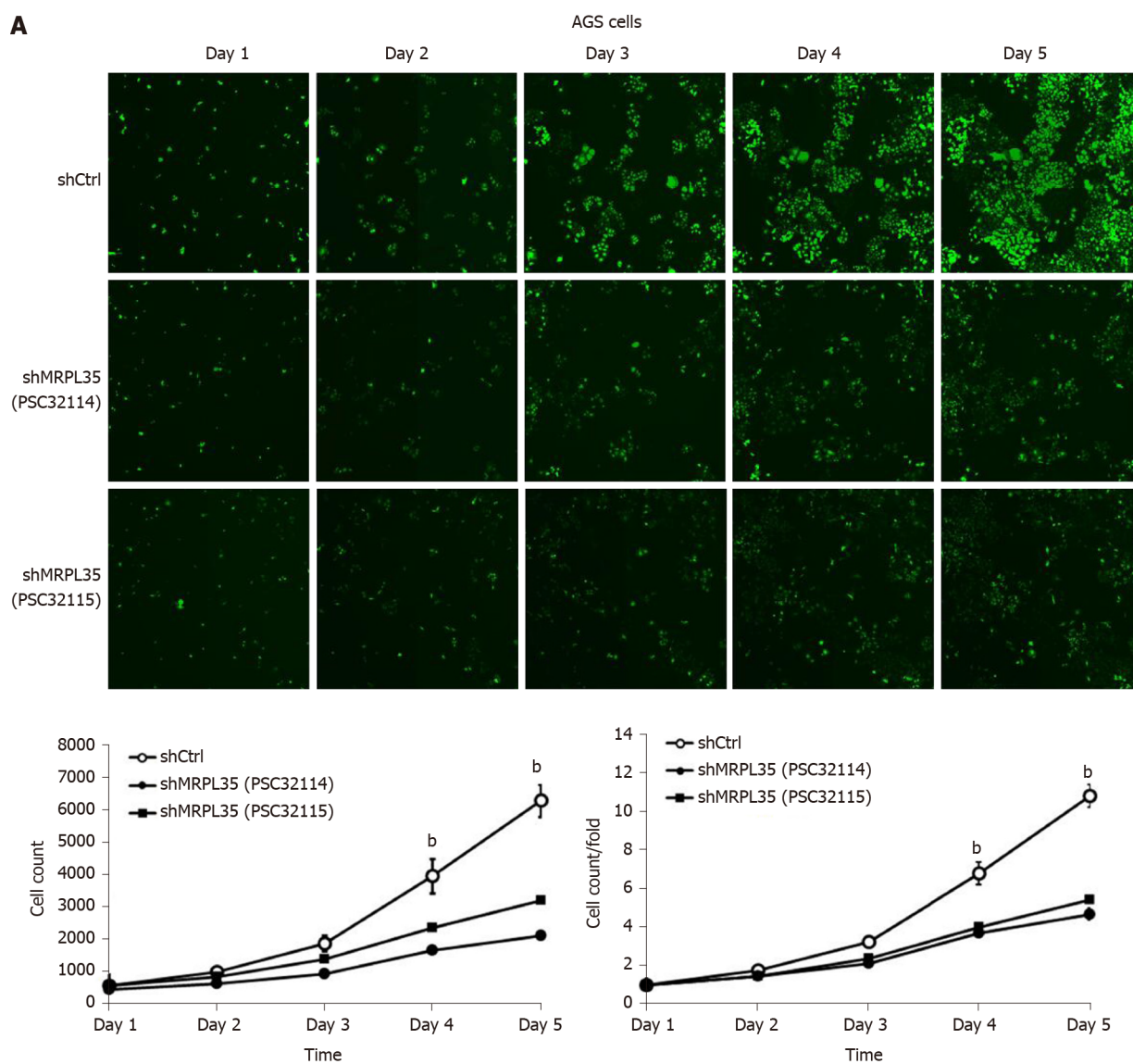


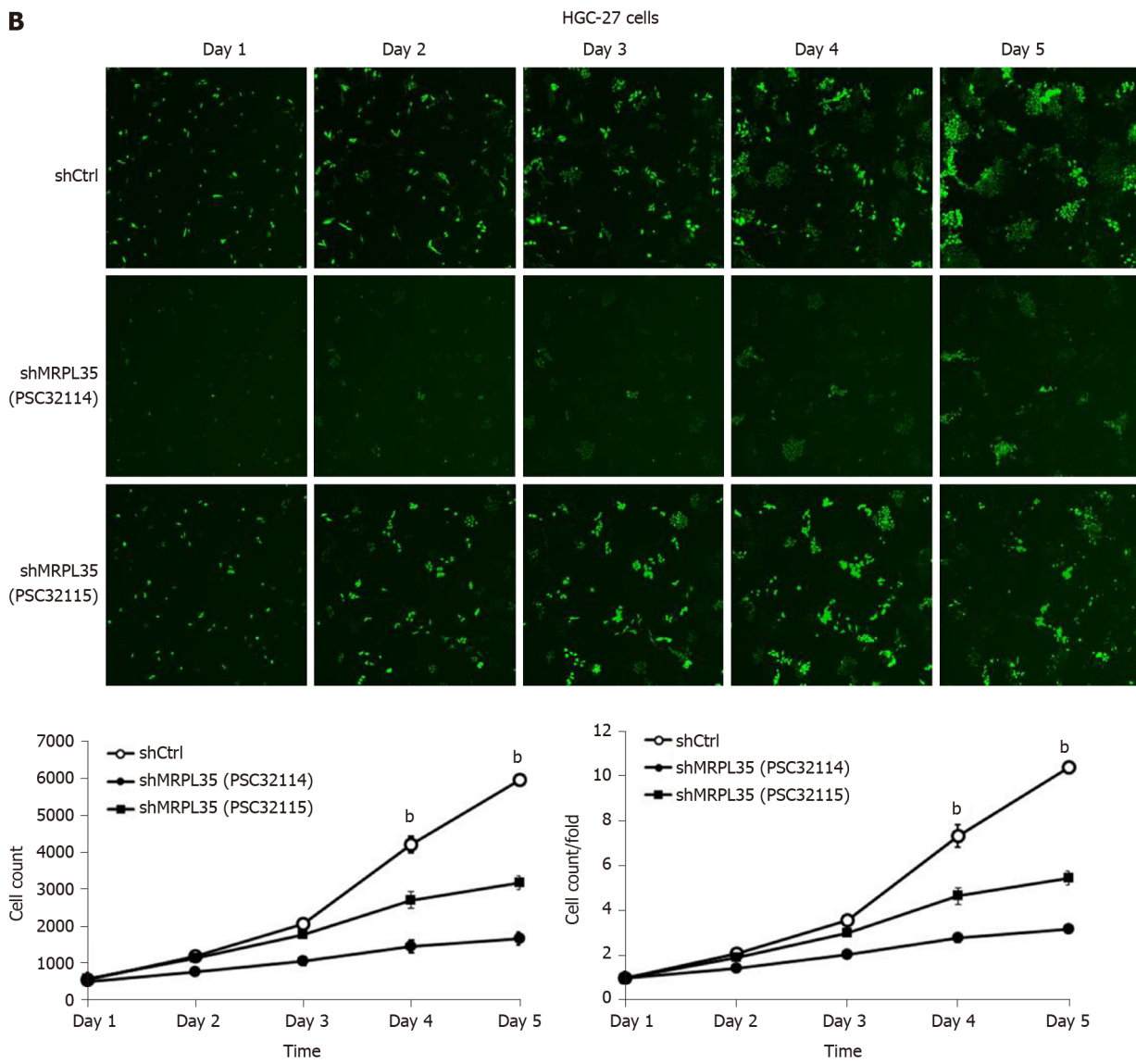


**Figure 3** The expression of MRPL35 in gastric carcinoma cells. A: Quantitative reverse transcription-polymerase chain reaction (qRT-PCR) detection of MRPL35 in gastric carcinoma cell lines (AGS, NCI-N87, MKN-45 and HGC-27); B and C: shCtrl (negative control virus) and shMRPL35 (lentiviral particles of MRPL35) (PSC32114 or PSC32115) infected AGS cells (B) and HGC-27 cells (C) at 72 h with bright and fluorescent micrographs (100 × magnification); D and E: qRT-PCR was used to analyze the expression of MRPL35 in AGS cells (D) and HGC-27 cells (E) infected with shCtrl and shMRPL35; F: Western blot was used to detect the expression of MRPL35 in AGS cells transfected with shCtrl and shMRPL35, and GAPDH (glyceraldehyde-3-phosphate dehydrogenase) was used as an internal control.  $n = 3$ .  $^bP < 0.01$ . shCtrl: Negative control virus; shMRPL35: Lentiviral particles of MRPL35; GAPDH: Glyceraldehyde-3-phosphate dehydrogenase; GFP: Green fluorescent protein.



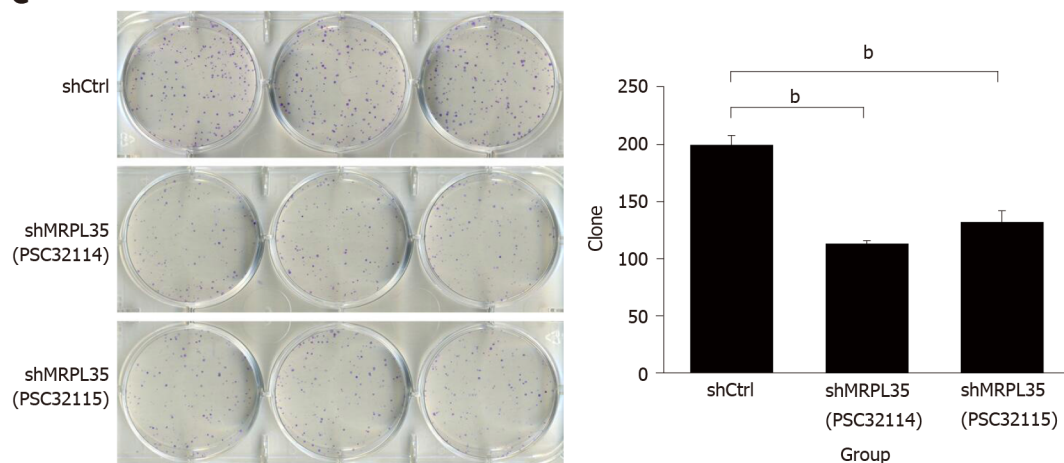
**A**



**B**

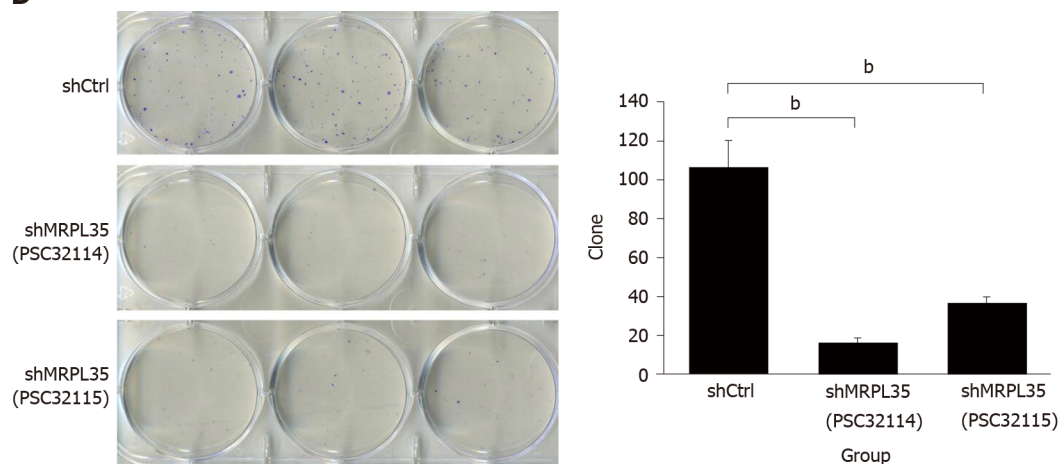
**C**

AGS cells



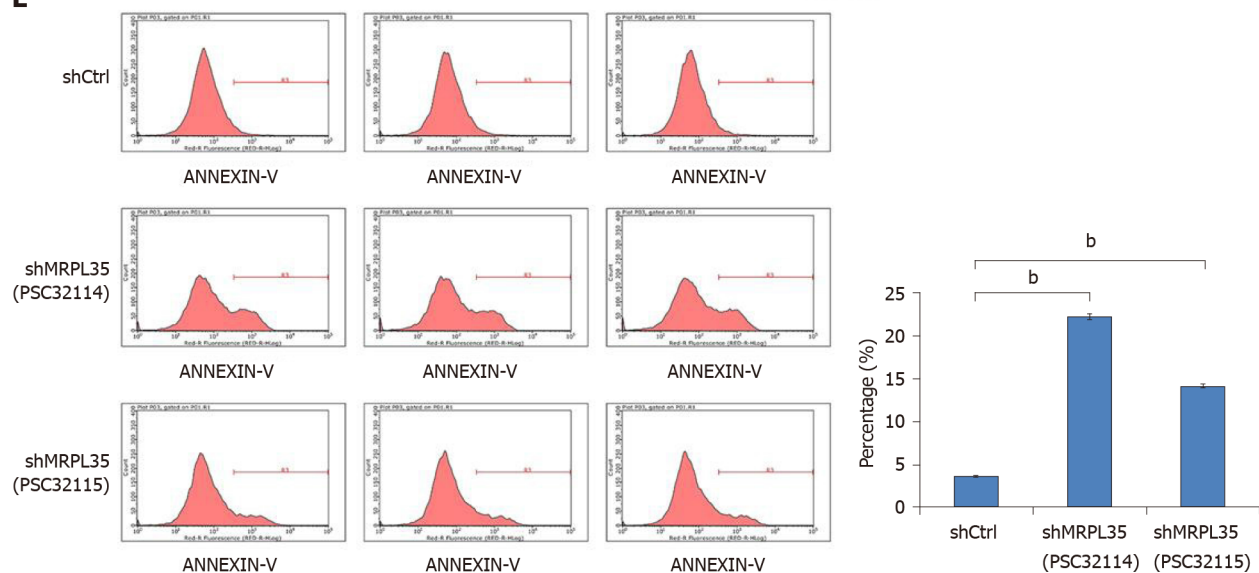
**D**

HGC-27 cells



**E**

AGS cells



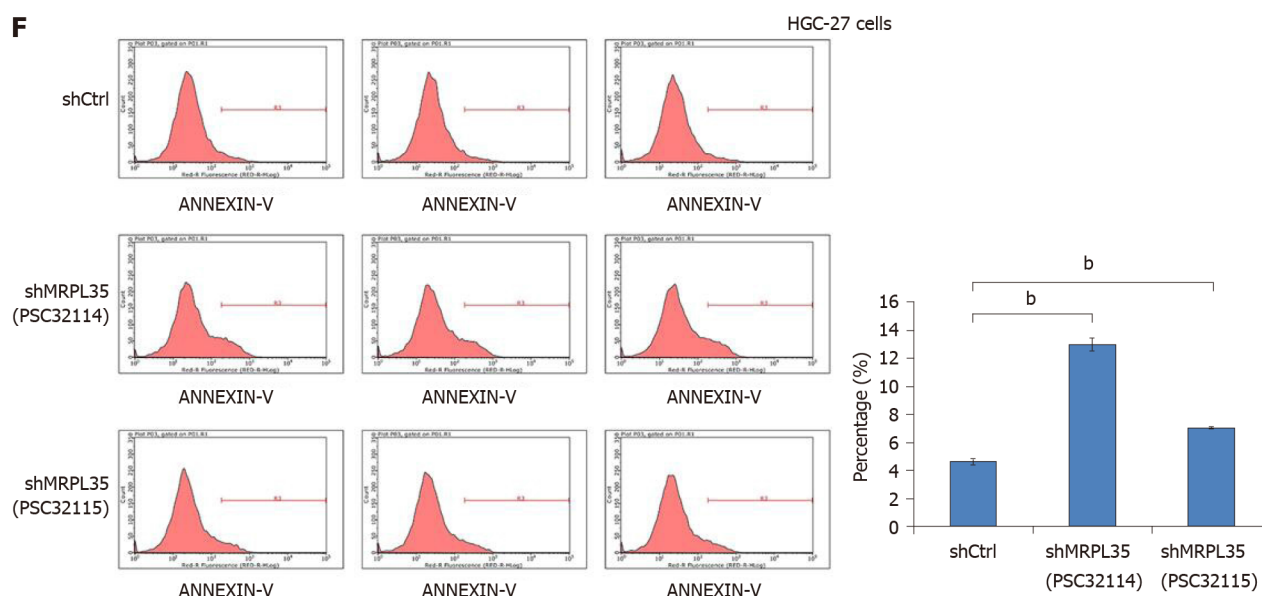


**Figure 4 Knockdown of MRPL35 inhibits gastric carcinoma cell proliferation and monoclonal formation and promotes gastric carcinoma cell apoptosis.** A and B: The Celigo cell count assay was used to analyze the proliferation of AGS cells (A) and HGC-27 cells (B) transfected with shCtrl (negative control virus) and shMRPL35 (lentiviral particles of MRPL35); C and D: Colony formation assay of shCtrl and shMRPL35 infected AGS cells (C) and HGC-27 cells (D); E and F: Flow cytometry analysis of apoptosis of shCtrl and shMRPL35 infected AGS cells (E) and HGC-27 cells (F).  $n = 3$ .  $^bP < 0.01$ . shCtrl: Negative control virus; shMRPL35: Lentiviral particles of MRPL35.

cancer<sup>[19]</sup>. Indeed, the tumor growth rate in the experimental group was slow, and the tumor was smaller than that in the control group, which was the same as our experimental results. The gastrointestinal tract contains the mouth, esophagus, stomach, small intestine, and large intestine. The cells contained in these tissues were developed from the endoderm of the early embryo. Perhaps because the esophagus, stomach, and large intestine all come from the endoderm, the inhibitory effects of MRPL35 in GC, esophageal cancer, and colorectal cancer are similar.

Furthermore, the PICK1 protein contains a PDZ domain, which binds to a variety of membrane proteins and organizes the subcellular localization of adaptor protein<sup>[20]</sup>. It may also participate in receptor aggregation by acting on the level of receptor internalization. Decreased expression of MRPL35 regulates the expression of MRPL27, reducing the expression of PICK1. The protein encoded by *BCL-XL* belongs to the BCL-2 protein family<sup>[21]</sup>. It can be used as an anti- or pro-apoptotic regulator involved in various cell activities and regulation of the opening of the mitochondrial outer membrane channel (VDAC). MRPL35 regulates the expression of BCL-XL by regulating the family member BAX. AGR2 encodes a member of the disulfide isomerase family of endoplasmic reticulum protein and plays a role in cell migration, cell differentiation, and growth, and is associated with cancer progression<sup>[22]</sup>. Consequently, the expression of MRPL35 and MRPL2 is altered, which in turn, affects that of AGR2. These results fully indicated that MRPL35 might be an oncogene, and the correlation between MRPL35 and GC is worthy of in-depth exploration.

In short, the current study suggested that MRPL35 has a causal correlation with GC, and related downstream proteins of MRPL35 have been identified. Nevertheless, the current study has some deficiencies. At present, only a few studies have investigated MRPL35, which is not sufficient to clarify its role as a therapeutic target for GC. On the premise that there are no relevant studies on MRPL35 and GC, follow-up research would be divided into three stages. In the first stage, the correlation between *PICK1*, *BCL-XL*, and *AGR2* genotype and GC phenotype would be explored. In the second stage, the correlation between MRPL35 and its downstream proteins *PICK1*, *BCL-XL*, and *AGR2* would be examined. In the third stage, the mechanism underlying the interaction between MRPL35 and *PICK1*, *BCL-XL*, and *AGR2* would be assessed, and two modes of action were considered: Direct and through tool protein. Also, covalent and non-covalent interactions occurred between the proteins. Anyway, our study aimed to provide a scientific basis for the treatment of GC and find effective drug target for the early prevention of GC.



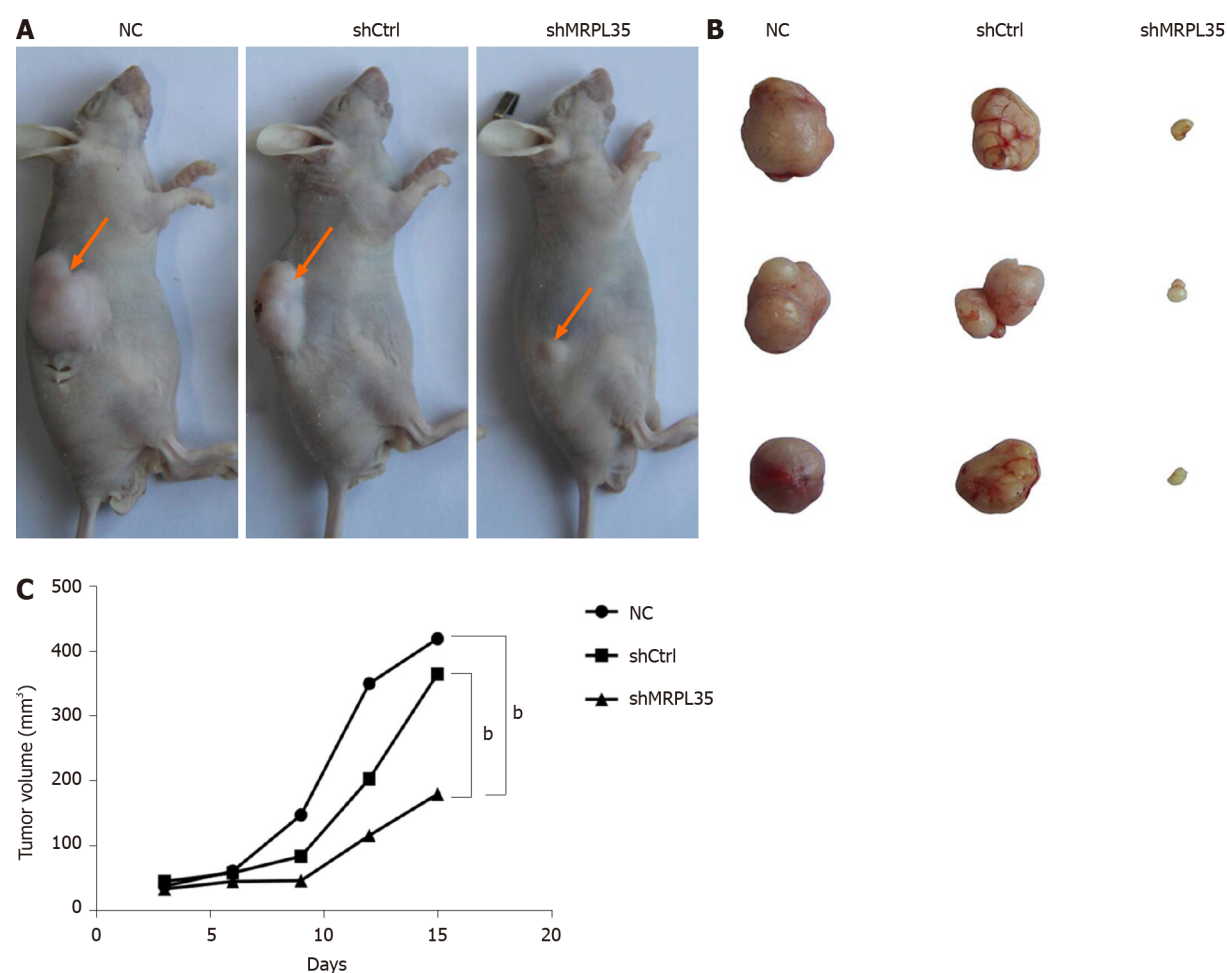


**Figure 5 Knockdown of *MRPL35* inhibits tumor formation in nude mice.** A: Nude mouse gastric carcinoma xenograft model; B: Subcutaneously transplanted tumor in nude mice; C: Tumor growth curve of transplanted tumor model.  $n = 30$ . <sup>b</sup> $P < 0.01$ . NC: Negative control; shCtrl: Negative control virus; shMRPL35: Lentiviral particles of MRPL35.

## CONCLUSION

MRPL35 is related to esophageal cancer and colorectal cancer, and has not been reported in GC. Our experimental data combined with the data in the public tumor database show that MRPL35 is of extraordinary importance in GC tissues and cells, which has also been verified in nude mice. The expression of MRPL35 in GC tissues is higher than that of the matched adjacent tissues, and knockdown of *MRPL35* can inhibit the proliferation of GC cells and induce apoptosis. This suggests that MRPL35 is a potential target for the treatment of GC, and it is necessary to further study the effect of MRPL35 on GC.



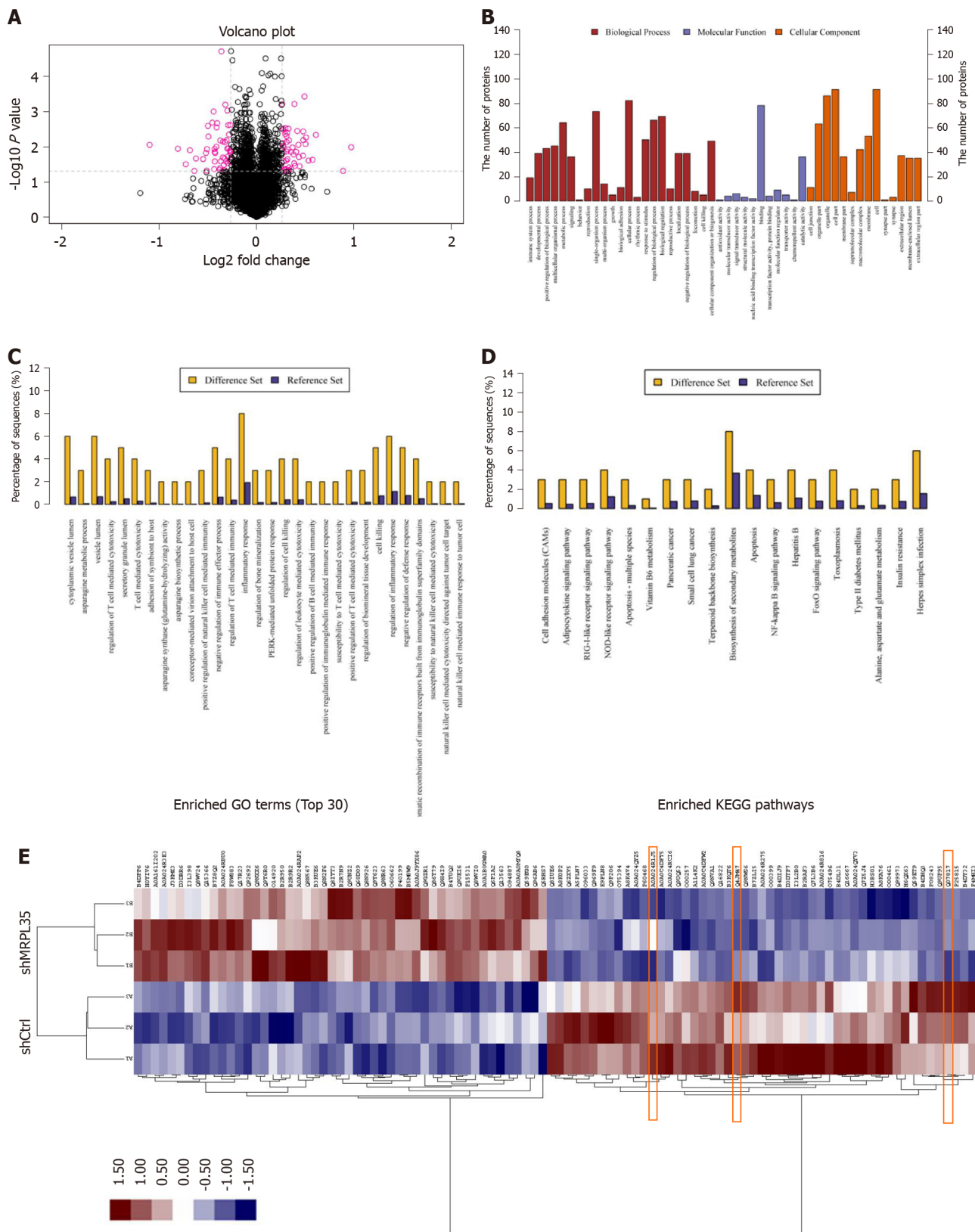


**Figure 6 Proteomic and bioinformatic analysis of identified proteins.** A: A total of 5993 proteins were identified by isobaric tags for relative and absolute quantification. Red circle indicates 100 differentially expressed proteins (DEPs); B: The result of Gene Ontology annotation. The identified proteins were categorized into three types: Biological process, molecular function, and cellular component; C: Enriched Gene Ontology annotation statistics of DEPs; D: Enriched KEGG pathway statistics of DEPs; E: Protein cluster analysis of DEPs. The red box part is AGR2, PICK1, and BCL-XL. shCtrl: Negative control virus; shMRPL35: Lentiviral particles of MRPL35.

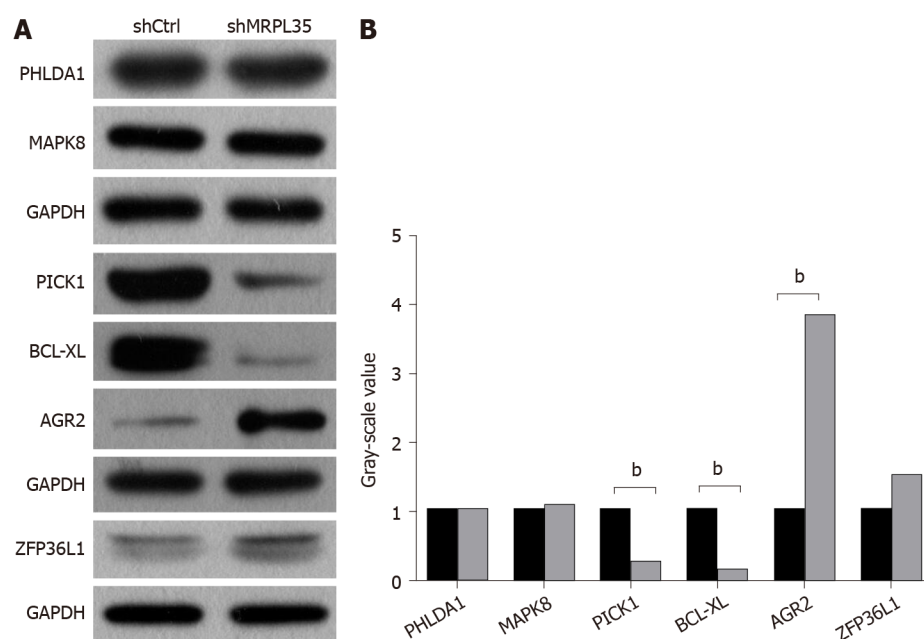


**Figure 7** Expression of related proteins in AGS cells after knockdown of *MRPL35*. A and B: The expression of PHLDA1, MAPK8, PICK1, BCL-XL, AGR2, and ZFP36L1 proteins was detected by Western blot. GAPDH was used as an internal control. A: Western blot images; B: Gray-scale value.  $n = 3$ .  $^bP < 0.01$ . shCtrl: Negative control virus; shMRPL35: Lentiviral particles of MRPL35.

## ARTICLE HIGHLIGHTS

### Research background

Gastric carcinoma (GC) is one of the most common cancers, and the existing treatment methods cannot meet the treatment needs for GC. At the same time, MRPL35, a member of the large subunit family of mitochondrial ribosomal protein, shows the characteristics of oncogene in certain cancers.

### Research motivation

The existing treatment methods for GC mainly include drugs, chemotherapy, and surgery, all of which have certain defects. Finding new therapeutic targets will be of great benefit to patients with GC.

### Research objectives

The present study aimed to explore the correlation between MRPL35 and GC, and the effect of knockdown of MRPL35 on GC cells.

### Research methods

The expression of MRPL35 in GC and the effect of MRPL35 on the prognosis of GC were evaluated based on data from public databases. Immunohistochemistry staining and pathological factors analysis were performed on 64 pairs of GC tissues and matched adjacent tissues. The effect of MRPL35 on the proliferation and apoptosis of GC cells was determined by Celigo cell count assay, flow cytometry, and tumor formation experiment in BABL/c nude mice. The related proteins that changed after knockdown of MRPL35 was identified by proteomic analysis and tested by Western blot.

### Research results

The expression of MRPL35 was up-regulated in GC and high expression of MRPL35 was associated with a poor survival in GC. The expression of MRPL35 in GC tissues was increased in comparison with matched adjacent tissues, which was related to age, lymph node metastasis, and pathological tumor-node-metastasis stage. Knockdown of MRPL35 inhibited GC cell proliferation and colony formation and induced apoptosis. After knockdown of MRPL35, the expression of PICK1 and BCL-XL protein decreased, and that of AGR2 protein increased.

### Research conclusions

MRPL35 is up-regulated in GC, and knockdown of MRPL35 could inhibit the proliferation of GC cells and induce apoptosis.

### Research perspectives

MRPL35 can be used for targeted therapy of GC, and can also be used as a new biomarker for GC.

## ACKNOWLEDGEMENTS

The authors would like to acknowledge Sun J for statistical analysis assistance.

## REFERENCES

- 1 Ferlay J, Colombet M, Soerjomataram I, Mathers C, Parkin DM, Piñeros M, Znaor A, Bray F. Estimating the global cancer incidence and mortality in 2018: GLOBOCAN sources and methods. *Int J Cancer* 2019; **144**: 1941-1953 [PMID: 30350310 DOI: 10.1002/ijc.31937]
- 2 Bray F, Ferlay J, Soerjomataram I, Siegel RL, Torre LA, Jemal A. Global cancer statistics 2018: GLOBOCAN estimates of incidence and mortality worldwide for 36 cancers in 185 countries. *CA Cancer J Clin* 2018; **68**: 394-424 [PMID: 30207593 DOI: 10.3322/caac.21492]
- 3 Song Z, Wu Y, Yang J, Yang D, Fang X. Progress in the treatment of advanced gastric cancer. *Tumour Biol* 2017; **39**: 1010428317714626 [PMID: 28671042 DOI: 10.1177/1010428317714626]
- 4 Slagter AE, Vollebergh MA, Jansen EPM, van Sandick JW, Cats A, van Grieken NCT, Verheij M. Towards Personalization in the Curative Treatment of Gastric Cancer. *Front Oncol* 2020; **10**: 614907 [PMID: 33330111 DOI: 10.3389/fonc.2020.614907]
- 5 Brown A, Amunts A, Bai XC, Sugimoto Y, Edwards PC, Murshudov G, Scheres SHW, Ramakrishnan V. Structure of the large ribosomal subunit from human mitochondria. *Science* 2014; **346**: 718-722 [PMID: 25278503 DOI: 10.1126/science.1258026]
- 6 Box JM, Kaur J, Stuart RA. MrpL35, a mitospecific component of mitoribosomes, plays a key role in cytochrome c oxidase assembly. *Mol Biol Cell* 2017; **28**: 3489-3499 [PMID: 28931599 DOI: 10.1091/mbc.E17-04-0239]
- 7 Alshabi AM, Vastrad B, Shaikh IA, Vastrad C. Identification of Crucial Candidate Genes and Pathways in Glioblastoma Multiform by Bioinformatics Analysis. *Biomolecules* 2019; **9** [PMID: 31137733 DOI: 10.3390/biom9050201]
- 8 Zhang L, Lu P, Yan L, Yang L, Wang Y, Chen J, Dai J, Li Y, Kang Z, Bai T, Xi Y, Xu J, Sun G, Yang T. MRPL35 Is Up-Regulated in Colorectal Cancer and Regulates Colorectal Cancer Cell Growth and Apoptosis. *Am J Pathol* 2019; **189**: 1105-1120 [PMID: 30862482 DOI: 10.1016/j.ajpath.2019.02.003]
- 9 Wang AF, Zhang Q, Zhang DM, Xiu YT, Ding YM, Liu LL. Effect of silencing mitochondrial ribosomal protein L35 gene on the growth of human esophageal carcinoma TE-1 cells. *Jilin Daxue Xuebao* 2019; **45**: 28-32
- 10 Wang YT. Preliminary study on the role of MRPL35 protein in the development of colorectal cancer. M.Sc. Thesis, Shanxi Medical University. 2017. Available from: <https://kns.cnki.net/KXRead/Detail?TIMESTAMP=637472036637783203&DBCODE=CJFQ&TABLEName=CJFDLAST2019&FileName=BQEB201901006&RESULT=1&SIGN=hPoiLoUIMEDInsKQkf7paQxOVMS%3d>
- 11 Gopisetty G, Thangarajan R. Mammalian mitochondrial ribosomal small subunit (MRPS) genes: A putative role in human disease. *Gene* 2016; **589**: 27-35 [PMID: 27170550 DOI: 10.1016/j.gene.2016.05.008]
- 12 Buchynska LG, Iurchenko NP, Kashuba EV, Brieieva OV, Glushchenko NM, Mints M, Lukianova NY, Chekhun VF. Overexpression of the mitochondrial ribosomal protein S18-2 in the invasive breast carcinomas. *Exp Oncol* 2018; **40**: 303-308 [PMID: 30593750]
- 13 Lee J, Seol MY, Jeong S, Lee CR, Ku CR, Kang SW, Jeong JJ, Shin DY, Nam KH, Lee EJ, Chung WY, Jo YS. A metabolic phenotype based on mitochondrial ribosomal protein expression as a predictor of lymph node metastasis in papillary thyroid carcinoma. *Medicine (Baltimore)* 2015; **94**: e380 [PMID: 25590838 DOI: 10.1097/MD.0000000000000380]
- 14 Lazar V, Suo C, Orear C, van den Oord J, Balogh Z, Guegan J, Job B, Meurice G, Ripoché H, Calza S, Hasmats J, Lundberg J, Lacroix L, Vielh P, Dufour F, Lehtiö J, Napieralski R, Eggermont A, Schmitt M, Cadranet J, Besse B, Girard P, Blackhall F, Validire P, Soria JC, Dessen P, Hansson J, Pawitan Y. Integrated molecular portrait of non-small cell lung cancers. *BMC Med Genomics* 2013; **6**: 53 [PMID: 24299561 DOI: 10.1186/1755-8794-6-53]
- 15 Kim MJ, Yoo YA, Kim HJ, Kang S, Kim YG, Kim JS, Yoo YD. Mitochondrial ribosomal protein L41 mediates serum starvation-induced cell-cycle arrest through an increase of p21(WAF1/CIP1). *Biochem Biophys Res Commun* 2005; **338**: 1179-1184 [PMID: 16256947 DOI: 10.1016/j.bbrc.2005.10.064]

- 16 **Gao Y**, Li F, Zhou H, Yang Y, Wu R, Chen Y, Li W, Li Y, Xu X, Ke C, Pei Z. Down-regulation of MRPS23 inhibits rat breast cancer proliferation and metastasis. *Oncotarget* 2017; **8**: 71772-71781 [PMID: 29069745 DOI: 10.18632/oncotarget.17888]
- 17 **Ong JR**, Bamodu OA, Khang NV, Lin YK, Yeh CT, Lee WH, Cherng YG. SUMO-Activating Enzyme Subunit 1 (SAE1) Is a Promising Diagnostic Cancer Metabolism Biomarker of Hepatocellular Carcinoma. *Cells* 2021; **10** [PMID: 33477333 DOI: 10.3390/cells10010178]
- 18 **Sun Z**, Zhu Y, Aminbuhe, Fan Q, Peng J, Zhang N. Differential expression of APE1 in hepatocellular carcinoma and the effects on proliferation and apoptosis of cancer cells. *Biosci Trends* 2018; **12**: 456-462 [PMID: 30473552 DOI: 10.5582/bst.2018.01239]
- 19 **Yan LH**. The effect of down-regulation of MRPL35 and RASGRF2 on tumor growth and metastasis of colorectal carcinoma xenograft model in nude mice. M.Sc. Thesis, Shanxi Medical University. 2018. Available from: <https://kns.cnki.net/KXReader/Detail?TIMESTAMP=637472036637783203&DBCODE=CJFQ&TABLEName=CJFDLAST2019&FileName=BQEB201901006&RESULT=1&SIGN=hPOiLoUIMEDInsKQkf7paQxOVMS%3d>
- 20 **Lei B**, Wang D, Zhang M, Deng Y, Jiang H, Li Y. miR-615-3p promotes the epithelial-mesenchymal transition and metastasis of breast cancer by targeting PICK1/TGFBRI axis. *J Exp Clin Cancer Res* 2020; **39**: 71 [PMID: 32336285 DOI: 10.1186/s13046-020-01571-5]
- 21 **Qi G**, Yu N, Xu K, Xie X, Mao Y, Chen X, Ran X, Lin G, Hu C. Grass carp (*Ctenopharyngodon idella*) Bcl-xl: transcriptional regulation and anti-apoptosis analysis. *Fish Physiol Biochem* 2020; **46**: 483-500 [PMID: 31836954 DOI: 10.1007/s10695-019-00668-9]
- 22 **Li J**, Hu J, Luo Z, Zhou C, Huang L, Zhang H, Chi J, Chen Z, Li Q, Deng M, Chen J, Tao K, Wang G, Wang L, Wang Z. AGR2 is controlled by DNMT3a-centered signaling module and mediates tumor resistance to 5-Aza in colorectal cancer. *Exp Cell Res* 2019; **385**: 111644 [PMID: 31614132 DOI: 10.1016/j.yexcr.2019.111644]



## Basic Study

# Mitochondrial pathway of the lysine demethylase 5C inhibitor CPI-455 in the Eca-109 esophageal squamous cell carcinoma cell line

Xiao-Jie Xue, Fei-Rong Li, Jing Yu

**ORCID number:** Xiao-Jie Xue 0000-0003-0315-1253; Fei-Rong Li 0000-0003-0166-8064; Jing Yu 0000-0001-5836-5334.

**Author contributions:** Xue XJ analyzed the data, drafted the article, and contributed to study design; Li FR contributed to data gathering; Yu J contributed to study design, editing, and revising the paper; all authors read and approved the final manuscript.

**Supported by** Young Talents Project of Hubei Provincial Health Commission, No. WJ2019H449.

### Institutional review board

**statement:** The study was reviewed and approved by Hubei cancer hospital, Tongji Medical College, Huazhong University of Science and Technology (approval No. LLHBCH2020LW-027).

**Conflict-of-interest statement:** The authors declare that they have no competing interests..

**Data sharing statement:** No additional data are available.

**Open-Access:** This article is an open-access article that was selected by an in-house editor and fully peer-reviewed by external reviewers. It is distributed in accordance with the Creative

**Xiao-Jie Xue, Fei-Rong Li**, Department of Clinical Laboratory, Huangshi Central Hospital, Affiliated Hospital of Hubei Polytechnic University, Edong Healthcare Group, Huangshi 435000, Hubei Province, China

**Xiao-Jie Xue**, Hubei Key Laboratory of Kidney Disease Pathogenesis and Intervention, Huangshi 435000, Hubei Province, China

**Xiao-Jie Xue**, Medical College, Wuhan University of Science and Technology, Wuhan 430081, Hubei Province, China

**Jing Yu**, Department of Laboratory Medicine, Hubei Cancer Hospital, Tongji Medical College, Huazhong University of Science and Technology, Wuhan 430079, Hubei Province, China

**Corresponding author:** Jing Yu, PhD, Doctor, Department of Laboratory Medicine, Hubei Cancer Hospital, Tongji Medical College, Huazhong University of Science and Technology, No. 116 Zhuodaquan South Road, Wuhan 430079, Hubei Province, China.  
[yujings9774@sina.com.cn](mailto:yujings9774@sina.com.cn)

## Abstract

### BACKGROUND

Esophageal cancer is a malignant tumor of the digestive tract that is difficult to diagnose early. CPI-455 has been reported to inhibit various cancers, but its role in esophageal squamous cell carcinoma (ESCC) is unknown.

### AIM

To investigate the effects and mechanism of the lysine demethylase 5C inhibitor, CPI-455, on ESCC cells.

### METHODS

A methyl tetrazolium assay was used to detect the inhibitory effect of CPI-455 on the proliferation of Eca-109 cells. Apoptosis, reactive oxygen species (ROS), and mitochondrial membrane potential were assessed by flow cytometry. Laser confocal scanning and transmission electron microscopy were used to observe changes in Eca-109 cell morphology. The protein expression of P53, Bax, lysine-specific demethylase 5C (KDM5C), cleaved Caspase-9, and cleaved Caspase-3 were assayed by western blotting.

### RESULTS



Commons Attribution NonCommercial (CC BY-NC 4.0) license, which permits others to distribute, remix, adapt, build upon this work non-commercially, and license their derivative works on different terms, provided the original work is properly cited and the use is non-commercial. See: <http://creativecommons.org/licenses/by-nc/4.0/>

**Manuscript source:** Unsolicited manuscript

**Specialty type:** Gastroenterology and hepatology

**Country/Territory of origin:** China

**Peer-review report's scientific quality classification**

Grade A (Excellent): 0  
Grade B (Very good): 0  
Grade C (Good): C  
Grade D (Fair): 0  
Grade E (Poor): 0

**Received:** January 8, 2021

**Peer-review started:** January 8, 2021

**First decision:** February 11, 2021

**Revised:** February 14, 2021

**Accepted:** March 24, 2021

**Article in press:** March 24, 2021

**Published online:** April 28, 2021

**P-Reviewer:** Casella C

**S-Editor:** Gao CC

**L-Editor:** Filipodia

**P-Editor:** Li JH



Compared with the control group, CPI-455 significantly inhibited Eca-109 cell proliferation. Gemcitabine inhibited Eca-109 cell proliferation in a concentration- and time-dependent manner. CPI-455 caused extensive alteration of the mitochondria, which appeared to have become atrophied. The cell membrane was weakly stained and the cytoplasmic structures were indistinct and disorganized, with serious cavitation when viewed by transmission electron microscopy. The flow cytometry and western blot results showed that, compared with the control group, the mitochondrial membrane potential was decreased and depolarized in Eca-109 cells treated with CPI-455. CPI-455 significantly upregulated the ROS content, P53, Bax, Caspase-9, and Caspase-3 protein expression in Eca-109 cells, whereas KDM5C expression was downregulated.

## CONCLUSION

CPI-455 inhibited Eca-109 cell proliferation *via* mitochondrial apoptosis by regulating the expression of related genes.

**Key Words:** Lysine-specific demethylase 5C; CPI-455; Esophageal squamous cell carcinoma; Caspase; P53

©The Author(s) 2021. Published by Baishideng Publishing Group Inc. All rights reserved.

**Core Tip:** This study confirmed that the lysine demethylase 5C inhibitor CPI-455 inhibited the proliferation of Eca-109 esophageal squamous cell carcinoma cells. CPI-455 played a role in esophageal squamous cell carcinoma cells proliferation and invasion that may have been associated in part with p53, Bax, Caspase-9, and Caspase-3 expression. CPI-455 induced Eca-109 cell apoptosis *via* a mitochondria-mediated intrinsic apoptotic signaling pathway by regulating the expression of related genes.

**Citation:** Xue XJ, Li FR, Yu J. Mitochondrial pathway of the lysine demethylase 5C inhibitor CPI-455 in the Eca-109 esophageal squamous cell carcinoma cell line. *World J Gastroenterol* 2021; 27(16): 1805-1815

**URL:** <https://www.wjgnet.com/1007-9327/full/v27/i16/1805.htm>

**DOI:** <https://dx.doi.org/10.3748/wjg.v27.i16.1805>

## INTRODUCTION

Esophageal cancer is a common digestive tract cancer, of which esophageal squamous cell carcinoma (ESCC) and esophageal adenocarcinoma represent the main histological types<sup>[1,2]</sup>. The incidence of esophageal cancer is relatively high, ranking seventh worldwide. ESCC accounts for more than 90% of esophageal cancers. As it is difficult to diagnose ESCC early due to a lack of specific clinical symptoms and insufficient preventive measures, it is often diagnosed at an advanced stage and has a poor prognosis. In addition, the 5-yr postoperative survival rate is less than 50%<sup>[3-5]</sup>. The lysine-specific demethylase 5C (KDM5C) inhibitor, CPI-455, regulates the apoptosis and proliferation of tumor cells by regulating the methylation state of lysine in KDM5C<sup>[6]</sup>. CPI-455 activity been reported in cervical<sup>[7]</sup>, gastric<sup>[8]</sup>, and prostate cancer<sup>[9]</sup>, and in other diseases<sup>[10,11]</sup>; but not in the treatment of esophageal cancer. In this study, human ESCC Eca-109 cells were used as a research model to preliminarily study the effect and mechanism of CPI-455 against ESCC and to explore novel approaches for the treatment and prevention of ESCC.

## MATERIALS AND METHODS

### Cell lines

Eca-109 human esophageal cancer cells and HPT-1A normal human esophageal epithelial cells were provided by the Cell Resource Center of the Shanghai Life Sciences Institute, Chinese Academy of Sciences (Shanghai, China). Other materials

included CPI-455 (MSDS, 1628208-23-0; Gibco, Ltd., United States), DMEM and RPMI 1640 cell culture media and fetal bovine serum (Gibco, Ltd). Anti-human P53 (cat no. sc-6243), Bax, KDM5C (cat no. sc-81623), Caspase-9 (cat no. 9746), Caspase-3 (cat no. 9502), GAPDH (glyceraldehyde-3-phosphate dehydrogenase, cat no. sc-47778) polyclonal antibody (1:200; Abcam, United Kingdom) were used for western blotting. Annexin V-fluorescein isothiocyanate (FITC)/propidium iodide (PI) apoptosis detection kits (cat no. F7250) were from Sigma-Aldrich (United States). polyvinylidene difluoride (PVDF) membranes were from Biyuntian Biotech (China) and bicinchoninic acid (BCA) protein quantitative detection kits were from Thermo Fisher (United States). An Epics Ultra flow cytometer (Beckman Coulter, United States), JEM-100sx transmission electron microscope (Jeol Ltd., Japan), and a TCS SP2 laser confocal microscope (Leica, Germany) were used.

### **Cell culture**

Eca-109 cells were cultured in DMEM and HET-1A cells were cultured in RPIM-1640 medium. Both were supplemented with 10% pre-inactivated FBS, 100 U/mL penicillin, and 100 U/mL streptomycin. Cells were adherently cultured in a 37 °C constant temperature incubator with a volume fraction of 5% CO<sub>2</sub> and 95% humidity; 0.25% trypsin-EDTA was used for cell digestion and passage. Cell growth in the culture flask was observed every 1-2 d, and the cell culture medium was replaced for passage culture.

### **Methyl tetrazolium assay**

For assay of growth and the logarithmic phase, cells were collected by trypsin digestion and centrifugation and 90 mL of a single cell suspension ( $3 \times 10^3$ /mL) were inoculated into 96-well culture plates and cultured at 37 °C in an atmosphere containing 5% CO<sub>2</sub> overnight to ensure adherence. When the cells grew to the appropriate density, the supernatant was discarded and 100 mL of the CPI-455 KDM5C inhibitor was added to each well, giving a final concentration of 15 mmol/L. The plates were cultured in an atmosphere containing 5% CO<sub>2</sub> at 37 °C for 0, 24, 48, 72, and 96 h (5 wells/time point). Following this, the cells were collected and centrifuged at 150 g for 10 min. The supernatant was discarded and the precipitate was washed once with phosphate buffered saline (PBS). A total of 200 µL of serum-free RPMI-1640 medium was added, followed by addition of 10 µL of methyl tetrazolium (MTT; 5 mg/mL). Following culture for a further 4 h, the supernatant was removed and 150 µL DMSO was added to each well to dissolve the purple crystals. The optical density (OD) was read at 490 nm after the crystals had completely dissolved. The survival rate was calculated as  $S\% = (\text{OD of the experimental group} / \text{OD of the control group}) \times 100$ .

### **Laser confocal scanning microscope assay of the ectropion of membrane phosphatidylserine**

The fluorescence of cell smears and suspension cultures after polylysine treatment was observed by confocal microscopy. Red (488/590 + 42 nm) and green (488/530 + 30 nm) dual channel detection and differential interference contrast imaging were performed. A total of 100 fields of vision were screened and 30 typical fields of vision were selected for inclusion in the preliminary statistical analysis. Annexin V-FITC (fluorescein isothiocyanate), PI double staining was performed and the fluorescence of Eca-109 cell membranes and necrotic nuclei was observed and analyzed as described above. DAPI (4', 6-diamidino-2-phenylindole, dihydrochloride) was used to stain the nuclei in cell smears and glycerol patches and analyzed by fluorescence microscopy, as described above.

### **Terminal deoxynucleotidyl transferase dUTP nick end labeling (TUNEL) assay of nucleation and DNA fragmentation of Eca-109 cells**

Eca-109 cells ( $5 \times 10^6$ /mL) were seeded in 24-well plates and cultured for 48 h. Cell smears were prepared from 50 µL of cell suspension on polylysine-treated slides that were fixed with 4% paraformaldehyde at room temperature for 30-60 min and washed twice with PBS. After treatment with terminal deoxynucleotidyl transferase and termination, the preparations were washed four times with PBS and incubated with FITC-labeled antibody for 30 min. Nuclei were stained with PI (1.0 g/mL) and the preparations were sealed with glycerin-mounted coverslips and marked. The cells were observed with a confocal laser scanning microscope, with FITC and PI dual channel fluorescence at an excitation wavelength of 490 nm and an emitted wavelength of 520 nm).

### Flow cytometry assay of reactive oxygen species (ROS)

Eca-109 cells were cultured in a six-well plates ( $3 \times 10^5$  cells/well), treated with 15  $\mu\text{mol/L}$  CPI-455 for 48 h, and collected. The cells were washed three times in PBS, centrifuged for 5 min, and the supernatant was discarded. The cells were resuspended in serum-free medium, dichloro-dihydro-fluorescein diacetate (DCFH-DA) was added to a final concentration of 10  $\text{mmol/L}$ , and the plates were incubated at 37 °C for 40 min. The cells were centrifuged for 10 min, and the pellet was collected, washed, and resuspended in precooled PBS. The cells were centrifuged to obtain a pellet and were stained for fluorescence detection. Each assay was performed in triplicate.

### Flow cytometry assay of mitochondrial membrane potential

Cells were harvested ( $2 \times 10^6/\text{mL}$ ) at scheduled times after treatment with 15  $\mu\text{mol/L}$  CPI-455 for 48 h. The Mitocapture dye and antibody incubation solutions were freshly prepared. The cells were washed and centrifuged and the mitochondria were stained. The cells were immediately transferred to collecting tubes for flow cytometry.

### Western blotting assay of P53, Bax, KDM5C, cleaved Caspase-9, and cleaved Caspase-3

Eca-109 cells were cultured for 48 h, collected, and centrifuged at 150 g for 5 min ( $r = 6$  cm). Total protein was extracted using a protein extraction kit. The supernatant was collected, and the protein concentration was determined using a BCA protein kit. Proteins were separated by sodium dodecyl sulfate-polyacrylamide gel electrophoresis (SDS-PAGE) and transferred to PVDF membranes. After blocking in 5% skim milk at room temperature for 2 h, anti-human mouse P53, Bax, KDM5C, Caspase-9, Caspase-3, and GAPDH monoclonal antibodies (1:1000; Santa Cruz Biotechnology, Inc., United States) were added and the membranes were incubated overnight at 4 °C and then with horseradish peroxidase (HRP)-labeled mouse secondary antibody (1:3,000; Origene Technologies Inc., China). The films were developed, fixed, scanned and analyzed using Image J software to calculate the gray values. Protein expression of the target protein was reported relative to GAPDH protein expression.

### Statistical analysis

GraphPad Prism 6.0 software was used to statistical analyze the data. The data were reported as means  $\pm$  SD. All assays were repeated independently three times. Between-group differences were compared with independent samples *t*-tests. One-way analysis of variance was used to compare data with normal distributions. Least significant difference (LSD)-*t*-tests were used for pairwise comparisons of multiple groups. The significance level was = 0.05.

## RESULTS

### CPI-455 inhibits Eca-109 cell proliferation

The MTT results demonstrated that CPI-455 significantly inhibited the proliferation of Eca-109 cells in a time- and a concentration-dependent manner. The CPI-455 LD<sub>50</sub> was 15  $\text{mol/L}$  CPI-455 at 48 h. Therefore, the 48 h concentration of 15  $\text{mol/L}$  CPI-455 was selected for the follow-up procedures (Figure 1).

### CPI-455 induces Eca-109 cell apoptosis

The laser confocal scanning microscopy results showed that prior to CPI-455 treatment, the Eca-109 cells had developed a complete mitochondrial structure. Mitocapture revealed a bright red color and "pipe-like network" that surrounded the nuclear lobule and was distributed throughout the entire cell. Following treatment with CPI-455 (15  $\mu\text{mol/L}$ ) for 48 h, both groups showed the presence of dye in the cytoplasm, with red mitochondrial staining and green cytoplasmic staining. Some cells contained visible "point and flake" red-stained mitochondria scattered in the cytoplasm, not present in clusters surrounding the nucleus, and gradually merging to form a "structureless aggregation". Substantial changes to the mitochondrial structure were observed, which appeared to indicate mitochondrial atrophy. Following CPI-455 treatment, the Eca-109 cell membranes were weakly stained and the internal cytoplasmic structures indistinct and disorganized, with severe cavitation (Figure 2A and B).

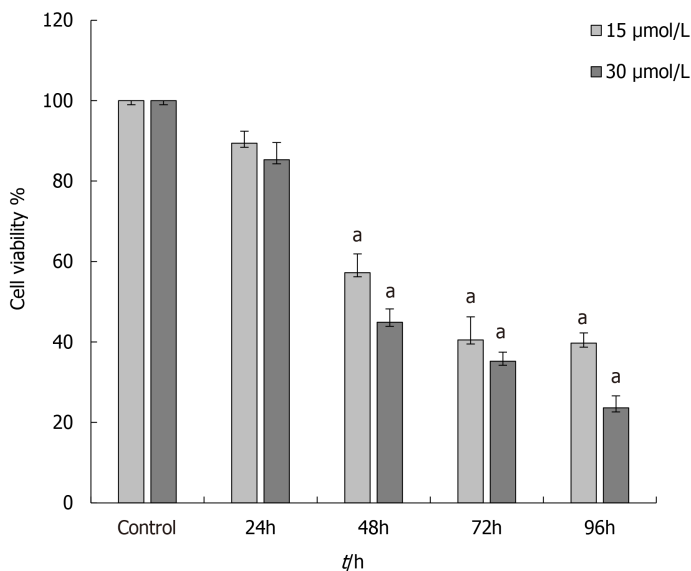


**Figure 1** Eca-109 cell viability following treatment with CPI-455 at different times and concentrations. Data are expressed as means  $\pm$  SE ( $n = 3$ ). <sup>a</sup> $P < 0.05$  vs control.

TUNEL and laser confocal scanning microscopy showed green fluorescence generated by the combination of FITC and the staining of 3'-OH terminal fragments produced by DNA fragmentation in the nucleus of apoptotic cells. Red fluorescence was emitted by PI-stained nuclei, which revealed the location of cells. Double-positive cells were seen in cells treated with CPI-455. Most Eca-109 cells in the CPI-455 group were double-positive for FITC and PI fluorescence. Most Eca-109 cells in the control group were negative for FITC and positive for PI, indicating that TUNEL assay of the CPI-455-stimulated group was positive. In terms of cell morphology, compared with the control group, most Eca-109 cells in the control group had a lower nuclear staining density, an unclear nuclear boundary, and larger nuclei. However, most ECA-109 cells in gemcitabine group had dense chromatin and small nuclei (Figure 2C and D).

#### **CPI-455 upregulates ROS content, P53, Bax, Caspase-9, and Caspase-3 expression and downregulates KDM5C expression and mitochondrial membrane potential in Eca-109 cells**

Flow cytometry was used to detect the effect of CPI-455 on the level of ROS in Eca-109 cells. With an extension of the induction time, the level of intracellular ROS in the Eca-109 cells was increased significantly, with statistically significant differences observed at 24, 48, and 72 h ( $P < 0.01$ , Figure 3). Compared with the control group, the mitochondrial membrane potential was depolarized and decreased ( $P < 0.01$ , Figure 4). The western blot results found increased expression of p53, Bax, Caspase-9, and Caspase-3 at 24, 48, and 72 h following CPI-455 treatment (Figure 5). However, KDM5C protein expression in the treated cells was significantly decreased compared with the controls ( $P < 0.01$ , Figure 6).

## **DISCUSSION**

Esophageal cancer is a digestive tract malignant tumor that is difficult to diagnose early. The most common treatments are surgery, radiotherapy, chemotherapy, and biologically targeted therapy<sup>[12]</sup>. The prognosis remains poor. The occurrence and development of esophageal cancer is complex and involves multiple gene changes, commonly resulting from histone methylation and epigenetic regulation of tumor-related genes.

CPI-455 is a KDM5C inhibitor that modulates the apoptosis and proliferation of tumor cells by regulating the lysine methylation status KDM5C. Recent reports have confirmed that the anti-tumor effect of CPI-455 in ovarian, breast, stomach, lung, and liver cancer is achieved by inducing the apoptosis and autophagy of tumor cells *via* modulating KDM5C gene transcription and expression<sup>[13,14]</sup>. In this study, the anti-Eca-109 effect of CPI-455 was studied and the associated mechanism was explored.



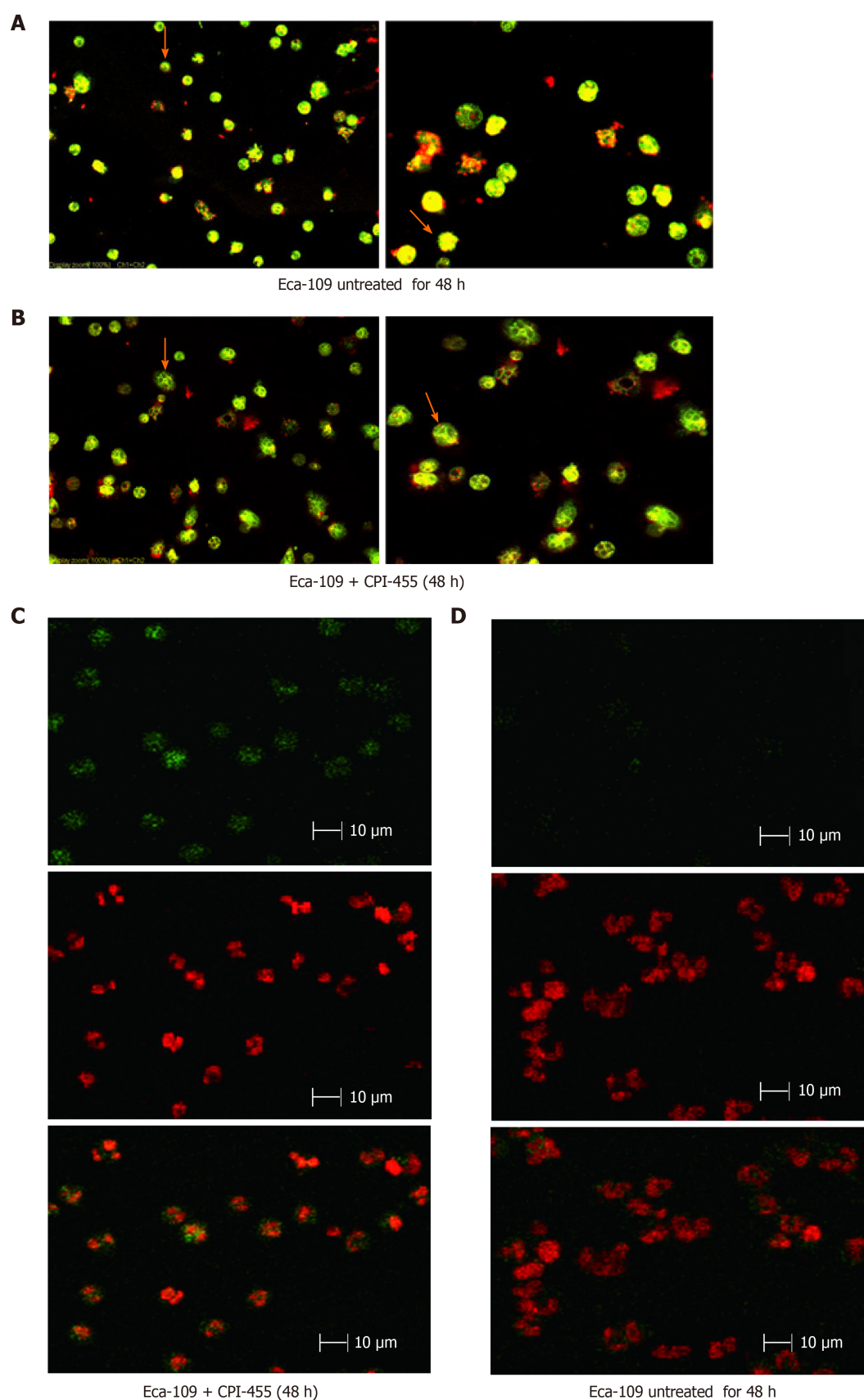


**Figure 2** Changes in Eca109 cells after 48 h culture with and without CPI-455 treatment. Left panels show the morphology of the mitochondria of Eca109 cells. A: Arrows indicate mitochondria with complete and clear structure. B: Arrows indicate mitochondria with a fuzzy structure and weak staining of cells. Right panels show TUNEL assay results (bar = 10  $\mu$ m) and laser confocal scanning microscopy  $\times$  600 of nuclear staining and DNA fragmentation of Eca109 cells C: without, and D: with CPI-455 treatment. Data are reported as means  $\pm$  SE ( $n = 3$ ).



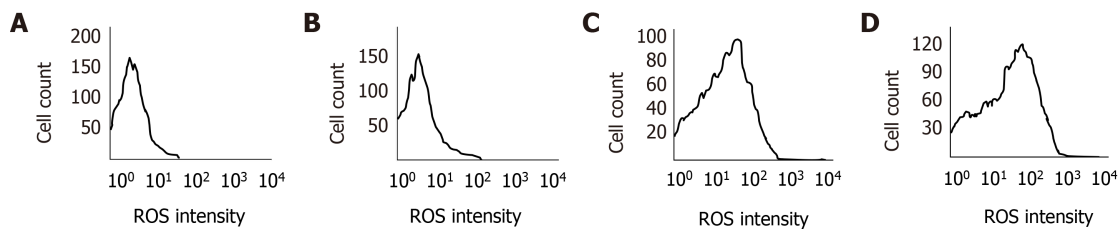


**Figure 3** Eca-109 induced by CPI-455 is dependent on the generation of reactive oxygen species. A: Eca109 untreated (0 h); B: Eca-109 induced by CPI-455 for 24 h; C: Eca-109 induced by CPI-455 for 48 h; D: Eca-109 induced by CPI-455 for 72 h. Data are reported as means  $\pm$  SE ( $n = 3$ ). ROS: Reactive oxygen species.

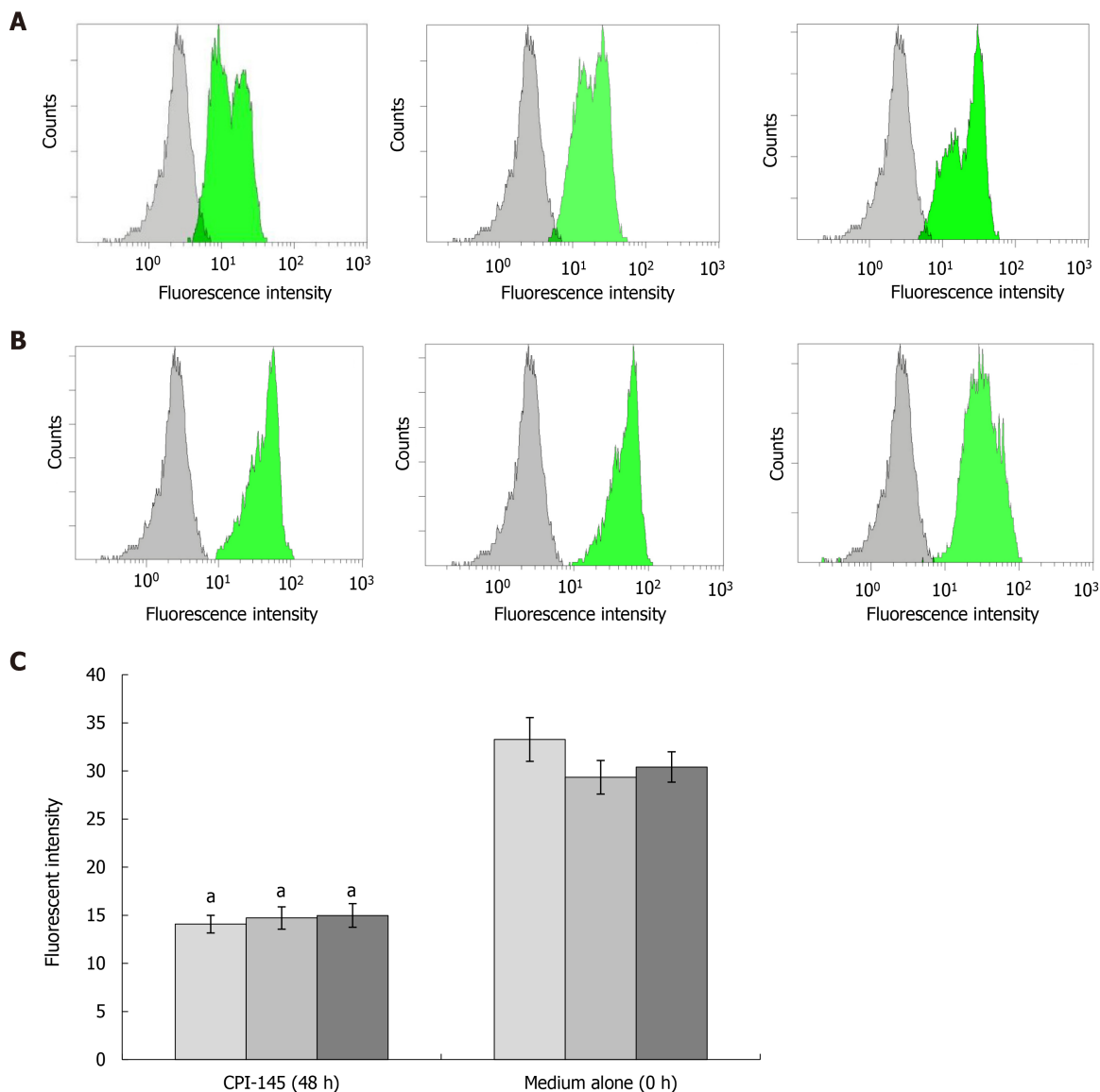


**Figure 4** Mitochondrial membrane potential assayed by flow cytometry. A: Eca109 untreated (0 h); B: Eca109 treated with CPI-455 for 48 h; C: Gray scale results of membrane potential energy of mitochondria (Blue: Results of the first assay; Red: Results of the second assay; Green: Results of the third assay). Data are reported as means  $\pm$  SE ( $n = 3$ ). <sup>a</sup> $P < 0.05$  vs control.

The study results found that CPI-455 inhibited the proliferation of esophageal cancer cells in a time-and concentration-dependent manner. However, at its effective concentration, CPI-455 was less toxic to normal esophageal cells than to Eca-109 cells. The inhibitory effect of CPI-455 on Eca-109 cell proliferation was confirmed by the assay of cell-membrane permeability by laser confocal scanning microscopy. This finding indicates that CPI-455 has favorable effects by inhibiting Eca-109 cell

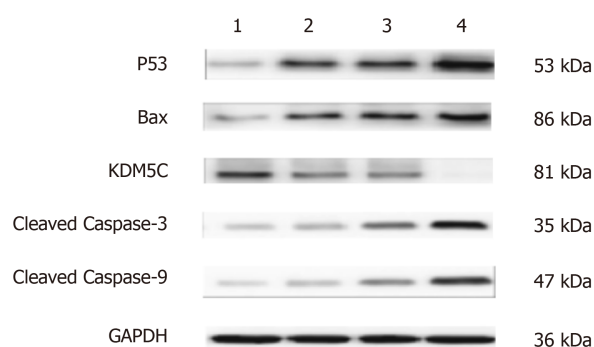


**Figure 5** Western blot assays of p53, Bax, lysine-specific demethylase 5C, cleaved Caspase 3, and cleaved Caspase 9 protein expression in Eca-109 cells. Lane 1: Eca109 untreated (0 h); Lane 2: Eca109 induced by CPI-455 for 24 h; Lane 3: Eca109 induced by CPI-455 for 48 h; Lane 4: Eca109 induced by CPI-455 for 72h. KDM5C: Lysine-specific demethylase 5C; GAPDH: Glyceraldehyde-3-phosphate dehydrogenase.

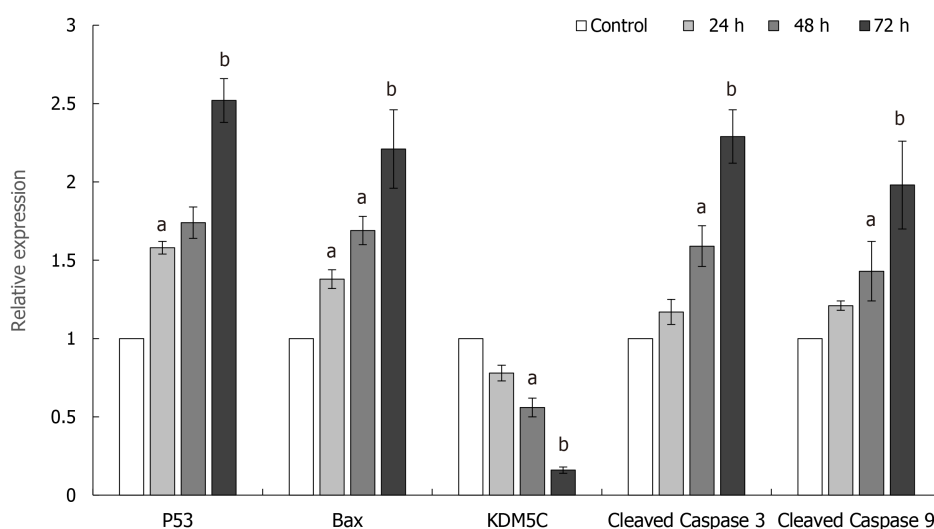


**Figure 6** Densitometry analysis of the immunoblotting data of P53, Bax, lysine-specific demethylase 5C, cleaved Caspase 3, and cleaved Caspase 9 proteins in Eca-109 cells. Data are reported as means  $\pm$  SE ( $n = 3$ ). <sup>a</sup> $P < 0.05$  vs control; <sup>b</sup> $P < 0.01$  vs control.

proliferation and growth, as well as the selective killing on ESCC cells (Figures 1 and 2).

Flow cytometry was used to determine the ROS content of Eca-109 cells, which is considered to be the by-product of oxygen consumption and cell metabolism. Previous studies have found that various chemotherapy drugs can induce an increase in the ROS content in tumor cells, and that at a certain level, ROS can induce the apoptosis of tumor cells<sup>[15-18]</sup>. Decrease of the mitochondrial membrane potential is the initial manifestation of the hypoxia apoptosis cascade<sup>[19]</sup>. In this study, the level of intracellular ROS significantly increased in treated Eca-109 cells (Figure 3), and depolarization of mitochondrial membrane was increased compared with controls (Figure 4). CPI-455 significantly induced the apoptosis of Eca-109 cells.

Previous studies have confirmed that the mechanism by which tumor cell apoptosis is induced varies widely depending on the various pathways that are involved. These includes mitochondrial pathways, which play an important role in the maintenance of stability, and those involving activation of multiple upstream and downstream genes (e.g., p53 and Bax). Activation of Caspase-2, 3, and 9 on the mitochondrial membrane is linked to the activation of mitochondrial apoptotic pathways<sup>[22-24]</sup>.

Therefore, the inhibitory effect of the KDM5C inhibitor, CPI-455, on Eca-109 cell proliferation may be related to the downregulation of KDM5C expression, activation of Caspase-3 and Caspase-9, change in mitochondrial membrane permeability, promotion of ROS production, depolarization of the mitochondrial membrane, release of the proapoptotic proteins, Bax and p53, in the mitochondria into the cytoplasm, and induction of tumor cell apoptosis (Figures 5 and 6). The above results indicate that CPI-455 induced apoptosis through an ROS-dependent mitochondrial signaling

pathway<sup>[25]</sup>.

Our study had some limitations, the mechanism involved in inducing apoptosis of tumor cells is extensive, and the mitochondrial apoptosis pathway is only one of them that plays an important role in maintaining cell stability. The mechanism has not been fully elucidated and needs further study. The results of this study provide a theoretical basis for the application of CPI-455 for the treatment of ESCC.

## CONCLUSION

CPI-455 inhibited ECA-109 cell proliferation *via* the mitochondrial apoptosis pathway by regulating the expression of related genes.

## ARTICLE HIGHLIGHTS

### Research background

Esophageal cancer is a malignant tumor of the digestive tract that is difficult to diagnose early. Although CPI-455 is reported to inhibit various cancers, the role of CPI-455 in esophageal squamous cell carcinoma (ESCC) is unknown.

### Research motivation

KDM5C, a lysine-specific demethylase 5C, inhibited ESCC proliferation and invasion, which may be partly associated with the expression of p53, Bax, Caspase-9, and Caspase-3. Mitochondria-mediated intrinsic apoptotic signaling plays an important role in the process of Eca-109 cell apoptosis induced by CPI-455.

### Research objectives

The study objective was to investigate the effect and mechanism of the KDM5C inhibitor, CPI-455, on ESCC cells.

### Research methods

The changes in proliferation, apoptosis, ROS content, and mitochondrial membrane potential of Eca-109 cells induced by CPI-455 were observed. The expression of P53, Bax, Caspase-9, Caspase-3, and KDM5C in Eca-109 cells was assayed.

### Research results

CPI-455 inhibited Eca-109 cell proliferation. P53, Bax, Caspase-9, and Caspase-3 were upregulated in Eca-109 cells, and KDM5C was significantly downregulated, by CPI-455. CPI-455 increased the level of intracellular ROS in Eca-109 cells, and decreased the mitochondrial membrane potential compared with the control group.

### Research conclusions

CPI-455 inhibited Eca-109 cell proliferation *via* the mitochondrial apoptosis pathway by regulating the expression of related genes.

### Research perspectives

CPI-455 might be a potential candidate for the development of novel chemotherapeutic agents to treat ESCC.

## ACKNOWLEDGEMENTS

We thank all the members of Department of Clinical Laboratory, Huangshi Central Hospital, Affiliated Hospital of Hubei Polytechnic University, Edong Healthcare Group and Department of Laboratory Medicine, Hubei cancer hospital, Tongji Medical College, Huazhong University of Science and Technology.

## REFERENCES

- 1 **Samson P**, Lockhart AC. Biologic therapy in esophageal and gastric malignancies: current therapies and future directions. *J Gastrointest Oncol* 2017; **8**: 418-429 [PMID: [28736629](#) DOI: [10.21037/jgo.2016.11.13](#)]
- 2 **Feng RM**, Zong YN, Cao SM, Xu RH. Current cancer situation in China: good or bad news from the 2018 Global Cancer Statistics? *Cancer Commun (Lond)* 2019; **39**: 22 [PMID: [31030667](#) DOI: [10.1186/s40880-019-0368-6](#)]
- 3 **Sohda M**, Kuwano H. Current Status and Future Prospects for Esophageal Cancer Treatment. *Ann Thorac Cardiovasc Surg* 2017; **23**: 1-11 [PMID: [28003586](#) DOI: [10.5761/ates.ra.16-00162](#)]
- 4 **Yan CY**, Chen LQ. [Retrospect of 2019: focus on the surgical treatment for adenocarcinoma of esophagogastric junction]. *Zhonghua Wei Chang Wai Ke Za Zhi* 2020; **23**: 20-25 [PMID: [31958926](#) DOI: [10.3760/cma.j.issn.1671-0274.2020.01.004](#)]
- 5 **Abbas G**, Krasna M. Overview of esophageal cancer. *Ann Cardiothorac Surg* 2017; **6**: 131-136 [PMID: [28447001](#) DOI: [10.21037/acs.2017.03.03](#)]
- 6 **Fu YD**, Huang MJ, Guo JW, You YZ, Liu HM, Huang LH, Yu B. Targeting histone demethylase KDM5B for cancer treatment. *Eur J Med Chem* 2020; **208**: 112760 [PMID: [32883639](#) DOI: [10.1016/j.ejmech.2020.112760](#)]
- 7 **Zhang Y**, Li X, Zhang J, Mao L. E6 hijacks KDM5C/Lnc\_000231/miR-497-5p/CCNE1 axis to promote cervical cancer progression. *J Cell Mol Med* 2020; **24**: 11422-11433 [PMID: [32818316](#) DOI: [10.1111/jcmm.15746](#)]
- 8 **Xu L**, Wu W, Cheng G, Qian M, Hu K, Yin G, Wang S. Enhancement of Proliferation and Invasion of Gastric Cancer Cell by KDM5C Via Decrease in p53 Expression. *Technol Cancer Res Treat* 2017; **16**: 141-149 [PMID: [26858085](#) DOI: [10.1177/1533034616629261](#)]
- 9 **Hong Z**, Wu G, Xiang ZD, Xu CD, Huang SS, Li C, Shi L, Wu DL. KDM5C is transcriptionally regulated by BRD4 and promotes castration-resistance prostate cancer cell proliferation by repressing PTEN. *Biomed Pharmacother* 2019; **114**: 108793 [PMID: [30921702](#) DOI: [10.1016/j.biopha.2019.108793](#)]
- 10 **Talebizadeh Z**, Shah A, DiTacchio L. The potential role of a retrotransposed gene and a long noncoding RNA in regulating an X-linked chromatin gene (KDM5C): Novel epigenetic mechanism in autism. *Autism Res* 2019; **12**: 1007-1021 [PMID: [31087518](#) DOI: [10.1002/aur.2116](#)]
- 11 **Wei G**, Deng X, Agarwal S, Iwase S, Distech C, Xu J. Patient Mutations of the Intellectual Disability Gene KDM5C Downregulate Netrin G2 and Suppress Neurite Growth in Neuro2a Cells. *J Mol Neurosci* 2016; **60**: 33-45 [PMID: [27421841](#) DOI: [10.1007/s12031-016-0770-3](#)]
- 12 **Hirano H**, Kato K. Systemic treatment of advanced esophageal squamous cell carcinoma: chemotherapy, molecular-targeting therapy and immunotherapy. *Jpn J Clin Oncol* 2019; **49**: 412-420 [PMID: [30920626](#) DOI: [10.1093/jco/hyz034](#)]
- 13 **Peng Y**, Alexov E. Cofactors-loaded quaternary structure of lysine-specific demethylase 5C (KDM5C) protein: Computational model. *Proteins* 2016; **84**: 1797-1809 [PMID: [27696497](#) DOI: [10.1002/prot.25162](#)]
- 14 **Denis H**, Van Grembergen O, Delatte B, Dedeurwaerder S, Putmans P, Calonne E, Rothé F, Sotiriou C, Fuks F, Deplus R. MicroRNAs regulate KDM5 histone demethylases in breast cancer cells. *Mol Biosyst* 2016; **12**: 404-413 [PMID: [26621457](#) DOI: [10.1039/c5mb00513b](#)]
- 15 **Bertero E**, Maack C. Calcium Signaling and Reactive Oxygen Species in Mitochondria. *Circ Res* 2018; **122**: 1460-1478 [PMID: [29748369](#) DOI: [10.1161/CIRCRESAHA.118.310082](#)]
- 16 **Zhelev Z**, Ivanova D, Bakalova R, Aoki I, Higashi T. Inhibition of the Pentose-phosphate Pathway Selectively Sensitizes Leukemia Lymphocytes to Chemotherapeutics by ROS-independent Mechanism. *Anticancer Res* 2016; **36**: 6011-6020 [PMID: [27793928](#) DOI: [10.21873/anticancer.11190](#)]
- 17 **Shen J**, Li ZJ, Hang ZF, Xu SF, Liu QQ, Tang H, Zhao XW. Insights into the Effect of Reactive Oxygen Species Regulation on Photocatalytic Performance via Construction of a Metal-Semiconductor Heterojunction. *J Nanosci Nanotechnol* 2020; **20**: 3478-3485 [PMID: [31748041](#) DOI: [10.1166/jnn.2020.17405](#)]
- 18 **Shukla H**, Chitrakar R, Bibi HA, Gaje G, Koucheiki A, Trush MA, Zhu H, Li YR, Jia Z. Reactive oxygen species production by BP-1,6-quinone and its effects on the endothelial dysfunction: Involvement of the mitochondria. *Toxicol Lett* 2020; **322**: 120-130 [PMID: [31953210](#) DOI: [10.1016/j.toxlet.2020.01.011](#)]
- 19 **Chan CK**, Supriady H, Goh BH, Kadir HA. Elephantopus scaber induces apoptosis through ROS-dependent mitochondrial signaling pathway in HCT116 human colorectal carcinoma cells. *J Ethnopharmacol* 2015; **168**: 291-304 [PMID: [25861953](#) DOI: [10.1016/j.jep.2015.03.072](#)]
- 20 **Chamani E**, Rezaei Z, Dastjerdi K, Javanshir S, Khorsandi K, Mohammadi GA. Evaluation of some genes and proteins involved in apoptosis on human chronic myeloid leukemia cells (K562 cells) by *datura innoxia* leaves aqueous extract. *J Biomol Struct Dyn* 2020; **38**: 4838-4849 [PMID: [31709925](#) DOI: [10.1080/07391102.2019.1691661](#)]
- 21 **Eslami F**, Mahdavi M, Babaei E, Hussen BM, Mostafavi H, Shahbazi A, Hidayat HJ. Down-regulation of Survivin and Bcl-2 concomitant with the activation of caspase-3 as a mechanism of apoptotic death in KG1a and K562 cells upon exposure to a derivative from ciprofloxacin family. *Toxicol Appl Pharmacol* 2020; **409**: 115331 [PMID: [33171188](#) DOI: [10.1016/j.taap.2020.115331](#)]
- 22 **An N**, Sun Y, Ma L, Shi S, Zheng X, Feng W, Shan Z, Han Y, Zhao L, Wu H. Helveticoside

- Exhibited p53-dependent Anticancer Activity Against Colorectal Cancer. *Arch Med Res* 2020; **51**: 224-232 [PMID: [32147288](#) DOI: [10.1016/j.arcmed.2020.02.007](#)]
- 23 **Gao G**, Chang F, Zhang T, Huang X, Yu C, Hu Z, Ji M, Duan Y. Naringin Protects Against Interleukin 1 $\beta$  (IL-1 $\beta$ )-Induced Human Nucleus Pulposus Cells Degeneration *via* Downregulation Nuclear Factor kappa B (NF- $\kappa$ B) Pathway and p53 Expression. *Med Sci Monit* 2019; **25**: 9963-9972 [PMID: [31927560](#) DOI: [10.12659/MSM.918597](#)]
  - 24 **Hou XF**, Xu LP, Song HY, Li S, Wu C, Wang JF. *ECRG2* enhances the anti-cancer effects of cisplatin in cisplatin-resistant esophageal cancer cells *via* upregulation of *p53* and downregulation of *PCNA*. *World J Gastroenterol* 2017; **23**: 1796-1803 [PMID: [28348485](#) DOI: [10.3748/wjg.v23.i10.1796](#)]
  - 25 **Li J**, Wu DD, Zhang JX, Wang J, Ma JJ, Hu X, Dong WG. Mitochondrial pathway mediated by reactive oxygen species involvement in  $\alpha$ -hederin-induced apoptosis in hepatocellular carcinoma cells. *World J Gastroenterol* 2018; **24**: 1901-1910 [PMID: [29740205](#) DOI: [10.3748/wjg.v24.i17.1901](#)]





## Observational Study

# Health-related quality of life after curative resection for gastric adenocarcinoma

Jan Grosek, Hana Zavrtanik, Aleš Tomažič

**ORCID number:** Jan Grosek 0000-0001-9832-4596; Hana Zavrtanik 0000-0003-0469-3978; Aleš Tomažič 0000-0002-1063-8636.

**Author contributions:** Grosek J and Tomažič A made substantial contributions to the conception and design of the study; Zavrtanik H contributed to the acquisition, analysis and interpretation of the data; all authors participated in drafting the manuscript; Grosek J and Tomažič A revised it critically; all authors read and approved the final version of the manuscript.

**Institutional review board statement:** The study was approved by the National Medical Ethics Committee of Republic of Slovenia (approval No. 0120-315/2019/3).

**Informed consent statement:** All study participants, or their legal guardian, provided informed written consent prior to study enrollment.

**Conflict-of-interest statement:** The authors declare that they have no financial or non-financial competing interests.

**Data sharing statement:** No additional data are available.

**STROBE statement:** The authors

**Jan Grosek, Hana Zavrtanik, Aleš Tomažič,** Department of Abdominal Surgery, University Medical Centre Ljubljana, Ljubljana 1000, Slovenia

**Jan Grosek, Aleš Tomažič,** Medical Faculty, University of Ljubljana, Ljubljana 1000, Slovenia

**Corresponding author:** Aleš Tomažič, MD, PhD, Chief Doctor, Professor, Surgeon, Department of Abdominal Surgery, University Medical Centre Ljubljana, Zaloška cesta 7, Ljubljana 1000, Slovenia. [ales.tomazic@kclj.si](mailto:ales.tomazic@kclj.si)

## Abstract

### BACKGROUND

With improved survival in gastric cancer patients, health-related quality of life has become an important clinical endpoint alongside primary oncological outcomes.

### AIM

To investigate health-related quality of life after various surgical procedures for gastric cancer treatment.

### METHODS

The validated Slovenian version of the European Organization for Research and Treatment of Cancer Quality of Life Core Questionnaire (QLQ-C30) and its gastric cancer-specific module (QLQ-STO-22) was sent for self-completion to patients that underwent curative resection for gastric adenocarcinoma between January 2014 and December 2018 at our centre. In total, 116 patients responded. Scores were compared between patients after subtotal distal *vs* total gastrectomy and patients after subtotal distal gastrectomy with Billroth II *vs* Roux-en-Y reconstruction.

### RESULTS

Interestingly, the extent of resection did not influence daily functioning; however, more dysphagia and eating restrictions were reported in patients after total gastrectomy when compared to patients after subtotal distal gastrectomy. Moreover, patients with Billroth II reconstruction after subtotal distal resection experienced worse physical and role functioning and reported more pain, fatigue and reflux compared to Roux-en-Y reconstruction.

### CONCLUSION

Based on our results, Roux-en-Y reconstruction after subtotal distal gastrectomy

have read the STROBE Statement-checklist of items, and the manuscript was prepared and revised according to the STROBE Statement-checklist of items.

**Open-Access:** This article is an open-access article that was selected by an in-house editor and fully peer-reviewed by external reviewers. It is distributed in accordance with the Creative Commons Attribution NonCommercial (CC BY-NC 4.0) license, which permits others to distribute, remix, adapt, build upon this work non-commercially, and license their derivative works on different terms, provided the original work is properly cited and the use is non-commercial. See: <http://creativecommons.org/licenses/by-nc/4.0/>

**Manuscript source:** Invited manuscript

**Specialty type:** Gastroenterology and hepatology

**Country/Territory of origin:** Slovenia

**Peer-review report's scientific quality classification**

Grade A (Excellent): 0  
Grade B (Very good): B, B, B  
Grade C (Good): C, C, C  
Grade D (Fair): 0  
Grade E (Poor): 0

**Received:** January 31, 2021

**Peer-review started:** January 31, 2021

**First decision:** February 22, 2021

**Revised:** March 5, 2021

**Accepted:** April 13, 2021

**Article in press:** April 13, 2021

**Published online:** April 28, 2021

**P-Reviewer:** Endo S, Mishra TS, Panduro-Correa V, Toyoshima O

**S-Editor:** Gao CC

**L-Editor:** A

**P-Editor:** Liu JH



should be preferred over Billroth II reconstruction. The data obtained from this study will help surgeons when preoperatively informing their patients about expected functional outcomes after gastrectomy and enable them to ensure proper supportive care of their patients in the postoperative period.

**Key Words:** Gastric cancer; Quality of life; Roux-en-Y; Billroth II; Gastrectomy

©The Author(s) 2021. Published by Baishideng Publishing Group Inc. All rights reserved.

**Core Tip:** Quality of life assessment is an important tool to guide and evaluate treatment interventions, especially after a major surgery like gastrectomy. We conducted a cross-sectional survey among patients with gastric adenocarcinoma treated at our centre to provide insight into overall wellbeing after curative resection. The information provided will guide surgeons in selecting an optimal treatment approach and informing patients about expected treatment outcomes.

**Citation:** Grosek J, Zavrtanik H, Tomažič A. Health-related quality of life after curative resection for gastric adenocarcinoma. *World J Gastroenterol* 2021; 27(16): 1816-1827

**URL:** <https://www.wjgnet.com/1007-9327/full/v27/i16/1816.htm>

**DOI:** <https://dx.doi.org/10.3748/wjg.v27.i16.1816>

## INTRODUCTION

Gastrectomy is a major operation that alters the physiological functions of the digestive tract. Consequently, patients that undergo this treatment commonly experience a broad range of metabolic disorders, including malnutrition, weight loss and several postgastrectomy symptoms that negatively impact patients' wellbeing<sup>[1]</sup>. With modern gastrectomy techniques and other treatment modalities, survival in gastric cancer patients has improved and health-related quality of life (HRQoL) has become an important aspect when evaluating treatment outcomes<sup>[2]</sup>.

Various surgical procedures have been described for achieving oncological radicality in gastric cancer. In previous comparative studies, subtotal distal gastrectomy was associated with shorter operative duration, reduced postoperative complications and better recovery when compared to total gastrectomy<sup>[3-6]</sup>. On the other hand, total gastrectomy could still be performed safely with low morbidity while reducing the risk of inadequate safety margins or remnant carcinoma<sup>[7,8]</sup>. Following subtotal distal gastrectomy, there is no consensus regarding the best type of reconstruction<sup>[9,10]</sup>. Billroth II reconstruction is often performed due to its simplicity, but associated reflux gastritis and esophagitis have been the limiting concerns. Roux-en-Y reconstruction is a recommended alternative, but it can result in delayed gastric emptying, nausea, vomiting and abdominal pain<sup>[11]</sup>. Selection of the procedure is usually made based on tumour location, preoperative staging, the patient's general physical status and the surgeon's preference. In addition, quality of life assessment has become an increasingly important index for evaluating and selecting treatment interventions. Patient-reported measures regarding their physical and emotional state after treatment as opposed to objectively defined short-term perioperative outcomes should be taken into consideration to achieve optimal care.

We conducted a cross-sectional survey among patients with gastric adenocarcinoma treated at a tertiary referral centre to provide insight into overall wellbeing after curative resection. The European Organization for Research and Treatment of Cancer (EORTC) Quality of Life Core Questionnaire (QLQ-C30) and its gastric cancer-specific module (QLQ-STO-22) were used to assess HRQoL<sup>[12]</sup>. Its various aspects were compared among different surgical procedures.

## MATERIALS AND METHODS

### Patients

Patients with gastric cancer that underwent curative resection at the Ljubljana University Medical Centre between January 2014 and December 2018 were recruited for the study. Patients were eligible for inclusion if they were older than 18, had undergone curative subtotal distal or total gastrectomy for histologically confirmed adenocarcinoma, and had not undergone previous gastric surgery. We excluded patients that were deemed unable to answer the questionnaires, provided questionnaires with missing items that prevented final scoring, suffered from other gastrointestinal diseases (*e.g.*, chronic inflammatory bowel disease, exocrine pancreatic insufficiency or cholestasis) or other malignant diseases, had undergone emergency or palliative surgery, or had experienced disease recurrence. The study was approved by the National Medical Ethics Committee of Republic of Slovenia (No. 0120-315/2019/3; July 9, 2019). Patients that met the inclusion criteria and provided written informed consent were included for further analysis.

### Data collection

Data on the patients included demographics, comorbidities, American Society of Anesthesiologists score, tumour stage, type of resection, type of reconstruction, postoperative complications, hospital stay, histopathological characteristics of the tumour, cancer recurrence and possible (neo)adjuvant therapy and were collected from electronic patient records.

### Surgery

All patients underwent open gastrectomy, either subtotal distal or total, depending on the tumour location and preoperatively determined tumor-node-metastasis stage. Gastric adenocarcinoma was confirmed upon histopathological examination of the specimen.

After total gastrectomy, reconstruction was performed with Roux-en-Y esophagojejunostomy in all cases. After subtotal distal gastrectomy, either a Billroth II or Roux-en-Y anastomosis was constructed. Braun enteroenterostomy was routinely performed in all cases of Billroth II gastrojejunostomy. Billroth I reconstruction was not performed in our patient cohort due to the surgeon's preference and lack of early-stage gastric cancer.

### HRQoL assessment

To assess postoperative HRQoL of our patient cohort, the validated Slovenian versions of the EORTC QLQ-C30 (version 0.3) and QLQ-STO-22 were used<sup>[12]</sup>.

The EORTC QLQ-C30 questionnaire consists of 30 questions divided into five functional scales (physical, role, cognitive, emotional and social), three symptom scales (fatigue, pain, and nausea and vomiting), the global health status/quality of life scale and six single items to report other complaints (dyspnoea, loss of appetite, insomnia, constipation, diarrhoea and financial difficulties).

The EORTC QLQ-STO22 is a gastric cancer-specific module to assess HRQoL of patients with adenocarcinoma of the stomach. It comprises 22 questions divided into five multi-item scales (dysphagia, chest and abdominal pain, reflux, eating restrictions and anxieties) and four single items (dry mouth, taste problems, body image and hair loss).

A study description with an informed consent form plus the EORTC QLQ-C30 and EORTC QLQ-STO-22 questionnaires were sent to the patients for self-completion.

All completed questionnaires were scored and linearly transformed to a 0-100 scale according to the EORTC QLQ-C30 Scoring Manual<sup>[13]</sup>. On the functional scale higher scores represent better functioning, whereas on the symptom scale higher scores indicate higher symptom burden. Missing values were processed as follows: if at least half of the items from the scale were answered, the missing items were assumed to have values equal to the average of the completed items on the scale.

HRQoL was compared between patients after subtotal distal *vs* total gastrectomy and between patients after subtotal distal gastrectomy with Billroth II *vs* Roux-en-Y reconstruction.

### Statistical analysis

Means with standard deviation as well as medians with interquartile ranges of EORTC QLQ-C30 and EORTC QLQ-STO-22 scores were obtained. The Shapiro-Wilk test was used to test the normal distribution of the data.

The time that elapsed from surgery to completion of the questionnaires was compared among different surgical procedures using the Kruskal-Wallis test and Mann-Whitney *U* test.

Scores of EORTC QLQ-C30 and EORTC QLQ-STO-22 of patients after subtotal distal *vs* total gastrectomy and Billroth II *vs* Roux-en-Y reconstruction were compared with the Mann-Whitney *U* test.

To assess the correlation between the type of operation and general health status adjusted for some demographic and clinical characteristics of patients, multiple linear regression was used. The assumptions of absence of multicollinearity (assessed by variance inflation factor), normal distribution of the residuals and homoscedasticity were met.

A double-sided *P* value of  $< 0.05$  was considered statistically significant. All statistical analyses were performed using SPSS 27.0 (IBM Corporation, Armonk, NY, United States).

## RESULTS

### Patients

Invitations for study participation were sent to 234 patients. A total of 116 (49.6%) patients that provided informed consent with completed questionnaires were further analyzed. There were 63 men and 53 women 44 to 88 years old. Ten questionnaires had missing items. In six questionnaires, only one item was missing. In four questionnaires, there were two missing items, which were not part of the same scale.

The time that elapsed from surgery to completion of the questionnaires is shown in [Table 1](#) and was not statistically different among different surgical procedures ( $P = 0.161$ ).

Respondents and non-respondents did not differ significantly according to sex, type of gastric resection, type of reconstructive procedure and postoperative complications. Respondents were younger ( $P = 0.016$ ) and had a significantly less advanced disease stage ( $P = 0.001$ ). The baseline characteristics of patients eligible for inclusion are presented in [Table 2](#).

### EORTC QLQ-C30 questionnaire evaluation

**Patients after total *vs* subtotal distal gastrectomy:** No statistically significant differences were observed in HRQoL of patients after total gastrectomy when compared to patients after subtotal distal gastrectomy. The details are shown in [Table 3](#).

**Patients after subtotal distal gastrectomy with Billroth II *vs* Roux-en-Y reconstruction:** HRQoL of patients after subtotal distal gastrectomy with Billroth II reconstruction was significantly lower on the physical ( $P = 0.038$ ) and role functioning ( $P = 0.034$ ) scale when compared to patients with Roux-en-Y reconstruction. Patients with Billroth II reconstruction also reported more pain ( $P = 0.01$ ) and fatigue ( $P = 0.028$ ). No differences were observed between the two groups in global health status/quality of life scores ( $P = 0.635$ ). The details are summarized in [Table 4](#).

Reported scores on different functional scales and the global health status/quality of life scale among various surgical procedures are presented in [Figure 1](#). Patients after subtotal distal gastrectomy with Roux-en-Y reconstruction scored highest on cognitive, role functioning and physical scales when compared to patients after total gastrectomy or subtotal distal gastrectomy with Billroth II reconstruction.

**Quality of life and type of surgery:** The type of surgery was significantly associated with the stage of the disease ( $P = 0.002$ ) ([Table 5](#)). Patients with stage III gastric adenocarcinoma underwent either total gastrectomy (43.9%) or subtotal distal gastrectomy with Billroth II reconstruction (41.3%) rather than Roux-en-Y reconstruction (22.2%).

When adjusted for demographic data, disease stage and postoperative complications in a multiple linear regression model, no statistically significant differences in the global health status/quality of life scale were observed among different surgical procedures. Global health status/quality of life scores were significantly negatively associated with disease stage ( $\beta = -0.21$ ,  $P = 0.029$ ; [Table 6](#)).

Patients with Roux-en-Y reconstruction had significantly higher scores on the emotional ( $\beta = 0.24$ ,  $P = 0.041$ ), role functioning ( $\beta = 0.24$ ,  $P = 0.034$ ) and physical scale ( $\beta = 0.23$ ,  $P = 0.048$ ) when compared to patients after Billroth II reconstruction, even

**Table 1** The time elapsed from surgery to completion of the questionnaires among different surgical procedures

	Median (IQR), yr
Total gastrectomy	3 (2-4)
Subtotal distal gastrectomy	3 (2-4)
Billroth II reconstruction	3 (1-4)
Roux-en-Y reconstruction	2.5 (1-4)

The difference among total gastrectomy, subtotal distal gastrectomy with Billroth II reconstruction and Roux-en-Y reconstruction was not statistically significant ( $P = 0.161$ , Kruskal-Wallis test), nor was the difference among total and subtotal distal gastrectomy ( $P = 0.056$ , Mann-Whitney  $U$  test). IQR: Interquartile range.

**Table 2** Baseline characteristics of patients eligible for inclusion ( $n = 234$ )

	Respondents ( $n = 116$ )	Non-respondents ( $n = 118$ )	$P$ value
Gender, $n$ (%)			0.192
Male	63 (54.3)	74 (62.7)	
Female	53 (45.7)	44 (37.3)	
Age at surgery (yr, median, IQR)	66 (58-74)	72 (63-78)	0.016
Performed procedure, $n$ (%)			0.299
Total gastrectomy	43 (37.1)	55 (46.6)	
Distal-Billroth II	26 (22.4)	20 (16.9)	
Distal-Roux-Y	47 (40.5)	43 (36.4)	
Postoperative complications, $n$ (%)			
Yes	28 (24.1)	38 (32.2)	0.170
TNM stage, $n$ (%)			0.001
0	3 (2.6)	4 (3.4)	
I	52 (44.8)	25 (21.2)	
II	32 (27.6)	36 (30.5)	
III	29 (25.0)	53 (44.9)	

IQR: Interquartile range; TNM: Tumor-node-metastasis.

when adjusted for other variables in a regression model (Table 7).

### **EORTC QLQ STO-22 questionnaire evaluation**

**Patients after total vs subtotal distal gastrectomy:** Patients after total gastrectomy reported more dysphagia ( $P = 0.020$ ) and eating restrictions ( $P = 0.017$ ) when compared to patients after subtotal distal gastrectomy. No differences were found in other scales of the EORTC QLQ STO-22 questionnaire (Table 8).

**Patients after subtotal distal gastrectomy with Billroth II vs Roux-en-Y reconstruction:** Patients after subtotal distal gastrectomy with Billroth II reconstruction reported more problems with reflux when compared to patients with Roux-en-Y reconstruction. No differences were found in other scales of the EORTC QLQ STO-22 questionnaire (Table 9).

## **DISCUSSION**

The results of this cross-sectional survey show that the type of gastric resection influences different aspects of HRQoL. Patients after total vs subtotal gastrectomy had similar functional scores, but the former experienced more dysphagia and eating



**Table 3 European Organization for Research and Treatment of Cancer Quality of Life Core Questionnaire (QLQ-C30) questionnaire scores by the type of resection (Mann-Whitney *U* test)**

	Subtotal gastrectomy (n = 73)		Total gastrectomy (n = 43)		P value
	mean (SD)	Median (IQR)	mean (SD)	Median (IQR)	
Functional scales					
Physical functioning	79.9 (21.4)	87 (67-100)	80.3 (19.5)	87 (73-100)	0.954
Role functioning	80.2 (26.7)	100 (67-100)	77.9 (26.1)	83 (67-100)	0.509
Cognitive functioning	81.9 (21.6)	83 (67-100)	82.9 (19.7)	83 (67-100)	0.842
Emotional functioning	82.1 (20.5)	92 (75-100)	76.1 (21.5)	79 (58-96)	0.116
Social functioning	81.5 (22.5)	83 (67-100)	73.7 (26)	83 (50-100)	0.115
Symptoms					
Dyspnoea	10.5 (22.1)	0 (0-0)	10.8 (21.5)	0 (0-0)	0.869
Insomnia	28.7 (29.1)	33 (0-33)	27.8 (28.1)	33 (0-33)	0.917
Appetite loss	10 (19.7)	0 (0-0)	12.3 (20.6)	0 (0-33)	0.489
Nausea/vomiting	10.7 (17.4)	0 (0-17)	4.7 (9.8)	0 (0-0)	0.079
Constipation	10.5 (22.1)	0 (0-0)	6.9 (13.6)	0 (0-0)	0.665
Diarrhoea	13.6 (22.7)	0 (0-33)	19.3 (24.4)	0 (0-33)	0.141
Fatigue	30.5 (23.3)	22 (17-33)	34.2 (23.4)	33 (22-50)	0.263
Pain	18.3 (22.4)	17 (0-33)	17.9 (21.6)	17 (0-33)	0.906
Financial problems	16.4 (26.7)	0 (0-33)	27.1 (32.8)	0 (0-67)	0.069
Global health status	66.6 (22.9)	67 (50-83)	67.4 (19.9)	67 (58-83)	0.846

IQR: Interquartile range; SD: Standard deviation.

restrictions. At the same time, patients after subtotal gastrectomy with Billroth II (compared to Roux-en-Y) reconstruction reported worse physical and role functioning scores and complained of symptoms such as pain, fatigue and reflux. However, these differences appear to be clinically less relevant because similar global health scores were reported by patients after different surgical procedures. The information provided should guide the surgeon on the optimal treatment approach after considering oncological feasibility of the technique. Moreover, it should be used to inform patients about expected functional sequelae.

Previous studies evaluated longitudinal changes of HRQoL after gastrectomy for gastric cancer and used preoperative scores as a reference<sup>[14-21]</sup>. However, these scores are highly influenced by circumstances surrounding the diagnosis as well as symptoms associated with the disease itself, such as nausea and vomiting, dysphagia, postprandial fullness, loss of appetite, fatigue due to anaemia and so on, resulting in worse HRQoL<sup>[16,17]</sup>. In their multicentre study, Brenkman *et al*<sup>[22]</sup> compared EORTC QLQ-C30 scores of patients after gastrectomy to a Dutch reference population and concluded that global HRQoL is more or less comparable between the two cohorts despite patients' worse scores on several functional and symptom scales. Similarly, Lee *et al*<sup>[23,24]</sup> found no significant difference in global HRQoL between patients more than 5 years after surgery for gastric cancer and healthy volunteers awaiting a routine screening exam.

A limited number of studies focused on HRQoL after various surgical procedures<sup>[5,11,15,16,18,20]</sup>. Hence, we opted to conduct a cross-sectional analysis to compare HRQoL after various types of gastric resection and to evaluate the actual life quality deviation caused by surgical treatment. Based on our results, the type of reconstruction appeared to have a greater effect on HRQoL than the extent of gastric resection, which is somehow unexpected. Our data show that proximal gastric preservation has marginal advantages for improving patients' quality of life by reducing dysphagia and eating restrictions postoperatively whereas no differences in daily functioning were found. In line with our finding, subtotal distal gastrectomy was generally better tolerated in several previous studies, especially due to a higher

**Table 4 European Organization for Research and Treatment of Cancer Quality of Life Core Questionnaire (QLQ-C30) questionnaire scores by the type of reconstruction (Mann-Whitney *U* test)**

	Billroth II ( <i>n</i> = 26)		Roux-Y ( <i>n</i> = 47)		<i>P</i> value
	mean (SD)	Median (IQR)	mean (SD)	Median (IQR)	
Functional scales					
Physical functioning	73.1 (23)	73.5 (53-93)	83.7 (19.6)	92 (73-100)	0.038
Role functioning	70.5 (31.4)	67 (50-100)	85.5 (22.4)	100 (67-100)	0.034
Cognitive functioning	76.9 (26.3)	83 (67-100)	84.7 (18.3)	83 (83-100)	0.301
Emotional functioning	74.9 (27.7)	83 (58-100)	86 (14)	92 (75-100)	0.220
Social functioning	79.5 (25.9)	83 (67-100)	82.6 (20.5)	83 (67-100)	0.792
Symptoms					
Dyspnoea	16.7 (30.3)	0 (0-33)	7 (15.4)	0 (0-0)	0.285
Insomnia	37.1 (33.2)	33 (0-67)	24 (25.8)	33 (0-33)	0.102
Appetite loss	12.8 (25.1)	0 (0-33)	8.4 (16.2)	0 (0-0)	0.651
Nausea/vomiting	15.4 (22.1)	0 (0-33)	8.1 (13.8)	0 (0-17)	0.194
Constipation	19.2 (31.5)	0 (0-33)	5.6 (12.5)	0 (0-0)	0.054
Diarrhoea	14.1 (31.6)	0 (0-0)	13.3 (16.4)	0 (0-33)	0.200
Fatigue	41 (28.6)	33 (22-67)	24.6 (17.5)	22 (17-33)	0.028
Pain	28.9 (28.1)	17 (0-50)	12.4 (16.1)	0 (0-17)	0.010
Financial problems	19.2 (28.6)	0 (0-33)	14.8 (25.8)	0 (0-33)	0.510
Global health status	68.2 (24.7)	67 (50-83)	65.7 (22)	67 (50-83)	0.635

IQR: Inter-quartile range; SD: Standard deviation.

**Table 5 Surgery type among different stages of the disease**

	Total gastrectomy, <i>n</i> (%)	Subtotal-Billroth II, <i>n</i> (%)	Subtotal-Roux-Y, <i>n</i> (%)	<i>P</i> value
Stage				0.002
0	4 (4.1)	3 (6.5)	0 (0)	
I	25 (25.5)	14 (30.4)	38 (42.2)	
II	26 (26.5)	10 (21.7)	32 (35.6)	
III	43 (43.9)	19 (41.3)	20 (22.2)	

symptom burden reported with total gastrectomy such as nausea and vomiting, dysphagia, eating restrictions and reflux<sup>[16,21]</sup>. In subtotal gastrectomy, gastric physiology is at least partly preserved, possibly leading to superior HRQoL. However, several studies found no difference in global HRQoL between the two groups<sup>[5,15,18,25]</sup>. A possible explanation for this finding is the time interval from the surgical procedure. HRQoL changes over time are well documented. In longitudinal analyses, significantly worse scores on almost all HRQoL scales were observed 1 mo to 6 mo postoperatively compared to the preoperative scores<sup>[14-17,20]</sup>. Several functional scales recovered to the baseline by 1 year after surgery, however, symptoms such as nausea and vomiting, reflux and eating restrictions persisted even 5 years after surgery<sup>[19,23,24]</sup>. In a long-term analysis by Lee *et al*<sup>[25]</sup>, HRQoL inferiority of patients after total gastrectomy when compared to subtotal distal gastrectomy generally disappeared beyond 5 years postoperatively, remaining inferior only in eating restrictions. In our study, the median time interval from the surgery to the completion of the questionnaires was 3 years, possibly diminishing some differences between the two groups.

Regarding the type of digestive tract reconstruction after subtotal distal gastrectomy, the choice of the technique is often driven by the surgeon's preferences,

**Table 6 Association between surgery type and global health status scores adjusted for demographic and clinical characteristics**

	$\beta$ (P value)
Male	-0.11 (0.229)
Age (yr)	-0.05 (0.625)
Total <i>vs</i> Billroth II	-0.001 (0.990)
Roux-Y <i>vs</i> Billroth II	-0.08 (0.492)
Postoperative complications-yes	-0.15 (0.116)
Stage II/III <i>vs</i> 0/I	-0.21 (0.029)

$\beta$ : Standardized regression coefficient.

**Table 7 Association between surgery type and scores on functional scales adjusted for demographic and clinical characteristics**

	Emotional		Social		Role		Physical		Cognitive	
	$\beta$	P value	$\beta$	P value	$\beta$	P value	$\beta$	P value	$\beta$	P value
Male	0.01	0.901	0.10	0.254	0.09	0.334	0.16	0.089	0.04	0.666
Age (yr)	0.09	0.343	0.05	0.557	0.08	0.379	-0.09	0.343	0.18	0.054
Total <i>vs</i> Billroth II	0.04	0.729	-0.11	0.343	0.15	0.199	0.15	0.201	0.16	0.194
Roux-Y <i>vs</i> Billroth II	0.24	0.041	0.04	0.763	0.24	0.034	0.23	0.048	0.17	0.154
Postoperative complications yes	-0.03	0.730	-0.13	0.150	-0.15	0.101	-0.10	0.292	0.01	0.915
Saage II/III <i>vs</i> 0/I	-0.17	0.062	-0.20	0.031	-0.27	0.003	-0.16	0.079	-0.09	0.324

$\beta$ : Standardized regression coefficient.

**Table 8 European Organization for Research and Treatment of Cancer Quality of Life Core Questionnaire gastric cancer-specific module (QLQ STO-22) questionnaire scores by the type of resection (Mann-Whitney U test)**

	Subtotal gastrectomy (n = 60)		Total gastrectomy (n = 51)		P value
	mean (SD)	Median (IQR)	mean (SD)	Median (IQR)	
Dysphagia	11.1 (15.8)	11 (0-11)	17.2 (17.1)	11 (0-33)	0.020
Pain	19.7 (17.9)	17 (8-33)	23.3 (20.9)	17 (8-33)	0.477
Reflux	16 (20.9)	11 (0-22)	22.7 (23.6)	11 (0-44)	0.089
Eating restrictions	14.7 (17.4)	8 (0-17)	21.6 (18.2)	17 (8-33)	0.017
Anxiety	33.1 (23.4)	33 (17-44)	31.4 (25.8)	22 (11-44)	0.591
Dry mouth	24.1 (28.5)	33 (0-33)	24.7 (28.3)	33 (0-33)	0.871
Taste	6.4 (18.1)	0 (0-0)	11.6 (21.7)	0 (0-33)	0.109
Body image	18.7 (29.9)	0 (0-33)	20.1 (27.4)	0 (0-33)	0.567
Hair loss	16.4 (27.9)	0 (0-33)	8.7 (20.9)	0 (0-0)	0.124

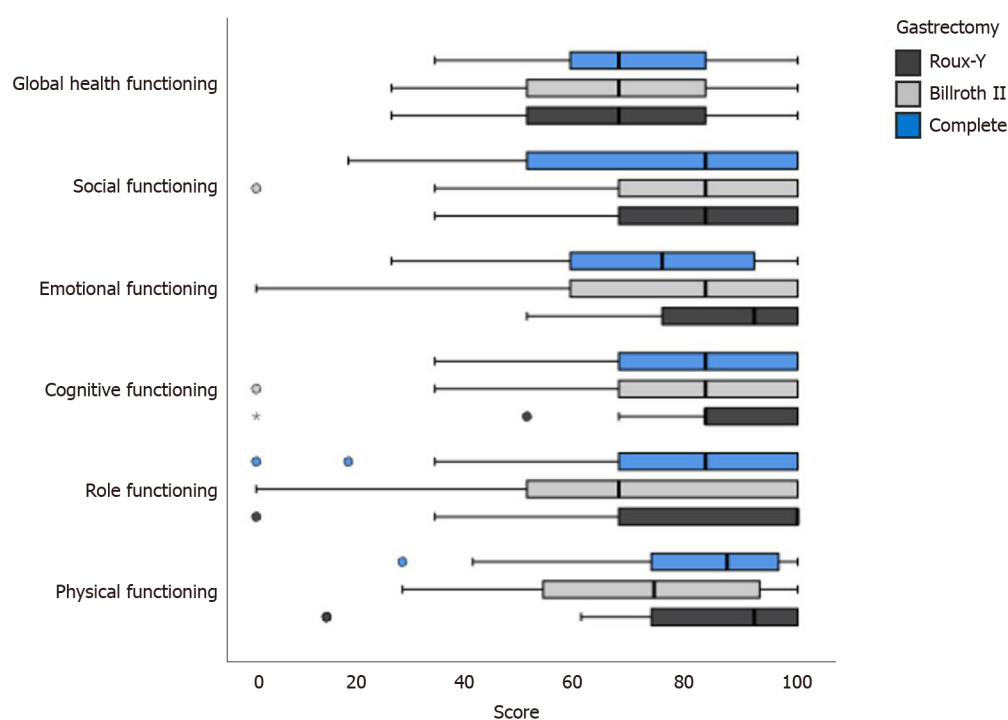
IQR: Interquartile range; SD: Standard deviation.

and no clear recommendations exist in the current literature<sup>[9-11]</sup>. Several studies suggested Roux-en-Y reconstruction to be superior to Billroth II reconstruction in terms of preventing bile reflux and remnant gastritis, thus allowing better quality of life<sup>[10,26-28]</sup>. However, in a proportion of patients, Roux-en-Y may be associated with a Roux stasis syndrome causing delayed gastric emptying with postprandial pain, nausea and vomiting<sup>[29,30]</sup>. Our results are partly in line with previous studies reporting reduced HRQoL following Billroth II *vs* Roux-en-Y reconstruction<sup>[10,26-28]</sup>. Patients after

**Table 9 European Organization for Research and Treatment of Cancer Quality of Life Core Questionnaire gastric cancer-specific module (QLQ STO-22) questionnaire scores by the type of reconstruction (Mann-Whitney *U* test)**

	Billroth II ( <i>n</i> = 18)		Roux-Y ( <i>n</i> = 42)		<i>P</i> value
	mean (SD)	Median (IQR)	mean (SD)	Median (IQR)	
Dysphagia	15.8 (22.3)	5.5 (0-22)	8.5 (10.2)	11 (0-11)	0.526
Pain	24.3 (23.9)	17 (8-33)	17.2 (13.3)	17 (8-25)	0.471
Reflux	28.5 (26.3)	22 (0-44)	9.1 (13)	0 (0-11)	0.001
Eating restrictions	22.3 (22.8)	17 (0-42)	10.4 (11.7)	8 (0-17)	0.069
Anxiety	36.6 (26.9)	33 (22-55)	31.2 (21.3)	33 (11-44)	0.541
Dry mouth	23 (26.3)	33 (0-33)	24.7 (29.9)	0 (0-33)	0.965
Taste	11.5 (26.6)	0 (0-0)	3.5 (10.3)	0 (0-0)	0.247
Body image	26.8 (36.5)	0 (0-33)	14.1 (24.8)	0 (0-33)	0.127
Hair loss	14.1 (27)	0 (0-33)	17.7 (28.6)	0 (0-33)	0.541

IQR: Inter-quartile range; SD: Standard deviation.

**Figure 1** Median scores with interquartile ranges of functional scales and global health status/quality of life scale based on the type of surgery.

Billroth II reconstruction scored lower on some of the functional scales and reported more pain, fatigue and reflux symptoms. This occurred despite routine construction of Braun anastomosis, which supposedly diverts bile from the remnant stomach, relieving reflux symptoms, dumping syndrome or other disturbances in food intake<sup>[31]</sup>. Although patients after Billroth II reconstruction were more likely to have a higher disease stage than those after Roux-en-Y reconstruction, statistically significant superiority of the Roux-en-Y procedure on the emotional, role and physical functioning scale remained after adjustment for demographic data, disease stage and postoperative complications.

### Study limitations

This study has some limitations. First, the cross-sectional nature does not allow

longitudinal assessment of HRQoL. Nonetheless, we believe this kind of design allows us to gain important insight into the overall HRQoL of patients following gastrectomy, which represents the basis for clinical decision making. Second, the number of participating patients is relatively low (116), representing 49.6% of patients that were eligible for study inclusion. Third, mail surveys lack data related to the actual health status of the patient. We did not see the patients to obtain their health status objectively; therefore, their subjective measures could not be compared to their actual physical findings. Nonetheless, HRQoL is a multimodal construct of physical, psychological and social wellbeing in relation to disease treatment. Therefore, objective and subjective measures are not necessarily related. Even if a patient is objectively well, he or she may at the same time be subjectively unwell, which should be addressed separately from objective measures.

## CONCLUSION

Our study shows that patients after gastrectomy for gastric cancer experience several functional and symptom complaints affecting quality of life. Based on our results, with regard to HRQoL, subtotal distal gastrectomy with Roux-en-Y reconstruction should be preferred over subtotal distal gastrectomy with Billroth II reconstruction. Patients should be informed preoperatively about expected functional sequelae after surgery and should be regularly monitored postoperatively to ensure proper symptomatic and supportive care.

## ARTICLE HIGHLIGHTS

### **Research background**

Gastrectomy is a major operation that alters the physiological functions of the digestive tract. Consequently, these patients experience malnutrition, weight loss and several postgastrectomy symptoms that negatively impact patients' wellbeing.

### **Research motivation**

With improved survival in gastric cancer patients, health-related quality of life has become an important clinical endpoint alongside oncological outcomes.

### **Research objectives**

The aim of this study was to investigate health-related quality of life after various surgical procedures for gastric cancer treatment.

### **Research methods**

Patients that underwent curative resection for gastric adenocarcinoma at a tertiary centre between January 2014 and December 2018 were recruited for inclusion in this cross-sectional survey. The validated Slovenian version of the European Organization for Research and Treatment of Cancer Quality of Life Core Questionnaire (QLQ-C30) and its gastric cancer specific module (QLQ-STO-22) were sent to all eligible patients for self-completion. The scores of both questionnaires were compared between patients after subtotal distal *vs* total gastrectomy and patients after subtotal distal gastrectomy with Billroth II *vs* Roux-en-Y reconstruction using the Mann-Whitney *U* test. The association between the type of operation and general health status adjusted for some demographic and clinical characteristics was assessed with multiple linear regression.

### **Research results**

Out of 234 patients that were eligible for study inclusion, 116 (49.6%) patients completed the questionnaires. No statistically significant differences were observed in scores on global or functional scales among patients after total or subtotal distal gastrectomy. However, patients after total *vs* subtotal gastrectomy did experience more dysphagia ( $P = 0.020$ ) and eating restrictions ( $P = 0.017$ ). Patients after subtotal distal gastrectomy with Billroth II reconstruction reported significantly worse scores on the physical ( $P = 0.038$ ) and role functioning ( $P = 0.034$ ) scales and had more problems with pain ( $P = 0.010$ ), fatigue ( $P = 0.028$ ) and reflux ( $P = 0.001$ ). When adjusted for demographic data, disease stage and postoperative complications, no



differences were observed in reported global health status/quality of life scores among different surgical procedures. However, Roux-en-Y was superior over Billroth II reconstruction in emotional ( $\beta = 0.24$ ,  $P = 0.041$ ), role ( $\beta = 0.24$ ,  $P = 0.034$ ) and physical ( $\beta = 0.23$ ,  $P = 0.048$ ) functioning when adjusted for other variables in a regression model.

### Research conclusions

Patients after gastrectomy for gastric cancer experience several functional and symptom complaints. Based on our results, subtotal distal gastrectomy with Roux-en-Y reconstruction should be preferred over subtotal distal gastrectomy with Billroth II reconstruction.

### Research perspectives

The data obtained from this study will help surgeons when preoperatively informing their patients about expected functional outcomes after gastrectomy and enable them to ensure proper supportive care for their patients in the postoperative period.

## REFERENCES

- 1 **Davis JL**, Ripley RT. Postgastrectomy Syndromes and Nutritional Considerations Following Gastric Surgery. *Surg Clin North Am* 2017; **97**: 277-293 [PMID: [28325187](#) DOI: [10.1016/j.suc.2016.11.005](#)]
- 2 **van den Boorn HG**, Stroes CI, Zwinderman AH, Eshuis WJ, Hulshof MCCM, van Etten-Jamaludin FS, Sprangers MAG, van Laarhoven HWM. Health-related quality of life in curatively-treated patients with esophageal or gastric cancer: A systematic review and meta-analysis. *Crit Rev Oncol Hematol* 2020; **154**: 103069 [PMID: [32818901](#) DOI: [10.1016/j.critrevonc.2020.103069](#)]
- 3 **Ji X**, Yan Y, Bu ZD, Li ZY, Wu AW, Zhang LH, Wu XJ, Zong XL, Li SX, Shan F, Jia ZY, Ji JF. The optimal extent of gastrectomy for middle-third gastric cancer: distal subtotal gastrectomy is superior to total gastrectomy in short-term effect without sacrificing long-term survival. *BMC Cancer* 2017; **17**: 345 [PMID: [28526077](#) DOI: [10.1186/s12885-017-3343-0](#)]
- 4 **Kong L**, Yang N, Shi L, Zhao G, Wang M, Zhang Y. Total vs subtotal gastrectomy for distal gastric cancer: meta-analysis of randomized clinical trials. *Onco Targets Ther* 2016; **9**: 6795-6800 [PMID: [27853375](#) DOI: [10.2147/OTT.S110828](#)]
- 5 **Goh YM**, Gillespie C, Couper G, Paterson-Brown S. Quality of life after total and subtotal gastrectomy for gastric carcinoma. *Surgeon* 2015; **13**: 267-270 [PMID: [25127442](#) DOI: [10.1016/j.surge.2014.07.002](#)]
- 6 **Ahmad R**, Schmidt BH, Rattner DW, Mullen JT. Factors influencing readmission after curative gastrectomy for gastric cancer. *J Am Coll Surg* 2014; **218**: 1215-1222 [PMID: [24680567](#) DOI: [10.1016/j.jamcollsurg.2014.02.015](#)]
- 7 **Tran TB**, Hatzaras I, Worhunsky DJ, Vitiello GA, Squires MH 3rd, Jin LX, Spolverato G, Votanopoulos KI, Schmidt C, Weber S, Bloomston M, Cho CS, Levine EA, Fields RC, Pawlik TM, Maithel SK, Norton JA, Poultsides GA. Gastric remnant cancer: A distinct entity or simply another proximal gastric cancer? *J Surg Oncol* 2015; **112**: 877-882 [PMID: [26511335](#) DOI: [10.1002/jso.24080](#)]
- 8 **Hanyu T**, Wakai A, Ishikawa T, Ichikawa H, Kameyama H, Wakai T. Carcinoma in the Remnant Stomach During Long-Term Follow-up After Distal Gastrectomy for Gastric Cancer: Analysis of Cumulative Incidence and Associated Risk Factors. *World J Surg* 2018; **42**: 782-787 [PMID: [28924721](#) DOI: [10.1007/s00268-017-4227-9](#)]
- 9 **Tran TB**, Worhunsky DJ, Squires MH, Jin LX, Spolverato G, Votanopoulos KI, Cho CS, Weber SM, Schmidt C, Levine EA, Bloomston M, Fields RC, Pawlik TM, Maithel SK, Norton JA, Poultsides GA. To Roux or not to Roux: a comparison between Roux-en-Y and Billroth II reconstruction following partial gastrectomy for gastric cancer. *Gastric Cancer* 2016; **19**: 994-1001 [PMID: [26400843](#) DOI: [10.1007/s10120-015-0547-3](#)]
- 10 **He L**, Zhao Y. Is Roux-en-Y or Billroth-II reconstruction the preferred choice for gastric cancer patients undergoing distal gastrectomy when Billroth I reconstruction is not applicable? *Medicine (Baltimore)* 2019; **98**: e17093 [PMID: [31770192](#) DOI: [10.1097/MD.00000000000017093](#)]
- 11 **So JB**, Rao J, Wong AS, Chan YH, Pang NQ, Tay AYL, Yung MY, Su Z, Phua JNS, Shabbir A, Ng EKW. Roux-en-Y or Billroth II Reconstruction After Radical Distal Gastrectomy for Gastric Cancer: A Multicenter Randomized Controlled Trial. *Ann Surg* 2018; **267**: 236-242 [PMID: [28383294](#) DOI: [10.1097/SLA.0000000000002229](#)]
- 12 **Aaronson NK**, Ahmedzai S, Bergman B, Bullinger M, Cull A, Duez NJ, Filiberti A, Flechtner H, Fleishman SB, de Haes JC. The European Organization for Research and Treatment of Cancer QLQ-C30: a quality-of-life instrument for use in international clinical trials in oncology. *J Natl Cancer Inst* 1993; **85**: 365-376 [PMID: [8433390](#) DOI: [10.1093/jnci/85.5.365](#)]
- 13 **Fayers P**, Aaronson NK, Bjordal K, Groenvold M, Curran D, Bottomley A. EORTC QLQ-C30 Scoring Manual. 3rd ed. Brussels: European Organization for Research and Treatment of Cancer, 2001

- 14 Avery K, Hughes R, McNair A, Alderson D, Barham P, Blazeby J. Health-related quality of life and survival in the 2 years after surgery for gastric cancer. *Eur J Surg Oncol* 2010; **36**: 148-154 [PMID: 19836921 DOI: 10.1016/j.ejso.2009.09.008]
- 15 Karanickolas PJ, Graham D, Gönen M, Strong VE, Brennan MF, Coit DG. Quality of life after gastrectomy for adenocarcinoma: a prospective cohort study. *Ann Surg* 2013; **257**: 1039-1046 [PMID: 23665970 DOI: 10.1097/SLA.0b013e31828c4a19]
- 16 Kim AR, Cho J, Hsu YJ, Choi MG, Noh JH, Sohn TS, Bae JM, Yun YH, Kim S. Changes of quality of life in gastric cancer patients after curative resection: a longitudinal cohort study in Korea. *Ann Surg* 2012; **256**: 1008-1013 [PMID: 23154395 DOI: 10.1097/SLA.0b013e31827661c9]
- 17 Kong H, Kwon OK, Yu W. Changes of quality of life after gastric cancer surgery. *J Gastric Cancer* 2012; **12**: 194-200 [PMID: 23094232 DOI: 10.5230/jgc.2012.12.3.194]
- 18 Park S, Chung HY, Lee SS, Kwon O, Yu W. Serial comparisons of quality of life after distal subtotal or total gastrectomy: what are the rational approaches for quality of life management? *J Gastric Cancer* 2014; **14**: 32-38 [PMID: 24765535 DOI: 10.5230/jgc.2014.14.1.32]
- 19 Yu W, Park KB, Chung HY, Kwon OK, Lee SS. Chronological Changes of Quality of Life in Long-Term Survivors after Gastrectomy for Gastric Cancer. *Cancer Res Treat* 2016; **48**: 1030-1036 [PMID: 27004956 DOI: 10.4143/crt.2015.398]
- 20 Kobayashi D, Kodera Y, Fujiwara M, Koike M, Nakayama G, Nakao A. Assessment of quality of life after gastrectomy using EORTC QLQ-C30 and STO22. *World J Surg* 2011; **35**: 357-364 [PMID: 21104250 DOI: 10.1007/s00268-010-0860-2]
- 21 Kwon OK, Yu B, Park KB, Park JY, Lee SS, Chung HY. Advantages of Distal Subtotal Gastrectomy over Total Gastrectomy in the Quality of Life of Long-Term Gastric Cancer Survivors. *J Gastric Cancer* 2020; **20**: 176-189 [PMID: 32596001 DOI: 10.5230/jgc.2020.20.e17]
- 22 Brenkman HJF, Tegels JJW, Ruurda JP, Luyer MDP, Kouwenhoven EA, Draaisma WA, van der Peet DL, Wijnhoven BPL, Stoot JHMB, van Hillegersberg R; LOGICA Study Group. Factors influencing health-related quality of life after gastrectomy for cancer. *Gastric Cancer* 2018; **21**: 524-532 [PMID: 29067597 DOI: 10.1007/s10120-017-0771-0]
- 23 Lee SS, Chung HY, Yu W. Quality of life of long-term survivors after a distal subtotal gastrectomy. *Cancer Res Treat* 2010; **42**: 130-134 [PMID: 20948917 DOI: 10.4143/crt.2010.42.3.130]
- 24 Lee SS, Chung HY, Kwon OK, Yu W. Quality of life in cancer survivors 5 years or more after total gastrectomy: a case-control study. *Int J Surg* 2014; **12**: 700-705 [PMID: 24866069 DOI: 10.1016/j.ijsu.2014.05.067]
- 25 Lee SS, Chung HY, Kwon OK, Yu W. Long-term Quality of Life After Distal Subtotal and Total Gastrectomy: Symptom- and Behavior-oriented Consequences. *Ann Surg* 2016; **263**: 738-744 [PMID: 26501699 DOI: 10.1097/SLA.0000000000001481]
- 26 Rauser S, Mangano A, Galli F, Rovera F, Boni L, Dionigi G, Dionigi R. Quality of life after gastrectomy for cancer evaluated via the EORTC QLQ-C30 and QLQ-STO22 questionnaires: surgical considerations from the analysis of 103 patients. *Int J Surg* 2013; **11** Suppl 1: S104-S109 [PMID: 24380539 DOI: 10.1016/S1743-9191(13)60028-X]
- 27 Cai Z, Zhou Y, Wang C, Yin Y, Shen C, Yin X, Chen Z, Zhang B. Optimal reconstruction methods after distal gastrectomy for gastric cancer: A systematic review and network meta-analysis. *Medicine (Baltimore)* 2018; **97**: e10823 [PMID: 29768387 DOI: 10.1097/MD.00000000000010823]
- 28 Lee MS, Ahn SH, Lee JH, Park DJ, Lee HJ, Kim HH, Yang HK, Kim N, Lee WW. What is the best reconstruction method after distal gastrectomy for gastric cancer? *Surg Endosc* 2012; **26**: 1539-1547 [PMID: 22179454 DOI: 10.1007/s00464-011-2064-8]
- 29 Hoya Y, Mitsumori N, Yanaga K. The advantages and disadvantages of a Roux-en-Y reconstruction after a distal gastrectomy for gastric cancer. *Surg Today* 2009; **39**: 647-651 [PMID: 19639429 DOI: 10.1007/s00595-009-3964-2]
- 30 Otsuka R, Natsume T, Maruyama T, Tanaka H, Matsuzaki H. Antecolic reconstruction is a predictor of the occurrence of roux stasis syndrome after distal gastrectomy. *J Gastrointest Surg* 2015; **19**: 821-824 [PMID: 25693423 DOI: 10.1007/s11605-015-2770-y]
- 31 Hwang HK, Lee SH, Han DH, Choi SH, Kang CM, Lee WJ. Impact of Braun anastomosis on reducing delayed gastric emptying following pancreaticoduodenectomy: a prospective, randomized controlled trial. *J Hepatobiliary Pancreat Sci* 2016; **23**: 364-372 [PMID: 27038406 DOI: 10.1002/jhbp.349]



## Surrogate markers of mucosal healing in inflammatory bowel disease: A systematic review

Monica State, Lucian Negreanu, Theodor Voiosu, Andrei Voiosu, Paul Balanescu, Radu Bogdan Mateescu

**ORCID number:** Monica State 0000-0003-4961-3476; Lucian Negreanu 0000-0003-3042-0754; Theodor Voiosu 0000-0003-3250-4900; Andrei Voiosu 0000-0001-8579-9314; Paul Balanescu 0000-0002-6000-1123; Radu Bogdan Mateescu 0000-0002-2607-8653.

**Author contributions:** State M, Balanescu P contributed to study design; State M, Voiosu T, Voiosu A and Balanescu P contributed to data acquisition, analysis and interpretation; State M, Voiosu T, Voiosu A, Negreanu L and Mateescu RB contributed to writing of this article; Negreanu L, State M and Mateescu RB contributed to editing, reviewing and final approval of the article.

**Conflict-of-interest statement:** The authors have no conflicts of interest to declare.

**PRISMA 2009 Checklist statement:** The authors have read the PRISMA 2009 Checklist, and the manuscript was prepared and revised according to the PRISMA 2009 Checklist.

**Open-Access:** This article is an open-access article that was selected by an in-house editor and fully peer-reviewed by external reviewers. It is distributed in accordance with the Creative Commons Attribution

**Monica State, Theodor Voiosu, Andrei Voiosu, Radu Bogdan Mateescu,** Department of Gastroenterology, Colentina Clinical Hospital, Bucharest 020125, Romania

**Lucian Negreanu,** Department of Gastroenterology, Emergency University Hospital, Bucharest 050098, Romania

**Lucian Negreanu, Theodor Voiosu, Andrei Voiosu, Paul Balanescu, Radu Bogdan Mateescu,** Carol Davila University of Medicine and Pharmacy, Bucharest 020021, Romania

**Paul Balanescu,** Department of Internal Medicine and Research Methodology, Colentina Clinical Hospital, Bucharest 020125, Romania

**Corresponding author:** Lucian Negreanu, MD, Assistant Professor, Department of Gastroenterology, Emergency University Hospital, Splaiul Independentei 169, Bucharest 050098, Romania. [negreanu\\_99@yahoo.com](mailto:negreanu_99@yahoo.com)

### Abstract

#### BACKGROUND

Mucosal healing (MH) has emerged as a key therapeutic target in inflammatory bowel disease (IBD), and achievement of this goal is documented by endoscopy with biopsy. However, colonoscopy is burdensome and invasive, and substitution with an accurate noninvasive biomarker is desirable.

#### AIM

To summarize published data regarding the performance of noninvasive biomarkers in assessing MH in IBD patients.

#### METHODS

We conducted a systematic review of studies that reported the performance of biomarkers in diagnosing MH in patients with IBD. The main outcome measure was to review the diagnostic accuracy of serum and fecal markers that showed promising utility in assessing MH.

#### RESULTS

We screened 1301 articles, retrieved 46 manuscripts and included 23 articles for full-text analysis. The majority of the included manuscripts referred to fecal markers (12/23), followed by circulatory markers (8/23); only 3/23 of the included manuscripts investigated combined markers (serum and/or fecal markers). Fecal calprotectin (FC) was the most investigated fecal marker for

NonCommercial (CC BY-NC 4.0) license, which permits others to distribute, remix, adapt, build upon this work non-commercially, and license their derivative works on different terms, provided the original work is properly cited and the use is non-commercial. See: <http://creativecommons.org/licenses/by-nc/4.0/>

**Manuscript source:** Invited manuscript

**Specialty type:** Gastroenterology and hepatology

**Country/Territory of origin:** Romania

**Peer-review report's scientific quality classification**

Grade A (Excellent): 0  
Grade B (Very good): B  
Grade C (Good): C  
Grade D (Fair): 0  
Grade E (Poor): 0

**Received:** January 27, 2021

**Peer-review started:** January 27, 2021

**First decision:** February 25, 2021

**Revised:** March 2, 2021

**Accepted:** April 7, 2021

**Article in press:** April 7, 2021

**Published online:** April 28, 2021

**P-Reviewer:** Chao X, Zhang Q

**S-Editor:** Gao CC

**L-Editor:** A

**P-Editor:** Liu JH



assessing MH. In ulcerative colitis, for cutoff levels ranging between 58 mcg/g and 490 mcg/g, the sensitivity was 89.7%-100% and the specificity was 62%-93.3%. For Crohn's disease, the cutoff levels of FC ranged from 71 mcg/g to 918 mcg/g (sensitivity 50%-95.9% and specificity 52.3%-100%). The best performance for a serum marker was observed for the endoscopic healing index, which showed a comparable accuracy to the measurement of FC and a higher accuracy than the measurement of serum C-reactive protein.

## CONCLUSION

Several promising biomarkers of MH are emerging but cannot yet substitute for endoscopy with biopsy due to issues with reproducibility and standardization.

**Key Words:** Inflammatory bowel disease; Ulcerative colitis; Crohn's disease; Biomarkers; Serum; Fecal; Mucosal healing

©The Author(s) 2021. Published by Baishideng Publishing Group Inc. All rights reserved.

**Core Tip:** Identification of performant biomarkers that can substitute for repeated and cumbersome invasive procedures is a priority. Although therapeutic success in both Crohn's disease and ulcerative colitis remains to be clearly defined, mucosal healing has been one of the main therapeutic targets stipulated by recent recommendations. In inflammatory bowel disease mucosal healing, several serum- and fecal-based markers have shown promising results; however, a multimarker may improve the diagnostic accuracy of any single independent biomarker.

**Citation:** State M, Negreanu L, Voiosu T, Voiosu A, Balanescu P, Mateescu RB. Surrogate markers of mucosal healing in inflammatory bowel disease: A systematic review. *World J Gastroenterol* 2021; 27(16): 1828-1840

**URL:** <https://www.wjgnet.com/1007-9327/full/v27/i16/1828.htm>

**DOI:** <https://dx.doi.org/10.3748/wjg.v27.i16.1828>

## INTRODUCTION

Endoscopic inspection plays a pivotal role in the diagnosis and monitoring of inflammatory bowel disease (IBD). According to current guidelines and recommendations, each individual patient is likely to undergo several endoscopic evaluations during the course of their disease, sometimes at relatively short intervals. Endoscopy is crucial to establish a diagnosis and to evaluate disease extent and severity. Endoscopic reassessment is recommended on a case-by-case basis in patients not responding to treatment or with frequent relapse and remains the gold standard for confirming the response to treatment<sup>[1]</sup>.

Although therapeutic success in both Crohn's disease (CD) and ulcerative colitis (UC) remains to be clearly defined, mucosal healing (MH) has been one of the main therapeutic targets stipulated by recent recommendations<sup>[2]</sup>. MH is associated with lower risks of relapse, hospitalization and surgery<sup>[3,4]</sup>. While there is currently no clear consensus regarding the definition of MH despite the many proposed scoring systems for endoscopic activity in IBD, most experts agree that a Mayo endoscopic subscore of 0 or 1 or a SES-CD (simple endoscopic score for CD) less than 3 constitutes an acceptable measure of MH, both of which have been widely used in recent clinical trials of UC and CD, respectively<sup>[5,6]</sup>.

Invasive procedures, such as colonoscopy, have a great impact on patients. Patients with IBD report significantly more embarrassment and burden from the bowel preparation phase and more pain during the colonoscopy<sup>[7]</sup>. Although the risk of complications related to colonoscopy in IBD patients is very low (< 1%), it is higher than that in other groups of patients<sup>[8,9]</sup> and involves significant costs<sup>[10]</sup>. Therefore, identifying reliable surrogate noninvasive markers for disease activity is desirable to reduce patient burden and costs.

In recent years, a wealth of publications regarding various noninvasive biomarkers in IBD have reported conflicting results on various clinical endpoints. The aim of this

systematic review was to evaluate published data regarding the diagnostic accuracy of biomarkers in assessing MH in IBD patients.

## MATERIALS AND METHODS

### Rationale

We conducted a systematic review of studies that reported on the accuracy of noninvasive biomarkers in diagnosing MH in patients with colonic IBD with the aim of identifying and assessing the diagnostic accuracy of these biomarkers. Neither imaging markers nor urine-based markers were included in this analysis. Studies investigating the role of C-reactive protein (CRP) in detecting MH were also not included, as a comprehensive analysis regarding this subject was recently published<sup>[11]</sup>. In this review, 30 eligible publications regarding CRP were included. CRP positively correlated with the endoscopic activity of the disease, yielding correlation coefficients from 0.29 to 0.63 for UC and from 0.31 to 0.71 for CD. At the time of this publication, no new data have emerged; thus, reanalysis of published data is unnecessary at this time.

### Literature search

A structured search was conducted on December 12, 2020 of the PubMed (MEDLINE) database. Our search terms included the following medical subject headings (Mesh) and text words: For IBD: inflammatory bowel disease, ulcerative colitis, Crohn's disease; For MH: mucosal healing, endoscopic remission, colonoscopy, sigmoidoscopy, remission induction; For biomarkers: biomarker, predict\*, clinical, laborator\*, serol\*, serum, fecal\*, feces, blood, cytokine\*. The entire search algorithm was the following: (((((((((((marker\*[tw])) OR (biomarker\*[tw])) OR ("Biomarkers"[Mesh])) OR (predict\*[tw])) OR (clinical[tw])) OR (laborator\*[tw])) OR (serol\* [tw])) OR ("Serum"[Mesh])) OR (fecal\* [tw])) OR ("Feces"[Mesh])) OR (blood [tw])) OR ("Blood"[Mesh])) OR (cytokine\* [tw])) OR ("Cytokines"[Mesh])) AND ("Colonoscopy"[Mesh Terms] OR "Sigmoidoscopy"[Mesh Terms] OR "Remission Induction"[Mesh Terms] OR ("mucosal"[Text])) OR "endoscopic remission"[Text Word])) AND ((((((inflammatory bowel disease [tw]) OR (ulcerative colitis [tw])) OR (Crohn's disease [tw])) OR ("Inflammatory Bowel Diseases"[Mesh])) OR ("Colitis, Ulcerative"[Mesh])) OR ("Crohn's Disease"[Mesh]))).

### Inclusion criteria

All manuscripts published from January 2010, with the full text version available online, either *via* open access or pay per view, were included in the screening process. To avoid potential bias related to the use of older generation endoscopes and to account for the evolving definition of "mucosal healing", we restricted our review to manuscripts published in the last 10 years.

### Exclusion criteria

Manuscripts concerning pediatric patients, veterinary studies, noncolonic CD, unspecified IBD, narrative reviews, case reports and research that did not include an endoscopic evaluation to confirm MH and a clear definition of MH were not included.

### Data extraction

These criteria were applied for the title screening process, followed by a full-text read of the filtered results. For all articles that met the criteria, using an a priori designed extraction form, two independent reviewers collected data regarding the type of study that was conducted, the investigated marker and its source (serum, feces) and the marker accuracy in predicting MH and the definition of MH considered for each study. The reference sections of the included studies were analyzed to retrieve relevant studies not identified by the original search.

Articles included in the final analysis were evaluated for quality and risk of bias using the Cochrane Risk of Bias Tool<sup>[12]</sup> and the Methodological Index for Non-Randomized Studies criteria<sup>[13]</sup> (Supplementary Tables 1 and 2).

Our review was registered on PROSPERO (December 19, 2020) and is currently awaiting publication on the registry site. Reporting of the review was conducted using the PRISMA guidelines. The statistical methods of this study were reviewed by a biomedical statistician at Colentina Clinical Hospital.



## RESULTS

In total, 1301 articles were retrieved with the search strategy, and 46 manuscripts were included for full-text analysis (Figure 1)<sup>[14]</sup>. After excluding studies that did not provide a clear definition of MH and studies that did not report at least a measure of performance for the investigated markers, 23 articles were included for complete data extraction and final analysis. Another reason for exclusion was reference to unclear characteristics of the study populations (ileal or colonic CD); MH was not one of the stated endpoints.

The selected manuscripts were further categorized by the source of investigated markers (fecal, serum). Studies investigating the performance of combined markers were discussed separately. Of 23 studies, 14 referred to prospective cohorts, with only 2 having a multicentric design. We also included 5 retrospective cohort analyses, 2 cross-sectional cohort studies, one case-control pilot study and a post hoc analysis of a clinical trial. The number of patients included in each study ranged from 20 to 311. The majority of included manuscripts referred to fecal markers (12/23), followed by circulatory markers (7/23), and only 4/23 investigated combined markers (serum and/or fecal markers). Most studies were performed in patients with UC (13/23): 7/12 studies investigated fecal markers, 4/7 studies investigated circulatory markers, and only one of the 3 included studies investigated combined markers. For CD patients, only 2/12 studies investigated fecal markers, and 2 studies referred to combined markers. Seven studies included both UC and CD patients (3/12 studies dedicated to fecal-based markers and 4/7 studies investigating circulatory markers).

For the definition of MH in CU patients, a Mayo endoscopic score (MES) of 0/0-1, UCEIS (UC endoscopy index of severity) of 0 or a Matts score of 1-2 (MH) Matts = 1/MES = 0 (complete MH) was applied. For CD patients, the MH definition was variable among studies: a SES-CD < 2/ $\leq$  2/ $\leq$  3/3-7, CDEIS (CD activity index)  $\leq$  4, or absence of mucosal lesions was used.

### Role of fecal biomarkers in detecting MH

Of the 23 studies included in this analysis, 12 investigated the association between fecal marker levels and MH.

**Fecal calprotectin:** Calprotectin is an antimicrobial protein mainly secreted by neutrophils that remains stable for several days at room temperature<sup>[15]</sup> and has been widely investigated in IBD patients for disease activity detection. In 9/12 studies, the authors investigated fecal calprotectin (FC) performance in assessing MH. Two studies compared FC and fecal immunochemical test (FIT) performance, and one investigated immune fecal occult blood test (iFOBT). Most studies were conducted in cohorts of UC patients (6/9) that involved a low number of participants (minimum 44, maximum 128). There was a large variation in the selected optimal cutoff values, and several commercial assays were used (ELISA, QPOCT).

In UC, the reported cutoff levels of FC for MH detection ranged between 58 mcg/g (sensitivity 89.7% and specificity 93.3%) and 490 mcg/g (sensitivity 100% and specificity 62%). For CD, the cutoff levels of FC ranged from 71 mcg/g (sensitivity 95.9% and specificity 52.3%) to 918 mcg/g (sensitivity 50% and specificity 100%) (Table 1).

**FIT:** Another fecal marker widely investigated for the assessment of IBD patients is FIT, which quantifies the globin (protein) component of hemoglobin found in stool. Quantitative FIT estimates the degree of colonic inflammation by measuring the concentration of hemoglobin in feces using an antibody that targets human hemoglobin<sup>[16]</sup>. When compared to FC, the specificity for MH in UC was similar, but FIT appeared to be more sensitive than FC for predicting MH (95% *vs* 77% for MES = 0 in a study by Hiraoka *et al.*<sup>[17]</sup>, 98.0% *vs* 78.4% for MES = 0, 94.9%, *vs* 74.6% for UCEIS 0-1 in a study by Ryu *et al.*<sup>[18]</sup>). One of the main advantages of using FIT over FC refers to cutoff values of FIT, which are relatively stable and almost equivalent to the cutoff values used in colorectal cancer screening<sup>[19]</sup>.

**iFOBT:** In addition to FIT, another fecal marker is the iFOBT, which measures the heme (nonprotein) component of hemoglobin from blood in the stool. This method has many limitations that cause false-positive results. Food and medication, as well as blood from dietary sources or upper GI bleeding, can result in a positive test<sup>[20]</sup>. When compared to FC in a retrospective analysis in UC patients, iFOBT showed higher sensitivity and specificity for assessing MH (80.6% and 100% *vs* 74.1% and 84.2%, respectively)<sup>[21]</sup>.

**Table 1 Synthetic presentation of data on fecal marker performance in detecting mucosal healing**

Ref.	Study type	Investigated marker	MH definition	CU/CD	Number of patients	AUC	95%CI	Sn (%)	Sp (%)	Cutoff level
E Penna <i>et al</i> <sup>[22]</sup>	Prospective cohort	FC	SES-CD $\leq 2$	CD	65 + 21 individuals in the control group	0.77	0.65-0.88	96	78	155 mcg/g
Hiraoka <i>et al</i> <sup>[17]</sup>	Prospective cohort	FC	MES = 0	UC	84	0.67	0.56 - 0.78	77	67	180 mcg/g
Hiraoka <i>et al</i> <sup>[17]</sup>	Prospective cohort	FIT	MES = 0	UC	84	0.62	0.50- 0.74	95	62	NA
Lee <i>et al</i> <sup>[23]</sup>	Prospective cohort	FC-ELISA; FC-QPOCT	MES = 0; SES-CD < 4	UC + CD	93	0.88	NANA	81.8(ELISA); 85.7 (QPOCT)	100 ELISA; 100 QPOCT	201 mcg/g ELISA; 150.5 mcg/g QPOCT
Urushikubo <i>et al</i> <sup>[24]</sup>	Cross-sectional, observational	FC	MES = 0; REI = 0; UCEIS = 0	UC	50	0.823; 0.780; 0.777	0.707-0.939; 0.658-0.903; 0.645-0.909	100; 100; 88	62; 70; 71	490 mcg/g; 288 mcg/g; 288 mcg/g
Ryu <i>et al</i> <sup>[18]</sup>	Retrospective cohort	FIT	MES = 0; UCEIS = 0-1	UC	128	NA	NA	98.0; 94.9	37.4; 38.3	100 ng/mL
Ryu <i>et al</i> <sup>[18]</sup>	Retrospective cohort	FC	MES = 0; UCEIS = 0-1	UC	128	NA	NA	78.4; 74.6	74.4; 76.5	170 mcg/g
Lin <i>et al</i> <sup>[25]</sup>	Multicentric prospective cohort	FC	UCEIS < 3; CDEIS < 6	UC + CD	88	0.87; 0.74	NA	88; 50	75; 100	191 mcg/g; 918 mcg/g
Vázquez Morón <i>et al</i> <sup>[26]</sup>	Prospective cohort	FC	SES-CD $\leq 2$	CD	71	NA	NA	95.9	52.3	71 mcg/g
Ryu <i>et al</i> <sup>[27]</sup>	Retrospective cohort	FIT	MES = 0-1	UC	63	0.81	0.59-0.94	73.33	81.82	< 7 ng/mL
Hassan <i>et al</i> <sup>[28]</sup>	Prospective cohort	FC	MES = 0-1	UC	44	0.949	0.838-0.992	89.7	93.3	58 mcg/g
Kostas <i>et al</i> <sup>[29]</sup>	Retrospective cohort	FC	MES = 0-1; absence of mucosal lesions for CD	UC + CD	149	0.956	NA	91.9	87.2	174 mcg/g
Yen <i>et al</i> <sup>[21]</sup>	Retrospective cohort	FC	MES = 0-1	UC	50	0.812	NA	74.19	84.21	156 mcg/g
Yen <i>et al</i> <sup>[21]</sup>	Retrospective cohort	iFOBT	MES = 0-1	UC	50	0.906	NA	80.65	100	$\leq 43$ ng/mL
Kristensen <i>et al</i> <sup>[30]</sup>	Prospective cohort	FC	MES = 0-1	UC	20	NA	NA	82.4	100	250 mcg/g

UC: Ulcerative colitis; CD: Crohn's disease; FC: Fecal calprotectin; FIT: Fecal immunoassay test; MES: Mayo endoscopic subscore; UCEIS: Ulcerative colitis endoscopy index of severity; REI: Rachmilewitz endoscopic index; M2-PK: M2 pyruvate kinase, iFOBT: Immune fecal occult blood test; NA: Not available; QPOCT: Quantitative point-of-care test; AUC: Area under the curve; CI: Confidence interval; Sn: Sensitivity; Sp: Specificity.

A systematic presentation of the data regarding fecal marker performance discussed in this review is listed in [Table 1](#).

### Role of circulatory biomarkers in detecting MH

We analyzed 7 studies discussing the role of various serum biomarkers in detecting MH. Four of 7 studies were conducted in UC cohorts; in 3 of the 7 studies, both UC and CD patients were included. We identified 3 studies that investigated the utility of trefoil factor 3 (TFF3) as a marker for MH in patients with UC, but only one study met the inclusion criteria. TFF3 is a mucin-associated peptide that is widely expressed in a tissue-specific manner in the gastrointestinal tract and is predominantly secreted by goblet cells of the small and large intestine<sup>[31]</sup>. In a study by Nakov *et al*<sup>[32]</sup>, the TFF3

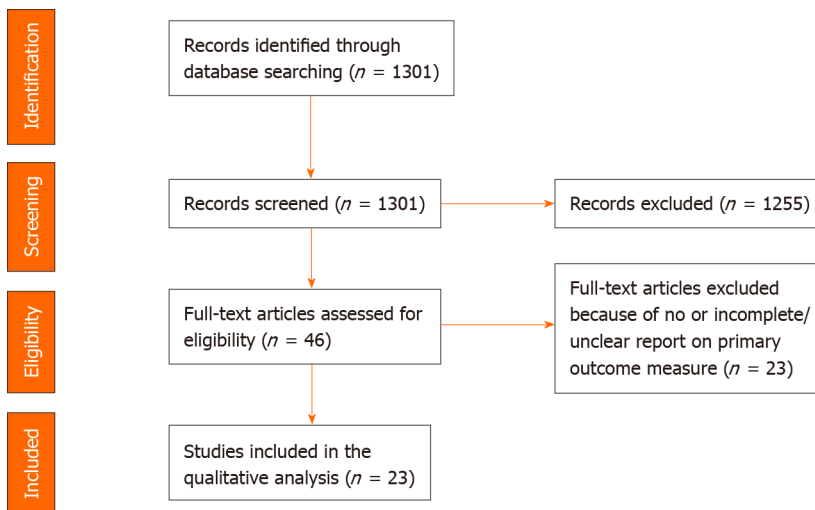


Figure 1 Flow chart of the manuscripts included in the final analysis according to the PRISMA reporting guidelines.

cutoff level of 6.74 ng/mL indicated complete MH (MES = 0; UCEIS = 0), with a sensitivity and specificity of 87.9% and 86.9% in patients with UC, respectively. An interesting aspect is that the area under the receiver operating characteristics (ROC) curve (AUC) of TFF3 + CRP showed higher accuracy than the AUC of TFF3 alone ( $Z = 2.210$ ,  $P = 0.027$ ) for predicting complete MH. However, when investigated in CD patients treated with tumor necrosis factor (TNF)- $\alpha$  antagonists, TFF3 was not a convenient or reliable surrogate marker of MH<sup>[33]</sup>.

Budzynska *et al*<sup>[34]</sup> investigated serum neutrophil gelatinase-associated lipocalin (NGAL), a low-molecular-weight protein released from activated neutrophils and the intestinal epithelium, whose mRNA expression is increased in inflamed intestinal tissue. NGAL performed well in UC patients and was able to distinguish endoscopically active from inactive UC, with an AUC-ROC of 0.758 (sensitivity 96% and specificity 54%). However, NGAL levels showed no significant relationship with either the clinical or endoscopic activity of CD.

In a study by Planell *et al*<sup>[35]</sup>, transcriptional changes in whole-blood samples from UC patients were investigated. A significant correlation with the degree of endoscopic activity was observed in several genes, including *haptoglobin* (HP), *CD177*, *GPR84*, and *S100A12*. Within the subset of genes whose expression best correlates with endoscopic disease severity, HP was the best gene to predict mucosal lesions. The logistic regression model for endoscopic activity prediction (endoscopic Mayo score: 0 *vs*  $\geq 1$ ) demonstrated a significant effect of HP ( $P < 0.001$ ), with an odds ratio of 1.9 [95% confidence interval (CI): 1.35-2.78] and an AUC = 0.75 (95%CI: 0.64-0.85). Defining a cutoff of -2.9 DCt, the sensitivity and specificity were 63.5% and 80.0%, respectively.

Nicotinamide phosphoribosyltransferase (Nampt) is another serum marker showing good potential in assessing MH. Nampt is an intracellular enzyme that is primarily associated with the induction and persistence of inflammatory responses. In a study by Neubauer *et al*<sup>[36]</sup>, serum Nampt in UC positively correlated with its clinical and endoscopic activity as well as with proinflammatory cytokines. Serum Nampt  $\leq 1.54$  ng/mL was a good indicator of MH (sensitivity 76%, specificity 75%, AUC 0.768).

One recent study proposed serum amyloid A (SAA) as a surrogate marker for MH. Both SAA and CRP are mainly secreted from the liver, but SAA is reported to be more effective than CRP in diseases other than IBD<sup>[37]</sup>. The diagnostic accuracy of SAA for MH was superior to that of CRP. SAA levels  $< 5.8$  could discriminate mucosal inflammation from MH, with a sensitivity of 72.2%, specificity of 85%, and accuracy of 79.9%. In contrast, CRP levels  $< 0.060$  could distinguish mucosal inflammation from MH, with a sensitivity of 62%, specificity of 75%, and accuracy of 70.4%<sup>[38]</sup>.

Dierckx *et al*<sup>[39]</sup> investigated glycoprotein acetylation (GlycA) in the serum or plasma of patients with IBD. GlycA is a novel nuclear magnetic resonance biomarker that summarizes the signals originating from glycan groups of certain acute-phase glycoproteins. In this study, GlycA concentration in both CD and UC patients achieving MH dropped back to HC levels ( $P = 0.90$ ,  $P = 0.910$ ) and showed potential to identify MH even in patients without elevated CRP. This should therefore be tested in large prospective cohorts.

Serum levels of leucine-rich alpha-2 glycoprotein, investigated in a prospective setting, were significantly higher in endoscopically active patients with UC having extensive and left-sided colitis than in those with MH, although marker performance measures were not clearly reported<sup>[40]</sup>.

A systematic presentation of the data regarding serum marker performance discussed in this review is listed in [Table 2](#).

### Role of combined biomarkers in detecting MH

Because of the suboptimal performance of individual noninvasive markers at detecting MH, further combining fecal and serum biomarkers in panels has been attempted to increase accuracy in several studies.

A multicentric international study conducted by D'Haens *et al*<sup>[41]</sup> aimed to develop and validate a multimarker, serologic, algorithm-based diagnostic test that could reflect the severity of endoscopic inflammation in CD patients. The endoscopic healing index (EHI) model includes serum concentrations of 13 biomarkers: angiopoietin 1 (ANG1) and 2 (ANG2); carcinoembryonic antigen-related cell adhesion molecule 1; CRP; SAA1; interleukin (IL) 7; transforming growth factor  $\alpha$ ; vascular cell adhesion molecule 1; extracellular matrix metalloproteinase inducer; and matrix metalloproteinases 1 (MMP1), 2 (MMP2), 3 (MMP3), and 9 (MMP9). EHI was constructed as a scale of 0-100 arbitrary units of EHI activity, with a higher score indicating more severe disease activity. The EHI identified patients with resolution of endoscopic disease activity, with good overall accuracy, although with variation between the 2 cohorts assessed. The EHI AUC-ROC values were comparable to the measurement of FC (0.950 *vs* 0.923  $P = 0.147$  in validation cohort 1 and 0.803 *vs* 0.854,  $P = 0.298$  in validation cohort 2) and higher than that of serum CRP.

Other serum markers that have shown promising results are anti-inflammatory serum cytokine profiles. Gubatan *et al*<sup>[42]</sup> reported that the serum cytokine ratio IL-4 + IL-10/IL-17A + TNF- $\alpha$  has the ability to identify UC patients with baseline histologic MH (AUC of 0.641,  $P = 0.044$ ). A serum cytokine ratio IL-4 + IL-10/IL-17A + TNF- $\alpha$  threshold of 0.1522 had the greatest sensitivity (52.6%, 95%CI: 35.8-69.0) and specificity (75.0%, 95%CI: 56.6-88.5), with a positive likelihood ratio of 2.015.

Other authors have tried to evaluate the combined role of serum, fecal and clinical scores in detecting MH. A post hoc analysis from the CALM study<sup>[43]</sup> reported the performance of the combination of FC, CRP and clinical disease activity index (CDAI) in detecting MH. Using the cutoffs FC < 250  $\mu$ g/g, CRP < 5 mg/L, and CDAI < 150, it had a sensitivity/specificity of 72%/63% and positive/negative predictive values of 86%/42% for CDEIS < 4 and no deep ulcers 48 wk after randomization. Data regarding the performance of combined biomarkers are listed in [Table 3](#).

Cytokines, such as IL-6 and soluble IL-2 receptor (sIL-2R), have been shown to modulate the intestinal immune system. Mavropoulou *et al*<sup>[44]</sup> analyzed serum IL-6 and sIL-2R levels in a cohort of IBD patients. They evaluated the correlation between these laboratory markers and clinical and endoscopic disease activity status in IBD patients. In this study, serum levels of sIL-2R ( $P < 0.001$ ) and CRP ( $P = 0.003$ ) as well as FC values ( $P < 0.001$ ) were associated with endoscopic remission in UC patients by univariate analysis. For CD patients, the threshold value for IL-6 to discriminate patients with endoscopic remission or active disease was 5.5 pg/mL, with an AUC-ROC of 0.80 (95%CI: 0.71-0.89).

## DISCUSSION

Over the past decade, the standard of care and management of IBD have greatly improved as a result of newly approved drugs as well as a wide array of invasive and noninvasive diagnostic tools. Novel “treat-to-target” strategies have recently been shown to impact disease progression and improve outcomes for IBD patients. MH has been one of the main targets suggested as part of current therapeutic goals<sup>[42]</sup>. Compared to previous strategies that focused on symptom control, recent studies have shown that achieving MH is associated with lower risks of relapse, hospitalization and surgery<sup>[3,4]</sup>. However, because MH is objectivated by intrusive colonoscopy, it is becoming increasingly apparent that surrogate noninvasive markers are needed for close and efficient disease monitoring and control. A reliable surrogate marker for MH would have a significant clinical impact, by reducing the number of endoscopic evaluations required during the course of disease.

Based on our findings, other than FC, which has a clear established role in current real-life clinical practice, none of the biomarkers was accurate enough to replace

**Table 2 Synthetic presentation of data on serum marker performance in detecting mucosal healing**

Ref.	Study type	Investigated marker	MH definition	CU/CD	Number of patients	AUC	95%CI	Sn (%)	Sp (%)	Cutoff level
Shinzaki <i>et al</i> <sup>[40]</sup>	Prospective cohort	LRG	Matts = 1-2 (MH); Matts = 1/MES = 0 (complete MH)	CU	129	0.849; 0.759	NA	NA	NA	NA
Dierckx <i>et al</i> <sup>[39]</sup>	Case control pilot study	GlycA	MES = 0-1; SES-CD ≤ 2	CU + CD	58 + 10 healthy controls	NA	NA	NA	NA	NA
Neubauer <i>et al</i> <sup>[36]</sup>	Prospective cohort	S-Nampt	MES = 0-1; NA for CD	CU + CD	240 + 40 non-IBD controls	0.768	0.67-0.85	76	75	≤ 1.54 ng/mL
Planell <i>et al</i> <sup>[35]</sup>	Cross-sectional cohort + case control	HP	MES = 0	UC	126 + 20 healthy controls + 16	0.75	0.64-0.85	63.5	80	-2.9 DCt
Nakov <i>et al</i> <sup>[32]</sup>	Prospective cohort	TFF3	MES = 0; UCEIS = 0	UC		0.927	0.877-0.976	87.9	86.9	6.74
Budzyńska <i>et al</i> <sup>[34]</sup>	Prospective cohort	NGAL	MES = 0-1; SES-CD = 3-7	UC + CD	120	0.79; 0.608	0.65-0.93; NA	96; 48	50; 83	43.6 ng/mL; 72.5 ng/mL
Wakai <i>et al</i> <sup>[38]</sup>	Retrospective cohort	Serum amyloid A	MES = 0-1	UC	108	0.807	0.748-0.867	72.2	85	< 5.8

UC: Ulcerative colitis; CD: Crohn's disease; LRG: Leucine-rich alpha-2 glycoprotein; GlycA: Glycoprotein acetylation; Nampt: Nicotinamide phosphoribosyltransferase; HP: Haptoglobin; TFF3: Trefoil factor 3; NGAL: Serum neutrophil gelatinase-associated lipocalin; NA: Not available; SES-CD: Simple endoscopic score for Crohn's disease; AUC: Area under the curve; CI: Confidence interval; Sn: Sensitivity; Sp: Specificity.

endoscopy. The most accurate serum marker was a multimarker based on 13 serum proteins, called the EHI, which showed comparable accuracy to the measurement of FC and higher accuracy than the measurement of serum CRP. We observed that most studies focused on assessing individual markers among a small number of patients in a wide variety of study designs and heterogeneous groups of patients.

However, endoscopic activity scores and MH definitions are not homogenous, which could represent an impediment in establishing the performance of various investigated markers. Additionally, there are several commercial assays for FC and other marker measurements available, making the establishment of cutoff values an insurmountable obstacle. Few studies compared the investigated markers to FC, which has been widely investigated and is commonly used in clinical practice.

It is mandatory to assess MH at different key time points during the disease course, especially to gauge the response to therapy or to address newly developed symptoms. FC has emerged as one of the few noninvasive tools commonly used in IBD clinical practice, and there is now considerable evidence confirming the good accuracy of FC in detecting MH<sup>[2]</sup>.

Even though some factors may influence its concentration (*e.g.*, the amount of mucus and blood in stool<sup>[45]</sup>), FC is one of the most sensitive noninvasive tools in differentiating IBD from functional disorders<sup>[46]</sup>. For IBD patients, different cutoff levels have been proposed for diagnostic purposes to differentiate between endoscopic active and nonactive disease, histologic healing<sup>[47]</sup> or prediction of relapse<sup>[2]</sup>, but a consensus has not yet been established. At present, an FC level over 250 mcg/g is considered to indicate active colonic inflammation<sup>[48]</sup>, while levels below 100 mcg/g may indicate endoscopic remission<sup>[49]</sup>.

One major limitation of FC use refers to the so-called "gray zone" level between 100 mcg/g and 250 mcg/g, which is difficult to interpret. Bodelier *et al*<sup>[50]</sup> investigated the occurrence of indefinite FC levels in a real-life IBD cohort and studied the additional value of a combination of biochemical markers and clinical activity indices. In the studied cohort, 24% of CD and 15% of UC patients had FC in this "gray zone". Finally, if given the option, patients usually prefer blood over fecal tests<sup>[51]</sup>, and this further limits the widespread use of FC in clinical practice.

Some of the circulatory markers investigated in the studies included in this review showed promising results. However, none of the investigated blood- or fecal-based markers showed great accuracy for MH prediction and therefore cannot replace endoscopy at this point.



**Table 3 Synthetic presentation of data on combined marker performance in detecting mucosal healing**

Ref.	Study type	Investigated marker	MH definition	CU/CD	Number of patients	AUC	95%CI	Sn (%)	Sp (%)	Cutoff level
Reinisch <i>et al</i> <sup>[43]</sup>	Post hoc analysis of clinical trial	FC, CRP and CDAI	CDEIS < 4	CD	244	0.68,	0.62-0.74	74	64	FC < 250 mcg/g, CRP < 5 mg/L, and CDAI < 150
D'Haens <i>et al</i> <sup>[41]</sup>	Prospective-specimen collection, retrospective-blinded-evaluation	EHI	SES-CD of $\leq 2$ and $\leq 1$ in each segment	CD	311 in 2 cohorts (116 + 195)	0.962; 0.693	0.942-0.982; 0.619-0.767	97.1; 83.2 (for cutoff of 20)	100; 87.8 (cutoff of 50)	$\leq 20$
Gubatan <i>et al</i> <sup>[42]</sup>	Prospective cohort	IL-4 + IL-10/IL-17A + TNF- $\alpha$	Geboes Histologic Grade of < 3	CU	70	0.641		52.6	75	0.1522
Mavropoulou <i>et al</i> <sup>[44]</sup>	Prospective cohort	sIL-2R (CU); IL-6 (CD); FC (UC); FC (CD)	MES = 0-1; SES-CD $\leq 3$	UC + CD	299 (84 + 145)	0.80; 0.80; 0.92; 0.84	0.68-0.91; 0.71-0.89; 0.86-0.99; 0.76-0.92	63; 69; 91; 70	85; 80; 89; 100	< 646 IU/mL; < 5.5 pg/mL; < 340 mg/kg; < 180 mg/kg

EHI: Endoscopic healing index measuring 13 proteins in blood [angiopoietin 1 (ANG1) and 2 (ANG2), carcinoembryonic antigen-related cell adhesion molecule 1, C-reactive protein, serum amyloid A1, interleukin 7, transforming growth factor  $\alpha$ , vascular cell adhesion molecule 1, extracellular matrix metalloproteinase inducer, and matrix metalloproteinases 1 (MMP1), 2 (MMP2), 3 (MMP3), and 9 (MMP9)]; UC: Ulcerative colitis; CD: Crohn's disease; AUC: Area under the curve; CI: Confidence interval; Sn: Sensitivity; Sp: Specificity; SES-CD: Simple endoscopic score for Crohn's disease; CRP: C-reactive protein; CDAI: Crohn's disease activity index; sIL-2R: Soluble interleukin 2 receptor; MES: Mayo endoscopic subscore; FC: Fecal calprotectin.

An ideal marker or multimarker should be noninvasive, sensitive, disease-specific, easy to perform, cost-effective<sup>[52]</sup> and ideally patient-friendly; such a marker remains to be identified by future research.

An important observation concerns newly established therapeutic targets in IBD management, which could soon be included as a standard of care achievement of histologic healing. Several studies have already assessed the performance of biomarkers in detecting this endpoint, such as the study conducted by Gubatan *et al*<sup>[42]</sup>, which explored the accuracy of serum cytokines in assessing histologic healing, defined as a Geboes Histologic Grade of < 3. There is evidence that FC levels correlate more closely with histological evaluation than macroscopic findings, suggesting that this biological marker is more sensitive than endoscopy<sup>[53]</sup>.

Widely used serum markers, such as CRP, white blood cell count, and erythrocyte sedimentation rate, combined with clinical activity scores are currently used in IBD monitoring. This approach lacks the diagnostic accuracy needed for decision making in patients with UC, and colonoscopy is still required for proper evaluation of disease activity.

For future research, a combined marker approach benchmarked against a well-investigated marker, such as FC, could be a promising alternative to endoscopic examination.

There are certain limitations to our analysis. We decided not to include data on CRP or imaging markers (magnetic resonance imaging, ultrasound) in detecting MH. A previous comprehensive analysis regarding the role of CRP in this setting was recently published by Krzystek-Korpaczka *et al*<sup>[11]</sup>. In this review of 30 studies, there was a large variation in the selected optimal cutoff values, ranging from 0.4 mg/L to 28 mg/L. CRP performance as an MH marker displayed better sensitivity than specificity for CD, with respective median values of 79.5% *vs* 61%, and better specificity than sensitivity for UC, with respective median values of 82% *vs* 66%<sup>[1]</sup>. CRP is a widely used marker in clinical practice for IBD monitoring, but it still fails to provide sufficient accuracy to replace endoscopy as an independent marker for MH. Expanding the search to imaging modalities would have diluted the information provided and was beyond the scope of our paper. Both magnetic resonance imaging and ultrasound are indispensable tools in IBD management, but operator-dependent

and costly, limiting their widespread use and accessibility. Our search was we relied exclusively on PubMed (MEDLINE) database for identification of potentially eligible studies.

## CONCLUSION

Various biomarkers for MH are currently under investigation and show promising results. However, at present, no biomarker is accurate enough to replace endoscopy. Therefore, it is our strong belief that future high-quality studies should further focus on establishing panels of biomarkers that would have higher predictive values than biomarkers alone.

## ARTICLE HIGHLIGHTS

### Research background

Mucosal healing (MH) has been one of the main therapeutic targets stipulated by recent recommendations. MH is associated with lower risks of relapse, hospitalization and surgery. In recent years, a wealth of publications regarding various noninvasive biomarkers for MH have reported conflicting results.

### Research motivation

MH is objectivated by intrusive colonoscopy, and it is becoming increasingly apparent that surrogate noninvasive markers are needed for close and efficient disease monitoring and control. A reliable surrogate marker for MH would have a significant clinical impact, by reducing the number of endoscopic evaluations required during the course of disease.

### Research objectives

We aimed to summarize published data regarding the performance of noninvasive biomarkers in assessing MH in inflammatory bowel disease patients.

### Research methods

We conducted a systematic review of studies that reported the performance of biomarkers in diagnosing MH in patients with inflammatory bowel disease. The main outcome measure was to review the diagnostic accuracy of serum and fecal markers that showed promising utility in assessing MH.

### Research results

We screened 1301 articles, retrieved 46 manuscripts and included 23 articles for full-text analysis. Fecal calprotectin (FC) was the most investigated fecal marker for assessing MH. The best performance for a serum marker was observed for the endoscopic healing index, which showed a comparable accuracy to the measurement of FC and a higher accuracy than the measurement of serum C-reactive protein.

### Research conclusions

Several promising biomarkers of MH are emerging but cannot yet substitute for endoscopy with biopsy due to issues with reproducibility and standardization.

### Research perspectives

For future research, a combined marker approach benchmarked against a well-investigated marker, such as FC, could be a promising alternative to endoscopic examination.

## REFERENCES

- 1 Annese V, Daperno M, Rutter MD, Amiot A, Bossuyt P, East J, Ferrante M, Götz M, Katsanos KH, Kiefflich R, Ordás I, Repici A, Rosa B, Sebastian S, Kucharzik T, Eliakim R; European Crohn's and Colitis Organisation. European evidence based consensus for endoscopy in inflammatory bowel disease. *J Crohns Colitis* 2013; 7: 982-1018 [PMID: 24184171 DOI: 10.1016/j.crohns.2013.09.016]
- 2 Maaser C, Sturm A, Vavricka SR, Kucharzik T, Fiorino G, Annese V, Calabrese E, Baumgart DC,

- Bettenworth D, Borralho Nunes P, Burisch J, Castiglione F, Eliakim R, Ellul P, González-Lama Y, Gordon H, Halligan S, Katsanos K, Kopylov U, Kotze PG, Krustinš E, Laghi A, Limdi JK, Rieder F, Rimola J, Taylor SA, Tolan D, van Rheeën P, Verstockt B, Stoker J; European Crohn's and Colitis Organisation [ECCO] and the European Society of Gastrointestinal and Abdominal Radiology [ESGAR]. ECCO-ESGAR Guideline for Diagnostic Assessment in IBD Part 1: Initial diagnosis, monitoring of known IBD, detection of complications. *J Crohns Colitis* 2019; **13**: 144-164 [PMID: 30137275 DOI: 10.1093/ecco-jcc/jjy113]
- 3 **Froslic KF**, Jahnsen J, Moum BA, Vatn MH; IBSEN Group. Mucosal healing in inflammatory bowel disease: results from a Norwegian population-based cohort. *Gastroenterology* 2007; **133**: 412-422 [PMID: 17681162 DOI: 10.1053/j.gastro.2007.05.051]
  - 4 **Ardizzone S**, Cassinotti A, Duca P, Mazzali C, Penati C, Manes G, Marmo R, Massari A, Molteni P, Maconi G, Porro GB. Mucosal healing predicts late outcomes after the first course of corticosteroids for newly diagnosed ulcerative colitis. *Clin Gastroenterol Hepatol* 2011; **9**: 483-489. e3 [PMID: 21195796 DOI: 10.1016/j.cgh.2010.12.028]
  - 5 **Boal Carvalho P**, Cotter J. Mucosal Healing in Ulcerative Colitis: A Comprehensive Review. *Drugs* 2017; **77**: 159-173 [PMID: 28078646 DOI: 10.1007/s40265-016-0676-y]
  - 6 **Klenske E**, Bojarski C, Waldner M, Rath T, Neurath MF, Atreya R. Targeting mucosal healing in Crohn's disease: what the clinician needs to know. *Therap Adv Gastroenterol* 2019; **12**: 1756284819856865 [PMID: 31236140 DOI: 10.1177/1756284819856865]
  - 7 **Denters MJ**, Schreuder M, Depla AC, Mallant-Hent RC, van Kouwen MC, Deutekom M, Bossuyt PM, Fockens P, Dekker E. Patients' perception of colonoscopy: patients with inflammatory bowel disease and irritable bowel syndrome experience the largest burden. *Eur J Gastroenterol Hepatol* 2013; **25**: 964-972 [PMID: 23660935 DOI: 10.1097/MEG.0b013e328361dcd3]
  - 8 **Navaneethan U**, Parasa S, Venkatesh PG, Trikudanathan G, Shen B. Prevalence and risk factors for colonic perforation during colonoscopy in hospitalized inflammatory bowel disease patients. *J Crohns Colitis* 2011; **5**: 189-195 [PMID: 21575880 DOI: 10.1016/j.crohns.2010.12.005]
  - 9 **Kim SY**, Kim HS, Park HJ. Adverse events related to colonoscopy: Global trends and future challenges. *World J Gastroenterol* 2019; **25**: 190-204 [PMID: 30670909 DOI: 10.3748/wjg.v25.i2.190]
  - 10 **Petryszyn PW**, Witczak I. Costs in inflammatory bowel diseases. *Prz Gastroenterol* 2016; **11**: 6-13 [PMID: 27110304 DOI: 10.5114/pg.2016.57883]
  - 11 **Krzystek-Korpacka M**, Kempinski R, Bromke M, Neubauer K. Biochemical Biomarkers of Mucosal Healing for Inflammatory Bowel Disease in Adults. *Diagnostics (Basel)* 2020; **10** [PMID: 32498475 DOI: 10.3390/diagnostics10060367]
  - 12 **Higgins JP**, Altman DG, Gøtzsche PC, Jüni P, Moher D, Oxman AD, Savovic J, Schulz KF, Weeks L, Sterne JA; Cochrane Bias Methods Group; Cochrane Statistical Methods Group. The Cochrane Collaboration's tool for assessing risk of bias in randomised trials. *BMJ* 2011; **343**: d5928 [PMID: 22008217 DOI: 10.1136/bmj.d5928]
  - 13 **Slim K**, Nini E, Forestier D, Kwiatkowski F, Panis Y, Chipponi J. Methodological index for non-randomized studies (minors): development and validation of a new instrument. *ANZ J Surg* 2003; **73**: 712-716 [PMID: 12956787 DOI: 10.1046/j.1445-2197.2003.02748.x]
  - 14 **Moher D**, Liberati A, Tetzlaff J, Altman DG; PRISMA Group. Preferred reporting items for systematic reviews and meta-analyses: the PRISMA statement. *PLoS Med* 2009; **6**: e1000097 [PMID: 19621072 DOI: 10.1371/journal.pmed.1000097]
  - 15 **Naess-Andresen CF**, Egelanddsal B, Fagerhol MK. Calcium binding and concomitant changes in the structure and heat stability of calprotectin (L1 protein). *Clin Mol Pathol* 1995; **48**: M278-M284 [PMID: 16696022 DOI: 10.1136/mp.48.5.m278]
  - 16 **Kato J**, Hiraoka S, Nakarai A, Takashima S, Inokuchi T, Ichinose M. Fecal immunochemical test as a biomarker for inflammatory bowel diseases: can it rival fecal calprotectin? *Intest Res* 2016; **14**: 5-14 [PMID: 26884729 DOI: 10.5217/ir.2016.14.1.5]
  - 17 **Hiraoka S**, Inokuchi T, Nakarai A, Takashima S, Takei D, Sugihara Y, Takahara M, Harada K, Okada H, Kato J. Fecal Immunochemical Test and Fecal Calprotectin Results Show Different Profiles in Disease Monitoring for Ulcerative Colitis. *Gut Liver* 2018; **12**: 142-148 [PMID: 28873508 DOI: 10.5009/gnl17013]
  - 18 **Ryu DG**, Kim HW, Park SB, Kang DH, Choi CW, Kim SJ, Nam HS. Clinical implications of fecal calprotectin and fecal immunochemical test on mucosal status in patients with ulcerative colitis. *Medicine (Baltimore)* 2019; **98**: e17080 [PMID: 31490411 DOI: 10.1097/MD.00000000000017080]
  - 19 **Navarro M**, Hijos G, Sostres C, Lué A, Puente-Lanzarote JJ, Carrera-Lasfuentes P, Lanás A. Reducing the Cut-Off Value of the Fecal Immunochemical Test for Symptomatic Patients Does Not Improve Diagnostic Performance. *Front Med (Lausanne)* 2020; **7**: 410 [PMID: 32984360 DOI: 10.3389/fmed.2020.00410]
  - 20 **Hubbard RA**, Johnson E, Hsia R, Rutter CM. The cumulative risk of false-positive fecal occult blood test after 10 years of colorectal cancer screening. *Cancer Epidemiol Biomarkers Prev* 2013; **22**: 1612-1619 [PMID: 23868091 DOI: 10.1158/1055-9965.EPI-13-0254]
  - 21 **Yen HH**, Chen MW, Chang YY, Huang HY, Hsu TC, Chen YY. Predictive values of stool-based tests for mucosal healing among Taiwanese patients with ulcerative colitis: a retrospective cohort analysis. *PeerJ* 2020; **8**: e9537 [PMID: 32742803 DOI: 10.7717/peerj.9537]
  - 22 **E Penna FGC**, Rosa RM, da Cunha PFS, de Souza SCS, de Abreu Ferrari ML. Faecal calprotectin is the biomarker that best distinguishes remission from different degrees of endoscopic activity in

- Crohn's disease. *BMC Gastroenterol* 2020; **20**: 35 [PMID: [32054445](#) DOI: [10.1186/s12876-020-1183-x](#)]
- 23 **Lee YW**, Lee KM, Lee JM, Chung YY, Kim DB, Kim YJ, Chung WC, Paik CN. The usefulness of fecal calprotectin in assessing inflammatory bowel disease activity. *Korean J Intern Med* 2019; **34**: 72-80 [PMID: [29347813](#) DOI: [10.3904/kjim.2016.324](#)]
  - 24 **Urushikubo J**, Yanai S, Nakamura S, Kawasaki K, Akasaka R, Sato K, Toya Y, Asakura K, Gonai T, Sugai T, Matsumoto T. Practical fecal calprotectin cut-off value for Japanese patients with ulcerative colitis. *World J Gastroenterol* 2018; **24**: 4384-4392 [PMID: [30344422](#) DOI: [10.3748/wjg.v24.i38.4384](#)]
  - 25 **Lin WC**, Wong JM, Tung CC, Lin CP, Chou JW, Wang HY, Shieh MJ, Chang CH, Liu HH, Wei SC; Taiwan Society of Inflammatory Bowel Disease Multicenter Study. Fecal calprotectin correlated with endoscopic remission for Asian inflammatory bowel disease patients. *World J Gastroenterol* 2015; **21**: 13566-13573 [PMID: [26730169](#) DOI: [10.3748/wjg.v21.i48.13566](#)]
  - 26 **Vázquez Morón JM**, Pallarés Manrique H, Machancoses FH, Ramos Lora M, Ruiz Frutos C. Accurate cut-offs for predicting endoscopic activity and mucosal healing in Crohn's disease with fecal calprotectin. *Rev Esp Enferm Dig* 2017; **109**: 130-136 [PMID: [28071062](#) DOI: [10.17235/reed.2017.4542/2016](#)]
  - 27 **Ryu DG**, Kim HW, Park SB, Kang DH, Choi CW, Kim SJ, Nam HS. Assessment of disease activity by fecal immunochemical test in ulcerative colitis. *World J Gastroenterol* 2016; **22**: 10617-10624 [PMID: [28082814](#) DOI: [10.3748/wjg.v22.i48.10617](#)]
  - 28 **Hassan EA**, Ramadan HK, Ismael AA, Mohamed KF, El-Attar MM, Alhelali I. Noninvasive biomarkers as surrogate predictors of clinical and endoscopic remission after infliximab induction in patients with refractory ulcerative colitis. *Saudi J Gastroenterol* 2017; **23**: 238-245 [PMID: [28721978](#)]
  - 29 **Kostas A**, Siakavellas SI, Kosmidis C, Takou A, Nikou J, Maropoulos G, Vlachogiannakos J, Papatheodoridis GV, Papaconstantinou I, Bamias G. Fecal calprotectin measurement is a marker of short-term clinical outcome and presence of mucosal healing in patients with inflammatory bowel disease. *World J Gastroenterol* 2017; **23**: 7387-7396 [PMID: [29151692](#) DOI: [10.3748/wjg.v23.i41.7387](#)]
  - 30 **Kristensen V**, Røseth A, Ahmad T, Skar V, Moum B. Fecal Calprotectin: A Reliable Predictor of Mucosal Healing after Treatment for Active Ulcerative Colitis. *Gastroenterol Res Pract* 2017; **2017**: 2098293 [PMID: [29225617](#) DOI: [10.1155/2017/2098293](#)]
  - 31 **Podolsky DK**, Lynch-Devaney K, Stow JL, Oates P, Murgue B, DeBeaumont M, Sands BE, Mahida YR. Identification of human intestinal trefoil factor. Goblet cell-specific expression of a peptide targeted for apical secretion. *J Biol Chem* 1993; **268**: 6694-6702 [PMID: [8454642](#)]
  - 32 **Nakov R**, Velikova T, Nakov V, Gerova V, Tankova L. Trefoil Factor 3 is Highly Predictive of Complete Mucosal Healing Independently and in Combination with C-Reactive Protein in Patients with Ulcerative Colitis. *J Gastrointest Liver Dis* 2019; **28**: 169-174 [PMID: [31204414](#) DOI: [10.15403/jgld-177](#)]
  - 33 **Eder P**, Stawczyk-Eder K, Korybalska K, Czepulis N, Luczak J, Lykowska-Szuber L, Krela-Kazmierczak I, Linke K, Witowski J. Trefoil factor-3 is not a useful marker of mucosal healing in Crohn's disease treated with anti-TNF- $\alpha$  antibodies. *World J Gastroenterol* 2017; **23**: 135-140 [PMID: [28104989](#) DOI: [10.3748/wjg.v23.i1.135](#)]
  - 34 **Budzynska A**, Gawron-Kiszka M, Nowakowska-Dulawa E, Spiewak J, Lesinska M, Kukla M, Waluga M, Hartleb M. Serum neutrophil gelatinase-associated lipocalin (NGAL) correlates with clinical and endoscopic activity in ulcerative colitis but fails to predict activity in Crohn's disease. *J Physiol Pharmacol* 2017; **68**: 859-865 [PMID: [29550798](#)]
  - 35 **Planell N**, Masamunt MC, Leal RF, Rodríguez L, Esteller M, Lozano JJ, Ramírez A, Ayrizono MLS, Coy CSR, Alfaro I, Ordás I, Visvanathan S, Ricart E, Guardiola J, Panés J, Salas A. Usefulness of Transcriptional Blood Biomarkers as a Non-invasive Surrogate Marker of Mucosal Healing and Endoscopic Response in Ulcerative Colitis. *J Crohns Colitis* 2017; **11**: 1335-1346 [PMID: [28981629](#) DOI: [10.1093/ecco-jcc/jjx091](#)]
  - 36 **Neubauer K**, Bednarz-Misa I, Walecka-Zacharska E, Wierzbicki J, Agrawal A, Gamian A, Krzystek-Korpacka M. Oversecretion and Overexpression of Nicotinamide Phosphoribosyltransferase/Pre-B Colony-Enhancing Factor/Visfatin in Inflammatory Bowel Disease Reflects the Disease Activity, Severity of Inflammatory Response and Hypoxia. *Int J Mol Sci* 2019; **20** [PMID: [30621173](#) DOI: [10.3390/ijms20010166](#)]
  - 37 **Raynes JG**, Cooper EH. Comparison of serum amyloid A protein and C-reactive protein concentrations in cancer and non-malignant disease. *J Clin Pathol* 1983; **36**: 798-803 [PMID: [6863571](#) DOI: [10.1136/jcp.36.7.798](#)]
  - 38 **Wakai M**, Hayashi R, Tanaka S, Naito T, Kumada J, Nomura M, Takigawa H, Oka S, Ueno Y, Ito M, Chayama K. Serum amyloid A is a better predictive biomarker of mucosal healing than C-reactive protein in ulcerative colitis in clinical remission. *BMC Gastroenterol* 2020; **20**: 85 [PMID: [32245401](#) DOI: [10.1186/s12876-020-01229-8](#)]
  - 39 **Dierckx T**, Verstockt B, Vermeire S, van Weyenbergh J. GlycA, a Nuclear Magnetic Resonance Spectroscopy Measure for Protein Glycosylation, is a Viable Biomarker for Disease Activity in IBD. *J Crohns Colitis* 2019; **13**: 389-394 [PMID: [30312386](#) DOI: [10.1093/ecco-jcc/jjy162](#)]
  - 40 **Shinzaki S**, Matsuoka K, Iijima H, Mizuno S, Serada S, Fujimoto M, Arai N, Koyama N, Morii E, Watanabe M, Hibi T, Kanai T, Takehara T, Naka T. Leucine-rich Alpha-2 Glycoprotein is a Serum

- Biomarker of Mucosal Healing in Ulcerative Colitis. *J Crohns Colitis* 2017; **11**: 84-91 [PMID: 27466171 DOI: 10.1093/ecco-jcc/jjw132]
- 41 **D'Haens G**, Kelly O, Battat R, Silverberg MS, Laharie D, Louis E, Savarino E, Bodini G, Yarur A, Boland BS, Afif W, Li XJ, Hale M, Ho J, Kondragunta V, Huang B, Kuy C, Okada L, Hester KD, Bray KR, Mimms L, Jain A, Singh S, Collins A, Valasek MA, Sandborn WJ, Vermeire S, Dulai PS. Development and Validation of a Test to Monitor Endoscopic Activity in Patients With Crohn's Disease Based on Serum Levels of Proteins. *Gastroenterology* 2020; **158**: 515-526. e10 [PMID: 31711925 DOI: 10.1053/j.gastro.2019.10.034]
  - 42 **Gubatan J**, Mitsuhashi S, Longhi MS, Zenlea T, Rosenberg L, Robson S, Moss AC. Higher serum vitamin D levels are associated with protective serum cytokine profiles in patients with ulcerative colitis. *Cytokine* 2018; **103**: 38-45 [PMID: 29324259 DOI: 10.1016/j.cyto.2017.12.023]
  - 43 **Reinisch W**, Panaccione R, Bossuyt P, Baert F, Armuzzi A, Hébuterne X, Travis S, Danese S, Sandborn WJ, Schreiber S, Berg S, Zhou Q, Kligys K, Neimark E, Suleiman AA, D'Haens G, Colombel JF. Association of Biomarker Cutoffs and Endoscopic Outcomes in Crohn's Disease: A Post Hoc Analysis From the CALM Study. *Inflamm Bowel Dis* 2020; **26**: 1562-1571 [PMID: 32105310 DOI: 10.1093/ibd/izaa025]
  - 44 **Mavropoulou E**, Mechie NC, Knoop R, Petzold G, Ellenrieder V, Kunsch S, Pilavakis Y, Amanzada A. Association of serum interleukin-6 and soluble interleukin-2-receptor levels with disease activity status in patients with inflammatory bowel disease: A prospective observational study. *PLoS One* 2020; **15**: e0233811 [PMID: 32470973 DOI: 10.1371/journal.pone.0233811]
  - 45 **Calafat M**, Cabré E, Mañosa M, Lobatón T, Marín L, Domènech E. High within-day variability of fecal calprotectin levels in patients with active ulcerative colitis: what is the best timing for stool sampling? *Inflamm Bowel Dis* 2015; **21**: 1072-1076 [PMID: 25793326 DOI: 10.1097/MIB.0000000000000349]
  - 46 **Mumolo MG**, Bertani L, Ceccarelli L, Laino G, Di Fluri G, Albano E, Tapete G, Costa F. From bench to bedside: Fecal calprotectin in inflammatory bowel diseases clinical setting. *World J Gastroenterol* 2018; **24**: 3681-3694 [PMID: 30197475 DOI: 10.3748/wjg.v24.i33.3681]
  - 47 **Cannatelli R**, Bazarova A, Zardo D, Nardone OM, Shivaji U, Smith SCL, Gkoutos G, Ricci C, Gui XS, Ghosh S, Iacucci M. Fecal Calprotectin Thresholds to Predict Endoscopic Remission Using Advanced Optical Enhancement Techniques and Histological Remission in IBD Patients. *Inflamm Bowel Dis* 2020 [PMID: 32592477 DOI: 10.1093/ibd/izaa163]
  - 48 **D'Haens G**, Ferrante M, Vermeire S, Baert F, Noman M, Moortgat L, Geens P, Iwens D, Aerden I, Van Assche G, Van Olmen G, Rutgeerts P. Fecal calprotectin is a surrogate marker for endoscopic lesions in inflammatory bowel disease. *Inflamm Bowel Dis* 2012; **18**: 2218-2224 [PMID: 22344983 DOI: 10.1002/ibd.22917]
  - 49 **Molander P**, Färkkilä M, Ristimäki A, Salminen K, Kemppainen H, Blomster T, Koskela R, Jussila A, Rautiainen H, Nissinen M, Haapamäki J, Arkkila P, Nieminen U, Kuusma J, Punkkinen J, Kolho KL, Mustonen H, Sipponen T. Does fecal calprotectin predict short-term relapse after stopping TNF $\alpha$ -blocking agents in inflammatory bowel disease patients in deep remission? *J Crohns Colitis* 2015; **9**: 33-40 [PMID: 25052347 DOI: 10.1016/j.crohns.2014.06.012]
  - 50 **Bodelier AG**, Jonkers D, van den Heuvel T, de Boer E, Hameeteman W, Masclee AA, Pierik MJ. High Percentage of IBD Patients with Indefinite Fecal Calprotectin Levels: Additional Value of a Combination Score. *Dig Dis Sci* 2017; **62**: 465-472 [PMID: 27933473 DOI: 10.1007/s10620-016-4397-6]
  - 51 **Osborne JM**, Flight I, Wilson CJ, Chen G, Ratcliffe J, Young GP. The impact of sample type and procedural attributes on relative acceptability of different colorectal cancer screening regimens. *Patient Prefer Adherence* 2018; **12**: 1825-1836 [PMID: 30271126 DOI: 10.2147/PPA.S172143]
  - 52 **Vermeire S**, Van Assche G, Rutgeerts P. Laboratory markers in IBD: useful, magic, or unnecessary toys? *Gut* 2006; **55**: 426-431 [PMID: 16474109 DOI: 10.1136/gut.2005.069476]
  - 53 **Theede K**, Holck S, Ibsen P, Ladelund S, Nordgaard-Lassen I, Nielsen AM. Level of Fecal Calprotectin Correlates With Endoscopic and Histologic Inflammation and Identifies Patients With Mucosal Healing in Ulcerative Colitis. *Clin Gastroenterol Hepatol* 2015; **13**: 1929-36. e1 [PMID: 26051392 DOI: 10.1016/j.cgh.2015.05.038]





## Managing esophagocutaneous fistula after secondary gastric pull-up: A case report

Johan F Lock, Stanislaus Reimer, Sebastian Pietryga, Rafael Jakubietz, Sven Flemming, Alexander Meining, Christoph-Thomas Germer, Florian Seyfried

**ORCID number:** Johan F Lock 0000-0002-9007-3937; Stanislaus Reimer 0000-0002-6356-7632; Sebastian Pietryga 0000-0002-9457-5416; Rafael Jakubietz 0000-0002-1471-9986; Sven Flemming 0000-0002-6304-3169; Alexander Meining 0000-0002-0127-4922; Christoph-Thomas Germer 0000-0003-3539-6132; Florian Seyfried 0000-0002-5915-8692.

**Author contributions:** Lock JF, Pietryga S, Flemming S and Seyfried F wrote the manuscript; Seyfried F led overall treatment; Seyfried F, Lock JF and Jakubietz R performed revisional surgery; Reimer S and Meining A led endoscopic treatment. Lock JF, Pietryga S and Flemming S prepared the figures; Germer CT, Meining A and Jakubietz R supported infrastructure and organizational issues; all authors read and approved the final manuscript.

**Informed consent statement:** A written consent for publication was obtained from the patient for all potentially identifiable clinical data and accompanying images.

**Conflict-of-interest statement:** The authors declare that they have no competing interests.

**CARE Checklist (2016) statement:** The authors have read the CARE

**Johan F Lock, Sebastian Pietryga, Sven Flemming, Christoph-Thomas Germer, Florian Seyfried,** Department of General, Visceral, Transplantation, Vascular and Pediatric Surgery, University Hospital Würzburg, Würzburg 97080, Germany

**Stanislaus Reimer, Alexander Meining,** Department of Gastroenterology, University Hospital Würzburg, Würzburg 97080, Germany

**Rafael Jakubietz,** Department of Trauma-, Hand-, Plastic- and Reconstructive Surgery, University Hospital Würzburg, Würzburg 97080, Germany

**Corresponding author:** Sven Flemming, MD, Academic Research, Senior Research Fellow, Surgeon, Department of General, Visceral, Transplantation, Vascular and Pediatric Surgery, University Hospital Würzburg, Oberdürrbacher Str. 6, Würzburg 97080, Germany. [flemming\\_s@ukw.de](mailto:flemming_s@ukw.de)

### Abstract

#### BACKGROUND

Gastric pull-up (GPU) procedures may be complicated by leaks, fistulas, or stenoses. These complications are usually managed by endoscopy, but in extreme cases multidisciplinary management including reoperation may be necessary. Here, we report a combined endoscopic and surgical approach to manage a failed secondary GPU procedure.

#### CASE SUMMARY

A 70-year-old male with treatment-refractory cervical esophagocutaneous fistula with stenotic remnant esophagus after secondary GPU was transferred to our tertiary hospital. Local and systemic infection originating from the infected fistula was resolved by endoscopy. Hence, elective esophageal reconstruction with free-jejunal interposition was performed with no subsequent adverse events.

#### CONCLUSION

A multidisciplinary approach involving interventional endoscopists and surgeons successfully managed severe complications arising from a cervical esophagocutaneous fistula after GPU. Endoscopic treatment may have lowered the perioperative risk to promote primary wound healing after free-jejunal graft interposition.

Checklist (2016), and the manuscript was prepared and revised according to the CARE Checklist (2016).

**Open-Access:** This article is an open-access article that was selected by an in-house editor and fully peer-reviewed by external reviewers. It is distributed in accordance with the Creative Commons Attribution NonCommercial (CC BY-NC 4.0) license, which permits others to distribute, remix, adapt, build upon this work non-commercially, and license their derivative works on different terms, provided the original work is properly cited and the use is non-commercial. See: <http://creativecommons.org/licenses/by-nc/4.0/>

**Manuscript source:** Unsolicited manuscript

**Specialty type:** Surgery

**Country/Territory of origin:** Germany

**Peer-review report's scientific quality classification**

Grade A (Excellent): A  
Grade B (Very good): B  
Grade C (Good): 0  
Grade D (Fair): 0  
Grade E (Poor): 0

**Received:** December 21, 2020

**Peer-review started:** December 21, 2020

**First decision:** January 23, 2021

**Revised:** February 5, 2021

**Accepted:** March 16, 2021

**Article in press:** March 16, 2021

**Published online:** April 28, 2021

**P-Reviewer:** Couto-Worner I, Eysselein VE

**S-Editor:** Liu M

**L-Editor:** Webster JR

**P-Editor:** Liu JH



**Key Words:** Esophageal fistula; Gastric fistula; Esophageal stenosis; Esophageal perforation; Endoscopic vacuum therapy; Free-jejunal graft; Autogenous jejunum transplantation; Case report

©The Author(s) 2021. Published by Baishideng Publishing Group Inc. All rights reserved.

**Core Tip:** Gastric pull-up (GPU) reconstruction after esophagectomy may be complicated by leaks, fistulas, and stenoses. In such cases, endoscopic interventions, including endoscopic vacuum therapy, stenting, or dilatation, are the corrective treatments of choice, but surgery is preferred when esophageal reconstruction becomes necessary. Here, we report a case of esophageal reconstruction after a secondary GPU procedure by combining endoscopic and surgical techniques to perform subtotal esophageal resection and reconstruction using a free-jejunal graft interposition.

**Citation:** Lock JF, Reimer S, Pietryga S, Jakubietz R, Flemming S, Meining A, Germer CT, Seyfried F. Managing esophagocutaneous fistula after secondary gastric pull-up: A case report. *World J Gastroenterol* 2021; 27(16): 1841-1846

**URL:** <https://www.wjnet.com/1007-9327/full/v27/i16/1841.htm>

**DOI:** <https://dx.doi.org/10.3748/wjg.v27.i16.1841>

## INTRODUCTION

Gastric pull-up (GPU) procedures may be complicated by leaks, fistulas, and stenoses. In such cases, restoration of the esophagus and adequate recovery of alimentation becomes challenging<sup>[1]</sup>. Endoscopic interventions, including endoscopic vacuum therapy (EVT), stenting, or dilatation, are the corrective treatments of choice<sup>[2]</sup>, but surgery is preferred when esophageal reconstruction becomes necessary<sup>[3]</sup>. Here, we report a case of esophageal reconstruction after a secondary GPU procedure by combining endoscopic and surgical techniques.

## CASE PRESENTATION

### Chief complaints

A 70-year-old male patient underwent emergency esophageal diversion after injury to the cervical esophagus during spinal surgery.

### History of present illness

Six months later, retrosternal GPU procedure was performed but postoperative anastomotic leakage occurred. The leakage was successfully managed by endoscopy and the patient was discharged with a fully covered esophageal stent in place. Three weeks later, local cervical infection and sepsis developed. At this time, our tertiary university hospital was contacted for patient transfer.

### History of past illness

Notable previous illnesses were arterial hypertension, non-active smoking status and an ischemic stroke with incomplete senso-motoric hemiparesis. Furthermore, the patient had a thyroidectomy in the past and open prostatectomy due to prostate cancer.

### Personal and family history

The patient had no family history that was related to the present illness.

### Physical examination

On admission, the patient showed clear signs of malnutrition and systemic inflammation with jugular and cervical phlegmon.

### Laboratory examinations

Initial laboratory data revealed a hemoglobin level of 6.7 g/dL, white blood cell count of 6400 cells/ $\mu$ L, and platelet count of  $210 \times 10^3/\mu$ L. The creatinine level was 0.76 mg/dL, unremarkable liver and cholestasis parameters, and albumin level was 2.8 g/dL.

### Imaging examinations

A chest computed tomography (CT) scan and endoscopy revealed a dislodged esophageal stent, with the proximal flare abutting an extraesophageal air and fluid-filled cavity (Figure 1). During stent removal, a partially epithelialized esophageal perforation 2 cm distal to the pharynx with an infected cavity (Figure 1B and C) as well as a 5 cm-long stenosis of the remaining esophagus were detected.

## FINAL DIAGNOSIS

Diagnosis of cervical esophagocutaneous fistula and anastomotic stenosis after GPU with signs of chronic malnutrition and systemic inflammation.

## TREATMENT

The patient received calculated antibiotic treatment and was transferred to the intensive care unit. An immediate endoscopy was carried out, and the dislocated stent (partially covered metal stent, length 80 mm, diameter 18 mm) was removed. Endoscopy showed an old, partially epithelialized and wide esophageal perforation 2 cm distal of the pharynx with an infected cavity behind it. Distal of the fistula, a long-segment (5 cm) stenosis of the esophagus ranging up to the esophago-gastrostomy was confirmed. Notably, the perforation and the fistula cavity were likely to be a secondary injury due to the dislocated cervical stent tulip (diameter 24 mm). After pus evacuation and debridement of the fistula, a fully covered self-expanding metal stent (length 100 mm, diameter 20 mm) was inserted in order to cover the fistula and to treat the stenosis. Due to an expected long-term course, a percutaneous jejunal feeding catheter was surgically inserted to ensure sufficient enteral nutrition. The first re-endoscopy revealed a slippage of the stent so that the cranial fistula ostium was not sufficiently covered. The stent position was successfully corrected but dislocated again during follow-up.

Thus, endoscopic management was switched to EVT. An EsoSponge system (B. Braun Melsungen, Germany) was placed into the esophagocutaneous fistula ostium (cavity). The jugular and cervical phlegmon resolved during EVT within two weeks and repeated endoscopic balloon dilatation was performed to resolve the esophageal stenosis. However, it became obvious that endoscopic management could not resolve the broad and rigid fistula with the concomitant partially obliterated esophagus. The issue was discussed interdisciplinarily and the therapeutic aim of endoscopy was redefined: Profound consolidation of the cervical infection and cleaning of the fistula cavity until salvage surgery (Figure 1D).

The cervical phlegmon resolved within two weeks, allowing subtotal esophageal resection and reconstruction using a free-jejunal graft interposition according to Ott *et al*<sup>[4]</sup>. Pre-operative work up included CT angiography to establish the feasibility of vascular reconstruction. Partial sternotomy was necessary to provide access to the esophagus and the stomach (Figure 2A). After resection of the cervical esophagus and fistula, the exploration confirmed that the GPU could not be mobilized up to the pharynx. Thus, laparotomy was performed and a suitable jejunal segment was harvested. The left carotid artery and the left jugular vein were used as recipient vessels. The graft was implanted in an isoperistaltic position. The cervical anastomosis was performed in an end-to-end fashion and the upper mediastinal gastro-jejuno-stomy in a side-to-side fashion (Figure 2B). A part of the upper sternum was resected to avoid any pressure on the graft and gastrojejunostomy. The soft tissue defect was covered with a sternocleidomastoid muscle flap. Abdominal reconstruction was achieved by an end-to-end jejunostomy.

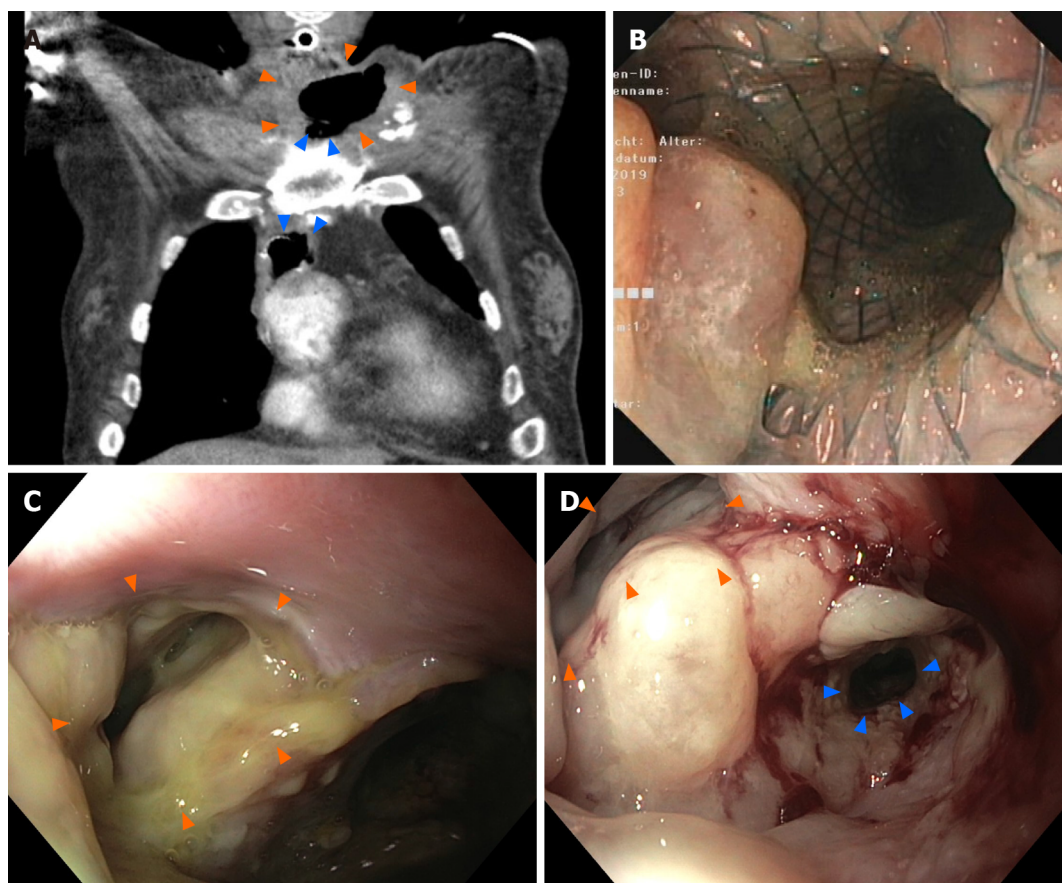


**Figure 1 Preoperative findings.** A: Contrast-enhanced computed tomography with oral and intravenous contrast application showing the jugular abscess (indicated by orange arrowheads) and the fully covered self-expandable metallic stent with its proximal end in the fistula (indicated by blue arrowheads); B: Endoscopy showing fully covered self-expandable metallic stent placed in the distal stenotic esophagus with the esophagocutaneous fistula directly orally of the stent. The fistula orifice is partially covered by the stent flare; C: Endoscopy after stent extraction with the large prestenotic fistula orifice (indicated by orange arrowheads); fistula filled with pus; D: Endoscopy after endoscopic vacuum therapy with cleaned fistula (indicated by orange arrowhead). The fistula is entirely epithelized. The distal esophagus segment remains stenotic (indicated by blue arrowheads).

## OUTCOME AND FOLLOW-UP

The postoperative course was uneventful. Oral alimentation was reestablished accompanied with daily speech therapy. Anastomotic healing was confirmed radiologically and endoscopically and the patient was transferred to a rehabilitation clinic in good clinical condition.

## DISCUSSION

Esophagectomy with diversion and later reconstruction of the upper gastrointestinal (GI) tract is reserved for complex esophageal disease<sup>[5]</sup>. Despite numerous advantages over alternative reconstruction techniques, anastomotic complications following GPU procedures occur in up to 12% of cases<sup>[6]</sup>.

Managing anastomotic leakage or stricture of GPU can be extremely challenging because of local tissue damage from previous surgery or chronic infection<sup>[4,7]</sup>. Endoscopic management of leaks, fistulas and stenosis in the upper GI tract has therefore not only become a valuable tool, but the standard approach for successful management even in complex situations<sup>[8,9]</sup>. Here, it is extremely important to carefully consider and constantly evaluate the local tissue and wound conditions. In our case, the constant pressure caused by the stent itself may have further deteriorated the esophageal wall and, thus, may have caused perforation and fistula with abscess formation since no external drainage had been established.

The surgical options available for the management of a complicated GPU procedure are limited and usually contain a high risk of morbidity and mortality<sup>[5]</sup>. Esophageal reconstruction with a free jejunal graft was introduced by Seidenberg and colleagues



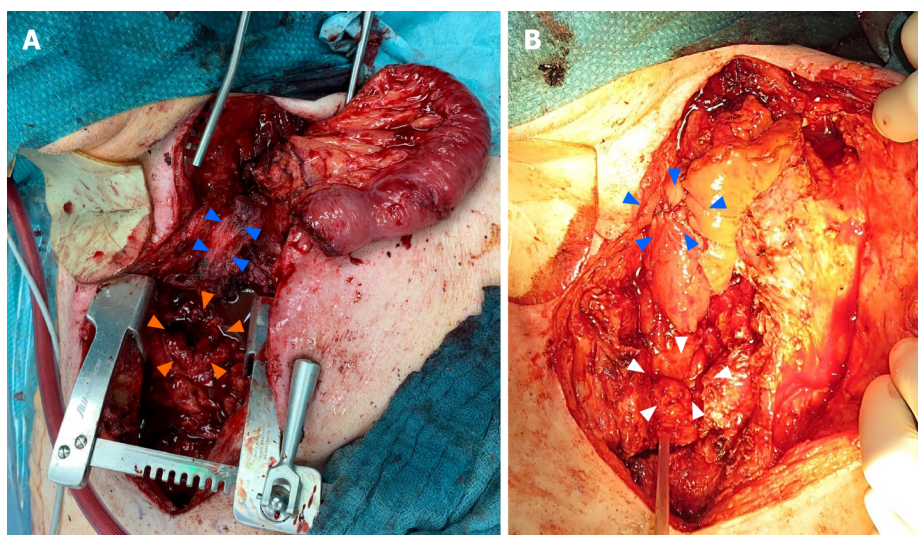


**Figure 2 Findings during surgery.** A: Free jejunal segment after reperfusion before intestinal anastomosis; orange arrowheads indicating the orifice of the gastric pull-up; blue arrowheads indicating the stenotic distal esophagus; B: Free jejunal segment after intestinal anastomosis; blue arrowheads at the mesentery of the free jejunal graft indicating the proximal esophago-jejunostomy; white arrowheads indicating distal jejuno-gastrostomy.

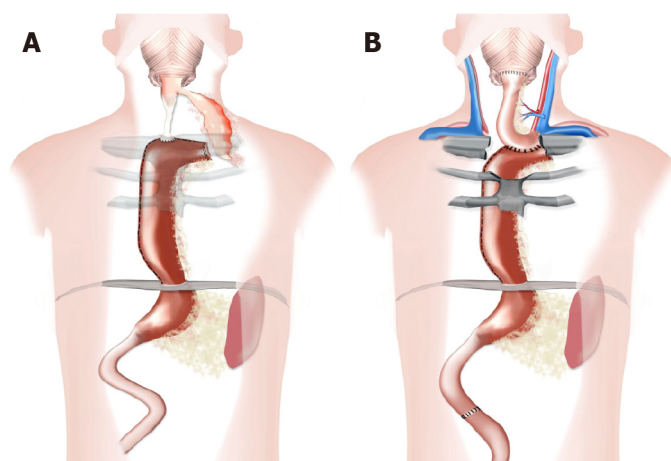


**Figure 3 Anatomic schemes.** A: Anatomy on admission; B: Reconstruction after surgery.

in 1959 and later modified by Siewert and colleagues in 2008 for treating cancer of the cervical esophagus<sup>[4,10]</sup>. The use of a salvage option after failed GPU has also been described<sup>[12]</sup>. Recent data regarding follow-up results in esophageal reconstruction strongly suggest the superiority of intestinal flaps over other reconstructions such as skin flaps.

High failure rates for secondary attempts after failed esophageal reconstruction have been described<sup>[1]</sup>, with a complication rate in excess of 70%<sup>[11]</sup>. However, free jejunal grafts have considerable advantages. They are usually easy to harvest, provide low donor-site morbidity, have good size approximation to the cervical esophagus, tolerate reflux well, and have a low rate of peptic ulceration incidence<sup>[12]</sup>. Disadvantages include the need for transient ischemia that requires advanced microsurgical skills for swift revascularization and a challenging surgical site environment because of previous surgery and infection.

## CONCLUSION

A multidisciplinary approach involving interventional endoscopists and surgeons was necessary to enable successful salvage management. Despite prior complications, operations and chronic infection, restoration and reconstruction of the esophagus was ultimately achieved (Figure 3). Thus, patients with chronic postoperative fistulas or



stenoses of the esophagus should be referred to specialized centers in a timely manner.

## ACKNOWLEDGEMENTS

We would like to thank Mrs. Anna Maria Kellersmann for preparation of **Figure 3** and Dr. Mohammed Hankir for proofreading the manuscript.

## REFERENCES

- 1 **Okazaki M**, Asato H, Takushima A, Nakatsuka T, Ueda K, Harii K. Secondary reconstruction of failed esophageal reconstruction. *Ann Plast Surg* 2005; **54**: 530-537 [PMID: [15838216](#) DOI: [10.1097/01.sap.0000155280.50178.fc](#)]
- 2 **Scognamiglio P**, Reeh M, Karstens K, Bellon E, Kantowski M, Schön G, Zapf A, Chon SH, Izbicki JR, Tachezy M. Endoscopic vacuum therapy vs stenting for postoperative esophago-enteric anastomotic leakage: systematic review and meta-analysis. *Endoscopy* 2020; **52**: 632-642 [PMID: [32316043](#) DOI: [10.1055/a-1149-1741](#)]
- 3 **Moore JM**, Hooker CM, Molena D, Mungo B, Brock MV, Battafarano RJ, Yang SC. Complex Esophageal Reconstruction Procedures Have Acceptable Outcomes Compared With Routine Esophagectomy. *Ann Thorac Surg* 2016; **102**: 215-222 [PMID: [27217296](#) DOI: [10.1016/j.athoracsur.2016.02.039](#)]
- 4 **Ott K**, Lordick F, Molls M, Bartels H, Biemer E, Siewert JR. Limited resection and free jejunal graft interposition for squamous cell carcinoma of the cervical oesophagus. *Br J Surg* 2009; **96**: 258-266 [PMID: [19224522](#) DOI: [10.1002/bjs.6437](#)]
- 5 **DiPierro FV**, Rice TW, DeCamp MM, Rybicki LA, Blackstone EH. Esophagectomy and staged reconstruction. *Eur J Cardiothorac Surg* 2000; **17**: 702-709 [PMID: [10856863](#) DOI: [10.1016/s1010-7940\(00\)00408-5](#)]
- 6 **Butskiy O**, Rahmanian R, White RA, Durham S, Anderson DW, Prisman E. Revisiting the gastric pull-up for pharyngoesophageal reconstruction: A systematic review and meta-analysis of mortality and morbidity. *J Surg Oncol* 2016; **114**: 907-914 [PMID: [27774626](#) DOI: [10.1002/jso.24477](#)]
- 7 **Suga H**, Okazaki M, Sarukawa S, Takushima A, Asato H. Free jejunal transfer for patients with a history of esophagectomy and gastric pull-up. *Ann Plast Surg* 2007; **58**: 182-185 [PMID: [17245146](#) DOI: [10.1097/01.sap.0000235432.09523.eb](#)]
- 8 **Laukoetter MG**, Mennigen R, Neumann PA, Dhayat S, Horst G, Palmes D, Senninger N, Vowinkel T. Successful closure of defects in the upper gastrointestinal tract by endoscopic vacuum therapy (EVT): a prospective cohort study. *Surg Endosc* 2017; **31**: 2687-2696 [PMID: [27709328](#) DOI: [10.1007/s00464-016-5265-3](#)]
- 9 **Seyfried F**, Reimer S, Miras AD, Kenn W, Germer CT, Scheurlen M, Jurowich C. Successful treatment of a gastric leak after bariatric surgery using endoluminal vacuum therapy. *Endoscopy* 2013; **45** Suppl 2: E267-E268 [PMID: [24008459](#) DOI: [10.1055/s-0033-1344569](#)]
- 10 **Seidenberg B**, Rosenak SS, Hurwitt ES, Som ML. Immediate reconstruction of the cervical esophagus by a revascularized isolated jejunal segment. *Ann Surg* 1959; **149**: 162-171 [PMID: [13627972](#) DOI: [10.1097/00000658-195902000-00002](#)]
- 11 **Sacak B**, Orfanotis G, Nicoli F, Liu EW, Ciudad P, Chen SH, Chen HC. Back-up procedures following complicated gastric pull-up procedure for esophageal reconstruction: Salvage with intestinal flaps. *Microsurgery* 2016; **36**: 567-572 [PMID: [26679742](#) DOI: [10.1002/micr.22520](#)]
- 12 **Gaur P**, Blackmon SH. Jejunal graft conduits after esophagectomy. *J Thorac Dis* 2014; **6** Suppl 3: S333-S340 [PMID: [24876939](#) DOI: [10.3978/j.issn.2072-1439.2014.05.07](#)]



Published by **Baishideng Publishing Group Inc**  
7041 Koll Center Parkway, Suite 160, Pleasanton, CA 94566, USA

**Telephone:** +1-925-3991568

**E-mail:** [bpgoffice@wjgnet.com](mailto:bpgoffice@wjgnet.com)

**Help Desk:** <https://www.f6publishing.com/helpdesk>

<https://www.wjgnet.com>

